

VOLUME 10 / June 2020

# detritus

Multidisciplinary Journal for Waste Resources & Residues

Editor in Chief:  
RAFFAELLO COSSU

[detritusjournal.com](http://detritusjournal.com)

an official journal of:

**iwwg**  
international waste working group

  
CISA



ISSN 2611-4135 / ISBN 9788862650670  
DETRITUS - Multidisciplinary Journal for Waste Resources & Residues

Detritus is indexed in:

- Emerging Sources Citation Index (ESCI), Clarivate Analytics, Web of Science
- Scopus, Elsevier
- DOAJ Directory of Open Access Journals
- Google Scholar

© 2020 CISA Publisher. All rights Reserved

The journal contents are available on the official website: [www.detritusjournal.com](http://www.detritusjournal.com)

Open access articles under CC BY-NC-ND license (<http://creativecommons.org/licenses/by-nc-nd/4.0/>)

Legal head office: Cisa Publisher - Eurowaste Srl, Via Beato Pellegrino 23, 35137 Padova - Italy / [www.cisapublisher.com](http://www.cisapublisher.com)

Graphics and layout: Elena Cossu, Anna Artuso - Studio Arcoplan, Padova / [studio@arcoplan.it](mailto:studio@arcoplan.it)

Printed by Cleup, Padova, Italy

Front page photo credits: 'Life and waste' courtesy of Nafiul Islam, Bangladesh

For subscription to printed version, advertising or other commercial opportunities please contact the Administration Office at [administration@eurowaste.it](mailto:administration@eurowaste.it)

Papers should be submitted online at <https://mc04.manuscriptcentral.com/detritusjournal>

Instructions to authors may be found at <https://detritusjournal.com/guide-for-authors/>

For any enquiries and information please contact the Editorial Office at [editorialoffice@detritusjournal.com](mailto:editorialoffice@detritusjournal.com)

Registered at the Court of Padova on March 13, 2018 with No. 2457

**[www.detritusjournal.com](http://www.detritusjournal.com)**

VOLUME 10 / June 2020

# detrītus

Multidisciplinary Journal for Waste Resources & Residues

Editor in Chief:

RAFFAELLO COSSU

[detrītusjournal.com](http://detrītusjournal.com)

an official journal of:

**iwwg**  
international waste working group

  
CISA



Detritus - Multidisciplinary Journal for Waste Resources and Residues - is aimed at extending the "waste" concept by opening up the field to other waste-related disciplines (e.g. earth science, applied microbiology, environmental science, architecture, art, law, etc.) welcoming strategic, review and opinion papers. **Detritus is indexed in Emerging Sources Citation Index (ESCI) Web of Science, Scopus, Elsevier, DOAJ Directory of Open Access Journals and Google Scholar.** Detritus is an official journal of IWWG (International Waste Working Group), a non-profit organisation established in 2002 to serve as a forum for the scientific and professional community and to respond to a need for the international promotion and dissemination of new developments in the waste management industry.

#### EDITOR-IN-CHIEF:

**Raffaello Cossu**, University of Padova, Italy  
E-mail: raffaello.cossu@unipd.it

#### ASSOCIATE EDITORS:

**Damià Barcelo**, ICRA Catalan Institute for Water Research, Spain  
E-mail: damia.barcelo@idaea.csic.es

**Pierre Hennebert**, INERIS, France  
E-mail: pierre.hennebert@ineris.fr

**Anders Lagerkvist**, Lulea University of Technology, Sweden  
E-mail: anders.lagerkvist@ltu.se

**Michael Nelles**, University of Rostock, Germany  
E-mail: michael.nelles@uni-rostock.de

**Abdul-Sattar Nizami**, King Abdulaziz University, Saudi Arabia  
E-mail: nizami\_pk@yahoo.com

**Mohamed Osmani**, Loughborough University, United Kingdom  
E-mail: m.osmani@lboro.ac.uk

**Alessandra Poletti**, University of Rome "La Sapienza", Italy  
E-mail: alessandra.poletti@uniroma1.it

**Marina Rigillo**, University of Naples "Federico II", Italy  
E-mail: marina.rigillo@unina.it

**Marco Ritzkowski**, TuTech Innovation GmbH, Germany  
E-mail: m.ritzkowski@tuhh.de

**Howard Robinson**, Phoenix Engineering, United Kingdom  
E-mail: howardr@phoenix-engineers.co.uk

**Rainer Stegmann**, TuTech Innovation GmbH, Germany  
E-mail: stegmann@tuhh.de

**Hans van der Sloot**, Hans Van der Sloot Consultancy, The Netherlands  
E-mail: hans@vanderslootconsultancy.nl

**Ian Williams**, University of Southampton, United Kingdom  
E-mail: i.d.Williams@soton.ac.uk

**Jonathan Wong**, Hong Kong Baptist University, Hong Kong  
E-mail: jwong@hkbu.edu.hk

**Hideki Yoshida**, Muroran Institute of Technology, Japan  
E-mail: gomigomi@mmm.muroran-it.ac.jp

**Aoran Yuan**, University of Birmingham, United Kingdom  
E-mail: Yuanhr@ms.giec.ac.cn

**Liangtong Tony Zhan**, Zheijangu University, China  
E-mail: zhanlt@zju.edu.cn

**Christian Zurbuegg**, Eawag/Sandec, Switzerland  
E-mail: christian.zurbuegg@eawag.ch

#### EDITORIAL OFFICE:

**Gioia Burgello**, Eurowaste Srl, Italy  
E-mail: editorialoffice@detritusjournal.com

#### MANAGING EDITORS:

**Werner Bidlingmaier**, Bauhaus-University Weimar  
Portraits  
werner.bidlingmaier@uni-weimar.de

**Elena Cossu**, Studio Arcoplan, Italy  
A photo, a fact, an emotion  
E-mail: studio@arcoplan.it

**Maria Cristina Lavagnolo**, University of Padova, Italy  
Info from the global world  
E-mail: mariacristina.lavagnolo@unipd.it

**Alberto Pivato**, University of Padova, Italy  
Environmental Forensics, Research to industry and industry to research,  
E-mail: alberto.pivato@unipd.it

**Roberto Raga**, University of Padova, Italy  
Books Review  
E-mail: roberto.raga@unipd.it

**Marco Ritzkowski**, TuTech Innovation GmbH, Germany  
New projects  
E-mail: m.ritzkowski@tuhh.de

**Rainer Stegmann**, TuTech Innovations GmbH, Germany  
Waste and Art  
E-mail: stegmann@tuhh.de

#### EDITORIAL ADVISORY BOARD:

**Mohammad Alamgir**, Khulna University of Engineering & Technology, Bangladesh

**Luca Alibardi**, Cranfield University, UK

**Andreas Bartl**, Vienna University of Technology, Austria

**Luciano Butti**, B&P Avvocati, Italy

**Dezhen Chen**, Tongji University, China

**Christophe Cord'Homme**, CNIM Group, France

**Hervé Corvellec**, Lund University, Sweden

**Frederic Coulon**, Cranfield University, UK

**Francesco Di Maria**, University of Perugia, Italy

**Lisa Doeland**, Radboud University Nijmegen, The Netherlands

**George Ekama**, University of Capetown, South Africa

**Marco Frey**, Sant'Anna School of Advance Studies, Italy

**Dieter Gerten**, Potsdam Institute for Climate Impact Research and Humboldt University of Berlin, Germany

**Apostolos Giannis**, Nanyang Technological University, Singapore

**Ketil Haarstad**, Norwegian Institute for Bioeconomy, Norway

**Uta Krogmann**, Rutgers University, USA

**Jianguo Liu**, Tsinghua University, China

**Wenjing Lu**, Tsinghua University, China

**Claudio Fernando Mahler**, COPPE/UFRJ, Brazil

**Marco Ragazzi**, University of Trento, Italy

**Jörg Römbke**, ECT GmbH, Germany

**Natalia Sliusar**, Perm National Research Polytechnic University, Russia

**Evangelos Voudrias**, Democritus University of Thrace, Greece

**Casta Zecena**, Universidad de San Carlos de Guatemala, Guatemala

## Editorial

# “CLOSING THE LOOP” OF THE CIRCULAR ECONOMY AND COVID19

The COVID-19 pandemic has placed considerable pressure on the waste management system and has challenged the Circular Economy, highlighting the already clearly evident contradictions and fragilities of the system.

The acknowledged principles underlying the Circular Economy are based on a series of assumptions including a limited availability of natural resources and a need to restrict emissions that impact on an environment at risk of being irreversibly compromised. Accordingly, the resulting aim of the Circular Economy is to maintain the value of products over an extended period of time, to reduce the use of non-renewable primary materials and to minimise impacts by preventing the generation of wastes (“Zero Waste”) through use of environmentally-friendly technologies.

Wastes therefore have been identified as a boundless new source of resources combined with the dual perspective of removing the problem of providing for their disposal. Thus, following establishment of the Circular Economy through the defining of measures of intervention and the enactment of national and international legislation, wastes have been definitively legitimised to substitute for non-renewable resources. This process had indeed already been launched worldwide through the “Kobe 3Rs Action Plan” (2008), with wastes evolving from useless foul-smelling dross into pieces of gold. And following decades of striving to ‘close the loop’ (Otterpohl et al., 1997) with the aim of fostering a sustainable closure of the material loop, conscious of the limitations of the industrial cycles and recirculation, all at once the world economy – in severe recession and seeking new development models – ‘copied and pasted’ this circular vision, defining it “an opportunity to rethink our economic future” and adopting the same to decline a new means of ensuring the future survival of the planet. The Circular Economy framework is nowadays seen as a key approach to achieve some of the United Nations Sustainable Development Goals (SDGs), such as goal 12- to ensure sustainable consumption and production patterns.

However, this attempt to portray the ‘new’ economy as the solution for all environmental concerns and promoter of a generational solidarity also serves to highlight both the original sin and potential Achilles heel of the system. Although worthy of having introduced the concept of the circularity of resources worldwide, this approach, globally deemed perfect (economically, socially and environmentally), has however failed to succeed to stimulate the marked change required to detach itself from the need for a conti-

nual rise in use of consumer goods and supply of services to affirm global development.

Indeed, SDGs, in conjunction with the aims of a Circular Economy, are directed along a similar trend, as depicted by sustainable development goal n.8, the aims of which translate into a global GDP growth of 3% per year (Hickel, 2019). In this context, the global use of primary materials is projected to almost double from 89 Gt in 2017 to 167 Gt in 2060, where the strongest growth in material use will occur in emerging and developing economies. The high demand for materials implies a similar rate of increase in use of both primary and secondary materials, although the high labour costs of secondary technologies, the need to continually update recycling technologies and the somewhat scarce quality of some fractions hamper a rapid and solid penetration of secondary materials despite an increase of competition in the area of recycling (data from OECD, 2019). The recycling industry, currently a tenth of the size of the mining sector in terms of GDP share, is likely to become more competitive and grow, although remaining a much smaller industry than the mining of primary materials.

For specific municipal waste streams, the market of secondary materials has certainly offered development opportunities to new recycling industries, although the combined effect of a rise in separate collection, the closure of a series of international markets and an ongoing trade war between China and the US, have all complicated the exploitation of growing volumes of materials. This excess supply has resulted in a depreciation of secondary materials (e.g.: the average price of cardboard has plummeted by 90% over the last year), and thus in a difficulty to close the cycle, at times even forcing a return to processing the materials as wastes (Maragoni, 2020).

Whatever the reason, an increase in waste production will be witnessed in forthcoming decades, particularly in those countries in which the Circular Economy is proposed as a development model of extreme efficacy in overcoming disparities. In 2016, a total of 2.1 billion tons of municipal wastes were produced worldwide, with a predicted 70% increase by the year 2050 (the

Sub-Saharan Africa is expected to see waste level approximately triple); the sole EU produced a total of 5t per inhabitant, 4% of which were hazardous waste (World Bank and Eurostat data).

Despite the efforts made to unite the starting point with the end point of this material loop, unfortunately, closure of the Circular Economy loop will only prove feasible if we finally concede that the Circular Economy as envisaged to

date does not provide a solution to the waste problem and does not contribute towards reducing disparities. We risk witnessing a further increase in forms of environmental colonialism: still today, electronic wastes originating from a series of industrialised nations (including the US, France, Germany, Switzerland, Korea and the Netherlands) end up in the Agbogbloshie landfill (Ghana). Indeed, Africa, in spite of the key statement made during the Bamako Conference (1991) against the importation of electronic wastes, continues to act as sink for a dubious separate collection of electronic wastes from throughout the world, with Ghana and Nigeria leading the depressing rank of importer nations (Poltronieri, 2019).

However, to identify waste recycling as the focal point of a Circular Economy whilst at the same time advocating the aim of Zero Waste is a sort of oxymoron.

The contradictions and fragilities highlighted have become even more evident during the recent COVID-19 pandemic.

Although a mean decrease of 20% was registered in municipal solid waste during the lockdown period, largely due to the lack of waste generated by traders and the restaurants field, the slowing down of a series of industrial activities and the shutting down of yet others, together with the closure of foreign markets have prevented separately collected wastes from finding an appropriate collocation. This in turn has led to a saturation of storage both in recycling plants and, in some cases, in thermal treatment plants. Contrary to both the latter and to landfills however, recycling fails to provide an outlet for the waste materials, that must be collected in any case.

An inverse situation has been created with regard to medical wastes, which in some contexts have increased three-fold, with the related management being on the verge of collapsing due to the unexpected deluge of volumes to be handled. The demagogic choice made by many European countries to limit (or even prevent), based on the principles of the Circular Economy, the construction of facilities, is at risk of becoming crucial in a sector in which thermal treatment plays a key role in guaranteeing safety and protection.

During the post-pandemic period, we will also need to deal with the disposal of personal protective equipment (face masks, gloves, plexiglass shields) and other plastic materials used in public spaces (plastic beakers, cutlery and cups used in the hospitality and other industries), items manufactured using mixed materials and deemed indispensable in the start-up of economic activities, to enable people to return to the office or to factories, to sit in a restaurant or to access retail shops.

There is therefore an evident conflict between the pathway identified by the Circular Economy (e.g.: European Strategy for Plastics in a Circular Economy, 2018) tending towards a reduction of single use plastics, and the need

to increase use of the latter over the forthcoming months, or even years. In Italy, the quantities of materials needed by workers throughout the various sectors, taking into account that some will continue to work from home, has been estimated in the use of more than 900 million face masks each month in the work place, another 100 million during travel, and more than 500 million gloves. It has also been estimated that schools will use a total of 400 million face masks each month, in addition to single-use lunch boxes with plastic plates and cutlery (estimates from Politecnico di Torino).

Solutions to these evident conflicts and contradictions have been put forward by the waste management sector involved in dealing with issues raised by the pandemic, in the interest of pursuing an efficient and non-demagogic closure of the Circular Economy loop.

Concomitant to the development of recycling plants aimed at improving performance and better defining End of Waste criteria, it is fundamental that the important contribution provided by the energy from waste sector in recovery of materials and provision of an alternative outlet to recycling, including both sustainable landfilling and geological repository (Cossu, 2016), should be acknowledged: in this way, residues from both recycling and emergencies such as the current COVID-19 pandemic could be allocated final or temporary storage. A system therefore that envisages a return to the land and a more flexible closure of the material loop, thus reinforcing the concept of resilience held so dear by the Circular Economy.

Effectively, we merely need to acknowledge that the Circular Economy is not perfect and does not comprise a superior form of 'ethics' to those adhered to by previous economic models.

Maria Cristina Lavagnolo  
University of Padova, Italy  
mariacristina.lavagnolo@unipd.it

## REFERENCES

- Cossu R. (2016). Back to Earth Sites: From "nasty and unsightly" landfilling to final sink and geological repository. *Waste Management* 55, 1-2; <http://dx.doi.org/10.1016/j.wasman.2016.07.028>
- Hickel J. (2019). The contradiction of the sustainable development goals: Growth versus ecology on a finite planet. *Sustainable Development*, 27 (5) 873-884. <https://doi.org/10.1002/sd.1947>
- Maragoni A. (2020). Quale nuovo equilibrio per le filiere del riciclo? *Staffetta Quotidiana*, on line magazine. Available on line at: <https://www.staffettaonline.com/articolo.aspx?id=344211>.
- Otterpohl R., Grottker M., Lange J. (1997). Sustainable water and waste management in urban areas. *Water Science and Technology*, 35 (9) 121-133. [https://doi.org/10.1016/S0273-1223\(97\)00190-X](https://doi.org/10.1016/S0273-1223(97)00190-X)
- Poltronieri F. (2019). In questa infernale discarica tossica del Ghana finiscono i nostri rifiuti elettronici. *EURONEWS*. Available on line at: <https://it.euronews.com/2019/07/26/in-questa-infernale-discarica-tossica-del-ghana-finiscono-i-nostri-rifiuti-elettronici>

# EVALUATION OF NEW SMALL-SCALE COMPOSTING PRACTICES WITH ENERGY RECOVERY

Roberto Guião de Souza Lima Jr.<sup>1</sup> and Claudio Fernando Mahler<sup>2,\*</sup>

<sup>1</sup> Department of Environmental Engineering, University Center of Volta Redonda, UniFOA, Volta Redonda, Rio de Janeiro, Brazil

<sup>2</sup> Department of Civil Engineering, Federal University of Rio de Janeiro, UFRJ, Rio de Janeiro, Brazil

## Article Info:

Received:  
6 June 2019  
Revised:  
13 February 2020  
Accepted:  
17 February 2020  
Available online:  
5 March 2020

## Keywords:

Decentralized composting  
Minimum impact  
Energy recovery  
Leachate and gas emissions

## ABSTRACT

This study involves the evaluation of new composting systems for the treatment of organic solid waste (OSW) that has low environmental impact. Two composting devices were developed, with four types of management, and their behavior was analyzed regarding temperature, gas production, moisture, leachate and percolated water production, compost maturation, nutrient presence, pH and water heating, which can be seen as an energy gain in addition to the economic viability of the process. The proposed composting techniques kept the waste at thermophilic temperatures for more than 20 days, with no significant emission of CH<sub>4</sub>, under aerobic conditions by passive aeration, without leachate generation. These results can be partially attributed to the suspension of the compost on pallets, the residue composition chosen in the experiments and the boundary conditions of the compartments. The energy recovery test, through water recirculation inside the compost, presented temperatures that reached 51°C after 24 h of recirculation, and were maintained throughout the process, 20 days, demonstrating its effectiveness. The proposed composting models are environmentally viable, minimizing gas emissions and leachate generation compared to landfill or industrial composting plants. They can be used in industrial kitchens, residential complexes, shopping malls and other small and medium solid waste generators. In addition, the solution presented in this study avoids the transportation of waste over medium and long distances, which also brings a significant reduction in energy expenses, and in the case of landfills, it avoids occupation for long periods, thus reducing emissions of gases and leachate, whose control and treatment are expensive.

## 1. INTRODUCTION

On site composting of organic solid waste (OSW) is an advantageous alternative to landfill disposal due to its aerobic feature, minimizing emissions by transport and degradation in the landfill, as well as leachate production and the corresponding need for treatment (Pires, Martin and Ni-Bin, 2011). However, scaling issues are relevant, as discussed by Martinez-Blanco et al. (2010) through life-cycle analysis, showing the environmental advantages of small-scale composting in comparison to industrial scale, because even predominantly aerobic composting can be a source of CH<sub>4</sub>, NH<sub>3</sub>, NO<sub>3</sub>, N<sub>2</sub>O and SO<sub>2</sub>.

In this context, unwanted emissions can be minimized or avoided depending on the operation, as reported in Amlinger and Peyr Cuhls (2008), Andersen et al. (2010a), Zuokaite and Zigmontiene (2013) and Ermolaev et al. (2014). For example, home composting with higher frequency of disturbance compared to lower frequency

increases GHG emissions (Andersen et al., 2010a; 2011; 2012). The same was observed by Ahn et al. (2011) with respect to CH<sub>4</sub> in waste from a system that integrates agriculture with pasture and forest. This latter finding was a surprise, because the authors believed that the greater the number of turnings, the more aerobic the condition would be, leading to less formation of CH<sub>4</sub>.

This phenomenon can be explained by the difficulty of keeping homogeneity of the ideal environmental conditions during solid state fermentation, contributing to the formation of sites with lower oxygenation and production of CH<sub>4</sub>, whose release is facilitated by revolving the compost material (Durand, 2003). On the other hand, when minimizing the frequency of disturbance or operating under controlled static conditions, methanotrophic microorganisms oxidize up to 98% of the CH<sub>4</sub> produced in the composting, as observed by Jackel, Thummes and Kampfer (2005) and Ignatius and Miller (2009). This is economically and technically viable in small-scale operations.

\* Corresponding author:  
Claudio Fernando Mahler  
email: mahler@coc.ufrj.br



Ignatius Bettio and Miller (2009a) also drew attention to emission mitigation potential and obtaining carbon credits, considering the sum of the different small-scale static composting projects. The generated organic compound also has ecological advantages over traditional chemical fertilizers (Andersen et al., 2012), adds value to the process and acts as a soil conditioner (Kiehl, 1998).

The economic difficulties and the fragility of public policies for waste management in Brazil are reflected by the fact that around 70% of municipalities still dispose of waste in dumps (IBGE, 2010). There is also a shortage of equipment appropriate for on-site treatment of OSW generated by apartment buildings, industrial kitchens, supermarkets, schools and others. In this study, we developed and tested the performance of new composter models and composting strategies with minimal impact, easy installation and operation, without proliferation of vectors or odors, focusing on the treatment of food scraps and plant trimmings. We also tested the energy use of composting for water heating, seeking to add value to the process.

## 2. METHODOLOGY

Two composter models were tested for 60 days, called 1 and 2, using two gabions measuring 4 m long x 1 m wide and 1 m high, each divided into four compartments (A, B, C and D), each with volume of 1 m<sup>3</sup> (Figure 1). The composters were covered with HDPE tarps to control moisture from rain and the compartments were covered on two sides by drainage mats, composed of geotextile filters, and had a three-dimensional plastic drainage core with 90% voids. The composters were also supported on pallets, increasing the passive aeration on all sides, including the base via thermal convection (chimney effect), as described in Münnich et al. (2006) and Andersen et al. (2010b). A HDPE membrane was installed below the pallets for soil protection and collection of leachates.

Composter 1 was also fitted with a drainage tube with diameter of 200 mm and holes along its entire length, arranged vertically in the center of each of its compartments, simulating a chimney to increase passive aeration of organic solid wastes (Figure 1).

The residues added in compartments A, B, C and D of each composter were inoculated as described in Table 1 and covered with a 5 cm layer of dried leaves after each OSW supply, to help maintain temperature and moisture as well as combat vectors such as flies.

The waste material was formulated experimentally of 33.3% food waste, 33.3% grass or leaves and 33.3% ground tree trunks (by volume), totaling approximately 500 kg of OSW per compartment.

The composters were operated statically, without disturbance. In other words, with each new input, only the top layer of dried leaves was removed, to allow the new material to contact the material already composted.

The compartments were monitored for temperature and moisture at points 10, 25 and 50 cm away from the wall or 40, 25 and 0 cm from the center and 25, 50 and 75 cm deep in each compartment, using a thermometer and Reotemp analog moisture meter with 90 cm rod for a total of 1.800 readings during 60 days of monitoring.



FIGURE 1: Composters 1 and 2 and their compartments A, B, C, D.

The percentages of CH<sub>4</sub> and O<sub>2</sub> gases were measured at 10, 25 and 50 cm from the wall or 40, 25 and 0 cm from the center and 30 and 60 cm depth in each compartment, using a Dräger X-AM7000 gas analyzer connected to a 1 meter metal rod (1,200 readings).

The same gas analyzer was used to determine the emissions from each compartment, associated with an Agilent Technologies model ADM200 flowmeter and a pyramidal flow chamber, covering the entire surface area of each compartment, as described in Andersen et al. (2010a).

The data were grouped into treatment pairs, considering the mean values of compartments A, B, C and D of composters 1 and 2, namely, 1A and 2A, 1B and 2B, 1C and 2C, and 1D and 2D. These were treated as repetitions since the differences between composters 1 and 2 concerning the presence of the central aeration (composter 1 only) were the same for all four treatments, henceforth simply called compartments A, B, C and D. Data were also evaluated considering composter 1 and 2 individually to identify variations between them, comprising the averages of data obtained from compartments A, B, C and D of each composter together, since the differences between these

TABLE 1: Management strategies of the compartments.

Compartments	Inoculation Strategy
A	OSW inoculated with 10% of its volume of compost after each input.
B	OSW inoculated with 10% of its volume of compost in the first input.
C	OSW inoculated with 10% of its wet weight with liquid inoculum EM® in every contribution (EM®: lactic acid bacteria, phototrophic bacteria and yeasts).
D	Control compartment receiving OSW without external inoculant.



compartments were also common to both composters. The pH, carbon/nitrogen ratio (C/N) and nutrients P, K, Na and Mg in the waste before intake and after 60 days of composting were evaluated, in duplicate samples, following the methods described in Andrade and Abreu (2006). Leachate generated in composters 1 and 2, independent of the compartment, was evaluated for pH and COD after 60 days, with samples in duplicate, following the Standard Methods D520 (Standard Methods, 1997).

Comparisons between the above parameters were made by analysis of variance (ANOVA) at a significance level of 95%, with prior verification of normality and homoscedasticity of the variables, as suggested by Sokal and Rohlf (2012). Since most of the data did not meet these requirements, we used base-ten logarithmic transformation [Log (x + 1)] prior to ANOVA, followed by the Tukey test to compare the means, at 95% confidence level (p < 0.05).

Data on variations of depth and distance from the wall of the compartments were analyzed separately for all compartments and composters, for a better understanding of their behavior considering the differences between treatments and composters.

To test the energy use for water heating, a composter with total volume of 2 m<sup>3</sup> was used. Two waste compositions were studied, expressed in volume: (i) composition: 33.3% food waste, 33.3% grass and leaves (dry and green) and 33.3% ground trunks; (ii) composition: 50% ground trunks and 50% green grass.

This composter was equipped with a 44 m copper coil with diameter of 12.70 mm, immersed in the OSW to a depth of 50 cm from the bottom, through which 300 liters of water was circulated by an electric pump 24 hours after the intake of OSW, between the composter and a boiler with thermal insulation. The temperature was measured outside (air temperature) and at the water outlet of the composter.

### 3. RESULTS AND DISCUSSION

#### 3.1 Temperature

Compartments A, B, C and D exhibited average temper-

atures that were mesophilic and reached maximums that were thermophilic, close to 70°C (Figure 2a), which were maintained for more than 20 consecutive days, enough for waste hygiene (USEPA, 1992). Significantly lower temperatures were observed in compartments A compared to C and D, which may have been caused by the 10% compost added as inoculum in these compartments, lowering their temperature to improve the porosity and consequently the oxygenation of OSW, in the same manner as observed in soils, where the addition of compost favors the formation of granules (Kiehl, 1998).

Among the composters, significantly higher temperatures were observed in composter 2 (Figure 2b), attributed to the absence of a central chimney.

Inside composter 1's compartments, the highest temperatures were observed 25 cm away from the wall or 25 cm from the center, against 50 cm in the compartments of composter 2, showing the influence of the chimney present in compartments 1 as a differential element with respect to passive cooling. In vertical evaluation, there was a common pattern in the compartments of composters 1 and 2 regarding the highest average temperature at 25 cm depth, compared to 50 and 75 cm. This result is probably related to the positioning of the composters on pallets, in contrast to traditional layouts, as noted by Jackel, Thummes and Kampfer (2005) and Ignatius et al. (2009b). This design helps establishment of the chimney effect and consequent redistribution of heat by the system, positively influencing the passive oxygenation and minimizing the formation of anaerobic sites, which result in the generation of CH<sub>4</sub> and leachate (Münnich et al., 2006) (Figure 3).

#### 3.2 Gases

The percentage of CH<sub>4</sub> was between 0.0 and 2.6% in the waste, with the highest average being lower than 0.2% in treatment D (Figure 4a). This minimization of CH<sub>4</sub> generation contrasts with the findings of Ignatius et al. (2009b), who studied composters with sizes, OSW composition and input regimes very similar to those of the present study. They found an average value of up to 15% CH<sub>4</sub> in central areas of their compost piles, about 6 times more than

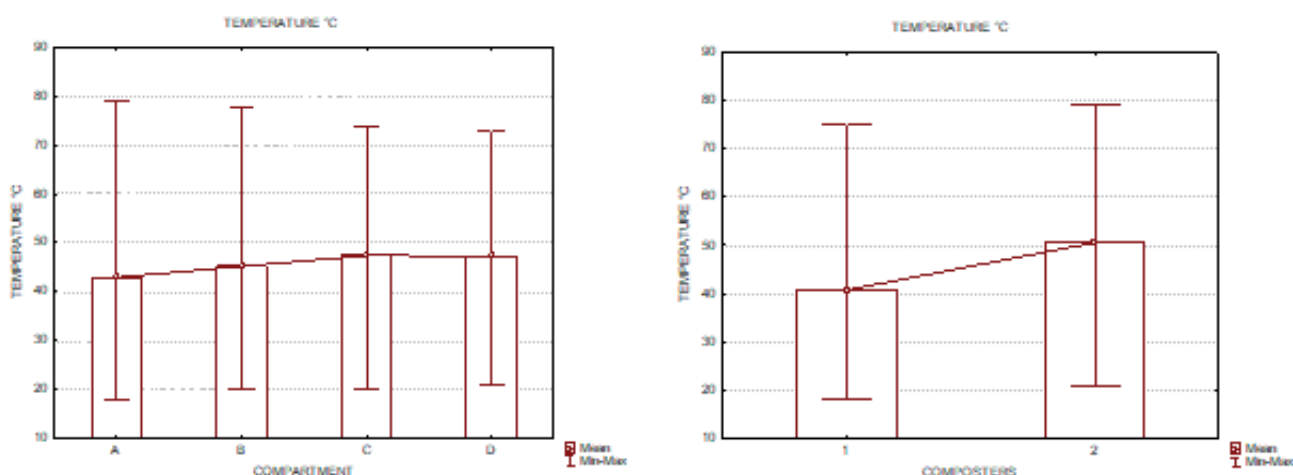


FIGURE 2a/2b : Average, minimum and maximum temperature per compartment and composter, respectively, in °C.

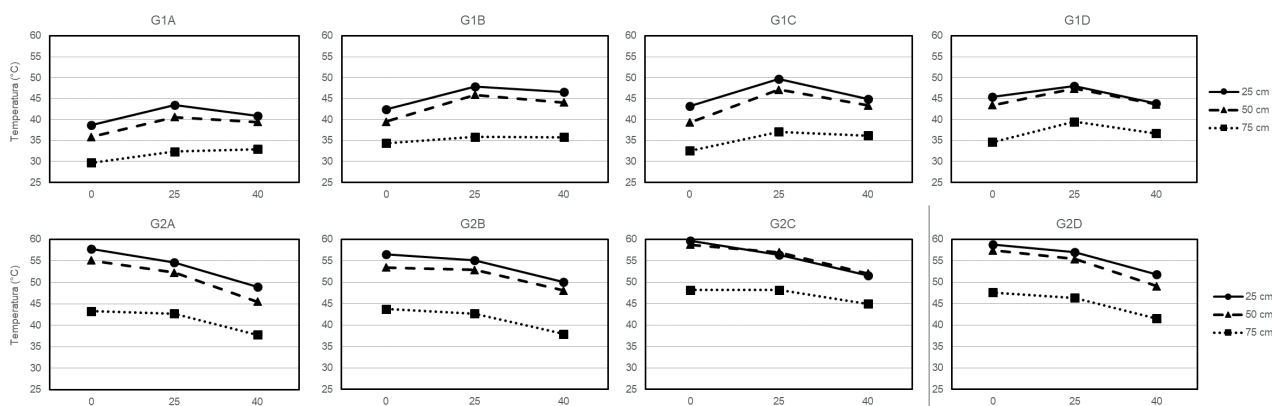


FIGURE 3: Average temperature in °C within the compartments 40, 25 and 0 cm from the center, and 25, 50 and 75 cm depth.

the highest maximum result in the central areas of this study. This positive result can be related to the efficient passive aeration, the result of the adopted materials and management strategies, ensuring aerobic conditions in all compartments, even those without chimney, since the generation of  $\text{CH}_4$  is directly related to the establishment of anaerobic conditions in the OSW (Munnich et al., 2006), usually related to high moisture and low penetration of  $\text{O}_2$  (Jiang et al., 2011; Kiehl, 1998).

However, even with little generation of  $\text{CH}_4$ , we observed significantly lower percentage of the gas in treatment A compared to C and D. This can be attributed to the addition of compost in maturation as inoculum at each input in treatment A, suggesting the efficiency of micro methanotrophic organisms present in the OSW to colonize and oxidize the  $\text{CH}_4$  produced. This was also noted by Jackel, Thummes and Kampfer (2005) and Rose et al. (2012), investigating minimization of  $\text{CH}_4$  emissions in composting and landfills with final compost coverage.

Regarding composters, both generated low percentages of  $\text{CH}_4$  (Figure 4b), although composter 1 showed significantly lower values than composter 2. This can be attributed to increased oxygenation and predominance of mesophilic temperatures in 1, since methanogenic microorganisms grow best at thermophilic temperatures and

methanotrophic ones find better conditions for growth and  $\text{CH}_4$  oxidation at mesophilic temperatures (Jackel et al., 2005).

Horizontally, within composter 1 the highest average  $\text{CH}_4$  values were observed in the waste 25 cm from the center of the composter, due to the central aeration of these compartments. In composter 2, without central aeration, the highest percentages of  $\text{CH}_4$  predominated at the center of the composter. Variations in  $\text{CH}_4$  according to depth did not exhibit a characteristic pattern, with larger values changing between 30 and 60 cm deep, although higher values predominated at 60 cm (Figure 5).

$\text{CH}_4$  emissions were sparse and minimal in all measurements, close to the minimum detection limit of 0.01%, and 5% reading error of the gas analyzer used. So, since all treatments proved to be effective in minimizing the production of  $\text{CH}_4$  and/or metabolizing the gas, we considered the emissions from all compartments to be negligible. This finding is similar to those reported by Jackel et al. (2005) and Ignatius et al. (2009b), where up to 98% of the produced  $\text{CH}_4$  was oxidized by methanotrophic communities. Further corroborating this assumption is that the average temperatures varied between 40 and 50°C in all compartments, the optimal range for activity of methanotrophic microorganisms, as already discussed. Thus, considering

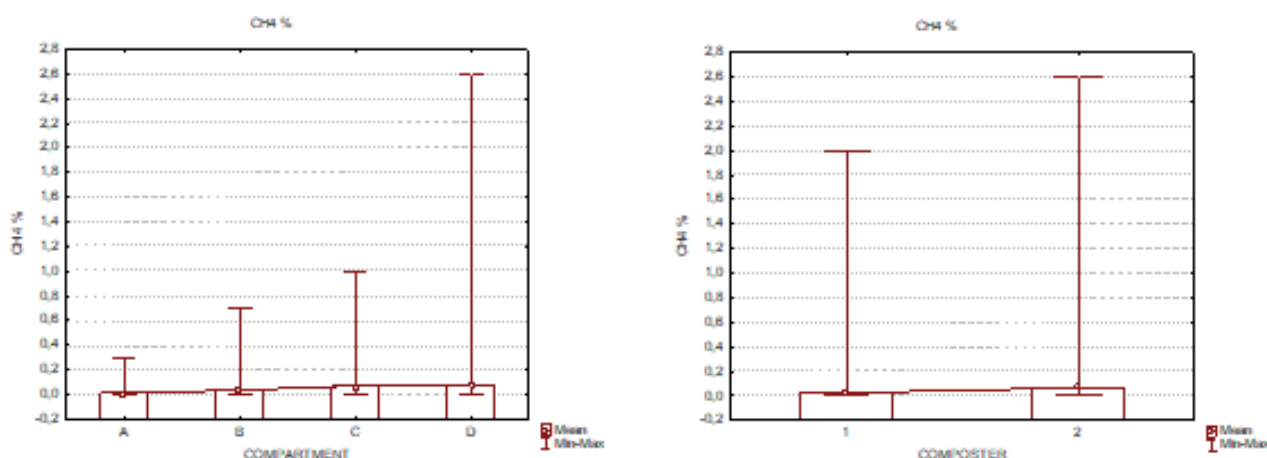


FIGURE 4a/4b: Maximum, minimum and average percentage of  $\text{CH}_4$  by compartment and composter, respectively.

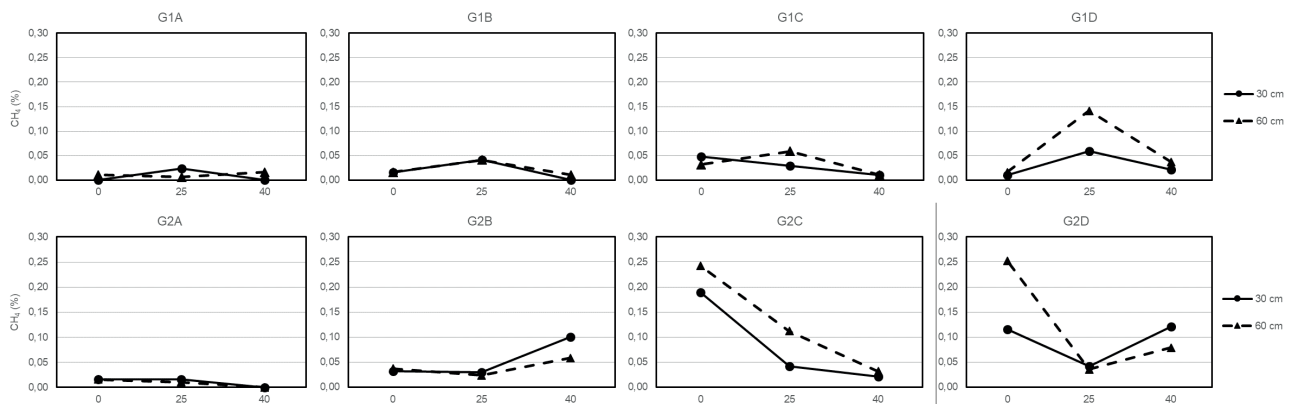


FIGURE 5: Average percentage of CH<sub>4</sub> at 40, 25 and 0 cm from the center, and 30 and 60 cm depth.

the emission of 600 kg of CO<sub>2</sub> eq./metric ton of ground OSW (USEPA, 2005), the 4 tons of OSW composted in this experiment avoided the emission of 2.4 tons CO<sub>2</sub> eq.. Furthermore, the absence of the need to transport the waste to a landfill prevented the emission of 87 kg of CO<sub>2</sub> eq., considering the emission of 2.9 kg CO<sub>2</sub> / l of diesel oil and the consumption of 7.5 L of diesel oil per ton of transported waste (Mahler, 2012). When discounting emissions that could theoretically be avoided in landfills by capture, burning and/or use for energy generation of CH<sub>4</sub>, and assuming maximum efficiency between 30% and 40% of emissions avoided, as observed by Viana (2011) and Maciel and Juca (2011), respectively, the emissions avoided by on-site composting would diminish by 34%.

Many aspects contribute together to minimize the generation of CH<sub>4</sub> from composting. Size, density, input intensity and presence of methanotrophic microorganisms are the most relevant parameters (Jackel et al, 2005). They are directly related to the oxygenation and temperature of the system and inversely proportional to the variation of the generation of CH<sub>4</sub>.

Since the present study investigated static operation, we believe the combination of a high proportion of structuring material and the positioning of the composters on pallets were important, by helping to establish efficient

passive aeration, as evidenced by the mean O<sub>2</sub> between 17 and 20% among compartments and composters (Figures 6a and 6b). These values were sufficient to ensure that all treatments presented suitable aerobic conditions in the composting process, defined as above 5% O<sub>2</sub> by Kiehl (1998) and above 10% by Miller (1993).

However, the solid organic waste present in treatments A and B exhibited significantly higher average O<sub>2</sub> percentages than in treatments C and D. This can be attributed to addition of compost as inoculum, which assists entry of O<sub>2</sub> by increasing the porosity of the waste, especially in treatment A, as discussed in the item on temperature.

In static windrow piles, the O<sub>2</sub> concentration also depends on the intensity of consumption by microorganisms and their replacement via passive aeration, which is influenced by the porosity of the material in the pile, moisture and the internal heat (Randle and Flegg, 1978). In this regard, it is noteworthy that the lowest average temperature and the highest average percentage of O<sub>2</sub> were observed in compartment 1A, which to some extent minimized the influence of temperature difference with respect to increased passive aeration and maximized the influence of possible increase in the porosity of the OSW due to the use of compost as inoculum. Also confirming the influence of the compost on the oxygenation of OSW is the fact that

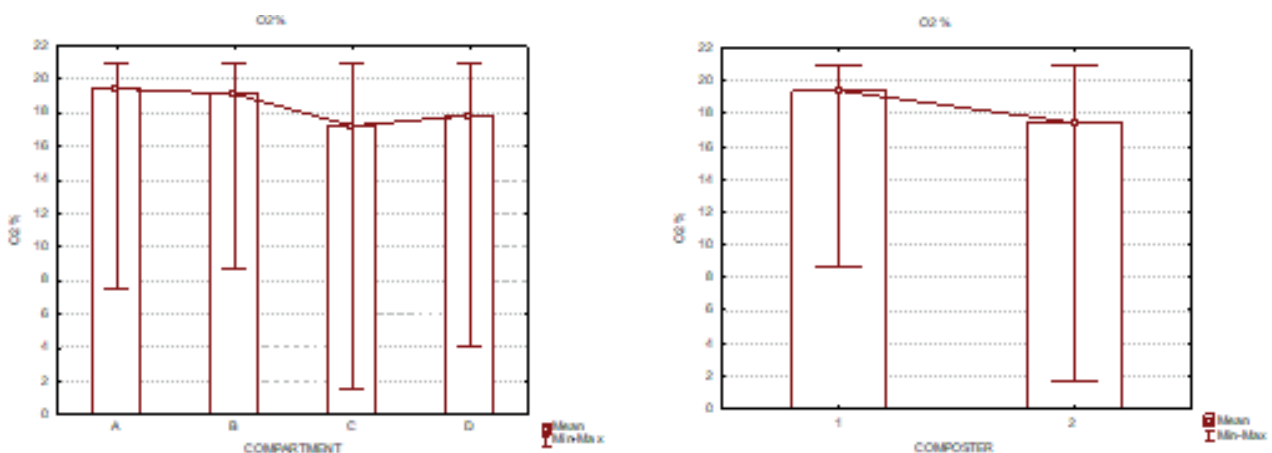


FIGURE 6a/6b: Maximum, minimum and average percentage of O<sub>2</sub> by compartment and composter, respectively.

compartment 2A, without chimney and inoculated with compost, presented an average  $O_2$  value compatible with those observed in compartments 1C and 1D, equipped with central chimney, despite the higher moisture in 2A.

Between composters, higher  $O_2$  percentage was expected in composter 1, due to the presence of the central chimney, facilitating oxygenation and moisture loss. This effect is supported by the higher moisture observed in composter 2, which is discussed below.

### 3.3 Moisture

Taking all the compartments together, the average moisture was near 60%, with significantly smaller differences for treatment A compared to the other treatments. This can be attributed to the use of compost as inoculum, since the increase in oxygenation attributed to the presence of compost favored drying even with the lower temperatures observed in A in comparison with the other treatments. Between the composters, the lowest average moisture in the waste was observed in composter 1, about 50%, versus about 70% in composter 2, attributed to the central aeration in composter 1.

Thus, the average moisture levels in the compartments and composters were between the minimum and maximum levels considered ideal for composting, of 50 and 70%, as suggested by Jiang et al. (2011), Kiehl (1998) and Brazil (2009), indicating proper maintenance of this parameter. Composting with moisture above 70% reduces  $O_2$  by excess water in waste macropores, while moisture below 50% reduces microbial activity, which ceases entirely below around 40% (Kiehl, 1998).

From an environmental point of view, Jiang et al. (2011) suggested that 65% moisture is the optimal value to minimize GHG emissions, the closest value to those attained by treatments B, C and D and composter 2, although compartment A in composter 2 was closest to 65% moisture.

It is noteworthy that the B compartments, although not differing in moisture significantly in relation to C and D, achieved significantly better performance with respect to  $O_2$  than C and D, similar to the A compartments. This aspect confirms again the importance of the type of inoculation applied to the compost mass regarding the adequacy of environmental parameters.

### 3.4 Leachate and percolated water

There was no generation of leachate in the composters and only a small amount of percolated water was produced, resulting from the external supply of water for wetting the compartments. This characteristic is attributed to the same aspects of maintenance of aerobic conditions discussed above, since the generation of leachate and  $CH_4$  is directly related to the establishment of anaerobic conditions (Munnich et al., 2006).

The leachates generated presented average COD of  $116.5 \text{ mg L}^{-1}$ , so they were suitable for reuse to wet the composters or as liquid fertilizer. They could also be discarded, considering that according to the average COD/BOD ratio of 2/1, suggested by Jordan and Person (2005), the average value of DBO for the leachate in question would be  $55.5 \text{ mg L}^{-1}$ , meeting the effluent discharge standards

set by CONAMA (2005) for BOD of up to  $60 \text{ mg l}^{-1}$  (there are no limits for wastewater discharge based on COD in Brazilian federal regulations).

Such COD values contrast with  $9,870 \text{ mg L}^{-1}$  obtained in traditional residential composting (Andersen et al., 2011). Obviously, such differences are understandable, since the comparison is between percolated water from wetting compost piles and leachate.

The average pH values of the leachate from composters 1 and 2, after 60 days, were 7.1 and 7, respectively, meeting the pH limit for disposal of waste according to CONAMA (2005).

### 3.5 Maturation of the compost

The C/N ratio  $<20$  is an indicator of stability for organic fertilizer class C according to Brasil (2009). In this regard, most of the treatments had C/N ratio indicating stability after 60 days, except for the D compartments, where the C/N averaged nearly 21, significantly smaller than D, suggesting the advantage of inoculation with compost with respect to degradation of organic solid wastes.

Between the composters, both had C/N  $<20$ , indicating stability of the material after 60 days. But composter 1 had C/N ratio significantly higher than composter 2, a result which may have been influenced by higher temperatures reached in composter 2. The average initial value of the C/N ratio of fresh OSW was 26/1.

### 3.6 pH

The pH of the wastes from treatments A, B and C, which received no inoculum, reached average values higher than 7 after 60 days, which was not observed in D, with pH below neutral (see Table 2). This aspect suggests composting without addition of inoculum is slower, although usually this process demands 90 to 120 days (Kiehl, 1998).

Treatment A presented significantly higher pH than C and D, which reinforces the idea that adding inoculum improves compost maturation.

However, residues in all compartments reached the reference value of  $\text{pH} > 6.5$ , described in Brasil (2009) and Giró (1994), suggesting that the material could complete its process of degradation in contact with the ground.

Both composters reached neutral pH after 60 days, with no significant differences, indicating that the differences in the temperature and oxygenation, derived from their mor-

**TABLE 2:** pH of OSW (before composting) and after 60 days of composting.

Sample	pH
Fresh OSW	5.6
Compartment A	7.5
Compartment B	7.3
Compartment C	7.1
Compartment D	6.7
References	<6.5a 6.5/8b

References: a) Brasil (2009), organic fertilizer from municipal solid waste; b) Giró (1994), mixed organic waste (public parks, gardens and homes)

phology (presence or absence of central chimney) did not affect the pH value.

### 3.7 Vectors

All treatments were effective in preventing the proliferation of flies and mice, a fact related to the maintenance of thermophilic temperatures, management strategy based on periodic OSW input and daily coverage with dry material, as suggested by Ignatius and Miller (2009). However, composter 2 was more efficient than 1 in combating flies, probably due to the higher temperatures. Particularly noteworthy is compartment 2A, which remained completely free of flies. This may be related to the use of compost every contribution, also suggesting its effectiveness in minimizing odors that attract vectors.

### 3.8 Water heating

The use of composting for heating water was appropriate because the 300 liters of water recirculated through the OSW reached 51°C after 24 h and remained at this temperature for 8 consecutive days in composter 1, with average ambient temperature of 21°C and maximum temperature of 71°C inside the composter. In composter 2, the same volume of water reached a temperature of 42°C after 24 hours in circulation and remained at that temperature for 15 consecutive days, with a mean ambient temperature of 23°C and maximum temperature of 62°C inside the composter.

However, the recirculation strategy depended on energy for pumping water and use of composter 1 would require frequent load changes. On the other hand, Jean Pain (1972) and Native Power (2013) suggested the passage of water only once through OSW, in long plastic hoses, and the use only of shredded trunks due to the longer degradation time of this material, (up to six months), which cheapens and facilitates the implementation of such systems, known in Germany as "Biomeiler".

## CONCLUSIONS

Two composting devices were developed, with four different types of management in each, and their behavior was studied regarding temperature, gas production, moisture, leachate and percolated water production, compost maturation, nutrient presence, pH. and water heating.

Both composters and all four treatments studied were effective considering health and environmental aspects, more so for composter 2 (without central chimney) and treatment A (10% compost added) (see Table 1) in relation to combatting vectors and degradation of OSW as well as for neutralization of CH<sub>4</sub> more efficiently, suggesting the use of model 2A in practical applications.

Overall, the maturation of the compound was satisfactory, with a C / N ratio <20 in almost all cases, indicating system stability after 60 days.

As for the pH, in all compost neutral values were reached after 60 days. In addition, the composters did not attract vectors, such as flies and mice.

The eight studied cases of composters reached temperatures of up to almost 80°C in some cases, and had

negligible CH<sub>4</sub> gas emission and release of leachate and percolated water.

There were no oxygen deficiencies in composter 2, making it unnecessary to use central aeration.

The good results of the experiments can be attributed mainly to the suspension of composters on pallets, the waste composition and boundary conditions adopted.

The energy recovery process showed that the water heating worked very well, reaching temperatures up to 51°C after 24 h of recirculation, for long periods, more than 20 days, with temperatures near 70°C, showing that this process can be a potential energy source.

The proposed composting model is environmentally feasible, because it minimizes gas emission and leachate generation compared to the landfill deposition or industrial composting plants.

## ACKNOWLEDGMENTS

The authors would like to thank CAPES, CNPq, FAPERJ and UNIFOA for supporting this study.

## REFERENCES

- Ahn, H.K.; Mulbry, W.; White, J.W.; Kondrad, S.I. Pile mixing increases greenhouse gas emissions during composting of dairy manure. *Bioresource Technology*, v.102, 2011, p. 2904–2909.
- Amlinger, F.; Peyr, S.; Cuhls, C. Green house gas emissions from composting and mechanical biological treatment. *Waste Management e Research*, v.26, 2008, p. 47-60.
- Andersen, J. K.; Boldrin, A.; Christensen, T. H.; Scheutz, C. Greenhouse gas emissions from home composting of organic household waste. *Waste Management*, v. 30, n.12, 2010a, p.2475–2482.
- Andersen, J. K.; Boldrin, A.; Christensen, T. H.; Scheutz, C. Quantification of greenhouse gas emission from windrow composting of garden waste. *Journal of Environmental Quality*, v.39, 2010b, p.713-724.
- Andersen, J. K.; Boldrin, A.; Christensen, T. H.; SCHEUTZ, C. Mass balance and life cycle inventory of home composting of organic waste. *Waste Management*, v.31, n. 9-10, 2011, p.1934-1943.
- Andersen, J.K.; Boldrin, A.; Christensen, T. H.; Scheutz, C. Home composting as an alternative treatment option for organic household waste in Denmark: An environmental assessment using life cycle assessment-modelling. *Waste Management*, v.32, n.1, 2012, p.31-40.
- Andrade, J.C.; Abreu, M.; Falcão, A.A. *Protocols of Chemical Analysis. Chemical analysis of solid waste for monitoring and agro-environmental studies.* Agronomic Institute, Campinas, 2006, p.121-158. (in Portuguese)
- Brasil. Ministry of Agriculture, Livestock and Supply of Agricultural Defense Secretariat, n.d. Normative Instruction No. 25 of 23 July 2009. Available at: <<http://sistemasweb.agricultura.gov.br/sislegis/action/detalhaAto.do?method=consultarLegislacaoFederal>>. Access: 28 November 2014. (in Portuguese)
- CONAMA. Ministry of Environment, 2005. CONAMA No 357 of 17 March 2005. Available at: <<http://www.mma.gov.br/port/conama/res/res05/res35705.pdf>>. Accessed on: 22 Mar. 2014. (in Portuguese)
- Durand, A. Bioreactor designs for solid state fermentation. *Biochemical Engineering Journal*, v.13, n. 2-3, 2003, p.113-125.
- EM® (2012). Efficient Microorganism. Available at: <<http://www.em-la.com>>. Accessed on 10 May 2012.
- Ermolaev, E.; Sundberg, C.; Pell, M.; Håkan, J. Greenhouse gas emissions from home composting in practice. *Bioresource Technology*, v.151, 2014, p.174-182.
- Giró F. Qualitat proposed legislation to composted per municipals to Residus Catalunya (in Catalan). Residus Board. Generalitat de Catalunya; 1994. (in Spain)
- IBGE - Brazilian Institute of Geography and Statistics. (2010) Census 2010 Rio de Janeiro: IBGE. Available at: <[www.ibge.gov.br](http://www.ibge.gov.br)>. Access: 10 April 2013.

- Inácio, C. T.; Bettio, D. B.; Miller, P. R. mitigation potential of methane emissions through composting projects on a small scale. In: Brazilian Congress of Organic Waste. Anais ... Victory: SBCS, 2009a. CD ROM. (in Portuguese)
- Inácio, C. T.; Procópio, A. S.; Teixeira, C.; Miller, P. R. O<sub>2</sub> dynamics, CO<sub>2</sub> and CH<sub>4</sub> in static windrow composting during the thermophilic phase. In: Brazilian Congress of Organic Waste. Anais ... Victory: SBCS, 2009b. CD ROM. (in Portuguese)
- Inácio, C. T.; Miller, P. R. Composting, science and practice for organic waste management. 1st ed. Rio de Janeiro: Embrapa Solos, 2009. 156p. (in Portuguese)
- Jackel, U.; Thummes, K.; Kampfer, P. Thermophilic methane production and oxidation in compost. *FEMS Microbiol. Ecolgy*, v.52, n. 2, 2005, p.175-184.
- Jiang, T.; Schuchardt, F.; Li, G.; Guo, R.; Zhao, Y. Effect of C/N rate and moisture conten on ammonia and greenhouse gas emission during the compost. *Journal of Environmental Sciences*, v.23, n. 10 , 2011, p.1754-1760.
- Jordão, E. P.; Pessoa, C. A. Domestic sewage treatment. 4 ed. Rio de Janeiro: Ed. ABES, 2005. 932p. (in Portuguese)
- Kiehl, E. J. Composting Manual: Maturation and Compost Quality. 4th ed. Piracicaba: Ed. Edmar José Kiehl, 1998. 171p. (in Portuguese)
- Maciel, F. J., Jucá, J. F. T. Evaluation of landfill gas production and emissions in a MSW large-scale Experimental Cell in Brazil. *Waste Management* v.31, p. 966-977, 2011.
- Mahler, C.f. Urban waste. 1 ed. Rio de Janeiro: Ed. Revan, 2012. 189 p. (in Portuguese)
- Martínez-Blanco, J.; Colón, J.; Gabarrell, X.; Font, X.; Sánchez, A.; Artola, A.; Rieradevall, J. The use of life cycle assessment for the comparison of biowaste composting at home and full scale. *Waste Management*, v.30, n. 6 , 2010, p.983-994.
- Miller, F. C. Composting as a process base on the control of ecologically selective factors. In: METTING, F. B., *Soil microbial ecology: application in agricultural and environmental management*. New York, NY, Marcel Dekker Inc., p. 515 – 541, 1993.
- Münnich, K.; Mahler, C. F.; Fricke, K. Pilot Project of mechanical-biological treatment of waste in Brazil. *Waste Management (Elmsford)*, v.26, n. 2 , 2006, p.150-157.
- Native Power (2013). Available in: <<http://www.native-power.de>>. Access in: 12 mar. 2013.
- Pain, J. (1972) Another kind of garden. Available in: <[http://library.uniteddiversity.coop/Permaculture/Another\\_Kind\\_of\\_Garden-The\\_Methods\\_of\\_Jean\\_Pain.pdf](http://library.uniteddiversity.coop/Permaculture/Another_Kind_of_Garden-The_Methods_of_Jean_Pain.pdf)>. Acesso em: 24 fev. 2014.
- Pires, A.; Martinho, G.; Ni-Bin, C. Solid state management in European countries. A review of systems analysis techniques. *Journal of Environmental Manegement*, v.92, n. 4, 2011, p.1033-1050.
- Rose, J. L.; Mahler, C.f.; Izzo, R. L. S. Comparison of the methane oxidation rate in four media. *Revista Brasileira de Ciência do Solo (Printed)*, v. 36, 2012, p. 803-812.
- Randle, J.; Flegg, M. Oxygen measurements in a Mushroom Compost Stack. *Scientia horticulturae*. v.8, n. 4, 1978, p. 315-323.
- Sokal, R. R.; Rohlf, F. J. *Biometry: The principles and practice of statistics in biological research*. 4.ed. W. H. Freeman and Co, 2012. 937p.
- Standard Methods. Standard Methods for the examination of water and wastewater, Method D 5220 Chemical Oxygen Demand (COD), 1997.
- Teixeira, L.b.; Germano, V.l.c; Oliveira, R.f. De; Furlan Junior, J. Composting process from urban organic waste into static windrow with natural ventilation. Belém: Embrapa Amazônia Oriental, 2004. 7p. (Embrapa Amazônia Oriental. Circular Técnica, 33). (in Portuguese)
- USEPA- United States Environmental Protection Agency. Environmental regulation and technology control of pathogens and vector attraction in sewage sludge. Under 40 CRF. Part 503. EPA-625/R-92/013, 1992. Available in: < [http://water.epa.gov/scitech/wastetech/biosolids/upload/2007\\_05\\_31\\_625r92013\\_625R92013.pdf](http://water.epa.gov/scitech/wastetech/biosolids/upload/2007_05_31_625r92013_625R92013.pdf) >. Acesso em: 19 mai. 2013.
- USEPA- United States Environmental Protection Agency. Landfill gas emissions model (LandGEM) version 3.02 user's guide. Washington: Office of Research and Development, EPA-600/R-05/047, 2005. 48p.
- Viana, T.a.p. Analysis of the methane emission estimates for landfills in CDM projects in Brazil. Dissertation (MSc) - 2011 State University of Rio de Janeiro, Faculty of Engineering. (in Portuguese).
- Zuokaite, E.; Zigmontiene, A. Application of a natural cover during sewage sludge composting to reduce gaseous emissions. *Polish Journal of Environmental Studies*, v.22, n.2, 2013, p.621-626.

# EVALUATION OF TEMPERATURE CHANGES IN ANAEROBIC DIGESTION PROCESS

Senem Önen Cinar \* and Kerstin Kuchta

Institute of Environmental Technology and Energy Economics, Hamburg University of Technology, Harburger Schloßstr. 36, 21079 Hamburg, Germany

## Article Info:

Received:  
15 July 2019  
Revised:  
5 December 2019  
Accepted:  
21 January 2020  
Available online:  
5 March 2020

## Keywords:

Anaerobic digestion  
Temperature effect  
Temperature adaptation  
Optimization

## ABSTRACT

The study examines the effect of temperature fluctuations on biogas production efficiency in biogas plants with the aim of evaluating the temperature flexibility of the process. Laboratory scale batch reactors were prepared with the chosen substrate (Dried Distillers Grains with Soluble, DDDS) and the study was conducted in three batches. A biogas formation potential test was implemented in each batch in a temperature-controlled room and in a temperature controlled water bath. The temperature changes took place on the third day of tests to evaluate the effect of 5°C, 10°C and 15°C increases on biogas production efficiency in separate test sets. Batch experiments showed that it is possible to ensure process recovery after 5°C and 10°C increases. Overall, the specific biomethane production was obtained between 364 - 412 Nml CH<sub>4</sub> / g oDM. Unlike 5°C and 10°C increases, after 15°C increase a lower methane content was obtained. These results show that it is possible to have flexible temperature operation in the process, even with high-temperature increases.

## 1. INTRODUCTION

Anaerobic digestion is a microbiological process which supplies energy production and evaluation of organic waste as a resource. Moreover, upgraded biogas is used as a vehicle fuel, and it is possible to inject in natural gas grids. Although it is a beneficial process in various ways, further development is necessary for this process in order to reduce energy consumption and improve process stability (J.B. Holm-Nielsen, 2009) (Ye Chen, 2007). Within the four successive stages (hydrolysis, acidogenesis, acetogenesis, and methanogenesis) of anaerobic digestion, organic material is converted into gas mixture in the absence of oxygen (FNR, 2010). Although the steady operation is possible in a single environment, there are different kinds of active microorganisms in each stage. Other parameters to supply stability of the process are continuous and consistent feeding, a stable temperature, constant stirring, and continuous monitoring (FNR, 2010) (Drosg, 2013).

The active microorganisms in the process of anaerobic digestion are divided into three temperature ranges due to their optimal growth rate temperatures: psychrophilic (<25°C), mesophilic (37°C - 42°C) and thermophilic (>50°C) (FNR, Biogas, 2013). Concerning the temperature, the dependence of both enzymatic reactions, and microorganisms' growth rates, temperature effect on reaction kinetics

in the process cannot be neglected (Gerardi M. H., 2003). There are various studies that compare the efficiency of thermophilic and mesophilic anaerobic digestion which show that thermophilic digestion is a better option to digest easily degradable substrates in a short time (Streitwieser, 2017) (Demirel Burak, 2008) (Moset Veronica, 2015). According to Zhang, a higher methane yield and volatile solid removal efficiency can be obtained in thermophilic conditions as compared to mesophilic conditions from soybean curd residue (Le Zhang, 2019). After incubation of the maize silage and cattle manure at 20°C, 30°C and 40°C, higher biogas generation was observed at higher temperatures (Dominika Kufka, 2019). Although higher biogas production can be observed at higher temperatures, however, the mesophilic temperature range is preferable due to its stability and low energy consumption (Rafaela Franqueto, 2019). Furthermore, the effect of one-step and stepwise temperature changes on biogas production has also been studied in various ways to see the adaptation of the process after readjustment to initial operation temperatures (Wu Man-chang, 2006) (El-Mashad Hamed M., 2004) (Iranpour R., 2002).

According to other studies, the temperature shocks and fluctuations in the biogas plant are to be avoided (FNR, 2010) (El-Mashad Hamed M., 2004). Thermal shocks are more effective on system stability at higher temperatures (>55°C) than at lower temperatures (K. Kundu, 2014). Sim-



\* Corresponding author:  
Senem Önen Cinar  
email: senem.oenen@tuhh.de



ilarly, the process is more sensitive to temperature changes within 15-20°C as compared to the range within 20-35°C (Deng, 2014). On the other hand, in some situations, temperature fluctuations cannot be prevented. Recently, a study by Matteo examined the overheating problem of small-scale digesters in summer with different gasometer dome materials. It showed that the temperature in the biogas reactor can reach 45°C due to the overheating problems (Matteo Bavutti, 2014). Since biogas plants generally do not have cooling systems, it is possible to have higher temperatures than expected inside the reactors because of increasing summer temperatures outside. Therefore, extra heat energy gained from high ambient temperatures or solar radiation can be considered an energy source which can enable the operation of biogas plants without heating.

The purpose of this study was to examine the temperature flexibility of the process in case of overheating problems or the operation of the plant using ambient heat in the summer season. A biogas formation potential test was implemented to the chosen substrate in order to evaluate the effect of temperature changes on biogas formation efficiency. Furthermore, the biogas formation efficiency of changing temperature conditions was compared to stable temperature conditions for each batch of the experiment.

### 1.1 Highlights

- Increasing ambient temperature in summer causes temperature management problems in biogas plants;
- Obtaining temperature flexibility in an anaerobic digestion process can give an opportunity to decrease the energy requirement of the plant;
- 5°C, 10°C and 15°C temperature increases were evaluated with biogas formation potential tests in the laboratory;
- Adaptation of an anaerobic digestion process to 5°C and 10°C temperature increases were achievable.

## 2. MATERIALS AND METHODS

### 2.1 Feedstock and preparation

DDGS-Pellets were supplied by Crop Energies AG. They are mainly used as concentrated feed material for animals. Studied substrate contains 327 g/ kg DM (dry matter) crude protein, 79 g/ kg DM crude fiber, 77 g/ kg DM crude lipids, 78 g/ kg DM starch sugar, 455 mg/g DM TOC (total organic carbon), 13184 mg/l (1 g in 100 ml distilled water dissolved) COD (chemical oxygen demand), 49.69 mg/g DM TKN (total Kjeldahl nitrogen), 136 mg/l (1 g in 100 ml distilled water dissolved) NH<sub>4</sub>-N, 24 mg/l (1 g in 100 ml distilled water dissolved) HCO<sub>3</sub><sup>-</sup> and 62 g/ kg DM crude ash. The feed material described is produced from wheat, barley, molasses, triticale, and corn (Protigrain, 2019). Implemented analytical methods for feedstock/digestate sample analyses are summarized in Table 1. The feed material is stored at room temperature in a plastic container until the experiment is conducted. The pellets were reduced in size before being mixed with inoculum. The inoculum was obtained from waste water treatment plant in Hamburg

and was stored in an air-conditioned room (36°C±0.5) before the tests.

For each batch, blank, reference, and substrate-inoculum mixtures were prepared in three parallels, according to VDI 4630 (VDI, 2014). Reference-inoculum (substrate: cellulose) and pellets-inoculum mixtures were prepared obtaining the oDM (organic dry matter) ratio between substrate and inoculum as given in Equation 1.

$$\frac{oDM_{substrate}}{oDM_{inoculum}} \leq 0.5 \quad (1)$$

Where *oDM<sub>substrate</sub>* is organic dry matter mass of substrate (g), and *oDM<sub>inoculum</sub>* is organic dry matter mass of inoculum (g) (VDI, 2014).

### 2.2 Experimental setup and procedures

The experimental part of this study includes three batches of biogas formation potential tests. For each batch, biogas formation potential of pellets was analysed with different temperature increases (5°C, 10°C and 15°C). Considering the biogas formation quality difference of inoculum, the analyses at 36°C were repeated for each batch in order to have a reference for the comparison of the situation with stable temperature management. The biogas formation potential of samples was determined according to German standard procedure (VDI, 2014) as a batch test in three parallels. The lab-scale 500 mL glass reactors were used with a gastight apparatus and eudiometer, as described in Figure 1. After the implementation of size reduction to the substrate, substrate-inoculum mixtures were prepared as mentioned in Equation 1.

The three batches of experiments were all started at 36°C. On the third day, temperature increases of 5°C, 10°C and 15°C occurred, as explained in Figure 1. All experiments were conducted in a temperature-controlled room at 36± 0.5°C. In order to increase the temperature of the reactors, a thermostatic water bath was used continuously from the third day of the experiment onwards. The water level in the water bath was constantly kept higher than the fill levels in the reactors. To supply homogeneity inside the reactors and prevent precipitation, daily shaking was implemented.

At the beginning of the test, the produced biogas quantity was recorded daily, later two to three- days every week. The temperature of the room and water bath and the pressure were recorded daily. The test duration for all experiments was a minimum of 21 days, depending on the biogas generation amount (less than 0.5% of the total volume that was produced up to that time) on the last days of the test.

The specific fermentation gas production was calculated as explained in the following equations.

$$V_{tr,N} = V \cdot \frac{(p-p_w) \cdot T_N}{p_N \cdot T} \quad (2)$$

Where *V<sub>tr,N</sub>* is the volume of dry gas in the normal state (ml<sub>N</sub>), *V* is the volume of the gas as read off (ml), *p* is the pressure of the gas phase at the time of reading (hPa), *p<sub>w</sub>* is the vapor pressure of the water as a function of the temperature of ambient space (hPa), *T<sub>N</sub>* is the normal temperature (273°K), *p<sub>N</sub>* is the normal pressure (1013 hPa), and *T*



**TABLE 1:** Conducted analytical analyses for the substrate and inoculum.

Parameter	Method	Equipment	Standard/ Norm
Dry matter content (DM)	Drying at 105°C during 24 hours	Drying oven	DIN 38414 – S2 (DIN, 1985)
Organic Dry Matter Content (oDM)	Dried samples from DM test were treated in muffle furnace at 220°C within 20 minutes, at 300°C within 30 minutes and at 550°C oven 5 hours	Oven	DIN 38409- H1- 3 (DIN, 1987)
Total organic carbon (TOC)	Thermal oxidation of organic carbon to CO <sub>2</sub> , infrared spectroscopic measurement of CO <sub>2</sub> (TC) Expulsion of inorganic carbon (TIC) as CO <sub>2</sub> with phosphoric acid, quantification of CO <sub>2</sub> via infrared spectroscopy	Analyser multi N/C 2000	DIN EN 1484 (DIN, 2019)
Chemical oxygen demand (COD)	Oxidation with potassium di-chromate in % weight of silver sulphate (catalyst), photometric determination of excess potassium dichromate	Digestion block; HT 200 Photometer; DR 3900	ISO 15705 (ISO, 2002)
Total Kjeldahl nitrogen (TKN)	Transfer of the organically bounded nitrogen compounds, ammonium, nitrate and nitrite by digesting the sample with Kjeldahl tablets Distillation of the ammonia formed after the addition of strong liquor in a template of hydrochloric acid and determination of analytical end point	Digestion block, distillation apparatus; vapodest 2 semiautomatic Titration programme; Schott	A 2.2.1 (Methodenbuch)
Ammonium (NH <sub>4</sub> -N)	Ammonium nitrogen is distilled off from the weakly basic solution as ammonia (NH <sub>3</sub> ), collected in boric acid solution and determined by measurement	Distillation apparatus: Vapodest 2 semiautomatic Titration programme; Schott	DIN 38406-E5-2 (DIN, 1983)
Hydrocarbonate (HCO <sub>3</sub> )	Titration with 0.1 N hydrochloric acid solution to pH 4.3	Titration unit consisting of the components T100, TA10, TM120	DIN 38409-7 (H7) (DIN)

is the temperature of the fermentation gas of the ambient space (°K) (VDI, 2014).

$$V_s = \frac{\sum V_n \cdot 10^4}{m_{DM.oDM}} \quad (3)$$

Where  $V_s$  is the specific fermentation gas production relative to organic dry mass during the test period (l<sub>N</sub>/kg oDM), is the net gas volume of the substrate during the test period (ml<sub>N</sub>),  $m$  is the mass of the weighted substrate or reference substrate (g), DM is the dry matter content of the inoculum or substrate (%), oDM is the loss on ignition of the sample or inoculum (%) (VDI, 2014).

The volume fractions of methane and carbon dioxide were determined to depend on the regular intervals with Gas Chromatography (HP 6890 Agilent) with the help of a thermal conductivity detector. Moisture correction for gas components was conducted as in Equation 4, since all biogas content measurements were conducted with water vapor containing biogas.

$$C_{tr,korr} = C_{CH_4(CO_2)} \frac{100}{C_{CH_4} + C_{CO_2}} \quad (4)$$

Where  $C_{tr,korr}$  is corrected concentration of the biogas components in dry gas (%),  $C_{CH_4(CO_2)}$  is measured concentration of biogas components in the gas (%),  $C_{CH_4}$  is measured methane concentration in the gas (%),  $C_{CO_2}$  is measured carbon dioxide concentration in the gas (%) (VDI, 2014).

### 3. RESULTS AND DISCUSSION

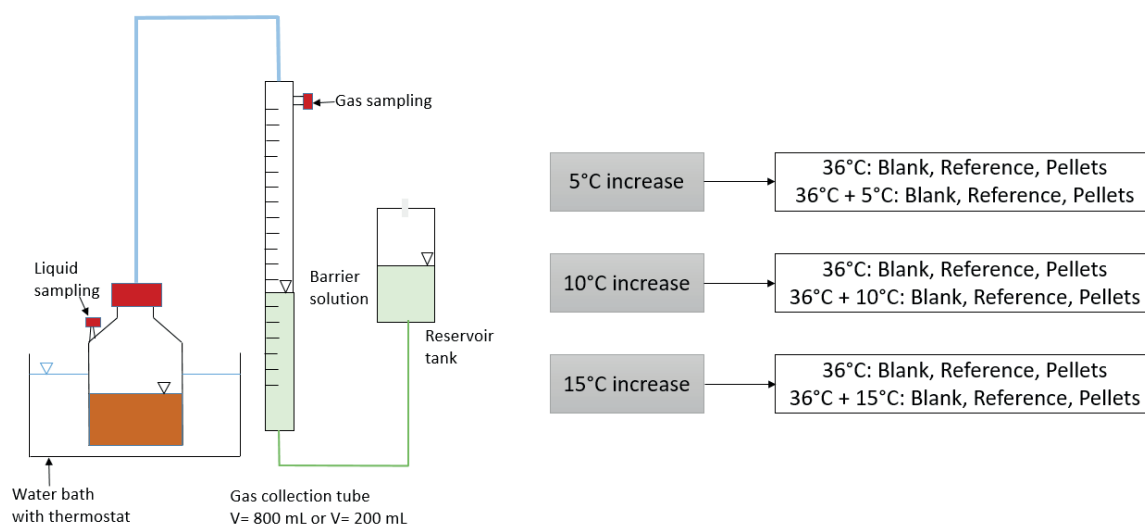
#### 3.1 Results of DM and oDM Analyses

Table 2 presents the results of DM and oDM content analyses of inoculum and pellets. Moreover, DM and oDM contents of cellulose are presented in Table 2 as well. Because the used inoculum samples were taken from the wastewater treatment plant at different times, DM and oDM contents of inoculum were analysed for each batch. The oDM content of inoculum varied between 62.3% and 64.4%; that shows the suitability of inoculum for the test, according to VDI 4630 (VDI, 2014).

#### 3.2 Biogas Generation

The batches were entitled as A (5°C increase), B (10°C increase), and C (15°C increase), and the results will now be presented with those classifications. With all batches, the test continued until no significant amount of biogas production was observed anymore. The temperature-increased cases were compared to the stable temperature operation cases for each batch.

In batch A, there was no significant difference between the specific biogas production amounts of the substrate at 36°C (600.20±23.34 Nml/ g oDM) and at 41°C (591.37±23.34 Nml/ g oDM), because the operating temperature was kept in the mesophilic temperature range. As shown in Figure 2, similar cumulative specific fermentation gas production curves were obtained. Compared



**FIGURE 1:** Experimental set-up for determination of biogas formation potential and experimental plan.

to the temperature-increased test, at 36°C, 42 Nml higher biomethane generation was obtained. The biogas generation from inoculum was higher at 41°C than at stable conditions, and the acceleration in biogas production of the samples at 41°C can be explained with the temperature increase on day three, as presented in Figure 2.

In batch B, the difference was higher than in batch A. Approximately 70 Nml/ g oDM biogas production difference was obtained from the samples at 36°C and 46°C. Although higher biogas production was observed at 46°C for the inoculum samples, a 23 Nml CH<sub>4</sub>/ g oDM higher biomethane was obtained from the pellets at 36°C. Similar to batch A, acceleration in specific biogas production from pellets and from inoculum was observed on day three, as shown in Figure 3.

The 15°C temperature increase was studied in batch C. A quite different biogas generation graph was obtained from that last test compared to the first two. Retarded degradation was observed in inoculum samples at 51°C with approximately 200 Nml/ g oDM higher biogas production than in inoculum samples at 36°C (see Figure 4). A 23 Nml CH<sub>4</sub>/ g oDM higher biomethane production than in the temperature-increased case was obtained at a stable temperature from pellets. As mentioned before, higher biogas formation can be observed at higher temperatures (Le Zhang, 2019) (Moset Veronica, 2015). The specific biogas production of inoculum sample after 15°C temperature increase was higher than other inoculum samples' productions. That can be explained with higher biogas production effi-

ciencies at higher temperatures after a specific time period of acclimatization. An adaptation of the microorganisms after a 15°C temperature increase could be obtained within 15 days, as represented in Figure 4. The 10°C temperature increase caused instability in reactors. Because a 46°C operation temperature neither supplies an optimum living environment for mesophilic, nor for thermophilic microorganisms.

There are two types of enzymes degrading substrate in the biogas production process: endoenzymes and exoenzymes. Endoenzymes are produced by all bacteria, but exoenzymes are just produced by specific bacteria. Furthermore, enzymes degrade only a specific substrate or group of substrates. Therefore, a high diversity of bacteria is needed to ensure the degradation of specific types of substrate (Gerardi M. H., 2003). The reaction rate of enzymatic reactions depends on the pH and the temperature of the reactor. If the temperature increases beyond the optimum temperature ranges, the reaction can stop due to the denaturation of enzymes (Caballero-Arzápalo, 2015). Most of the enzymes are stable in the mesophilic range up to 37°C and become unstable a few degrees beyond, between 40°C and 50°C (Bisswanger, 2008). Based on this study, the highest biomethane generations are obtained at 36°C, due to the suitability for enzymes of that temperature in the reaction.

As presented in Figure 5, the specific bio methane production of pellets at all temperature scenarios varied between 364.15±11.84 and 420.48±16.93 Nml CH<sub>4</sub>/ g oDM. In each case, a higher biomethane production was obtained at a stable temperature as compared to a temperature-changed situation. A change in operation temperatures led to instability in the process in each batch and caused lower specific biomethane production after temperature increases, as shown in Figure 5. The highest standard deviation was observed after 10°C temperature increase, which can be explained with the adaption challenges of microorganisms to the temperature between mesophilic and thermophilic temperature ranges. The highest difference between the methane contents of stable and un-

**TABLE 2:** DM and oDM content of substrates and inoculum.

	DM [%]	oDM [%]
Pellets	89.3±0.14	93.6±0.03
Inoculum (used for 5°C increase batch)	2.81±0.10	62.34±0.52
Inoculum (used for 10°C increase batch)	3.42±0.25	64.38±0.08
Inoculum (used for 15°C increase batch)	3.13±0.02	64.36±0.22
Cellulose (reference sample's substrate)	96.65	100.00

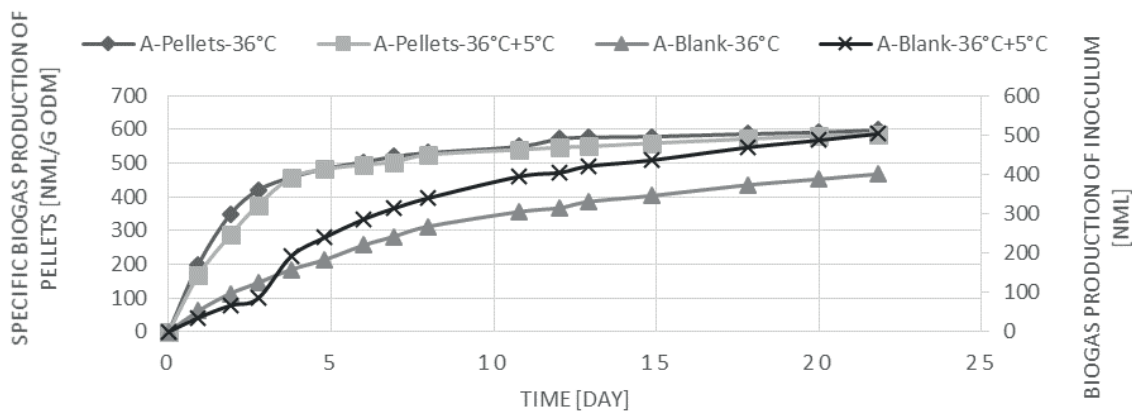


FIGURE 2: Specific fermentation gas production - 5°C increase.

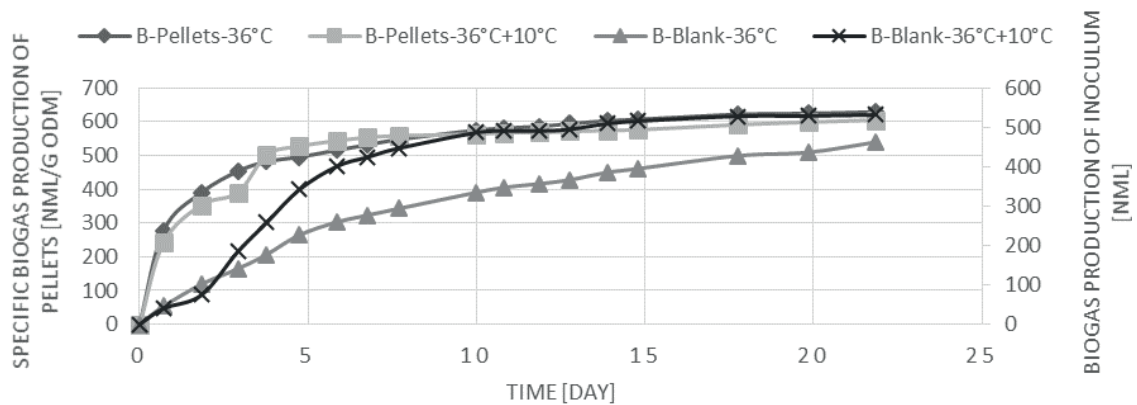


FIGURE 3: Specific fermentation gas production - 10°C increase.

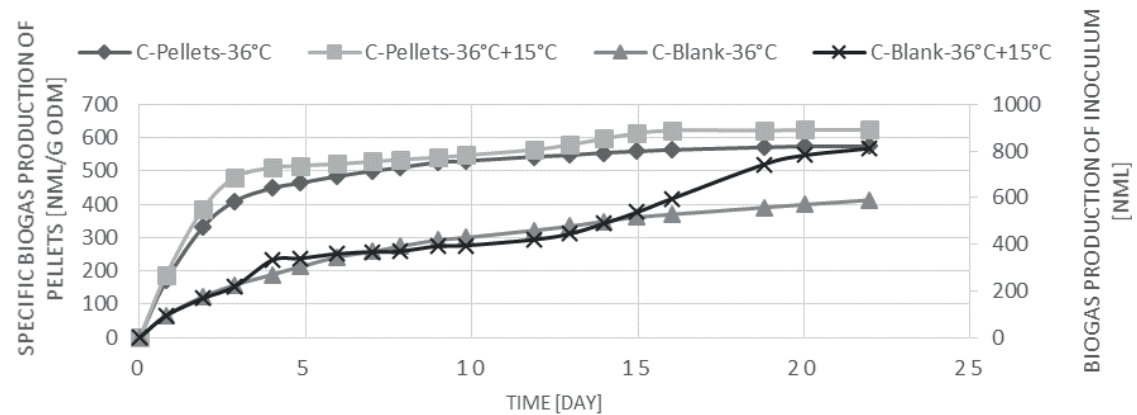


FIGURE 4: Specific fermentation gas production - 15°C increase.

stable temperature conditions was observed after a 15°C temperature increase, as depicted in Figure 6, which shows adaption problems of the process after an abrupt temperature change.

### 3.3 Results of pH Measurements

As mentioned in materials and methods part, the pH of each reactor was measured before and after the test. The results are presented in Table 3. Before starting the experiment, slightly different pH values between the same

samples was observed. Those differences were caused by impurities in inoculum sample. In each batch, higher pH values were obtained at higher temperatures as compared to stable conditions (36°C). The concentration of ammonia strongly depends on the process temperature, hence increasing the temperature and temperature fluctuations led to an increase of ammonia concentration (Al Seadi, Rutz, & Prassl, 2008) (FNR, Biogas, 2013). Therefore, it can cause pH increases, which were analysed at increased temperatures in the samples. Furthermore, hydrolysis and

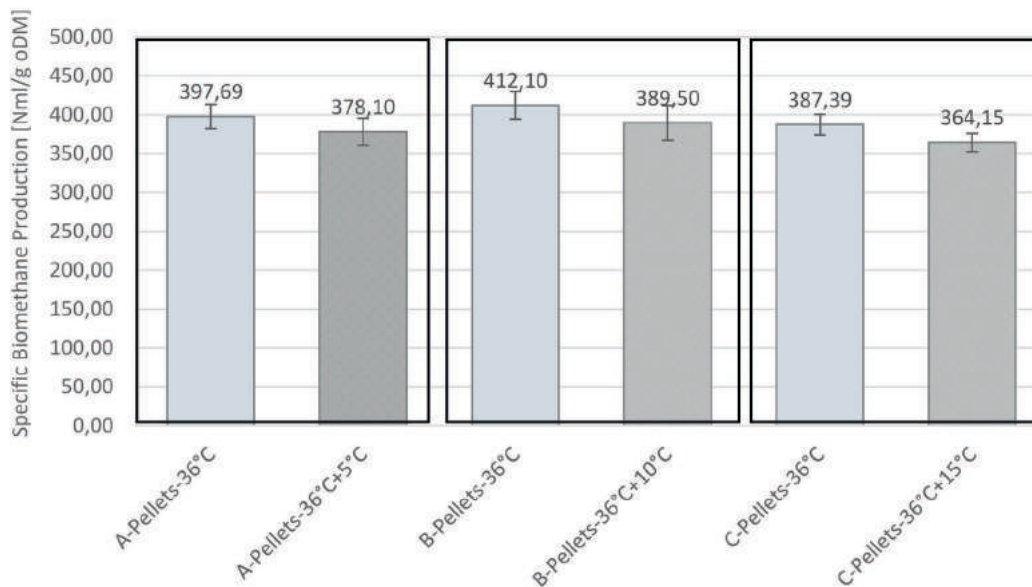


FIGURE 5: Specific bio-methane production of samples.

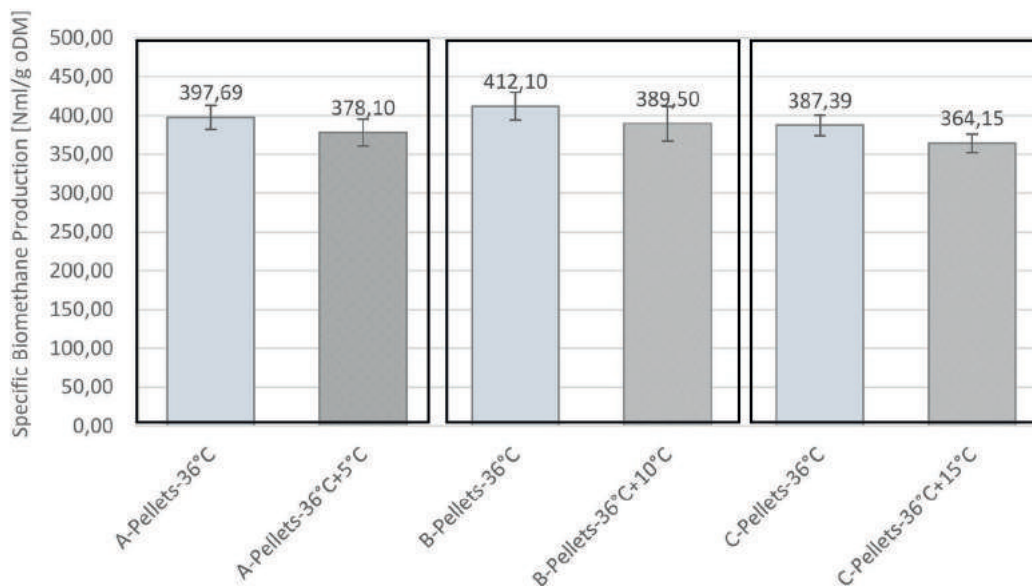


FIGURE 6: Methane content of biogas.

acidogenesis were negatively affected by higher temperatures due to the increasing concentration of ammonia (El-Mashad Hamed M., 2004). Overall, the pH and methane content of batch C showed that the process could not be adapted to temperature change successfully.

Considering all the results obtained from both pure inoculum and substrate analyses, the adaption of the pure inoculum samples to new operation temperatures was easier than mixed inoculum-feedstock samples. That can be caused by adaption challenges of enzymes that facilitate the degradation of the substrate within the whole process (Gerardi M. H., 2003). The results showed that without the inhibition of the process, the adaption to new conditions could be possible after 5°C temperature increases with a lower biomethane generation than in stable condi-

tions. In the anaerobic digestion process, methanogens are the most sensitive group to temperature changes and other disturbances. Moreover, it is necessary to supply a balance between acetogens and methanogens in order to obtain stable biogas formation (Teimour Amani, 2010) (Gerber, 2009) (Caballero-Arzápalo, 2015). After 10°C and 15°C temperature increases, methanogens are affected negatively by changing the environment. Due to the high standard deviation of the methane content after a 10°C temperature increase, a detailed study is needed to get a clearer idea about the effect of operation at 46°C. Varying results were observed after a 15°C increase for pure inoculum and inoculum-substrate mixture samples. On the one hand, an adaption of the inoculum sample at thermophilic conditions can be possible after a specific time of acclima-

**TABLE 3:** pH values before and after the test.

	Sample	pH- beginning	pH - end
1 <sup>st</sup> set	Blank-36°C	7.59±0.009	7.60±0.017
	Blank-36°C+5°C		7.70±0.053
	Pellets-36°C	7.50±0.024	7.46±0.012
	Pellets-36°C+5°C		7.57±0.016
2 <sup>nd</sup> set	Blank-36°C	7.59±0.026	7.60±0.020
	Blank-36°C+10°C		7.72±0.081
	Pellets-36°C	7.51±0.021	7.51±0.017
	Pellets-36°C+10°C		7.68±0.084
3 <sup>rd</sup> set	Blank-36°C	7.63±0.011	7.64±0.119
	Blank-36°C+15°C		7.81±0.219
	Pellets-36°C	7.54±0.017	7.57±0.033
	Pellets-36°C+15°C		7.91±0.058

tization, but on the other hand, the temperature increase has caused process inhibition in the inoculum-substrate mixture samples. In further studies, the effect of temperature changes should be analysed with detailed microbiological studies concerning both samples.

#### 4. CONCLUSIONS

This study examined the effect of temperature changes on biogas formation efficiency at different temperature ranges. It was found that an adaptation of the process to the new conditions is possible after 5°C and 10°C increases. Similar (higher than 64%) methane content was observed in biogas from all reactors in the first two batches A and B. However, the highest standard deviation was obtained after a 10°C increase. After a 15°C increase, methane content was lower than in stable conditions and in the other batches, as well. Not only a decrease in methane content, but also high increases in the pH values were recorded in batch C, caused by the adaptation problem of the process. Specific biomethane production amounts fluctuated in the range of 364-420 Nml CH<sub>4</sub>/ g oDM, with the highest 10% dissimilarity. The specific biogas formation graphs showed that similar biogas generation could be obtained despite the destruction of the process by temperature changes, except in the case of a 15°C temperature increase as in batch C. After each temperature change, pH value increases were observed, but did not exceed 8 and stayed in the optimum range 7 and 8. According to pH values obtained after the test, there was no inhibition observed in the test reactors. Hence our results indicate that the temperature fluctuations can be adapted by the process. Further research is needed to get detailed information about a 15 °C increase at the reactor temperature.

#### ACKNOWLEDGEMENTS

We are immensely grateful to the students and staff from the Institute of Environmental Technology and Energy Economics for their support. Special thanks to the German Academic Exchange Service (DAAD) for their scholarship for the researcher.

#### REFERENCES

- Al Seadi, T., Rutz, D., & Prassl, H. (2008). Biogas handbook.
- Bisswanger, H. (2008). Enzyme Kinetics: Principles and Methods. Wiley-VCH Verlag GmbH & Co. KGaA .
- Caballero-Arzápalo, N. (2015, September 10). Untersuchungen zum anaeroben Abbauprozess ausgewählter Abfallsubstrate mit Hilfe spezieller Mikroorganismen und Enzyme. München.
- Demirel Burak, S. P. (2008). The roles of acetotrophic and hydrogenotrophic methanogens during anaerobic conversion of biomass to biomethane. *Reviews in Environmental Science and Biotechnology*, 173-190.
- DIN. (n.d.). German standard methods for the examination of water, waste water and sludge - Parameters characterizing effects and substances (group H) - Part 7: Determination of acid and base-neutralizing capacities (H 7) , 2005.
- DIN. (1983). German standard methods for the examination of water, waste water and sludge; cations (group E); determination of ammonia-nitrogen (E 5) .
- DIN. (1985, 11). German standard methods for the examination of water, waste water and sludge; sludge and sediments (group S); determination of water content, of dry residue and of solids content (S 2).
- DIN. (1987). Deutsche Einheitsverfahren zur Wasser-, Abwasser- und Schlammuntersuchung; Summarische Wirkungs- und Stoffkenngrößen (Gruppe H); Bestimmung des Gesamttrockenrückstandes, des Filtrat-trockenrückstandes und des Glührückstandes (H 1).
- DIN. (2001). Bestimmung des Glühverlustes der Trockenmasse, DIN EN 12879 (S 3a) 2001-02, 2001.
- DIN. (2001). Bestimmung des Trockenrückstandes und des Wassergehalts, DIN EN 12880 (S 2a) 2001-2,2001.
- DIN. (2019). Water analysis - Guidelines for the determination of total organic carbon (TOC) and dissolved organic carbon (DOC); German version EN 1484:1997.
- Dominika Kufka, M. B. (2019). Stable isotopes of C and H in methane fermentation of agriculture substrates at different temperature conditions. *Open Geosciences*.
- Drosg, B. (2013). Process monitoring in biogas plants. *IEA Bioenergy* .
- Ei-Mashad Hamed M., Z. G. (2004). Effect of temperature and temperature fluctuation on thermophilic anaerobic digestion of cattle manure. *Bioresource technology*, 191-201.
- FNR. (2010). Guide to Biogas: From production to use. Rostock: FNR, Abt. Öffentlichkeitsarbeit.
- FNR. (2013). Biogas. Fachagentur Nachwachsende Rohstoffe e.V. (FNR).
- Gerardi, M. H. (2003). *The Microbiology of Anaerobic Digestion*. Wiley-Interscience .
- Gerber, M. (2009). Ganzheitliche stoffliche und energetische Modellierung des Biogasbildungsprozesses . Bochum.
- Iranpour R., C. H. (2002). Changing Mesophilic Wastewater Sludge Digestion into Thermophilic Operation at Terminal Island Treatment Plant. *Water and Environment Research*, 497-507.
- ISO. (2002). Water quality – Determination of the chemical oxygen demand index (ST-COD) – Small-scale sealed-tube method.
- J.B. Holm-Nielsen, T. A.-P. (2009). The future of anaerobic digestion and biogas utilization. *Bioresource Technology*, pp. 5478-5484.
- Jabłoński, S., Rodowicz, P., & Łukaszewicz, M. (2015). Methanogenic archaea database containing physiological and biochemical characteristics. *International journal of systematic and evolutionary microbiology* , 1360–1368.
- K. Kundu, I. B. (2014, January 30). Impact of abrupt temperature increase on the performance of an anaerobic hybrid bioreactor and its intrinsic microbial community. *Bioresource Technology*, pp. 72-79.
- Kayode Feyisetan Adekunle, J. O. (2015). A Review of Biochemical Process of Anaerobic Digestion. *Advances in Bioscience and Biotechnology*, 205-212.
- Le Zhang, K.-C. L.-H. (2019, September ). Mesophilic and thermophilic anaerobic digestion of soybean curd residue for methane production: Characterizing bacterial and methanogen communities and their correlations with organic loading rate and operating temperature. *Bioresource Technology*.
- Liangwei Deng, H. Y. (2014, August 7). Kinetics of temperature effects and its significance to the heating strategy for anaerobic digestion of swine wastewater. *Applied Energy*, pp. 349-355.

- Matteo Bavutti, L. G. (2014). Thermal stabilization of digesters of biogas plants by means of optimization of the surface radiative properties of the gasometer domes. 68th Conference of the Italian Thermal Machines Engineering Association, (pp. 1344-1353).
- Methodenbuch, D. V. (n.d.). Bestimmung von Gesamt-Stickstoff nach KJELDAHL.
- Moset Veronica, P. M. (2015). Mesophilic versus thermophilic anaerobic digestion of cattle manure: methane productivity and microbial ecology. *Microbial biotechnology*.
- Protigrain, C. A. (2019, May 13). Retrieved from [http://www.cropenergies.com/de/Lebens-Futtermittel/ProtiGrain/Qualitaet/ProtiGrain-2011-DE\\_1.pdf](http://www.cropenergies.com/de/Lebens-Futtermittel/ProtiGrain/Qualitaet/ProtiGrain-2011-DE_1.pdf)
- Rafaela Franqueto, J. D. (2019). Effect of Temperature Variation on Codigestion of Animal Waste and Agricultural Residue for Biogas Production. *BioEnergy Research*.
- Streitwieser, D. A. (2017). Comparison of the anaerobic digestion at the mesophilic and thermophilic temperature regime of organic wastes from the agribusiness. *Bioresource Technology*, 985-992.
- Suryawanshi, P. C., Chaudhari, A. B., & Kothari, R. M. (2010). Thermophilic anaerobic digestion. The best option for waste treatment. *Critical reviews in biotechnology*, 31-40.
- Teimour Amani, M. N. (2010). Anaerobic digestion from the viewpoint of microbiological, chemical, and operational aspects - A review. *Environmental Reviews*.
- VDI. (2014). Vergärung organischer Stoffe Substratcharakterisierung, Probenahme, Stoffdatenerhebung, Gärversuche, VDI 4630.
- Wu Man-chang, S. K. (2006). Influence of temperature fluctuation on thermophilic anaerobic digestion of municipal organic solid waste. *Journal of Zhejiang University*, 180-185.
- Ye Chen, J. J. (2007). Inhibition of anaerobic digestion process: A review. *Bioresource Technology*, pp. 4044-4064.

# UTILIZATION OF DEMOLITION WOOD AND MINERAL WOOL WASTES IN WOOD-PLASTIC COMPOSITES

Petri Jetsu<sup>1,\*</sup>, Markku Vilkki<sup>2</sup> and Ismo Tiihonen<sup>3</sup>

<sup>1</sup> VTT Technical Research Centre of Finland Ltd, P.O.Box 1603, FI-40101 Jyväskylä, Finland

<sup>2</sup> Conenor Ltd, Poukamankatu12, FI-15240 Lahti, Finland

<sup>3</sup> Ismo Tiihonen, Saahkarintie 176, FI-77700 Rautalampi, Finland

## Article Info:

Received:  
4 September 2019  
Revised:  
20 December 2019  
Accepted:  
14 January 2020  
Available online:  
5 March 2020

## Keywords:

Demolition waste wood  
Demolition waste mineral wool  
Wood-plastic composites  
Extrusion  
Mechanical properties

## ABSTRACT

Wood and mineral wool fractions from demolished buildings were sorted into different categories and processed to the suitable grain size needed for the manufacturing of wood-plastic composites. Processed construction and demolition waste materials mixed with plastics and additives were extruded into hollow test bars using a conical rotary extruder. Test specimens needed for measurements were cut from test bars. The results showed that the mechanical performance of wood-plastic composites based on construction and demolition waste wood, and mineral wool was at a good level and comparable to commonly used wood-plastic composites in decking applications. The highest strength properties of wood-plastic composites were achieved with a plywood fraction and the lowest with materials containing a particle/fibre board fraction. The mechanical performance can be improved by utilizing mineral wool in the formulation of wood-plastic composites. A material mixture containing several wood fractions as well as mineral wool also gave good strength properties. Only a minor reduction in strength properties was measured when recycled plastic was utilized meaning that wood-plastic composites suitable for many types of applications can be produced entirely from recycled materials.

## 1. INTRODUCTION

Construction and demolition waste (CDW) is one of the most significant waste streams in the European Union (EU) representing a 25-30% share of all waste generation in the EU (European Commission, 2018). Recent studies concluded that EU28 countries generated approximately 351 million tons of CDW (excluding excavation materials) in 2012 (Deloitte, 2017). Especially in the Nordic countries, the proportion of CDW wood can be very high, reaching the 25-30% level (Bio by Deloitte, 2015). However, the recycling rate of CDW wood is low and the material is currently being mainly used in energy recovery purposes (Bio by Deloitte, 2015). At the moment, CDW wood is used to some extent in particle boards, ground covers and animal beddings, for example (Bio Intelligent Service, 2011). The utilization of CDW wood in the production of pulp, wood panels and bio-fuels was studied in DEMOWOOD project (Era-learn), and in wood-plastic composite (WPC) production in the IRCOW project (Garcia et al., 2013).

The exact volume of CDW mineral wool currently in use in the buildings stock is challenging to define due to the lack of reliable data. However, Väntsi and Kärki (2014) estimated with the model introduced by Müller et al. (2009)

that the annual mass of CDW mineral wool in EU27 countries might exceed 2.5 million tons in 2019. Despite several options for mineral wool waste recycling, it is commonly disposed of at landfill, due to a lack of widely available recycling systems (Väntsi, 2015). Currently recycling opportunities for mineral wool waste are related, for example, to recycling it in mineral wool production (Holbek, 1987; European Commission, 2004) and its utilization in the production of cement-based composites (Cheng et al., 2011), hybrid particleboards (Mamiński, et al., 2011), ceiling tiles (Dunser, 2007), composite ceramics (Balkevičius and Pranckevičienė, 2008) and wood-plastic composites (Väntsi and Kärki, 2014; Väntsi, 2015). At the moment almost all mineral wool wastes will be deposited in landfills in Finland. However some companies offer recycling solution, which is based on crushing the mineral wool panels to mineral-wool loose material. Mineral wool is classified non-hazardous material, but there is a limit for long-term dust exposure and in very dustable work personal protective equipment should be used.

The Waste Framework Directive (WFD) 2008/98/EC, amended by Directive /2018, states that reuse, recycling and other material recovery of non-hazardous CDW should be increased to 70% in the EU by 2020 (European Parlia-



ment and Council, 2008). On the other hand the Landfill Directive 1999/31/EC requires that EU countries should reduce landfilling of biodegradable municipal waste to 35% of the total amount of biodegradable municipal waste existing in 1995 by 2016 (European Parliament and Council, 1999). Tightening regulations together with environmental benefits achieved by CDW recycling will raise the need to increase the recycling rate of CDW significantly in the future. According to the amendment of the WFD, the Commission shall consider setting the recycling targets for construction and demolition waste and its material-specific fractions by 31 December 2024 (European Parliament and Council, 2008). In practice, this means that in future there might be specific recycling targets, e.g. for wood waste.

In recent years, WPCs have started rapidly gaining popularity in the construction and automotive sectors. The global markets for WPCs were approximately 2 million tons in 2014 and the volumes are growing rapidly (Chen, 2014). The three leading regions are North America, Asia and Europe and the main applications are decking and railings (Chen, 2014). CDW materials are not yet largely used in WPC-manufacturing because of the common challenges related to recycling of CDW materials like ensuring raw material purity and steady availability as well as processing and transportation cost issues (Dolan et al., 1999; Väntsi and Kärki, 2014). However if these challenges can be solved, the utilization of CDW materials in WPCs can offer many benefits for WPC producers, including improved environmental performance, improved material efficiency and even improved cost competitiveness.

The objective of this investigation was to determine the potential of CDW wood and CDW mineral wool as a raw material for WPCs. The influence of different CDW wood fractions as well as CDW glass and stone wool on the mechanical properties of WPCs was clarified. Bending and impact strength measurements were used as standard methods, to evaluate the performance of the produced WPC materials.

## 2. MATERIALS AND METHODS

### 2.1 Raw materials and processing

CDW wood and mineral wools from demolished buildings were transported to the handling terminal for pre-treatment. CDW wood was sorted by hand into four different categories according to origin and purity: clean wood fraction, painted wood fraction, plywood fraction and particle/fibre board fraction. CDW mineral wool was sorted by hand into glass and stone wool fractions. The composition of glass and stone wool is different. Glass wool is made from silica sand, limestone and soda ash or recycled glass. Stone wool is made from volcanic rock like basalt. Addition to these basic raw materials mineral wools contain additives like resin binders (European Mineral Wool Manufacturers Association, 2018). Based on the origin of rock or sand the composition of stone or glass wool can vary. The end use application effects also on the composition of mineral wool. Bigger impurities like stones, concrete pieces, metal and plastic particles as well as pressure impregnated wood include preservatives

(classified to hazardous material) were also removed from CDW wooden and mineral wool fractions by hand at this stage. CDW wooden fractions were further processed with pre- and post-crusher to downsize the particle size of raw materials to a suitable size for the refining process. Pre- and post-crushing was not needed for CDW mineral wools.

Wooden materials were fed to a pre-crusher unit, supplied with an electrically driven fixed hammer mill. The technical specifications of the pre-crusher and post-crusher were as follows: The rotor speed of the pre-crusher was 1000 1/min and power 75 kW. The feeding table was 1.6 m wide and it is equipped with belt conveyor and upper feeding roller. The processing capacity was 100–250 loose m<sup>3</sup>/h depending on fed material. The post-crusher was located in the same line as the pre-crusher and was fed with the feedstock coming from the pre-crusher by a belt conveyor. The electrically driven post-crusher was a high speed swinging blade hammer mill with a rotor speed of 1250 1/min and power of 160 kW. The processing capacity and width were the same as in the pre-crusher unit. A magnetic separator was used for removing magnetic metals from post-crushed materials.

At the pre-crushing phase, the average particle size of sorted CDW wooden fractions was decreased below 0.5x0.5 m. A post-crusher with a screen mesh size of 70 mm downsized the average particle size of CDW wooden fractions below 80 mm.

Cleaning operations of post-crushed CDW wood were continued with an air separator where non-magnetic and magnetic metal particles, gravel and sand were removed. The air separator was equipped with a vibrating feeder table, from where the material was dropped in a thin (thickness 1-3 cm) uniform layer. Magnetic separation was located at the beginning of the material free fall and after that a laminar horizontal airflow began to separate the falling material. Heavier particles like concrete, stones, metals, glass etc. fall vertically away from airflow and the lighter wood particles fly horizontally with air-flow. Separation to wood and reject (heavier particles) categories was done by adjusting the position of the separation wall located inside the air separator. The separated wood material was transported with belt conveyors to the pre-refining phase.

The hammer mill used in the pre-refining phase was equipped with swinging blade hammers and a 10 mm screen. The pre-refiner was powered by a 400 kW diesel engine. The post-refiner was a swinging blade hammer mill equipped with a 4 mm screen, powered by a 50 kW diesel engine. Two magnetic separators were located between the pre- and post-refiners and after post-refiner.

At the pre-refining phase, the particle size of CDW wooden and mineral wool fractions was downsized below 10 mm by hammer mill (screen mesh size 10 mm). The particle size of CDW wooden and mineral wool fractions was reduced to below 4 mm by hammer mill (screen mesh size 4 mm) at the post-refining phase. Finally, refined CDW wooden and mineral wool fractions were dried to dry solid content of 80-85% by waste heat coming from post-refining process.



## 2.2 Composite processing: raw materials, mixing, extrusion

In addition to the processed CDW wood and mineral wool fractions, the raw materials used in the production of extruded WPC test bars are presented in Table 1.

The main production phases of the fibre-plastic composites were mixing and extruding. At the mixing phase, agglomerates consisted of CDW wooden and mineral wool fractions, plastic and additives, which were formed by high-speed mixer unit. CDW wooden material, which contains 15-20% of moisture, was also dried at the mixing phase to a dry solid content above 98%. The agglomerates were extruded into 1 m long hollow test bars 60 x 40 mm in size with 8 mm wall thickness using a conical rotary Conex®-extruder type CWE 380-1.

The high-speed (batch) mixer unit consisted of two separate bowls; an upper (hot) bowl, 100 litres in size, for mixing and a lower (cold) bowl, 200 litres in size, with a water circulation jacket for cooling. The diameter of the mixing bowl was 800 mm and it was equipped with three mixing blades. The cooling bowl was equipped with one mixing blade and its diameter was 1000 mm. In these experiments the loading batch quantity was 30 kg of total mixture and the mixing speed used was 1350 rpm in the mixing bowl. During the mixing cycle of approximately 25 minutes, the temperature in the mixing bowl and the load on the mix-

ing bowl motor were measured. Both temperature and drive load measurement data were used to monitor the agglomeration rate of the mixture and when the agglomeration was completed agglomerates were discharged into the cooling bowl. After a cooling time of approximately ten minutes, agglomerates were ready to be discharged into the container from the cooling bowl.

A Conex®-extruder CWE 380-1 consists of a rotating conical rotor with spiral groove geometry and holes for mixing the material composition fed from two sides at 3 and 9 o'clock positions via placed screw feeders. The rotor diameter is 380 mm at the feeding side and 100 mm at the tip. The rotor is surrounded on both sides from inside and outside by heated (electrical and/or oil circulation) stationary stators with "mirror shaped" groove geometry to match the rotor geometry. Each stator heating is divided into two individual sections; the feeding zone and the melting zone. In these experiments, the temperature of the feeding zone was set to 120°C and the melting zone to 160°C. The rotational speed of the rotor was 5 rpm and the flight clearance (gap) between the rotor and stators was 0.5 mm.

Overall 14 different WPC materials based on CDW wood and mineral wool fractions were extruded for further studies (Table 2).

**TABLE 1:** Raw materials used in the production of WPCs.

	Trade name, description	Form	Supplier
Polypropylene	BC245MO, copolymer, MFR 3.5 g/10 min *	Granules	Borealis
Recycled polypropylene	Consumer bottles, mixed colors, MFR 1 g/10 min *	Flakes	Swerec
Talc	Finntalc M30, filler	Powder	Mondo Minerals
Maleic anhydride acid (PP-g-MAH)	Licocene® PP MA 7452, coupling agent	Granules	Clariant
Blend of modified fatty acid ester	Struktol® TPW 113, processing aid	Granules	Struktol

\* MFR: Melt Flow Rate

**TABLE 2:** Extruded WPC materials. Numbers in the table indicate the amount of materials (percentage by weight).

	Abbr.	1	2	3	4	5	6	7	8	9	10	11	12	13	14
<b>Wood fractions</b>															
Clean wood	W	60		63	58	63	58								63
Painted wood	PW		63						19	48	38	48	38		
Plywood	PLY								17					68	
Particle/fibre board	MDF							63	17						
<b>Mineral wool fractions</b>															
Stone wool	SW			5	10				5			20	30		
Glass wool	GW					5	10		5	20	30				
<b>Plastic</b>															
Polypropylene virgin	PP	27	25	25	25	25	25	25	25	25	25	25	25	25	
Polypropylene recycled	PPr														25
<b>Additives</b>															
Talc		5	5					5	5						5
Processing aid		6	5	5	5	5	5	5	5	5	5	5	5	5	5
Coupling agent		2	2	2	2	2	2	2	2	2	2	2	2	2	2

### 2.3 Testing

The particle sizes of CDW wooden fractions were determined according to the ISO 17827-2:2016 standard (ISO 17827-2:2016, 2016). In this method CDW wooden fractions are screened through vertically positioned and horizontally oscillating sieves with square apertures to sort wooden particles mechanically into descending size classes. The sizes of apertures of sieves from top to bottom are 16.0 mm, 8.0 mm, 4.0 mm, 2.0 mm, 1.0 mm, 0.71 mm, 0.5 mm, 0.315 mm, 0.250 mm, 0.180 mm, 0.125 mm, 0.090 mm and 0.063 mm. Total amount of analysed wooden material was 50 g per fraction. The fibre dimensions of CDW glass and stone wool were analysed by the L&W FiberMaster fibre analyser. Measured fibre quantity was approximately 5300 fibres for glass wool and 3000 fibres for stone wool.

Test specimens for flexural and impact strength measurements were cut from WPC test bars and they were kept under standard conditions (23°C, 50% relative humidity) for at least five days before testing. Flexural tests were performed according to the ISO-178 standard using an Instron 4505 Universal Tensile Tester (Instron Corp., Canton, MA, USA) with a 1 kN load cell and a 1 mm/min cross-head speed (ISO-178, 2019). Test specimen thickness was 8.5±1 mm, width 20±1.5 mm and length 200±2 mm. The impact strength was measured using a Charpy Ceast 5.5 Impact Strength Machine according to the ISO-179 standard (ISO-179, 2010). The test was performed on un-notched specimen, which thickness was 8±1 mm, width 10.5±1 mm and length 80±2 mm. Each value obtained represented the average of five samples in flexural test and the average of ten samples in impact test. Standard deviation was used to quantify the amount of variation of parallel measurements.

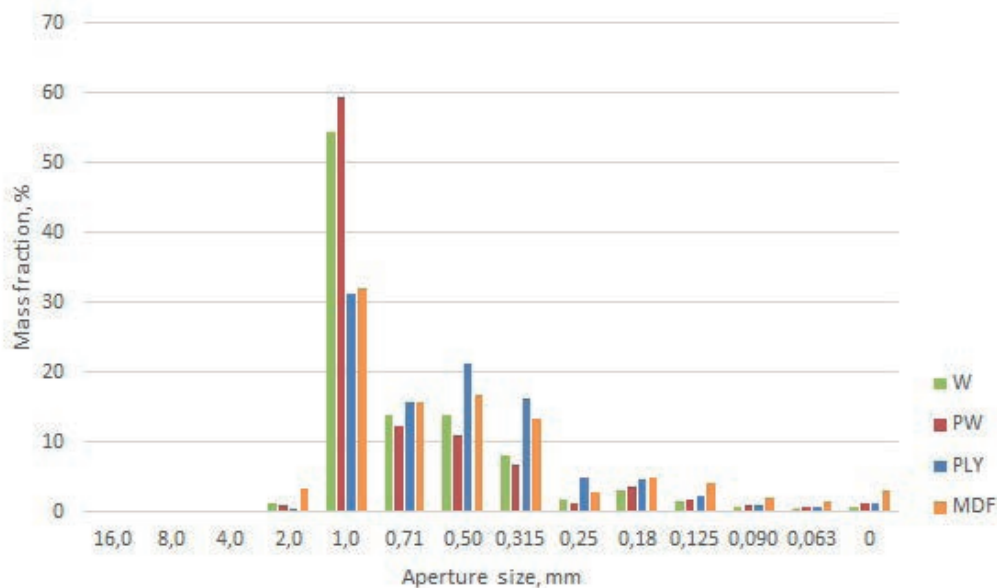
### 3. RESULTS

Particle size distributions of refined CDW wooden fractions and length distributions of refined CDW mineral wool

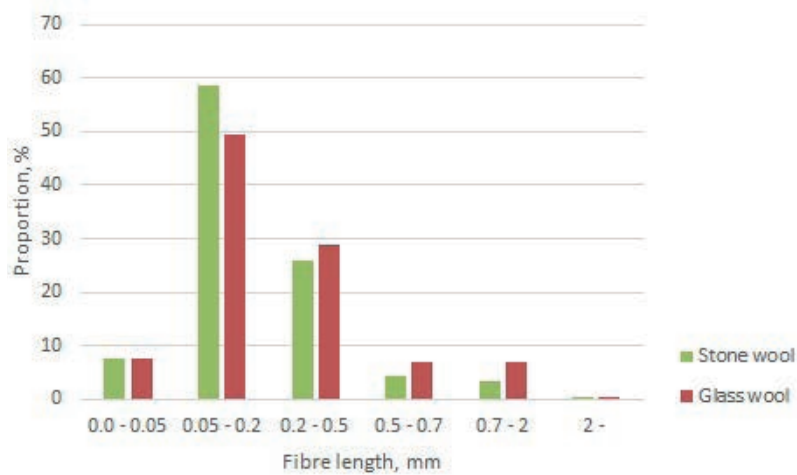
fractions are shown in Figure 1 and Figure 2. It can be seen from Figure 1 that there is a clear difference in particle size distributions between CDW wood and building board fractions. For clean wood and painted wood fractions a particle size between 1-2 mm represented a proportion over 50% of the total mass. However, the same particle size fraction represented only about a 30% proportion for the plywood and particle/fibre board fractions. The share of particles varying between 0.3-1 mm was 30 to 35% for CDW wooden fractions and 45 to 55% for CDW building board fractions. It should be also noted that the proportion of particles smaller than 0.18 mm was clearly highest in the MDF fraction. The average particle size for clean wood, painted wood, plywood and particle/fibre board fractions were 1.10 mm, 1.14 mm, 0.85 mm and 0.90 mm respectively.

The highest amount of CDW stone and glass wool material fell into the 0.05-0.5 mm fibre length category (Figure 2). The proportion of this category was approximately 85% for the stone and 78% for the glass wool fraction. The proportion of fibres longer than 0.5 mm was higher in the glass wool material than in the stone wool material. The length weighted average fibre lengths and widths for glass wool were 0.53 mm and 14.40 µm and for stone wool 0.39 mm and 16.30 µm respectively.

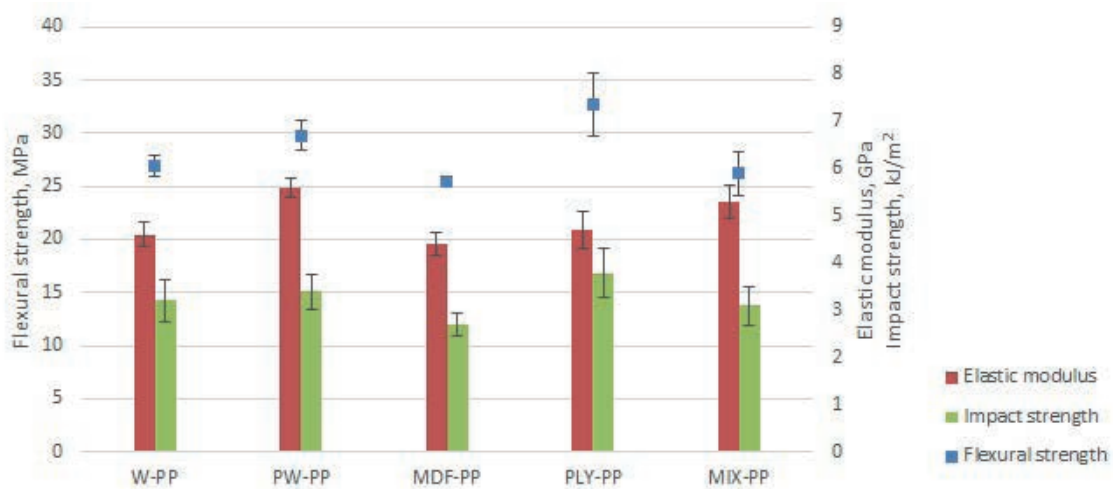
The flexural and impact strength results of WPC materials containing CDW wooden fractions correlated closely to each other (Figure 3). The lowest strengths were achieved with materials containing a particle/fibre board (MDF) fraction and the highest with materials containing a plywood (PLY) fraction. It was noted that the MDF fraction included hard particles like melamine particles, which can be assumed to cause defects (weak points) in WPCs. The dust content of MDF fraction was also much higher than the other CDW wooden fractions leading to reduced reinforcement capability. The PLY fraction gave slightly better results vs. other tested materials. This could be from the influence of adhesives used in PLY manufacturing promoting



**FIGURE 1:** Particle size distributions of refined CDW wooden fractions: clean wood (W), painted wood (PW), plywood (PLY) and particle/fibre board (MDF).



**FIGURE 2:** Length weighted length distributions of refined CDW glass and stone wool fractions.



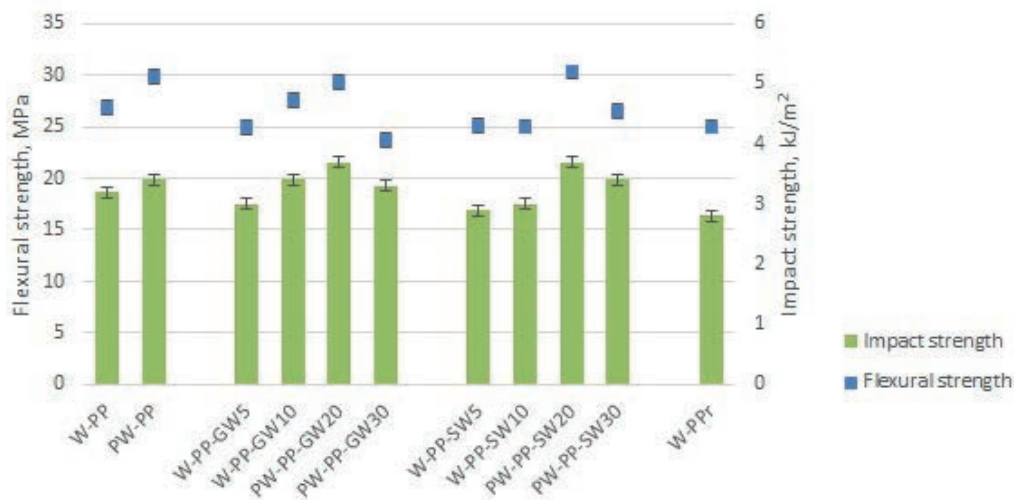
**FIGURE 3:** Flexural strength, impact strength and elastic modulus of WPCs based on CDW wooden materials. Error bars represent standard deviation. CDW fractions are clean wood (W), painted wood (PW), particle/fibre board (MDF), plywood (PLY) and mixed CDW material (MIX). Polymer matrix in all cases is polypropylene (PP).

improved coupling between the natural fibres and polymer matrix. Based on the flexural and impact strength results of the painted wood (PW) fraction we can conclude that there is no need to remove paints or lacquers, for example, from the surfaces of wood before WPC production. Mixed CDW material (MIX), where both mineral wool fractions and all other CDW wooden fractions except clean wood (W) fraction were used, also gave good strength results meaning that there is no need, necessarily, for CDW wood sorting before the production of WPCs and CDW mineral wools can be processed together with CDW wooden fractions in the production of WPCs.

Generally speaking, compared to commercially available products (Haider and Leßlhuber, 2015), the flexural strengths of the produced WPC materials were at a good level, above 25 MPa, and the elastic moduli of all WPCs were high, above 4 GPa (Figure 3). In fact, elastic modulus values over 5 GPa are exceptional high. The impact strength level of the produced WPC materials was quite low, which is a typical feature for high filled WPC materials.

As we can see from Figure 4 the mechanical properties of WPCs based on CDW wood can be improved by utilizing CDW mineral wools in the production of WPC materials. The results indicated that there was an optimum dosage level (near 20%) for CDW mineral wools, where the highest flexural and impact strength was achieved. However it seemed that a 30% dosage level of CDW mineral wool was already too much, leading to deterioration of mechanical properties.

The results achieved differ somewhat from the earlier findings by Väntsi et al. (2014). They concluded that the dosage of CDW stone wool had a positive effect on impact strength of WPCs, but a negative effect on flexural strength. Cui et al. reported that the effect of glass fibres on the impact strength of WPCs could be a positive or negative depending on the glass fibre type (Cui and Tao, 2008). Findings related to flexural strength are inconsistent, i.e. the addition of glass fibres can reduce (Ashrafi et al., 2011) or improve (Valente et al, 2011) the flexural strength of WPCs. One of the main factors affecting the mechanical properties of WPCs is the interfacial adhesion between the



**FIGURE 4:** Flexural and impact strength of WPCs containing CDW glass wool (GW) or stone wool (SW). Number behind the abbreviation meaning the share of glass or stone wool. Error bars represent standard deviation. Reference materials are clean wood (W) and painted wood (PW) containing WPCs without mineral wool. Polymer matrix is virgin polypropylene (PP) or recycled (PPr) polypropylene.

filler materials and the polymer matrix (Cui and Tao, 2008; Petinakis et al., 2009; Ashrafi et al., 2011; Valente et al., 2011; Poletto et al., 2011) and this adhesion can vary, for example with the glass fibre type.

A small reduction in flexural and impact strengths of WPCs can be noticed when recycled polypropylene is utilized (Figure 4). However, for several applications a strength reduction of this magnitude is not significant, meaning that in many cases WPCs can be totally produced from recycled raw materials. Of course, it should be noted that the mechanical properties of WPCs based on the recycled plastics depend heavily on the quality of the recycled plastics (Kazemi-Najafi, 2013).

#### 4. CONCLUSIONS

We showed that the mechanical performance of wood-plastic composites based on construction and demolition waste wood and mineral wool was at a good level and comparable to commonly used wood-plastic composites in decking applications, and therefore offers very attractive raw material alternatives for wood-plastic composite production. The highest strength properties of wood-plastic composites were achieved with a plywood fraction and the lowest with materials containing a particle/fibre board fraction. The mechanical performance can be improved by utilizing mineral wools in the production of wood-plastic composites. It seemed that the optimum dosage level of mineral wool is approximately 20%. Material mixtures containing different wood fractions as well as mineral wool also gave good strength properties meaning that there is a possibility to utilize a relatively compact processing concept without many sorting phases. It is obvious that significant cost savings at the raw material processing phase can be achieved by simplifying the processing concept. Only a minor reduction in strength properties was noticed when recycled plastic was used, offering savings to raw material costs. The results showed that wood-plastic composites could be produced totally from

recycled materials thus promoting the circular economy and reducing waste in the construction and demolition sectors. In addition wood-plastic composites are recyclable i.e. all materials can be re-used or processed by plastic processes to new products.

#### ACKNOWLEDGEMENTS

This research is part of the HISER project ([www.hiser-project.eu](http://www.hiser-project.eu)). The HISER project has received funding from the European Union's Horizon 2020 research and innovation program under grant agreement No. 642085.

#### REFERENCES

- Ashrafi, M., Vaziri, A., Nayeb-Hashemi, H., (2011). Effect of processing variables and fiber reinforcement on the mechanical properties of wood plastic composites. *Journal of Reinforced Plastics and Composites*, 30:1939-45.
- Balkevičius, V., Pranckevičienė, J., (2008). Investigation of properties of composite ceramics. *Materials Science*, April, 14(1).
- Bio by Deloitte (2015). Construction and Demolition Waste Management in FINLAND/SWEDEN/ - Factsheets. Contract study for European Commission: [http://ec.europa.eu/environment/waste/studies/mixed\\_waste.htm#deliverables](http://ec.europa.eu/environment/waste/studies/mixed_waste.htm#deliverables)
- Bio Intelligent Service (2011). Service contract on management of construction and demolition waste. Final report, Task 2, Contract study for EC: <https://publications.europa.eu/en/publication-detail/-/publication/0c9eefc-d07a-492e-a7e1-6d355b16dde4>
- Chen, J., (2014). Wood-plastic composites: technologies and global markets. Market report, BCC Research.
- Cheng, A., Lin, W-T., Huang, R., (2011). Application of rockwool waste in cement-based composites. *Materials and design*, vol. 32, no. 2, pp. 636-642.
- Cui Y-H., Tao J., (2008). Fabrication and mechanical properties of glass fiber-reinforced wood plastic hybrid composites. *Journal of Applied Polymer Science*, 112:1250-7.
- Deloitte (2017). Resource Efficient use of mixed wastes - Improving management of construction and demolition waste. Contract study for European Commission: [http://ec.europa.eu/environment/waste/studies/pdf/CDW\\_Final\\_Report.pdf](http://ec.europa.eu/environment/waste/studies/pdf/CDW_Final_Report.pdf)
- Dolan, P., Lampo, R., Dearborn, J., (1999). Concepts for reuse and recycling construction and demolition waste. Technical report, Construction Engineering Research Laboratories, U.S. Army corps of Engineers.

- Dunser, A., (2007). Characterisation of mineral wastes, resources and processing technologies - Integrated waste management for production of construction material. Case study: waste mineral fiber in ceiling tile manufacture: [http://www.smartwaste.co.uk/filelibrary/Ceiling\\_tiles\\_waste\\_mineral\\_wool.pdf](http://www.smartwaste.co.uk/filelibrary/Ceiling_tiles_waste_mineral_wool.pdf)
- ERA-LEARN <https://www.era-learn.eu/network-information/networks/woodwisdom-net-2/sustainable-competitive-processing-and-end-use/optimisation-of-material-recycling-and-energy-recovery-from-waste-and-demolition-wood-in-different-value-chains>
- European Commission (2004). Waste injection into the melting furnace in stone wool production. [http://ec.europa.eu/environment/life/project/Projects/index.cfm?fuseaction=home.showFile&rep=file&fil=LIFE02\\_ENV\\_FIN\\_000328\\_LAYMAN.pdf](http://ec.europa.eu/environment/life/project/Projects/index.cfm?fuseaction=home.showFile&rep=file&fil=LIFE02_ENV_FIN_000328_LAYMAN.pdf)
- European Commission (2018). Construction and Demolition Waste (CDW): [http://ec.europa.eu/environment/waste/construction\\_demolition.htm](http://ec.europa.eu/environment/waste/construction_demolition.htm) (Last updated September 9, 2018).
- European Mineral Wool Manufacturers Association (2018). <https://www.eurima.org/about-mineral-wool>
- European Parliament and Council (1999). Landfill Directive 1999/31/EC. 26<sup>th</sup> April.
- European Parliament and Council (2008). Waste Directive 2008/98/EC. 19<sup>th</sup> November.
- Garcia, M., Hidalgo, J., Vilkki, M., (2013). Opportunities for recycling C&DW into WPCs. Proceedings of the 6<sup>th</sup> international wood fibre polymer composites symposium, Biarritz.
- Haider, A., Leßlumer, J., (2015). Comparison of commercial European WPC-Deckings 2008 and 2014. 6<sup>th</sup> WPC & NFC Conference. 16 - 17 December, Cologne.
- Holbek K (1987), U.S. Patent no. 4,287,142.
- ISO 17827-2:2016 Solid biofuels – Determination of particle size distribution for uncompressed fuels – Part 2: Vibrating screen method using sieves with aperture of 3,15 mm and below
- ISO 178:2019 Plastics – Determination of flexural properties
- ISO 179-1:2010 Plastics – Determination of Charpy impact properties – Part 1: Non-instrumented impact test
- Kazemi-Najafi, S., (2013). Use of recycled plastics in wood plastic composites - a review. *Waste Management*, 33:1898-1905.
- Mamiński, M., Król, M., Jaskółowski, W., Borysiuk, P., (2011). Wood-mineral wool hybrid particleboards. *European Journal of wood and wood Products*, vol. 69, no. 2, pp. 337-339.
- Müller, A., Leydolph, B., Stanelle, K., (2009). Recycling mineral wool waste—Technologies for the conversion of the fiber structure. Part 1, *Interceram* 58:378–381.
- Petinakis, E., Yu, L., Edward, G., Dean, K., Liu, H.S., Scully, A.D., (2009). Effect of Matrix–Particle Interfacial Adhesion on the Mechanical Properties of Poly(lactic acid)/Wood-Flour Micro-Composites. *Journal of Polymers and the Environment*, 17, 83.
- Poletto, M., Zeni, M., Zattera, A.J., (2011). Effects of wood flour addition and coupling agent content on mechanical properties of recycled polystyrene/wood flour composites. *Journal of Thermoplastic Composite Materials*, 25: 821-833.
- Valente, M., Sarasini, F., Marra, F., Tirillò, J., Pulci, G., (2011). Hybrid recycled glass fibre/wood flour thermoplastic composites: manufacturing and mechanical characterization. *Composites Part A*, 42:649-657.
- Väntsi, O., (2015). Utilization of recycled mineral wool as filler in wood-plastic composites. Doctoral thesis, 9<sup>th</sup> October.
- Väntsi, O., Kärki, T., (2014). Mineral wool waste in Europe: A review of mineral wool waste quantity, quality and current recycling methods. *Journal of Material Cycles and Waste Management*, 16, pp. 62-72.
- Väntsi, O., Kärki, T., (2014). Utilization of recycled mineral wool as filler in wood-polypropylene composites. *Construction and Building Materials*, 55, pp. 220-226.

# CASE STUDY ON ENHANCED LANDFILL MINING AT MONT-SAINT-GUIBERT LANDFILL IN BELGIUM: MECHANICAL PROCESSING, PHYSICO-CHEMICAL AND MINERALOGICAL CHARACTERISATION OF FINE FRACTIONS <4.5 MM

Daniel Vollprecht <sup>1,\*</sup>, Juan Carlos Hernández Parrodi <sup>1,2</sup>, Hugo Lucas <sup>3</sup> and Roland Pomberger <sup>1</sup>

<sup>1</sup> Montanuniversität Leoben, Department of Environmental and Energy Process Engineering, 8700 Leoben, Austria

<sup>2</sup> Renewi Belgium SA/NV, NEW-MINE project, 3920 Lommel, Belgium

<sup>3</sup> RWTH Aachen University, IME Process Metallurgy and Metal Recycling, 52056 Aachen, Germany

## Article Info:

Received:

5 January 2020

Revised:

24 February 2020

Accepted:

25 February 2020

Available online:

31 March 2020

## Keywords:

Enhanced landfill mining

Fine fractions

Mechanical processing

Chemical composition

Mineralogical composition

Waste-to-material

## ABSTRACT

Fine fractions obtained by mechanical processing of excavated waste constitute a challenge for (enhanced) landfill mining projects. These fractions are mainly composed of humified organic and weathered inorganic compounds, whereas metals and calorific fractions are depleted. In this study we present data on the chemical composition and grain size distribution of the fine fractions <4.5 mm, as well as on the mineralogical composition of the two finest subfractions (0.18 to 0.5 mm and <0.18 mm). Chemical analyses indicate no trend regarding the enrichment or depletion of heavy metals in the different particle size ranges. Leaching from the finer fractions is somewhat higher than from the coarser fractions (i.e. 1.6 to 4.5 mm and 0.5 to 1.6 mm), although the fraction 0.18 to 0.5 mm shows the lowest overall leaching. Pseudo-total contents of Cu, Zn, Cd, Hg and Pb and leachable contents of Ni exceed Austrian limit values for the production of soil substitutes from wastes. Electron microprobe analyses indicate that Zn and Pb, which exceed limit values for pseudo-total content, are present as Fe-Zn alloy, ZnS and ZnSO<sub>4</sub>, and metallic Pb and Pb-Ca phosphate, respectively. In summary, dry-mechanical processing, which is a feasible method in the particle size range >4.5 mm, showed a limited effect in the range <4.5 mm. Removal of Pb- and Zn-containing phases is highly challenging due to the diverse mineralogy and fine grain size of few μm. Consequently, it seems unlikely that the Austrian limit values for soil substitutes can be met.

## 1. INTRODUCTION

Landfill mining, “a process for extracting [...] resources from waste materials that have previously been disposed of [...]” (Krook et al., 2012) was introduced in 1953 (Savage et al., 1993), whilst interest in this topic has increased significantly over the last 30 years. Although from an economic perspective landfill mining is largely not a feasible option (Laner et al., 2019), a combination of the process with environmental remediation may be promising (Frändgård et al., 2015), particularly when considering the value of ecosystem revitalisation (Bulakovs et al., 2017).

Fine fractions produced by mechanical processing of landfill mining materials are a major obstacle for an economically feasible (enhanced) landfill mining ((E)LFM) due to the predominant amounts and problematic characteristics (García López, et al., 2019; Hernández Parrodi, et al.,

2019b; Hernández Parrodi, Höllen, & Pomberger, 2018a; Hernández Parrodi, Höllen, & Pomberger, 2018b).

Fine fractions have been considered a potential substrate for intermediate or final cover layers for both operational landfills or closed and excavated landfills, which may represent a source of revenue (Hogland, 2010; Greedy, 2016). A previous study from the Austrian LAMIS project indicates that the fine fraction <20 mm has a permeability of only 5.45 10<sup>-8</sup> m/s, if it has been compacted to a density of 1.26 g/cm<sup>3</sup> at an optimal water content of 23.2% and a temperature of 22°C (Liebetegger, 2015). Another option is use as soil substitute or construction aggregates (Spooren et al., 2013). For the latter application, the organic material should be removed from the fine fractions (Quaghebeur, et al., 2013), e.g. by physico-chemical treatment (Bhatnagar, et al., 2017).



\* Corresponding author:

Daniel Vollprecht

email: daniel.vollprecht@unileoben.ac.at



Detritus / Volume 10 - 2020 / pages 26-43

<https://doi.org/10.31025/2611-4135/2020.13940>

© 2020 Cisa Publisher. Open access article under CC BY-NC-ND license

In the context of the NEW-MINE project a case study was conducted at Mont-Saint-Guibert (MSG) landfill in Belgium. Mechanical processing of the fine fractions 90 to 4.5 mm yielded median amounts of approx. 37.2 wt.% inert, 9.0 wt.% combustibles and 1.7 wt.% total metals in dry state of the total amount of fine fractions <90 mm (Hernández Parrodi et al., 2019c). In the latter case study, the extension of mechanical processing from a particle size of 10 mm to 4.5 mm increased the amount of recovered materials by around 10 wt.% (Hernández Parrodi et al., 2019c), thus representing an additional amount of resource potential in comparison with previous studies in which particle sizes below 10 mm were not processed (Wanka, Münnich, & Fricke, 2017). However, fine fractions <4.5 mm which, due to their fine grain size are not suitable for separation either manually or using sensor-based technologies, remain highly challenging (Küppers, et al., 2019). Direct sorting technologies such as magnetic and eddy-current separation may be applied in the recovery of ferrous and non-ferrous metals, respectively, down to a particle size of 4.5 mm (Hernández Parrodi et al., 2019c; Lucas et al., 2019); however, these materials only account for a small amount of the total quantity of fine fractions, leaving behind a large share of fine fractions <4.5 mm – composed mainly of weathered inorganic and decomposed organic matter (Hernández Parrodi, et al., 2019a).

In view of the characteristics of the fine fractions <4.5 mm, being a mixture of organic compounds and mineral phases, utilisation as a soil substitute has been discussed (Hernández Parrodi, Höllen, & Pomberger, 2018b; Hernández Parrodi et al., 2019c). Soils have been defined as the uppermost biologically active part of the Earth's crust, contributing to promoting soil functions (Scheffer & Schachtschabel, 2018). Soil sealing leads to a loss of these functions, thus constituting a major environmental concern (Scalenghe & Marsan, 2009). Additionally, approx. 25 million tons of excavated soils are landfilled in Austria every year (Federal Ministry for Sustainability and Tourism, 2017). Consequently, to maintain soil functions, soil substitute materials (Federal Ministry for Sustainability and Tourism, 2017) are produced for recultivation purposes. In Austria, legal requirements dictate the production of soil substitutes from waste, particularly to prevent recirculation of contaminants (Austrian Standards, 2013).

The fine fractions <4.5 mm of landfill mining materials are rich in both organic and inorganic contaminants compared to the bulk of excavated materials (Burlakovs et al., 2016). Results of tests conducted on these fractions show how most of the potentially toxic elements studied (As, Ba, Cd, Co, Cr, Cu, Fe, Mg, Mn, Ni, Pb, Sb and Zn) were bound to fractions of low extractability. This suggests that the fraction could be used as a low-risk cover material during environmental site remediation, landfill recultivation and land restoration, although further environmental analysis should first be performed due to the low mobility and leaching potential of toxic metals. In several countries total contents may also be used as limit values for the recycling of wastes inhibiting the utilization of wastes even at low leachability. A Swedish study reported how the total contents of zinc (Zn), barium (Ba) and chromium (Cr) in

fine fractions of landfilled material were above threshold values for contaminated soil (Jani et al., 2016). In this context, it should be considered that many metals may not only pose a threat to the environment, but also contribute to the resource potential of fine fractions (Burlakovs et al., 2018). An additional concern is associated with the presence of organic carbon, which may lead to the formation of methane (Mönkäre, Palmroth & Rintala, 2016). Thus, utilization of the entire fine fractions <4.5 mm for protection of natural resources might contradict the aim of waste management to protect human health and the environment by removing contaminants from a circular economy (Republic of Austria, 2002).

Consequently, to achieve all three aims of waste management, i.e. protection of human health, protection of the environment and protection of natural resources, separation of fine fractions <4.5 mm into a contaminant-depleted fraction for recycling as soil substitute and a contaminant-enriched fraction for disposal at a sanitary landfill is mandatory.

Advanced separation technologies for grain size ranges below 4.5 mm are state-of-the-art in mineral processing, e.g. flotation (Peleka, Gallios, & Matis, 2017), electrostatic separation (Kelly & Spottiswood, 1989) or selective leaching of individual mineral phases (Lane et al., 2016), although detailed knowledge of the phase composition of the material is required. Due to the frequent lack of relevant information with regard to fine fractions from landfill mining, often also associated with significantly higher costs, this study tested a more simple approach, i.e. the screening and dry abrasion of surface defilements (i.e. impurities).

The first working hypothesis for this treatment was based on the knowledge that contaminants are enriched in the finest fraction, thus implying that even in the range <4.5 mm separation between a clean coarser fraction and a contaminated finer fraction might be achieved.

The second working hypothesis referred to mobility of contaminants in the fine fraction: Although fine fractions of landfill mining materials are often described as soil-like material (Hernández Parrodi, Höllen, & Pomberger, 2018b; Hernández Parrodi et al., 2019c) no studies have been conducted to date to assess their mineralogical composition. However, detailed knowledge is not only necessary for advanced separation technologies, but also to gain a deeper understanding of the leachability of heavy metals related to their mineral host phases (Vollprecht, et al., 2019). Existing studies on the mobility of contaminants from LFM fine fractions (Burlakovs, et al., 2016) follow the approach of sequential extraction, but do not explicitly address mineralogy of the fine fraction.

Consequently, our second hypothesis suggests that the mineralogy of (E)LFM fine fractions is related to leachability, as is the case for other materials such as slags (Neuhold, et al., 2019) and rocks (Vollprecht, et al., 2019).

To summarise, we present here the first study of fine fractions from landfill mining, including a comprehensive mineralogical analysis with particular emphasis on inorganic contaminants present and related leaching behaviour.

## 2. MATERIALS AND METHODS

### 2.1 Materials

Fine fractions <4.5 mm were obtained from mechanical processing of fine fractions <90 mm from MSG landfill, Belgium, performed by Hernández Parrodi et al., 2019c (Figure 1). Fractions were produced after sieving composite samples of batches 1 and 2 of fine fractions <90 mm; first at 30 mm, subsequently at 10 mm and finally at 4.5 mm at optimal water content (15 wt.%) and in dry state. Additionally, particles ranging from 90 to 30 mm, 30 to 10 mm and 10 to 4.5 mm were sieved once more at 4.5 mm after a series of mechanical processing steps (i.e. extraction of ferrous and non-ferrous metals, density separation and sensor-based sorting), with the purpose of removing released surface defilements. The subsequently produced fractions <4.5 mm were combined with fine fractions <4.5 mm for further handling. Total amount of fine fractions <4.5 mm corresponded to 42.9 wt.% and 42.7 wt.% of fine fractions <90 mm at optimal water content and in dry state, respectively (Hernández Parrodi et al., 2019c). In turn, the fine fractions <90 mm accounted for approx. 77 wt.% of the total amount of processed material in raw state from the MSG landfill (Hernández Parrodi et al., 2019a). Additional details on the fine fractions <90 mm and mechanical processing, as well as further information about the sampling method and preparation of composite samples, are reported in Hernández Parrodi et al., 2019a and Hernández Parrodi et al., 2019c.

A total of six composite laboratory samples (n=6), containing both batch 1 and batch 2, were obtained from composite samples of the fine fractions <4.5 mm at optimal water content (n=3) and in dry (n=3) state, and the physico-chemical properties determined. In line with the properties detected and the findings of the study on particle size distribution and water content in the fine fractions <90 mm

performed by Hernández Parrodi et al., 2019c, additional mechanical processing of the fine fractions <4.5 mm was designed. The study of particle size distribution and water content revealed that in order to achieve adequate particle size classification of the fine fractions below 3 mm, further reduction of the water content is needed, particularly below 0.6 mm. Therefore, only composite samples of batches 1 and 2 of the fine fractions <4.5 mm in dry state were used for further mechanical processing. This suggests that the composite samples at optimal water content state would need to be dried and processed in the mechanical processing. It is important to note that the state referred to as “the dry state” does not correspond to a strictly dry state, but rather to an average water content of 1.5 wt.% due to absorption/adsorption of ambient moisture by the material throughout the whole mechanical processing.

Additionally, six soil samples were taken from the landfill and the surrounding area for comparison of determined heavy metal concentrations with geological background concentrations.

### 2.2 Mechanical Processing

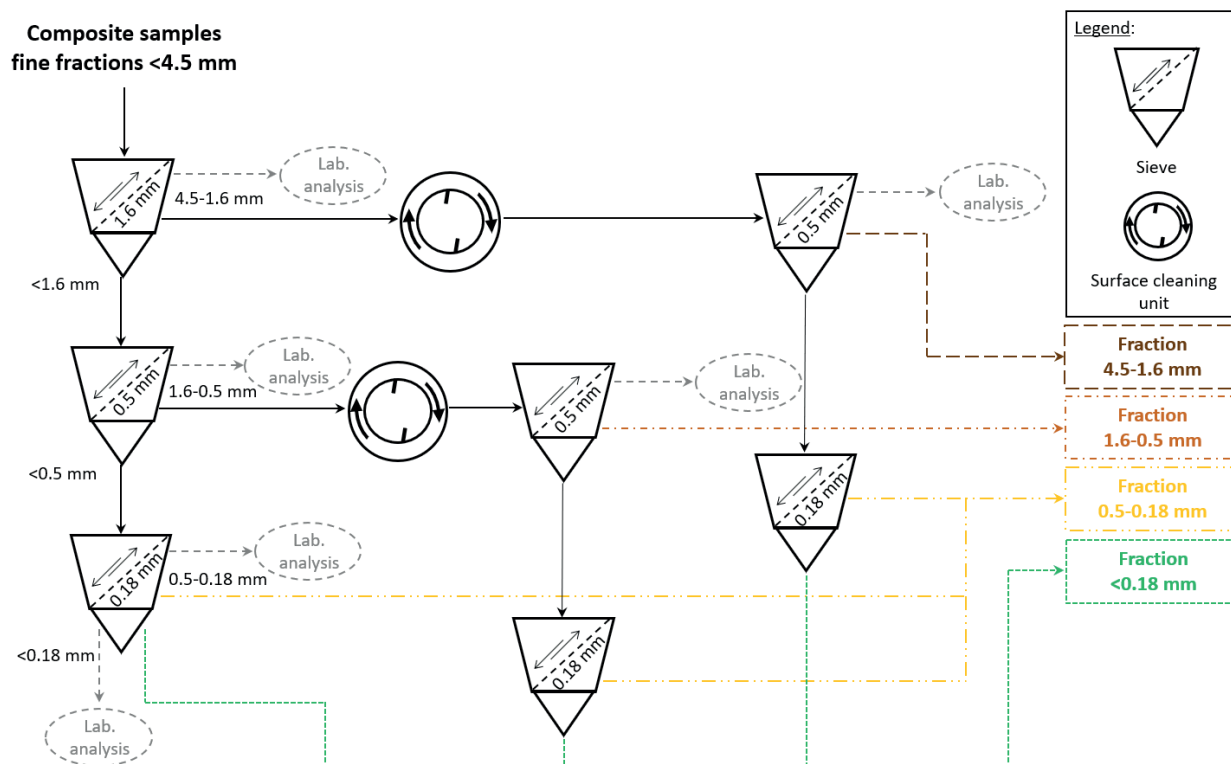
The fine fractions <4.5 mm were subjected to dry-mechanical processing consisting of particle size classification steps (i.e. sieving), followed by a surface cleaning process, driven by superficial erosion (surface attrition), and a second particle size classification step for elimination of loosened surface defilements and detritus. Figure 2 displays a graphic representation of the dry-mechanical processing applied.

A total of eight composite samples (n=8) of the fine fractions <4.5 mm of batch 1 (n=4) and batch 2 (n=4) in dry state were sieved further into four particle size ranges (i.e. 4.5 to 1.6 mm, 1.6 to 0.5 mm, 0.5 to 0.18 mm and <0.18 mm). The samples subsequently underwent chemical analysis to identify the particle size range(s) featuring



FIGURE 1: Location of the Mont-Saint-Guibert landfill.





**FIGURE 2:** Scheme of dry-mechanical processing of the fine fractions <4.5 mm.

the highest concentrations of pollutants and to determine whether the quality of fine fractions <4.5 mm could be improved through further mechanical processing. For this purpose, composite samples were further sieved in a vibratory sieve tower (Retsch AS 200) with woven wire test sieves and squared openings of 1.6 mm, 0.5 mm and 0.18 mm at an amplitude of 100%. Due to the amount of material, prior to sieving, each composite sample was divided into two or three subsamples. Each subsample was sieved for 1 minute to simulate an industrial sieving process, and the amounts of all particle size ranges determined using a precision scale (Sartorius ENTRIS6202-1S; resolution of 0.01 g). After sieving, three composite samples (n=3) were used to determine the physico-chemical properties of each of the four particle size ranges produced. In turn, four composite samples (n=4), including both batch 1 and batch 2, for each of the particle size ranges 4.5 to 1.6 mm and 1.6 to 0.5 mm (n=8) were further mechanically processed by surface cleaning. For this purpose, the particle size ranges 4.5 to 1.6 mm and 1.6 to 0.5 mm underwent further processing in a surface cleaning unit, which consisted of an automatic concrete mixer (Atika BM 125 S) rotated at a speed of 30 rpm with an inclination of 45° for 10 minutes for each composite sample (Figure 3). The objective of the surface cleaning process was to decrease the concentration of pollutants in the coarser particle size ranges (i.e. 4.5 to 1.6 mm and 1.6 to 0.5 mm), since it was assumed that the majority of pollutants would be present in the finer particle size ranges (0.5 to 0.18 mm and <0.18 mm), which would attach to the surface of the coarser particle size ranges as surface defilements.

One composite sample from each set of four was stored for future use in additional laboratory analyses or alternative processing steps. As shown in Figure 2, a dry surface cleaning process was followed by 1-minute sieving at 0.5 mm and 0.18 mm using the previously described vibrating sieve. Finally, the obtained composite samples were used to determine the physico-chemical properties of fractions subjected to the surface cleaning process, with the aim of analysing and evaluating effectiveness and performance.

### 2.3 Chemical Analyses

Three of the composite samples <4.5 mm were analysed for chemical composition (20 oxides) by means of X-ray fluorescence (XRF) spectrometry using fusion tablets according to DIN EN ISO 12667 at CRB GmbH, Hardegsen, Germany. Loss of ignition (LOI) was determined according to DIN EN ISO 26845 at 1025°C. The mean value of the three analyses was used for further considerations.

Three composite samples of each of the fractions 4.5 to 1.6 mm, 1.6 to 0.5 mm, 0.5 to 0.18 mm and <0.18 mm (n=12) were chemically analysed at the laboratory of the Chair of Waste Processing Technology and Waste Management (AVAW) of the Montanuniversität Leoben. Additionally, the chemical composition of three composite samples of each of the fractions 4.5 to 1.6 mm and 1.6 to 0.5 mm (n=6) was determined subsequent to dry surface cleaning to compare the concentrations of different pollutants prior to and following dry surface cleaning.

Chemical analyses were generally conducted according to ÖNORM S 2122 ("Soils from Wastes"), which was also taken as a basis for reference values of different parame-



**FIGURE 3:** Scheme of dry-mechanical processing of the fine fractions <4.5 mm.

ters to be complied with. Additionally, as no limit values for pseudo-total contents (aqua regia digestion) are provided in ÖNORM S2122, limit values for pseudo-total contents of contaminants for excavated soil landfills (Federal Ministry for Agriculture, Forestry, Environment and Water Management, 2008) and recycling of excavated soil (Federal Ministry for Sustainability and Tourism, 2017) were used for comparison. Samples were analysed for total carbon (TC), total organic carbon (TOC, both according to EN 13137), nitrogen (N), adsorbable organic halogens (AOX, according to DIN 38414-18), polycyclic aromatic hydrocarbons (PAHs, according to ÖNORM L 1200), polychlorinated biphenyls (PCBs, according to DIN 38414-20), the cohesion number (KH value, according to ÖNORM S2122-2) and the hydrocarbon index (according to ÖNORM EN 14039). TOC/N ratio was calculated according to ÖNORM S 2122-2. Furthermore, physical properties, including dry and wet density (ÖNORM S 2122-1) and water content (according to ÖNORM L 1062), were determined.

For the determination of pseudo-total metal content, samples were digested in aqua regia according to ÖNORM EN 13657. Metals were determined in the digested sample by means of inductively coupled plasma mass spectrometry (ICP-MS) according to ÖNORM EN ISO 17294-2.

Water-soluble constituents were determined according to ÖNORM L 1092 and ÖNORM S 2122-1. As the production of a saturated water extract was not possible, the following procedure was applied: 100 g air-dried sample was suspended in 500 g pure water and shaken for 2 h in an overhead shaker. Solids were separated from the solution by a centrifuge (15 min at 5,500 rotations per min) and subsequent filtration (0.45 µm). The resulting leachates were analysed for pH (according to ISO 10523), electric conductivity (according to DIN EN 27888), permanganate index ( $C_{ox}$ , according to ÖNORM EN ISO 8467), dissolved organic carbon (DOC, according to ÖNORM EN 1484), anions (i.e. fluoride, chloride, nitrate, sulphate and phosphate, according to DIN EN ISO 10304-1), ammonium (according to DIN 38406-5) and other cations (according to ÖNORM EN ISO 17294-2). Three composite samples (n=3) were analysed

for each parameter and the arithmetic mean, together with the standard error (confidence interval of 95%), were calculated based on the results of laboratory analysis.

Finally, the six soil samples obtained from the landfill and surrounding areas were analysed for Ba, Ge, Cd, Cr, Co, Cu, Ge, As, Hf, Sc, Li, Au, Ag by means of inductively coupled plasma optical emission spectrometry (ICP-OES) at the Chair of Process Metallurgy and Metal Recycling at RWTH Aachen University. Furthermore, S and C were determined in the same laboratory by combustion and subsequent determination of oxides in the off-gas.

## 2.4 Mineralogical Analyses

Modal mineral composition of the fractions <0.18 mm and 0.18 to 1.5 mm from batch 1 and batch 2 was investigated by means of X-ray powder diffraction (XRD) analysis. Two powdered samples (n=2) of each particle size range and batch were analysed using a PANalytical X'Pert Pro diffraction instrument (CoK $\alpha$  radiation ( $\lambda=1.79 \text{ \AA}$ )), 40 mA, 45 kV) and PANalytical HighScore Plus software package at the Institute of Applied Geosciences, Graz University of Technology. Diffractograms were automatically quantified using Rietveld refinement. Resulting net lower limits of detection were in the order of 2 - 5 wt.%, indicating the potential presence of minerals at lower concentrations, although not detectable by XRD.

The distribution of C, S, Pb, Si, Cu, Al, O, K, Ca, P, Zn, Na, Mg, Ba and Fe was determined for the same samples by electron probe microanalyses (EPMA) using the JEOL JXA 8200 instrument installed at the Chair of Resource Mineralogy, Montanuniversität Leoben. Polished sections were carbon coated (EMITECH K950X) to minimize charging under the electron beam. Element maps of mineral phases were conducted using wavelength-dispersive spectrometers (WDX). Heavy-metal containing phases were qualitatively analysed for chemical composition using energy dispersive spectrometers (EDX). The instrument was operated in high vacuum ( $<1.65 \cdot 10^{-5}$  mbar), with 15 kV acceleration voltage, 10 nA beam current (on Faraday cup), and with beam diameter set to spot size ( $\gg 1 \text{ \mu m}$ ).

### 3. RESULTS AND DISCUSSION

#### 3.1 Mechanical Processing

As described in Section 2 all composite samples of the fine fractions <4.5 mm in the dry state were initially sieved at 1.6 mm, 0.5 mm and 0.18 mm. Half of the resulting composite samples of particle size ranges 4.5 to 1.6 mm, 1.6 to 0.5 mm, 0.5 to 0.18 mm and <0.18 mm were used to determine the physico-chemical properties of fractions prior to the surface cleaning process. This process was undertaken to assess whether enrichment of any of the studied parameters, such as heavy metals, PAHs and PCBs, among others, occurred in the presence of any specific particle size distribution and, thus determine whether the same parameters could be concentrated in a certain particle size range by means of particle size classification. Additionally, the physico-chemical characteristics of each particle size range were used as a reference to evaluate the effects of the surface cleaning process. Figure 4 displays the general mass balance of the mechanical processing approach studied in this investigation. Figures for the general mass balance were calculated using the arithmetic mean of the four composite samples (n=4) processed in the tested mechanical processing, based on the average amount of fine fractions <4.5 mm (42.9 wt.%) versus the total quantity of fine fractions <90 mm processed in dry state in our previous study (Hernández Parrodi et al., 2019c).

The general mass balance in Figure 4 revealed amounts corresponding to approx. 13.9 wt.%, 10.8 wt.%, 12.7 wt.%

and 5.6 wt.% for the particle size ranges 4.5 to 1.6 mm, 1.6 to 0.5 mm, 0.5 to 0.18 mm and <0.18 mm, respectively. This highlighted a tendency of the amount of material to decrease in line with reduction in particle size, with the exception of particle size range 0.5 mm to 0.18 mm, featuring a higher amount than the particle size range 1.6 mm to 0.5 mm. Images of the obtained fractions are shown in Figure 5.

Directly after the initial sieving steps at 1.6 mm, 0.5 mm and 0.18 mm, composite samples of particle size ranges 4.5 mm to 1.6 mm and 1.6 mm to 0.5 mm were processed in the surface cleaning unit and subsequently sieved at 0.5 mm and 0.18 mm. An average material loss of approx. 1.2 wt.% due to surface cleaning and subsequent sieving was estimated, whereas an amount of about 3.4 wt.% of liberated surface defilements and detritus after the surface cleaning process was calculated, compared to the total amount of fine fractions <90 mm processed in the dry state. As only a modest average water content of 1.5 wt.% (Table 4) was determined in the processed composite samples, further influence of ambient moisture was deemed negligible in regards to general mass balance. Respective amounts of 0.9 wt.% and 0.7 wt.% of the fraction 0.5 mm to 0.18 mm were obtained in particle size ranges 4.5 mm to 1.6 mm and 1.6 mm to 0.5 mm after sieving at 0.18 mm, while quantities of 1.3 wt.% and 0.6 wt.% of the fraction <0.18 mm were yielded, respectively. Therefore, the dry-mechanical processing used in this study produced total amounts of approx. 11.7 wt.% fine fractions 4.5 mm to 1.6 mm (clean), 9.5 wt.% fine

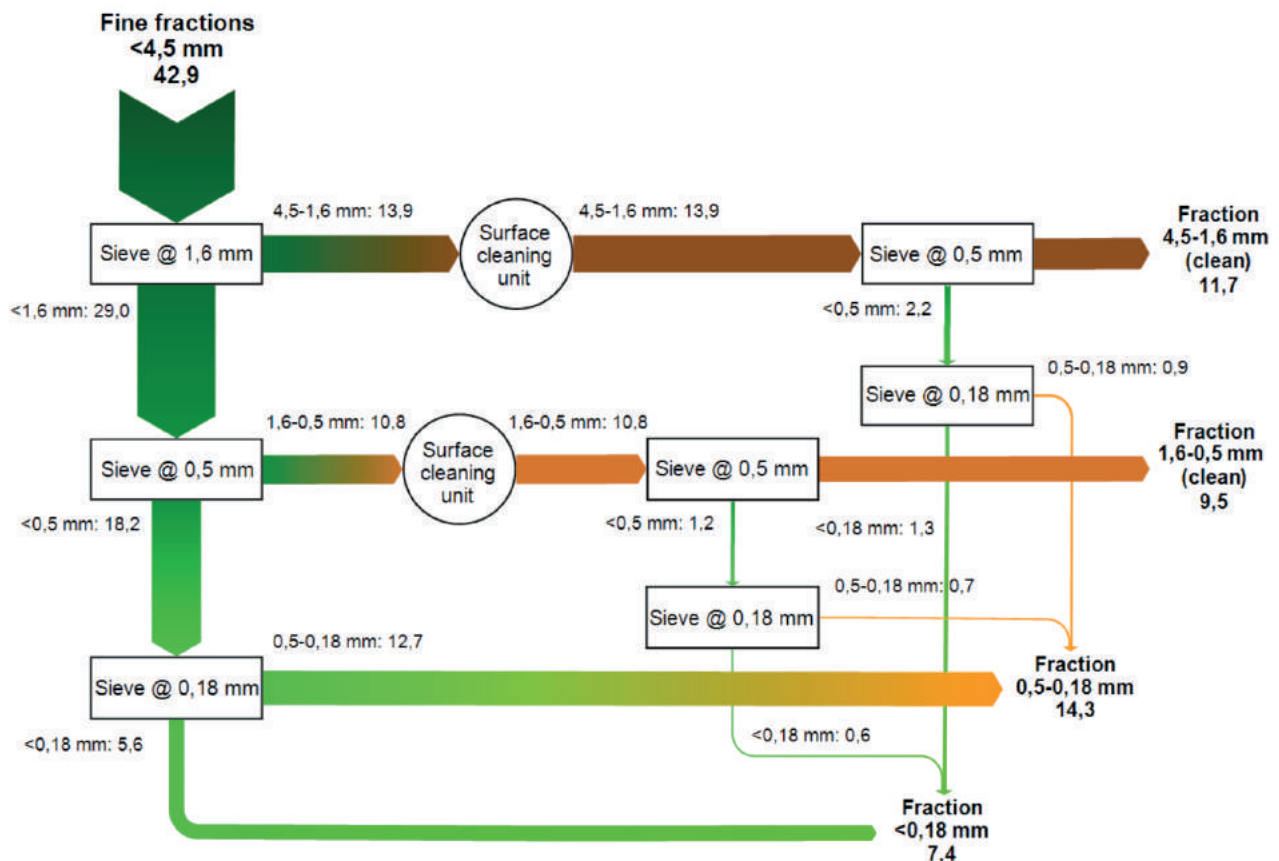


FIGURE 4: General mass balance of the mechanical processing of the fine fractions <4.5 mm, figures in wt.%.

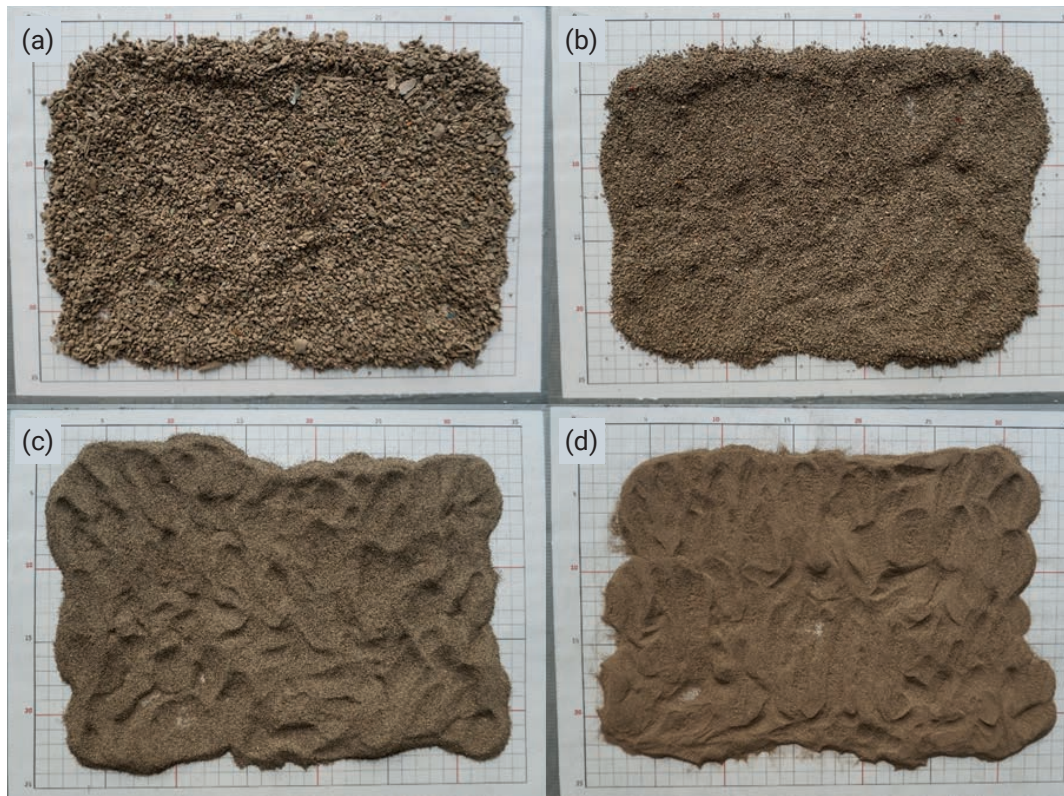
fractions 1.6 mm to 0.5 mm (clean), 14.3 wt.% fine fractions 0.5 mm to 0.18 mm and 7.4 wt.% fine fractions <0.18 mm. Images of the coarser particle size ranges 4.5-1.6 mm and 1.6-0.5 mm after the dry surface cleaning process and subsequent sieving at 0.5 mm and 0.18 mm are shown in Figure 6.

### 3.2 Chemical Analyses

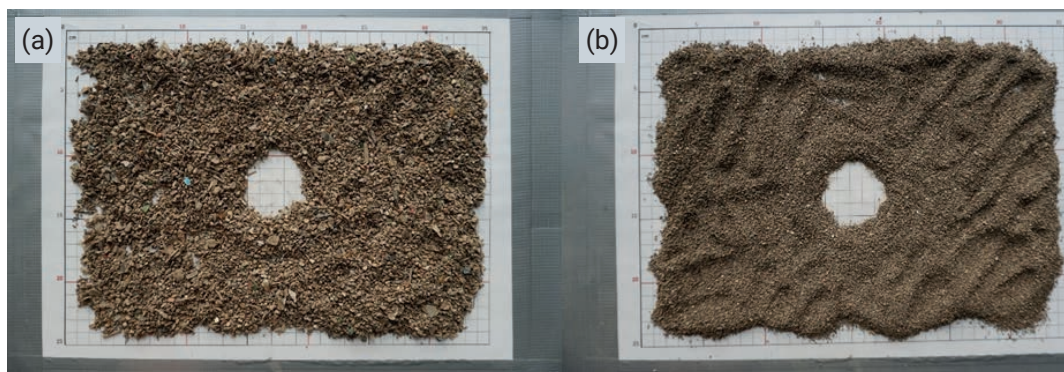
The chemical composition of the entire fine fraction <4.5 mm is displayed in Table 1.  $\text{SiO}_2$  represented the main chemical component at approx. 70 wt.%, followed by LOI (14 wt.%), CaO (5 wt.%),  $\text{Fe}_2\text{O}_3$  and  $\text{Al}_2\text{O}_3$  (each 4 wt.%). All other analysed chemical components were below 1 wt.%.

Compared to the average composition of the Earth's Crust (Taylor, 1964), samples were rich in  $\text{SiO}_2$ , but depleted in  $\text{Al}_2\text{O}_3$ . This suggests that either  $\text{SiO}_2$ -enriched materials, e.g. building sand, had been landfilled, or that  $\text{SiO}_2$  had become enriched following deposition in the landfill. However, usually due to weathering, not only  $\text{SiO}_2$ , but also  $\text{Al}_2\text{O}_3$  are found to be enriched, thus supporting the first hypothesis, i.e. landfilling of  $\text{SiO}_2$ -enriched materials.

Pseudo-total contents of chemical elements in the investigated samples are summarized in Table 2. The pseudo-total contents of almost all elements in the fraction 0.5 to 0.18 mm corresponded to approximately half the values obtained from the coarser (1.6 to 0.5 mm and 4.5 to 1.6



**FIGURE 5:** Particle size ranges (a) 4.5 to 1.6 mm, (b) 1.6 to 0.5 mm, (c) 0.5 to 0.18 mm and (d) <0.18 mm of the fine fractions <4.5mm after first sieving steps.



**FIGURE 6:** Particle size ranges (a) 4.5 to 1.6 mm and (b) 1.6 to 0.5 mm of the fine fractions <4.5 mm after the dry surface cleaning process and second sieving step.

**TABLE 1:** Chemical composition (fusion tablet, data refer to dry matter (DM)) of the fine fractions < 4.5 mm.

Parameter	Unit	<4.5 mm_1	<4.5 mm_2	<4.5 mm_3	Mean
SiO <sub>2</sub>	wt. %	69.37	70.01	69.80	69.73
Al <sub>2</sub> O <sub>3</sub>	wt. %	4.00	3.98	4.00	3.99
Fe <sub>2</sub> O <sub>3</sub>	wt. %	4.52	4.41	4.48	4.47
Cr <sub>2</sub> O <sub>3</sub>	wt. %	0.01	0.01	0.01	0.01
MnO	wt. %	0.04	0.04	0.04	0.04
TiO <sub>2</sub>	wt. %	0.28	0.28	0.29	0.28
V <sub>2</sub> O <sub>5</sub>	wt. %	0.01	0.01	0.01	0.01
P <sub>2</sub> O <sub>5</sub>	wt. %	0.24	0.24	0.23	0.23
CaO	wt. %	4.90	4.76	4.85	4.84
MgO	wt. %	0.62	0.61	0.63	0.62
K <sub>2</sub> O	wt. %	0.79	0.79	0.83	0.80
Na <sub>2</sub> O	wt. %	0.37	0.38	0.38	0.38
SO <sub>3</sub>	wt. %	0.82	0.71	0.83	0.79
ZrO <sub>2</sub>	wt. %	0.02	0.02	0.02	0.02
NiO	wt. %	0.01	0.01	0.01	0.01
CuO	wt. %	0.02	0.03	0.02	0.02
ZnO	wt. %	0.11	0.11	0.11	0.11
Rb <sub>2</sub> O	wt. %	0.01	0.01	0.01	0.01
SrO	wt. %	0.02	0.02	0.02	0.02
BaO	wt. %	0.06	0.06	0.07	0.06
LOI	wt. %	13.72	13.47	13.32	13.50
Sum	wt. %	99.92	99.92	99.91	99.92

mm) and finer (<0.18 mm) fractions. The sum of all analytes accounts for 5.8 wt.% of the fraction 0.5 to 0.18 mm and 9.9 to 12.6 wt.% for the three other fractions. This can be explained by different dissolution behaviour of this fraction during aqua regia digestion. Silicon concentrations were below 0.1 wt.% for all fractions, although SiO<sub>2</sub> concentrations were about 70 wt.% according to XRF, in agreement with the fact that aqua regia does not dissolve silicate minerals. Consequently, it is suggested that the fraction 0.5 to 0.18 mm may be richer in silicate minerals. Considering the lack of oxygen analyses, it can be estimated that approx. 85 wt.% of the samples (exceeding 90% wt for the fraction 0.5 to 0.18 mm) are made up of silicates.

The main constituents were found to be Ca (2.4 wt.% in the fraction 0.5 to 0.18 mm, 4.4-4.8 wt.% in the other fractions), Fe (1.9 wt.% in the fraction 0.5 to 0.18 mm, 3.2 wt.% in the fraction <0.18 mm and 4.8-5.0 wt.% in the coarser fractions) and Al (0.7 wt.% in the fraction 0.5 to 0.18 mm, 1.1-1.3 wt.% in the other fractions). All other elements were below 1 wt.%. Ca and Fe concentrations substantially matched the results obtained by XRF, whereas Al concentrations were significantly lower in digested samples compared to XRF measurements. This suggests that Al is bound to silicate minerals, whereas Ca and Fe are bound to more soluble phases such as carbonates and hydroxides, respectively.

The recycling of fine fractions from EFLM as soil substitute is not directly regulated in Austria. Soil substitutes may

only be produced from a restricted list of wastes including excavated soil, but not specifically including (E)LFM materials. However, due to the soil-like character of the material, limit values for the recycling of excavated soil (Federal Ministry for Sustainability and Tourism, 2017) as soil substitute might be used as an approximation. Furthermore, limit values for excavated soil landfills (Federal Ministry for Agriculture, Forestry, Environment and Water Management, 2008), which are almost identical to limit values established for recycling, thus further supporting the need to assess environmental impact of the investigated material. Both these limit values and also concentrations detected refer to pseudo-total content obtained by aqua regia digestion.

In general, the pseudo-total contents of contaminants were in the same range as those observed for the Kudjape landfill, Latvia (Burlakovs et al., 2016). A comparison between determined values and limit values shows that pseudo-total contents of Cr, Co, As and Ni were below the limit values for all fractions, whereas determined values for Cu, Zn, Cd, Hg and Pb were above the limit values for all fractions (except Hg for the fraction 0.5 to 0.18 mm). This may imply either that Cr, As, Co and Ni are only present in very low concentrations or that they are bound to the silicates or other low-soluble phases such as oxides. In the case of As, present as oxyanion, also strong sorption in the acidic pH might play a role, as the mineral surfaces are charged positively in this pH range. Conversely, Cu, Zn, Cd, Hg and Pb represent chalcophilic elements, which are instead bound to sulphide minerals. Under oxidizing conditions, such as in aqua regia, these are easily dissolved. This suggests that this group of elements may be increasingly bound to sulphides or similar mineral phases, or adsorbed on surfaces of mineral or organic matter.

No trend was observed with regard to the enrichment or depletion of heavy metals in the different particle size ranges. This indicates the unsuitability of particle size classification in the range <4.5 mm as a means of achieving limit values for pseudo-total content of heavy metals in the investigated EFLM fine fractions. As certain heavy metals (e.g. Cd and Pb) are frequently present in glass products (especially in the past), and glass was not sorted out of these fractions, these elements might be bound to glass. Glass separation, e.g. by density separation, might represent a means of decreasing the content of these elements.

Furthermore, background concentrations of heavy metals in soil at the landfill site and surrounding areas should also be taken into account (Table 3), specifically to determine the extent to which the heavy metal concentrations should be attributed exclusively to waste disposed of at the landfill, and thus enable a conclusive assessment of heavy metal concentrations. Both investigated heavy metals and carbon content were below the limit value for excavated soil landfills in Austria (Federal Ministry for Agriculture, Forestry, Environment and Water Management, 2008). Consequently, the geogenic background concentration may be considered negligible.

In addition to heavy metals, organic contaminants were also found to partly exceed limit values for excavated soil landfills and recycling (Table 4). This was indeed the

**TABLE 2:** Pseudo-total contents of the investigated fine fractions (n=3, s=1σ), bold parameters are above threshold values, comparable data from Burlakovs et al (2016), limit values for excavated soil landfills according to (Federal Ministry for Agriculture, Forestry, Environment and Water Management, 2008), for recycling quality class BA according to (Federal Ministry for Sustainability and Tourism, 2017).

Parameter	Unit	4.5-1.6 mm	1.6-0.5 mm	0.5-0.18 mm	<0.18 mm	Burlakovs et al (2016)	Limit value for excavated soil landfills	Limit value for recycling (class BA)
Li	mg/kg DM	11±0	11±0	5±0	9±1		-	
Be	mg/kg DM	<10	<10	<10	<10		-	
B	mg/kg DM	32±2	36±2	17±2	26±2		-	
Na	mg/kg DM	747±75	827±69	347±17	587±57		-	
Mg	mg/kg DM	4867±173	4953±141	2263±154	3540±93	8700 - 10200	-	
Al	mg/kg DM	10567±962	12767±736	7310±1435	11167±728		-	
Si	mg/kg DM	770±317	977±105	630±88	507±133		-	
P	mg/kg DM	1353±112	1413±92	637±52	1080±97		-	
K	mg/kg DM	2187±107	2390±131	1370±57	2683±159		-	
Ca	mg/kg DM	44067±3437	47867±131	23933±10178	44500±9061		-	
Ti	mg/kg DM	210±20	223±17	117±7	217±17		-	
V	mg/kg DM	27±8	29±3	15±3	28±3		-	
Cr	mg/kg DM	96±17	107±7	45±4	76±0	54 - 123	300	300
Mn	mg/kg DM	477±66	510±11	197±24	323±29	313 - 383	-	
Fe	mg/kg DM	48300±7355	49867±3927	19400±2012	31633±1829	29600 - 53900	-	
Co	mg/kg DM	13±1	15±1	5±0	10±0	6 - 8	50	50
Ni	mg/kg DM	74±1	95±17	41±7	69±19	29 - 44	100	100
<b>Cu</b>	<b>mg/kg DM</b>	<b>770±663</b>	<b>430±137</b>	<b>133±7</b>	<b>197±13</b>	<b>191 - 362</b>	<b>100</b>	<b>100</b>
<b>Zn</b>	<b>mg/kg DM</b>	<b>1203±125</b>	<b>1260±147</b>	<b>567±36</b>	<b>953±79</b>	<b>1300 - 2000</b>	<b>500</b>	<b>500</b>
As	mg/kg DM	12±1	14±1	<10	12±1	4 - 6	50	50
Se	mg/kg DM	<10	<10	<10	<10		-	
Sr	mg/kg DM	150±11	167±7	86±2	153±7	120 - 479	-	
Mo	mg/kg DM	9±3	12±4	3±0	5±1		-	
Pd	mg/kg DM	<1	<1	<1	<1		-	
Ag	mg/kg DM	5±2	6±3	2±1	4±1		-	
<b>Cd</b>	<b>mg/kg DM</b>	<b>5±1</b>	<b>7±1</b>	<b>3±0</b>	<b>5±1</b>	<b>1</b>	<b>2</b>	<b>2</b>
Sn	mg/kg DM	220±60	293±46	106±13	177±24		-	
Sb	mg/kg DM	8±1	12±2	5±0	8±2		-	
Te	mg/kg DM	<2	<2	<2	<2		-	
Ba	mg/kg DM	663±68	763±73	350±49	577±51	246 - 420	-	
W	mg/kg DM	17±3	16±2	<1	<1		-	
<b>Hg</b>	<b>mg/kg DM</b>	<b>6±0</b>	<b>1±0</b>	<b>&lt;1</b>	<b>2±0</b>		-	<b>1</b>
Tl	mg/kg DM	<1	<1	<1	<1		-	
<b>Pb</b>	<b>mg/kg DM</b>	<b>670±23</b>	<b>1010±122</b>	<b>460±57</b>	<b>777±86</b>	<b>128 - 477</b>	<b>150</b>	<b>150</b>

case for TOC, hydrocarbon index and PAH, whereas PCB remained below limit values. Compared to ranges established by ÖNORM S 2122-2, the TOC/N ratio was rather high, although TOC was within established limits. Differences between legislations may be explained by the fact that in soils organic carbon is mainly present as humic substances which represent stable forms or carbon, whereas in organic wastes instable forms such as carbohydrates, proteins and lipids are present, which tend to form methane under anaerobic conditions in landfills. Ecological evaluation of use of the investigated samples as soil substitute,

both degree of humification, i.e. the conversion of instable to stable organic substances in the material, and redox regime in the planned application should be considered.

### 3.3 Leaching Behaviour

Water soluble constituents are displayed in Table 5. These constituents were determined using a liquid: solid ratio of 5:1 over a 2 h period to compare soluble concentrations to recommended values for regular soil according to ÖNORM S 2122-2. However, limit values for landfilling and recycling relate to a liquid: solid ratio of 10 and leaching

**TABLE 3:** Geogenic background concentrations of selected chemical elements (bdl: below detection limit).

Parameter / Unit	Ba	Ge	Cd	Cr	Co	Cu	Ga	As	Hf	Sc	Li	Au	C	S
Sample	ppm	ppm	ppm	ppm	ppm	ppm	ppm	ppm	ppm	ppm	ppm	ppm	wt. %	wt. %
1	188	bdl	bdl	158	18	14	bdl	11	bdl	92	134	45	0.08	0.012
2	367	bdl	2	67	13	14	bdl	9	bdl	34	128	39	1.15	0.027
3	198	bdl	bdl	72	12	15	bdl	9	bdl	30	118	28	0.85	0.021
4	377	bdl	bdl	143	13	14	bdl	7	bdl	33	128	32	0.82	0.020
5	224	bdl	bdl	83	11	10	bdl	5	bdl	30	117	28	0.42	0.011
6	194	bdl	2	84	12	9	bdl	8	bdl	29	115	29	0.32	0.016

**TABLE 4:** Physical and chemical parameters of the investigated fine fractions (n=3, s=1 $\sigma$ ), bold parameters are above threshold values, limit values for excavated soil landfills according to Federal Ministry for Agriculture, Forestry, Environment and Water Management (2008), for recycling quality class BA according to Federal Ministry for Sustainability and Tourism (2017).

Parameter	Unit	4.5-1.6 mm	1.6-0.5 mm	0.5-0.18 mm	<0.18 mm	Ranges according to ÖNORM S2122-2	Limit value for excavated soil landfills	Limit value for recycling (class BA)
AOX	mg/kg DM	255	285	218	293			
Cohesion number	1	71.40	87.60	54.37	61.10	41 - 90		
Wet density	g/cm <sup>3</sup>	0.72	0.74	1.09	0.95			
Dry density	g/cm <sup>3</sup>	0.71	0.72	1.08	0.94			
<b>TOC</b>	<b>% C DM</b>	<b>8.31</b>	<b>8.04</b>	<b>7.91</b>	<b>7.72</b>	<b>1.5-11.6</b>	<b>3.00</b>	<b>1.00</b>
Total-N	% DM	0.49	0.53	0.27	0.34			
C	% DM	9.95	10.80	10.16	10.38			
<b>TOC/N</b>	<b>1</b>	<b>17.83</b>	<b>15.20</b>	<b>28.93</b>	<b>22.83</b>	<b>9-14</b>		
<b>Hydrocarbon index</b>	<b>mg/kg DM</b>	<b>980</b>	<b>1,233</b>	<b>507</b>	<b>967</b>		<b>200</b>	<b>200</b>
<b>PAH (16/EPA)</b>	<b>mg/kg DM</b>	<b>17.80</b>	<b>17.73</b>	<b>6.38</b>	<b>7.68</b>		<b>4</b>	<b>4</b>
Polychlorinated biphenyles	mg/kg DM	0.33	0.47	<0.10	0.40			1
Water content (105 °)	wt. %	1.57	1.80	0.80	1.53		-	-

time of 24 h. Thus, no direct comparison is possible. However, in order to assess the mobility of chemical elements, a comparison with all three groups of values provides some orientation.

Electric conductivity of the leachate was lowest for the fraction 0.5 to 0.18 mm. This corresponds to the observation of the lowest solubility of this fraction in aqua regia, thus suggesting that the fraction is not only richer in silicates, but also in mineral phases which are soluble in aqua regia, but insoluble in water. In contrast to the observations made in aqua regia, for water extraction the finest fraction displayed a significantly higher percentage of soluble elements than other fractions. With the exception of fraction 0.5 to 0.18 mm, a general trend of increasing solubility with decreasing particle size was detected, likely caused by an increased surface area.

Generally speaking, and in agreement with the findings of a previous study (Burlakovs et al., 2016), the share of water soluble contaminants was approx. three orders of magnitude lower than pseudo-total content. Chloride, sodium and potassium concentrations in leachate exceeded the range recommended for soils, thus implying a risk of salinization of the soil. In order to remove soluble salts from fine

fractions, a washing process is suggested. Soluble nitrate and phosphate concentrations were also above recommended values for regular soil, displaying strong variations within one particle size range. Ammonium concentrations were found to be within the recommended range, suggesting that nitrification had taken place in the landfill due to microbiological activity. The high concentrations of nutrients may lead to eutrophication of the ground and surface waters in the vicinity of the potential application area. Thus, concentrations of these constituents should be decreased in the fine fractions <4.5 mm, e.g. by a washing process. Sulphate concentrations were above limit values for 10:1 leachates, although these cannot be directly applied.

Pseudo-total contents for nickel were below limit values, although with soluble concentrations above the recommended values for soils and in the range of the limit value for recycling of excavated soils. These values were in agreement with previous data (Burlakovs et al., 2016), implying that further treatment technologies should focus on immobilisation rather than on removal of Ni. For example, Rabelo Monich et al (2018) describe waste-derived glass ceramics obtained from plasma gasification of MSW with leachable concentrations of only 0.003 to 0.009 mg/kg DM, i.e. two

**TABLE 5:** Soluble concentrations (liquid: solid ratio (L/S) 5:1, data refer to dry matter (DM)) of investigated fine fractions (n=3, s=1 $\sigma$ ), bold parameters are above threshold values, limit values for excavated soil landfills (L/S 10:1) according to Federal Ministry for Agriculture, Forestry, Environment and Water Management (2008), for recycling quality class BA (L/S 10:1) according to Federal Ministry for Sustainability and Tourism (2017), recommended values for normal soil according to Austrian Standards (2013).

Parameter	Unit	4.5-1.6 mm	1.6-0.5 mm	0.5-0.18 mm	<0.18 mm	Limit value for excavated soil landfills	Limit value for recycling (class BA)	Recommended values for normal soil
pH	-	7.65±0.08	7.66±0.04	7.81±0.04	7.81±0.04	6.5-11	4.5-9.5	5.5- 8.8
Electric conductivity	[mS/m]	192±28	226±38	167±22	290±14	150	150	-
NH <sub>4</sub> <sup>+</sup>	[mg/kg DM]	83±61	61±4	32±4	70±8	10	10	7.5-75
F <sup>-</sup>	[mg/kg DM]	3.41±0.90	3.43±1.11	2.61±0.55	3.22±0.90	20	20	
Cl <sup>-</sup>	[mg/kg DM]	261±74	310±95	166±46	327±84	-	-	7.5-75
NO <sub>3</sub> <sup>-</sup>	[mg/kg DM]	287±379	328±450	165±208	332±440	443	443	37.5-150
PO <sub>4</sub> <sup>3-</sup>	[mg/kg DM]	10±6	9±3	5±2	12±3	15	15	0.1-2.25
SO <sub>4</sub> <sup>2-</sup>	[mg/kg DM]	4297±833	5700±1366	4501±1132	8834±190		2500	
TOC	[mg/kg DM]	344±18	416±28	257±26	471±20	200	100	15-338
B	[mg/kg DM]	1.75±0.25	2.00±0.28	1.20±0.18	1.90±0.19	-	-	0.226-0.525
Na	[mg/kg DM]	224±33	259±43	139±20	260±42	-	-	3-30
Mg	[mg/kg DM]	127±28	163±41	96±27	186±31	-	-	7.5-45
Al	[mg/kg DM]	0.33±0.08	0.42±0.06	0.55±0.16	0.45±0.06	-	-	0.075-0.750
Si	[mg/kg DM]	6.45±0.24	6.22±0.20	3.35±0.30	5.64±0.32	-	-	0.053-2.07
K	[mg/kg DM]	251±29	281±31	171±18	306±33	-	-	15-75
Ca	[mg/kg DM]	1727±265	2239±435	1649±383	3331±203	-	-	7.5-75
V	[mg/kg DM]	<0.005	<0.005	<0.005	<0.005	-	-	<0.045
Cr	[mg/kg DM]	0.01±0.00	0.02±0.00	0.01±0.00	0.02±0.00	1	0.5	<0.023
Mn	[mg/kg DM]	0.93±0.46	1.23±0.65	0.75±0.44	1.42±0.55			0.015-15
Fe	[mg/kg DM]	0.34±0.01	0.35±0.03	0.26±0.02	0.39±0.04			0.30-13.5
Co	[mg/kg DM]	0.03±0.01	0.04±0.01	0.02±0.01	0.05±0.01	1	1	0.002-0.075
Ni	[mg/kg DM]	0.34±0.18	0.39±0.19	0.23±0.09	0.42±0.19	-	0.4	<0.023
Cu	[mg/kg DM]	0.45±0.42	0.47±0.44	0.26±0.08	0.51±0.48		2	0.023-0.90
Zn	[mg/kg DM]	0.30±0.08	0.39±0.09	0.23±0.06	0.44±0.07	20	4	0.03-0.75
As	[mg/kg DM]	<0.05	0.06±0.00	<0.05	0.06±0.01	0.5	0.5	<0.011
Se	[mg/kg DM]	<0.05	<0.05	<0.05	<0.05	-	0.1	0.008-0.038
Mo	[mg/kg DM]	0.10±0.03	0.15±0.03	0.10±0.03	0.20±0.02	-	0.5	0.023-0.375
Cd	[mg/kg DM]	<0.005	0.005±0.00	<0.005	0.006±0.001	0.05	0.05	<0.005
Sn	[mg/kg DM]	0.01±0.00	0.01±0.00	0.01±0.00	0.01±0.00	2	2	<0.008
Ba	[mg/kg DM]	0.35±0.03	0.36±0.03	0.33±0.03	0.41±0.02	10	10	
Hg	[mg/kg DM]	<0.005	<0.005	<0.005	<0.005	0.01	0.01	<0.002
Tl	[mg/kg DM]	<0.005	<0.005	<0.005	<0.005			<0.002
Pb	[mg/kg DM]	0.01±0.00	0.01±0.00	<0.005	0.01±0.00	1	0.5	<0.075

orders of magnitude below the values obtained for fine fractions in this study. On the contrary, Cu, Pb, and Zn, which far exceeded limit values for pseudo-total contents, were characterised by very low leaching in the range of recommended values for soils, thus indicating how use of a removal technology to decrease total content may be more appropriate.

To summarize, with regard to leaching behaviour, the release of soluble salts from the investigated materials is more problematic than release of heavy metals. The low leaching of heavy metals from ELM fine fractions confirms previous data (Burlakovs et al., 2016).

### 3.4 Mineralogical Analyses

XRD analyses of each two samples of the finest particle size ranges (0.5 to 0.18 mm and <0.18 mm) indicate a composition of approx. 70 to 80 wt.% quartz ( $\alpha$ -SiO<sub>2</sub>), 10 wt.% calcite (CaCO<sub>3</sub>), 10% feldspars and minor amounts of kaolinite (Al<sub>4</sub>[(OH)<sub>8</sub>Si<sub>4</sub>O<sub>10</sub>]), illite ((K,H<sub>3</sub>O)Al<sub>2</sub>(Si<sub>3</sub>Al)O<sub>10</sub>((H<sub>2</sub>O,OH)<sub>2</sub>), siderite (FeCO<sub>3</sub>) and gypsum (CaSO<sub>4</sub>·2H<sub>2</sub>O) with no significant differences between the two particle size ranges (Figure 7, Table 6). The two samples from the fraction 0.5 to 0.18 mm displayed more consistent differences between each other than to the finest particle size



**TABLE 6:** Mineralogical composition of the particle size ranges 0.18 to 0.5 mm and <0.18 mm from batches 1 and 2 (n.d.: not detected).

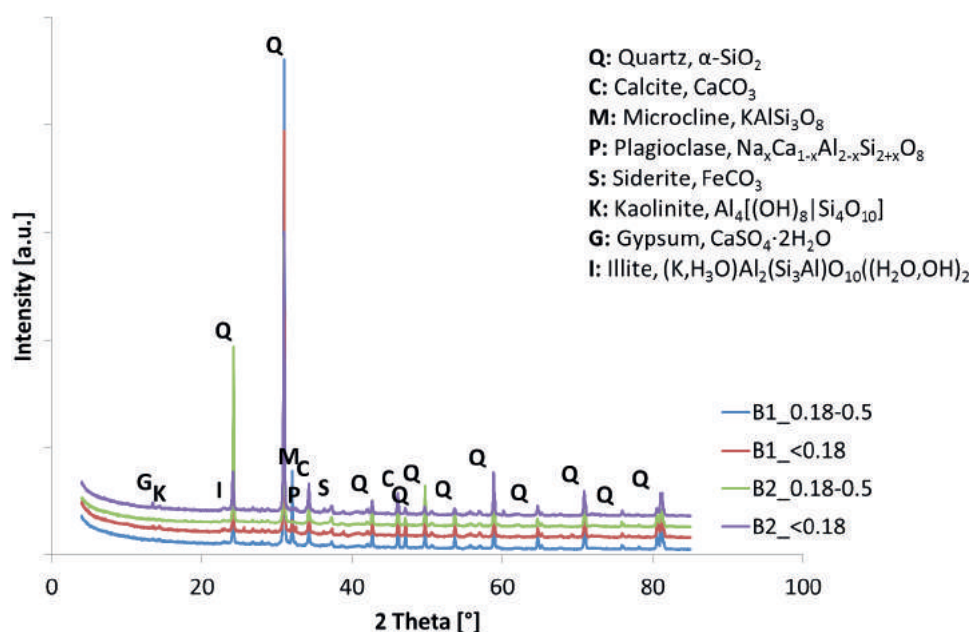
Phase	Unit	B1_0.18-0.5 mm	B1_<0.18 mm	B2_0.18-0.5 mm	B2_<0.18 mm
Quartz, SiO <sub>2</sub>	wt. %	80	73	80	72
Calcite, CaCO <sub>3</sub>	wt. %	6	10	10	13
Microcline, KAlSi <sub>3</sub> O <sub>8</sub>	wt. %	12	4		n.d.
Plagioclase, Na <sub>x</sub> Ca <sub>1-x</sub> Al <sub>2-x</sub> Si <sub>2+x</sub> O <sub>8</sub>	wt. %	n.d.	4	n.d.	3
Siderite, FeCO <sub>3</sub>	wt. %	1	1	2	2
Kaolinite, Al <sub>4</sub> [(OH) <sub>8</sub> ]Si <sub>4</sub> O <sub>10</sub> ]	wt. %	1	1	n.d.	1
Gypsum, CaSO <sub>4</sub> ·2H <sub>2</sub> O	wt. %	1	2	n.d.	3
Illite, (K,H <sub>3</sub> O)Al <sub>2</sub> (Si <sub>3</sub> Al)O <sub>10</sub> ((H <sub>2</sub> O,OH) <sub>2</sub> )	wt. %	n.d.	1	8	6

range <0.18 mm. Thus, the hypothesis that the fraction 0.5 to 0.18 mm may be enriched in silicates could not be confirmed mineralogically.

Microprobe EDX analyses of sample B1\_<0.18 mm (Figure 8) suggest that Pb is present in metallic form or as (hydr)oxide. Elemental distribution maps taken by WDX from the same area do not indicate oxygen in the respective area, indicating the presence of Pb in metallic form (Figure 9), also in agreement with the low leachability of Pb from the investigated sample. With respect to the potential utilization of the investigated sample as soil substitute, the risk of a release of significant amounts of Pb into ground water is very low, although a direct route from soil to (human) mouth cannot be excluded. It is indeed for this reason that technologies capable of removing Pb-containing particles should be considered. The elemental map of Pb (Figure 9), in combination with the backscattered electron image (Figure 8), suggest that the dimensions of individual metallic lead grains are only a few μm, although forming an agglomerate of approx. 100 μm in size. These agglomerates might be separated from the other particles due to their different density (Pb: 11.34 gcm<sup>-3</sup>; quartz: 2.65 gcm<sup>-3</sup>), e.g. by jigging or heavy-media separation.

Zinc is associated with S according to EDX analyses. WDX analyses revealed a complete absence of oxygen in the respective area, i.e. Zn is present as ZnS, either as sphalerite (α-ZnS) or wurtzite (β-ZnS). The observed low leaching of Zn (Table 5) indicates a high stability of these phases under the experimental conditions. However, it should be taken into account that ZnS might be oxidized by atmospheric oxygen and water, which yields dissolved Zn and sulphuric acid, thus potentially posing a long-term risk when using the investigated sample as soil substitute. Removal of ZnS grains is highly challenging due to their grain size of few μm and, compared to Pb, a less pronounced tendency to form agglomerates (Figure 8). Existing technologies to separate ZnS in this grain size, e.g. froth flotation (Peleka, Gallios, & Matis, 2017), are too expensive for use in the production of a soil substitute. Hence, maintaining reducing conditions through addition of biochar may represent an interesting option for use in ensuring low levels of Zn leaching (Houben, Evrard, & Sonnet, 2013).

Ba is associated with S according to EDX and also with O according to WDX, i.e. present as BaSO<sub>4</sub>, barite, which is characterized by a very low solubility (about 1.4 mg/L

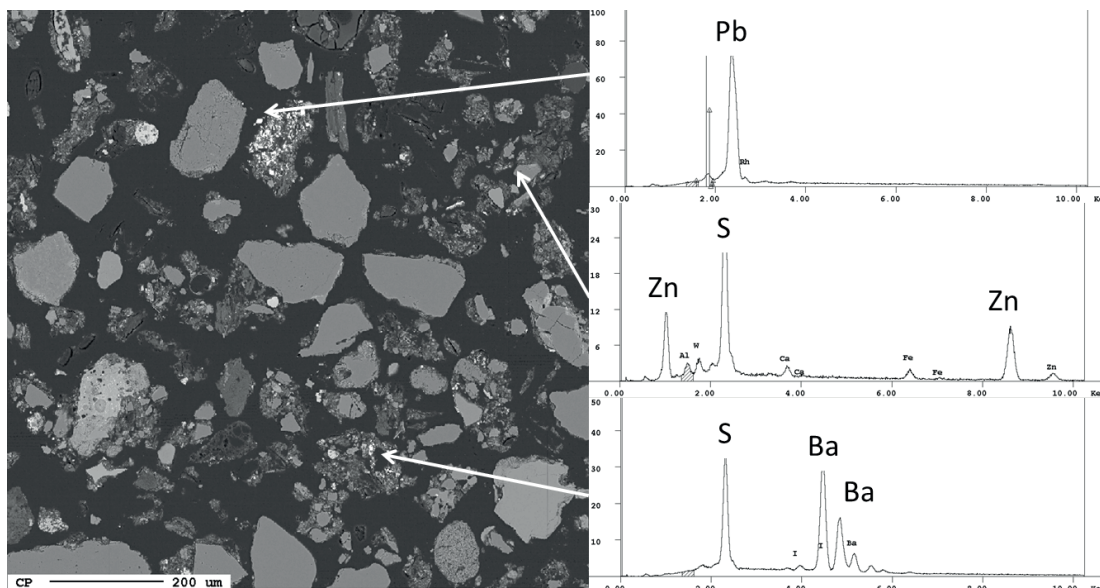


**FIGURE 7:** XRD patterns of the fine fractions 0.18 to 0.5 mm and <0.18 mm from batches 1 and 2.

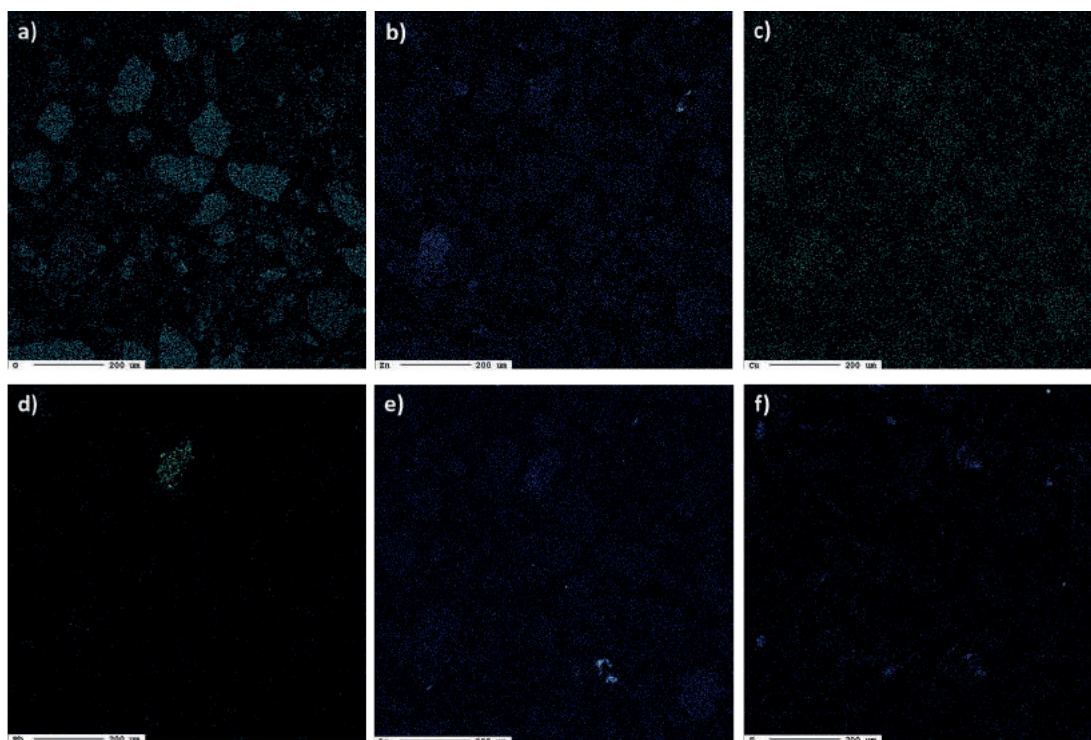
at 25°C (Blount, 1977)). This is in agreement with the observed low leaching of Ba (Table 5). In contrast to Zn, which may be mobilized due to oxidation of sulphide, the same is not observed with Ba, which occurs already as sulphate. Barite itself is not hazardous, thus the presence of Ba as barite does not pose an environmental risk when using the investigated sample as soil substitute.

Cu is diffusely distributed, which suggests its presence as an adsorbed species (Figure 9). The very low leaching of Cu from the investigated sample (Table 5) is in agreement

with the slightly alkaline pH of the leachate which favours adsorption of cations, e.g.  $\text{Cu}^{2+}$ , on the surfaces of minerals and organic matter. However, to avoid oral ingestion, e.g. by children, and ensure compliance with the threshold value for pseudo-total content of Cu, this element should be removed from the material prior to utilization as soil substitute. To desorb Cu from the surfaces, they will need to be charged positively, which can be done by acid washing and may prove to be an interesting option to condition the material for use as soil substitute.



**FIGURE 8:** Backscattered electron image (left) and EDX spot analyses of heavy metal bearing phases in sample B1\_<0.18 mm.



**FIGURE 9:** Elemental mapping of (a) oxygen, (b) Zn, (c) Cu, (d) Pb, (e) Ba, and (f) S in sample B1\_<0.18 mm.

In sample B1\_0.18-0.5 mm, Zn is associated with Fe, but not with S according to EDX analyses (Figure 10). WDX mappings indicate that no O is present in this grain, i.e. Zn is present as Fe-Zn alloy. However, it should be noted how only one Zn-containing grain was found in both B1\_<0.18 mm and B1\_0.18-0.5 mm, thus preventing any firm assumptions from being made with regard to Zn-containing phases in the particle size ranges. However, Zn leaching of this sample is similarly low in all fractions and both Fe-Zn alloys and ZnS are characterized by a low solubility. In both

samples, Zn-containing grains are in the range of a few  $\mu\text{m}$ . With respect to separation of Zn, presence of the latter in Fe-Zn alloys would enhance the use of additional technologies such as jigging or heavy-media separation, which cannot be used for ZnS.

EDX spectra of individual particles (Figure 10) and WDX elemental distribution maps (Figure 11) confirm the presence of Ba as barite and the diffuse distribution of Cu.

In contrast to sample B1\_<0.18 mm no Pb could be detected in sample B1\_0.18-0.5 mm.

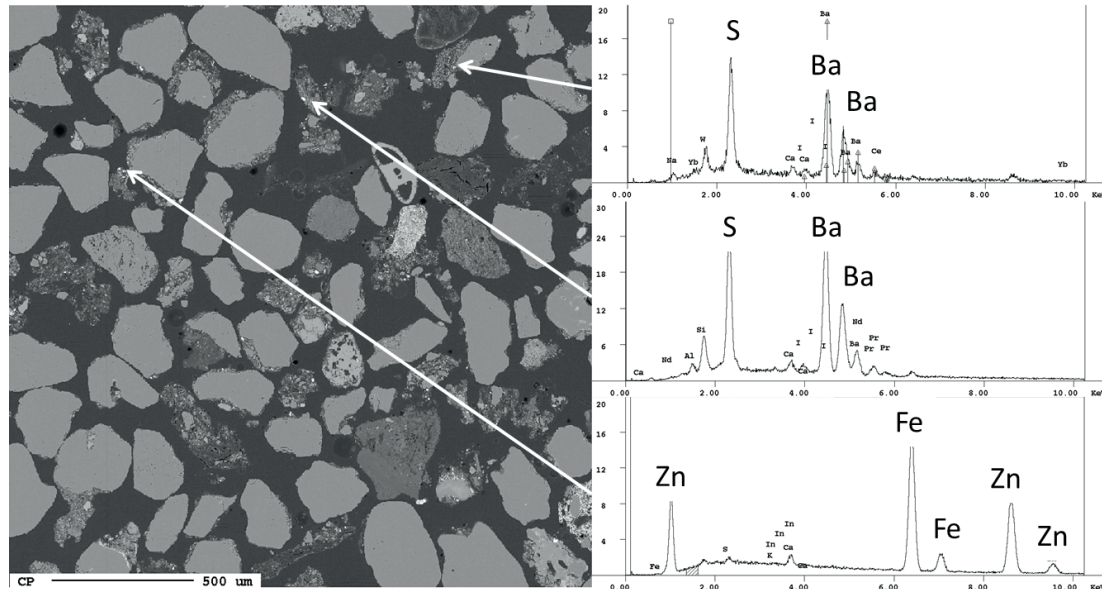


FIGURE 10: Backscattered electron image (left) and EDX spot analyses of heavy metal bearing phases in sample B1\_0.18-0.5 mm.

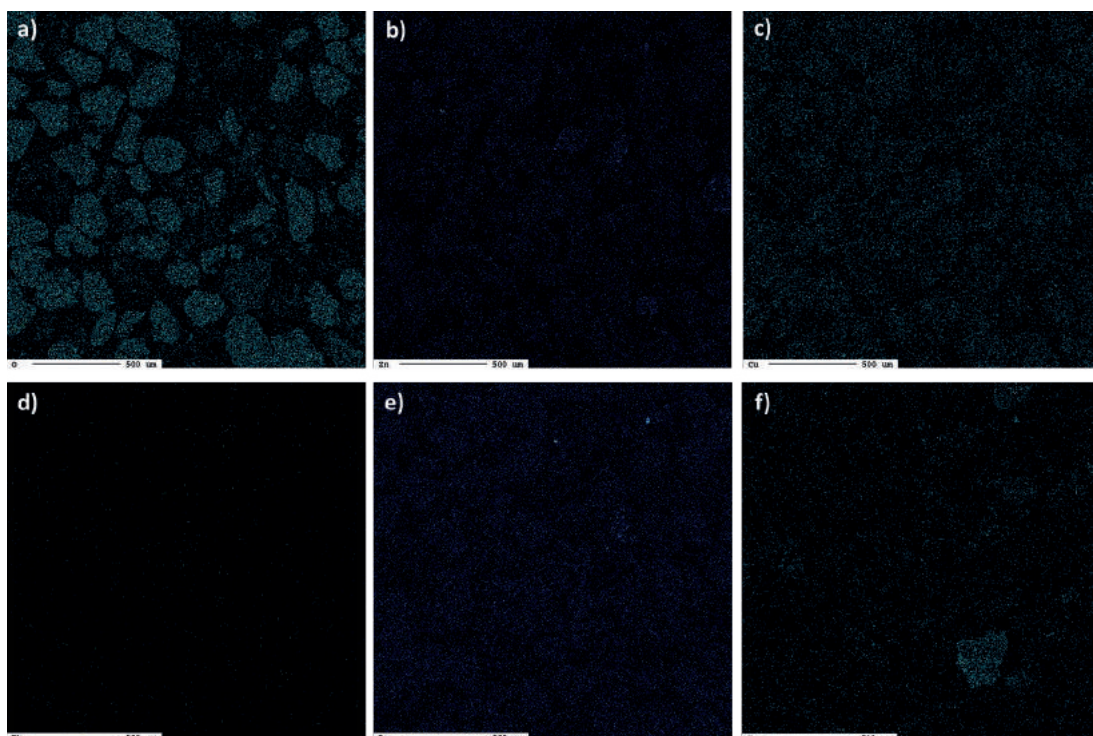
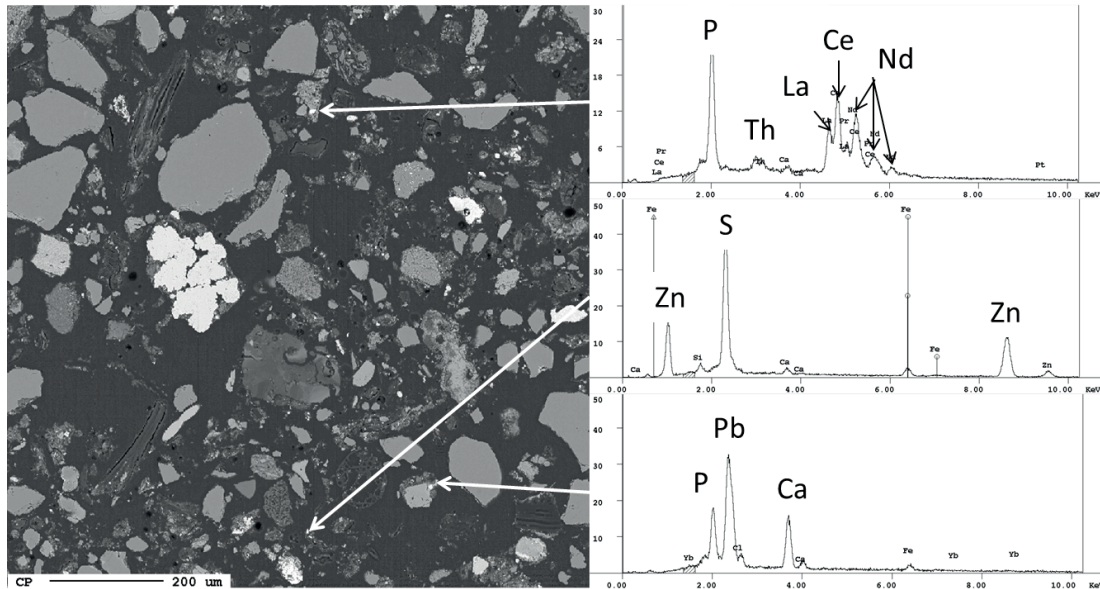


FIGURE 11: Elemental mapping of (a) oxygen, (b) Zn, (c) Cu, (d) Pb, (e) Ba, and (f) S in sample B1\_0.18-0.5 mm.

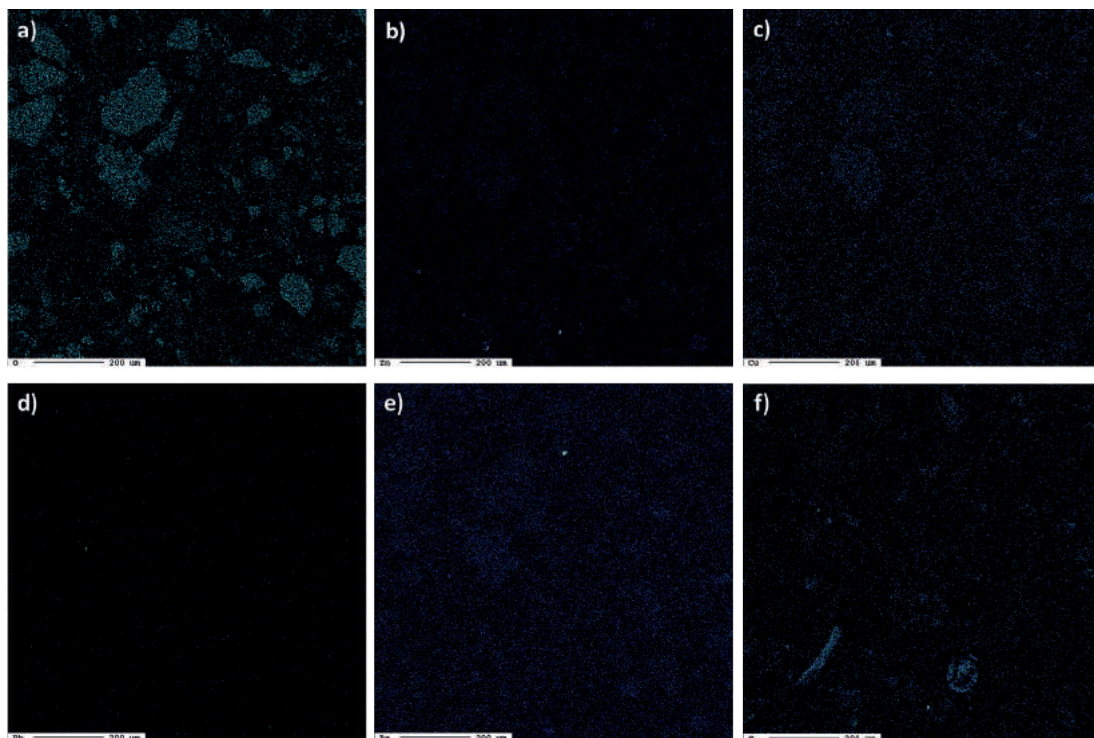
In sample B2-8\_<0.18 mm, EDX analyses (Figure 12) indicated the presence of monazite, (La,Ce,Nd)[PO<sub>4</sub>], the most important ore mineral for rare earth elements (REE). Cerium, Nd and La have been reported in MSW landfills in the range of 14-25 mg/kg, 8-12 mg/kg and 7-11 mg/kg, respectively (Gutiérrez-Gutiérrez et al., 2015), which is below the average concentrations in the continental crust (Taylor, 1964) and of no economic or ecological relevance. However, the mineralogical bonding of REE in MSW landfills has not to date been investigated. EDX analyses clearly indi-

cate that Thorium (Th) is incorporated in the investigated monazite grain, thus causing environmental concern due to its radioactivity. Considering that this grain with a size of few μm is the only one in the entire investigated sample, the environmental impact is negligible.

As in sample B1-8\_<0.18 mm, EDX analysis shows the association of Zn with S (Figure 12) and WDX elemental mapping (Figure 13) indicates the absence of O in this grain, meaning that Zn is present as zinc sulphate. As hydrogen cannot be measured, it remains unclear if the wa-



**FIGURE 12:** Backscattered electron image (left) and EDX spot analyses of heavy metal bearing phases in sample B2\_<0.18 mm.



**FIGURE 13:** Elemental mapping of (a) oxygen, (b) Zn, (c) Cu, (d) Pb, (e) Ba and (f) S in sample B2\_<0.18 mm.

ter-free zincosite ( $\text{ZnSO}_4$ ) or the water-containing phases gunningite ( $\text{ZnSO}_4 \cdot \text{H}_2\text{O}_2$ ), boyleite ( $\text{ZnSO}_4 \cdot 4\text{H}_2\text{O}_2$ ), goslarite or zinc melanterite (both  $\text{ZnSO}_4 \cdot 7\text{H}_2\text{O}_2$ ) are present. It is suggested that more oxidizing conditions were present in this sample compared to the other two samples, where Zn was present as ZnS. However, as leaching does not significantly differ between the samples, the difference in mineralogy does not seem to produce a significant impact on environmental performance. EDX pattern indicates the presence of a calcium lead phosphate (Figure 12), although

WDX mappings suggest the absence of Pb. As in the other samples, WDX mappings indicate the diffuse distribution of Cu within the sample.

In sample B2\_0.18-0.5 mm, EDX analyses confirmed the association of Zn and S (Figure 14). In contrast to the other samples, this phase is not present as individual grain, but forms a rim around a quartz grain. WDX mapping of O (Figure 15) also reveals the presence of oxygen in this rim, i.e. Zn is present as  $\text{ZnSO}_4$ , as in sample B2-8\_<0.18 mm. EDX patterns also confirmed the presence of Ba as barite,

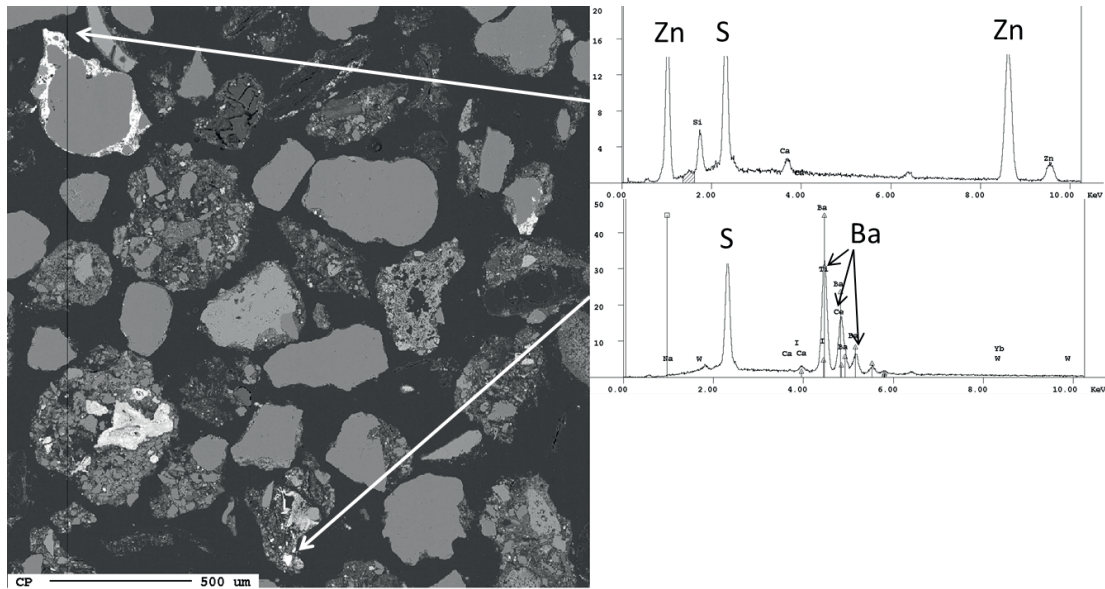


FIGURE 14: Backscattered electron image (left) and EDX spot analyses of heavy metal bearing phases in sample B2\_0.18-0.5 mm.

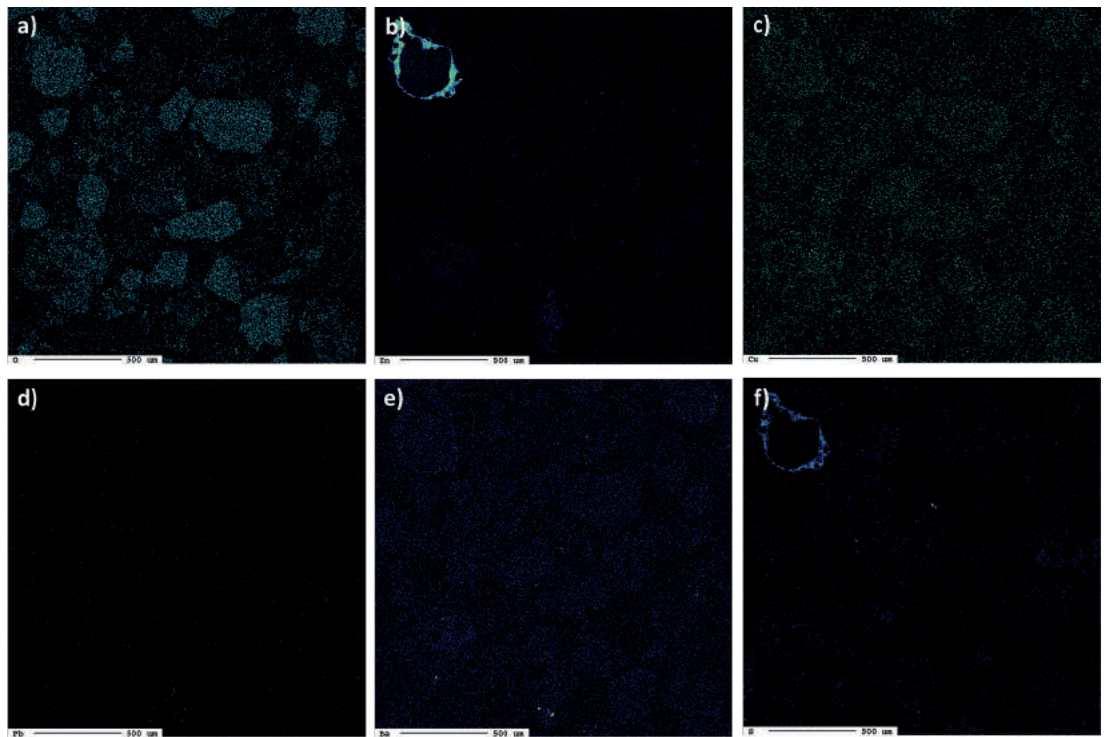


FIGURE 15: Elemental mapping of (a) oxygen, (b) Zn, (c) Cu, (d) Pb, (e) Ba and (f) S in sample B2\_0.18-0.5 mm.

BaSO<sub>4</sub>. Pb could not be detected in this sample, whereas Cu is randomly distributed in the same way as in other samples (Figure 15).

To summarize, mineralogical investigations confirm the presence of Pb as metal and as Pb-Ca phosphate, Zn as Fe-Zn alloy, sulphide and sulphate, Ba as barite, Cu adsorbed to mineral surfaces and REE as monazite. This stable incorporation (and in case of Cu, adsorption) explains the low leaching of heavy metals from the investigated samples. However, the mineralogical bonding of Ni, characterised by rather high leaching, is in agreement with observations from natural rocks (Vollprecht et al., 2019).

#### 4. CONCLUSIONS

Fine fractions are a major obstacle for the economic feasibility of (E)LFM. Although screening and density separation may be used to recover significant amounts of combustible and inert materials, the fine-grained soil-like materials remain an important challenge.

In this study, we refute our first working hypothesis according to which screening in the range <4.5 mm allows for a separation into a clean coarser fraction and a contaminated finer fraction. Conversely, we confirmed our second working hypothesis, i.e. that the mineralogy of ELMF fine fractions is related to their leachability, as several host phases for low-leaching elements such as a Fe-Zn alloy, ZnS and ZnSO<sub>4</sub>, metallic Pb and Pb-Ca phosphate, were identified.

Briefly, the main problematic factors in the recycling of ELMF fine fractions are represented by the high pseudo-total contents of organic carbon and heavy metals, in the present case study Cu, Zn, Cd, Hg and Pb, which hinder use of these fractions in countries in which limit values for pseudo-total contents have been established in environmental legislation. In countries regulating only the leachable contents of heavy metals, the utilization of fine fractions from (E)LFM seems more realistic, as this study shows that the majority of heavy metals is tightly bound in low-soluble mineral phases or strongly adsorbed to mineral surfaces.

A remaining challenge in the present case study is the rather high leaching of Ni, which may be encountered when using immobilization technologies. Further research is needed to investigate both the adverse effects of carbon speciation, such as methane formation, and beneficial effects including carbon sequestration in stable humic substances.

In a broader scope, future research on fine fractions from ELMF should be conducted to investigate alternative uses, e.g. as landfill liner (Liebetegger 2015) or other constituent in an "aftercare-free landfill". For this purpose, a low hydraulic conductivity and low leaching of heavy metals might be sufficient, particularly as the material would continue to be considered a waste, with no need to meet end-of-waste criteria need. Therefore, an intelligent use of the fine fractions to minimize aftercare needs seems to represent the most promising option. A saving on aftercare costs and consideration of the real estate/ecosystem services (Burlakovs et al., 2017) may provide new pathways for future ELMF projects and should be investigated.

#### ACKNOWLEDGEMENTS

This research was funded by the European Union Horizon 2020 research and innovation programme under the Marie Skłodowska-Curie grant agreement No. 721185 "NEW-MINE" (EU Training Network for Resource Recovery through Enhanced Landfill Mining; [www.new-mine.eu](http://www.new-mine.eu)). The authors thank Alexia Aldrian for chemical and Federica Zaccarini and Maik Zimmermann for electron microprobe analyses.

#### REFERENCES

- Austrian Standards, 2013. ÖNORM S2122-2. Soils from waste - Part 2: Evaluation on the basis of fractional analyses.
- Bhatnagar, A., Kaczala, F., Burlakovs, J., Kriipsalu, M., Hogland, M., Hogland, W., 2017. Hunting for valuables from landfills and assessing their market opportunities. A case study with Kudjape landfill in Estonia. *Waste Manag. Res.* 35(6), 627-635.
- Blount, C., 1977. Barite solubilities and thermodynamic quantities up to 300°C and 1400 bar. *Am. Min.* 62, 942-957.
- Burlakovs, J., Jani, Y., Kriipsalu, M., Vincevica-Gaile, ZH., Kaczala, F., Celma, G., Ozola, R., Rozina, L., Rudovica, V., Hogland, M., Viksna, A., Pehme, K.-M., Hogland, W., Klavins, M. 2018. On the way to 'zero waste' management: Recovery potential of elements, including rare earth elements, from fine fraction of waste. *J. Clean. Prod.* 186, 91-90.
- Burlakovs, J., Kriipsalu, M., Klavins, M., Bhatnagar, A., 2017. Paradigms on landfill mining: From dump site scavenging to ecosystem services revitalization. *Resour. Conserv. Recy.*, 123, 73-84.
- Burlakovs, J., Kaczala, F., Vincevica-Gaile, Z., Rudovica, V., Orupöld, K., Stapkevica, M., Bhatnagar, A., Kriipsalu, M., Hogland, M., Klavins, M., Hogland, W., 2016. Mobility of Metals and Valorization of Sorted Fine Fractions of Waste After Landfill Excavation. *Waste Biomass Valori.* 7(3), 593-602.
- Federal Ministry for Agriculture, Forestry, Environment and Water Management, 2008. Landfill Ordinance. <https://www.ris.bka.gv.at/GeltendeFassung.wxe?Abfrage=Bundesnormen&Gesetzesnummer=20005653>
- Federal Ministry for Sustainability and Tourism, 2017. Federal Waste Management Plan.
- Frändegård, P., Krook, J., Svensson, N., 2015. Integrating remediation and resource recovery: On the economic conditions of landfill mining. *Waste Manag.* 42, 137-147.
- García López, C., Ni, A., Hernández Parrodi, J., Küppers, B., Raulf, K., Pretz, T., 2019. Characterization of landfill mining material after ballistic separation to evaluate material and energy recovery potential. *Detritus* 8, 5-23.
- Greedy, D., 2016. Landfilling and landfill mining. *Waste Manag. Res.* 34(1), 1-2.
- Gutiérrez-Gutiérrez, S., Coulon, F., Jiang, Y., Wagland, S., 2015. Rare earth elements and critical metal content of extracted landfilled material and potential recovery opportunities. *Waste Manag.* 42, 128-136.
- Hernández Parrodi, J. C., García López, C., Küppers, B., Raulf, K., Vollprecht, D., Pretz, T., Pomberger, R., 2019a. Case study on enhanced landfill mining at Mont-Saint-Guibert landfill in Belgium: Characterization and potential of fine fractions. *Detritus* 8, 47-61.
- Hernández Parrodi, J. C., Höllen, D., Pomberger, R., 2018a. Characterization of fine fractions from landfill mining: A review of previous investigations. *Detritus* 2, 46-62.
- Hernández Parrodi, J. C., Höllen, D., Pomberger, R., 2018b. Potential and main technological challenges for material and energy recovery from fine fractions of landfill mining: A critical review. *Detritus* 3, 19-29.
- Hernández Parrodi, J. C., Lucas, H., Gigantino, M., Sauve, G., Esguerra, J. L., Einhäupl, P., Vollprecht, D., Pomberger, R., Friedrich, B., Van Acker, K., Krook, J., Svensson, N., Van Passel, S., 2019b. Integration of resource recovery into current waste management through (enhanced) landfill mining. *Detritus* 8, 141-156.
- Hernández Parrodi, J. C., Raulf, K., Vollprecht, D., Pretz, T., Pomberger, R., 2019c. Case study on enhanced landfill mining at Mont-Saint-Guibert landfill in Belgium: Mechanical processing of fine fractions for material and energy recovery. *Detritus* 8, 62-78.

- Hogland, W. H., 2010. Enhanced Landfill Mining - Material recovery, energy utilisation and economics in the EU (Directive) perspective. Proceedings of the 1st International Academic Symposium on Enhanced Landfill Mining, 4-6.
- Houben, D., Evrard, L., Sonnet, P., 2013. Mobility, bioavailability and pH-dependent leaching of cadmium, zinc and lead in a contaminated soil amended with biochar. *Chemosphere* 92(11), 1450-1457.
- Jani, Y., Kaczala, F., Marchand, C., Hogland, M., Kriipsalu, M., Hogland, W., Kihl, A., 2016. Characterisation of excavated fine fraction and waste composition from a Swedish landfill. *Waste Manag. Res.* 34(12), 1292-1299.
- Kelly, E. & Spottiswood, D., 1989. The theory of electrostatic separations: A review Part I. Fundamentals. *Miner. Eng.* 2(1), 33-46.
- Krook, J., Svensson, N., Eklund, M., 2012. Landfill mining: A critical review of two decades of research. *Waste Manag.* 32(3), 513-520.
- Küppers, B., Hernández Parrodi, J. C., García López, C., Pomberger, R., Vollprecht, D., 2019. Potential of sensor-based sorting in enhanced landfill mining. *Detritus* 8, 24-30.
- Lane, D., Cook, N., Grano, S., Ehrig, K., 2016. Selective leaching of penalty elements from copper concentrates: A review. *Miner. Eng.* 98, 110-121.
- Laner, D., Esguerra, J.L., Krook, J., Horttanainen, M., Kriipsalu, M., Rosendal, R.M., Stansiavljević, 2019. Systematic assessment of critical factors for the economic performance of landfill mining in Europe: What drives the economy of landfill mining. *Waste Manag.* 95, 674-686.
- Liebetegger, W., 2015. Landfill Mining - Charakterisierung der Fein- und heizwertreichen Fraktion. Master Thesis. Montanuniversität Leoben.
- Lucas, H., García López, C., Hernández Parrodi, J. C., Vollprecht, D., Raulf, K., Pomberger, R., Pretz, T., Friedrich, B., 2019. Quality assessment of non-ferrous metals in landfill mining: A case study in Belgium. *Detritus* 8, 79-90.
- Mönkäre, T. J., Palmroth, M. R., Rintala, J. A., 2016. Characterization of fine fraction mined from two Finnish landfills. *Waste Manag.* 47A, 34-39.
- Neuhold, S., van Zomeren, A., Dijkstra, J.J., van der Sloot, H.A., Drissen, P., Algermissen, D., Mudersbach, D., Schüler, S., Griessacher, T., Raith, J., Pomberger, R., Vollprecht, D., 2019. Investigation of Possible Leaching Control Mechanisms for Chromium and Vanadium in Electric Arc Furnace (EAF) Slags Using Combined Experimental and Modeling Approaches. *Minerals* 9, 525.
- Peleka, E., Gallios, G., Matis, K., 2017. A perspective on flotation: a review. *J. Chem. Technol. Biotechnol.* 93, 615-623.
- Quaghebeur, M., Laenen, B., Geysen, D., Nielsen, P., Pontikes, Y., van Gerwen, T., Spooren, J., 2013. Characterization of landfilled materials: screening of the enhanced landfill mining potential. *J. Clean. Prod.* 55, 72-83.
- Rabelo Monich, P., Rincón Romero, A., Höllen, D., Bernardo, E., 2018. Porous glass-ceramics from alkali activation and sinter-crystallization of mixtures of waste glass and residues from plasma processing of municipal solid waste. *J. Clean. Prod.* 188, 871-878.
- Republic of Austria, 2002. Bundesgesetz über eine nachhaltige Abfallwirtschaft (Abfallwirtschaftsgesetz 2002 – AWG 2002). BGBl. I Nr. 102/2002.
- Savage, G.M., Golueke, C.G., von Stein, E.L., 1993. Landfill mining: past and present. *Biocycle* 34, 58-61.
- Scalenghe, R. & Marsan, F., 2009. The anthropogenic sealing of soils in urban areas. *Landscape Urban Plan.* 90(1-2), 1-10.
- Scheffer, F. & Schachtschabel, P., 2018. Lehrbuch der Bodenkunde (17th Edition). Springer Spektrum.
- Spooren, J., van den Bergh, K., Nielsen, P., Quaghebeur, M., 2013. Landfilled fine grained mixed industrial waste: Metal recovery. *Acta Metall. Slovaca* 19(3), 160-169.
- Taylor, S., 1964. Abundance of chemical elements in the continental crust: a new table. *Geochim. Cosmochim. Acta* 28(8), 1,273-1,285.
- Vollprecht, D., Berger, M., Altenburger-Junker, I., Neuhold, S., Sedlazeck, K. P., Aldrian, A., Dijkstra, J.J., van Zomeren, A., Raith, J., 2019. Mineralogy and Leachability of Natural Rocks – A Comparison to Electric Arc Furnace Slags. *Minerals* 9, 501.
- Wanka, S., Münnich, K., Fricke, K., 2017. Landfill Mining - Wet mechanical treatment of fine MSW with a wet jigger. *Waste Manage.* 59, 316-323.

# CASE STUDY ON ENHANCED LANDFILL MINING AT MONT-SAINT-GUIBERT LANDFILL IN BELGIUM: PHYSICO-CHEMICAL CHARACTERIZATION AND VALORIZATION POTENTIAL OF COMBUSTIBLES AND INERT FRACTIONS RECOVERED FROM FINE FRACTIONS

Juan Carlos Hernández Parrodi <sup>1,2,\*</sup>, Daniel Vollprecht <sup>1</sup> and Roland Pomberger <sup>1</sup>

<sup>1</sup> Montanuniversität Leoben, Department of Environmental and Energy Process Engineering, 8700 Leoben, Austria

<sup>2</sup> Renewi Belgium SA/NV, NEW-MINE project, 3920 Lommel, Belgium

## Article Info:

Received:  
3 January 2020  
Revised:  
14 February 2020  
Accepted:  
19 February 2020  
Available online:  
31 March 2020

## Keywords:

Enhanced landfill mining  
Physico-chemical characterization  
Valorization routes  
Refuse derived fuel  
Substitute for construction  
aggregates  
Fine fractions

## ABSTRACT

The fine fractions account for the largest share of material recovered through (enhanced) landfill mining. These fractions typically present challenging characteristics for processing and valorization methods and, hence, they have been largely discarded in previous landfill mining projects. This situation has hindered the economic and environmental feasibility of landfill mining, since most of the excavated waste has been directed back into the landfill. Therefore, the fine fractions are one of the major challenges faced by (enhanced) landfill mining and suitable material and energy recovery schemes for these fractions need to be further developed and, if necessary, created. To this end, the physico-chemical characteristics of the “Combustibles” and “Inert” fractions recovered from the fine fractions <90 mm through a dry-mechanical process have been determined and their suitability for waste-to-material and waste-to-energy schemes has been evaluated in the MSG case study. The recovered “Combustibles” fractions represented 12.5 wt.% and 9.0 wt.% of the fine fractions <90 mm processed in the optimal water content and dry states, while the recovered “Inert” fractions accounted for 35.5 wt.% and 37.2 wt.%, respectively. According to the EN 15359:2011, the “Combustibles” fractions could be valorized as SRF in (co-)incineration, power and cement plants in both the optimal water content state and the dry state in the EU. However, in Austria these fractions can only be incinerated and not co-incinerated according to the Austrian Waste Incineration Ordinance (AVV), since in some cases they present concentrations of As, Cd, Co, Hg and Pb above the limit values. Therefore, in contrast to conventional (co-)incineration, the plasma gasification process proposed by the NEW-MINE project might offer a potential waste-to-energy valorization route for the combustible fractions obtained from the fine fractions of landfill-mined waste. As for the “Inert” fractions, there is no overarching legislation in the EU to regulate such materials yet in place and, hence, these fractions are solely subject to national or local regulations on recycling building materials. In Austria the “Inert” fractions would need further treatment in order to be valorized as a substitute for construction aggregates according to the Austrian Recycling Building Materials Ordinance (RBV), as they exceed the limit values for hydrocarbons, Cd, Pb, Zn, NH<sub>4</sub><sup>+</sup> and anionic surfactants in certain cases. Therefore, suitable waste-to-material valorization schemes for the recovered inert fractions from the fine fractions of landfill-mined waste are to be further developed, while appropriate overarching regulations need to be created at EU level.

## 1. INTRODUCTION

In many cases landfill mining (LFM) has failed as a business model and it has mainly been carried out within the framework of contaminated sites remediation to address the threat that landfills and dumpsites pose to the

health and well-being of the environment. However, the development of novel technologies is aiming to eventually bridge the gap between the practically possible and the economically feasible, and might gradually enable further material and energy recovery from landfill-mined material,

\* Corresponding author:  
Juan Carlos Hernández Parrodi  
email: [juan.carlos.parrodi@renewi.com](mailto:juan.carlos.parrodi@renewi.com)



as well as facilitate its integration into current waste management systems (Hernández Parrodi et al., 2019b). For this purpose, suitable valorization routes for the outputs of LFM need to be further developed and, if necessary, created. For example, in the case of the recovered combustible fractions some projects have investigated their traditional co-incineration in cement plants (Wolfsberger et al., 2015), whereas others have aimed for non-conventional routes of energy recovery through alternative thermo-chemical processes, such as pyrolysis and gasification, which might allow the upcycling of their residues into higher value glass-ceramics (Monich, Romero, Höllen, & Bernardo, 2018; Rabelo Monich, Vollprecht, & Bernardo, 2020) and inorganic polymer binders (Ascensão, Marchi, Segata, Faleschini, & Pontikes, 2019; Machiels et al., 2017). The latter approach is addressed in the enhanced landfill mining (ELFM) concept, which has been put to test in a case study at the Mont-Saint-Guibert (MSG) landfill site in Belgium. The MSG landfill case study is being carried out within the framework of the EU Training Network for Resource Recovery through Enhanced Landfill Mining - NEW-MINE. As defined by Jones et al., 2013, ELFM is the safe conditioning, excavation and integrated valorization of historic and/or future landfilled waste streams as both materials (Waste-to-Material (WtM)) and energy (Waste-to-Energy (WtE)), using innovative transformation technologies and respecting the most stringent social and ecological criteria.

One of the main challenges in (E)LFM are the fine fractions, since they present difficult characteristics for their processing and valorization, and can account for 40-80 wt.% of the total amount of landfill-mined waste (Hernández Parrodi, Höllen, & Pomberger, 2018a). The fine fractions have been frequently defined as the material with a particle size <60 mm to <10 mm in previous (E)LFM studies (Hernández Parrodi et al., 2018a); however, there is no convention in that regard to date. Furthermore, one commonly chosen alternative in prior projects has been to classify the fine fractions as a residual fraction and direct them back into the landfill (Bhatnagar et al., 2017; Kaartinen, Sormunen, & Rintala, 2013; Münnich, Fricke, Wanka, & Zeiner, 2013), which has had a critical impact on the economic and environmental feasibility of LFM projects. Therefore, the recovery of material and energy from the fine fractions has been included into the scope of the MSG case study. To this end a mechanical processing approach was designed and applied to the fine fractions in the optimal water content (owc) and dry states, according to the results of the material characterization of the fine fractions reported by Hernández Parrodi et al., 2019a and the strategies for WtM and WtE proposed in Hernández Parrodi, Höllen, & Pomberger, 2018b. In the MSG case study the fine fractions are the material with a particle size <90 mm and the owc state corresponds to a water content of around 15 wt.%. The owc state aims at minimizing material losses in the form of dust and small particle-sized and light materials, as well as decreasing the amount of energy required in the drying process. In addition, the owc should not compromise the effectivity and efficiency of a dry-mechanical processing approach. Hence, the mechanical processing approach of the MSG case study was tested in both the owc and dry

states, in order to study and evaluate the effects of the owc in terms of the processability of the fine fractions <90 mm and the quality of the produced material fractions. The tested approach consisted of a series of mechanical processing steps, which classified the fine fractions <90 mm into different material fractions and particle size ranges according to their physical properties, such as particle size, shape and density, among others, in order to enable material and energy recovery. The mechanical processing produced the following material fractions: "Fine fractions <4.5 mm", "Combustibles", "Inert", "Ferrous metals" and "Non-ferrous metals". Further details on the employed mechanical processing and produced fractions are reported by Hernández Parrodi, Raulf, Vollprecht, Pretz, & Pomberger, 2019c. The "Fine fractions <4.5 mm" were further mechanically processed and investigated by Vollprecht, Hernández Parrodi, Lucas, & Pomberger, 2020, while the quality of the extracted "Non-ferrous metals" was studied in Lucas et al., 2019. The recovery of ferrous metals from landfilled material has been successfully carried out in previous investigations (Van Vossen & Prent, 2011; Wagner & Raymond, 2015) and, therefore, the "Ferrous metals" fraction was not further investigated in the MSG case study. Sieving the excavated landfill material into different particle size ranges as a first treatment step, followed by sorting the coarse fractions into different waste types to characterize the material has been addressed in several previous (E)LFM investigations (García Lopez et al., 2019; Hogland, 2002; Hull, Krogmann, & Strom, 2005; Kurian, Esakku, Palanivelu, & Selvam, 2003; Quaghebeur et al., 2013; Stessel & Murphy).

The present study focuses on the obtained "Combustibles" and "Inert" fractions, which are intended to be valorized as an alternative fuel (i.e. refuse derived fuel (RDF)) and a substitute for construction aggregates (e.g. construction gravel), respectively. The main physico-chemical characteristics of each fraction, according to the applicable European Directives (i.e. 2000/76/EC on Incineration of Waste, EN 15359:2011 on Solid Recovered Fuels, 2008/98/EC on Waste and 1999/31/EC on Landfill of Waste) and Austrian ordinances (i.e. Waste Incineration Ordinance (Abfallverbrennungsverordnung – AVV) and Recycling Building Materials Ordinance (Recycling-Baustoffverordnung – RBV)), were determined in the owc and dry states. That information was used to evaluate the quality of the produced fractions in each state and determine their suitability for the intended WtM and WtE valorization routes, as well as to analyze the effects of the owc on the quality of each fraction.

## 2. MATERIALS AND METHODS

### 2.1 Site description, excavation works and mechanical pre-processing

The present case study was carried out at the landfill site "Centre d'enfouissement Technique de Mont-Saint-Guibert (CETeM)", which is located in the municipality of MSG, Belgium. This landfill served as one of the main disposal sites of municipal solid waste, non-hazardous industrial waste and construction and demolition waste in the province of Walloon Brabant (Bureau d'études gre-

isch (beg), 2002). The landfilled material was extracted by means of excavators and pre-processed with a ballistic separator (Stadler model STT 6000) directly after excavation. The ballistic separation was performed in two steps: firstly with screen paddles of 200 mm and secondly of 90 mm, from which representative samples were taken for further study. The fine fractions <90 mm of this case study were obtained from the second ballistic separation step and represented around 77 wt.% of the total amount of pre-processed material (~374 Mg). More detailed information about the landfill site, excavation works, mechanical pre-processing, sampling procedures and characteristics of the excavated material can be found in Garcia Lopez et al., 2019 and Hernández Parrodi et al., 2019a.

## 2.2 Mechanical processing of the Combustibles and Inert fractions

The “Combustibles” and “Inert” fractions were produced with the light and heavy fractions, respectively, which in turn were obtained from the density separation steps of the mechanical processing in the owc and dry states in Hernández Parrodi et al., 2019c. Previous to the density separation steps, the fine fractions <90 mm were subjected to particle size classification and ferrous and non-ferrous metals extraction. The particle size classification steps produced the particle size ranges 90-30 mm, 30-10 mm and 10-4.5 mm. The density separation method applied to those particle size ranges corresponds to windsifting. A cross-flow windsifter was employed in the particle size range 90-30 mm, whereas a zig-zag windsifter was used in the particle size ranges 30-10 mm and 10-4.5 mm. After density separation, both light and heavy fractions were sieved at 4.5 mm in order to remove loosened fine particles (i.e. impurities) throughout the mechanical processing. Subsequently, the heavy fractions were processed with near infrared (NIR) sorting to further extract combustible materials. The extracted combustible materials from the heavy fractions were added to the light fractions for joint valorization and to produce the “Combustibles” fraction. The heavy fractions after further removal of combustible materials were denominated the “Inert” fractions. Further information on the application of NIR sorting to the heavy fractions of the fine fractions <90 mm are reported in Küppers, Hernández Parrodi, Garcia Lopez, Pomberger, & Vollprecht, 2019 and Hernández Parrodi et al., 2019c.

The median values obtained from processing all composite samples of the fine fractions <90 mm (n=16) in the

owc (n=8) and dry (n=8) states were used to elaborate the general mass balance of the mechanical processing, which was reported and analyzed in Hernández Parrodi et al., 2019c.

### 2.2.1 Combustibles fractions

The general mass balance of the mechanical processing of the fine fractions <90 mm in Hernández Parrodi et al., 2019c reported total amounts of “Combustibles” of 12.5 wt.% in the owc state and 9.0 wt.% in the dry state. In turn, the mass distribution of the “Combustibles” fraction among the particle size ranges 90-30 mm, 30-0 mm and 10-4.5 mm in the owc state was about 4.6 wt.%, 5.0 wt.% and 2.5 wt.%, respectively. In the dry state, the particle size range 90-30 mm presented an amount of 4.1 wt.%, while 30-10 mm accounted for 2.7 wt.% and 10-4.5 mm for 2.0 wt.%. This information is shown as Sankey diagrams in Figure 1.

The physical appearance of each of the particle size ranges of the produced “Combustibles” fractions by the employed mechanical processing in the owc and dry states is displayed in Figure 2. In those images it can be seen that the “Combustibles” fractions were mainly composed of plastics, textiles, wood and paper & cardboard in both states, as well as that the presence of plastics and textiles seems to decrease with particle size. It is also clear that the owc state presents a higher amount of surface defilements (i.e. impurities) than the dry state. Composite samples of each of these fractions were used for the laboratory analyses performed in this study.

### 2.2.2 Inert fractions

As shown in Figure 3, the “Inert” fractions accounted for 35.5 wt.% of the total amount of produced fractions in the owc state; from which 15.3 wt.%, 15.6 wt.% and 6.3 wt.% corresponded to the particle size ranges 90-30 mm, 30-10 mm and 10-4.5 mm, respectively. In turn, the dry state showed a total amount of 37.2 wt.%, with 15.5 wt.% of the material present in the particle size range 90-30 mm, 13.0 wt.% in 30-10 mm and 8.1 wt.% in 10-4.5 mm.

Figure 4 displays photographs of the “Inert” fractions in the owc and dry states, in which it can be observed that these fractions are mostly comprised of concrete, bricks, stones and glass. The presence of concrete and bricks appears to decrease with particle size in both states. Similarly as for the “Combustibles” fractions, the “Inert” fractions show a greater amount of impurities in the owc state than in the dry state. Composite samples were used to deter-

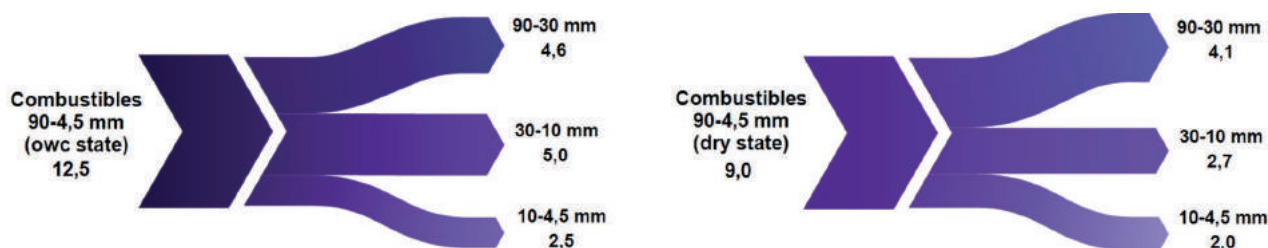


FIGURE 1: Mass distribution of the “Combustibles” fractions among particle size ranges in the owc and dry states [figures in wt.%] (Hernández Parrodi et al. 2019c).



FIGURE 2: “Combustibles” fractions in the owc and dry states (Hernández Parrodi et al. 2019c).

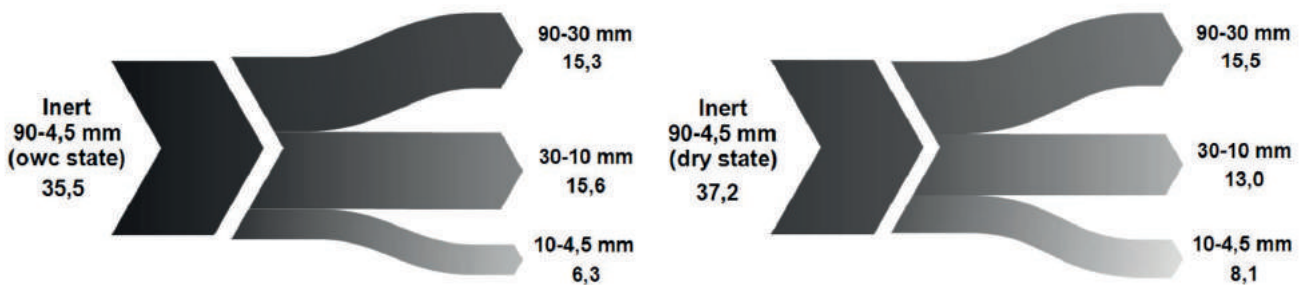


FIGURE 3: Mass distribution of the “Inert” fractions among particle size ranges in the owc and dry states [figures in wt. %] (Hernández Parrodi et al. 2019c).

mine the physico-chemical properties of these fractions as well.

### 2.3 Laboratory analyses

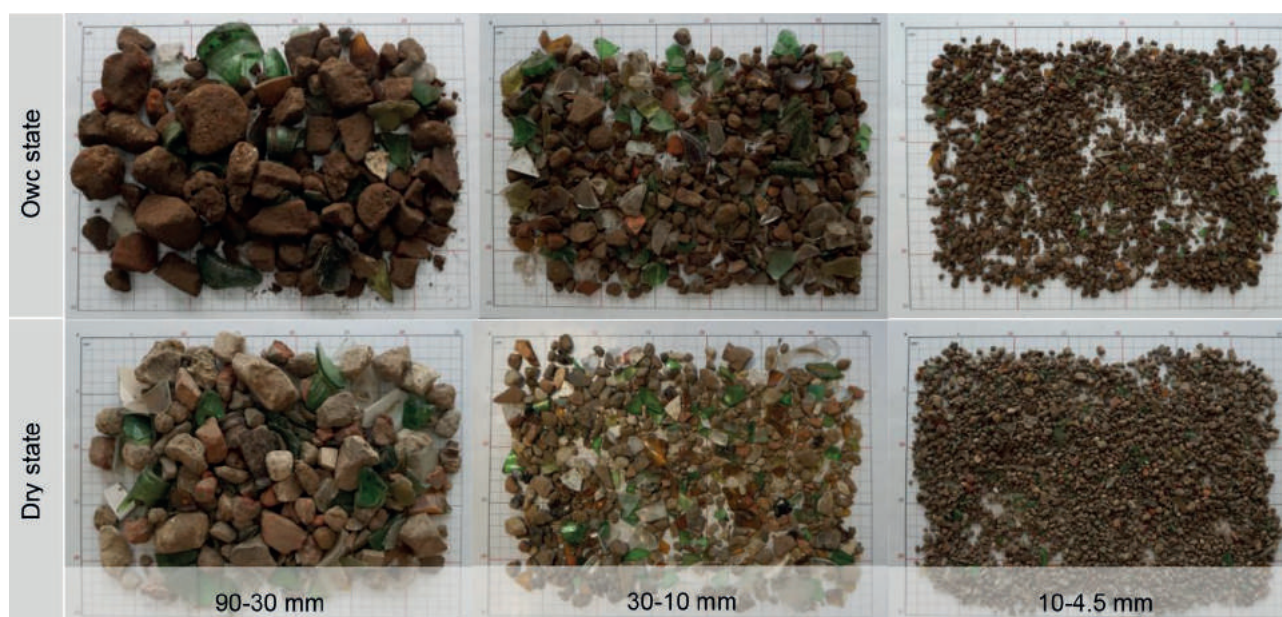
The determination of the physico-chemical characteristics of the “Combustibles” and “Inert” fractions was performed by the laboratory for environmental analyses of the Chair of Waste Processing Technology and Waste Management (AVAW) of the Montanuniversität Leoben, which is accredited as testing laboratory according to ISO/IEC 17025.

A total of 3 composite samples ( $n=3$ ) of each fraction (i.e. “Combustibles” and “Inert” fractions) of each particle size range (i.e. 90-30 mm, 30-10 mm and 10-4.5 mm) and of each state (i.e. owc and dry states) was analyzed in order to determine the pseudo-total contents (aqua regia digestion), among other parameters, of the “Combustibles” and “Inert” fractions. Additionally, the leachable concentrations of the “Inert” fractions were determined, as leaching tests are useful to determine the susceptibility of the fine fractions to serve alternative purposes (Kaczala et al., 2017). Depending on the reference taken for the limit values to be met, the arithmetic mean and standard error, with

a confidence interval of 95% ( $Ci= 95\%$ ), or the 50th percentile (median) and 80th percentile of the laboratory results were employed to describe each of the analyzed fractions. Box-and-whisker plots were elaborated with the 20th, 50th and 80th percentiles, as well as with the maximum and minimum values.

#### 2.3.1 Laboratory analyses of the Combustibles fractions

Solid matter laboratory analyses were performed to determine the main physico-chemical characteristics of the “Combustibles” fractions, as well as to individually evaluate their suitability for the production of RDF according to the EN 15359:2011 and the AVV. The results of each particle size range were also employed to calculate the physico-chemical characteristics and quality of the mixture of the 3 particle size ranges, in the original proportions in which they were generated by the mechanical processing, as a single particle size range (i.e. 90-4.5 mm). The original proportions in which the “Combustibles” fractions were generated were determined by ponderating the mass distribution of the owc and dry states presented in Figure 1. In the owc state, the median original proportions were about 38 wt.%, 41 wt.% and 21 wt.% of the particle size ranges 90-



**FIGURE 4:** "Inert" fractions in the owc and dry states (Hernández Parrodi et al. 2019c).

30 mm, 30-10 mm and 10-4.5 mm, respectively. The median original proportions in the dry state presented amounts of around 47 wt.% for the particle size range 90-30 mm, 31 wt.% for 30-10 mm and 22 wt.% for 10-4.5 mm.

The pseudo-total contents of heavy metals and other elements in the "Combustibles" fractions, as well as of additional parameters (e.g. dry matter (DM) content, net calorific value (NCV) and ash content (AC)), in the owc and dry states were determined according to the European Standard EN 15359:2011 on "Solid Recovered Fuels – Specifications and Classes" and the AVV. In the EU the EN 15359:2011 provides the overarching classification and specifications criteria for the production and utilization of solid recovered fuel (SRF), whereas the Directive on the Incineration of Waste (2000/76/EC) sets the emission limit values for waste (co-)incineration plants. The EN 15359:2011 employs parameters such as NCV, chlorine (Cl) and mercury (Hg) to determine if the material in question can be utilized as SRF and, given that the material meets the specifications, classifies the SRF according to its properties. The classification system of the EN 15359:2011 is shown in Table 1.

In Austria, the production and utilization of RDF (including SRF), as well as the emissions from co-incineration, cement and power plants, are further regulated in the

AVV. This ordinance sets the limit values for the contents of certain heavy metals (i.e. arsenic (As), cadmium (Cd), cobalt (Co), chromium (Cr), mercury (Hg), nickel (Ni), lead (Pb) and antimony (Sb)) in RDF depending on the type of application. Table 2 presents a summary of the limit values of the AVV for the corresponding heavy metals according to utilization type.

The determination of the DM content was done according to the DIN EN 14346 (Process A), while the DIN 51900-1 was followed to determine the NCV. The contents of Cl, fluorine (F), sulfur (S) and bromine (Br) were determined via calorimetric digestion (ÖNORM EN 14582) according to the DIN EN ISO 10304-1. The AC was determined following the ÖNORM EN 15403 and the heavy metals pseudo-total contents were determined through inductively coupled plasma - mass spectrometry (ICP-MS) according to the ÖNORM EN 15411. The total organic carbon (TOC) and polycyclic aromatic hydrocarbons ( $\Sigma 16$ PAHs/EPA) contents were determined according to the ÖNORM EN 13137 and the ÖNORM L 1200, respectively.

### 2.3.2 Laboratory analyses of the Inert fractions

Analogously to the "Combustibles" fractions, the particle size ranges 90-30 mm, 30-10 mm and 10-4.5 mm of the "Inert" fractions in the owc and dry states were subject

**TABLE 1:** Specifications and classes of SRF according to the EN 15359:2011.

Classification property	Statistical measure	Unit	Classes				
			1	2	3	4	5
NCV	Mean	[MJ/kg (ar)]	$\geq 25$	$\geq 20$	$\geq 15$	$\geq 10$	$\geq 3$
Cl	Mean	[wt.% (DM)]	$\leq 0.2$	$\leq 0.6$	$\leq 1$	$\leq 1.5$	$\leq 3$
Hg	Median	[mg/MJ (ar)]	$\leq 0.02$	$\leq 0.03$	$\leq 0.08$	$\leq 0.15$	$\leq 0.5$
	80 <sup>th</sup> percentile	[mg/MJ (ar)]	$\leq 0.04$	$\leq 0.06$	$\leq 0.16$	$\leq 0.3$	$\leq 1$

Notes: DM= dry matter, ar= as received.

**TABLE 2:** Limit values for the utilization of RDF according to the AVV.

Parameter	Unit	For use in co-incineration plants		For use in cement plants		For use in power plants <sup>1)</sup>	
		Median	80 <sup>th</sup> percentile	Median	80 <sup>th</sup> percentile	Median	80 <sup>th</sup> percentile
As	[mg/MJ (DM)]	1	1.5	2	3	2	3
Cd	[mg/MJ (DM)]	0.17	0.34	0.23	0.46	0.27	0.54
Co	[mg/MJ (DM)]	0.9	1.6	1.5	2.7	1.4	2.5
Cr	[mg/MJ (DM)]	19	28	25	37	31	46
Hg	[mg/MJ (DM)]	0.075	0.15	0.075	0.15	0.075	0.15
Ni	[mg/MJ (DM)]	7	12	10	18	11	19
Pb	[mg/MJ (DM)]	15	27	20	36	23	41
Sb	[mg/MJ (DM)]	7	10	7	10	7	10

Notes: DM= dry matter.

<sup>1)</sup> With a contribution of  $\leq 10\%$  of the thermal energy from the incineration of waste to the total thermal energy.

to solid matter analyses and, in addition, to leaching tests. The suitability of the “Inert” fractions for the production of a substitute for construction aggregates was evaluated according to the RBV and was performed per particle size range and as a single particle size range mixed in the original proportions in which the particle sizes were generated (only applicable to the solid matter analyses) as well, which were calculated by ponderating the mass distribution of the owc and dry states displayed in Figure 2. In the owc state, the median original proportions of the particle size ranges 90-30 mm, 30-10 mm and 10-4.5 mm corresponded to about 41 wt.%, 42 wt.% and 17 wt.%, whereas in the dry state they accounted for around 42 wt.%, 36 wt.% and 22 wt.%, respectively.

The solid matter analyses and leaching tests were carried out according to the RBV, which establishes the specifications, limit values and quality classes for the reuse and recycling of construction and demolition waste, as well as the allowed applications of such materials in Austria. However, the scope of this ordinance contains an exclusive lists of waste types which may be used for the production of recycled aggregates. Inert materials recovered through (E)LFM are not included in that list. Nevertheless, to this day the EU does not yet have an overarching directive to regulate this type of materials (Saveyn et al., 2014) and, therefore, the RBV was taken as a reference in this study. The RBV employs parameters, such as heavy metals (i.e. As, Cd, Co, Cr, Cu, Hg, Ni, Pb, and Zn), hydrocarbon index (KW index) and  $\Sigma 16\text{PAHs/EPA}$  content, in the solid matter to determine if the material in question is suitable to replace construction aggregates in certain applications, which are also defined in the same ordinance. As for the leaching tests, that ordinance sets the limit values for parameters such as pH, electric conductivity, TOC, KW index, Co, Cr, Cr, molybdenum (Mo), Ni, ammonium-N ( $\text{NH}_4^+$ ), chloride ( $\text{Cl}^-$ ), nitrite ( $\text{NO}_2^-$ ), sulfate ( $\text{SO}_4^{2-}$ ) and the methylene blue active substance assay (MBAS assay), among others. A synopsis of the classification system of the RBV for both solid matter and leachate analyses is presented in Table 3. The allowed applications of each of the quality classes in Table 3 are defined in the RBV as well, which are shown in Table 4.

Regarding the solid matter analyses, the S content of the “Inert” fractions was determined via inductively coupled plasma - optical emission spectrometry (ICP-OES) according to the ÖNORM EN ISO 11885. The concentrations of the heavy metals and other elements were determined via inductively coupled plasma - mass spectrometry (ICP-MS) and aqua regia digestion (ÖNORM EN 13657 (6.3)) according to the ÖNORM EN ISO 17294-2. For the determination of the KW index the ÖNORM EN 14039 was followed. Loss on ignition (LOI) was determined according to the DIN EN ISO 26845:2008-06 at 1025°C, deviating from the standard as individual determination. The chemical composition was determined through quantitative x-ray fluorescence (XRF) according to the DIN EN ISO 12677. DM, TOC and  $\Sigma 16\text{PAHs/EPA}$  contents were determined analogously to the “Combustibles” fractions.

As for the leaching tests, pH was determined according to the ISO 10523, while the DIN EN 27888 was used for the determination of the electric conductivity. The concentrations of  $\text{Cl}^-$ ,  $\text{NO}_2^-$ ,  $\text{SO}_4^{2-}$  and fluoride ( $\text{F}^-$ ) were determined following the DIN EN ISO 10304-1 and  $\text{NH}_4^+$  was determined according to the DIN 38406-5. The ÖNORM EN 903 was followed for the MBAS assay, whereas TOC and KW index were determined according to the DIN EN 1484-3 and the EN ISO 9377-2, respectively. The concentrations of Co, Cr, Cr, Mo and Ni were determined via leaching tests (ÖNORM EN 12457-4 (waste)) according to the ÖNORM EN ISO 17294-2 (ICP-MS).

### 3. RESULTS AND DISCUSSION

#### 3.1 Combustibles fractions

The results of the solid matter laboratory analyses of the “Combustibles” fractions for the parameters NCV, AC, Cl, F, S, Br, C, H, Hg and N, as well as DM, TOC and  $\Sigma 16\text{PAHs/EPA}$  contents, per particle size range (i.e. 90-30 mm, 30-10 mm, 10-4.5 mm and 90-4.5 mm (mixed in original proportions)) and state (i.e. the owc and dry states) are presented in Table 5.

The figures in Table 5 show that the DM content in the owc state, which was set prior to the experiments to 85.0 wt.%, varied between 86.7 wt.% and 74.5 wt.% among the particle size ranges and presented a tendency to decrease towards finer particle sizes. The dry state showed a varia-

**TABLE 3:** Limit values for the recycling of construction materials according to the RBV.

Parameter	Unit	Quality classes				
		U-A	U-B	U-E	H-B	
Leaching tests (L/S 10)	pH	[1]	7.5 <sup>1)</sup> - 12.5 <sup>2)</sup>			up to 12.5 <sup>2)</sup>
	Electric conductivity	[mS/m]	150			-
	Cr <sub>Tot</sub>	[mg/kg (DM)]	0.6	1	0.6	1
	Co	[mg/kg (DM)]	-	-	1	-
	Cu	[mg/kg (DM)]	1	2	1	2
	Mo	[mg/kg (DM)]	-	-	0.5	-
	Ni	[mg/kg (DM)]	0.4	0.6	0.4	-
	NH <sub>4</sub> <sup>+</sup>	[mg/kg (DM)]	4	8	4	8
	Cl <sup>-</sup>	[mg/kg (DM)]	800	1,000	800	1,000
	NO <sub>2</sub> <sup>-</sup>	[mg/kg (DM)]	-	2	-	-
	SO <sub>4</sub> <sup>2-</sup>	[mg/kg (DM)]	2,500	6,000	2,500	6,000
	TOC	[mg/kg (DM)]	100	200	100	200
	KW index	[mg/kg (DM)]	-	-	5	-
	MBAS assay	[mg/kg (DM)]	-	-	1	-
	Solid matter	As	[mg/kg (DM)]	-	-	50 / 200 <sup>4)</sup>
Pb		[mg/kg (DM)]	150	-	150 / 500 <sup>3), 4)</sup>	-
Cd		[mg/kg (DM)]	-	-	2 / 4 <sup>4)</sup>	-
Cr <sub>Tot</sub>		[mg/kg (DM)]	90 / 300 <sup>4)</sup>	90 / 700 <sup>4)</sup>	300 / 700 <sup>4)</sup>	90 / 700 <sup>4)</sup>
Co		[mg/kg (DM)]	-	-	50	-
Cu		[mg/kg (DM)]	90 / 300 <sup>4)</sup>	90 / 500 <sup>4)</sup>	100 / 500 <sup>4)</sup>	90 / 500 <sup>4)</sup>
Ni		[mg/kg (DM)]	60 / 100 <sup>5)</sup>	60	100	60
Hg		[mg/kg (DM)]	-	0.7	1 / 2 <sup>4)</sup>	0.7
Zn		[mg/kg (DM)]	-	450	500 / 1,000 <sup>4)</sup>	450
KW index		[mg/kg (DM)]	150	200	150	200
Σ16PAHs/EPA		[mg/kg (DM)]	12	20	12	20

Notes: DM= dry matter.

<sup>1)</sup> For natural non-contaminated rock the pH-range starts from 6.5.

<sup>2)</sup> If the pH value and/or the electrical conductivity are exceeded, freshly broken concrete containing recycling building materials can be subjected to rapid carbonation based on the ÖNORM S 2116-3 "Investigation of Stabilized Waste, Part 3: Rapid Carbonation", issued on January 1, 2010. In this case, the eluate must be examined again. In any case, the limit values must be observed after carbonation. This applies to both the pH value and electrical conductivity.

<sup>3)</sup> If the Pb content exceeds 150 mg/kg (DM), the Pb concentration in the eluate must be determined and a limit value of 0.3 mg/kg (DM) must be complied with.

<sup>4)</sup> The higher limit value applies if background concentrations can be demonstrated.

<sup>5)</sup> No limit value applies if background concentrations can be demonstrated.

tion of the DM content between 97.3 wt.% and 97.1 wt.% among the particle size ranges, which also presented a decreasing tendency (albeit very slight) towards finer particle sizes. This can be explained by the greater presence of impurities in the owc state than in the dry state, which tend to absorb/adsorb water and whose amount has also shown an increasing trend with the decrease in particle size. Furthermore, this information reveals that the material processed in the dry state with an initial DM content of 100.0 wt.% absorbed/adsorbed between 2.7 wt.% and 2.9 wt.% of moisture from the environment along the mechanical processing, which suggests that a closed moisture-free mechanical processing would be needed to maintain the water content below those levels. The calculated DM contents of the mixed single particle size range 90-4.5 mm accounted for 80.3 wt.% in the owc state and 97.2 wt.% in the dry state.

The NCV was significantly higher in the dry state than in the owc state although it was normalized to DM. This means that either during mechanical processing in the owc state calorific materials were lost to the fine fractions <4.5 mm or inert materials were lost to the same fraction during processing in the dry state. It is suggested that the latter is the case, i.e. inorganic materials remained attached to the calorific fractions in the owc state to a greater extent than in the dry state. The NCV was higher for coarser fractions, i.e. combustibles occurred rather in coarser particle size, and varied from 15.8 MJ/kg (DM) to 7.9 MJ/kg (DM) in the owc state and from 17.6 MJ/kg (DM) to 8.9 MJ/kg (DM) in the dry state. As a mixed single particle size range, the NCV of the "Combustibles" fractions accounts for 12 MJ/kg (DM) in the owc state and 14.4 MJ/kg (DM) in the dry state. The values of the NCV referring to the original substance (as received (ar)) are in the range of those us-

**TABLE 4:** Permitted use of recycled construction aggregates per quality class according to the RBV.

Class	Description	Unbound application <sup>1)</sup> without low permeable, bound top layer or base layer	Unbound application <sup>1)</sup> under low permeable, bound top layer or base layer	Production of concrete from the strength class C 12/15 on or strength class C 8/10 from the exposure class XC1 on	Production of asphalt
U-A	Aggregates for the unbound use, as well as for the hydraulic or bituminous bound use	Yes	Yes	Yes	Yes
U-B	Aggregates for the unbound use, as well as for the hydraulic or bituminous bound use	No	Yes <sup>2)</sup>	Yes	Yes
U-E	Aggregates for the unbound use, as well as for the hydraulic or bituminous bound use	Yes <sup>2), 3)</sup>	Yes <sup>2)</sup>	Yes	Yes
H-B	Aggregates exclusively for the production of concrete from the strength class C 12/15 on or from the strength class C 8/10 from the exposure class XC1 on	No	No	Yes	No

Notes:

<sup>1)</sup> Including manufacture of concrete under strength class C 12/15 or up to strength class C 8/10 under exposure class XC1.

<sup>2)</sup> Use according to § 13 Z1 (unless a water-legal license for the use of recycled building materials is not available in protected areas, not in designated zones of sanctuaries, not in designated protected areas, not in and immediately above groundwater and not in surface water).

<sup>3)</sup> Only in the trapezoid of the track body as a base layer (§ 13 Z 4).

able in fluidized bed incinerators (Sarc & Lorber, 2013) for the particle size ranges 90-30 mm and 30-10 mm, but below that range for the particle size range 10-4.5 mm. The ranges of NCV values of the “Combustibles” fractions are in the same range as those obtained for individual calorific fractions in a previous LFM project in Austria (Wolfsberger et al., 2015).

The AC is significantly higher for the samples processed in the owc state than for those processed in the dry state. This is associated with the presence of a larger amount of surface defilements in the owc state and the predominant inorganic nature of surface defilements. Contrary to the NCV, the AC of the “Combustibles” fractions increased with the decrease in particle size, which can also be explained by the increase in the amount of impurities as particle size decreased and the directly proportional correlation between the amount of impurities composed predominantly of inorganic compounds and the AC. In the dry state the AC reached values above 50 wt.% (DM) in the particle size range 10-4.5 mm, while it did as well in the particle size ranges 30-10 mm and 10-4.5 mm in the owc state. Amounts of 47.4 wt.% (DM) and 38.2 wt.% (DM) of AC were calculated for the mixed single particle size range 90-4.5 mm in the owc and dry states, respectively. The AC values of the “Combustibles” fractions were in the range of low quality supplier materials for RDF production from municipal solid waste and industrial or commercial waste (Sarc & Lorber, 2013), which show that the quality of the combustible materials obtained through LFM for the production of RDF might not be very far from that of more recent types of waste.

The Cl and S concentrations in the “Combustibles” fractions decreased with decreasing particle size in both the owc and dry states. As a mixed single particle size range, the concentrations of Cl and S are in the range of 0.9-1.2 wt.% and 0.5-0.6 wt.%, respectively, for both states; which is in agreement with commercial RDF (Sarc & Lorber, 2013). The determined concentrations were higher for the material processed in the dry state, which suggests that Cl and S are

enriched in combustible materials (e.g. as PVC for Cl and vulcanized plastics for S) and not in inorganic surface defilements. The F and B concentrations were insignificant. The C contents decreased with decreasing particle size in both the owc and dry states, and were higher for the fractions treated in the dry state, which suggests dominance of organic carbon. This can be confirmed by the TOC values, which indicated that practically the entire C content is organic. Amounts of 33.0 wt.% (DM) and 39.7 wt.% (DM) account for the C content of the mixed single particle size range in the owc and dry states, respectively. The H content showed the same tendency as Cl, S and C contents, both with respect to particle size and processing state, which suggests its presence in combustible materials. H presented concentrations in the range of 2.9-5.8wt.% (DM) in the owc state and 3.2-6.8 wt.% (DM) in the dry state. For N, which showed respective concentrations in the range of 1.0-2.0 wt.% (DM) and 0.9-1.4-wt.% (DM) in the owc and dry states, a decrease with decreasing particle size was observed; but not clear correlation with the processing state (i.e. owc and dry states) was identified. The concentrations of Σ16PAHs/EPA were in the range of 10.9-13.3 mg/kg (DM) in the owc state and 9.4-13.4 mg/kg (DM) in the dry state, and did not seem to be influenced by the processing state and are highest for the intermediate particle size range (i.e. 30-10 mm) in both states. As for the Hg concentrations, no significant variations between the owc and dry states for the particle size ranges 90-30 mm and 10-4.5 mm were shown. The particle size range 30-10 mm presented the highest concentrations of Hg in the owc state, while 10-4.5 mm did so in the dry state. The concentrations of Hg ranged from 0.06-0.30 mg/MJ (ar) in the owc state and from 0.07-0.20 mg/MJ (ar) in the dry state. The Hg concentrations are rather enriched in the finer particle size ranges, which suggests its association with surface defilements.

The pseudo-total contents of the heavy metals As, Cd, Co, Cr, Hg, Ni, Pb and Sb in the “Combustibles” fractions per particle size range and state, and as a single particle size range mixed in the original proportions of each particle

**TABLE 5:** Laboratory results of the solid matter analyses of the “Combustibles” fractions.

Parameter	Unit	90-30 mm				30-10 mm				10-4.5 mm				90-4.5 mm (mixed in original proportions)			
		Owc		Dry		Owc		Dry		Owc		Dry		Owc		Dry	
		Mean	Std. error	Mean	Std. error	Mean	Std. error	Mean	Std. error	Mean	Std. error	Mean	Std. error	Mean	Std. error	Mean	Std. error
DM	[wt.% (ar)]	86.70	1.69	97.27	0.83	77.17	1.90	97.20	0.11	74.53	0.43	97.13	0.07	80.24	0.81	97.22	0.41
NCV <sup>1)</sup>	[MJ/kg (DM)]	15.80	0.41	17.60	1.63	10.53	0.95	13.40	1.13	7.87	1.24	8.93	0.24	11.97	0.48	14.39	0.90
	[MJ/kg (ar)]	13.40	0.71	17.07	1.49	7.60	0.98	12.93	1.08	5.23	0.91	8.57	0.26	9.31	0.43	13.92	0.82
AC	[wt.% (DM)]	33.00	4.21	26.10	0.97	52.87	1.12	42.70	1.93	62.70	4.28	57.70	1.41	47.38	1.37	38.20	1.26
Cl	[wt.% (DM)]	1.48	1.16	1.91	0.69	0.63	0.16	0.73	0.28	0.16	0.01	0.16	0.01	0.86	0.47	1.16	0.37
F	[wt.% (DM)]	0.02	0.00	0.02	0.00	0.02	0.00	0.02	0.00	0.02	0.00	0.02	0.00	0.02	0.00	0.02	0.00
S	[wt.% (DM)]	0.58	0.29	0.74	0.12	0.46	0.07	0.40	0.02	0.41	0.04	0.38	0.03	0.50	0.12	0.55	0.04
Br	[wt.% (DM)]	0.02	0.00	0.02	0.01	<d.l.	-	<d.l.	-	<d.l.	-	<d.l.	-	-	-	-	-
C	[wt.% (DM)]	42.53	6.67	49.17	2.65	29.83	1.54	35.93	1.88	21.83	0.66	24.67	0.73	32.98	2.41	39.67	1.39
H	[wt.% (DM)]	5.82	1.05	6.80	0.75	3.84	0.18	4.53	0.22	2.90	0.08	3.18	0.05	4.40	0.35	5.30	0.39
N	[wt.% (DM)]	1.99	2.00	1.40	0.49	1.04	0.08	1.23	0.23	0.97	0.03	0.94	0.04	1.39	0.78	1.24	0.15
TOC	[wt.% C (DM)]	43.37	5.35	52.13	2.58	28.40	2.01	37.57	2.69	18.97	1.52	20.60	2.16	32.11	1.54	40.68	2.45
Σ16PA Hs/EPA	[mg/kg (DM)]	10.89	12.77	9.38	4.79	21.33	19.45	18.23	5.87	13.27	2.68	13.40	3.42	15.67	5.21	13.01	4.15
Parameter	Unit	Median	80 <sup>th</sup> percentile	Median	80 <sup>th</sup> percentile	Median	80 <sup>th</sup> percentile	Median	80 <sup>th</sup> percentile	Median	80 <sup>th</sup> percentile	Median	80 <sup>th</sup> percentile	Median	80 <sup>th</sup> percentile	Median	80 <sup>th</sup> percentile
Hg	[mg/MJ (ar)]	0.06	0.07	0.07	0.09	0.30	0.31	0.11	0.11	0.20	0.23	0.20	0.24	0.15	0.16	0.09	0.11
Ba	[mg/MJ (DM)]	61.39	239.49	21.02	22.05	112.97	218.92	66.42	83.88	136.02	147.46	102.99	103.66	89.94	217.66	42.38	49.18
Be	[mg/MJ (DM)]	<d.l.	-	<d.l.	-	<d.l.	-	<d.l.	-	<d.l.	-	<d.l.	-	<d.l.	-	<d.l.	-
Cu	[mg/MJ (DM)]	7.59	20.13	14.20	51.36	18.99	24.68	11.19	40.75	25.42	30.76	27.99	30.00	17.41	20.92	29.89	42.45
Mo	[mg/MJ (DM)]	0.89	0.92	0.57	0.64	0.52	0.62	0.37	0.38	0.92	1.09	0.88	1.09	0.81	0.82	0.55	0.57
Mn	[mg/MJ (DM)]	13.92	16.20	7.95	8.98	26.58	27.72	19.40	19.40	40.68	42.20	33.58	33.58	21.50	23.67	14.11	15.09
Se	[mg/MJ (DM)]	<d.l.	-	<d.l.	-	0.25	0.27	<d.l.	-	0.42	0.43	0.03	0.39	-	-	-	-
Tl	[mg/MJ (DM)]	<d.l.	-	<d.l.	-	<d.l.	-	<d.l.	-	<d.l.	-	<d.l.	-	<d.l.	-	<d.l.	-
V	[mg/MJ (DM)]	0.82	1.09	0.63	0.76	2.28	2.79	1.12	1.39	3.56	3.64	2.69	2.75	1.66	2.03	1.18	1.18
Zn	[mg/MJ (DM)]	77.22	92.41	56.82	62.27	131.96	132.53	163.43	178.66	179.24	186.10	150	153.36	112.43	112.54	102.09	103.89

Notes: <d.l. = amount below detection limit. ar= as received. DM= dry mass. n=3, std. error with Ci of 95%.<sup>1)</sup> The gross calorific value (GCV) was determined experimentally according to the DIN 51900-1. A fixed correction factor of f= 0.92, based on the GCV, was used for the calculation of the NCV according to the “AQS Richtlinie (2001)”.

size range are shown in the form of box-and-whisker plots in Figure 5.

The data in Figure 5 show that the concentrations of As, Cd, Co, Ni and Pb increase with decreasing particle size, which suggests that they are present in the inorganic defilements or adsorbed to their surfaces. For Cr, Hg, and Sb this trend is less pronounced. For As, Cd, Co, and mostly Pb and Ni, concentrations in the owc state processed samples are higher than in those processed in the dry state, which confirms their association with inorganic defilements.

Cr concentrations in the coarsest particle size range are higher for the material processed in the dry state, whereas in the finer particle size ranges they are higher for those materials processed in the owc state. This suggests that one part of Cr is present in larger particles, e.g. textiles due to tanning agents, whereas another part is present in fine-grained surface defilements.

After comparing the results with the limit values set in the AVV (Table 2), it was observed that the concentrations of the particle size range 90-30 mm in the owc state exten-



sively complied with the limit values of all heavy metals for use in power plants; except Pb, which was only exceeded for the 80th percentile by a minuscule amount. In turn, the same particle size in the dry state presented low concen-

trations of all heavy metals as well, failing only to comply with the median and 80th percentile limit values for Cd for use in power plants by small amounts. However, the median concentrations of Hg in the owc and dry states were

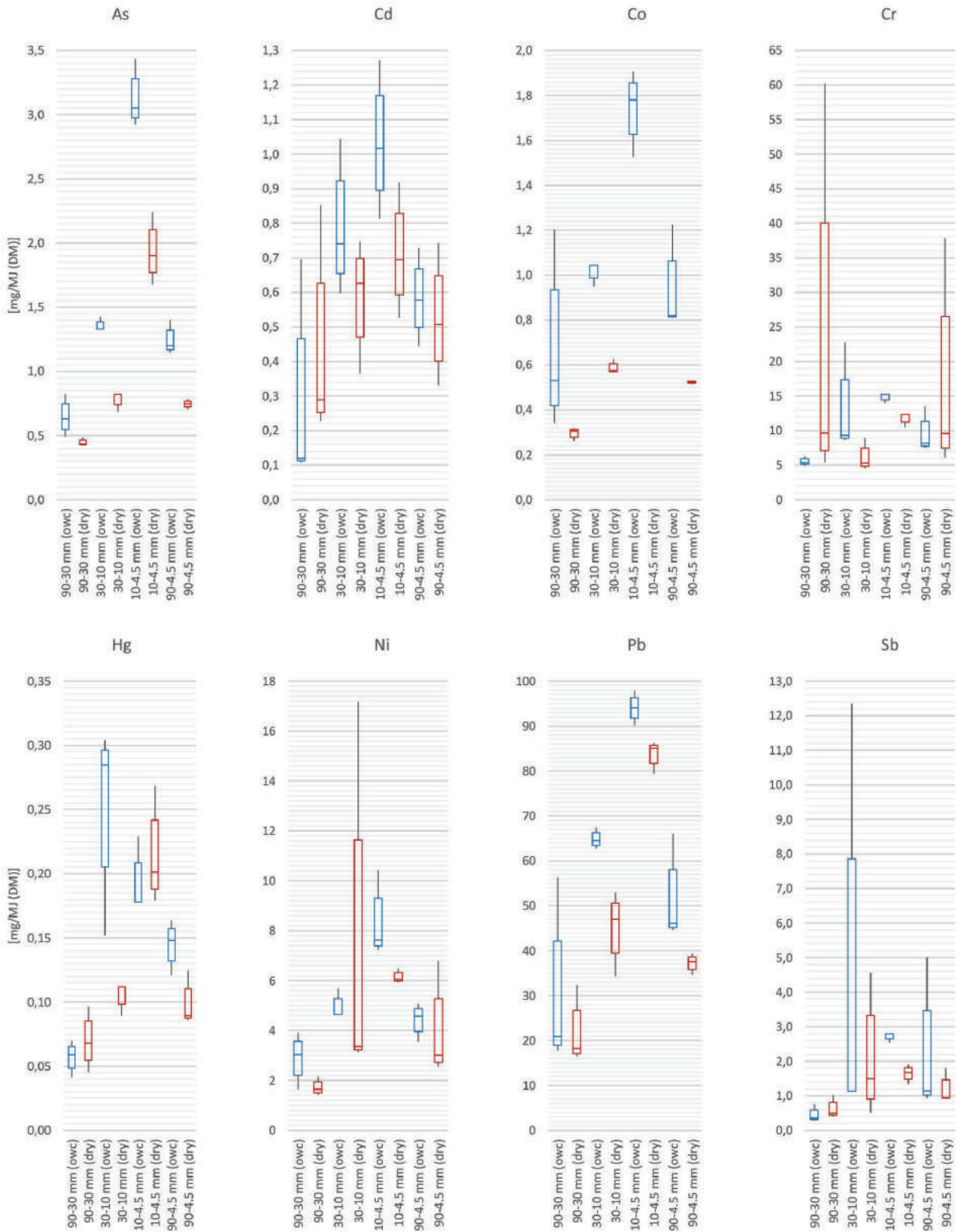


FIGURE 5: Heavy metals concentrations of the “Combustibles” fractions in the owc (blue) and dry (red) states.

close to that of the limit value and, hence, this element could also be problematic. The particle size range 30-10 mm failed to comply with the limit values of Cd and Pb for both median and 80th percentile in the owc and dry states. Additionally, that particle size range exceeded the median and 80th percentile limit values of Hg in the owc state, while in the dry state only the limit value for the median was exceeded. The concentrations of Cd, Hg and Pb of the particle size range 10-4.5 mm were above the limit values for the median and 80th percentiles in both owc and dry states. In the owc state, the concentration of As exceeded the median and 80th percentile limit values, while the median concentration of Co was above the limit value as well.

According to the previous data, it can be said that the quality of the "Combustibles" fractions tends to decrease with particle size. That can be explained by the presence of heavy-metal bearing fine-grained particles. If the particle size ranges 90-30 mm, 30-10 mm and 10-4.5 mm were to be mixed in the original proportions, the resulting single particle size range 90-4.5 mm of the "Combustibles" fractions would exceed the median and 80th percentile limit values for Hg and Pb in the owc state, while the median for Cd would also be above the limit value. In the dry state, the particle size range 90-4.5 mm would exceed the median and 80th percentile limit values of Cd, as well as the median limit values of Hg and Pb.

### 3.1.1 Valorization of Combustibles fractions as RDF

Previous investigations have shown that plastics from (E)LFM are most likely not suitable for recycling routes and, thus, their valorization should be directed to energy recovery through thermochemical processes, such as incineration, pyrolysis and gasification, or to the production of monomers and industrial chemical precursors (Canopoli, Fidalgo, Coulon, & Wagland, 2018). This might be the case, since LFM plastic waste is commonly characterized by its high ash, impurities and heavy metals contents (Canopoli et al., 2018).

In general, the "Combustibles" fractions recovered in the present case study could be valorized as SRF in (co-)incineration, power and cement plants in the EU, under certain circumstances depending on the type of plant and given that the corresponding plant complies with the applicable emission limit values established in the Directive on the Incineration of Waste (2000/76/EC), since the recovered "Combustibles" fractions meet the specifications set in the EN 15359:2011, in both the owc and dry states. Furthermore, the "Combustibles" fractions could be valorized mixed in one single particle size range (i.e. 90-4.5 mm) in their original proportions (i.e. 38 wt.% of 90-30 mm, 41 wt.% of 30-10 mm and 21 wt.% of 10-4.5 mm in the owc state; 47 wt.% of 90-30 mm, 31 wt.% of 30-10 mm and 22 wt.% of 10-4.5 mm in the dry state) or individually, separated in the particle size ranges of the mechanical processing (i.e. 90-30 mm, 30-10 mm and 10-4.5 mm). The latter approach is reasonable for those cases in which the coarser fraction can be incinerated at a lower price, or even for revenue, in co-incineration plants and only the finer fractions need to be incinerated at higher prices in incineration plants. Altogether, the "Combustibles" fractions corresponded to a

SRF of class-code NVC 5; CI 3; Hg 3 in the owc state and of NVC 4; CI 4; Hg 3 in the dry state. Individually, the particle size range 90-30 mm corresponds to a SRF of class-code NVC 3; CI 4; Hg 3, 30-10 mm to a class-code of NVC 5; CI 2; Hg 5 and 10-4.5 mm to one of NVC 5; CI 1; Hg 4 in the owc state. In the dry state, the particle size ranges 90-30 mm, 30-10 mm and 10-4.5 mm correspond to SRF of class-codes: NVC 3; CI 5; Hg 3, NVC 4; CI 3; Hg 3 and NVC 5; CI 1; Hg 4, respectively. Nevertheless, it is important to stress that legislation on waste may vary from country to country in the EU and additional restrictions, as well as stricter limit values can be applied. It is also relevant to note that the recovered combustible fractions from the fine fractions are likely to be valorized together with those recovered from the coarse fractions (i.e. the 2D >200 mm and 2D 200-90 mm fractions in the MSG case study), which might have a significant positive impact on the quality of the whole recovered combustible fraction, since the combustible fractions recovered from the coarse fractions of (E)LFM frequently present higher NCVs and lower amounts of organic and inorganic pollutants, and account for a considerable share of the processed material.

Some of the circumstances previously mentioned are that not all classes of SRF are suitable for all types of plants (refer to CEN / TR 15508). For example, if cement and lime kilns and power plants use 100% SRF as fuel and have an emission limit of Hg of 0.05 mg/m<sup>3</sup>, only SRF class Hg 1 is suitable for those plants. SRF with a class Hg 5 could only be used in those plants if this class of SRF represents less than 100% of the fuel mixture. For other SRF classes, the specific transfer factor for a given process and the proportion of SRF determine which classes can be used without improving the transfer conditions. Examples of transfer factors for existing processes are given in the CEN / TR 15508. Additionally, SRF should not be used as fuel if less heat energy is generated and available for the plant-related process, than is consumed during the combustion of the SRF and, therefore, is not available for the process. As a result, for example, the use of SRF class NCV 5 in systems that require a higher minimum heating value for energy production should be avoided.

However, in Austria, where regulations are stricter than in many other EU countries, the "Combustibles" fractions would need to be subjected to a cleaning process, in which the amount of surface defilements and impurities could be further reduced, in order to be valorized as RDF in co-incineration plants.

An alternative to both further cleaning for subsequent co-incineration and direct incineration is the use of pyrolysis and gasification as thermo-chemical valorization methods for the combustible fractions of landfill-mined material in order to produce syngas. Subsequently to the pyrolysis/gasification process, the molten ash residue is vitrified; producing a glassy slag. This is the principal approach in the NEW-MINE project, which proposes the utilization of plasma gasification as alternative thermo-valorization method for the high calorific fractions from landfill-mined waste. The plasma gasification investigated in the NEW-MINE project can cope with RDF materials with higher inorganic pollutant contents, since those pollutants can be immobilized in the

vitrified residue. The gasification process of SRF from municipal solid waste and industrial waste was studied in Zaini, Yang, & Jönsson, 2017; whereas the pyrolysis/gasification of RDF from landfill-mined waste was successfully tested in Zaini, García López, Pretz, Yang, & Jönsson, 2019 on a laboratory scale. It has also been demonstrated that thermal treatment of the glassy slag yielded glass-ceramics with very low leaching of Cr, Cu, Co, Cd and Ni (Rabelo Monich et al., 2020), as well as that inorganic polymer binders can be produced from the (semi-)vitreous material obtained as by-product in plasma gasification of waste materials (Ascensão et al., 2019; Machiels et al., 2017). Both glass-ceramics and inorganic polymers are higher value-added products that could be used to replace raw materials in construction applications, such as tiles, bricks and glass foams (Monich et al., 2018; Rabelo Monich, Dogrul, Lucas, Friedrich, & Bernardo, 2019; Rincón, Marangoni, Cetin, & Bernardo, 2016), as well as in the production of concrete (Ascensão et al., 2019; Machiels et al., 2017). Therefore, in contrast to conventional (co-)incineration, plasma gasification might offer a potential WtE valorization route for the combustible fractions obtained from the fine fractions of landfill-mined waste, which in the present case study accounted for 12.5 wt.% and 9.0 wt.% of the total amount of the fine fractions <90 mm in the owc and dry states, respectively.

### 3.2 Inert fractions

The chemical composition of the “Inert” fractions per particle size range (i.e. 90-30 mm, 30-10 mm, 10-4.5 mm) and state (i.e. owc and dry states) was determined through XRF analyses. This information is displayed graphically in the form of stacked columns in Figure 6.

The information in Figure 6 unveils that most of the “Inert” fractions was composed of silicon dioxide ( $\text{SiO}_2$ ), followed by aluminium oxide ( $\text{Al}_2\text{O}_3$ ), calcium oxide ( $\text{CaO}$ ), iron oxide ( $\text{Fe}_2\text{O}_3$ ) and sodium oxide ( $\text{Na}_2\text{O}$ ). Chemically, there are no significant differences between the samples processed in the owc state and those processed in the dry state. The LOI was higher for the finest particle size ranges, as moisture is mainly adsorbed by finer particles.  $\text{Al}_2\text{O}_3$  and  $\text{CaO}$  concentrations do not significantly change among particle size ranges, whereas  $\text{Fe}_2\text{O}_3$  increased with the decrease in particle size. This can be explained by the formation of iron hydroxides in the landfill due to the oxidation of  $\text{Fe}^{2+}$  to  $\text{Fe}^{3+}$  in the leachate and also by the corrosion of iron particles. A similar behavior is observed for Mn, which is explained analogously by the precipitation of Mn hydroxides due to the oxidation of  $\text{Mn}^{2+}/\text{Mn}^{3+}$  to  $\text{Mn}^{4+}$ . As Cr showed a similar tendency, it is suspected that Cr formed secondary Cr(III) phases as described in Sedlazeck, Höllen, Müller, Mischitz, & Gieré, 2017. Contrary as for Fe and Mn, the higher valent form of Cr was more soluble than the lower valent form.

Additionally, solid matter laboratory analyses were performed to the “Inert” fractions for parameters such as S, C, KW index, N and certain heavy metals (i.e. Cr, Co, Ni, Cu, Zn, As, Cd, Hg and Pb), as well as DM,  $\Sigma 16\text{PAHs}/\text{EPA}$  and TOC

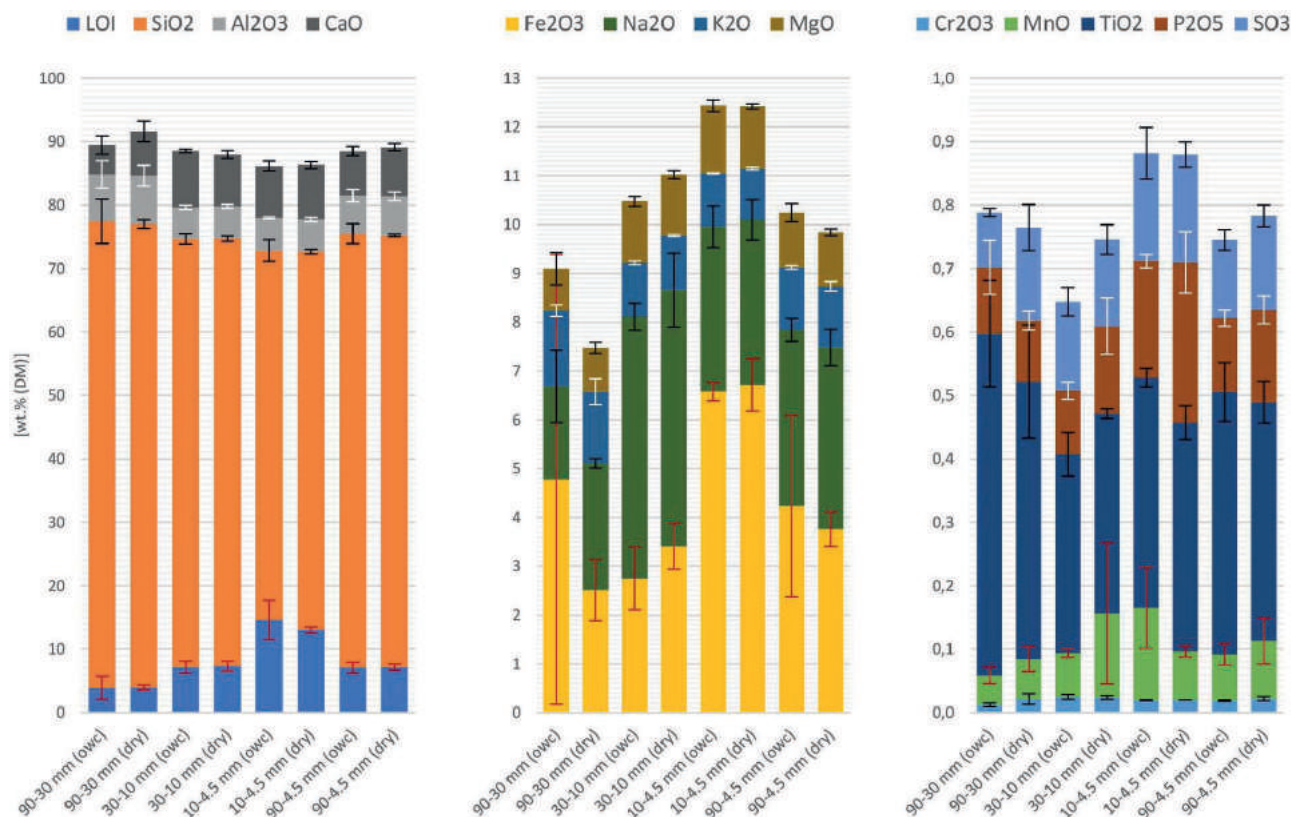


FIGURE 6: Chemical composition of the “Inert” fractions from XRF analyses in the owc and dry states.

contents, per particle size range and state. Table 6 presents a summary of the results of those laboratory analyses.

The results in Table 6 show that the particle size range 90-30 mm presented the best quality among all particle size ranges in both the owc and dry states, complying with all solid matter parameters for all quality classes (i.e. U-A, U-B, U-E and H-B from Table 3); except for the concentration of Pb in the dry state, which was slightly exceeded for all quality classes. However, the standard error of this parameter significantly exceeds the mean value itself and shows the strongest variation among all parameters for that state; suggesting the presence of outliers. Moreover, the amount of Pb was significantly exceeded in the particle size range 10-4.5 mm in both states, whereas the particle size range 30-10 mm complied with the limit value for all quality classes in both states as well. The concentration of Pb in the leaching tests of the "Inert" fractions as a mixed single particle size range 90-4.5 mm can be expected below 0.3 mg/kg (DM) in both states, since the highest concentration determined from all samples of all particle size ranges was 0.26 mg/kg (DM) (Table 7), which was one order of magnitude above those of all other samples. Provided that background concentrations of Pb in the site of application can be proven, a limit value of 500 mg/kg DM would apply to these fractions and, hence, all particle size ranges, except 10-4.5 mm in the dry state, would meet the limit value for all quality classes.

In terms of quality, the particle size range 30-10 mm followed 90-30 mm. In the dry state, the particle size range 30-10 mm complied with all parameters for all quality classes; except for the hydrocarbons content (KW index), which slightly exceeded the limit values for the quality classes U-A and U-E. In the owc state, this particle size range exceeded the limit values for hydrocarbons content for all quality classes, in which classes U-B and H-B were only slightly exceeded. The concentration of Cd in this particle size range exceeded the lower limit value for quality class U-E and presented the same value as the higher limit value (applicable if background concentrations can be demonstrated) in the owc state. However, the standard error of the Cd content in that state suggests outliers and, in addition, Cd content is not relevant for classes U-A, U-B and H-B. The Zn concentration was also exceeded by this particle size range in the owc state for classes U-A, U-B and H-B, as well as the lower limit value for class U-E; meaning that if background concentrations of Zn can be proven, the higher limit value for class U-E would not be exceeded.

The particle size range 10-4.5 mm showed the lowest quality, since the limit values for hydrocarbons, Zn, Cd and Pb were exceeded for all quality classes in both the owc and dry states. No significant differences were identified between the quality of both states in this particle size range; except for Pb, which presented a higher concentration in the dry state.

As a mixed single particle size range 90-4.5 mm, the "Inert" fractions would slightly exceed the limit values for hydrocarbons for the quality classes U-B and H-B in both owc and dry states, while the concentration of Pb would exceed the limit value for class U-A and the lower limit value for classes U-B, U-E and H-B only in the dry state. In the owc

state, the Zn content would exceed quality classes U-A, U-B and H-B, and the lower limit value of class U-E.

In general, it can be said that the dry state presented higher concentrations of Pb; nevertheless, a conclusive tendency cannot be confirmed due to the presence of outliers. In turn, the owc state showed consistently higher contents of hydrocarbons and Zn, which can be explained by the presence of impurities. For Cd no trend could be identified between both states.

The previous information reveals that the quality of the "Inert" fractions, in terms of the solid matter parameters analyzed, decreased with the decrease in particle size. This suggests that the quality decrease is associated with the presence of organic and inorganic impurities and, therefore, a cleaning step would be needed to reduce the concentrations of the problematic elements and compounds (especially those of hydrocarbons), and enable the utilization of the "Inert" fractions as substitute for construction aggregates in Austria. The elevated concentrations of Cd and Pb could be due to the presence of glass, since such elements have been commonly used in glass production as coloring and decorative agents in the past. Hence, the separation of glass from the "Inert" fractions, through a density separation or sensor-based sorting method, might reduce the concentrations of Cd and Pb.

In addition to the solid matter laboratory analyses, leaching tests were performed to samples of the "Inert" fractions according to the RBV. The results of the leaching tests are summarized in Table 7. After comparing the leaching tests parameters of the "Inert fractions" in Table 7 with the corresponding limit values set in the RBV, it was observed that the contents of  $\text{NH}_4^+$  significantly exceeded the limit values in almost every case; only the particle size range 30-10 mm in the owc state complied with the limit value of classes U-B and H-B, and exceeded the limit value of classes U-A and U-E by a minuscule amount. High concentrations of  $\text{NH}_4^+$  in landfills are in agreement with previous observations (Vollprecht, Frühauf, Stocker, & Ellersdorfer, 2019). Only with one exception, for the particle size range 90-30 mm, the amounts of  $\text{NH}_4^+$  were lower in the owc state than in the dry state.

The amounts of anionic surfactants determined by the MBAS assay, which are the active washing components of products such as soap or detergent, were very slightly above the limit values in the particle size ranges 30-10 mm in the owc state and 10-4.5 mm in both states, whereas the amounts in the particle size ranges 30-10 mm in the dry state and 90-30 mm in both states were below the detection limit. It should be noted that the limit value in the RBV for this parameter corresponds to the detection limit of the assay and, therefore, the measured amounts could correspond to outliers.

The pH value of the particle size range 10-4.5 mm in the owc state was very slightly below the limit value of quality classes U-A, U-B and U-E; however, this fraction is suitable for quality class H-B. Hence, pH is not regarded as a problematic parameter in this fraction.

The TOC content of the particle size range 10-4.5 mm in the dry state complied with the limit values for quality classes U-B and H-B, but slightly exceeded those of class-

**TABLE 6:** Laboratory results of the solid matter analyses of the “Inert” fractions.

Parameter	Unit	90-30 mm				30-10 mm				10-4.5 mm				90-4.5 mm (mixed in original proportions)			
		Owc		Dry		Owc		Dry		Owc		Dry		Owc		Dry	
		Mean	Std. error	Mean	Std. error	Mean	Std. error	Mean	Std. error	Mean	Std. error	Mean	Std. error	Mean	Std. error	Mean	Std. error
DM	[wt.%]	97.13	0.66	99.67	0.13	97.13	0.69	99.73	0.07	90.73	0.07	99.30	0.00	96.05	0.54	99.61	0.05
S	[mg/kg (DM)]	740.00	239.52	1,043.33	252.36	1,176.67	73.63	853.33	34.57	1,966.67	42.84	1,563.33	96.24	1,131.93	95.19	1,089.33	129.87
C	[wt.% (DM)]	1.42	0.45	1.47	0.06	3.33	0.74	3.66	0.48	6.24	0.39	6.32*	0.04	3.04	0.26	2.86	1.09
KW index	[mg/kg (DM)]	60.67	25.44	38.00	31.38	226.67	51.03	164.33	144.28	646.67	183.98	630.00	244.80	230.01	21.98	213.72	13.48
N	[wt.% (DM)]	0.15	0.01	0.14	0.01	0.20	0.01	0.21	0.02	0.35	0.04	0.33	0.05	0.20	0.00	0.21	0.01
Σ16PAHs/ EPA	[mg/kg (DM)]	0.25	0.43	1.70	2.27	0.68*	0.34	0.34*	0.44	3.35	0.76	8.59	6.23	0.86	0.38	2.68	1.66
TOC	[wt.% C (DM)]	0.27	0.08	0.26	0.04	1.60	0.49	2.25	0.61	4.56	0.36	4.85	0.19	1.56	0.18	1.99	0.19
Li	[mg/kg (DM)]	3.47	1.31	4.23	0.77	4.07	0.17	3.83	0.58	8.90	2.19	7.33	1.25	4.64	0.23	4.77	0.60
Be	[mg/kg (DM)]	<d.l.	-	<d.l.	-	<d.l.	-	<d.l.	-	<d.l.	-	<d.l.	-	<d.l.	-	<d.l.	-
Na	[mg/kg (DM)]	1,356.67	329.98	1,256.67	297.32	2,250.00	1,017.75	1,836.67	136.42	1,650.00	152.24	1,640.00	167.46	1,781.73	493.43	1,549.80	136.99
Mg	[mg/kg (DM)]	1,826.67	1,857.16	1,570.00	311.14	2,130.00	425.37	2,033.33	471.26	4,583.33	768.02	3,876.67	226.70	2,422.70	799.41	2,244.27	318.98
Al	[mg/kg (DM)]	5,643.33	843.36	6,620.00	1,082.80	6,270.00	373.43	6,276.67	892.49	9,440.00	1,211.45	9,136.67	1,324.14	6,551.97	299.83	7,050.07	448.93
Si	[mg/kg (DM)]	740.00	256.30	1,376.67	257.38	713.33	66.31	643.33	56.96	530.00	166.70	556.67	42.84	693.10	153.67	932.27	104.40
P	[mg/kg (DM)]	223.33	154.47	190.00	70.67	360.00	122.40	430.00	215.90	820.00	22.63	1,056.67	252.36	382.17	41.43	467.07	91.96
K	[mg/kg (DM)]	1,523.33	164.12	1,376.67	254.63	1,383.33	94.90	1,430.00	92.63	2,043.33	213.61	1,963.33	202.53	1,552.93	72.21	1,524.93	36.85
Ca	[mg/kg (DM)]	20,333.33	17,078.01	22,290.00	21,136.07	30,400.00	1,584.25	22,900.00	4,834.23	35,900.00	2,856.05	36,000.00	1,821.15	27,207.67	6,861.29	25,525.80	9,317.40
Ti	[mg/kg (DM)]	450.00	186.29	373.33	101.42	253.33	13.07	206.67	6.53	276.67	17.29	290.00	22.63	337.93	81.42	295.00	37.09
V	[mg/kg (DM)]	5.23	1.83	18.27	23.26	10.77	6.12	8.70	4.71	15.67	3.46	17.00	3.92	9.33	3.71	14.54	9.27
Cr	[mg/kg (DM)]	15.33	4.57	29.00	29.42	22.00	3.92	19.33	3.27	46.33	24.41	37.67	3.46	23.40	7.43	27.43	13.66
Mn	[mg/kg (DM)]	125.00	65.25	253.33	147.25	203.33	55.82	636.67	856.54	883.33	651.47	360.00	29.94	286.82	150.91	414.80	256.38
Fe	[mg/kg (DM)]	27,000.00	34,326.87	10,433.33	2,883.56	19,100.00	4,901.31	19,700.00	3,063.71	42,600.00	1,555.70	44,600.00	4,708.08	26,334.00	12,768.72	21,286.00	2,268.87
Co	[mg/kg (DM)]	4.40	1.02	2.60	0.79	3.30	0.34	2.57	0.17	7.57	1.75	5.57	0.57	4.48	0.23	3.24	0.35
Ni	[mg/kg (DM)]	8.73	1.21	7.43	0.17	14.00	1.13	11.33	1.73	31.33	6.23	26.33	3.97	14.79	1.99	13.00	0.79
Cu	[mg/kg (DM)]	10.50	5.39	9.60	2.40	31.33	14.42	52.67	26.74	74.33	19.93	84.00	35.30	30.10	7.35	41.47	14.59
Zn	[mg/kg (DM)]	83.00*	52.92	73.33	26.23	863.33	1,017.84	266.67	201.26	1,193.33	639.57	1,065.00*	499.80	588.15	323.91	283.00	186.87
As	[mg/kg (DM)]	30.67	40.51	<d.l.	-	<d.l.	-	<d.l.	-	<d.l.	-	<d.l.	-	-	-	<d.l.	-
Se	[mg/kg (DM)]	<d.l.	-	<d.l.	-	<d.l.	-	<d.l.	-	<d.l.	-	<d.l.	-	<d.l.	-	<d.l.	-
Sr	[mg/kg (DM)]	74.00	55.07	96.33	29.08	95.33	6.43	73.00	6.88	116.67	13.07	103.33	6.53	90.21	23.39	89.47	11.13
Mo	[mg/kg (DM)]	<d.l.	-	<d.l.	-	1.53	0.33	<d.l.	-	1.97	0.47	3.47	0.52	-	-	-	-
Pd	[mg/kg (DM)]	<d.l.	-	<d.l.	-	<d.l.	-	<d.l.	-	<d.l.	-	<d.l.	-	<d.l.	-	<d.l.	-
Ag	[mg/kg (DM)]	<d.l.	-	<d.l.	-	<d.l.	-	<d.l.	-	2.77	3.46	1.07	0.13	-	-	-	-
Cd	[mg/kg (DM)]	<d.l.	-	<d.l.	-	4.00	5.88	<d.l.	-	4.17	0.86	4.43	4.68	-	-	-	-
Sn	[mg/kg (DM)]	3.87	1.44	4.43	4.11	25.33	2.61	27.33	14.24	130.00	49.33	170.00	49.33	34.33	7.45	49.10	12.15
Sb	[mg/kg (DM)]	1.53	1.05	<d.l.	-	1.57	0.46	2.43	2.62	2.53	0.17	3.10	0.41	1.72	0.29	-	-
Te	[mg/kg (DM)]	<d.l.	-	<d.l.	-	<d.l.	-	<d.l.	-	<d.l.	-	<d.l.	-	<d.l.	-	<d.l.	-
Ba	[mg/kg (DM)]	77.33	42.36	106.67	6.53	105.00	14.97	104.33	26.21	840.00	594.82	360.00	79.21	218.61	116.05	161.56	20.08
W	[mg/kg (DM)]	<d.l.	-	<d.l.	-	<d.l.	-	<d.l.	-	<d.l.	-	<d.l.	-	<d.l.	-	<d.l.	-
Hg	[mg/kg (DM)]	<d.l.	-	<d.l.	-	<d.l.	-	<d.l.	-	<d.l.	-	<d.l.	-	<d.l.	-	<d.l.	-
Tl	[mg/kg (DM)]	<d.l.	-	<d.l.	-	<d.l.	-	<d.l.	-	<d.l.	-	<d.l.	-	<d.l.	-	<d.l.	-
Pb	[mg/kg (DM)]	34.00*	1.96	186.00	251.71	136.67	52.27	58.50*	26.46	250.00*	0.00	836.67	191.48	95.03	36.26	276.23	121.92

Notes: <d.l.= amount below detection limit. ar= as received. DM= dry mass. n=3, std. error with Ci of 95%.  
\*This parameter was determined from 2 measurements (n=2) instead of 3 (n=3).

es U-A and U-E.

Mixed as a single particle size range 90-4.5 mm, the “Inert” fractions are expected to comply with all parameters of the leaching tests: except for NH<sub>4</sub><sup>+</sup> and anionic surfactants.

The contents of NH<sub>4</sub><sup>+</sup> were generally larger in the owc state than in the dry state, which suggests that NH<sub>4</sub><sup>+</sup> is adsorbed to fine-grained particles which in turn are adhered to particles in the owc state and removed in the dry state. No

**TABLE 7:** Laboratory results of the leaching tests of the "Inert" fractions.

Parameter	Unit	90-30 mm				30-10 mm				10-4.5 mm			
		Owc		Dry		Owc		Dry		Owc		Dry	
		Mean	Std. error	Mean	Std. error	Mean	Std. error	Mean	Std. error	Mean	Std. error	Mean	Std. error
pH	[1]	9.13	0.17	10.30	0.69	8.23	0.69	8.87	0.46	7.27	0.26	7.70	0.00
Electric conductivity	[mS/m]	34.07	4.35	30.17	16.41	40.03	19.65	55.80	38.44	80.00	4.30	60.00	5.63
NH <sub>4</sub> <sup>+</sup>	[mg/kg (DM)]	30.67	14.06	20.00	8.98	4.40	1.58	29.33	1.31	16.00	2.99	64.33	9.62
Cl <sup>-</sup>	[mg/kg (DM)]	113.67	22.92	87.33	23.58	94.67	40.25	43.33	4.71	210.00	11.32	140.00	11.32
SO <sub>4</sub> <sup>2-</sup>	[mg/kg (DM)]	980.00	197.30	663.33	102.68	1,090.00	680.09	1,180.00	1,280.07	2,416.67	62.32	1,840.00	238.44
MBAS assay	[mg/kg (DM)]	<d.l.	-	<d.l.	-	1.23	0.36	<d.l.	-	1.07	0.13	1.07	0.13
TOC	[mg/kg (DM)]	52.00	9.09	49.90	20.68	50.23	12.77	58.77	17.60	96.17	2.52	125.67	8.03
KW index	[mg/kg (DM)]	<d.l.	-	<d.l.	-	<d.l.	-	<d.l.	-	0.51	0.02	<d.l.	-
NO <sub>2</sub> <sup>-</sup>	[mg/kg (DM)]	<d.l.	-	<d.l.	-	<d.l.	-	<d.l.	-	<d.l.	-	<d.l.	-
F	[mg/kg (DM)]	<d.l.	-	<d.l.	-	<d.l.	-	<d.l.	-	<d.l.	-	<d.l.	-
Li	[mg/kg (DM)]	0.05	0.02	0.05	0.02	0.05	0.02	0.03	0.01	0.08	0.01	0.04	0.01
Be	[mg/kg (DM)]	<d.l.	-	<d.l.	-	<d.l.	-	<d.l.	-	<d.l.	-	<d.l.	-
Na	[mg/kg (DM)]	89.67	14.77	64.00	13.34	95.67	28.09	63.33	10.51	183.33	6.53	133.33	6.53
Mg	[mg/kg (DM)]	28.67	12.41	10.57	7.73	42.67	23.26	23.67	15.20	103.00	6.88	66.00	8.84
Al	[mg/kg (DM)]	2.60	2.16	3.77	1.30	3.77	1.14	8.37	7.47	1.63	0.24	1.43	0.07
Si	[mg/kg (DM)]	59.00	18.70	135.00	103.09	25.33	3.64	27.33	11.78	19.00	1.13	23.67	1.73
P	[mg/kg (DM)]	0.64	0.47	0.23	0.10	0.22	0.07	0.56	0.30	0.30	0.04	0.74	0.12
K	[mg/kg (DM)]	100.67	9.22	86.33	10.45	109.33	40.51	113.33	26.13	213.33	6.53	220.00	11.32
Ca	[mg/kg (DM)]	546.67	180.47	466.67	243.32	1,013.33	567.65	713.33	523.16	1,486.67	199.35	996.67	444.99
Ti	[mg/kg (DM)]	0.02	0.01	0.04	0.02	0.01	0.00	0.02	0.01	0.02	0.00	0.02	0.01
V	[mg/kg (DM)]	0.07	0.03	0.76	1.11	0.01	0.00	0.07	0.06	<d.l.	-	<d.l.	-
Cr	[mg/kg (DM)]	<d.l.	-	0.02	0.00	<d.l.	-	<d.l.	-	<d.l.	-	<d.l.	-
Mn	[mg/kg (DM)]	0.05	0.03	0.04	0.03	0.09	0.08	0.06	0.05	0.31	0.05	0.57	0.17
Fe	[mg/kg (DM)]	0.64	0.21	0.65	0.54	0.59	0.12	0.88	0.44	1.51	0.57	1.24	0.55
Co	[mg/kg (DM)]	0.02	0.01	0.01	0.00	<d.l.	-	<d.l.	-	0.01	0.00	0.02	0.00
Ni	[mg/kg (DM)]	0.05	0.01	0.03	0.01	0.05	0.02	0.08	0.03	0.10	0.01	0.16	0.02
Cu	[mg/kg (DM)]	0.11	0.01	0.12	0.10	0.10	0.07	0.34	0.28	0.15	0.03	0.24	0.00
Zn	[mg/kg (DM)]	0.06	0.01	0.04	0.02	0.06	0.06	0.06	0.00	0.31	0.12	0.22	0.07
As	[mg/kg (DM)]	<d.l.	-	<d.l.	-	<d.l.	-	<d.l.	-	<d.l.	-	<d.l.	-
Se	[mg/kg (DM)]	<d.l.	-	<d.l.	-	<d.l.	-	<d.l.	-	<d.l.	-	<d.l.	-
Sr	[mg/kg (DM)]	1.07	0.13	0.93	0.37	1.51	0.89	1.09	0.89	2.63	0.17	2.07	0.17
Mo	[mg/kg (DM)]	0.13	0.09	0.09	0.05	0.05	0.02	0.06	0.01	0.06	0.01	0.15	0.02
Pd	[mg/kg (DM)]	<d.l.	-	<d.l.	-	<d.l.	-	<d.l.	-	<d.l.	-	<d.l.	-
Ag	[mg/kg (DM)]	<d.l.	-	<d.l.	-	<d.l.	-	<d.l.	-	<d.l.	-	<d.l.	-
Cd	[mg/kg (DM)]	<d.l.	-	<d.l.	-	<d.l.	-	<d.l.	-	<d.l.	-	<d.l.	-
Sn	[mg/kg (DM)]	<d.l.	-	<d.l.	-	<d.l.	-	<d.l.	-	<d.l.	-	0.02	0.00
Sb	[mg/kg (DM)]	0.01	0.00	0.01	0.00	0.03	0.03	0.03	0.03	0.03	0.01	0.05	0.02
Te	[mg/kg (DM)]	<d.l.	-	<d.l.	-	<d.l.	-	<d.l.	-	<d.l.	-	<d.l.	-
Ba	[mg/kg (DM)]	0.31	0.03	0.27	0.11	0.48	0.25	0.44	0.22	0.91	0.05	0.88	0.02
W	[mg/kg (DM)]	0.02	0.01	0.03	0.03	<d.l.	-	<d.l.	-	<d.l.	-	<d.l.	-
Hg	[mg/kg (DM)]	<d.l.	-	<d.l.	-	<d.l.	-	<d.l.	-	<d.l.	-	<d.l.	-
Tl	[mg/kg (DM)]	<d.l.	-	<d.l.	-	<d.l.	-	<d.l.	-	<d.l.	-	<d.l.	-
Pb	[mg/kg (DM)]	0.02	0.00	0.02	0.01	0.02	0.01	0.26	0.43	0.05	0.02	0.03	0.01

Notes: <d.l.= amount below detection limit. ar= as received. DM= dry mass. n=3, std. error with Ci of 95%.

clear trend was identified regarding the anionic surfactants among the particle size ranges and states.

The previous information suggests that, in general, the quality of the “Inert” fractions could be improved if handled as a mixed single particle size range (i.e. 90-4.5 mm). Nonetheless, the mixed single particle size range would very likely still exceed the limit values for  $\text{NH}_4^+$  for all quality classes.

### 3.2.1 Valorization of the Inert fractions as substitute for construction aggregates

Due to the lack of an overarching ordinance in the EU regarding the recycling of construction materials and aggregates, the employment of the “Inert” fractions obtained from landfill-mined waste as a substitute for construction aggregates either falls into a relative grey area of waste legislation in many of the EU countries, or is subjected to ordinances for materials other than landfill-mined waste. For instance, in Austria the “Inert” fractions would need further treatment in order to be valorized as a substitute for construction aggregates according to the RBV. None of the particle size ranges 90-30 mm, 30-10 mm and 10-4.5 mm were strictly suitable for that type of valorization individually, which as previously mentioned would result more problematic than the valorization of these fractions as a mixed single particle size range 90-4.5 mm. Hence, the “Inert” fractions could be valorized as a mixed single particle size range in Austria, provided that they are further processed in a cleaning treatment. This treatment is to be designed in such a way that the amount of anionic surfactants and  $\text{NH}_4^+$  are reduced and the limit values set in the RBV can be met. The content of  $\text{NH}_4^+$  could be significantly reduced with the implementation of a nitrification process, while the amount of anionic surfactants could be decreased by a washing step. As the problematic parameters in the “Inert” fractions were not exceeded by high amounts, the further treatment of these fractions in order to meet the corresponding limit values seems technically possible: nonetheless, this might render the (E)LFM process economics unfavorable. Furthermore, the valorization of the inert fractions in (E)LFM projects is of critical importance, since they can account for a significant share of the fine fractions; such as in this case study, in which they represent 35.5 wt.% and 37.2 wt.% in the owc and dry states, respectively. Similarly to the combustible fractions, both the recovered inert fractions from the coarse fractions (i.e. the 3D >200 mm and 3D 200-90 mm fractions in the MSG case study) and the fine fractions are likely to be valorized together and, hence, the quality of the overall recovered inert fractions might be substantially improved in this manner, as the inert fractions recovered from the coarse fractions commonly show lower amounts of surface defilements and account for a significant share of the processed material.

It is also relevant to stress, that inert materials obtained through (E)LFM are not precisely included into the scope of the RBV and, therefore, their employment as recycled construction aggregates is not guaranteed even if all specifications have been met. Moreover, additional specifications for this type of valorization, which were not investigated in this study, may apply in the RBV. Therefore, suitable WtM

schemes for the inert fractions recovered from the fine fractions of (E)LFM are to be further developed, while appropriate regulations need to be created at EU level.

## 4. CONCLUSIONS

The recovered “Combustibles” and “Inert” fractions from the fine fractions <90 mm of the MSG landfill case study corresponded to a material mainly composed of calorific fractions and a material constituted mostly by inorganic components, respectively. From an overarching perspective, the “Combustibles” fractions could be valorized as SRF in (co-)incineration, power and cement plants in the EU, under certain circumstances, since they meet the specifications established in the EN 15359:2011 in both the owc and dry states. These fractions could be valorized mixed in one single particle size range (i.e. 90-4.5 mm) in their original proportions or individually in particle size ranges (i.e. 90-30 mm, 30-10 mm and 10-4.5 mm). However, legislation on waste may vary from country to country in the EU and additional restrictions, as well as stricter limit values, can be applied in a specific member state. For example, in Austria these fractions can be incinerated, but not co-incinerated, according to the limit values for contaminants established in the AVV, as concentrations for As, Cd, Co, Hg and Pb were above the limit values in certain particle size ranges. In general, the quality of these fractions decreased with the decrease in particle size. As a mixed single particle size range only the concentrations of Cd, Hg and Pb exceeded the limit values.

In contrast to conventional (co-)incineration, the plasma gasification process proposed by the NEW-MINE project might offer an appealing WtE valorization route for the combustible fractions obtained from the fine fractions of landfill-mined waste, which in the present case study accounted for 12.5 wt.% and 9.0 wt.% of the total amount of the fine fractions in the owc and dry states, respectively. This valorization route could enable the upcycling of its residues into higher value-added products (e.g. glass-ceramics and inorganic polymers), in addition to the production of high quality energy carriers (e.g. hydrogen or methane): thus contributing to the economic and environmental feasibility of the project.

In Austria the “Inert” fractions would need further treatment in order to be valorized as a substitute for construction aggregates according to the RBV. None of the particle size ranges are strictly suitable for that type of valorization individually, as the contents of hydrocarbons, Cd, Pb, Zn,  $\text{NH}_4^+$  and anionic surfactants were above the limit values. As it was the case for the “Combustibles” fractions, the quality of the “Inert” fractions decreased as particle size decreased. The valorization of these fractions as a mixed single particle size range would be less problematic than as individual particle size ranges, since the limit values of less parameters (i.e. hydrocarbons, Pb and  $\text{NH}_4^+$ ) are expected to be exceeded in this way. Hence, the “Inert” fractions could be valorized as a mixed single particle size range in Austria, provided that they are further processed in a cleaning treatment. As the problematic parameters in this fraction were not exceeded by high amounts, the further treat-

ment of these fractions in order to meet the corresponding limit values seems technically possible. Furthermore, the valorization of the inert fractions in (E)LFM projects is of critical importance, since they can account for a significant share of the fine fractions; such as in this case study, in which they represent 35.5 wt.% and 37.2 wt.% in the owc and dry states, respectively. Therefore, suitable WtM valorization schemes for the inert fractions recovered from the fine fractions of (E)LFM are to be further developed and appropriate overarching regulations need to be created at EU level.

It is important to emphasize that both the combustible and inert fractions recovered from the fine fractions are likely to be valorized together with those recovered from the coarse fractions in (E)LFM projects and, therefore, the overall quality of the resulting fractions might be improved in this way, as the fractions recovered from the coarse fractions frequently show better quality and account for a significant share of the processed landfill-mined material.

In general, impurities were associated to the presence of organic and inorganic pollutants and, thus, to a decrease on the valorization potential of both the “Combustibles” and “Inert” fractions. Although the dry state visually presented a lower amount of surface defilements than the owc state, to process these fractions in the dry state did not suffice to comply with the corresponding Austrian limit values. Therefore, cleaning methods would be needed to remove the contaminants from the “Combustibles” and “Inert” fractions in Austria. However, it seems unlikely that those methods will be economically feasible, as prices of primary raw materials and regulations remain to be daunting obstacles for (E)LFM. The increasing market prices of primary raw materials, the development of a holistic legal framework for secondary raw materials and the raising public awareness will set the conditions to justify further material and energy recovery from the fine fractions from (E)LFM, as well as the employment of innovative waste processing and cleaning technologies.

## ACKNOWLEDGEMENTS

This research has been funded by the European Union’s Horizon 2020 research and innovation programme under the Marie Skłodowska-Curie grant agreement No. 721185 “NEW-MINE” (EU Training Network for Resource Recovery through Enhanced Landfill Mining; [www.new-mine.eu](http://www.new-mine.eu)). The authors wish to express their special gratitude to Renewi Belgium SA/NV, Stadler Anlagenbau GmbH, the Department of Processing and Recycling (IAR) of the RWTH Aachen University and the Chair of Waste Processing Technologies and Waste Management (AVAW) of the Montanuniversität Leoben, as well as its laboratory for environmental analyses, for their straightforward collaboration and support.

## REFERENCES

Ascensão, G., Marchi, M., Segata, M., Faleschini, F., & Pontikes, Y. (2019). Increasing the dimensional stability of CaO-FeOx-Al2O3-SiO2 alkali-activated materials: On the swelling potential of calcium oxide-rich admixtures. *Detritus*, 8(1), 91–100.

Bhatnagar, A., Kaczala, F., Burlakovs, J., Kriipsalu, M., Hogland, M., & Hogland, W. (2017). Hunting for valuables from landfills and assessing their market opportunities: A case study with Kudjape landfill in Estonia. *Waste Management & Research*, 35(6), 627–635.

Bureau d’études greisch (beg) (2002). Centre d’Enfouissement Technique de Mont-Saint-Guibert: Etude des conséquences de l’octroi du permis d’urbanisme du 29.10.01 sur les conditions d’exploitation du permis du 16.12.98.

Canopoli, L., Fidalgo, B., Coulon, F., & Wagland, S. T. (2018). Physico-chemical properties of excavated plastic from landfill mining and current recycling routes. *Waste management (New York, N.Y.)*, 76, 55–67.

Garcia Lopez, C., Ni, A., Hernández Parrodi, J. C., Küppers, B., Raulf, K., & Pretz, T. (2019). Characterization of landfill mining material after ballistic separation to evaluate material and energy recovery potential. *Detritus*, 8(1), 5–23.

Hernández Parrodi, J. C., Garcia Lopez, C., Küppers, B., Raulf, K., Vollprecht, D., Pretz, T., & Pomberger, R. (2019a). Case study on enhanced landfill mining at Mont-Saint-Guibert landfill in Belgium: Characterization and potential of fine fractions. *Detritus*, 8(1), 47–61.

Hernández Parrodi, J. C., Höllen, D., & Pomberger, R. (2018a). Characterization of fine fractions from landfill mining: A review of previous investigations. *Detritus*, 2(1), 46–62.

Hernández Parrodi, J. C., Höllen, D., & Pomberger, R. (2018b). Potential and main technological challenges for material and energy recovery from fine fractions of landfill mining: A critical review. *Detritus*, 3(1), 19–29.

Hernández Parrodi, J. C., Lucas, H., Gigantino, M., Sauve, G., Esguerra, J. L., Einhäupl, P., et al. (2019b). Integration of resource recovery into current waste management through (enhanced) landfill mining. *Detritus*, 8(1), 141–156.

Hernández Parrodi, J. C., Raulf, K., Vollprecht, D., Pretz, T., & Pomberger, R. (2019c). Case study on enhanced landfill mining at Mont-Saint-Guibert landfill in Belgium: Mechanical processing of fine fractions for material and energy recovery. *Detritus*, 8(1), 62–78.

Hogland, W. (2002). Remediation of an Old Landfill Site: Soil Analysis, Leachate Quality and Gas Production. *Environmental Science and Pollution Research*, 9(S1), 49–54.

Hull, R. M., Krogmann, U., & Strom, P. F. (2005). Composition and Characteristics of Excavated Materials from a New Jersey Landfill. *Journal of Environmental Engineering*, 131(3), 478–490.

Jones, P. T., Geysen, D., Tielemans, Y., Van Passel, S., Pontikes, Y., Blanpain, B., et al. (2013). Enhanced Landfill Mining in view of multiple resource recovery: a critical review. *Journal of Cleaner Production*, 55, 45–55.

Kaartinen, T., Sormunen, K., & Rintala, J. (2013). Case study on sampling, processing and characterization of landfilled municipal solid waste in the view of landfill mining. *Journal of Cleaner Production*, 55, 56–66.

Kaczala, F., Mehdinejad, M. H., Lääne, A., Orupöld, K., Bhatnagar, A., Kriipsalu, M., & Hogland, W. (2017). Leaching characteristics of the fine fraction from an excavated landfill: Physico-chemical characterization. *Journal of Material Cycles and Waste Management*, 19(1), 294–304.

Küppers, B., Hernández Parrodi, J. C., Garcia Lopez, C., Pomberger, R., & Vollprecht, D. (2019). Potential of sensor-based sorting in enhanced landfill mining. *Detritus*, 8(1), 24–30.

Kurian, J., Esakku, S., Palanivelu, K., & Selvam, A. (2003). Studies on landfill mining at solid waste dumpsites in India. *Proceedings Sardinia 2003. Ninth International Waste Management and Landfill Symposium*. 6-10 October, 2003. S. Margherita di Pula, Cagliari, Italy, 3, 248–255.

Lucas, H. I., Garcia Lopez, C., Hernández Parrodi, J. C., Vollprecht, D., Raulf, K., Pomberger, R., et al. (2019). Quality assessment of non-ferrous metals recovered from landfill mining: A case study in Belgium. *Detritus*, 8(1), 79–90.

Machiels, L., Arnout, L., Yan, P., Jones, P. T., Blanpain, B., & Pontikes, Y. (2017). Transforming Enhanced Landfill Mining Derived Gasification/Vitrification Glass into Low-Carbon Inorganic Polymer Binders and Building Products. *Journal of Sustainable Metallurgy*, 3(2), 405–415.

Monich, P. R., Romero, A. R., Höllen, D., & Bernardo, E. (2018). Porous glass-ceramics from alkali activation and sinter-crystallization of mixtures of waste glass and residues from plasma processing of municipal solid waste. *Journal of Cleaner Production*, 188, 871–878.



- Münnich, K., Fricke, K., Wanka, S., & Zeiner, A. (2013). Landfill Mining: A contribution to conservation of natural resources? Proceedings Sardinia 2013. Fourteenth International Waste Management and Landfill Symposium. 30 Sep. - 4 Oct., 2013. S. Margherita di Pula, Cagliari, Italy.
- Quaghebeur, M., Laenen, B., Geysen, D., Nielsen, P., Pontikes, Y., van Gerwen, T., & Spooren, J. (2013). Characterization of landfilled materials: screening of the enhanced landfill mining potential. *Journal of Cleaner Production*, 55, 72–83.
- Rabelo Monich, P., Dogrul, F., Lucas, H., Friedrich, B., & Bernardo, E. (2019). Strong porous glass-ceramics from alkali activation and sinter-crystallization of vitrified MSWI bottom ash. *Detritus*, 8(1), 101–108.
- Rabelo Monich, P., Vollprecht, D., & Bernardo, E. (2020). Dense glass-ceramics by fast sinter-crystallization of mixtures of waste-derived glasses. *International Journal of Applied Ceramic Technology*, 17(1), 55–63.
- Rincón, A., Marangoni, M., Cetin, S., & Bernardo, E. (2016). Recycling of inorganic waste in monolithic and cellular glass-based materials for structural and functional applications. *Journal of chemical technology and biotechnology (Oxford, Oxfordshire : 1986)*, 91(7), 1946–1961.
- Sarc, R., & Lorber, K. E. (2013). Production, quality and quality assurance of Refuse Derived Fuels (RDFs). *Waste management (New York, N.Y.)*, 33(9), 1825–1834.
- Saveyn, H., Eder, P., Garbarino, E., Muchova, L., Hjelmar, O., van der Sloot, H., et al. (2014). Study on methodological aspects regarding limit values for pollutants in aggregates in the context of the possible development of end-of-waste criteria under the EU Waste Framework Directive: Final report. EUR, Scientific and technical research series: Vol. 26769. Luxembourg: Publications Office.
- Sedlazeck, K. P., Höllen, D., Müller, P., Mischitz, R., & Gieré, R. (2017). Mineralogical and geochemical characterization of a chromium contamination in an aquifer - A combined analytical and modeling approach. *Applied Geochemistry*, 87, 44–56.
- Stessel, R. I., & Murphy, R. J. Processing of material mined from landfills. In *Mechanical Engineering Publications LTD 1992 – National Waste Processing Conference* (p. 101).
- Van Vossen, W. J., & Prent, O. J. (2011). Feasibility study: Sustainable material and energy recovery from landfills in Europe. *Proceedings Sardinia 2011. Thirteenth International Waste Management and Landfill Symposium. 3-7 October 2011. S. Margherita di Pula, Cagliari, Italy*, 247–248.
- Vollprecht, Frühauf, Stocker, & Ellersdorfer (2019). Ammonium Sorption from Landfill Leachates Using Natural and Modified Zeolites: Pre-Tests for a Novel Application of the Ion Exchanger Loop Stripping Process. *Minerals*, 9(8), 471.
- Vollprecht, D., Hernández Parrodi, J. C., Lucas, H., & Pomberger, R. (2020). Case study on enhanced landfill mining at Mont-Saint-Guibert landfill in Belgium: Mechanical processing, physico-chemical and mineralogical characterization of fine fractions <4.5 mm. *Detritus*, In press.
- Wagner, T. P., & Raymond, T. (2015). Landfill mining: Case study of a successful metals recovery project. *Waste Management*, 45, 448–457.
- Wolfsberger, T., Aldrian, A., Sarc, R., Hermann, R., Höllen, D., Budischowsky, A., et al. (2015). Landfill mining: Resource potential of Austrian landfills - Evaluation and quality assessment of recovered municipal solid waste by chemical analyses. *Waste Management & Research*, 33(11), 962–974.
- Zaini, I. N., García López, C., Pretz, T., Yang, W., & Jönsson, P. G. (2019). Characterization of pyrolysis products of high-ash excavated-waste and its char gasification reactivity and kinetics under a steam atmosphere. *Waste management (New York, N.Y.)*, 97, 149–163.
- Zaini, I. N., Yang, W., & Jönsson, P. G. (2017). Steam gasification of solid recovered fuel char derived from landfill waste: A kinetic study. *Energy Procedia*, 142, 723–729.

## SILVER RECOVERY FROM END-OF-LIFE PHOTOVOLTAIC PANELS

Larisse Suzy Silva de Oliveira <sup>1</sup>, Maria Tereza Weitzel Dias Carneiro Lima <sup>2</sup>, Luciana Harue Yamane <sup>1</sup> and Renato Ribeiro Siman <sup>1,\*</sup>

<sup>1</sup> Department of Environmental Engineering, Federal University of Espírito Santo, Fernando Ferrari Avenue 514, Goiabeiras, Vitória, 29075-910, Brazil

<sup>2</sup> Department of Chemistry, Federal University of Espírito Santo, Fernando Ferrari Avenue 514, Goiabeiras, Vitória, 29075-910, Brazil

### Article Info:

Received:  
11 November 2019  
Revised:  
17 February 2020  
Accepted:  
24 February 2020  
Available online:  
31 March 2020

### Keywords:

Photovoltaic panel  
Silver recovery  
Hydrometallurgical  
E-waste  
Recycling

### ABSTRACT

The growth of the photovoltaic sector has stood out among renewable sources of energy, due to technological innovations that have brought about cost reductions. Thus, this paper aimed to analyze the technical feasibility of silver recovery from photovoltaic cells using acid leaching, followed by an evaluation of the chemical and electrochemical precipitation processes to analyze their efficiencies. As a primary objective of this work, the gravimetric composition and the metal concentration (Ag, Al, Pb, Cu, and Fe) in the photovoltaic cells were first determined, developing the basis for future research on photovoltaic panels recycling. Subsequently, the influence of HNO<sub>3</sub> concentration (1-10 mol/L), temperature (25-60°C), and reaction time were evaluated. A new research application used a statistical tool, the Central Composite Rotational Design (CCRD), as well as samples of different brands and models of photovoltaic panels, in order to ensure the experimental validity. As a highlight, the analysis of the composition of the photovoltaic cells, applying the HNO<sub>3</sub> leaching, showed that up to 6.87 kg of silver can be recovered per ton of photovoltaic cells. It was possible to solubilize 100% of the silver contained in the photovoltaic cells using the optimal parameters. Silver precipitation by addition of HCl and Na<sub>2</sub>CO<sub>3</sub>, as well as electroprecipitation, made it possible to extract more than 99% of silver in solution, being a primary novelty of this study. Therefore, the studied pathway allowed for the recovery of 99.98% of the silver present in the photovoltaic cells.

## 1. INTRODUCTION

The development of alternative energy sources has been explored in order to increase energy supply and to replace or reduce the exploitation of non-renewable sources. Among the renewable sources of energy, solar energy from photovoltaic panels is one of the most used and efficient methods (Europe, 2018). It is estimated that an installed power of 26.7MW allows for saving about 560,700 t of Carbon dioxide equivalent (tCO<sub>2</sub>eq) during the lifetime of the photovoltaic system, as an alternate to fossil fuels. If the photovoltaic panels were recycled instead of being landfilled, it can additionally save about 1600-2400 tCO<sub>2</sub>eq. (D'Adamo et al., 2017).

Rapid development of the photovoltaic industry has presented a global challenge with respect to the recycling of valuable components from end-of-life photovoltaic panels, due to the approximate 30 year lifespan of these panels (Song et al., 2020).

It is estimated that by the year 2050, 78 million tons of photovoltaic panels will need to be disposed of around the world, but information about their destinations (recy-

cling) and final disposal are still scarce (Weckend, Wade, & Heath, 2016). According to Domínguez & Geyer (2019), there will be 800 thousand metric tons (Mt) of end-of-life photovoltaic panels in need of disposal between 2030 and 2060 in the United States alone. Table 1 shows some estimates of photovoltaic panels waste.

Due to this potential generation of end-of-life photovoltaic panels in the coming years, some studies evaluating different recycling processes and routes have been conducted. They have especially focused on crystalline silicon panels, representing 85-90% of the market due to low prices and mature manufacturing technology (Song et al., 2020).

Silicon photovoltaic panels are composed of an aluminum frame, tempered glass, a silicon photovoltaic cell with metal filaments that are wrapped in two layers of encapsulating material, and a backsheet (Tammamo et al., 2016). The main metals present in photovoltaic panels are lead, copper, aluminum, and silver (Dias et al., 2016). The composition of a silicon photovoltaic panel (a) and its cell (b) is shown in Figure 1.

\* Corresponding author:  
Renato Ribeiro Siman  
email: renato.siman@ufes.br

**TABLE 1:** Estimates of photovoltaic panel waste generation.

Area	Year	Tonnes	Reference
World	2030	8 millions	Weckend et al. (2016)
	2030	1.7 millions	Gangwar et al. (2019)
	2035	1 million	International Energy Agency (2013)
	2038	1.9 millions	Paiano (2015)
	2050	60 millions	Gangwar et al. (2019)
	2050	78 millions	Weckend et al., 2016
Czech republic	2025	545 thousand	Kumar & Sarkan (2013)
Europe	2020	18 thousand	Larsen (2009)
Italy	2050	8 millions	Paiano (2015)
EUA	2050	9.57 millions	Monier & Hestin (2011)
EUA	2060	9.8 millions	Domínguez & Geyer (2019)
Spain	2030	100 thousand	Santos & Alonso-García (2018)
Spain	2050	700 thousand	Santos & Alonso-García (2018)

Materials such as aluminum, silicon, gold, steel, and copper represent around 75% of the total value of a photovoltaic panel system (including inverters, transformers, cabling, and mouting), but Figure 1 shows the composition for only the photovoltaic panel and cell (Domínguez & Geyer, 2019).

Although several studies have been carried out with the aim of recovering silicon, aluminum, or glass in photovoltaic panels (Azeumo et al., 2019; Dias et al., 2017; Fiandra et al., 2019), exploration of silver extraction methods is of more recent interest, and there is still a need to improve the feasibility of processes (Kuczyńska-Łażewska et al., 2018). Additionally, Apergis & Apergis (2019) analyzed the role of solar energy production in driving silver prices, pointing out that higher silver prices due to decreases in supply could negatively affect promotion of solar energy sources and their sustainable growth.

In this sense, Deng, Chang, Ouyang, & Chong (2019) suggested that value recovery, including recovering intact silicon wafers and silver, should be a pursued in order to

make high-value recycling more attractive, in addition to current mass recovery of glass and the aluminium frame carried out by recyclers. Dias et al. (2016) studied the extraction of silver from photovoltaic modules via the solubilization of silver in nitric acid. This process was followed by precipitation with addition of sodium chloride, where recovery of 94% of silver was achieved. In a second test, the samples were submitted to pyrolysis prior to the acid leaching process, and silver recovery was 92%.

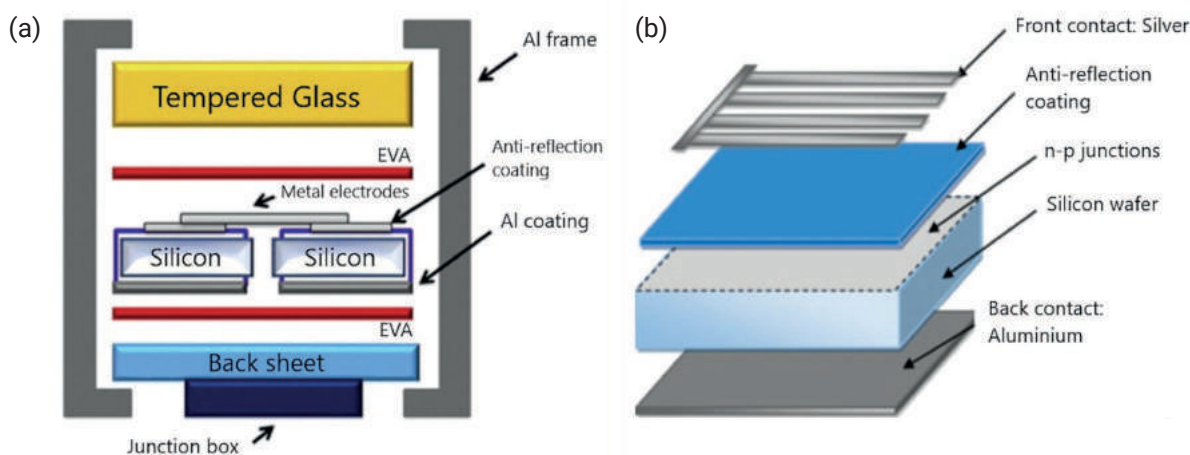
Kuczyńska-Łażewska et al. (2018) analyzed the silver and aluminium extraction from the solar cell using acid and basic leaching process with HNO<sub>3</sub> and NaOH at different concentrations and temperatures. They concluded that there is no justified need for highly corrosive substances, such as hydrofluoric acid, strong oxidising agents, or temperatures above 60°C, except for removal of metals from the solar cell surface.

Moreover, silver concentration was investigated by Song et al. (2020) using high voltage fragmentation and by Nevala et al. (2019) using electro-hydraulic fragmentation as a substitutes for mechanical methods to dismantle end-of-life photovoltaic panels. This was done to concentrate valuable metals on specific particle size fractions in order to facilitate the separation and recovery of metals.

Therefore, it is possible to use several techniques to recycle and recover the metals present in photovoltaic panels, and it is necessary to evaluate technical, economic, and environmental aspects to choose the routes to be used.

In the review performed by Padoan, Altamari, & Paganelli (2019) comparing solutions proposed over the past two decades to recycle photovoltaic panels, it was highlighted that energy consumption in a recycling process is less than that spent in the manufacturing of a new panel, and recovery techniques are in constant development.

Del Pero et al. (2019) performed a Life Cycle Assessment of a recycling process (mobile pilot scale) of solar panels waste. The investigation of all Life Cycle stages showed that recycling from different material fractions (aluminum, glass, copper, silicon, and plastics) allows for achieving great environmental benefits, due to avoided production of new materials and energy. Also, according to



**FIGURE 1:** Composition of a panel (a) and a silicon photovoltaic cell (b) of first generation. Adapted from KANG et al. (2012); So; Yu (2015). Legend: EVA - ethylene-vinyl acetate.

Sica et al. (2018), the photovoltaic sector may be one of the biggest contributors to the circular economy, applying the metaphor of natural systems to the production of goods and services. They estimated that about 42 new photovoltaic panels can be produced by the recycling of 100 used photovoltaic panels.

The photovoltaic sector is trying to improve photovoltaic panels design from an ecological perspective. Some producers are investing in research to find less hazardous materials and production processes with low environmental impact in order to reduce risks for the human health and environment (Sica et al., 2018).

In this sense, the present study evaluates the feasibility of a novel route to selectively extract and recover the silver from photovoltaic cells by nitric acid leaching, followed by selective silver precipitation (chemical and electrochemical). Comparison of silver precipitation processes by addition of HCl and electroprecipitation as the last step of the proposed route is the primary study novelty.

Although few studies have used electrochemical or chemical precipitation to recover silver from photovoltaic panels (Lee, et al., 2013; Yousef et al., 2019), the present study contributes an analysis of three different models of photovoltaic panels, using three units of each model and three samples of each unit (triplicate). With this number of samples and using statistic tools in a Central Composite Rotational Design (CCRD) to generate response surfaces and perform analysis of variance (ANOVA), the obtained results are more consistent and reliable.

Progress in the reuse processes for the photovoltaic panels components will allow for the minimization of environmental impacts generated from its inadequate disposal, such as the reduction of carbon footprint, and also to reduce the consumption of resources from primary sources (Yousef et al., 2019).

## 2. MATERIALS AND METHODS

The experimental procedure began with the experimental design and with the collection of the end-of-life photo-

voltaic panels. Afterwards, the gravimetric composition of the photovoltaic panels (STEP 1) was determined. The photovoltaic cells were removed by manual and thermal separation, followed by the characterization stage (STEP 2) and acid leaching tests (STEPS 3 and 4). Finally, the recovery of silver in solution was performed using chemical and electrochemical precipitation (STEP 5).

### 2.1 End-of-life photovoltaic panels

Three photovoltaic panels were donated by the Solar Brasil Tecnologia & Energia Fotovoltaica Ltda (São Paulo, Brazil) company, presenting damaged protection glass.

In order to allow for comparison of the results, 6 photovoltaic panels of two different models (3 of each) were acquired. In this way, 9 photovoltaic panels (three models) formed of polycrystalline silicon (1st generation) were analyzed. Table 2 shows the main characteristics of the panels, and Figure 2 illustrates an example of each photovoltaic panel model used in the research.

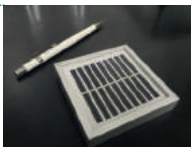

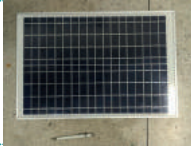
### 2.2 Step 1 - Gravimetric composition of end-of-life photovoltaic panels

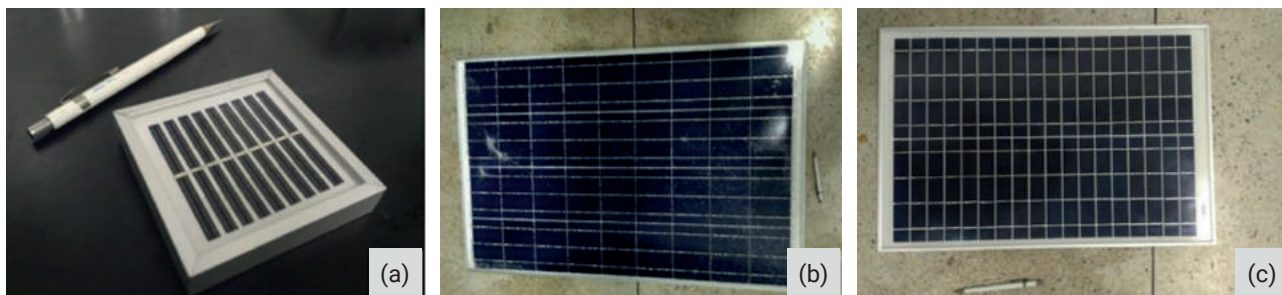
The photovoltaic panels were individually weighed on a balance (brand Marte/50 kg scale). Using manual separation, each model of photovoltaic panels was analyzed for the percentages of aluminum, glass, photovoltaic cells, and polymeric material that compose them. To do so, photovoltaic cell size portions of each photovoltaic panels were sampled.

Using the average composition of the photovoltaic cells analyzed, the ratio of glass and polymer was calculated to estimate the weight of the panel edges that did not contain photovoltaic cells. The weight of the photovoltaic cells was subtracted from the photovoltaic panel total, and the proportions obtained between polymers and glass were used to estimate the weight of these components in areas where there were no photovoltaic cells.

To separate the glass, polymers, and photovoltaic cells, nine portions (defined by cell size) of each photovoltaic panel model were placed in the muffler oven (Linn

**TABLE 2:** Main characteristics of the photovoltaic panels used in the research.

Model	Model image	Brand	Potency (W)	Dimensions (cm) (Length x Width x Thickness)	Weight (kg)	N° of photovoltaic cells	Effective area - cell area (m <sup>2</sup> )
A		Star Solar (Guangzhou)	0.5	8 x 8 x 1.2	0.13	18	0.027
B		Yingli	95	102 x 66 x 3	8.0	36	0.584
C		Komaes	20	50 x 35 x 2.5	2.4	36	0.146



**FIGURE 2:** Models of photovoltaic panels used for research. Legend: (a) Star solar, (b) Yingli, and (c) Komaes.

Elektro Therm) for 20 min at a temperature of 600°C, using a method adapted from Dias et al. (2016) and Kang et al. (2012). The obtained material was weighed before and after the time in the muffle oven for determination of the polymer fraction. The glass, metal filaments, and photovoltaic cells were then manually separated and weighted.

### 2.3 Step 2 - Characterization of photovoltaic cells

The photovoltaic panels were fractionated manually and subjected to thermal separation for removal of the ethylene-vinyl acetate (EVA) polymer film. The samples were placed in the muffle oven at a temperature of 600°C for 20 min. The photovoltaic cells were then manually separated and comminuted in a porcelain mortar. This process is illustrated in Figure 3.

The photovoltaic cells of each photovoltaic panel were used in the determination of Ag, Cu, Al, Fe, and Pb in Steps 2 and 3. The metals were chosen according to the composition of photovoltaic panels already reported in the literature (Dias et al., 2016; Kuczyńska-Lażewska et al., 2018a; Latunussa et al., 2016).

The characterization of the metals was carried out initially using aqua regia, which is commonly used for the determination of the metallic composition of e-waste (Dias et al., 2016; Hubau et al., 2019).

Nine photovoltaic cells comminuted from each photovoltaic panel model were digested in aqua regia, composing twenty-seven characterization tests in total. The nitric and hydrochloric acids used were previously distilled to ultrapurify them and minimize contamination of the samples. Also, all glassworks were cleaned and decontaminated by treatment in alkaline detergent solution (5% v/v) for 24h, in acidic solution (15% v/v) for 24 h, and then rinsed with ultrapure water.

The samples were digested in triplicate using Erlenmeyer flasks with a nominal capacity of 250 mL. The samples were maintained in the solution for 2h at a ratio of 0.05 g/mL and, then, filtered on a filter paper (Unifil) with 1-2 µm particle retention.

Before the filtration process, the weights of the filter paper, crucibles, and samples were measured on an analytical balance (Quimis/Q-500L210C). After filtration, the filter paper containing the insoluble fraction was oven dried (Logen Scientific) in a ceramic crucible for 48 h at 70°C. Then, it was transferred to a desiccator for cooling in a moisture-free atmosphere and was again weighed in analytical balance.

The mass balance was then calculated. From the difference between the calculated mass of metals and the total weight of the sample, the mass of the silicon present in the photovoltaic cells can be estimated.

Aliquots of the liquid fraction obtained after filtration were sent for quantitative determination of Cu by the Inductively Coupled Plasma Spectrometry (ICP-MS) (Perkin Elmer/Nexlon 300D), as well as for the determination of Ag, Pb, Fe, and Al by Flame Atomic Absorption Spectrometry (FAAS) (Analytik Jena/Zeenit 700). Both tests were performed in the Atomic Spectroscopy Laboratory at the Federal University of Espírito Santo in Brazil.

As silver can react with the hydrochloric acid present in aqua regia to form a precipitate (AgCl) (Dias et al., 2016; Yang et al., 2017), a complementary silver solubilization test was performed using the nitric acid. The results obtained in this test were used as a reference for the silver extraction in the following stages. The experiment was performed using only photovoltaic cell samples from the photovoltaic panel model that presented a higher concentration of silver during the characterization process with aqua regia.

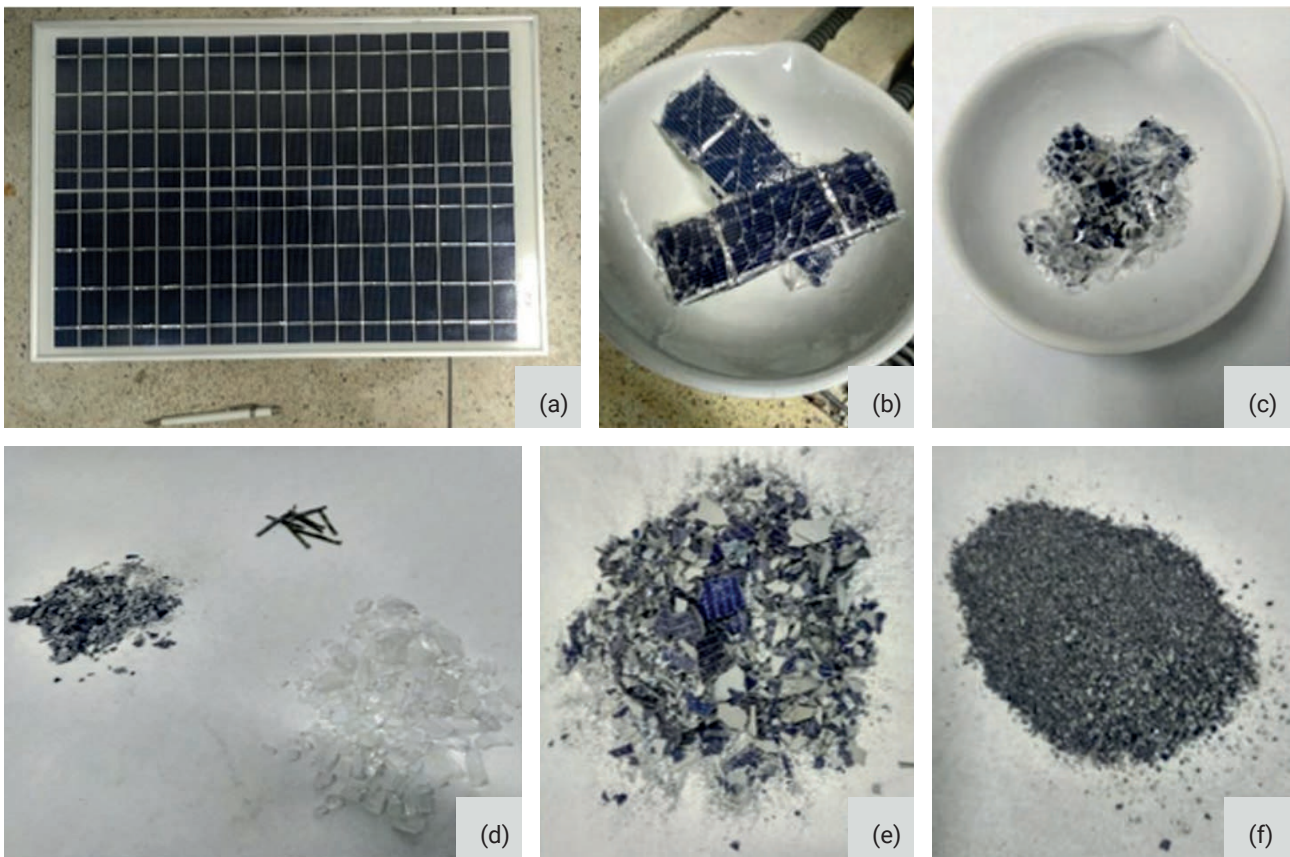
The results obtained by leaching with nitric acid, used as a reference for the concentration of silver in the photovoltaic cells, was performed under a temperature of 55°C and concentration of 2.3 mol/L of HNO<sub>3</sub>. These conditions were established after different tests to optimize the solubilization of silver.

### 2.4 Step 3 - Nitric acid leaching of photovoltaic cells

In Step 3, the comminuted photovoltaic cells, which were mechanically processed in Step 2 and stored, were used. These samples were homogenized and quartered for each model of photovoltaic cells, obtaining samples of 5 g each. Silver acid leaching was then carried out using nitric acid at different concentrations and controlled temperatures.

The solid-liquid ratio used was 0.05 g/mL, and in order to minimize energy costs, no magnetic stirring was used. In acid leaching, nitric acid was used at different concentrations (1-10 mol/L), simulating a range of room temperature (25°C) to higher temperatures (60°C). The optimal temperature (42°C) for the solubilization of silver, suggested by Rojas & Martins (2010) and by Dias et al. (2016), was also tested.

Erlenmeyer flasks with nominal capacity of 250 mL were placed on a shaker with heating control (Tecnal/TE-0853). All procedures were performed inside a laboratory



**FIGURE 3:** Process of separation and comminution of photovoltaic cells. Legend: a) Photovoltaic panel; b) Separated photovoltaic samples; c) Photovoltaic samples after the muffler oven; d) Manual separation of glass, metal filaments, and photovoltaic cells; e) Separated photovoltaic cells; f) Comminuted photovoltaic cells.

fume hood with forced ventilation, and the temperature of the acid leaching system was monitored using a mercury thermometer (Inco term, -10/+110°C).

The analytical balance was used to weigh samples of comminuted material. After 2 hours, each of the leached solutions obtained was filtered using filter paper with particle retention of 1-2 µm and were analyzed by FAAS to determine Ag, Pb, and Al concentrations.

Considering that results from Joda & Rashchi (2012) and Motta (2018) showed that the Central Composite Rotational Design (CCRD) can be used to optimize the amount of tests and leaching inputs and also reach results similar to those obtained by the complete factorial method, the CCRD was used for the experimental design of the acid leaching stage.

The number of experiments was determined by the CCRD using two factors: nitric acid concentration and tem-

perature. Table 3 presents the alpha values generated by the model between the maximum values (10 mol/L; 60°C) and minimum values (1 mol/L; 25°C).

Applying the CCRD, 4 vertex points, 4 axial points, and 3 replicates were used for the center, totaling 11 experiments per model of photovoltaic panel, as shown in Table 4.

From the experimental results, a mathematical model was determined, and response surfaces were generated.

**TABLE 3:** Maximum parameters adopted and corresponding alpha values.

Parameters	Codes	Alpha values (α)				
		-1.41	-1	0	1	1.41
HNO <sub>3</sub> concentration (mol/L)	X1	1	2.3	5.5	8.7	10
Temperature (°C)	X2	25	30	42	55	60

**TABLE 4:** Tests stipulated by the CCRD.

Experiment (n°)	HNO <sub>3</sub> concentration (mol/L)	Temperature (°C)
1	2.3	30
2	8.7	30
3	2.3	55
4	8.7	55
5	1	42
6	10	42
7	5.5	25
8	5.5	60
9	5.5	42
10	5.5	42
11	5.5	42

Using a statistical tool of analysis of variance (ANOVA), the significance and adequacy of the model was tested. For analysis of the data, the Fischer variation ratio (F value) was also applied, providing a statistically valid measure of how well the factors describe the variation in the mean data.

## 2.5 Step 4 - Analysis of nitric acid leaching of silver versus time

The combination of temperature and nitric acid concentration, identified in Step 3 as more efficient for acid leaching of silver, was adopted in a new experiment. In this experiment, three quartered samples of 5 g of the photovoltaic panel model C were used. To optimize the testing time, 10 mL aliquots were sampled every 30 min for analysis in order to construct the silver extraction ratio curve with respect to the reaction time. With the results of the triplicates, the extraction averages were calculated for each time period.

The aliquots were filtered and used for analysis by FAAS to determine the Ag, Pb, and Al concentration. The leached solutions were separated so that the one with the highest solubilization of silver was used in Step 5.

## 2.6 Step 5 - Silver recovery by precipitation

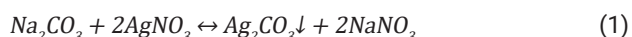
This step aimed to determine the silver recovery by chemical and electrochemical precipitation while comparing the obtained results.

### 2.6.1 Chemical precipitation of silver

In the chemical precipitation, the sodium carbonate and hydrochloric acid reagents were used, which were selected based on the information from Vogel (1981) regarding their effectiveness on silver precipitation.

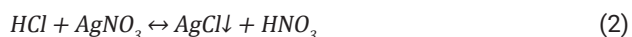
After the acid leaching, about 200 mL of the solution obtained in the optimum silver extraction conditions were separated for the precipitation step.

A solution of 0.1 mol/L sodium carbonate ( $\text{Na}_2\text{CO}_3$ ) was added to 50 mL of the sample to precipitate silver carbonate ( $\text{Ag}_2\text{CO}_3$ ), according to the reaction presented in Equation 1:



The amount of sodium carbonate solution added was calculated by stoichiometry, augmenting with an additional 20% (v/v) from the calculated value. This was based on the silver concentration determined by FAAS.

In another 50 mL of the sample, a 37% hydrochloric acid solution (HCl) was added to precipitate the silver chloride (AgCl), according to the reaction presented in Equation 2:



The amount of hydrochloric acid solution added was also calculated by stoichiometry, augmenting with an additional 20% (v/v) from the calculated value. This was based on the silver concentration determined by FAAS. The solutions were filtered by quantitative filter paper with 1-2  $\mu\text{m}$  particle retention, and an aliquot of the solution was removed for ICP-MS analysis to determine the residual silver concentration of each experiment.

### 2.6.2 Electrochemical silver precipitation

In this test, 50 mL of the leached solutions were submitted to an electrochemical process for the precipitation of silver in solution.

A platinum plate (7cm×2cm) was used as a positive electrode, a steel plate (7cm×2cm) was used as a negative electrode, and the current density was 60 A/m<sup>2</sup>. Based on the analyses performed by Lee et al. (2013) and Raju, Chung, & Moon (2009), the test was maintained for 1 h. The space between the electrodes was 30 mm, and the temperature was 21°C. The pH of the solution at the time of the experiment was 2.5. To perform the experiment, the electrolytic cell was mounted in a 100 mL glass vessel with the platinum electrode and the stainless-steel electrode used as anode and cathode, respectively.

The electrodes were connected to a digital electric source (Minipa/MPS-3005, 30V/5A) to provide direct current, and the voltage and current were monitored using a multimeter (Minipa/MA-149). The leached solution was then filtered via quantitative filter paper with particle retention of 1-2  $\mu\text{m}$ , and the liquid fraction was analyzed by FAAS to determine the residual silver concentration.

## 3. RESULTS AND DISCUSSION

Following the five steps described in section 2, it was possible to achieve and discuss some results that are presented in sections 3.1 to 3.5. The experimental planning and its results were analyzed with the support of statistical tools and professionals in order to ensure its reability.

### 3.1 Step 1 - Gravimetric composition of end-of-life photovoltaic panels

Table 5 shows the average composition of each analyzed material for the three photovoltaic panel models, presenting the standard deviation and the mean. The composition of each panel is also shown in Figure 4.

Latunussa et al. (2016) observed that the photovoltaic panel consisted of 70% glass, 18% aluminum frame, 5.1% EVA (polymer), 3.7% photovoltaic cell, and 1.5% backsheets polymer, among other materials.

These data corroborate the result obtained in this stage of the research, showing differences regarding the percentage of glass and aluminum for Model A. The photovoltaic panel of Model A was made with a glass of lower resistance; however, it had a reinforced aluminum frame, justifying

**TABLE 5:** Statistical analysis of the gravimetric composition of the photovoltaic panel models (percentage by mass).

Variable (%)	Aluminum Frame	Glass	Cell	Filaments	Polymers
Panel A	49.98	36.73	1.91	0.35	11.04
Panel B	12.68	70.9	4.89	0.65	10.88
Panel C	14.86	68.16	4.01	0.87	12.10
Mean	25.84	58.60	3.60	0.62	11.34
Standard deviation	20.93	18.99	1.53	0.26	0.67

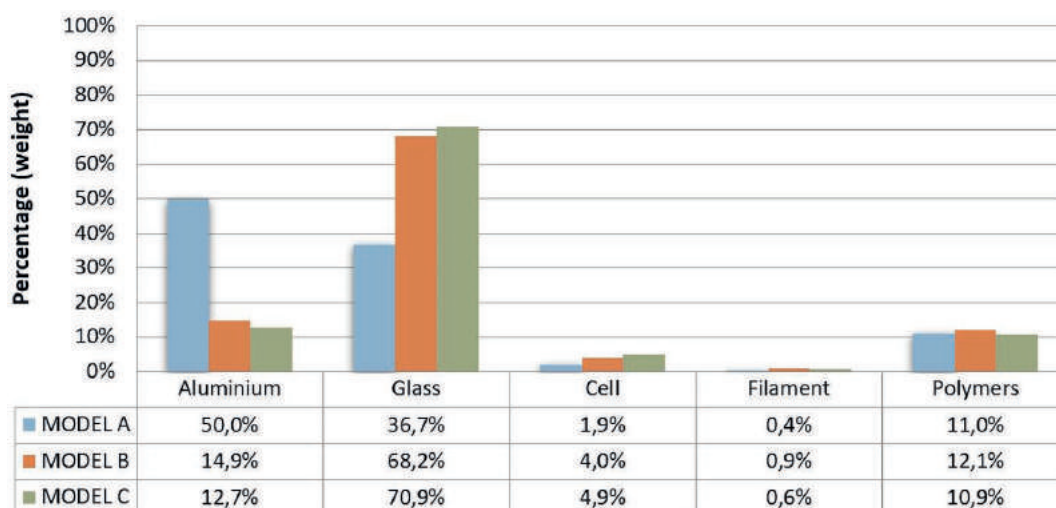


FIGURE 4: Gravimetric composition of analyzed photovoltaic panels (percentage by mass).

fying the obtained result. The other observed differences resulted from variation in the model and manufacturer of photovoltaic panels.

The fraction where the silver is found (photovoltaic cell) is superior in the composition of photovoltaic panels when compared to the percentage of PCB from e-waste, which is widely studied for the recovery of metals (Hubau et al., 2019; Motta, 2018; Rebelllo, 2018). Photovoltaic panels also have less heterogeneity than other e-wastes. For example, the composition of the photovoltaic panels is more than 80% glass and aluminum frame, which are materials that can be separated and recycled. Thus, determination of the gravimetric composition of the photovoltaic panels indicates the relevance of studies aimed at the recycling these materials.

### 3.2 Step 2 - Characterization of photovoltaic cells

Table 6 summarizes the characterization results for the photovoltaic cells of the three models and shows the average concentration of each metal, the metals not identified in this study, and the fraction of silicon of the cells.

According to Paiano (2015), other metals such as zinc and tin can also be part of photovoltaic cells, possibly be-

ing components of the metals fraction not identified in the present work.

For Model A, the silver presented a concentration of 0.29 kg/ton in photovoltaic cells. Model B presented about 0.86 kg of silver per ton in photovoltaic cells. Approximately 2.6 kg of silver per ton of photovoltaic cells were found in Model C.

From the results obtained in the characterization with aqua regia, Model C of the photovoltaic panels was selected for use in a leaching test with nitric acid because it presented a higher concentration of silver. Figure 5 shows the composition of photovoltaic panel C, considering the new silver concentration result obtained through nitric acid leaching.

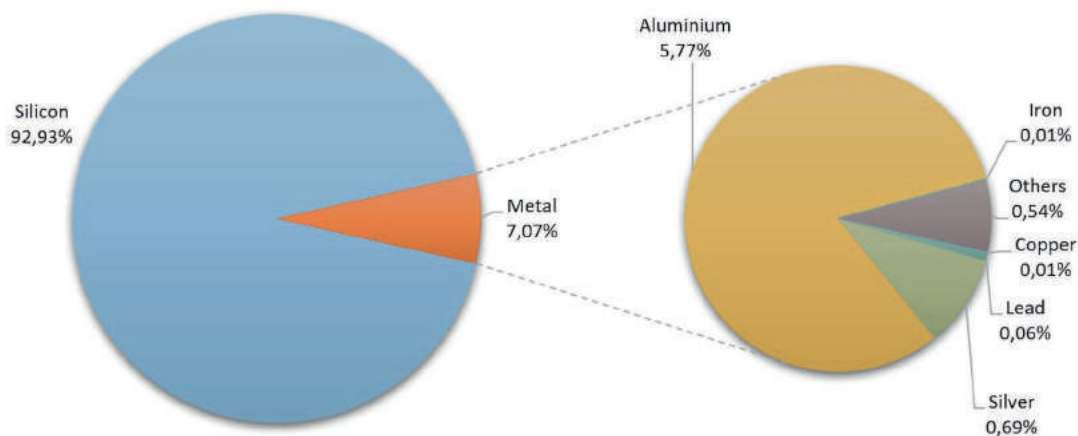
Using this reference value for silver, it is inferred that it is possible to recover up to 6.87 kg of silver in one ton of photovoltaic cells. This result is close to the one found by Chen et al. (2020), reporting 5.7 kg of silver in one ton of photovoltaic cells. Based on these results and aiming at the recycling of silver, the characterization with nitric acid should be preferentially used, since it allows for greater solubilization of this metal in relation to the digestion with aqua regia.

TABLE 6: Characterization of the photovoltaic cells of the different models of photovoltaic panels.

Variable (%)	Composition of the photovoltaic cell (% by mass)						
	Silver (Ag)	Copper (Cu)	Aluminium (Al)	Lead (Pb)	Iron (Fe)	Other metals	Silicon (Si)
Model A	0.03	1.20	3.30	0.13	<DL	3.78	91.55
$\sigma$ A	0.01	0.69	0.84	0.10	-	9.71	3.04
Model B	0.09	0.02	6.73	0.27	0.005	2.18	90.71
$\sigma$ B	0.01	0.02	0.83	0.18	0.001	10.87	1.64
Model C	0.26	0.01	5.77	0.06	0.006	0.96	92.93
$\sigma$ C	0.07	0.01	0.63	0.02	0.005	6.81	0.43
Mean	0.13	0.41	5.27	0.15	0.004	2.31	91.73
$\sigma$	0.12	0.69	1.77	0.11	0.003	1.41	1.12

Legend:  $\sigma$  = Standard deviation; DL = detection limit (LQferro = 0.316 mg/L)





**FIGURE 5:** Characterization of the photovoltaic cells from Photovoltaic Panel Model C, considering the silver concentration obtained in the solubilization with nitric acid.

Padoan et al. (2019) provided a review on the recycling of photovoltaic panels and showed that literature presents an Ag concentration in photovoltaic panels that ranges between 60-525 mg/kg. The present research observed 336 mg/kg, which is a result that is close to the average proposed by Padoan et al (about 300 mg/kg).

Regarding silver, it is possible to observe that the concentration range in photovoltaic cells reported in the different studies (0.08-1.67%) is higher than that found in PCB (0.06-0.21%) (Kasper et al., 2011; Lee et al., 2013; Olson et al., 2013). According to the U.S. Geological Survey (2015), economically viable extraction of silver from ore requires a minimum concentration of 0.07% by mass. Thus, the importance of silver recovery from photovoltaic cells is justified, according to the experiments performed in the present study because its concentration in photovoltaic cells is up to 0.69%.

### 3.3 Step 3 - Nitric acid leaching of photovoltaic cells

In the nitric acid leaching stage, only Model C of the photovoltaic panels was studied, since it presented a high-

er concentration of silver, according to Step 2. Each experiment at this stage was performed for 2 hours. The results obtained for the silver acid leaching experiments of the photovoltaic cells, as well as the parameters used, are presented in Table 7.

Table 7 also shows the results for solubilized aluminum and lead concentrations, and these elements were determined together with silver because they presented higher concentrations than the other metals in the characterization step.

From the statistical analysis using ANOVA, the values of the statistically significant coefficients were generated. From these, it was possible to create a mathematical model (Equation 3), which indicates the percentage of silver extraction as a function of temperature and acid concentration.

$$\text{Silver solubilization (\%)} = -0.39 \times [\text{HNO}_3]^2 - 0.015 \times [T]^2 + 5.24 \times [\text{HNO}_3] + 1.77 \times T \quad (3)$$

The mathematical model for the CCRD presented an  $R^2 = 0.99$ . In this sense, based on the  $R^2$  value, the CCRD

**TABLE 7:** Results of silver, lead, and aluminum concentration obtained in the acid leaching tests with 2h of duration for Model C of photovoltaic panel.

Experiment (n°)	Concentration of HNO <sub>3</sub> (mol/L)	Temperature (°C)	Ag		Al		Pb	
			mg/L	%	mg/L	%	mg/L	%
1	2.3	30	171.08	50	2492.75	74	42.25	30
2	8.7	30	203.25	59	2525.00	75	3.22	2
3	2.3	55	254.18	74	3490.00	100	55.00	39
4	8.7	55	234.73	68	2845.00	85	42.03	30
5	1	42	<DL	<DL	1686.75	50	16.70	12
6	10	42	207.85	60	2665.00	80	72.38	52
7	5.5	25	180.13	52	2252.75	67	46.43	33
8	5.5	60	218.53	63	3352.50	100	47.00	34
9	5.5	42	243.20	71	2637.50	79	52.30	37
10	5.5	42	208.83	61	3095.00	92	41.98	30
11	5.5	42	216.60	63	2757.50	82	84.08	60

Legend: DL = Detection limit (DL Ag = 0.07754)

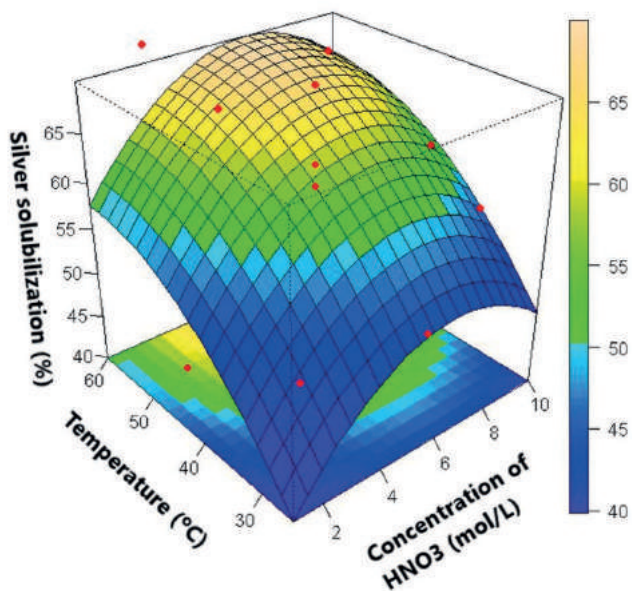


FIGURE 6: Contour curve for the central composite rotational design model - Model C.

model can be used as a predictive model (Joda & Rashchi, 2012). Figure 6 shows the contour curve generated from the mathematical model obtained with the significant parameters and using the software Action.

The yellow-orange color area in the graph shown in Figure 6 shows the combination of temperature and nitric acid concentration, obtaining better silver solubilization (60-70%). The response surface generated from the results suggests, among the ranges of parameters analyzed, that temperatures between 50-60°C combined with HNO<sub>3</sub> concentration between 2-10 mol/L are better applicable for the solubilization of silver present in photovoltaic cells. Using the Minitab software, the main effects graph was generated, as shown in Figure 7.

As observed in Figure 7, there is no great variation in the silver solubilization percentage (60-63%) in the nitrate acid concentration range of 2.3-10 mol/L, and therefore, it was de-

cidated to adopt 55°C and an HNO<sub>3</sub> concentration of 2.3 mol/L as optimum parameters, considering that this test allowed for the solubilization of 74% of the silver. These parameters were further defined in order to minimize the use of nitric acid, since a lower concentration of the reagent is used.

In their study, Joda & Rashchi (2012) used a CCRD and performed acid leaching, obtaining up to 87.3% of silver solubilization with temperatures between 60-70°C and HNO<sub>3</sub> concentrations between 3-4 mol/L. They also observed the increase in PCB silver extraction by increasing the HNO<sub>3</sub> concentration.

These parameters are also close to those calculated in the current research as optimal for silver extraction. It is well known that silver extraction can be obtained with nitric acid leaching (Deng et al., 2019; Tao & Yu, 2015; Yousef et al., 2019); however, parameters such as temperature, acid concentration, reaction time, and solid ratio still need to be explored, as many different results are obtained with the variation of this parameters (Dias et al., 2016; Shin et al., 2017; Yousef et al., 2019).

### 3.4 Step 4 - Analysis of nitric acid leaching of silver versus time

At this stage, the optimum conditions of temperature (55°C) and nitric acid concentration (2.3 mol / L), identified by the response surface method (Fig.6) and by the main effects graph for acid leaching of silver (Fig.7), were used in a new experiment. The aim was to analyze the reaction time of 2 h, based on the results of Dias et al. (2016), Joda & Rashchi (2012), and Lee et al. (2013). Figure 8 shows the percentages of extraction of Ag, Al, and Pb over time.

The values of silver extraction by time, presented in Figure 8, were calculated based on the relationship between the concentration of silver obtained in the reference leaching (nitric acid) and the results obtained by time in the present step. The solubilization of the other metals (Pb and Al) was compared with the average obtained in the characterization with aqua regia.

Rojas & Martins (2010) studied the recovery of Ag of jewelry scraps using concentrated nitric acid and conclud-

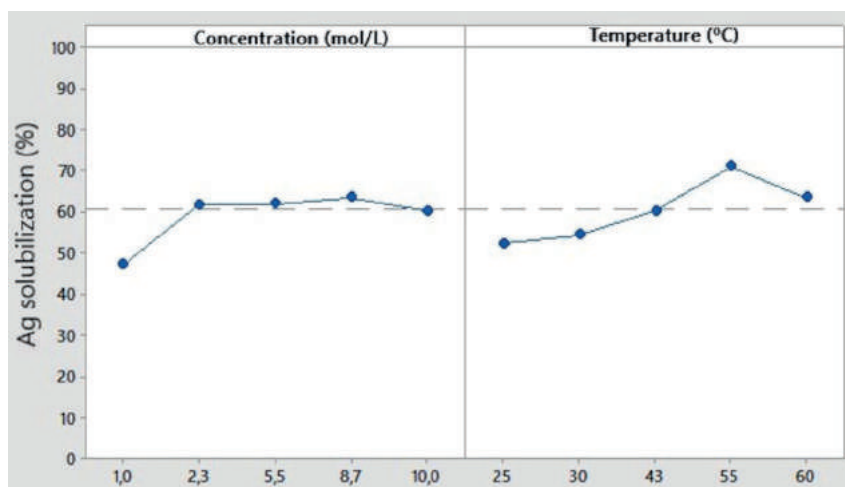


FIGURE 7: Main Effects for Ag Solubilization (%).

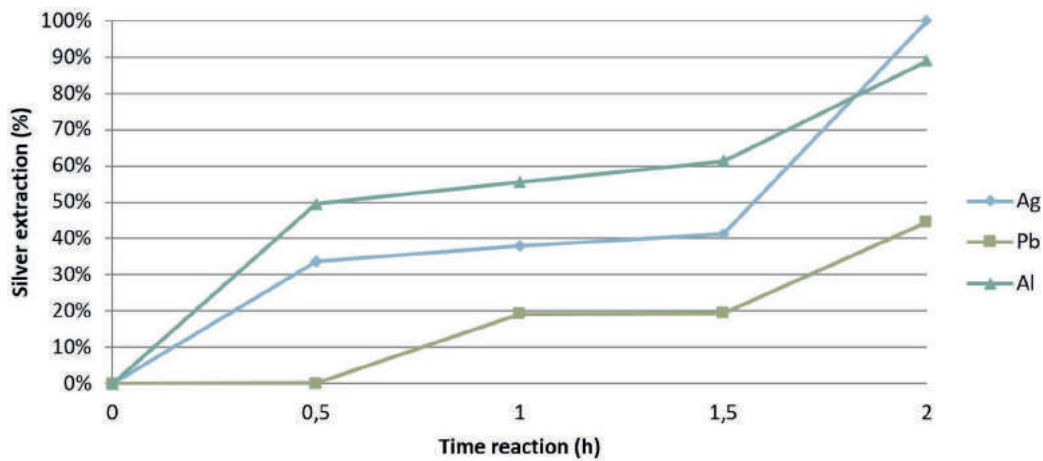


FIGURE 8: Percentage of Ag, Pb, and Al extraction versus time - Model C.

ed that about 2 hours at a temperature of 43°C was an ideal reaction time. These results corroborate those found in the present study, where the reaction time of 2 h with a temperature of 55°C was able to solubilize 95% of the silver present in the photovoltaic cell. Although the temperature used is 12°C higher than that used in the Rojas & Martins research, dilute nitric acid (2.3 mol/L) was used here.

Chen et al. (2020) used a 4 mol/L nitric acid concentration under the conditions of 80°C for 4 hours, and then, 3 mol/L sodium hydroxide at 70°C for 3 hours achieved a leaching efficiency of 99.7% of Ag and 99.9% of Al from photovoltaic solar panels. In the present study, Ag solubilization was achieved with less time reaction, a less concentrated acid, and a lower temperature. However, the Al leaching was lower than that achieved by Chen et al. (2020), who performed an extra leaching experiment with sodium hydroxide. Savvilitidou & Gidarakos (2019) also analyzed the extraction and concentration of silver from waste crystalline silicon photovoltaic panels. The leaching conditions used were a solid:liquid ratio of 0.02, 30% HNO<sub>3</sub>, controlled temperature of 20°C, constant agitation of 150 rpm for one hour experiment, and they achieved 93-100% of Ag leaching efficiency. Comparing with this experiment, both the results and the applied parameters are very similar. The temperature used by Savvilitidou & Gidarakos (2019) was lower, but a higher acid concentration was applied. Though their reaction time was lower, they used a magnetic stirrer, which was not used in the present study.

In order to apply Equation 3 from Step 3, the parameters used in other researches were added to the equation

to estimate the silver leaching results (Table 8). As the optimum result was obtained at Step 4 when the best conditions from Step 3 were applied to a new experiment, the equation results were the compared.

Some of the equation results underestimate the real silver leaching percentage obtained by the authors. This can be explained by the variation of other parameters (reaction time, solid liquid ratio, and agitation) that are not apply in the equation.

Considering that photovoltaic cells are mainly composed of Al, Ag, and Si, the remaining comminuted and filtered material after the acid leaching process will be mostly silicon, which can also be recovered (Lee et al., 2013; Padoan et al., 2019).

For silver reuse, it is important that its extraction occurs selectively, providing a metal of greater purity. However, about 88% of aluminum and 44% of lead was also solubilized. Thus, it is necessary to use other processes to separate these metals. Solubilization of Al and Pb indicates that nitric acid leaching can also be used to recover these metals that have additional economic value. Otherwise, the other metals like lead need to be removed to avoid contamination, as it is considered a potentially toxic metal.

### 3.5 Step 5 - Silver recovery by precipitation

In this step, the silver extraction was determined by chemical and electrochemical precipitation to compare these results. In order to perform this test, the leaching solution obtained in Step 4 was used with the following pa-

TABLE 8: Comparison between Silver leaching results estimated by Equation 3 and other researches that applied nitric acid leaching.

Reference	HNO <sub>3</sub> concentration (mol/L)	Temperature (°C)	Other parameters	Silver leaching results (%)	Silver leaching estimate by Equation 3 (%)
Present article	2.3	55	0.05 g/mL, 2 h	100	100
C.-H. Lee et al. (2018)	5	70	0.1 g/mL, 2 h	Not analyzed	100
Chen et al. (2020)	4	80	0.01 g/mL, 4 h	99.7	97
Savvilitidou & Gidarakos, (2019)	6.45	20	0.02 g/mL, 1 h, magnetic agitation	93	76
(Dias et al. (2016)	13.8	25	0.05 g/mL, 2 h, magnetic agitation	94	53

rameters: temperature of 55°C, concentration of HNO<sub>3</sub> of 2.3 mol/L, and reaction time of 2 hours. Figure 9 shows the percentage of silver extraction obtained by each evaluated method.

The chemical precipitation with sodium carbonate extracted about 48% of the silver in solution, suggesting that this is not a suitable reagent under the circumstances analyzed in this experiment. This was also the method with the highest precipitation of the other metals in solution (32% of Pb and 25% of Al), causing greater contamination of the precipitate.

The methods that presented the highest silver removal efficiency were electroprecipitation and the addition of hydrochloric acid, recovering 99.98% and 99.93%, respectively, of silver in solution.

Yousef et al. (2019) studied the Ag extraction from photovoltaic panels using nitric while adding HCl to the solution, and they achieved 97.65% of silver extraction. Lee et al. (2013) analyzed the silver precipitation by addition of HCl and by electroprecipitation. In its study, HCl was added to solution containing Ag. The reaction was maintained for 2h at different temperatures, obtaining the maximum recovery of 89.74% of Ag. In the electrochemical analysis, the experiment was conducted for 4h with 50 mL of the electrolytic solution with an electrical density of 60 A/m<sup>2</sup> at pH 5, obtaining a recovery of 87.44% of the silver in solution.

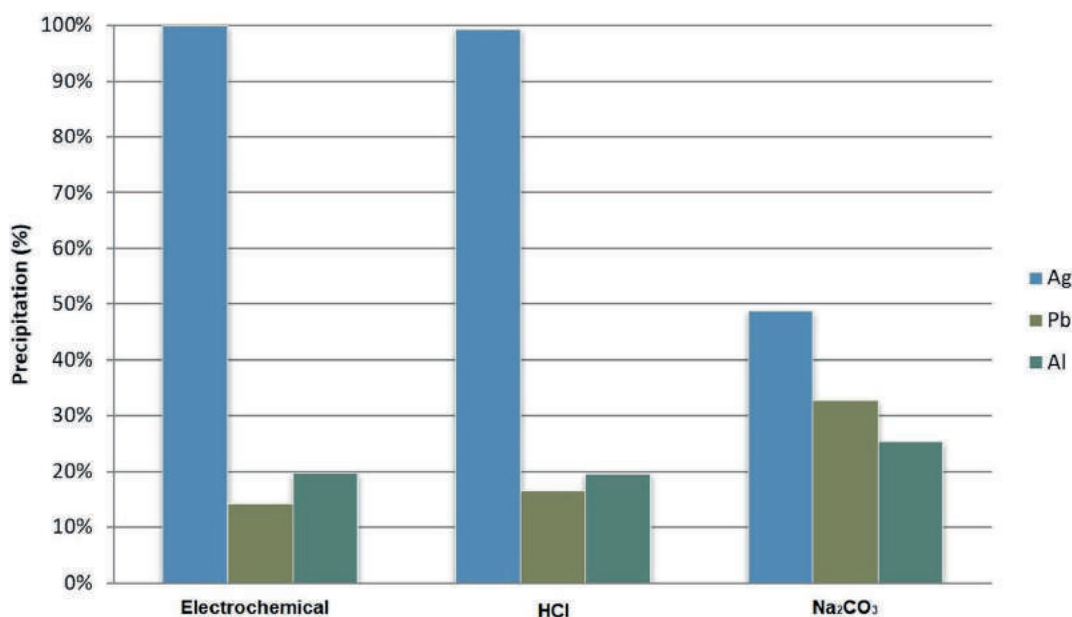
In the present study, it was possible to precipitate over 99% of the silver with the addition of HCl and reaction time of 5 min, which is more than what was obtained by both Lee et al. (2013) and Yousef et al. (2019). In the electrochemical assay, it was also possible to precipitate over 99% of the silver by applying a current density of 60 A/m<sup>2</sup> at a 2.5 pH and a reaction time of 1 h. Thus, in the present study, the results were better than those of Lee et al. (2013), although there was a shorter reaction time.

As observed, the electrochemical process and the chemical precipitation with addition of HCl were shown to be equivalent in relation to the silver extraction.

Chemical precipitation has higher costs for reagents. However, the development of processes allowing for the regeneration of the employed reactants could reduce the environmental impact and the processing costs of chemical methods (Padoan et al., 2019).

According to Prado & Ruotolo (2016), although there is energy consumption in the electrochemical process, it can still be economically attractive when comparing the prices of energy and metallic silver. However, the used parameters, such as electrode potential and the applied current, require strict control during electrolysis in order to avoid uncontrolled reactions and thus loss of recoverable silver (Prado & Ruotolo, 2016).

Electroprecipitation presents lesser contamination of lead in the precipitate, however, other factors should be analyzed to determine which is better, and there should also be more replicates of this experiment to ensure this is a phenomenon rather than some experiment error. When comparing the percentage of precipitation between the three procedures, it is observed that the electrochemical procedure and the chemical precipitation with HCl present very close values. This indicates that the two procedures are equivalent in terms of percentage of recovery. However, the Na<sub>2</sub>CO<sub>3</sub> chemical precipitation procedure differs greatly from the others. This result can be explained by the solubility of the salts. Ag<sub>2</sub>CO<sub>3</sub> is more soluble than AgCl under the same conditions, which results in a lower percentage of silver precipitation when carbonate is used. For lead, the situation is reversed, that is, PbCl<sub>2</sub> is much more soluble than PbCO<sub>3</sub>, and this results in less lead precipitation when HCl is used as a precipitant. Electrochemically, the lead reduction potential is very low, which makes it difficult to reduce and, consequently, makes its precipitation difficult.



**FIGURE 9:** Percentage of silver, lead, and aluminum extraction of photovoltaic cells from Photovoltaic Panel Model C by chemical precipitation (HCl and Na<sub>2</sub>CO<sub>3</sub>) and electroprecipitation.

Though it is of great importance the research on a laboratory scale to improve parameters of the photovoltaic panels recycling, it is also important to consider the issues to take it to the commercial scale. Zhang & Xu (2016) emphasized the importance of the analysis of factors such as: investment cost, wastewater generation, level of method industrialization, degree of toxicity of the materials used, and accessibility of these materials.

Mahmoudi et al. (2019) also said that to develop and scale up the current photovoltaic panel recycling, it is necessary to reduce the gas emission and temperature during the delamination process. This could be done by choosing a proper mixing ratio for the etching process, decrease the use of chemicals and its wastes production, and achieve a high level of purification. However, changing from a pilot level to the industrial scale is imperative to ensure the recycling of all the amount of photovoltaic panel waste that will be generated and to prove economic feasibility (Cucchiella et al., 2015). The economic feasibility of the recycling requires collaborative action of all stakeholders in the industry. Deng et al. (2019) highlights that the government authorities should consider cost and regulation changes to discourage landfill of PV modules. Also, the manufacturers should include recycling viability into photovoltaic panels design and consider how to use second-life materials in their production systems.

#### 4. CONCLUSIONS

The novelty of the present article was a statistical basis to compare the different parameters analyzed to improve the silver recovery from photovoltaic panels. The CCRD applications, as well as the use of samples of different brands and models of photovoltaic panels, are some of the highlights of this research.

Another main contribution of this work is the determination of the gravimetric composition of silicon photovoltaic panels, which was imperative in estimating the potential recovery of each component. According to the results, the fraction where the silver (photovoltaic cell) is found is superior in the photovoltaic panel composition when compared to the percentage of PCB from e-waste. Therefore, the importance of studying the metals recovery of photovoltaic cells is justified (material with lower heterogeneity than others e-waste, making the recycling easier).

Analysis of the photovoltaic cells, according to the results for leaching with  $\text{HNO}_3$ , presented greater solubilization of silver, showing that up to 6.87 kg of silver can be recovered per ton of photovoltaic cells.

One of the findings of this research proved that there is no need to use high nitric acid concentrations for silver leaching, reducing reagent costs, and disposal. The solubilization of silver using nitric acid in a solid-liquid ratio of 0.05 g/mL and 2 h of reaction time highlighted the following optimal parameters: temperature of 55°C and 2.3 mol/L of  $\text{HNO}_3$  concentration. The statistical evaluation indicated that the temperature and the concentration of nitric acid are significant factors in the solubilization of silver.

Regarding the reaction time for silver solubilization, it was possible to solubilize 100% of silver in solution over 2 hours using the optimum parameters obtained.

The electrochemical process and the chemical precipitation with addition of HCl were shown to be equivalent in relation to the silver extraction, and for the electroprecipitation test, there was less contamination of lead in the precipitate.

The recycling route studied achieved the goal of recovering up to 99.98% of the silver from photovoltaic cells by combining processes involving acid leaching by nitric acid followed by electroprecipitation process.

#### ACKNOWLEDGEMENTS

This research was supported by the Fundação de Amparo à Pesquisa e Inovação do Espírito Santo (FAPES), Espírito Santo, Brazil (Process nº 68781369/2014 and Process nº 83757392/2018). We would also like to thank Michael James Stablein of the University of Illinois Urbana-Champaign for his translation services and review of this paper.

#### REFERENCES

- Apergis, I., & Apergis, N. (2019). Silver prices and solar energy production. *Environmental Science and Pollution Research*, 26(9), 8525–8532. <https://doi.org/10.1007/s11356-019-04357-1>
- Azeumo, M. F., Germana, C., Ippolito, N. M., Franco, M., Luigi, P., & Settimio, S. (2019). Photovoltaic module recycling, a physical and a chemical recovery process. *Solar Energy Materials and Solar Cells*, 193, 314–319. <https://doi.org/10.1016/j.solmat.2019.01.035>
- Chen, W.-S., Chen, Y.-J., Yueh, K.-C., Cheng, C.-P., & Chang, T.-C. (2020). Recovery of valuable metal from Photovoltaic solar cells through extraction. *IOP Conference Series: Materials Science and Engineering*, 720, 012007. <https://doi.org/10.1088/1757-899X/720/1/012007>
- Cucchiella, F., D'Adamo, I., Lenny Koh, S. C., & Rosa, P. (2015). Recycling of WEEEs: An economic assessment of present and future e-waste streams. *Renewable and Sustainable Energy Reviews*, 51, 263–272. <https://doi.org/10.1016/j.rser.2015.06.010>
- D'Adamo, I., Miliacca, M., & Rosa, P. (2017). Economic Feasibility for Recycling of Waste Crystalline Silicon Photovoltaic Modules. *International Journal of Photoenergy*, 2017, 1–7. <https://doi.org/10.1155/2017/4184676>
- Del Pero, F., Delogu, M., Berzi, L., & Escamilla, M. (2019). Innovative device for mechanical treatment of End of Life photovoltaic panels: Technical and environmental analysis. *Waste Management*. <https://doi.org/10.1016/j.wasman.2019.06.037>
- Deng, R., Chang, N. L., Ouyang, Z., & Chong, C. M. (2019). A techno-economic review of silicon photovoltaic module recycling. *Renewable and Sustainable Energy Reviews*, 109(April), 532–550. <https://doi.org/10.1016/j.rser.2019.04.020>
- Dias, P., Javimczik, S., Benevit, M., & Veit, H. (2017). Recycling WEEE: Polymer characterization and pyrolysis study for waste of crystalline silicon photovoltaic modules. *Waste Management*, 60, 716–722. <https://doi.org/10.1016/j.wasman.2016.08.036>
- Dias, P., Javimczik, S., Benevit, M., Veit, H., & Bernardes, A. M. (2016). Recycling WEEE: Extraction and concentration of silver from waste crystalline silicon photovoltaic modules. *Waste Management*, 57, 220–225. <https://doi.org/10.1016/j.wasman.2016.03.016>
- Domínguez, A., & Geyer, R. (2019). Photovoltaic waste assessment of major photovoltaic installations in the United States of America. *Renewable Energy*, 133, 1188–1200. <https://doi.org/10.1016/j.renene.2018.08.063>
- Europe, S. P. (2018). *Global Market Outlook for Solar Power 2018-2022*. <http://www.solarpowereurope.org/wp-content/uploads/2018/09/Global-Market-Outlook-2018-2022.pdf>

- Fiandra, V., Sannino, L., Andreozzi, C., Corcelli, F., & Graditi, G. (2019). Silicon photovoltaic modules at end-of-life: Removal of polymeric layers and separation of materials. *Waste Management*, 87, 97–107. <https://doi.org/10.1016/j.wasman.2019.02.004>
- Gangwar, P., Kumar, N. M., Singh, A. K., Jayakumar, A., & Mathew, M. (2019). Solar photovoltaic tree and its end-of-life management using thermal and chemical treatments for material recovery. *Case Studies in Thermal Engineering*. <https://doi.org/10.1016/j.csite.2019.100474>
- Hubau, A., Chagnes, A., Minier, M., Touzé, S., Chapron, S., & Guezennec, A.-G. (2019). Recycling-oriented methodology to sample and characterize the metal composition of waste Printed Circuit Boards. *Waste Management*, 91, 62–71. <https://doi.org/10.1016/J.WASMAN.2019.04.041>
- International Energy Agency. (2013). Trends 2013 in Photovoltaic Applications: photovoltaic power systems programme. [http://www.iea-pvps.org/fileadmin/dam/public/report/statistics/FINAL\\_TRENDS\\_v1.02.pdf](http://www.iea-pvps.org/fileadmin/dam/public/report/statistics/FINAL_TRENDS_v1.02.pdf)
- Joda, N. N., & Rashchi, F. (2012). Recovery of ultra fine grained silver and copper from PC board scraps. *Separation and Purification Technology*, 92, 36–42. <https://doi.org/10.1016/j.seppur.2012.03.022>
- Kang, S., Yoo, S., Lee, J., Boo, B., & Ryu, H. (2012). Experimental investigations for recycling of silicon and glass from waste photovoltaic modules. *Renewable Energy*, 47, 152–159. <https://doi.org/10.1016/j.renene.2012.04.030>
- Kasper, A. C., Berselli, G. B. T., Freitas, B. D., Tenório, J. A. S., Bernardes, A. M., & Veit, H. M. (2011). Printed wiring boards for mobile phones: Characterization and recycling of copper. *Waste Management*, 31(12), 2536–2545. <https://doi.org/10.1016/j.wasman.2011.08.013>
- Kuczyńska-Lażewska, A., Klugmann-Radziemska, E., Sobczak, Z., & Klimczuk, T. (2018a). Recovery of silver metallization from damaged silicon cells. *Solar Energy Materials and Solar Cells*, 176, 190–195. <https://doi.org/10.1016/J.SOLMAT.2017.12.004>
- Kuczyńska-Lażewska, A., Klugmann-Radziemska, E., Sobczak, Z., & Klimczuk, T. (2018b). Recovery of silver metallization from damaged silicon cells. *Solar Energy Materials and Solar Cells*, 176, 190–195. <https://doi.org/10.1016/j.solmat.2017.12.004>
- Kumar, S., & Sarkan, B. (2013). Design for reliability with weibull analysis for photovoltaic modules. *Int. J. Curr. Eng. Technol*, 129–134.
- Larsen, K. (2009). End-of-life PV: then what? *Renewable Energy Focus*. [https://doi.org/10.1016/S1755-0084\(09\)70154-1](https://doi.org/10.1016/S1755-0084(09)70154-1)
- Latunussa, C. E. L., Ardente, F., Blengini, G. A., & Mancini, L. (2016). Life Cycle Assessment of an innovative recycling process for crystalline silicon photovoltaic panels. *Solar Energy Materials and Solar Cells*, 156, 101–111. <https://doi.org/10.1016/j.solmat.2016.03.020>
- Lee, C.-H., Chang, Y.-W., Popuri, S. R., Hung, C.-E., Liao, C.-H., Chang, J.-E., & Chen, W.-S. (2018). *Environmental Engineering and Management* (Vol. 17, Issue 3). [http://www.eemj.eu](http://www.eemj.icpm.tuiasi.ro/http://www.eemj.eu)
- Lee, C. H., Hung, C. E., Tsai, S. L., Popuri, S. R., & Liao, C. H. (2013). Resource recovery of scrap silicon solar battery cell. *Waste Management and Research*, 31(5), 518–524. <https://doi.org/10.1177/0734242X13479433>
- Mahmoudi, S., Huda, N., Alavi, Z., Islam, M. T., & Behnia, M. (2019). End-of-life photovoltaic modules: A systematic quantitative literature review. In *Resources, Conservation and Recycling*. <https://doi.org/10.1016/j.resconrec.2019.03.018>
- Monier, V., & Hestin, M. (2011). Study on Photovoltaic panels supplementing the impact assessment for a recast of the WEEE directive. In *Bio Intelligence Service* (Issue April).
- Motta, V. C. N. da. (2018). Extração de cobre de placas de circuito impresso de tablets por lixiviação ácida e precipitação seletiva. Federal University of Espírito Santo.
- Nevala, S. M., Hamuyuni, J., Junnila, T., Sirviö, T., Eisert, S., Wilson, B. P., Serna-Guerrero, R., & Lundström, M. (2019). Electro-hydraulic fragmentation vs conventional crushing of photovoltaic panels – Impact on recycling. *Waste Management*, 87, 43–50. <https://doi.org/10.1016/j.wasman.2019.01.039>
- Olson, C.L.; Geerligts, L.J.; Goris, M.J.A.A.; Bennett, I.J.; Clyncke, J. (2013). Current and future priorities for mass and material in silicon PV modules. *ECN Solar Energy*, 4629–4633.
- Padoan, F. C. S. M., Altimari, P., & Pagnanelli, F. (2019). Recycling of end of life photovoltaic panels: A chemical prospective on process development. *Solar Energy*, 177(December 2018), 746–761. <https://doi.org/10.1016/j.solener.2018.12.003>
- Paiano, A. (2015). Photovoltaic waste assessment in Italy. *Renewable and Sustainable Energy Reviews*, 41, 99–112. <https://doi.org/10.1016/j.rser.2014.07.208>
- Prado, P. F. A., & Ruotolo, L. A. M. (2016). Silver recovery from simulated photographic baths by electrochemical deposition avoiding Ag<sub>2</sub>S formation. *Journal of Environmental Chemical Engineering*, 4(3), 3283–3292. <https://doi.org/10.1016/j.jece.2016.06.035>
- Raju, T., Chung, S. J., & Moon, I. S. (2009). Electrochemical recovery of silver from waste aqueous Ag(I)/Ag(II) redox mediator solution used in mediated electro oxidation process. *Korean Journal of Chemical Engineering*, 26(4), 1053–1057. <https://doi.org/10.2478/s11814-009-0175-x>
- Rebellou, R. Z. (2018). Recuperação de ouro e prata de lâmpadas de LED inservíveis por lixiviação em tiouréia. Federal University of Espírito Santo.
- Rojas, C. E. B., & Martins, A. H. (2010). Reciclagem de sucata de jóias para a recuperação hidrometalúrgica de ouro e prata. *Metalurgia & Materiais*, 1–7.
- Santos, J. D., & Alonso-García, M. C. (2018). Projection of the photovoltaic waste in Spain until 2050. *Journal of Cleaner Production*, 196, 1613–1628. <https://doi.org/10.1016/j.jclepro.2018.05.252>
- Savvilitidou, V., & Gidakos, E. (2019). Pre-concentration and recovery of silver and indium from crystalline silicon and copper indium selenide photovoltaic panels. *Journal of Cleaner Production*, xxx, 119440. <https://doi.org/10.1016/j.jclepro.2019.119440>
- Shin, J., Park, J., & Park, N. (2017). A method to recycle silicon wafer from end-of-life photovoltaic module and solar panels by using recycled silicon wafers. *Solar Energy Materials and Solar Cells*, 162(September 2016), 1–6. <https://doi.org/10.1016/j.solmat.2016.12.038>
- Sica, D., Malandrino, O., Supino, S., Testa, M., & Lucchetti, M. C. (2018). Management of end-of-life photovoltaic panels as a step towards a circular economy. *Renewable and Sustainable Energy Reviews*, 82, 2934–2945. <https://doi.org/10.1016/J.RSER.2017.10.039>
- Song, B. P., Zhang, M. Y., Fan, Y., Jiang, L., Kang, J., Gou, T. T., Zhang, C. L., Yang, N., Zhang, G. J., & Zhou, X. (2020). Recycling experimental investigation on end of life photovoltaic panels by application of high voltage fragmentation. *Waste Management*, 101, 180–187. <https://doi.org/10.1016/j.wasman.2019.10.015>
- Tammara, M., Salluzzo, A., Rimauro, J., Schiavo, S., & Manzo, S. (2016). Experimental investigation to evaluate the potential environmental hazards of photovoltaic panels. *Journal of Hazardous Materials*, 306, 395–405. <https://doi.org/10.1016/J.JHAZMAT.2015.12.018>
- Tao, J., & Yu, S. (2015). Review on feasible recycling pathways and technologies of solar photovoltaic modules. *Solar Energy Materials and Solar Cells*, 141, 108–124. <https://doi.org/10.1016/j.solmat.2015.05.005>
- U.S. Geological Survey. (2015). Mineral Commodity Summaries 2015. US Geological Survey, 196. <https://doi.org/10.3133/70140094>
- Vogel, A. I. (1981). *Química analítica qualitativa* (5th ed.). Ed. Mestre Jou. <https://books.google.com.br/books?id=VJ02QwAACAAJ>
- Weckend, S., Wade, A., & Heath, G. (2016). *End of Life Management: Solar Photovoltaic Panels*. Paris, France: International Energy Agency (IEA). <https://doi.org/10.2172/1561525>
- Yang, E.-H., Lee, J.-K., Lee, J.-S., Ahn, Y.-S., Kang, G.-H., & Cho, C.-H. (2017). Environmentally friendly recovery of Ag from end-of-life c-Si solar cell using organic acid and its electrochemical purification. *Hydrometallurgy*, 167, 129–133. <https://doi.org/10.1016/j.hydromet.2016.11.005>
- Yousef, S., Tatarians, M., Denafas, J., Makarevicius, V., Lukošiuūtė, S.-I., & Kruopienė, J. (2019). Sustainable industrial technology for recovery of Al nanocrystals, Si micro-particles and Ag from solar cell wafer production waste. *Solar Energy Materials and Solar Cells*, 191, 493–501. <https://doi.org/10.1016/J.SOLMAT.2018.12.008>
- Zhang, L., & Xu, Z. (2016). A review of current progress of recycling technologies for metals from waste electrical and electronic equipment. *Journal of Cleaner Production*, 127, 19–36. <https://doi.org/10.1016/j.jclepro.2016.04.004>

# END-OF-LIFE MANAGEMENT OF PHOTOVOLTAIC PANELS IN AUSTRIA: CURRENT SITUATION AND OUTLOOK

Tudor Dobra \*, Martin Wellacher and Roland Pomberger

Montanuniversitaet Leoben, Department of Environmental and Energy Process Engineering, Chair of Waste Processing Technology and Waste Management, Franz-Josef-Straße 18, A-8700, Leoben, Austria

## Article Info:

Received:  
27 August 2019  
Revised:  
2 January 2020  
Accepted:  
27 January 2020  
Available online:  
5 March 2020

## Keywords:

Photovoltaic panel  
End-of-life  
WEEE legislation  
Recycling  
Waste prognosis

## ABSTRACT

In recent years the end-of-life (EOL) management of photovoltaic (PV) panels has started to attract more attention. By including PV panels in the WEEE Directive in 2012 the European Union has introduced a concrete legislative framework regarding EOL for this sector. Several research investigations into specialized PV recycling processes have been conducted over the last years, although very few of the findings have been implemented on a commercial level up to now. Nowadays, recycling usually still takes place in general recycling plants for flat glass or waste electronics. In this work, the current situation regarding EOL management of PV panels in Austria is analysed by literature research and interviews with stakeholders relevant to the EOL of PV panels. The legislative framework (including national peculiarities) and its influence on current procedures regarding collection and subsequent treatment is shown. Furthermore, current recycling processes are described and a country specific prognosis model is created to assess the future development of waste quantities. Results show that the amount of PV panel waste arising in Austria at the moment is very small and therefore no dedicated recycling takes place. However, quantities will considerably rise in the upcoming years and will act as the main driving force for the implementation of an improved EOL management system including specialised recovery processes.

## 1. INTRODUCTION

The role of renewable energy sources has, in view of a sustainable energy supply, steadily increased and become more important in recent years. One key technology in this field is photovoltaics (PV). Worldwide PV capacity has increased from 1.5 GW in 2000 to over 500 GW in 2018 (Jäger-Waldau 2018), with projections of a further increase to over 4.500 GW in 2050 (Weckend et al. 2016). While the PV industry has drawn continuous attention and achieved improvements relating to issues like increased cell efficiency and lowered production costs, end-of-life (EOL) aspects have started to attract widespread attention only recently. This can be attributed to the long lifetime of PV panels and the thereby created gap between the time when a panel is being put into operation and its emergence as waste at EOL.

The European Union (EU) has introduced PV specific legislation by updating the Directive on waste electrical and electric equipment (WEEE) in 2012 and including PV in its scope (European Commission 2012). The directive contains important aspects like extended producer responsibility (EPR) in regard to financing the collection,

treatment, recovery and disposal of WEEE, obligations relating to registration, information and reporting as well as targets for collection and recovery including recycling. As with all EU directives, each member state had to transpose its contents into national law (EUR-Lex 2018). In the field of WEEE and especially for PV this resulted in several country specific regulations, which influence the organisation of collection and recovery regarding EOL panels. When talking about EOL of PV panels, a distinction between the various technologies is important, as the different material contents (valuable as well as hazardous) are of significance for the recycling process. For this work, two main classifications are considered and distinguished – crystalline silicon (c-Si) panels and thin-film panels (e.g. CdTe, CIGS). Further details on the different technologies, their structure and the materials contained within can be found in Lunardi et al. (2018). At the moment, only few specialised recycling facilities for PV panels exist on a commercial level (Xu et al. 2018). This is mainly due to the fact that the amount of currently generated waste is low. As a result, stand-alone recycling plants are not economically feasible (Cucchiella et al. 2015; D'Adamo et al. 2017). For c-Si panels the processing at EOL nowadays



\* Corresponding author:  
Tudor Dobra  
email: tudor.dobra@unileoben.ac.at



takes place in existing recycling plants, e.g. flat glass recycling plants as well as general WEEE recycling plants. The process consists of mechanical separation of the major components (glass, metals and plastics) and usually does achieve legal compliance even without PV specific investments (Wambach 2017; Weckend et al. 2016). Thin-film panels are currently processed by combining mechanical and chemical steps. For CdTe panels, the company First Solar has established a (commercial) process that includes shredding the module, etching of the semiconductor layer, solid/liquid separation and subsequent purification of the different fractions, namely glass, laminate material and the semiconductor metals Cadmium and Tellurium (Komoto and Lee 2018). Looking ahead, several studies predict a high increase in the amount of PV waste on a global scale as well as for different regions during the coming years (Paiano 2015; Peeters et al. 2017; Santos and Alonso-García 2018). Associated with this, a lot of research regarding new PV specific recycling options has been conducted recently (Lunardi et al. 2018; Xu et al. 2018).

Currently Austria is not one of the key PV markets, measured by already installed capacity. However, the steady increase in installations over the last years, combined with high goals regarding future developments in this field, make it interesting for the primary PV industry as well as the EOL sector. The aim of this work is to depict the current EOL situation of PV panels in Austria, elaborate on the different factors that have an influence on it and show how they are interconnected. This includes (1) investigation of PV related legislation with focus on the national particularities and their effect on the EOL system, (2) examination of current practices in regard to collection and recovery of EOL panels and (3) a country specific waste prognosis. This information can subsequently be used as the basis for future developments regarding a sustainable EOL management of PV panels.

## 2. MATERIALS AND METHODS

### 2.1 Legislative Framework

The WEEE Directive as well as the main documents for the national transposition in Austria were screened for information regarding photovoltaics. In addition, the corresponding regulations in other European countries, especially those relevant to the PV industry (Germany, Italy, France, Spain and the UK) were checked to identify similarities and differences between different implementations of the WEEE Directive throughout Europe. Additionally, relevant stakeholders in Austria were interviewed. This included:

- 2 PV panel producers,
- 3 waste management companies (that have received EOL panels for treatment),
- 2 WEEE compliance schemes and
- the national coordinating institution for WEEE, the so called Elektroaltgeraete Koordinierungsstelle (EAK).

Furthermore, information made available by European stakeholders (primarily compliance schemes) was used

as a reference, mainly for double checking the information from the corresponding national legislative documents.

### 2.2 Current EOL management of PV panels

The main research method regarding current EOL practices were the qualitative interviews with the Austrian stakeholders mentioned in 2.1. The aim was to obtain information regarding the PV market in Austria (in general) with a focus on the emergence, collection and subsequent treatment of EOL PV panels on a national level. Although no fixed questionnaire was used, the following questions are an overview of the main aspects discussed with all interview partners:

- What quantities of PV waste are currently emerging in Austria and how is the collection organized?
- How does the treatment of EOL panels look like in Austria? What materials are recovered?
- How does the legislative framework influence the EOL management?
- How do you expect the Austrian PV market to develop in the coming years (installed capacity, used technology)?
- What, if any, changes do you expect regarding the EOL situation in Austria in the coming years and which factors will be the main drivers?

In addition, publications by the EAK as well as the National Waste Management Plan and its corresponding status reports were consulted. Literature about the progress in other countries along with ongoing research regarding EOL management of PV was also considered. Although there is no direct applicability for the current situation in Austria, this information can be relevant for future developments.

### 2.3 PV panel waste prognosis

The waste prognosis model is composed of two parts, namely the creation of an adequate Weibull function and the specification of the installed PV panel mass in the considered timeframe (2000 to 2050). Those aspects as well as the actual calculations are subsequently explained.

#### 2.3.1 Weibull model

The Weibull distribution was originally proposed in 1937 to estimate machinery lifetime. Nowadays, the distribution is a broadly used statistical model in reliability engineering and life-time data analysis (Ng and Wang 2009). It is considered to be the most suitable approach to describe discard behaviour for electrical and electronic equipment (EEE) and has been applied frequently in scientific literature (Forti et al. 2018). In its easiest form, it only takes the wear out phase into account. This simplification is appropriate for this case, as a population of panels from many different manufacturers is assumed (Kleiss 2016). Therefore the cumulative failure probability ( $p_{cumm}$ ) after a certain operational time can be described with Equation 1, according to Wambach and Sander (2015) and Weckend et



al. (2016). The specific failure probability ( $p_{\text{spec}}$ ) in a certain year  $x$  can be calculated by Equation 2.

$$F(x) = p_{\text{cumm,after } x \text{ years}} = 1 - e^{-\left(\frac{x}{\beta}\right)^\alpha} \quad (1)$$

Equation 1: Simplified Weibull function (wear out only)

$$p_{\text{spec,in year } x} = p_{\text{cumm,after } x \text{ years}} - p_{\text{cumm,after } (x-1) \text{ years}} \quad (2)$$

Equation 2: Failure probability in a certain year ( $x$  years after installation)

The two relevant parameters for Equation 1 are the shape factor  $\alpha$  and the characteristic lifetime  $\beta$ . These values were adopted from Weckend et al. (2016) and are  $\alpha = 5.3759$  for the Regular Loss Scenario and  $\alpha = 2.4928$  for the Early Loss Scenario with a characteristic lifetime of  $\beta = 30$  years in both cases. The assumption regarding lifetime was also supported by the interviewed stakeholders. The main difference between the considered scenarios is that the Regular Loss Scenario includes no early attrition, while the Early Loss Scenario also considers defects during the lifespan e.g. during transportation and installation. Further details on the scenarios can be found in Weckend et al. (2016). The obtained values fall in line with several other publications. Forti et al. (2018) for example mention an  $\alpha$ -value of 3.5 (which sits in the middle of the two scenarios from Weckend et al. (2016)). Considering the lifetime ( $= \beta$ ), they suggest 25 years, which is also a common value found in literature.

### 2.3.2 Yearly installed PV panel mass

Historic data regarding installed PV capacity in Austria is available in Biermayr et al. (2018) for the timeframe 2000 to 2017 (shown in Figure 1). Installation numbers before 2000 were very small and therefore negligible. From 2018 on, a yearly capacity increase projection based on the qualitative research (compare to 2.2) was used. An average value of 400 MW of new PV capacity per year from 2020 to 2050 was deemed reasonable by the stakeholders ques-

tioned. For the transition years, values of 250 MW for 2018 and 300 MW for 2019 were used.

The conversion from installed PV-power to panel-mass was based on values taken from Weckend et al. (2016). Between each of the directly adopted values (see Table 1), a linear integration was done to simulate a steady decline in average weight to power ratio over the corresponding years.

### 2.3.3 Calculation of projected waste

By multiplying the mass of PV panels installed in a certain year with the specific failure probability for all subsequent years (here, relative values e.g. 5 years after installation are used), a yearly waste distribution for those panels was achieved. The summation of all values arising in the same year (here, absolute values like 2025 are considered), results in the total waste amount for each year.

## 3. RESULTS AND DISCUSSION

### 3.1 Legislative Framework

In Austria the transposition of the European WEEE Directive was achieved by updating the Elektroaltgeräteeverordnung (EAG-VO) in 2014. The EPR as well as the definition of a producer, which includes (1) manufacturers, (2) resellers, (3) importers and (4) direct sellers (by distance communication) were unalteredly adopted. In general, EEE can be classified as business to consumer (B2C) or business to business (B2B) products. The B2C classification applies to equipment intended to be used in private households and to equipment used in other areas which, because of its nature and quantity, is similar to that for private households. Equipment not meeting the aforementioned characteristics is classified as B2B. All PV panels put on the market are classified as B2B products in Austria, not considering whether they are actually used by businesses or private households. The arising waste is therefore always classified as professional waste. This is in stark contrast to most EU member states where PV pan-

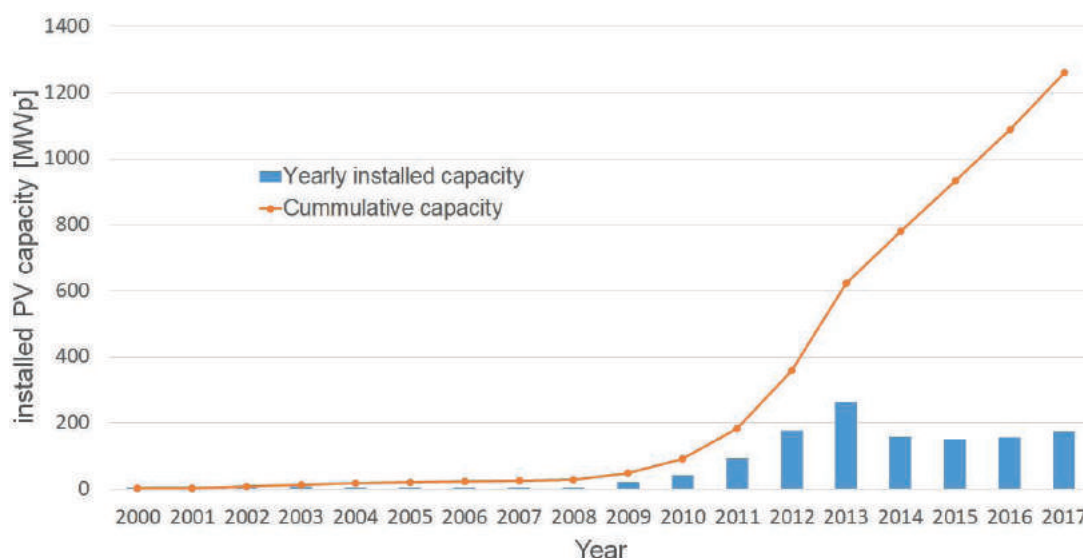


FIGURE 1: Installed PV capacity in Austria from 2000 to 2017 according to Biermayr et al. (2018).

**TABLE 1:** Weight to power ratio of PV panels according to Weckend et al. (2016).

Year	Weight to power ratio [t/MW]
2000	110
2005	100
2010	90
2015	70
2030	60
2050	45

els are classified as B2C products, e.g. the UK and France (GOV.UK 2018; Solar Waste, n.d.) or a differentiated system with both B2B and B2C classification is used as it is the case in Germany and Italy (Deutscher Bundestag 2015; Malandrino et al. 2017).

While all EOL PV panels are considered professional waste, a distinction is made between historic and new PV panels. This is of relevance when determining who is responsible for financing the collection and treatment at the EOL stage. In this regard the date on which the panel was put on the market is relevant, with the 1<sup>st</sup> of July 2014 being the cut-off date. For PV panels put on the market in Austria before this date, the responsibility lies with their owner at the EOL stage when no replacement with new equivalent products takes place. However, if the old panels are substituted, the producer of the new panels is responsible for financing the collection and treatment of the old ones. In case of panels put on the market after the cut-off date, the responsibility of financing the EOL costs lies with the original producer whether or not a replacement with new panels takes place. These aforementioned stipulations were taken from the WEEE directive, although the exact cut-off date is a national particularity.

In regards to the six WEEE categories specified in the European directive, Austria has implemented an adaptation with six modified categories. PV panels are a separate "collection and treatment category" and have specific recycling targets, although the values are equal to those for large equipment, which is where PV panels are classified in the WEEE directive. Those targets, as of the 15<sup>th</sup> of July 2018, are (1) 85 w. % in regard to recovery and (2) 80 w. % concerning preparation for re-use and recycling. However, the target regarding collection (65 w. % of EEE put on the market on average in the last three years in the respective member state) is not applied to the different categories but rather across the sum of all WEEE (European Commission 2012). The share of PV panels in regard to all EEE put on the market is currently about 3.35 w. %, while their share regarding collection is even lower with 0.02 w. % (EAK 2018).

### 3.2 Current EOL Management of PV panels

#### 3.2.1 EPR and Collection of EOL PV panels

The previously mentioned B2B classification of all PV panels on the one hand simplifies the EOL requirements for producers. Contrary to the case of B2C EEE no financial guarantee is needed and it is not compulsory to take part in a compliance scheme as a producer of historic waste. On the other hand, this setup does not really encourage the im-

plementation of a nationwide solution but rather facilitates stand-alone approaches that are feasible for the individual producers. This is further supported by the previously mentioned fact that PV panels make up only 0.02 w. % of collected EEE.

In regard to PV panels put on the market today, three options are available to producers for fulfilment of the EPR:

1. Implementation a self-organised take-back
2. Taking part in a compliance scheme on a voluntary basis
3. Usage of the compliance scheme as a service provider

In case of the self-organised system all responsibilities, including the obligatory documentation and reporting to the authorities, are assumed by the producer directly. Old PV panels are first taken back by the producer and subsequently handed over to a treatment facility. Taking part in a compliance scheme works in the same way as it does for other WEEE. At the time of putting the panels on the market, a fee, in relation to the amount of panels, is paid to the compliance scheme. By doing so, most of the responsibilities are transferred to the scheme. At the moment the fee for PV panels is 0.12 Euro per piece for several compliance schemes in Austria (ERA 2018; Interseroh 2018). The last option can be seen as a merged solution between the other two, where no fee is paid upfront but rather the costs arise at the time the compliance scheme is used as a service provider when EOL is reached. In this case, individual agreements are established between the producer and the compliance scheme as to what aspects of the EPR are covered by the service and what parts the producer has to fulfil themselves. The stakeholder interviews have shown that nowadays the self-organised system and the service provider system are the ones primarily used by Austrian PV panel producers. The amount of licensed PV panels, meaning the use of a classical compliance scheme, is marginal.

#### 3.2.2 Treatment of EOL PV panels

According to the EAK in 2016 and 2017 a total of 12 respectively 22 tonnes of PV panel waste was reported and collected (EAK 2017, 2018), although the actual number might be higher due to the fact that a part of the arising PV waste is reported under a wrong category or not reported at all. As previously mentioned, this amount makes up only 0.02 w. % of all collected EEE. These very low quantities are the main reason why no dedicated recycling plant for PV panels exists in Austria. As a consequence, no uniform way of treatment for EOL panels is used at the moment (BMNT 2018). Although a flat glass recycling plant is available, treatment of PV panels is not performed at this facility as it is the case in other European countries e.g. Germany and Belgium. The recovery and recycling process in Austria is performed by different parties including waste management companies (usually those already active in WEEE treatment) and the scrap industry. An individual recycling approach, dependent on the type of panel (c-Si or thin-film) and its condition (e.g. broken glass plate, electrical fault) is implemented. Usually panels are stored until a

reasonable number of similar panels is reached, regarding the aforementioned criteria (technology and condition). Details about the recoverable materials depending on the different technologies can be found in Lunardi et al. (2018). Treatment in most cases starts with a manual step for removing the aluminium frame (if applicable) and the junction box with cables. Subsequently, mechanical processes are applied for crushing the panel and separating it into different streams containing profitable materials (e.g. metals, glass) that can be sold. Valuable materials, e.g. silver in c-Si panels or the semiconductor material from thin-film panels are not specifically recovered. At the moment it is unclear how long this treatment system will remain feasible, but stakeholders agree that the rise in waste quantities will at some point induce the need for a more autonomous EOL management system for PV panels. According to some stakeholders, the increase in waste could also lead to the adoption of more specific legislation regarding the recycling process (e.g. the need to recover certain valuable materials or to remove hazardous ones), although they do not think it will happen in the next years.

### 3.3 Waste projections

Figure 2 shows the probability of failure in a certain year after installation for both applied scenarios (Regular Loss and Early Loss). The Regular Loss distribution shows a higher and more concentrated peak, meaning that most failures will occur in a shorter timespan during the latter part of the product life, while the Early Loss distribution shows failures that are spread out more evenly over the whole lifetime.

The results of the prognosis model can be seen in Figure 3. The waste prognosis shows a significant increase of PV panel waste in Austria for the upcoming years, e.g. an increase by a factor of 30 to 200 in a 10-year-timespan (2016 to 2025) depending on which scenario is considered. The threshold of 2.000 tonnes per year will be reached in 2031 (Regular Loss) or in 2024 (Early Loss) respectively. This can be seen as the critical amount in regard to the construction of a specialized PV recycling plant, when considering the fact that a currently active commercial plant in France treated around 1.800 t in 2018 (Veolia 2018). Comparing the Austrian prognosis to those of other regions, a similar trend can be observed regarding the relative distri-

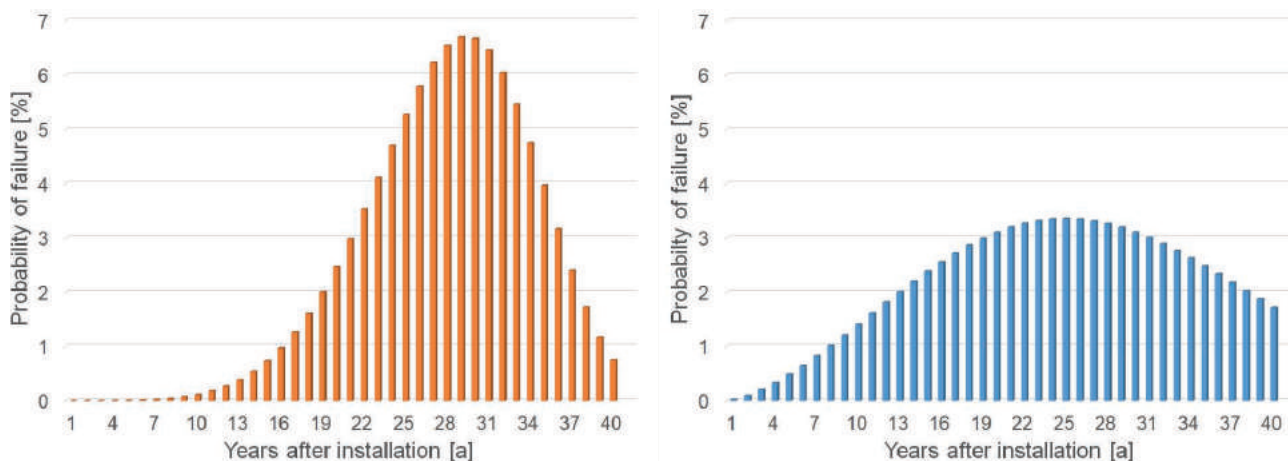


FIGURE 2: Specific probability of failure according to Weibull function (a) Regular Loss scenario, (b) Early Loss scenario.

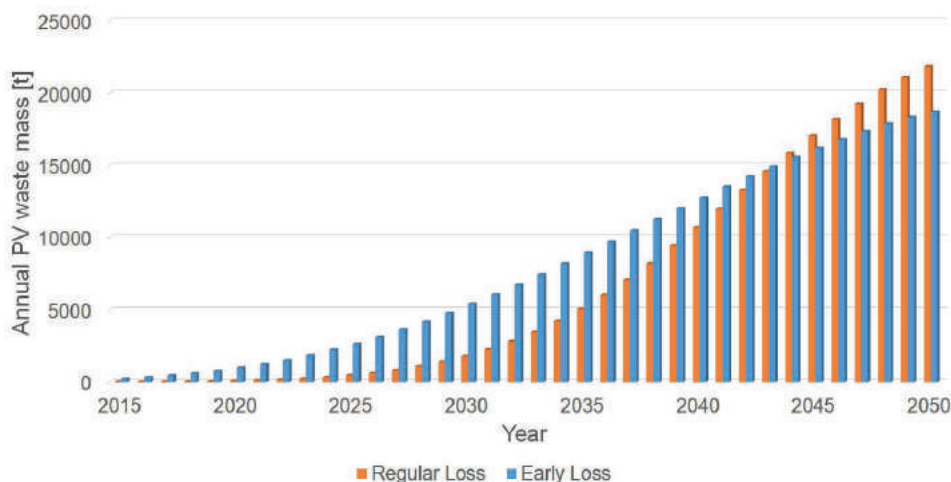


FIGURE 3: PV panel waste projection for Austria.

bution of PV panel waste for the coming years although the absolute values for Austria are lower. This was expected and can be explained by the lower amount of installed PV capacity. It is important to note that there are several uncertainties regarding this prognosis, the main ones being (1) the projection of future installed capacity and (2) the non-inclusion of one-time effects like repowering, meaning the replacement of still working panels with new ones with higher efficiency. While these uncertainties have to be kept in mind, it has to be noted that the capacity projection is rather conservative (e.g. PV Austria (2018) indicates a much larger growth in the coming years) and does not influence the short-time prognosis significantly, as only a small amount of those panels will emerge as waste in the next years. Additionally, repowering is probably not as big of a factor in Austria compared to other countries like Italy or Spain because most installations are not operated as commercial plants and are therefore not mainly profit oriented. A comparison shows that the waste quantities according to the Regular Loss Scenario for 2016 and 2017 correspond rather well with the real numbers published by the EAK (EAK 2017, 2018). Therefore, the present prognosis can be seen as a good basis in regard to future waste quantities. Still, continuous monitoring and evaluation of the EOL situation should be performed. The collection of more statistical data (e.g. if the real lifetime corresponds with the 30 years that have been assumed) will enable a more reliable and precise forecast, which in turn will be a more concrete basis for future decisions.

#### 4. CONCLUSIONS AND OUTLOOK

The situation regarding EOL management of PV panels in Austria was investigated. Concerning the legal framework for photovoltaic waste, it was shown that although legislation in all EU member states is based on the WEEE-Directive, specific national characteristics exist and influence the way EOL processes are set up. The applied B2B classification for all PV panels in Austria (in combination with the different options available for EPR fulfilment) enables a flexible approach for the producers but also somewhat hinders the implementation of nationwide EOL solutions. Stakeholder interviews showed that at the moment collection and subsequent treatment of EOL panels in Austria is performed in a decentralized way by several different parties. The applied recycling technologies are not PV specific but rather combinations of manual and mechanical process steps accounting for the type and condition of the respective panels. As this approach complies with the mandatory recycling rates, there is (at least currently) no need or incentive for change in this regard. The applied prognosis model however shows a significant increase in PV panel waste for the upcoming years. Even the more conservative approach (Regular Loss) predicts an increment of the factor 30 from 2016 to 2025. This increase is also seen as the main driver regarding changes to the EOL management system and adoption of PV specific recycling technologies, by the interviewed stakeholders. These will be important for guaranteeing the long-term reliability of EOL activities while potentially also increasing

the economic potential of recycling processes. Therefore, it is necessary to continuously monitor the EOL situation, in order to obtain more reliable data. This will enable more precise predictions, which subsequently should be used as reference for future decisions regarding the EOL management of PV panels.

#### ACKNOWLEDGEMENTS

This research was performed within the project PVRe<sup>2</sup> and has received funding from the Austrian Research Promotion Agency FFG (Energieforschungsprogramm 2017 - Leitprojekte, FFG No. 867267, Klima- und Energiefonds). The authors would like to thank Gernot Oreski and Gabriele Eder for their contributions to this work.

#### REFERENCES

- Biermayr, P., Dißauer, C., Eberl, M., Enigl, M., Fechner, H., Fischer, L., et al. (2018). *Innovative Energietechnologien in Österreich Marktentwicklung 2017*, Vienna: BMVIT. [https://nachhaltigwirtschaften.at/resources/iea\\_pdf/reports/marktstatistik-2017-endbericht.pdf](https://nachhaltigwirtschaften.at/resources/iea_pdf/reports/marktstatistik-2017-endbericht.pdf).
- BMNT. (2018). *Die Bestandaufnahme der Abfallwirtschaft in Österreich - Statusbericht 2018*, Vienna. <https://www.bmnt.gv.at/dam/jcr:aacdf932-476d-408e-aa00-06ede1a8a6fd/Statusbericht%202018.pdf>. Accessed: 18 February 2019.
- Cucchiella, F., D'Adamo, I., & Rosa, P. (2015). End-of-Life of used photovoltaic modules: A financial analysis. *Renewable and Sustainable Energy Reviews*, 47, (552–561). doi:10.1016/j.rser.2015.03.076
- D'Adamo, I., Miliacca, M., & Rosa, P. (2017). Economic Feasibility for Recycling of Waste Crystalline Silicon Photovoltaic Modules. *International Journal of Photoenergy*, 2017, (6, 1–6). doi:10.1155/2017/4184676
- Deutscher Bundestag. (2015). Gesetz über das Inverkehrbringen, die Rücknahme und die umweltverträgliche Entsorgung von Elektro- und Elektronikgeräten. ElektroG.
- Elektroaltgeräte Koordinierungsstelle. (2017). *Tätigkeitsbericht 2016* (EAK, Ed.), Vienna. [https://www.eak-austria.at/presse/TB/Taetigkeitsbericht\\_2016.pdf](https://www.eak-austria.at/presse/TB/Taetigkeitsbericht_2016.pdf). Accessed: 20 February 2019.
- Elektroaltgeräte Koordinierungsstelle. (2018). *Tätigkeitsbericht 2017* (EAK, Ed.), Vienna. [https://www.eak-austria.at/presse/TB/Taetigkeitsbericht\\_2017.pdf](https://www.eak-austria.at/presse/TB/Taetigkeitsbericht_2017.pdf). Accessed: 18 February 2019.
- ERA. (2018). *Tarifübersicht, ERA Elektro Recycling Austria*. [https://www.era-gmbh.at/fileadmin/user\\_upload/ERA\\_Tarifuebersicht\\_ab\\_01\\_2019.pdf](https://www.era-gmbh.at/fileadmin/user_upload/ERA_Tarifuebersicht_ab_01_2019.pdf). Accessed: 15 February 2019.
- EUR-Lex. (2018). *EU directives*. <https://eur-lex.europa.eu/legal-content/EN/TXT/?uri=LEGISSUM%3A114527>. Accessed: 26 February 2019.
- European Commission. (2012). *Directive 2012/19/EU of the European Parliament and of the Council of 4 July 2012 on waste electrical and electronic equipment (WEEE)*. WEEE Directive.
- Forti, V., Baldé, K., & Kühr, R. (2018). *E-waste Statistics: Guidelines on Classifications, Reporting and Indicators*, second edition (United Nations University, Ed.).
- GOV.UK. (2018). *Electrical and electronic equipment (EEE) covered by the WEEE regulations*. <https://www.gov.uk/government/publications/electrical-and-electronic-equipment-eee-covered-by-the-weee-regulations/electrical-and-electronic-equipment-eee-covered-by-the-weee-regulations>. Accessed: 20 February 2019.
- Interseroh. (2018). *Tarifübersicht 2019, Interseroh Austria*. [https://www.interseroh.at/fileadmin/PDF/Kundeninfo\\_Sonstige\\_AT/EAG-Tarife\\_Jaen\\_2019\\_AT.pdf](https://www.interseroh.at/fileadmin/PDF/Kundeninfo_Sonstige_AT/EAG-Tarife_Jaen_2019_AT.pdf). Accessed: 15 February 2019.
- Jäger-Waldau, A. (2018). *PV Status Report 2018* (Publications Office of the European Union, Ed.). [http://publications.jrc.ec.europa.eu/repository/bitstream/JRC113626/pv\\_status\\_report\\_2018\\_online.pdf](http://publications.jrc.ec.europa.eu/repository/bitstream/JRC113626/pv_status_report_2018_online.pdf). Accessed: 14 February 2019.
- Kleiss, G. (2016). Estimating future recycling quantities of PV modules in the European Union. In *WIP* (Ed.), *Proceedings of the EU PVSEC 2016* (Munich) (pp. 2365–2368).
- Komoto, K., & Lee, J.-S. (2018). *End-of-Life Management of Photovoltaic Panels: Trends in PV Module Recycling Technologies*. Report IEA-PVPS T12-10:2018, International Energy Agency.

- Lunardi, M. M., Alvarez-Gaitan, J. P., Bilbao, J. I., & Corkish, R. (2018). A Review of Recycling Processes for Photovoltaic Modules. In B. Zaidi (Ed.), *Solar Panels and Photovoltaic Materials* (pp. 9–27). InTech.
- Malandrino, O., Sica, D., Testa, M., & Supino, S. (2017). Policies and Measures for Sustainable Management of Solar Panel End-of-Life in Italy. *Sustainability*, 9, (4, 481). doi:10.3390/su9040481
- Ng, H. K. T., & Wang, Z. (2009). Statistical estimation for the parameters of Weibull distribution based on progressively type-I interval censored sample. *Journal of Statistical Computation and Simulation*, 79, (2, 145–159). doi:10.1080/00949650701648822
- Paiano, A. (2015). Photovoltaic waste assessment in Italy. *Renewable and Sustainable Energy Reviews*, 41, (99–112). doi:10.1016/j.rser.2014.07.208
- Peeters, J. R., Altamirano, D., Dewulf, W., & Dufloy, J. R. (2017). Forecasting the composition of emerging waste streams with sensitivity analysis. A case study for photovoltaic (PV) panels in Flanders. *Resources, Conservation and Recycling*, 120, (14–26). doi:10.1016/j.resconrec.2017.01.001
- Photovoltaic Austria Federal Association. (2018). Konzept: 100.000 Dächer- und Speicherprogramm als Beitrag zu 100 % erneuerbarem Strom (PV Austria, Ed.). <https://www.pvaustria.at/wp-content/uploads/2019-02-04-PVA-Management-Summary-PVA-Konzept-100.000>. Accessed: 18 February 2019.
- Santos, J. D., & Alonso-García, M. C. (2018). Projection of the photovoltaic waste in Spain until 2050. *Journal of Cleaner Production*, 196, (1613–1628). doi:10.1016/j.jclepro.2018.05.252
- Solar Waste. (n.d.). European WEEE Directive in your country. <http://www.solarwaste.eu/in-your-country/france/>. Accessed: 20 February 2019.
- Veolia. (2018). Planet #October 2018 EN. [https://www.veolia.cn/sites/g/files/dvc146/f/assets/documents/2018/11/Planet\\_Magazine\\_October\\_2018.pdf](https://www.veolia.cn/sites/g/files/dvc146/f/assets/documents/2018/11/Planet_Magazine_October_2018.pdf). Accessed: 26 February 2019.
- Wambach, K. (December 2017). Life Cycle Inventory of Current Photovoltaic Module Recycling Processes in Europe, IEA-PVPS.
- Wambach, K., & Sander, K. (2015). Perspectives of management of End-of-Life photovoltaic modules. In WIP (Ed.), *Proceedings of the EU PVSEC 2015 (Hamburg)* (pp. 3073–3078).
- Weckend, S., Wade, A., & Heath, G. (June 2016). End-of-Life management solar photovoltaic panels, IRENA & IEA-PVPS.
- Xu, Y., Li, J., Tan, Q., Peters, A. L., & Yang, C. (2018). Global status of recycling waste solar panels: A review. *Waste management (New York, N.Y.)*, 75, (450–458). doi:10.1016/j.wasman.2018.01.036

# CHARACTERISATION OF BACTERIAL DIVERSITY IN FRESH AND AGED SEWAGE SLUDGE BIOSOLIDS USING NEXT GENERATION SEQUENCING

Karen R. Little <sup>1</sup>, Han Ming Gan <sup>2</sup>, Aravind Surapaneni <sup>3</sup>, Jonathan Schmidt <sup>3</sup> and Antonio F. Patti <sup>1,\*</sup>

<sup>1</sup> School of Chemistry, Monash University, Clayton, VIC 3800, Australia

<sup>2</sup> School of Life and Environmental Sciences, Deakin University, Geelong, VIC 3220, Australia

<sup>3</sup> South East Water, Frankston, VIC 3199, Australia

## Article Info:

Received:  
11 August 2019  
Revised:  
23 January 2019  
Accepted:  
27 January 2020  
Available online:  
5 March 2020

## Keywords:

Biosolids  
Sewage sludge  
Bacteria  
Next generation sequencing

## ABSTRACT

Sewage sludge, often referred to as biosolids, is generated in large quantities by wastewater treatment plants. It contains macro- and micronutrients which are essential for plant growth and so represents a valuable agricultural resource. Prior to land application, pathogens are carefully monitored to reduce the risk of crop and soil contamination, however, to date there has been limited investigation of agriculturally beneficial bacteria indigenous to the biosolids. This study investigated shifts in the composition of the bacterial community alongside the physicochemical properties of biosolids of increasing age, from freshly dewatered to those stockpiled for approximately four years. With stockpiling, there was a significant increase in ammonium content, ranging from 801 mg/kg in the fresh biosolids to 8,178 mg/kg in the stockpiled biosolids and a corresponding increase in pH ranging from 6.93 to 8.21. We detected a ten-fold increase in Firmicutes, from 4% relative abundance in the fresh biosolids compared to 40% in the older, stockpiled biosolids. Plant growth promoting bacteria (PGPB) of the Proteobacteria family, particularly of the *Devosia* and *Bradyrhizobium* genera were identified in the freshly dewatered and the older, stockpiled biosolids. Land application of the biosolids studied here could reduce fertiliser costs, provide a means of pH correction to acidic soils and a potential source of bacteria beneficial for crop growth.

## 1. INTRODUCTION

Australia produces approximately 300,000 tonnes of dry sewage sludge biosolids annually. Approximately 55% of this is applied to agricultural land, 30% stored in landfill and 15% is composted, used for land rehabilitation, landscaping or incinerated (Australian & New Zealand Biosolids Partnership, 2016).

The agricultural benefits of applying biosolids to soil are the addition of nutrients, particularly nitrogen and phosphorus and to increase organic matter. Beneficial effects have been demonstrated on crop yield and nutrition (Cooper, 2005; Ferraz, Momentel, & Poggiani, 2016; Petersen, Petersen, & Rubæk, 2003; Warman & Termeer, 2005) and soil physicochemical properties (Bevacqua & Mellano, 1993; Gómez-Muñoz, Magid, & Jensen, 2017; Qiong, Li, Cui, & Wei, 2012; Tamoutsidis, Papadopoulos, Tokatlidis, Zotis, & Mavropoulos, 2002) in a range of soil and crop types.

Advances in high-throughput 16S rDNA amplicon sequencing technologies provide a considerable amount of taxonomic information and have changed our understanding of microbial diversity in the environment. Given the importance of microbes to influence crop growth and nutrient availability in soil, consideration needs to be given to the composition of the microbial community indigenous to the biosolids as well as effects on the soil microbial community following land application. A growing awareness of inoculation with plant growth promoting bacteria (PGPB) represents an important strategy for sustainable management and reduction of negative environmental impacts. Within the broad range of PGPB, the Proteobacteria phylum is the most represented, with a number of bacteria classified to this phylum capable of forming symbiotic relationships with leguminous plants. Some of these bacteria are also capable of producing phytohormones (Hershey, Lu, Zi, & Peters, 2014; Nagel, Bieber, Schmidt-Dannert, Nett, & Peters, 2018) and solubilizing inorganic phosphate (Z. Dai et

\* Corresponding author:  
Antonio Frank Patti  
email: tony.patti@monash.edu

al., 2019), thereby promoting plant growth in a number of ways.

A number of studies have focused on pathogen detection and abundance in biosolids (Bibby & Peccia, 2013; Bibby, Viau, & Peccia, 2010; Irwin et al., 2017; Karpowicz, Novinscak, Bärlocher, & Filion, 2010; Rouch, Fleming, Deighton, Blackbeard, & Smith, 2008; Viau & Peccia, 2009a, 2009b; Yergeau et al., 2016), risks to human health during land application due to bioaerosol generation (Herrmann, Grosser, Farrar, & Brobst, 2017; Paez-Rubio et al., 2007), and effects on the indigenous soil microbial community following land application (Hu, Pang, Yang, Zhao, & Cao, 2019; Mossa, Dickinson, West, Young, & Crout, 2017; Schlatter et al., 2019). To our knowledge, identification of bacterial diversity in biosolids of different ages and more importantly identification of agriculturally beneficial bacteria in biosolids stockpiles has not been investigated.

The aims of this study were:

- To investigate the bacterial diversity and community composition of the biosolids from a wastewater treatment plant, ranging from freshly dewatered sludge to that stockpiled for a period of four years.
- To identify if agriculturally relevant bacteria (PGPB) were present in the aged biosolids.

## 2. MATERIALS AND METHOD

### 2.1 Biosolids collection

The Boneo wastewater treatment plant is located 83 km from Melbourne, on Victoria's Mornington Peninsula. The plant accepts domestic wastewater and tankered waste including leachate from the local landfill sites and serves a population equivalent of approximately 47,800 people. The annual median inflow of domestic wastewater to the plant is 10 ML day<sup>-1</sup>, however, there is significant seasonal variation due to the number of holiday homes in the area. Wastewater treatment is via a twin stream activated sludge process. Waste activated sludge from the bioreactors is drawn from the return activated sludge (RAS) underflow from the clarifiers and treated via aerobic digestion for approximately 10 days. The treated sludge is transferred to an anaerobic storage lagoon for further digestion to reduce volatile solids. Most of the sludge from the anaerobic lagoon is pumped to a continuously mixed storage tank of approximately 10 m<sup>3</sup> capacity that supplies feed sludge to the belt press for dewatering. Dewatered sludge from the belt press is conveyed into one of the three enclosed solar drying sheds where it is distributed over the drying floor by a mechanical tiller and dried to > 50% dry solids. After a predetermined period of time, equivalent to three months in summer and ten months during the winter season, the sludge is harvested and transported to the biosolids stockpile area. Surplus sludge from the anaerobic lagoon that exceeds the capacity of the belt press/solar drying shed route is pumped to an open-air sludge drying pan. After approximately one year in the drying pan the sludge is removed, usually at the end of summer when the sludge is at its driest, and transported to the biosolids stockpile area. Once stockpiled, the biosolids remain in a

static state without mechanical turning or aeration. Typically, the dried sludge from the sludge drying pan and the solar dryers from the Boneo wastewater treatment plant is stockpiled for greater than three years to achieve the highest treatment grade (Grade T1). The treatment grades in accordance with the Environmental Protection Authority (EPA) Publication 943 (EPA Victoria, 2004) are determined according to three main criteria: (i) adoption of a prescribed treatment process with minimum performance criteria (e.g. temperature/time); (ii) microbiological limits to demonstrate that the treatment processes are operating effectively; and (iii) measures for controlling bacterial regrowth, vector attraction and generation of nuisance odours. Grade T1 (< 100 Escherichia g<sup>-1</sup> dry solids, < 1 Salmonella spp. 50 g<sup>-1</sup> dry solids, ≤ 1 enteric virus 100 g<sup>-1</sup> dry solids) represents the highest quality grade and from a microbiological perspective is suitable for unrestricted use, whereas restrictions on end use apply to T2 and T3 biosolids (EPA Victoria, 2004). Recently, Irwin et al (2017) verified the sludge treatment processes at the Boneo wastewater treatment plant and concluded that this plant achieved T1 grade biosolids with respect to prescribed log reductions for a range of pathogens (> 3 log<sub>10</sub> enteric virus and > 2 log<sub>10</sub> Ascaris ova in addition to achieving the E. coli and Salmonella criteria as above), after a stockpiling/storage period of one year. Shortening the storage time from three years to one year reduces overall site odour potential, improves site aesthetics as well as reduces the total area of land required for stockpiling. Only biosolids from the solar dryer route were investigated in this study as biosolids from the drying pans are inadvertently mixed with clay liner from the drying pan during harvest.

The biosolids stockpile sampling equipment was decontaminated using the Environmental Protection Agency Victoria (EPA) approved triple wash procedure (Extran® solution followed by rinsing with tap water then de-ionised water), between each sample core to avoid cross-contamination. Disposable gloves and boot covers were worn during the sampling of stockpiles and were replaced between each sample location within a stockpile. Samples were placed into sterile bags and stored on ice. Upon arrival at Monash University they were stored at - 20°C until physicochemical analysis and DNA extraction were performed.

The biosolids samples were collected from five points within the sludge treatment process and identified according to the period of time elapsed post-dewatering. The first sampling point was at the conveyor belt, which transported the dewatered biosolids into the solar drying shed. Six grab samples of approximately 250-300 g each were combined to form a composite sample of approximately 1.6 kg, which was identified as week 0 (t=0). The second sampling point was in the solar drying shed, furthest away from the incoming dewatered sludge, where the biosolids had been turned and dried by mechanical tillering for one week. Six grab samples of approximately 150-200 g each were collected from the width of the shed floor and combined to form a composite sample of approximately 1.1 kg. This sample was identified as week 1 (t=1). Over a period of time, the biosolids are moved from the drying shed to outdoor stockpiles. Prior to transporting the biosolids to

the stockpile area, six grab samples of approximately 200 g each were collected and combined to form a composite sample of approximately 1.2 kg, which was identified as week 2 (t=2). Portable percussion sampling equipment was used to collect cores from biosolids stockpiles which had been established in 2015 and 2012, with biosolids additions made to each stockpile within that year. Five replicate cores were collected from regular intervals along the length of each stockpile. Once the sample had been extruded from the coring tool, a portion of biosolids was retained from depths of 0.7 and 1.5 m from the 2015 stockpile, and 1.5 m and 2 m from the 2012 stockpile. These depths represented mid-depth and 1 m from the base of the pile and will be collectively referred to henceforth as Depth 1 and Depth 2, respectively. Biosolids sampled from the 2015 and 2012 stockpiles will be referred to as 52 weeks and 208 weeks, respectively. The total number of biosolids samples collected from the site was 23 (1 each from 0, 1 and 2 weeks, 10 from 52 weeks and 10 from 208 weeks). All of the biosolids were collected on the same day (26th October 2016). The waste-water treatment process at the site hasn't changed since 2012 hence it is justifiable to compare the fresh biosolids (0, 1 and 2 weeks) to the 2015 (52 weeks) and 2012 (208 weeks) biosolids.

## 2.2 Biosolids physiochemical properties

The pH and EC of the biosolids were determined in 5 g sub samples suspended in deionised water (1:5 W/V) following shaking for 1 h using a TPS WP81 meter and probe (TPS Pty Ltd, Springwood, Qld). Total C and N were determined by dry combustion (Vario microcube, Elementar). Approximately 5 g of each sample was dried at 105°C for 48 h and moisture loss determined from the loss of mass before and after drying. A portion of each sample was submitted to ALS, Scoresby, Victoria for ammonium, nitrate, Olsen P and total K analysis.

## 2.3 DNA extraction and sequencing analysis

Genomic DNA was extracted from each biosolids sample in triplicate using the PowerSoil® DNA Isolation Kit (MoBio Laboratories, Carlsbad, CA), following the manufacturer's procedure with the only exception being a double wash with Solution C5 on the spin filter prior to DNA elution. Yields and purity of the DNA were determined by NanoDrop (Thermoscientific) at 260 and 280 nm. PCR amplification was carried out on the purified DNA (~20 ng input) using KAPA HiFi HotStart ReadyMix (Kapa Biosystems, South Africa) and primers targeting the V3-V4 region of microbial 16S rRNA gene. (Bartram, Lynch, Stearns, Moreno-Hagelsieb, & Neufeld, 2011; Klindworth et al., 2012). The forward and reverse primers were synthesized to contain partial Illumina adaptor sequence on their 5' ends (TCGTCGGCAGCGTCAGATGTGTATAA-GAGACAG and GTCTCGTGGGCTCGGAGATGTGTATAAGAGACAG for forward and reverse primers, respectively) that enable the addition of Illumina dual index barcode in the second PCR step. The first PCR conditions involved an initial denaturation step at 95°C for 3 min followed by 25 cycles of 95°C for 30 sec, 55°C for 30 sec and 72°C for 30 sec and ended with an extension step at 72°C for 5 min. The PCR prod-

ucts were purified using 0.8x volume of AmpureBead XP (Beckman Coulter, Danvers, MA) and were then used as the template for the second PCR step with similar cycling condition followed by another round of purification using 0.6x volume of AmpureBead XP (Beckman Coulter, Danvers, MA). Each library was individually quantified using Qubit dsDNA BR Assay Kit (Invitrogen, Santa Clara, CA), normalized, pooled, denatured and sequenced on the MiSeq (2 x 250 bp paired-end run) located at the Monash University Malaysia Genomics Facility.

## 2.4 Bioinformatics

Primer sequences were trimmed from the 5' end of each read using cutadapt version 1.14 (Martin, 2011). The trimmed pair-end reads were quality-trimmed and merged using the fastq\_mergepairs command as implemented in USEARCH v9 (Edgar & Flyvbjerg, 2015). The overlapped reads were subsequently dereplicated, clustered at 97% identity cut off and chimera-filtered using UPARSE (Edgar, 2013). Taxonomy assignment, abundance estimation, and diversity metric calculation were performed using QIIME 1.8 (Caporaso et al., 2010).

## 2.5 Statistical analysis

Bacterial abundance data was arcsine transformed and the normality assessed by the Shapiro-Wilk test. At the phylum level of classification, phyla with less than 2% abundance were categorised as 'Other'. Significant differences in abundance at the phylum level between the biosolids of increasing age were identified by Kruskal-Wallis followed by pairwise comparisons by Dunn's multiple comparison test. Significant differences in the bacterial alpha diversity were identified by the Kruskal-Wallis test. Significant differences in the relative abundance of bacteria at the genus classification level were identified by Analysis of Similarities (ANOSIM) with Bray Curtis distance index and genera contributions to dissimilarity identified by Similarity Percentage analysis (SIMPER). Shared operational taxonomic units (OTUs) were identified using the "compute\_core\_microbiome.py" command (default setting) in QIIME and the Venn diagram constructed using VENNY (Oliveros, 2015).

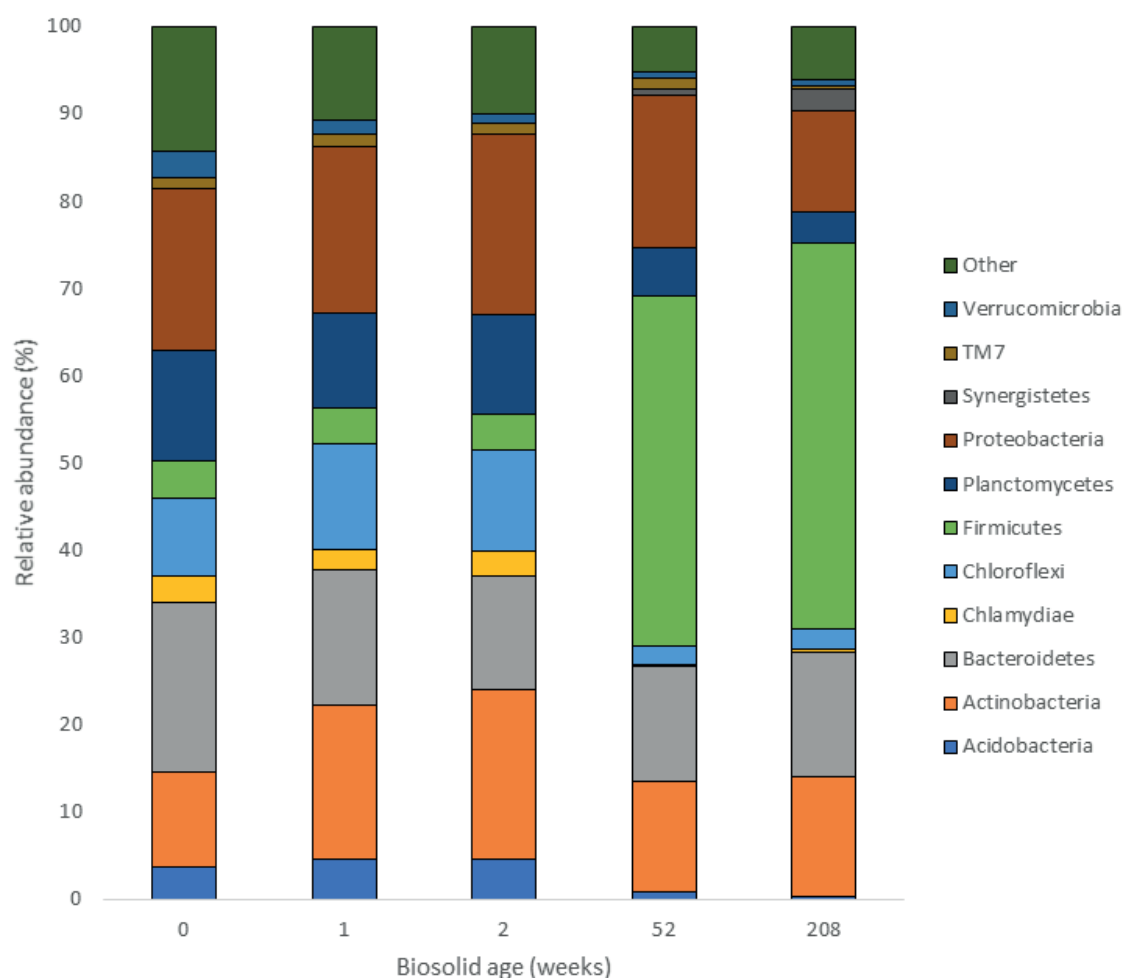
The normality of the biosolids physicochemical data was assessed by the Shapiro-Wilks test and significant differences were identified by ANOVA and Tukey's Honestly Significant Difference (HSD) using IBM SPSS Statistics for Windows, Version 23.0. Armonk, NY: IBM Co. Canonical correspondence analysis was used to identify the physicochemical properties associated with changes in bacterial abundance and Spearman's rank-order correlation was used to confirm the relationship using PAST - Paleontological statistics software package for education and data analysis.

# 3. RESULTS

## 3.1 Relative bacterial abundance at the phylum level of classification

The allocation of sequences to phyla is generally considered robust, particularly if correction procedures are implemented to remove biases and errors (Edgar, 2013; Edgar





**FIGURE 1:** Relative abundance of the bacterial phyla in the biosolids according to age (weeks) irrespective of sampling depth. Phyla with less than 2% of the overall abundance were categorised as Other.

& Flyvbjerg, 2015). Irrespective of the sampling depth and biosolids age, the dominant phyla were Firmicutes, Actinobacteria, Bacteroidetes and Proteobacteria. (Figure 1). The phyla Acidobacteria Chlamydiae, Planctomycetes, Synergistetes, TM7 and Verrucomicrobia were also detected but at lower abundances. The most dramatic increase was in the abundance of Firmicutes which increased ten-fold from 4.2% in the fresh biosolids to 40 to 44% in the stockpiled biosolids. The abundance of Actinobacteria was variable, with no clear trend, ranging from 10.9 to 19.3% and the abundance of Proteobacteria decreased with stockpiling from 18.5 to 20.4% in the fresh biosolids to 11.5% in the stockpiled biosolids.

The abundance of the less dominant phyla Acidobacteria, Chlamydiae, Chloroflexi, Planctomycetes and Verrucomicrobia all decreased significantly with increasing biosolids age. The abundance of Synergistetes increased significantly with biosolids stockpiling time from 0.13% in the fresh biosolids to 2.5% in the stockpiled biosolids. There were significant differences in the relative abundance of phyla with biosolids age, with the exception of Bacteroidetes (Table 1).

The relative abundance of each phylum at the two sampling depths was determined in the stockpiled biosolids (52

and 208 weeks). Within the 52 weeks stockpile there were significant decreases in Acidobacteria, Proteobacteria and Planctomycetes with increasing depth (Table 2). There were significant increases with depth in the abundance of Firmicutes and Synergistetes. In the 208 weeks stockpile, there were significant increases in Acidobacteria, Actinobacteria, Bacteroidetes, Chlamydiae, Planctomycetes, and TM7 with increasing depth. There were significant decreases in Bacteroidetes, Synergistetes, and Verrucomicrobia phyla.

### 3.2 Bacterial alpha diversity

Bacterial alpha diversity significantly decreased with increasing age of the biosolids as indicated by chao1 ( $p < 0.01$ ), observed OTUs ( $p < 0.01$ ) and Shannon index ( $p < 0.01$ ) (Figure 2). For each measure of alpha diversity, there was no significant difference between the 52 and 208 weeks old biosolids. There were significant differences between all other pairwise combinations.

### 3.3 Biosolids physicochemical properties

The pH of the biosolids was significantly higher in the older stockpiled biosolids compared to the fresh biosolids, ranging from 8.21 to 6.93, respectively (Table 3). There was a significant increase in the ammonium content of the bio-

**TABLE 1:** Pairwise comparisons of the relative abundance of bacterial phylum in the fresh (0, 1 and 2 week) and stockpiled (52 and 208 weeks) biosolids as determined by Kruskal-Wallis followed by Dunn's multiple comparison test. The abbreviation 'ns' refers to not significant. \* p<0.05, \*\* p<0.01

Phylum	Kruskal-Wallis p value	Biosolids age (weeks)				
		1	2	52	208	
Acidobacteria	**	0	ns	ns	0.04	0.01
		1		ns	0.01	<0.01
		2			ns	0.02
		52				ns
		208				ns
Actinobacteria	*	0	0.04	0.02	ns	ns
		1		ns	0.04	ns
		2			0.01	0.03
		52				ns
		208				ns
Bacteroidetes	ns					
Chlamydiae	**	0	ns	ns	<0.01	<0.01
		1		ns	<0.01	0.01
		2			<0.01	<0.01
		52				ns
		208				ns
Chloroflexi	**	0	ns	ns	<0.01	0.01
		1		ns	0.02	0.03
		2			<0.01	<0.01
		52				ns
		208				ns
Firmicutes	**	0	ns	ns	<0.01	<0.01
		1		ns	<0.01	<0.01
		2			<0.01	<0.01
		52				ns
		208				ns
Planctomycetes	**	0	ns	ns	0.03	<0.01
		1		ns	ns	<0.01
		2			ns	<0.01
		52				<0.01
		208				<0.01
Proteobacteria	**	0	ns	ns	ns	ns
		1		ns	ns	0.04
		2			ns	0.02
		52				0.02
		208				0.02
Synergistetes	**	0	ns	ns	ns	0.04
		1		ns	ns	0.02
		2			ns	<0.01
		52				<0.01
		208				<0.01
TM7	**	0	ns	ns	ns	0.04
		1		ns	ns	0.01
		2			ns	0.03
		52				<0.01
		208				<0.01
Verrucomicrobia	**	0	ns	ns	<0.01	<0.01
		1		ns	0.03	<0.01
		2			ns	0.04
		52				ns
		208				ns

solids with stockpiling, with 801 mg/kg in the fresh biosolids compared to up to 8,178 mg/kg in the stockpiled biosolids. Analysis by ANOVA indicated significant differences in nitrate between the biosolids but this was not significant

**TABLE 2:** Bacterial phylum relative abundance at two depths in the 52 and 208 weeks old biosolids stockpiles. The values presented are Kruskal-Wallis mean rank. The abbreviation 'ns' refers to not significant. \* p<0.05, \*\* p<0.01

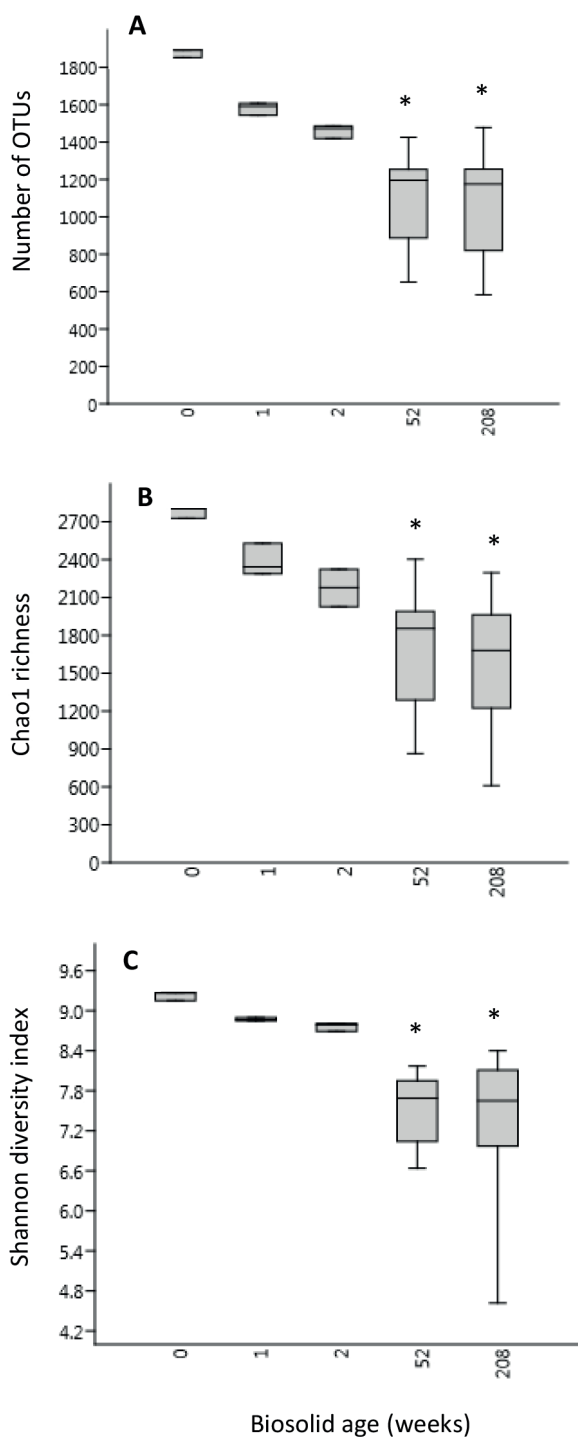
Biosolids age (weeks)	Bacterial phylum	Depth 1	Depth 2	p value	
52	Acidobacteria	16.00	14.33	**	
	Actinobacteria	17.29	11.33	ns	
	Bacteroidetes	14.48	17.89	ns	
	Chlamydiae	14.26	18.39	ns	
	Chloroflexi	13.95	19.11	ns	
	Firmicutes	15.14	16.33	**	
	Planctomycetes	15.62	15.22	**	
	Proteobacteria	15.90	14.56	**	
	Synergistetes	14.38	18.11	*	
	TM7	17.38	11.11	*	
	Verrucomicrobia	14.67	17.44	ns	
	208	Acidobacteria	10.47	20.53	**
		Actinobacteria	10.00	21.00	**
		Bacteroidetes	19.40	11.60	**
		Chlamydiae	12.13	18.87	**
Chloroflexi		14.67	16.33	ns	
Firmicutes		14.07	16.93	ns	
Planctomycetes		9.83	21.17	**	
Proteobacteria		14.93	16.07	ns	
Synergistetes		12.00	10.00	**	
TM7		10.00	21.00	**	
Verrucomicrobia	18.67	12.33	*		

by Tukey's HSD due to the conservative nature of the analysis. There were no significant changes in Olsen P, total N, total C or K with stockpiling. There was a significant decrease in moisture with stockpiling. Canonical Correspondence Analysis (CCA) (Figure 3) indicated that the change in abundance of Firmicutes may have been influenced by ammonium concentration and total K. This was indicated by the close proximity of Firmicutes abundance to the quantitative explanatory variables ammonium and total K, in the direction of increasing concentration. Spearman correlation confirmed this, with ammonium content being the main driver of Firmicutes abundance changes and less so influenced by pH, K and total N (Table 4).

### 3.4 Genera in the Firmicutes phylum

Analysis by ANOSIM with Bray-Curtis distance index indicated that at the genus classification, the composition of the Firmicutes phylum in the fresh (weeks 0, 1 and 2 combined) biosolids was significantly different to that of the stockpiled (weeks 52 and 208 combined) biosolids (Table 5). Pairwise comparison indicated significant differences in Firmicutes community composition with depth in 52 weeks biosolids stockpile while the composition of the 208 weeks stockpile is more consistent.

Bacteria community compositional differences were identified by SIMPER. Only genera that contributed to greater than 5% dissimilarity have been reported. Comparisons were made between the composition of the fresh biosolids



**FIGURE 2:** Observed OTUs (A), Chao1 (B) and Shannon index (C) of the fresh (0, 1 and 2 week) and stockpiled (52 and 208 weeks) biosolids. \* indicates that these values are not significantly different by Dunn's Multiple Comparison test. All other pairwise combinations are significantly different.

and the 52 weeks biosolids at sampling depth 1. The largest contributor to dissimilarity was Tepidimicrobium with 19.53% contribution, increasing in abundance from 0.08 to 11.10%, respectively (Table 6). Bacillus accounted for a 15.4% contribution, followed by Caldicoprobacter (11.08%), Anoxybacillus (6.78%), Desulfotomaculum (6.32%) and Paenibacillus (6.25%).

**TABLE 3:** Physicochemical properties of the fresh and stockpiled biosolids. Mean values are presented and values in parentheses represent standard error. Values in rows with the same lower case letter are not significantly different at  $p=0.05$  as assessed by Tukey's HSD.

	Biosolid age (weeks)				
	Fresh	52 Depth 1	52 Depth 2	208 Depth 1	208 Depth 2
pH	7.39 <sup>b</sup> (0.07)	6.93 <sup>c</sup> (0.22)	8.10 <sup>a</sup> (0.03)	8.21 <sup>a</sup> (0.02)	8.01 <sup>a</sup> (0.02)
Ammonium (mg/kg)	801 <sup>c</sup> (71)	4655 <sup>b</sup> (797)	8178 <sup>a</sup> (1424)	7280 <sup>a</sup> (440)	6327 <sup>ab</sup> (439)
Nitrate (mg/kg)	0.45 (0.27)	2444 (1125)	249 (247)	15 (15)	98 (43)
Total K (mg/kg)	2333 (296)	4040 (517)	3225 (423)	3840 (287)	3440 (341)
Olsen P (mg/kg)	2433 (521)	1232 (98)	3300 (1903)	1540 (144)	878 (122)
Total C (%)	21.57 (2.65)	25.31 (2.69)	28.01 (1.58)	21.60 (0.87)	20.62 (1.38)
Total N (%)	3.37 (0.24)	3.82 (0.45)	4.41 (0.32)	4.02 (0.30)	3.40 (0.25)
Moisture (%)	49.03 <sup>a</sup> (2.25)	34.07 <sup>b</sup> (1.91)	32.62 <sup>b</sup> (3.34)	38.00 <sup>ab</sup> (2.47)	38.77 <sup>b</sup> (1.31)

Comparisons were made between the composition of the 52 weeks biosolids at sampling depths 1 and 2 (Table 7). Sporosarcina was the largest contributor to dissimilarity at 12.37% with an increase in the mean from 1.1 to 6.77%, respectively. The next largest contributor was Bacillus at 11.63%, followed by Caldicoprobacter (8.82%) Tepidimicrobium (8.71%), Anoxybacillus (6.01%), Clostridium (5.90%) and Geobacillus (5.87%).

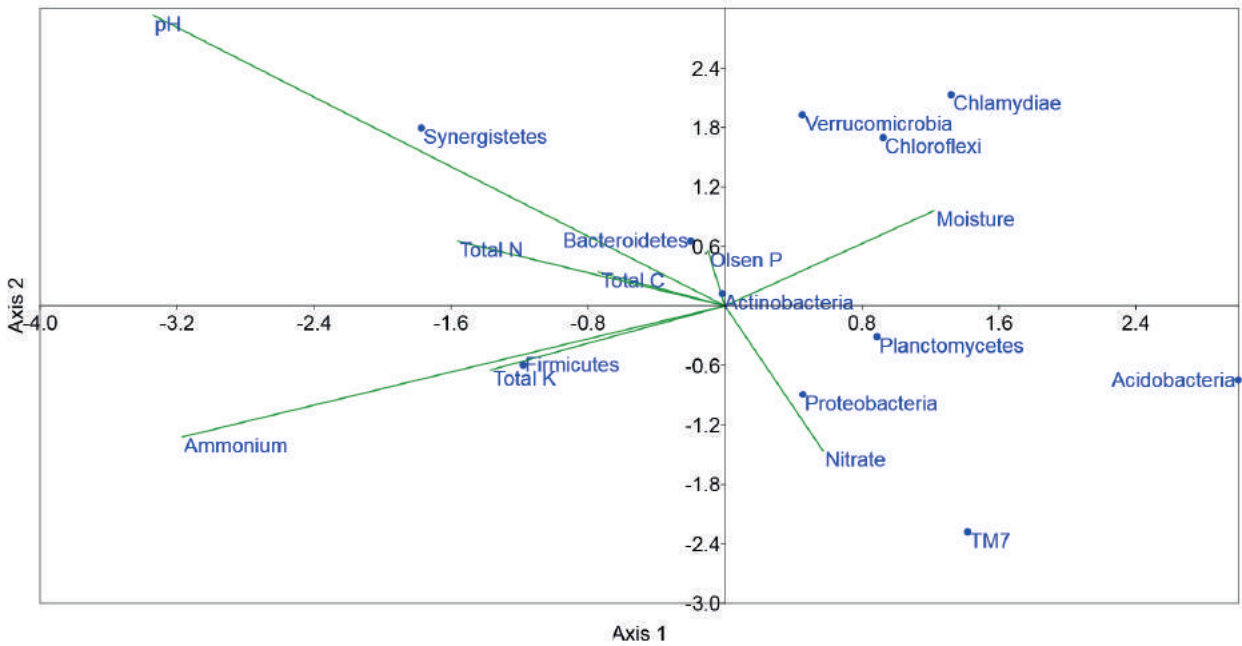
### 3.5 Shared Operational Taxonomic Units (OTUs)

Twelve OTUs were present in all of the collected biosolids, from fresh to stockpiled (Table 8). These were predominantly classified to the Proteobacteria phylum, with Actinobacteria and Firmicutes also represented.

## 4. DISCUSSION

Next generation sequencing was used to characterise the bacterial community in fresh, dewatered (0, 1 and 2 weeks old) and stockpiled biosolids (52 and 208 weeks old). Significant shifts in the composition of the bacterial community with stockpiling were detected, correlating to changes in the physicochemical properties of the biosolids. To our knowledge this is the first culture-independent study of bacterial community shifts with physicochemical properties assessment over time comparing freshly dewatered biosolids to those stored in unmanaged stockpiles.

The dominant phyla identified in the fresh and stockpiled biosolids were similar to those detected in other studies, although in varying proportions (Bibby et al., 2010; Novinscak, Filion, Surette, & Allain, 2008; Yergeau et al., 2016). Yergeau et al. (2016) found that in dewatered sludge, the dominant phyla were Bacteroidetes, Proteobacteria and Firmicutes, but a comparatively lower abundance of Actinobacteria. Conversely, Novinscak, DeCoste, Surette, and Filion (2009) demonstrated that in biosolids stored in



**FIGURE 3:** Canonical Correspondence Analysis (CCA) of the physicochemical properties of the biosolids regardless of age and the relative abundance of bacteria classified to the phylum level. The green lines indicate the direction of increase of each quantitative explanatory variable.

windrows, the abundance of Firmicutes decreased significantly with Proteobacteria becoming the dominant phyla however the management practices e.g. turning and aeration were not described. In comparison to the phyla identified in agricultural soils, depending on management practices, Proteobacteria would be expected to dominate the community with lower abundances of phyla including Ac-

idobacteria, Actinobacteria, Verrucomicrobia, Bacteroidetes, Chloroflexi and Firmicutes, (Bibby et al., 2010; Janssen, 2006; Shange, Ankumah, Ibekwe, Zabawa, & Dowd, 2012). The persistence and functionality of biosolids indigenous bacteria once applied to land would depend on a range of factors including environmental conditions, the crop and soil type and competition for resources from the soil indig-

**TABLE 4:** Spearman's rank order correlation coefficients. Values in bold highlight significant correlations where \*\* p<0.01 and \*p<0.05.

Phylum	pH	Ammonium (mg/kg)	Nitrate (mg/kg)	K (mg/kg)	Olsen P (mg/kg)	C (%)	N (%)	Moisture (%)
Acidobacteria	<b>-0.81**</b>	<b>-0.83**</b>	0.34	-0.31	-0.031	-0.28	<b>-0.53**</b>	0.17
Actinobacteria	-0.12	-0.27	0.09	-0.26	-0.24	-0.20	-0.38	0.15
Bacteroidetes	0.14	-0.26	-0.15	-0.05	0.30	0.34	0.46	0.04
Chlamydiae	-0.09	<b>-0.54**</b>	-0.38	<b>-0.54**</b>	0.06	0.07	-0.25	<b>0.44*</b>
Chloroflexi	-0.20	<b>-0.61**</b>	-0.50	-0.23	0.15	0.03	-0.15	0.40
Firmicutes	<b>0.57**</b>	<b>0.81**</b>	-0.18	0.49*	-0.06	0.23	<b>0.46*</b>	-0.35
Planctomycetes	<b>-0.68**</b>	<b>-0.73**</b>	<b>0.44*</b>	<b>-0.46*</b>	-0.12	0.02	<b>-0.46*</b>	0.18
Proteobacteria	<b>-0.62**</b>	<b>-0.43**</b>	0.17	-0.28	-0.04	-0.29	<b>-0.52*</b>	0.27
Synergistetes	<b>0.70**</b>	<b>0.67**</b>	<b>-0.69**</b>	0.28	-0.04	0.02	0.37	-0.08
TM7	<b>-0.74**</b>	<b>-0.64**</b>	<b>0.67**</b>	-0.37	-0.17	-0.05	<b>-0.47*</b>	0.05
Verrucomicrobia	-0.01	<b>-0.60**</b>	-0.11	<b>-0.44*</b>	0.34	0.27	0.02	0.28

**TABLE 5:** Pairwise comparisons of the composition of the Firmicutes phylum at the genus level where \*p<0.01 and \*\*p<0.001. The abbreviation 'ns' refers to not significant.

	Biosolid age (weeks)			
	Depth 1 (52)	Depth 2 (52)	Depth 1 (208)	Depth 2 (208)
Fresh (0, 1 and 2 weeks pooled)	**	**	**	**
52 weeks, Depth 1	-	*	*	*
52 weeks, Depth 2	-	-	ns	ns
208 weeks, Depth 1	-	-	-	ns

**TABLE 6:** SIMPER analysis of the fresh biosolids compared to the 52 weeks biosolids at sampling depth 1.

Taxon	Average dissimilarity	Contribution (%)	Cumulative (%)	Mean Fresh	Mean 52 weeks, Depth 1
Tepidimicrobium	17.62	19.53	19.53	0.08	11.10
Bacillus	13.90	15.40	34.93	0.23	9.20
Caldicoprobacter	10.00	11.08	46.01	0.10	6.34
Anoxybacillus	6.12	6.78	52.79	<0.01	3.56
Desulfotomaculum	5.71	6.32	59.11	0.03	3.62
Paenibacillus	5.64	6.25	65.37	0.06	3.22

**TABLE 7:** SIMPER analysis of the 52 weeks biosolids sampled at depth 1 compared to depth 2.

Taxon	Average dissimilarity	Contribution (%)	Cumulative (%)	Mean 52 weeks, Depth 1	Mean 52 weeks, Depth 2
Sporosarcina	3.97	12.37	12.37	1.10	6.77
Bacillus	3.74	11.63	24.00	9.20	11.10
Caldicoprobacter	2.84	8.82	32.82	6.34	9.49
Tepidimicrobium	2.80	8.71	41.53	11.10	10.80
Anoxybacillus	1.93	6.01	47.55	3.56	1.37
Clostridium	1.90	5.90	53.45	2.74	4.73
Geobacillus	1.89	5.87	59.31	2.44	4.40

**TABLE 8:** Shared OTUs between the fresh and stockpiled biosolids. Values in parentheses represent  $\pm$  standard error based on relative abundance.

OTU ID	Phylum	Classification level	Classification	Abundance within the phylum (%)	Mean times detected Fresh	Mean times detected 52 weeks	Mean times detected 208 weeks
4	Actinobacteria	Genus	Mycobacterium	18.86	446.67 (34.26)	224.00 (30.23)	593.33 (71.57)
216	Actinobacteria	Genus	Microbacterium	0.95	7.44 (1.08)	14.17 (2.25)	7.80 (1.22)
84	Firmicutes	Family	Clostridiaceae	0.86	55.89 (4.47)	47.57 (6.72)	43.27 (5.31)
17	Firmicutes	Family	Clostridiaceae	1.77	135.00 (7.08)	86.60 (11.50)	93.80 (11.69)
85	Firmicutes	Genus	Turicibacter	0.74	53.22 (3.46)	38.77 (5.76)	34.90 (5.03)
42	Firmicutes	Family	Clostridiaceae	1.71	127.56 (9.09)	81.50 (11.86)	90.93 (13.47)
59	Proteobacteria	Genus	Mesorhizobium	3.87	44.56 (4.33)	126.57 (14.43)	58.17 (5.35)
69	Proteobacteria	Genus	Hyphomicrobium	1.70	25.56 (2.64)	45.27 (6.52)	40.90 (5.96)
898	Proteobacteria	Genus	Hyphomicrobium	0.47	4.22 (0.60)	12.43 (3.28)	12.63 (2.46)
1403	Proteobacteria	Family	Bradyrhizobium	0.30	4.33 (0.71)	5.50 (0.67)	8.40 (1.45)
217	Proteobacteria	Order	Rhizobiales	0.41	4.11 (0.72)	7.57 (0.97)	13.87 (1.77)
578	Proteobacteria	Genus	Devosia	0.55	2.00 (0.37)	15.53 (2.53)	14.33 (2.10)

enous microbes (Deng et al., 2019; Trabelsi, Mengoni, Ben Ammar, & Mhamdi, 2011).

In terms of the physicochemical properties of the fresh and stockpiled biosolids, total N and total K were within the range of that found in other studies of 20-80 g/kg and 1-6 g/kg, respectively (Cogger, Forge, & Neilsen, 2006). The P was lower in our study compared to 15-30 g/kg measured by Cogger et al. (2006), however we measured plant available P (Olsen P) rather than total P. The biosolids stockpiles accumulate over a period of time, with no turning or aeration and so regions within the stockpiles transition in their exposure to the atmosphere, becoming anaerobic after a period of time being aerobic. The dramatic increase in ammonium content from the fresh biosolids to the older, stockpiled biosolids along with low levels of nitrate indicate a limitation in the oxidation of ammonium to nitrate. The significant increase in pH, ammonium and decrease in nitrate at the two depths in the 52 weeks stockpile indicates the development of environmental and ecological

niches while in the 208 weeks stockpile there was more consistency in terms of the physicochemical and bacterial community composition with depth. The decrease in bacterial diversity with increasing biosolids age was likely due to environmental stress induced by high concentrations of ammonium and increased pH (Lauber, Hamady, Knight, & Fierer, 2009).

Firmicutes produce endospores and can persist in a wide range of environments for long periods of time, explaining their prevalence in high ammonium and alkaline pH conditions in our study. The significant shift in the composition of the Firmicutes phylum with stockpiling was attributed primarily to genera Tepidimicrobium and Sporocarcina. Tepidimicrobium is a protein degrader, identified in anaerobic digestates and as also demonstrated here, tolerant to elevated ammonium concentrations (Huang et al., 2013; Li et al., 2017). Conversely X. Dai et al. (2016) demonstrated a decrease in the abundance of Tepidimicrobium and Firmicutes in general with increasing ammonium stress in

anaerobic digestion of sewage sludge with the ammonium level artificially raised to 6000 mg N/L. Tepidimicrobium is a strict anaerobe so is not likely to persist once the biosolids are applied to agricultural land. Sporosarcina requires high ammonium and alkaline pH conditions for growth. (Mörsdorf & Kaltwasser, 1989). Species of this genus are commonly found in fertile soils, may produce urease to assist the breakdown of urea and are aerobic or facultatively anaerobic so could persist once the stockpiled biosolids have been distributed from the stockpile (Editorial, 2015). Paenibacillus and Bacillus increased in relative abundance with stockpiling and depending on the species, could be of agricultural benefit if added to an agricultural system. Paenibacillus are known to promote plant growth by a range of strategies including symbiotic N<sub>2</sub> fixation, the production of auxin and the control of pathogens (Grady, MacDonald, Liu, Richman, & Yuan, 2016; McSpadden Gardener, 2004). The Bacillus genus consists of species with a wide range of functions which may be pathogenic or beneficial. Species may be aerobic or facultative anaerobic so may persist either as endospores or functioning bacteria following land application would need to be monitored.

Despite changes in the physicochemical composition of the biosolids with increasing age, agriculturally beneficial nitrogen fixing bacteria belonging to the genus Devosia and Bradyrhizobium (Wolińska et al., 2017) were detected. The abundance of Rhizobium increases with increasing pH due to increased availability of nutrients such as Mo (Lowendorf, Baya, & Alexander, 1981). While to our knowledge there have been no previous reports of direct detection in biosolids, a study conducted by Cousin, Grant, Dixon, Beyene, and van Berkum (2002) isolated Bradyrhizobium from soil plots to which biosolids had been applied but not from the untreated control plots. It was concluded that the rhizobium may have been introduced with the biosolids. Although these bacteria represent a relatively small proportion of the phylum, their presence is important for plant growth promotion however their ability to form nodules after application to crops will depend on the species of rhizobium, soil conditions and compatibility with the crop (Slattery & Pearce, 2001).

The bacterial community in the stockpiled biosolids had a similar composition to that of an anaerobic digester, dominated by Firmicutes with Actinobacteria, Bacteroidetes and Proteobacteria (De Vrieze et al., 2015). In addition to use in agriculture, there could be potential for bioprospecting the biosolids for inoculant for anaerobic digestion and composting (Slimane, Fathya, Assia, & Hamza, 2014). Bacteria detected in the biosolids including Anoxybacillus, a cellulolytic thermophile, speeds up composting by increasing the duration of the thermophilic phase (Ghafari, Sepahi, Razavi, Malekzadeh, & Haydarian, 2011) and likewise, Geobacillus has demonstrated a similar effect (Sarkar et al., 2010).

## 5. CONCLUSIONS

The stockpiled biosolids in this study are an alkaline product with elevated ammonium content and along with the presence of beneficial bacteria make the application of

biosolids to agricultural land an attractive option, potentially reducing fertiliser costs and pH correction in acidic soils. For any valorisation study, pathogen content needs to be monitored. Field trials in a range of soil types are needed to determine the persistence of agriculturally relevant microbes and soil physicochemical properties, particularly pH and available nutrients such as ammonium, nitrate and phosphorus. This study was limited to one wastewater treatment plant and this could be extended to additional plants and biosolid stockpiles. The potential for using the biosolids as an inoculant for anaerobic digestion and composting could also be investigated.

## REFERENCES

- Australian & New Zealand Biosolids Partnership. (2016). Australian & New Zealand Biosolids Partnership. Retrieved from <https://www.biosolids.com.au/>
- Bartram, A. K., Lynch, M. D., Stearns, J. C., Moreno-Hagelsieb, G., & Neufeld, J. D. (2011). Generation of multimillion-sequence 16S rRNA gene libraries from complex microbial communities by assembling paired-end Illumina reads. *Applied and environmental microbiology*, 77(11), 3846-3852.
- Bevacqua, R. F., & Mellano, V. J. (1993). Sewage sludge compost's cumulative effects on crop growth and soil properties. *Compost science & utilization*, 1(3), 34-37.
- Bibby, K., & Peccia, J. (2013). Identification of viral pathogen diversity in sewage sludge by metagenome analysis. *Environmental Science & Technology*, 47(4), 1945-1951.
- Bibby, K., Viau, E., & Peccia, J. (2010). Pyrosequencing of the 16S rRNA gene to reveal bacterial pathogen diversity in biosolids. *Water Research*, 44(14), 4252-4260.
- Caporaso, J. G., Kuczynski, J., Stombaugh, J., Bittinger, K., Bushman, F. D., Costello, E. K., . . . Gordon, J. I. (2010). QIIME allows analysis of high-throughput community sequencing data. *Nature Methods*, 7(5), 335-336.
- Cogger, C., Forge, T., & Neilsen, G. (2006). Biosolids recycling: Nitrogen management and soil ecology. *Canadian Journal of Soil Science*, 86(4), 613-620.
- Cooper, J. L. (2005). The effect of biosolids on cereals in central New South Wales, Australia. 1. Crop growth and yield. *Australian Journal of Experimental Agriculture*, 45(4), 435-443. doi:<http://dx.doi.org/10.1071/EA03099>
- Cousin, C., Grant, J., Dixon, F., Beyene, D., & van Berkum, P. (2002). Influence of biosolids compost on the bradyrhizobial genotypes recovered from cowpea and soybean nodules. *Archives of Microbiology*, 177(5), 427-430. doi:10.1007/s00203-002-0401-y
- Dai, X., Yan, H., Li, N., He, J., Ding, Y., Dai, L., & Dong, B. (2016). Metabolic adaptation of microbial communities to ammonium stress in a high solid anaerobic digester with dewatered sludge. *Scientific Reports*, 6.
- Dai, Z., Liu, G., Chen, H., Chen, C., Wang, J., Ai, S., . . . Tang, C. (2019). Long-term nutrient inputs shift soil microbial functional profiles of phosphorus cycling in diverse agroecosystems. *The ISME Journal*, 1-14.
- De Vrieze, J., Gildemyn, S., Vilchez-Vargas, R., Jáuregui, R., Pieper, D. H., Verstraete, W., & Boon, N. (2015). Inoculum selection is crucial to ensure operational stability in anaerobic digestion. *Applied Microbiology and Biotechnology*, 99(1), 189-199.
- Deng, S., Wipf, H. M.-L., Pierroz, G., Raab, T. K., Khanna, R., & Coleman-Derr, D. (2019). A Plant Growth-Promoting Microbial Soil Amendment Dynamically Alters the Strawberry Root Bacterial Microbiome. *Scientific Reports*, 9(1), 1-15.
- Edgar, R. C. (2013). UPARSE: highly accurate OTU sequences from microbial amplicon reads. *Nature Methods*, 10(10), 996-998.
- Edgar, R. C., & Flyvbjerg, H. (2015). Error filtering, pair assembly and error correction for next-generation sequencing reads. *Bioinformatics*, 31(21), 3476-3482.
- Editorial, B. (2015). Sporosarcina. In *Bergey's Manual of Systematics of Archaea and Bacteria*: John Wiley & Sons, Ltd.

- EPA Victoria. (2004). Guidelines for Environmental Management, Biosolids Land Application.
- Ferraz, A. d. V., Momentel, L. T., & Poggiani, F. (2016). Soil fertility, growth and mineral nutrition in *Eucalyptus grandis* plantation fertilized with different kinds of sewage sludge. *New Forests*, 47(6), 861-876.
- Ghaffari, S., Sepahi, A. A., Razavi, M. R., Malekzadeh, F., & Haydarian, H. (2011). Effectiveness of inoculation with isolated *Anoxybacillus* sp. MGA110 on municipal solid waste composting process. *African Journal of Microbiology Research*, 5(30), 5373-5378.
- Gómez-Muñoz, B., Magid, J., & Jensen, L. S. (2017). Nitrogen turnover, crop use efficiency and soil fertility in a long-term field experiment amended with different qualities of urban and agricultural waste. *Agriculture, Ecosystems & Environment*, 240, 300-313.
- Grady, E. N., MacDonald, J., Liu, L., Richman, A., & Yuan, Z.-C. (2016). Current knowledge and perspectives of *Paenibacillus*: a review. *Microbial Cell Factories*, 15(1), 203.
- Herrmann, R. F., Grosser, R. J., Farrar, D., & Brobst, R. B. (2017). Field studies measuring the aerosolization of endotoxin during the land application of Class B biosolids. *Aerobiologia*. doi:10.1007/s10453-017-9480-8
- Hershey, D. M., Lu, X., Zi, J., & Peters, R. J. (2014). Functional conservation of the capacity for ent-kaurene biosynthesis and an associated operon in certain rhizobia. *Journal of bacteriology*, 196(1), 100-106.
- Hu, Y., Pang, S., Yang, J., Zhao, X., & Cao, J. (2019). Changes in soil microbial community structure following amendment of biosolids for seven years. *Environmental Pollutants and Bioavailability*, 31(1), 24-31. doi:10.1080/26395940.2019.1569478
- Huang, Y., Sun, Y., Ma, S., Chen, L., Zhang, H., & Deng, Y. (2013). Isolation and characterization of *Keratinibaculum paraultunense* gen. nov., sp. nov., a novel thermophilic, anaerobic bacterium with keratinolytic activity. *FEMS Microbiology Letters*, 345(1), 56-63. doi:10.1111/1574-6968.12184
- Irwin, R., Surapaneni, A., Smith, D., Schmidt, J., Rigby, H., & Smith, S. R. (2017). Verification of an alternative sludge treatment process for pathogen reduction at two wastewater treatment plants in Victoria, Australia. *Journal of water and health*, 15(4), 626-637.
- Janssen, P. H. (2006). Identifying the dominant soil bacterial taxa in libraries of 16S rRNA and 16S rRNA genes. *Applied and environmental microbiology*, 72(3), 1719-1728.
- Karpowicz, E., Novinscak, A., Bärlocher, F., & Filion, M. (2010). qPCR quantification and genetic characterization of *Clostridium perfringens* populations in biosolids composted for 2 years. *Journal of applied microbiology*, 108(2), 571-581.
- Klindworth, A., Pruesse, E., Schweer, T., Peplies, J., Quast, C., Horn, M., & Glöckner, F. O. (2012). Evaluation of general 16S ribosomal RNA gene PCR primers for classical and next-generation sequencing-based diversity studies. *Nucleic Acids Research*, gks808.
- Lauber, C. L., Hamady, M., Knight, R., & Fierer, N. (2009). Pyrosequencing-based assessment of soil pH as a predictor of soil bacterial community structure at the continental scale. *Applied and environmental microbiology*, 75(15), 5111-5120.
- Li, N., Xue, Y., Chen, S., Takahashi, J., Dai, L., & Dai, X. (2017). Methanogenic population dynamics regulated by bacterial community responses to protein-rich organic wastes in a high solid anaerobic digester. *Chemical Engineering Journal*, 317, 444-453. doi:https://doi.org/10.1016/j.cej.2017.02.098
- Lowendorf, H. S., Baya, A. M., & Alexander, M. (1981). Survival of *Rhizobium* in acid soils. *Applied and environmental microbiology*, 42(6), 951-957.
- Martin, M. (2011). Cutadapt removes adapter sequences from high-throughput sequencing reads. *EMBnet. journal*, 17(1), pp. 10-12.
- McSpadden Gardener, B. B. (2004). Ecology of *Bacillus* and *Paenibacillus* spp. in Agricultural Systems. *Phytopathology*, 94(11), 1252-1258. doi:10.1094/PHYTO.2004.94.11.1252
- Mörsdorf, G., & Kaltwasser, H. (1989). Ammonium assimilation in *Proteus vulgaris*, *Bacillus pasteurii*, and *Sporosarcina ureae*. *Archives of Microbiology*, 152(2), 125-131. doi:10.1007/bf00456089
- Mossa, A.-W., Dickinson, M. J., West, H. M., Young, S. D., & Crout, N. M. J. (2017). The response of soil microbial diversity and abundance to long-term application of biosolids. *Environmental Pollution*, 224, 16-25. doi:https://doi.org/10.1016/j.envpol.2017.02.056
- Nagel, R., Bieber, J. E., Schmidt-Dannert, M. G., Nett, R. S., & Peters, R. J. (2018). A Third Class: Functional Gibberellin Biosynthetic Operon in Beta-Proteobacteria. *Frontiers in Microbiology*, 9(2916). doi:10.3389/fmicb.2018.02916
- Novinscak, A., DeCoste, N., Surette, C., & Filion, M. (2009). Characterization of bacterial and fungal communities in composted biosolids over a 2 year period using denaturing gradient gel electrophoresis. *Canadian journal of microbiology*, 55(4), 375-387.
- Novinscak, A., Filion, M., Surette, C., & Allain, C. (2008). Application of molecular technologies to monitor the microbial content of biosolids and composted biosolids. *Water Science and Technology*, 57(4), 471-477. doi:10.2166/wst.2008.019
- Oliveros, J. C. (2015). VENN. An interactive tool for comparing lists with Venn Diagrams. 2007. In.
- Paez-Rubio, T., Ramarui, A., Sommer, J., Xin, H., Anderson, J., & Peccia, J. (2007). Emission rates and characterization of aerosols produced during the spreading of dewatered class B biosolids. *Environmental Science & Technology*, 41(10), 3537-3544.
- Petersen, S. O., Petersen, J., & Rubæk, G. H. (2003). Dynamics and plant uptake of nitrogen and phosphorus in soil amended with sewage sludge. *Applied Soil Ecology*, 24(2), 187-195.
- Qiong, L., Li, J.-m., Cui, X.-l., & Wei, D.-p. (2012). On-farm assessment of biosolids effects on nitrogen and phosphorus accumulation in soils. *Journal of Integrative Agriculture*, 11(9), 1545-1554.
- Rouch, D. A., Fleming, V., Deighton, M., Blackbeard, J., & Smith, S. R. (2008). Evaluating pathogen risks in production of biosolids in Victoria. Paper presented at the AWA Biosolids Specialty IV Conference.
- Sarkar, S., Banerjee, R., Chanda, S., Das, P., Ganguly, S., & Pal, S. (2010). Effectiveness of inoculation with isolated *Geobacillus* strains in the thermophilic stage of vegetable waste composting. *Bioresource Technology*, 101(8), 2892-2895.
- Schlatter, D. C., Paul, N. C., Shah, D. H., Schillinger, W. F., Bary, A. I., Sharratt, B., & Paulitz, T. C. (2019). Biosolids and Tillage Practices Influence Soil Bacterial Communities in Dryland Wheat. *Microbial Ecology*, 78(3), 737-752. doi:10.1007/s00248-019-01339-1
- Shange, R. S., Ankumah, R. O., Ibekwe, A. M., Zabawa, R., & Dowd, S. E. (2012). Distinct Soil Bacterial Communities Revealed under a Diversely Managed Agroecosystem. *PLoS one*, 7(7), e40338. doi:10.1371/journal.pone.0040338
- Slattery, J., & Pearce, D. (2001). The impact of background rhizobial populations on inoculation response. *Inoculates and nitrogen fixation of legumes in Vietnam. ACIAR Proceeding*(109e), 37-45.
- Slimane, K., Fathya, S., Assia, K., & Hamza, M. (2014). Influence of Inoculums/Substrate Ratios (ISRs) on the Mesophilic Anaerobic Digestion of Slaughterhouse Waste in Batch Mode: Process Stability and Biogas Production. *Energy Procedia*, 50, 57-63. doi:http://dx.doi.org/10.1016/j.egypro.2014.06.007
- Tamoutsidis, E., Papadopoulos, I., Tokatlidis, I., Zotis, S., & Mavropoulos, T. (2002). Wet sewage sludge application effect on soil properties and element content of leaf and root vegetables. *Journal of plant nutrition*, 25(9), 1941-1955.
- Trabelsi, D., Mengoni, A., Ben Ammar, H., & Mhamdi, R. (2011). Effect of on-field inoculation of *Phaseolus vulgaris* with rhizobia on soil bacterial communities. *FEMS Microbiology Ecology*, 77(1), 211-222. doi:10.1111/j.1574-6941.2011.01102.x
- Viau, E., & Peccia, J. (2009a). Evaluation of the enterococci indicator in biosolids using culture-based and quantitative PCR assays. *Water Research*, 43(19), 4878-4887.
- Viau, E., & Peccia, J. (2009b). Survey of wastewater indicators and human pathogen genomes in biosolids produced by class A and class B stabilization treatments. *Applied and environmental microbiology*, 75(1), 164-174.
- Warman, P., & Termeer, W. (2005). Evaluation of sewage sludge, septic waste and sludge compost applications to corn and forage: yields and N, P and K content of crops and soils. *Bioresource Technology*, 96(8), 955-961.
- Wolińska, A., Kuźniar, A., Zielenkiewicz, U., Banach, A., Izak, D., Stępniewska, Z., & Błaszczak, M. (2017). Metagenomic Analysis of Some Potential Nitrogen-Fixing Bacteria in Arable Soils at Different Formation Processes. *Microbial Ecology*, 73(1), 162-176.
- Yergeau, E., Masson, L., Elias, M., Xiang, S., Madey, E., Huang, H., . . . Beaudette, L. (2016). Comparison of Methods to Identify Pathogens and Associated Virulence Functional Genes in Biosolids from Two Different Wastewater Treatment Facilities in Canada. *PLoS one*, 11(4), e0153554. doi:10.1371/journal.pone.0153554

# EFFECTS OF THE DIFFERENT IMPLEMENTATION OF LEGISLATION RELATING TO SEWAGE SLUDGE DISPOSAL IN THE EU

Torben Bauer <sup>1,\*</sup>, Linus Ekman Burgman <sup>2</sup>, Lale Andreas <sup>1</sup> and Anders Lagerkvist <sup>1</sup>

<sup>1</sup> Waste Science and Technology, Luleå University of Technology, 97187 Luleå, Sweden

<sup>2</sup> Technology and Social Change, Linköping University, 58183 Linköping, Sweden

## Article Info:

Received:  
13 December 2019  
Revised:  
3 March 2020  
Accepted:  
5 March 2020  
Available online:  
8 May 2020

## Keywords:

Sewage sludge  
Legislation  
Phosphorus recovery  
Nutrient recovery  
Land application

## ABSTRACT

The European Directive 86/278/EEC implemented in 1986 was a means adopted by the European Union to improve use of the valuables in sewage sludge by applying treated sludge on agricultural soils. To prevent an accumulation of pollutants, the Directive provided suggestions limiting concentrations of toxic elements in sewage sludge and agricultural soil. The Directive was implemented diversely throughout EU member states, with current national legislations only partly reflecting the initial intentions of the EU Directive from 30 years ago. This study demonstrates how the European Directive was implemented in three countries currently at different stages of replacing the agricultural application of sewage sludge with incineration (Netherlands, Germany and Sweden). Additionally, recent changes in the legislation with regards to the re-use and final disposal of sewage sludge in the three chosen member states are analysed. The aim was to investigate how each member state has solved the conflict between improvement of nutrient recovery from sludge and limitation of pollutants in agricultural soil. Based on this review, limit values are not necessarily reflected in application rates of sewage sludge in agriculture. Following changes in current legislation, phosphorus recovery will become a priority task. The recovery of other valuables from sewage sludge is currently not regulated in the legislation of the three member states investigated.

## 1. INTRODUCTION

Sewage sludge is produced in wastewater treatment plants. The sludge acts concomitantly as a sink for pollutants (toxic elements, organic contaminants, pathogens, residues of pharmaceuticals, micro plastic) and the stream, which accumulates organic matter and nutrients in the wastewater stream. In the EU-27, based on a 2005 calculation, 9.8 MtDS/year of sewage sludge were produced (Kelessidis & Stasinakis, 2012). By 2020, the amount of sewage sludge was expected to exceed 13 MtDS/year in the EU-27 following implementation of the Urban Waste Water Treatment Directive in member states joining the EU subsequent to 2004 (Kelessidis & Stasinakis, 2012). Currently, the main method applied in the treatment of sewage sludge is anaerobic digestion, which makes use of approx. 50% of the organic matter by producing biogas and partly addresses the issue of pollutants (Kelessidis & Stasinakis, 2012). Following anaerobic digestion, the sewage sludge is disposed of or reused in a series of different ways. The main re-use route in the EU is application on agricultural soil (45% directly and 7% after composting of the produced sludge (LeBlanc, Matthews, & Richard, 2008)). However,

although application on agricultural soil makes use of the nutrients contained in the sludge, it also diffuses the pollutants.

In addition to application on agricultural soil, the sludge can be reused in land reclamation or landfill covers. The most common disposal routes are incineration of dried sludge and landfilling. Marine disposal of sewage sludge was banned in EU in 1998 (Council of the European Communities, 1991; Kelessidis & Stasinakis, 2012).

Re-use and disposal routes differ considerably across the EU, particularly as the EU-Directive 86/278/EEC issued in 1986 only provides guidelines relating to the re-use and final disposal of sewage sludge. Figure 1 and Figure 2 provide an overview of the total amounts per year and capita and the disposal routes for sewage sludge in selected EU countries.

The Netherlands, Germany and Sweden were chosen for this comparative study in view of their objective to minimise or abolish the use of sludge in agriculture whilst continuing to re-use the valuables contained in the sludge. Accordingly, legislation in these countries is required to identify solutions for the disposal or elimination of pollutants, whilst allowing for re-use of valuables. This conflict

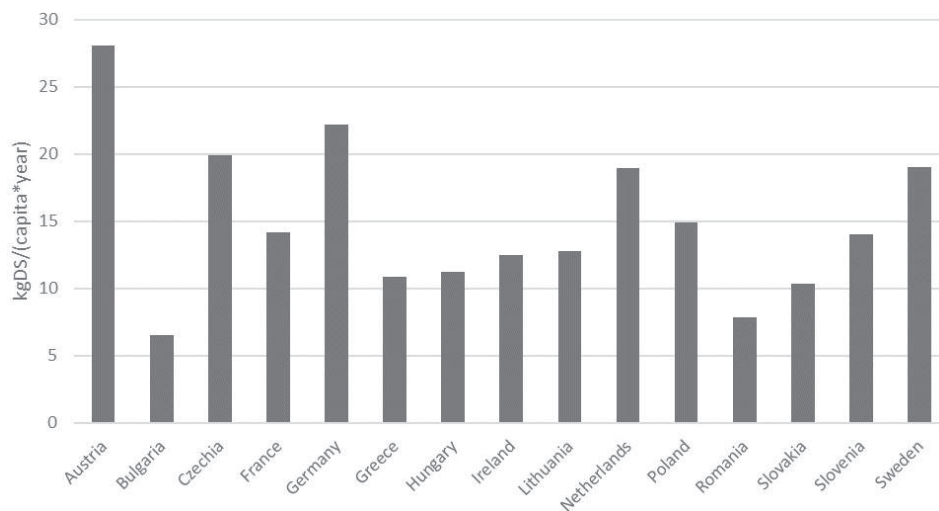
\* Corresponding author:  
Torben Bauer  
email: torben.bauer@ltu.se



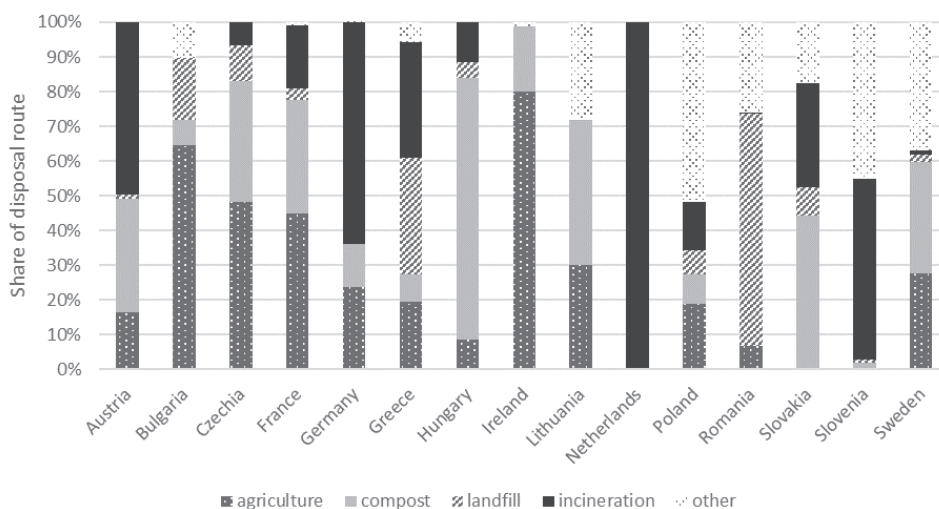
is examined herein. While the Netherlands progressed to an incineration-only strategy several years ago, Germany has also recently adhered to this trend and is currently reducing the share of land application in favour of incineration. Although Figure 2 shows a different approach in Sweden, a change from application in agriculture to incineration is also being debated in Sweden. The large share of “other” in Sweden indicates the usage of sewage sludge in landfill covers, seen as a form of land reclamation (Svinhufvud, 2017). For newer EU member countries such as Poland or Czechia, re-use and disposal routes differ widely with a focus on application in agriculture and landfilling. In the case of more recent EU-member states, it is unclear what the share of “other disposal route” represents (European Commission, 2004, 2017; Kelessidis & Stasinakis, 2012).

The aim of this study was to highlight the differences manifested in implementation of the EU Directive 86/278/EEC in the chosen member states. For this purpose, both

EU-level and national legislation from certain member states was analysed. The main focus was on limit values for toxic elements, as established both in the EU Directive and by national legislation, with a view to investigating how these limit values rule out certain re-use and disposal routes. In addition, the existence of limit values for organic pollutants and changes in legislation in recent years were analysed to clarify how the selected member states were attempting to improve nutrient recovery without disposing of pollutants on agricultural soil. This study was limited to the member states listed previously: the Netherlands served as an example of an incineration-only strategy; Germany was selected in the light of a recent (2017) change in legislation to promote a reduced application in agriculture and increased incineration in combination with phosphorus recovery. Finally, Sweden was chosen due to its reliance on application in agriculture, although in the presence of an ongoing policy process aimed at prohibiting all applications in agriculture whilst continuing to undertake phos-



**FIGURE 1:** Final disposal of sewage sludge in EU countries per year and capita. Countries were selected based on the amount of sludge to be disposed of being at least 20,000 tDS/year and availability of data for either 2014 or 2015 (Eurostat, 2015).



**FIGURE 2:** Share of each disposal route for sewage sludge in selected EU countries. Countries were selected based on the amount of sludge to be disposed of being at least 20,000 tDS/year and availability of data for either 2014 or 2015 (Eurostat, 2015).

phorus recovery (Government Offices of Sweden, 2018a).

The aims were achieved by means of a literature review of scientific articles, reports from authorities and legislation (laws and directives). The literature covers legislation enforced at both EU level as well as in each chosen member state. Table 1 provides an overview of the legislation assessed.

## 2. BACKGROUND AND LIMITATIONS

This study focussed on limit values and future strategies for the recovery of phosphorus from sludge. Although limit values represent a minor part of the legislation system, they form the core of the legislation, with disposal strategies being expressed in limit values in many countries. The phosphorus recovery strategies implemented in the chosen member states share the common features whereby applications in agriculture are no longer envisaged, but phosphorus is still recovered and reused. To achieve this, policy-makers develop long-term strategies which can no longer be expressed only in limit values. By analysing limit values and future phosphorus recovery strategies, assumptions relating to future sewage sludge re-use and disposal strategies in the member states can be made without the need to assess other parts of the legislation.

This paper did not take into account comparisons between the fertilising qualities of sludge, sludge based fertilizers and other commercial fertilizers. Phosphorus recovery was only addressed in terms of legislation strategies and no analysis of strategies focussing on circular phosphorus flows was conducted. Accordingly, no conclusions can be drawn with regard to the importance of phosphorus recovery strategies in, for example, a circular economy.

## 3. RESULTS & DISCUSSION

The legislation evaluated for the following chapter is shown in Table 1.

### 3.1 EU

The EU Directive 86/278/EEC dated June 1986 establishes rules and limits relating to the application of sewage sludge on agricultural soil for the purpose of recycling nutrients present in the sludge, but also limits the accumula-

tion of toxic elements in the soil. The Directive suggests that member states either set limits for concentrations of toxic elements in the sludge or set accumulation limits for toxic elements in the soil. Limit values for both cases can be found in the Directive, although member states may also opt to implement stricter regulations. In addition to limiting toxic elements, the Directive regulates the documentation of sludge usage as well as providing recommendations for nutrient needs of plants, quality of soil and sludge stabilization (Brown, Tsiarta, Watson, & Hudson, 2015; Council of the European Union, 1986a).

According to Brown (2015) the Directive has been implemented by all EU member states, with many setting stricter limits for concentrations of toxic elements in soil than the values suggested in the EU Directive (e.g. 20 member states have stricter values for Cd). An even higher number of member states have set more restrictive values for concentrations of toxic elements present in sludge used in agriculture (Kelessidis & Stasinakis, 2012). In contrast, the frequencies for soil testing vary considerably and have not been fully implemented in several member states (Brown et al., 2015).

### 3.2 Netherlands

In the Netherlands, the application of sewage sludge to agricultural soils had already been regulated prior to the introduction of the EU-Directive. In 1995, the EU-Directive was implemented into national legislation (Ruijter, 2018), and the limit values for toxic elements in soil were lower than values suggested in the EU-Directive. Even stricter values were implemented for concentrations of toxic elements in sludge (Zn, Cr, and Hg more than 10 times lower than in EU-Directive) (Brown et al., 2015). Since the values were much more restrictive than limit values established for other organic-based fertilizers, application in agriculture of sewage sludge became virtually impossible. Moreover, landfilling was also ruled out by setting the limit for total organic carbon in landfillable sludges below 5% (Ehlert et al., 2013). Limit values for organic contaminants were not implemented (Ehlert et al., 2013). As changes in local legislation were foreseeable, two mono-incinerators for sewage sludge were put into operation in 1993 and 1995 (Ruijter, 2018).

**TABLE 1:** Overview of the legislative documents examined and specification of the literature it was accessed through.

Country	Legal documents	Accessed via	Content
EU	EU-directive 86/278/EEC	Council of the European Union (1986) and secondary literature: Brown (2015); Kelessidis & Stasinakis (2012); European Commission (2004, 2017)	Suggestions for limit values (soil, sludge, dosage), application rates, re-use and disposal routes
NL	BOOM Decree and Fertiliser Decree incl. Implementation	Secondary literature: Brown (2015); Ehlert et al. (2013); de Boer et al. (2018); Ruijter (2018)	Limit values (soil, sludge), application rates
DE	Sewage sludge ordinance (AbfKlärV) 2015 and 2017; Fertilizer and Soil ordinance (DüMV and BBodSchV)	Bundesministerium für Umwelt (2015); Bundesregierung (2017c, 2017a, 2017b) and secondary literature: Brown (2015); van Aaken (2017)	Limit values (soil, sludge), application rates, phosphorus recovery strategy, sludge handling and transport
SE	Directives of Swedish environmental protection agency: SNFS 1994:2; SNFS 1998:4; SNFS 2001:5 Committee directive Dir. 2018:67	Government Offices of Sweden (2018); Naturvårdsverket (1994, 1998, 2001) and secondary literature: Brown (2015); Oberg & Mason-Renton (2018)	Limit values (soil, sludge dosage), application rates (by sludge dosage)

Today the two mono-incinerators treat 50% of the sewage sludge produced in the Netherlands. The rest is co-incinerated in bio-energy plants, cement production, municipal solid waste incinerators and in a German coal power plant. Phosphorus removal from wastewater has been mandatory in the Netherlands since 1995 (Ruijter, 2018). Phosphorus recovery from ash is tested in the mono-incinerators. In addition, phosphorus recovery by formation of struvite in the wastewater treatment process is tested. The regulations for fertilizers in the Netherlands have a category for recovered phosphorus, making it easier for recovered phosphorus to enter the market. Since 2015, the Netherlands have legislated on phosphorus recovery, although this has proved difficult to implement (de Boer, Romeo-Hall, Roomans, & Slootweg, 2018).

### 3.3 Germany

In Germany, the EU-Directive was implemented through the sewage sludge ordinance in 1992. The limits in the ordinance for concentrations of toxic elements in soil and sludge were stricter in some parts than the limit values suggested by the EU-Directive. In addition, limit values for organic contaminants (polychlorinated biphenyls (PCB)) and maximum amounts for application of sludge on agricultural soil were implemented (Brown et al., 2015; Bundesministerium für Umwelt, 2015; Council of the European Union, 1986a).

The German sewage sludge ordinance was updated in 2017. The limits for toxic elements in the soil were aligned with the federal soil protection ordinance and toxic element limits for sludge were matched with those of the fertilizer ordinance. Sludge limits remained as in the previous sewage sludge ordinance. Additionally, the mixing of sludges or ashes from sludge incineration was limited and documentation requirements for sludge production, transport, incineration and disposal were intensified. The average sewage sludge in Germany continues to meet the new toxic element limits for agricultural use. In addition to the adaptation of limits, a strategy for phosphorus recovery was introduced: from 2029 onwards, wastewater treatment plants with a capacity of more than 100.000 inhabitant equivalents phosphorus recovery will be mandatory if the sludge contains more than 20 g phosphorus per kg of sludge dry matter. For these treatment plants, application in agriculture of sludge will be forbidden from 2029 onwards. From 2032, these regulations will also apply for plants with a capacity of more than 50.000 inhabitant equivalent units. Smaller plants will not be required to recover phosphorus from sludge. Furthermore, the ordinance does not specify use of any particular technology or method for phosphorus recovery (Bundesministerium für Umwelt, 2017; Bundesregierung, 2017a, 2017b; van Aaken, 2017a).

### 3.4 Sweden

In Sweden, the EU-Directive was implemented in 1994 (Naturvårdsverket, 1994), and subsequent amendments made in 1998 and 2001 (Naturvårdsverket, 1998, 2001a). These amendments also addressed changes to the limit values of toxic elements relating to use of sewage sludge in agriculture. The Swedish legislation includes toxic ele-

ment limits for both soil and applied sludge. In contrast to the legislation enforced in the Netherlands and Germany, the toxic element content of the sludge is not regulated, but rather the quantity of toxic elements to be applied to agricultural soil is limited; this implies that highly contaminated sludges may be applied in low dosages.

It should also be highlighted how following recommendation by the Swedish farmers' association that members cease all agricultural application in 1999 (Bengtsson & Tillman, 2004), a voluntary certification, REVAQ, was established, which included stricter limit values (Malmqvist, Kärman, & Rydhagen, 2006). This form of limitation beyond state regulation represents the expression of a more deliberative mode of governing sewage sludge management, as seen in Sweden (Oberg & Mason-Renton, 2018).

The Swedish government and environmental protection agency has been working to develop phosphorus recovery strategies, stricter limit values for toxic elements and new limits for organic contaminants since 2012 (Bergqvist et al., 2013; Svinhufvud, 2017). Currently, the aim is to set up a new regulation for sewage sludge disposal banning the usage of sewage sludge on land, including agriculture, although allowing for phosphorus recovery (Government Offices of Sweden, 2018b). These goals are similar to those of the new German ordinance, which will likely serve as a template for the future Swedish ordinance.

### 3.5 Comparisons

In the Netherlands, the average sewage sludge in 2012 was characterised by lower concentrations of toxic elements for all seven toxic elements tested than average sludges in Germany or Sweden (Brown et al., 2015). Swedish and German sludges are comparable in their average concentrations of toxic elements (Brown et al., 2015), whilst sludges in the Netherlands do not meet the limits for application in agriculture.

Table 2 shows a comparison of limit values for toxic elements present in sludge. In the Netherlands, the limit values for toxic elements were approx. 5-10 times stricter than values established in Germany (1992 ordinance), as shown in Figure 3. Even following introduction of the new German ordinance in 2017, limit values in the Netherlands remain considerably stricter for the majority of toxic elements compared to German values. When comparing the dose of toxic elements on agricultural soil (given as mass flows of toxic elements per area), Sweden and the Netherlands have comparable values, with Swedish values being more restrictive in part. The German values for dosage of toxic elements are approx. 15 times higher. Although Sweden and the Netherlands adhere to similar dosage limits, sewage sludge may still be applied to agricultural soil in Sweden since limit values only relate to the dosage of toxic elements (mass flow of toxic elements to the soil), and not to the total concentrations of toxic elements in the sludge.

All values throughout the three countries were at least 10-fold, at times up to 100-fold, lower than values suggested in the EU-Directive. In the Netherlands this was due to the fact that both accumulation of toxic elements in the soil and pollution of water bodies must be prevented (Ehlert et al., 2013). All toxic elements applied to the soil

should be taken up by crops, resulting in no accumulation in the soil (Ehlert et al., 2013). Even for toxic elements that are not taken up by crops, accumulation should not exceed 1 % over a 100-year time frame (Ehlert et al., 2013).

Table 2 shows the maximum allowable concentrations of toxic elements in soil for application of sewage sludge in agriculture. Conversely to sludge dosage values, limits for soil are in the same range for all three countries and in line with recommendations of the EU-Directive.

Since Germany is the only country of the three to have implemented limit values for organic contaminants (PCB), no comparison is possible. Although the EU included limit values for organic contaminants in their draft for a new sewage sludge directive in the year 2000, and the Swedish environmental protection agency provided suggestions for limit values on organic contaminants in 2012, neither Sweden nor the Netherlands have implemented these (Bergqvist et al., 2013; European Union, 2000). One reason for this might be that the detection of organic contaminants is more complicated than for toxic elements (Aparicio, Santos, & Alonso, 2009). Moreover, an investigation conducted by the European Commission reported that organic contaminants (dioxins, PCBs, PAHs, TBT) should not be included in routine sewage sludge monitoring. The reason for this is that only very low quantities of organic contaminants are present in sewage sludge and have a low water solubility, thus making health problems due to leaching or plant uptake unlikely, particularly when compared to toxic elements (Langenkamp, Part, Erhardt, & Prueß, 2001). On the contrary, the report indeed suggests limit values for detergents (linear alkylbenzene sulphonates) for environmental reasons, ensuring the use of only aerobically and anaerobically degradable detergents (Langenkamp et al., 2001).

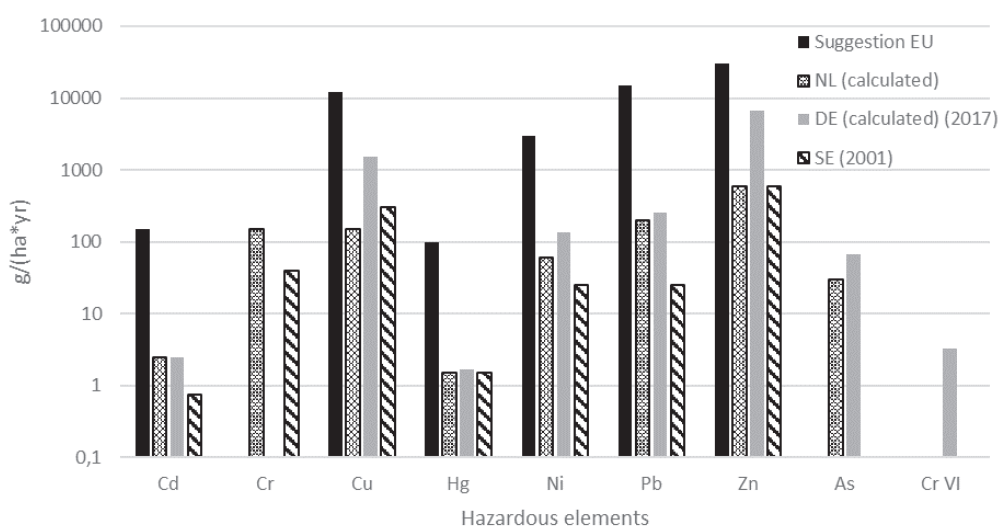
In all three countries, landfilling has been banned as an option for sewage sludge disposal. In the Netherlands and Germany, this has been achieved by allowing solely disposal of sludges with a TOC of less than 5 %. In Sweden, landfilling of organic waste is forbidden in general. In

**TABLE 2:** Maximum allowed amounts of toxic elements in sewage sludge which are to be applied to agricultural soil. Values for NL and DE are calculated by multiplication of limit concentrations for toxic elements in sewage sludge with maximum yearly dosage. All values are given in grams per hectare and year (g/(ha\*year)). (Brown et al., 2015; Bundesministerium für Umwelt, 2015, 2017; Bundesregierung, 2017a, 2017b; Council of the European Union, 1986a; Ehlert et al., 2013; Naturvårdsverket, 2001a).

	EU	NL	DE (2017)	SE (2001)
Cd	150	2.5	2.5	0.75
Cr		150		40
Cu	12,000	150	1503	300
Hg	100	1.5	1.7	1.5
Ni	3,000	60	134	25
Pb	15,000	200	251	25
Zn	30,000	600	6,680	600
As		30	67	
Cr (VI)			3.3	

**TABLE 3:** Maximum allowed concentrations of toxic elements in agricultural soil to which sewage sludge is to be applied. Values for Germany are dependent on physical soil properties (min: sand; max: clayey soil). Values given in mg/kg dry matter. (Brown et al., 2015; Bundesministerium für Umwelt, 2015, 2017; Bundesregierung, 2017a, 2017b; Council of the European Union, 1986a; Ehlert et al., 2013; Naturvårdsverket, 2001a).

	EU min.	EU max.	NL	DE (2017) min.	DE (2017) max.	SE
Cd	1	3	0.8	0.4	1.5	0.4
Cr			100	30	100	60
Cu	50	140	36	20	60	60
Hg	1	1.5	0.3	0.1	1	0.3
Ni	30	75	35	15	70	30
Pb	50	300	85	40	100	40
Zn	150	300	140	60	200	100



**FIGURE 3:** Graphical presentation of limits for concentrations of toxic elements given in Table 2 to emphasise the magnitude of differences. Note that the y-axis is in logarithmic scale.

contrast to Germany and the Netherlands however, Sweden allows the usage of sewage sludge in landfill covers. Approximately a quarter of all Swedish sludge is disposed of in this way (Svinhufvud, 2017). The issue however is raised as to whether this disposal route should be viewed as a form of landfilling.

A comparison of the Dutch and German legislation clearly reveals how the focus of German authorities is on nutrient recycling, with application in agriculture as a major disposal route for sewage sludge, whereas the Netherlands have concentrated mainly on the protection of surface waters from pollutants and uncontrolled nutrient flows. Although the limits in the new German ordinance are more restrictive, application in agriculture is only partly ruled out, and most sewage sludges can still be used in agriculture. The main focus of the new ordinance is on aligning a series of German ordinances, placing more focus on documentation and testing and setting up a long term strategy for phosphorus recovery. As soon as the new phosphorus recovery strategy is in place (2029 resp. 2032) application in agriculture will be forbidden for plants to which the strategy applies.

In Sweden, the focus is directed towards keeping contamination low by implementing limits as strict as the Netherlands, although not ruling out land application of sewage sludge. Due to the strict limitations for application in agriculture of sludge in Sweden, illegal or accidental overdosage of sewage sludge on agricultural soils may occur (Zachrisson, 2019). Since the possibility of sewage sludge application has been completely precluded in the Netherlands, overdosage is impossible and illegal applications are likely to be discovered. Germany may also be prone to illegal application or overdosage, however, due to the less strict limits for application on the one hand and limit values for sludge content rather than dosage on the other, illegal application or excessive dosage are less likely. In the absence of any official data, these considerations are mainly based on assumptions; they could however represent a field of interest for further research or policymaking.

A phosphorus recovery strategy is currently being developed in Sweden, with the German strategy acting, at least in part, as a guideline for the Swedish strategy. In Sweden, a total of 416 wastewater treatment plants are currently operational (André et al., 2016), most of which are relatively small in comparison to German plants, thus highlighting how collaborations in phosphorus recovery will be crucial. Since the new German ordinance establishes limitations regulating collaborations, particularly when mixing different sludges or ashes, difficulties may be encountered in setting up these collaborations or regional networks. However, in the case of smaller wastewater treatment plants (<50.000 inhabitant equivalent units) collaboration in implementing complex phosphorus recovery methods will be crucial. The latter is clearly evident in the incineration strategy of the Netherlands: although the Netherlands have 330 wastewater treatment plants, two mono-incinerators alone treat 50% of the produced sewage sludge. The implementation of phosphorus recovery strategies on the sites equipped with mono-incinerators is the most feasible means of nutrient recovery in the Netherlands (Ruijter,

2018). In Germany, a total of 9500 wastewater treatment plants are currently in operation, 9000 of which treat less than 50.000 inhabitant equivalents each. The treatment capacity of these plants corresponds to 40% of Germany's total wastewater treatment capacity (Durth, Kolvenbach, & Statistisches Bundesamt und DWA-Arbeitsgruppe KEK-1.2 "Statistik," 2014). The new phosphorus recovery strategy does not affect these plants, although it does make collaborations between plants more difficult. To promote phosphorus recovery by means other than in large plants and through application in agriculture, a series of technical and legal strategies should soon be introduced. These strategies should also consider the need for a combined or regional phosphorus recovery for the smaller plants. These innovations will of course imply a need for major adaptations to the German ordinance to ensure its suitability for use as a potential guideline for future legislation in Sweden.

Data present in literature has underlined the difficulties encountered in the Netherlands in implementing a policy strategy for phosphorus recovery. However, several pilot scale tests for phosphorus recovery are currently being conducted at wastewater treatment plants and mono-incinerators (Ruijter, 2018).

Since May 2014, the European commission has included phosphorus on the list of critical raw materials, leading to an increased focus on phosphorus recovery in some of the EU member states. In addition to phosphorus, sewage sludge also contains other valuables including potassium, nitrogen or metals. Since phosphorus recovery is not an indicator for the recovery of other valuables, none of the legislations examined is aimed at recovery of these valuables from sludge, thus implying that market demand will lead the potential extraction of other resources from sewage sludge. It is debatable whether a market demand for products obtained from sewage sludge may develop in the near future without a promoting legislation (Hukari, Hermann, & Nättorp, 2016). The potential recovery, not only of phosphorus, but also of other nutrients and energy from sludge could be achieved by combining thermal and biological treatments with the goal of separating different fractions from sewage sludge. This could simplify the subsequent extraction of nutrients and better address the issue of pollutants. Due to the need however for a more concentrated technical effort, regional collaborations will prove crucial in setting up this type of extraction, together with other advanced sludge treatments.

## 4. CONCLUSIONS

All three countries investigated adhered to different strategies when setting limits for sewage sludge application on agricultural soils. Major differences are present in limit values for sewage sludge applied in agriculture – however, limit values for the presence of toxic elements in soils to which sewage sludge may be applied are comparable. The authors therefore question the utility of limit values in relation to health issues, particularly in view of other sources highlighting the minor role played by toxicology in the defining of limit values for sewage sludge (Ehlert et al., 2013; Langenkamp et al., 2001). Overall, all three coun-

tries applied limit values as a tool to assist in steering the means of re-use and disposal of sewage sludge.

Although the Netherlands prohibited the application of sludge in agriculture more than 20 years ago, the average sludge in the Netherlands is still today less contaminated than average sludges in Sweden or Germany (Brown et al., 2015). Future research should be aimed at investigating why and how the Netherlands have succeeded in achieving a lower pollutant load in sewage sludge, and the knowledge exploited by other countries to reduce contamination of their sewage sludge.

In contrast to the Netherlands, Swedish ordinances permit the use of sewage sludge in low doses, providing for a system of voluntary deliberative certification; for this reason, application in agriculture is widely used. In contrast to the Netherlands and Germany, Sweden also uses large amounts (each approx. 25%) of the produced sewage sludge in landfill covers and soil production (Svinhufvud, 2017). It is debatable however whether this process constitutes re-use, as reported by the European Commission (2017), particularly with regard to nutrient recovery.

While the new German ordinance places particular emphasis on new methods of phosphorus recovery, it still leaves options open for the continued operations of small plants and use of lower grade sludges in the absence of phosphorus recovery after 2032. Indeed, application in agriculture will continue to be permitted. In this case, the intention of the policy makers is clear, although it may result in a loophole through which to bypass the new regulations (e.g. downgrading of sludges or downsizing of plants). It should be evaluated whether new rules for mixing of sludges and products from sludges, as well as transportation of sludges, might limit collaborations focused on the treatment of sewage sludge.

Despite the successful application of a series of technologies for use in phosphorus recovery, the legislative focus across the EU member states varies considerably (Abis, Calmano, & Kuchta, 2018; Tsybina & Wuensch, 2018; van Dijk, 2017). The performing of additional research in the field of nutrient recovery from sewage sludge and evaluation of potential related legislation will contribute towards setting clear goals and indicating a pathway towards the establishing of an EU-wide Directive. To date, the EU has issued a series of working documents on which to base a new Directive to replace the acknowledged outdated 1986 Directive (European Commission, 2010; European Union, 2000). The working documents focus on the agricultural usage of sewage sludge and new limit values, but not on phosphorus recovery (European Commission, 2010)

Lastly, it remains to be ascertained whether phosphorus should represent the sole resource to undergo recovery from sewage sludge, particularly as the issue of other resources present in sewage sludge are not considered in any legislation implemented throughout the three countries examined.

## ACKNOWLEDGEMENTS

The work was carried out under the auspices of Graduate School in Energy Systems, financed by the Swedish

Energy Agency. Economic support from the Swedish Research Council Formas, within the national research program Sustainable Spatial Planning, is also gratefully acknowledged (dnr. 2018-00194).

## REFERENCES

- Abis, M., Calmano, W., & Kuchta, K. (2018). Innovative technologies for phosphorus recovery from sewage sludge ash. *Detritus - Volume 1*, 1(1), 23. <https://doi.org/10.26403/DETRITUS/2018.23>
- André, A., Sundin, A. M., Linderholm, L., Borbas, I., Svinhufvud, K., Eklund, K., ... Rosenblom, T. (2016). *Wastewater treatment in Sweden 2016*. (Naturvårdsverket, Ed.). Retrieved from <https://www.naturvardsverket.se/Documents/publikationer6400/978-91-620-8809-5.pdf?pid=22471>
- Aparicio, I., Santos, J. L., & Alonso, E. (2009). Limitation of the concentration of organic pollutants in sewage sludge for agricultural purposes: A case study in South Spain. *Waste Management*, 29(5), 1747–1753. <https://doi.org/10.1016/j.wasman.2008.11.003>
- Bengtsson, M., & Tillman, A.-M. (2004). Actors and interpretations in an environmental controversy: the Swedish debate on sewage sludge use in agriculture. *Resources, Conservation and Recycling*, 42, 65–82. <https://doi.org/10.1016/j.resconrec.2004.02.004>
- Bergqvist, M., Gunnesby, U., Gårdstam, L., Hedlund, B., Karltorp, G., Kock, E., ... Åstrand, K. (2013). *Hållbar återföring av fosfor*. (Naturvårdsverket, Ed.), Rapport / Naturvårdsverket (Vol. 6580). Stockholm.
- Brown, M., Tsiarta, C., Watson, S., & Hudson, J. (2015). Final Implementation Report for the Directive 86/278/EEC on Sewage Sludge. Retrieved from [https://ec.europa.eu/environment/archives/waste/reporting/pdf/SS\\_dir\\_report\\_2010\\_2012.pdf](https://ec.europa.eu/environment/archives/waste/reporting/pdf/SS_dir_report_2010_2012.pdf)
- Bundesministerium für Umwelt. Klärschlammverordnung (AbfKlärV) (2015).
- Bundesministerium für Umwelt. Verordnung zur Neuordnung der Klärschlammverwertung, 2017 Bundesgesetzblatt § (2017).
- Bundesregierung. Bundes-Bodenschutz- und Altlastenverordnung (BBodSchV) (2017).
- Bundesregierung. Verordnung über das Inverkehrbringen von Düngemitteln, Bodenhilfsstoffen, Kultursubstraten und Pflanzenhilfsmitteln (Düngemittelverordnung - DüMV), 1 § (2017).
- Bundesregierung. Verordnung über die Verwertung von Klärschlamm, Klärschlammgemisch und Klärschlammkompost (Klärschlammverordnung - AbfKlärV) (2017). Germany.
- Council of the European Communities. European urban waste water treatment directive (UWWTD) (91/271/EEC) of 21 May 1991 (1991). Retrieved from <https://eur-lex.europa.eu/legal-content/EN/TXT/PDF/?uri=CELEX:31991L0271&from=EN>
- Council of the European Union. COUNCIL DIRECTIVE of 12 June 1986 on the protection of the environment, and in particular of the soil, when sewage sludge is used in agriculture, Official Journal of the European Communities § (1986).
- Council of the European Union. COUNCIL DIRECTIVE of 12 June 1986 on the protection of the environment, and in particular of the soil, when sewage sludge is used in agriculture, Official Journal of the European Communities § (1986). Retrieved from <http://data.europa.eu/eli/dir/1986/278/oj>
- de Boer, M. A., Romeo-Hall, A., Rooimans, T., & Slootweg, J. (2018). An Assessment of the Drivers and Barriers for the Deployment of Urban Phosphorus Recovery Technologies: A Case Study of The Netherlands. *Sustainability*, 10(6), 1790. <https://doi.org/10.3390/su10061790>
- Durth, A., Kolvenbach, F.-J., & Statistisches Bundesamt und DWA-Arbeitsgruppe KEK-1.2 "Statistik." (2014). *Abwasser und Klärschlamm in Deutschland – statistische Betrachtungen. Korrespondenz Abwasser, Abfall*, 61(12), 1106–1112. <https://doi.org/10.3242/kae2014.12.003>
- Ehlert, P. A. I., Posthuma, L., Römkens, P. F. A., Rietra, R. P. J. J., Winterse, A. M., van Wijnen, H., ... Groenenberg, J. E. (2013). Appraising Fertilisers: Origins of current regulations and standards for contaminants in fertilisers (Working Document 336). Retrieved from <http://www.wageningenur.nl/wotnatuurenmilieu/>
- European Commission. (2004). Implementation of Council Directive 91/271/EEC of 21 May 1991 concerning urban waste water treatment, as amended by Commission Directive 98/15/EC of 27 February 1998. Retrieved from <https://eur-lex.europa.eu/legal-content/EN/TXT/PDF/?uri=CELEX:52004DC0248&from=EN>

- European Commission. (2010). Working Document Sludge and Bio-waste.
- European Commission. (2017). 9th Technical assessment on UWWTD implementation. Annex V: National chapters. Retrieved from [http://ec.europa.eu/environment/water/water-urbanwaste/implementation/pdf/Annex\\_V.pdf](http://ec.europa.eu/environment/water/water-urbanwaste/implementation/pdf/Annex_V.pdf)
- European Union. (2000). Working Document on Sludge, 3rd draft (Vol. 80). Brussels.
- eurostat. (2015a). Sewage sludge production and disposal from urban wastewater. (E. European Commission, Ed.). Luxembourg. Retrieved from [https://ec.europa.eu/eurostat/tgm/graphCreator.do?tab=graph&a=6&cp=noValue&c=1&d=0&h=1&geo=2-39&x=geo&ww\\_tpar=2-7&y=ww\\_tpar&language=en&pcode=ten00030&plugin=1 Y3 - 2019-01-09 M4 - Citavi](https://ec.europa.eu/eurostat/tgm/graphCreator.do?tab=graph&a=6&cp=noValue&c=1&d=0&h=1&geo=2-39&x=geo&ww_tpar=2-7&y=ww_tpar&language=en&pcode=ten00030&plugin=1 Y3 - 2019-01-09 M4 - Citavi)
- eurostat. (2015b). Sewage sludge production and disposal from urban wastewater. (E. European Commission, Ed.). Luxembourg.
- Government Offices of Sweden. (2018a). Giftfri och cirkulär återföring av fosfor från avloppsslam. Retrieved from <https://www.regeringen.se/rattsliga-dokument/kommittedirektiv/2018/07/dir-201867/>
- Government Offices of Sweden. (2018b). Giftfri och cirkulär återföring av fosfor från avloppsslam.
- Hukari, S., Hermann, L., & Nättorp, A. (2016). From wastewater to fertilisers – Technical overview and critical review of European legislation governing phosphorus recycling. *Science of The Total Environment*, 542, 1127–1135. <https://doi.org/10.1016/j.scitotenv.2015.09.064>
- Kelessidis, A., & Stasinakis, A. S. (2012). Comparative study of the methods used for treatment and final disposal of sewage sludge in European countries. *Waste Management (New York, N.Y.)*, 32(6), 1186–1195. <https://doi.org/10.1016/j.wasman.2012.01.012> PM - 22336390
- Langenkamp, H., Part, P., Erhardt, W., & Prüeb, A. (2001). Organic Contaminants in Sewage Sludge for Agricultural Use. Retrieved from [https://ec.europa.eu/environment/archives/waste/sludge/pdf/organics\\_in\\_sludge.pdf](https://ec.europa.eu/environment/archives/waste/sludge/pdf/organics_in_sludge.pdf)
- LeBlanc, R. J., Matthews, P., & Richard, R. P. (2008). Global atlas of excreta, wastewater sludge, and biosolids management. *Proceedings of IWA Conference—Moving forward Wastewater biosolids sustainability technical managerial and public synergy June*. <https://doi.org/10.1080/17405629.2013.793597>
- Malmqvist, P.-A., Kärrman, E., & Rydhagen, B. (2006). Evaluation of the ReVAQ project to achieve safe use of wastewater sludge in agriculture. *Water Science and Technology*, 54(11–12), 129–135. <https://doi.org/10.2166/wst.2006.759>
- Naturvårdsverket. Kungörelse med föreskrifter om skydd för miljön, särskilt marken, när avloppsslam används i jordbruket (1994).
- Naturvårdsverket. Statens naturvårdsverks föreskrifter om ändring i kungörelsen (SNFS 1994:2) med föreskrifter om skydd för miljön, särskilt marken, när avloppsslam används i jordbruket (1998).
- Naturvårdsverket. Kungörelse med föreskrifter om skydd för miljön, särskilt marken, när avloppsslam används i jordbruket (2001). Sweden.
- Naturvårdsverket. Kungörelse med föreskrifter om skydd för miljön, särskilt marken, när avloppsslam används i jordbruket (2001). Sweden. Retrieved from <http://www.naturvardsverket.se/Documents/foreskrifter/nfs1994/snfs1994-02k.pdf>
- Oberg, G., & Mason-Renton, S. A. (2018). On the limitation of evidence-based policy: Regulatory narratives and land application of biosolids/sewage sludge in BC, Canada and Sweden. *Environmental Science and Policy*, 84, 88–96. <https://doi.org/10.1016/j.envsci.2018.03.006>
- Ruijter, J. A. (2018). Dutch Experience of sludge management and P-recovery pathways Content 1 . *Sewage water treatment in NL 2 . Sludge management*.
- Svinhufvud, K. (2017). Phosphorus: Strategies and Reuse Initiatives in Sweden. (Naturvårdsverket, Ed.). Vilnius.
- Tsybina, A., & Wuensch, C. (2018). Analysis of Sewage Sludge Thermal Treatment Methods in the Context of Circular Economy, 02, 3–15.
- van Aaken, L. (2017a). Klärschlammverordnung verkündet. (B. K. e.V., Ed.).
- van Aaken, L. (2017b). Klärschlammverordnung verkündet. (B. K. e.V., Ed.). Retrieved from [https://www.kompost.de/fileadmin/user\\_upload/Dateien/HUK\\_aktuell/2017/H\\_K-03-2017.pdf](https://www.kompost.de/fileadmin/user_upload/Dateien/HUK_aktuell/2017/H_K-03-2017.pdf)
- van Dijk, K. (2017). Nutrient recovery from wastewater: opportunities and challenges of EU regulatory context. Retrieved from [www.phosphorusplatform.eu](http://www.phosphorusplatform.eu)
- Zachrisson, N. (2019). Slamförbud riskerar spridning i det fördolda. Retrieved November 13, 2019, from <https://sverigesradio.se/sida/artikel.aspx?programid=406&artikel=7014613>

## BIOGAS FROM CASSAVA PEELS WASTE

Felix Aibuedefe Aisien <sup>1,\*</sup> and Eki Tina Aisien <sup>2</sup>

<sup>1</sup> Department of Chemical Engineering, University of Benin, Benin City, Nigeria

<sup>2</sup> Department of Environmental Management and Toxicology, University of Benin, Benin City, Nigeria

### Article Info:

Received:  
13 July 2019  
Revised:  
30 January 2020  
Accepted:  
4 February 2020  
Available online:  
5 March 2020

### Keywords:

Cassava peels  
Methane  
Biogas  
Biofertilizer  
Anaerobic digestion

### ABSTRACT

The increasing growth of cassava agro-industries in Nigeria has led to the enormous generation of cassava peels waste. The feasibility of generating biogas and biofertilizer for both domestic and agricultural applications from cassava peels waste inoculated with cow dung was investigated. Fresh and stale cassava peels were used in the study. Three pretreatment chemicals such as sodium hydroxide (NaOH), calcium hydroxide (Ca(OH)<sub>2</sub>) and ammonium chloride (NH<sub>4</sub>Cl) buffer solutions were used in pretreating the cassava peels and cow dung slurry. Six batch anaerobic biodigesters of 10-litre capacity each were used in this study for 40 days retention period. The pH, temperature, and volumes of biogas and methane produced were monitored and recorded daily. The fertilizer qualities (total solids, volatile solids, % phosphorus, % nitrogen, etc.) of the digester slurry and the digester sludge after 40 days digestion were determined using official methods of analysis of Association of Official Analytical Chemists (AOAC). The results showed that the amount of biogas generated is 2540 cm<sup>3</sup>/day. The stale cassava peels and cow dung slurry and the use of NH<sub>4</sub>Cl pretreatment chemical gave the best biogas production and methane yield of 104,961 cm<sup>3</sup> and 62.3% respectively. The digester sludge from the anaerobic digestion of cassava peels and cow dung showed and demonstrated good biofertilizer qualities.

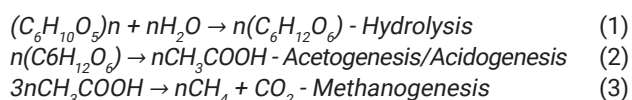
## 1. INTRODUCTION

The continuous increase in energy demands has been a serious problem resulting from increased population growth, urbanization, and industrialization worldwide. This problem is more pronounced in underdeveloped and developing countries where the social-economic situations are quite low. Lack of infrastructures for energy generation, transmission, and distribution, unavailability of nonrenewable energy sources such as fossil fuels, low technology for energy conversion from renewable energy sources such as biogas, and lack of funds for purchase of fossil fuels, infrastructural and technology developments in energy sectors have been implicated in the near energy crisis in most underdeveloped and developing countries (Aisien, et. al., 2010; Kwasi – Effah et. al., 2015). However, since energy can be obtained from renewable energy sources such as waste materials, the issue of poverty as it relates to the energy crisis in undeveloped and developing countries can be seriously reduced. The renewable energy source such as biogas production from anaerobic digestion of organic waste materials which can be sourced from municipal solid waste, agricultural waste, industrial waste, and household waste can provide enormous energy worldwide (Aisien et. al., 2007b; Igbum, et. al., 2019). Besides, biogas

can be produced from food waste (Huiru, et al., 2019). Biogas is a cheap form of renewable energy that can meet to a large extent the energy demands of the rural populace globally. It is a colourless flammable gas produced via anaerobic digestion of organic waste materials. It is a smokeless, hygienic and more convenient fuel to use than other solids fuels (Buren, 1979). The increased emphasis on the use of renewable energy from biogas over the nonrenewable energy source of fossil fuels, will not only reduce energy demands from fossil fuels which is becoming very expensive and can lead to energy crisis but will as well address the problems of greenhouse gas emissions, global warming, environmental pollution/degradation and health hazard (COP 21, 2015; Igbum, et. al., 2019). Biogas is a renewable energy source that is produced by the biological degradation of organic matters in the absence of oxygen. The biogas from anaerobic digestion of organic matters is a gas that comprises of methane (50-72 vol.%), carbon (IV) oxide (25-45 vol.%), nitrogen (>2 vol.%), hydrogen sulphide (>1 vol.%), water (2-7 vol.%) and oxygen (>2 vol.%) (Mel, et. al., 2015). There are three main biochemical processes involved in biogas production. These are hydrolysis, acidogenesis/acetogenesis and methanogenesis (Igwe, 2014) as indicated below.

\* Corresponding author:  
Felix Aibuedefe Aisien  
email: aibue.aisien@uniben.edu





Biogas energy has been successfully used for lighting, heating, cooking, power generation and fuel for vehicles. Besides, the sludge from anaerobic digestion of waste materials can serve as a biofertilizer for the improvement of soil fertility (Aisien et al., 2007).

Nigeria is the world's largest producer of cassava (*Manihot esculenta* Crantz), producing over 46 million tons of cassava per year (IITA -1). According to FAO (2001), about 250 to 300 kg of cassava peels is produced per tonne of fresh cassava root processed. Cassava peel accounts for 8-15 wt.% of the total dry matter of the root. Cassava peels composition consists of 20-31 wt.% hemicelluloses, 16 - 42 wt.% cellulose and 6-8 wt.% lignin. Other than fiber, peels also contain 81.9 - 93.9 wt.% organic matter and 4.1- 6.5 wt.% crude protein (Kongkiattikajorn and Sornvorawea, 2011). Analysis of mineral content of cassava peel indicated the following mineral content: 48.7 wt.% C; 1 wt.% N; 1.1 wt.% K; 1.6 wt.% P; 0.16 wt.% NO<sub>3</sub>; 0.15 wt.% Na; 0.9 wt.% Ca; 125 mg/kg Zn; 15 mg/kg Cu; 180 mg/kg Mn; 16.7 mg/kg Pb; 48.7 wt.% C/N; and 52.6 wt.% ash (Adelekan and Bamgboye, 2009).

The increase in population growth coupled with the low cost of living in Nigeria has led to a drastic increase in cassava utilization in garri, starch, fufu, lafu, and flour production. This has contributed to a tremendous increase in cassava peels waste generation. The other wastes from cassava processing in Nigeria include; cassava wastewater, sievates and offal (wastes from "foo-foo" production). International livestock research institute (ILRI), 2015 reported that approximately 98% of Nigeria's cassava peels annually are wasted due to constraints associated with drying and was concerned about its safe use, particularly the presence of hydrocyanide and mycotoxins-related food poisoning. The indiscriminate disposal of cassava peels in landfills/waste dump sites has led to serious environmental pollution. This waste degrades to produce noxious leachate that contaminates both surface and underground water sources and other products that cause air pollution. The effects of these pollution problems associated with the degradation of cassava peels in dumpsites include foul odor and sometimes poisonous and polluted air, which when inhaled by man or animals may result in infection and diseases that may take a long time to manifest. In the same vein, vegetation and soil around the cassava peels' dumpsites are rendered unproductive and devastated due to biological and chemical reactions taking place during the degradation of cassava peels. Cassava peels have been used as a feedstuff for various livestock. Besides, cassava peels have found applications in the production of reducing sugar, bioethanol, biogas and biofertilizer (Aisien et al., 2010; Anaeto, et al., 2013; Kongkiattikajorn and Sornvorawea, 2011 and Olanbiwoninu and Odufa, 2012).

Many types of research have been carried out with cassava peels waste alone and cassava peels with other waste materials especially animal wastes for biogas production.

Adelekan and Bamgboye (2009) and Ofoefule and Uzodimma (2009) reported that biogas production and methane yield improved significantly when cassava peels were combined with different animal wastes. They also stated that the ratio of cassava peels to animals waste that is, carbon to nitrogen ratio was very important to ensure increased production of biogas and methane yield. Besides, Ezekoye and Ezekoye (2009), Ilaboya et al. (2010), Ilori, et al., (2007) and Adeyanju, (2008) reported that the blending of cassava peels with other plants waste. They found out that there is the need to apply some small quantity of animal wastes as inoculum in other to achieve an appreciable increase in biogas production and methane yield. Bayitse et. al., 2014 reported that cassava peels co - digested with manure produce biogas and biofertilizer by optimizing carbon to nitrogen ratio. Nkodi et. al., 2018 and Olaniyan, et. al., 2017 stated that the combination of cassava peels with animal waste yield a larger volume of biogas compare with cassava peels alone. Besides, Sawyeer et. al., 2017; Onuorah, et. al., 2016 and Ben and Michael, 2018 reported that the appropriate carbon to nitrogen ratio must be maintained. They stated that cassava peel to the animal waste ratio of 30: 20 is required for maximum biogas yield. Olawale et. al., 2017 reported that the addition of cow dung (animal manure) lowered the C : N ratio of the cassava peels to value between 20: 1 and 30: 1, which make co-substrate ideal for anaerobic digestion. Many other researchers have appreciated the unique nature of cassava peels substrate in terms of high concentration of cyanide. They reported that for sufficient biogas production from cassava peels there must be an appropriate pretreatment method in place (Deepanraj et. al., 2014; Nkodi, et. al., 2016; Mel, et. al., 2015; Ben and Michael, 2018; Igbum, et. al., 2019; Onuorah, et. al., 2016, Shah, et. al., 2015; Gopinattan, et al., 2015). They employed various chemical pretreatment methods such as the use of alkalis (NaOH, KOH, NaHCO<sub>3</sub>, Ca(OH)<sub>2</sub>) of different concentration in the maintenance of the slurry/ substrate pH for optimum biogas production. However, the application of a buffer solution was not considered, which we believed would resist more change in slurry pH when compare with alkalis solutions. Another gap identified from previous studies on cassava peels conversion to biogas was that investigation on stale cassava peels bio-digestion was neglected. It is the stale cassava peels that are abundant in most cassava peels dumpsites that usually constitute its associated environmental pollution and health hazard. Therefore, this study is designed to address these gaps. The application of an acid buffer solution will be investigated together with the alkaline solution as pretreatment chemicals. Besides, fresh and stale cassava peels will be studied. A comparison will be made and the conclusion drawn.

Therefore, the focus of this study is to investigate the production of biogas from cassava peels, as a potential alternative source of energy using cow dung as an inoculum. Besides, to determine whether the digested sludge from the anaerobic digestion can be used as a source of biofertilizer. As a result of the identified gaps in previous research works on cassava peels for biogas production, the objective of the research was to investigate the effect

of the nature of cassava peels, (fresh and stale) and the applications of different pretreatment chemicals (alkaline and acid buffer solutions) on biogas production and methane yield.

## 2. MATERIALS AND METHODS

### 2.1 Materials collection

15kg each of fresh and stale cassava peels were collected with clean polythene bags from the Imuetinyan cassava processing mill and Orore Obazee cassava waste dump site in Benin city respectively. Cow dung (inoculum) were obtained from Egharevba slaughterhouse in Benin city. Anaerobic digesters designed and fabricated by Aisien et al, 2007 were collected from Chemical Engineering laboratory, University of Benin, Benin city.

### 2.2 Experimental design

Six (6) anaerobic digesters A, B, C, D, E, and F were used in the studies. A, B, and C were used for biogas production while D, E and F were for methane production for NaOH, Ca(OH)<sub>2</sub> and NH<sub>4</sub>Cl buffer solution pretreatment chemicals respectively.

### 2.3 Method

A 3.6kg fresh cassava peels were washed with clean tap water and the water was allowed to drain out for about 20 min. The washed fresh cassava peels were then ground with an electrically powered grinding machine using 5 litres of deionized water to form a slurry. Then a 4g cow dung was mixed with 1 litre of deionized water to produce a cow dung slurry, which will serve as inoculum. Both slurries were transferred to 10-litre plastic bowl and thoroughly mixed. Then, a 6 g/l NaOH solution was used as a pretreatment chemical and this was furtherly used to mixed the cassava peels and cow dung slurries in the bowl until the pH was 6.8. 4 litres each of the chemically pretreated mixed fresh cassava peels and cow dung slurries at pH 6.8 was charged immediately into two, 10-litre airtight anaerobic digesters A and D. The set up connected to digester A was simply a gas measuring cylinder to measure the volume of biogas produced daily by the displacement method. However, the digester D was designed to measure the volume of methane produced. Hence, the set up was connected via a 4 g/l NaOH solution container such that the released biogas, carbon (IV) oxide and other gases were made to pass through the container. In the process, carbon (IV) oxide and other gases except methane gas were absorbed. The resultant methane produced was daily monitored and measured by displacement method. Both anaerobic digestion processes were observed for 40 days. The temperature of the digesting slurry was daily monitored with a thermometer while that of the digester sludge was measured with a thermocouple. The pH of the digesting slurry was monitored with a Jowrey 3020 pH meter. A similar procedure was used for the stale cassava peels, except that the observed initial preparation of the stale cassava peels. This involved soaking of stale cassava peels in distilled water for 4 hours before blending. The essence of investigating the fresh and stale cassava peels was that both contribute

to the environmental pollution and health hazard associated with cassava peels waste management. As a matter of fact, in most cassava peels dumpsites, the population of the stale cassava peels far outweigh that the fresh cassava peels. The effects of different chemical pretreatment on cassava peel and cow dung slurry for biogas production was furtherly investigated using a similar procedure as that of NaOH above, but this time 10 g/l and 10.85 g/l for calcium hydroxide and ammonium chloride buffer respectively were used as the pretreatment chemicals. This is because of the high concentration of cyanide in the form of hydrogen cyanide (HCN) in cassava peels, especially during the bio-digestion process.

The fertilizing properties (total solids, volatile solids, % nitrogen, % phosphorus, % potassium, ammonium, and pH) were carried out in triplicate using official methods of analysis, AOAC (1990) on both the digester slurry and digester sludge before and after the 40 days anaerobic digestion respectively. Two sets of plastic bowls G and H containing garden soils and at least seven maize plants were used for the growth study. The cassava and cow dung digested sludge (biofertilizer) was added to plastic bowl G only, while plastic bowl H served as the control without biofertilizer. The bowls were well watered and were kept on a place that daily exposed them to sunlight. The height of the maize plants in plastic bowl G and H was observed for 4 weeks.

## 3. RESULTS AND DISCUSSION

The effects of the nature of cassava peels were investigated by anaerobic digestion of fresh cassava peels and cow dung and stale cassava peels and cow dung. Figure 1 shows the variation of biogas production from fresh and stale cassava peels and cow dung. The results show that for both fresh and stale cassava peels and cow dung, the biogas production started after 24 hrs. However, it was observed that in the first 5 days of the anaerobic digestion, the volume of biogas produced from stale cassava peels was significantly higher than the volume of biogas produced from fresh cassava peels. The high rate of production of hydrocyanic acid at the earlier stage of anaerobic digestion of the fresh cassava peels was the possible reason for the reduced volume of biogas production. Smith et. al., (1985) reported that the presence of cyanogenic glucosides in cassava peels could induce excess acid production and the release of cyanide, which is highly toxic to methanogenic arches, hence reduces biogas production. This was however different in the case of stale cassava peels substrate where there is little or no hydrocyanic acid left because of its initial degradation period. During this biodegradation period, the hydrocyanic acid produced, usually evaporate into the environment in the waste dumpsite. This result compares favorably with that reported by Cuzin and Labat, (1992) and Bayitse, et. al., (2014). Also, there was a gradual increase in biogas production for both fresh and stale cassava peels and cow dung digestion from the 5th day to the 11th day. During this period, there was no substantial difference between the volume of biogas produced from fresh and stale cassava peels and

cow dung. Besides, the 12th and 13th days experienced a drastic increase in biogas production from both fresh and stale cassava peels. The maximum biogas production was recorded on the 13th day. This is an indication of the absence of hydrocyanic acid from the fresh cassava peels after about 13th day digestion period. Between the 14th day and 23rd day of digestion, there was a drastic decrease in biogas production for both fresh and stale cassava peels. Beyond 23rd day, the volume of biogas produced gradually decreased to almost an insignificant volume for both fresh and stale cassava peels. This might have been as a result of depletion of nutrients in both cassava peels and cow dung and reduction of the population of methanogenic microorganisms in the digesting slurry (Nkodi, et. al., 2018). It can be concluded that the volume of biogas produced was in a fluctuating manner during 40 days anaerobic digestion. Besides, the result shows that the cumulative volume of biogas produced from fresh cassava and cow dung slurry and stale cassava peels and cow dung slurry are 95,592 cm<sup>3</sup> and 104,961cm<sup>3</sup> respectively. Therefore, the rate of biogas production was 2520 cm<sup>3</sup>/day and 2390 cm<sup>3</sup>/day for stale and fresh cassava peels respectively. The methane yields were 62% and 63% for stale and fresh cassava peels respectively. This results compared favourably with that reported by Ukpai and Nnabuchi (2012); Sawyerr, et. al., (2017) and Olaniyan, et. al., (2017).

The variation of pH with retention time for fresh and stale cassava peels and cow dung digestion is represented in Figure 2. The pH values varied from 6.2 to 7.5 and 6.7 to 7.8 for fresh cassava peels and cow dung slurry and stale cassava peels and cow dung slurry respectively. Smith et. al., (2007) and Mel, et. al., (2015) reported that the pH range of between 6.5 and 7.5 was required for optimum biogas production. The pH values were fluctuating within the 40 days anaerobic digestion period. The high pH values were only experienced after periodic adjustment. Thereafter, the pH value continuously decreased with retention time. The fluctuating pattern of pH may be attributed to

the biodegradation of compounds that are present in the cassava peels and cow dung slurry (Onuorah, et. al., 2016). The earlier decrease in pH value of the mixture (slurry) was probably due to the conversion of initial product to hydrolytic products such as glycerol, fatty acids, which includes acetic acids, propanoic acids and butyric acid and these acids depressed the pH values (Ozturk, et. al., 1991). McCarty and Smith, (1997) reported that the acid nature of the system will negatively affect the activity of methanogenic bacteria and may lead finally to their death. Also, it has been established by researchers that there is an almost direct relationship between pH and the volume of gas production in any anaerobic digestion system (Aisien et. al., 2007b and Ahmad et. al., 2003).

Figure 3 shows the variation of temperature with retention time for fresh and stale cassava peels and cow dung. The results show that the average temperature of the digesting slurry for both fresh cassava peels and cow dung and stale cassava peels and cow dung varied from 28oC to 35oC. This temperature range falls within the mesophilic temperature range which enabled the micro-organisms to attend a maximum performance for biogas production (Igwe, 2014), hence, favourable biogas production at this temperature range. However, the temperature values fluctuated within the 40 days retention time. The fluctuating pattern of temperature may be attributed to the energy generated during the biodegradation of compounds that are present in the cassava peels and cow dung slurry, and the fluctuating environmental temperature. It was observed that there was quite a direct relationship between biogas production, methane yield and temperature. The results reported by Aisien et. al., (2007), Ukpai and Nnabuchi (2012), Igbum, et. al., (2019) and Sawyerr, et. al., (2017) conform.

The effects of the different pretreatment chemicals such as alkaline (NaOH, Ca(OH)<sub>2</sub>) and buffer (NH<sub>4</sub>Cl) on the volume of biogas production for fresh and stale cassava peels and cow dung slurry is shown in Figure 4. The pattern of the results was similar to that observed in Fig-

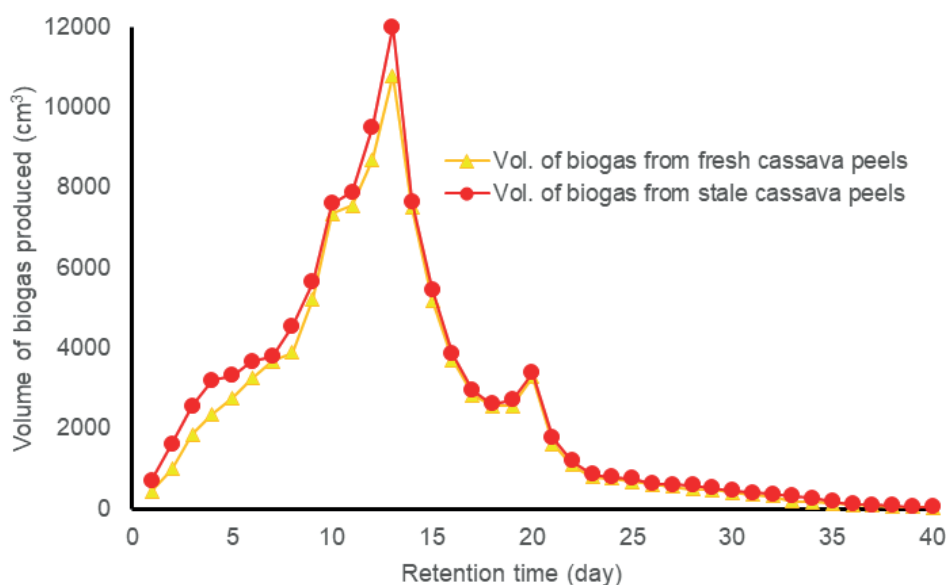


FIGURE 1: Variation of biogas produced with retention time from fresh and stale cassava peels and cow dung digestion.

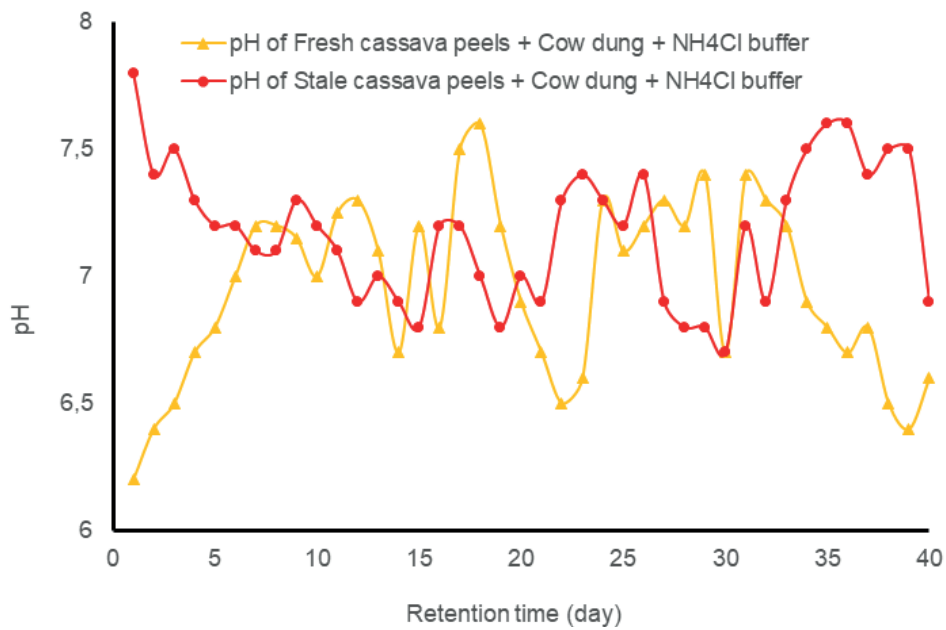


FIGURE 2: Variation of pH with retention time from fresh and stale cassava peels and cow dung digestion.

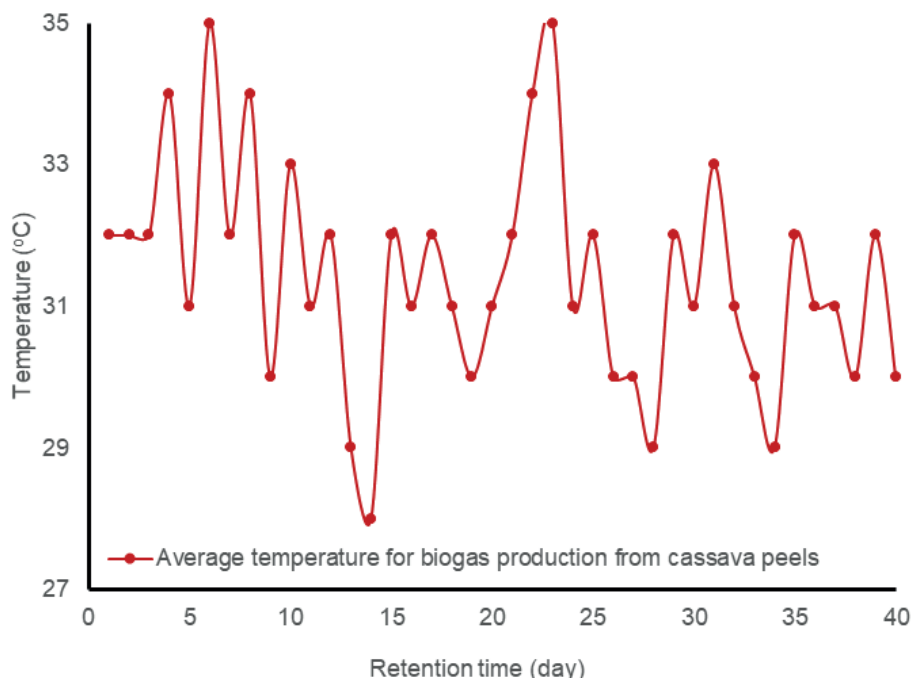


FIGURE 3: Variation of temperature with retention time for biogas production from fresh and stale cassava peels and cow dung.

ure 1. The use of NaOH pretreatment increased biogas production from cassava peels as reported by Ilaboya et al., (2010). Besides, Shah, et. al., (2015); Ben and Michael, (2018) and Gopinattan, et. al., 2015 reported that alkaline (NaOH and Ca(OH)<sub>2</sub>) pretreatment methods generally enhanced biogas production from cassava peels. However, there was no substantial difference in the volume of biogas produced from both NaOH and Ca(OH)<sub>2</sub> pretreatment chemicals as seen in Figure 4. This is an indication of the extent to which alkaline pretreatment chemicals can affect the change in biogas production. This might have been due

to the erratic nature of cassava peels and cow dung slurry, which produced hydrocyanic acid in the early period of the anaerobic digestion (Cuzin and Labat 1992; Igwe, 2014). The NH<sub>4</sub>Cl buffer pretreatment chemical showed a substantial increase when compared with the alkaline pretreatment chemicals. This is an indication of the contribution of the buffer in the stabilization of the slurry pH, being able to strongly resist the frequent change in pH resulting from the acidic nature of the slurry. Therefore, it is advisable to always apply buffer pretreatment chemicals rather than the alkaline pretreatment chemicals for a difficult substrate

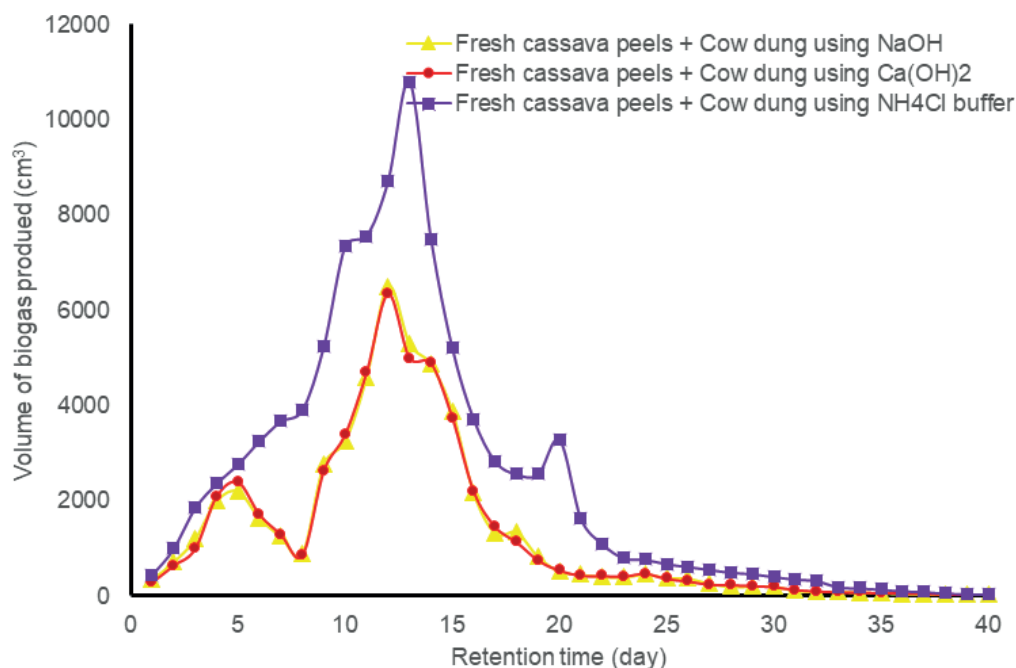


FIGURE 4: Variation of biogas produced with retention time using different pretreatment chemicals.

such as cassava peels to produce a substantially large volume of biogas and high yield of methane.

The cumulative volumes of biogas and methane, average pH and average temperature for the different chemical pretreatment methods for anaerobic digestion of fresh cassava peels and cow dung slurry are shown in Table 1. The cumulative volume of biogas and methane produced were 51,666 cm<sup>3</sup>, 33,700 cm<sup>3</sup>; 51,295 cm<sup>3</sup>, 32,310 cm<sup>3</sup> and 95,592 cm<sup>3</sup>, 58,890 cm<sup>3</sup> for NaOH, Ca(OH)<sub>2</sub> and NH<sub>4</sub>Cl chemical pretreatment methods respectively. The methane yield for NaOH, Ca(OH)<sub>2</sub> and NH<sub>4</sub>Cl chemical pretreatment methods were 53.3%, 58.7% and 62% respectively. The average pH and average temperature were 6.71, 32°C; 6.69, 31.4°C; and 7.00, 30.6°C for NaOH, Ca(OH)<sub>2</sub> and NH<sub>4</sub>Cl chemical pretreatment methods respectively. This shows that the acid buffer pretreatment method gave the most favourable results.

Figure 5 shows the pH variation patterns for the anaerobic digestion of fresh cassava peels and cow dung slurry using NaOH, Ca(OH)<sub>2</sub> and NH<sub>4</sub>Cl chemical pretreatment methods. The pH variation patterns using NaOH and Ca(OH)<sub>2</sub> chemical pretreatment methods were quite similar. It was observed that the pH gradually increased to a

particular level and then start decreasing to the lowest level until it was readjusted again to pH 6.8 using 8 M NaOH and Ca(OH)<sub>2</sub> solutions. This trend continues throughout the 40 days digestion period. However, the NaOH pretreatment method shows a slightly higher pH variation. The pattern for fresh cassava peels and cow dung using NH<sub>4</sub>Cl buffer pretreatment method was very different from that of NaOH and Ca(OH)<sub>2</sub> pretreatment methods. As for the NH<sub>4</sub>Cl buffer pretreatment method, the fluctuation of the slurry pH was not much and was within the pH range for optimum biogas production, hence it was not necessary to readjust the pH for optimum biogas production as in the case of alkaline pretreatment methods. This might be as a result of the buffering effect of NH<sub>4</sub>Cl buffer before the commencement of the anaerobic digestion. Table 1 shows that the average pH of 6.71, 6.69 and 7.0 for NaOH, Ca(OH)<sub>2</sub> and NH<sub>4</sub>Cl chemical pretreatment methods respectively. This result compared favourably with that reported by Wantanee and Sureelak, (2004). They reported that most researches on biogas production using cassava materials and animal's waste (inoculums), neutralizers have been applied to the slurry to bring the pH of the slurry to neutrality. Buren (1983) reported that the micro-organisms involved in

TABLE 1: The cumulative volumes of biogas and methane, average pH and the average temperature of fresh cassava peels to cow dung with different pretreatment chemical methods.

Fresh cassava peels to cow dung with different chemical pretreatment	Cumulative volume of biogas (cm <sup>3</sup> )	Cumulative volume of methane (cm <sup>3</sup> )	Average pH	Average temperature
Cassava peels and cow dung mixed slurries using NaOH pretreatment	51,666	33,700	6.71	32.0
Cassava peels and cow dung mixed slurries using Ca(OH) <sub>2</sub>	51,295	32,310	6.69	31.4
Cassava peels and cow dung mixed slurries using NH <sub>4</sub> Cl	95,592	58,890	7.00	30.6

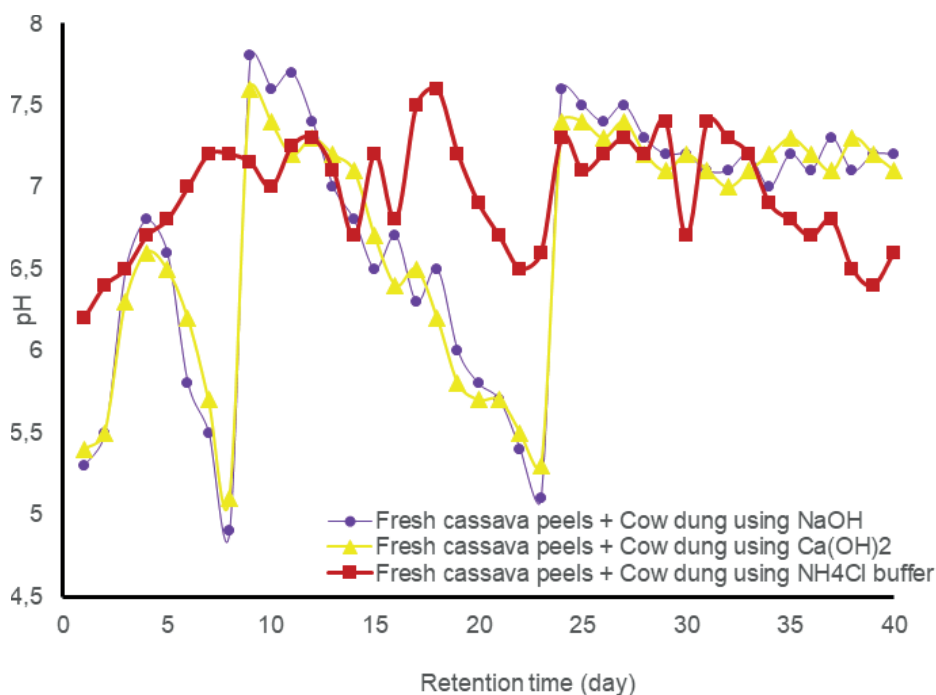


FIGURE 5: Variation of pH with retention time using different pretreatment chemicals.

anaerobic bio-digestion require a neutral or mildly alkaline environment, as a too-acidic or too-alkaline environment will be detrimental.

Table 2 shows the results of the chemical composition of cassava peels and cow dung slurry compared with cassava peels and cow dung digested sludge (biofertilizer) after 40 days anaerobic digestion. The fertilizer quality parameters (nitrogen, phosphorus and potassium) of the biofertilizer shows percentage increase of 75%, 79.35% and 50.77% for nitrogen, phosphorus and potassium respectively. However, there was 54.02%, 80.95% and 56.04% percent decrease in total solids, volatile acids and ammonia respectively. The pH of the digested sludge was within the limit for good biofertilizer. It has been reported that digested sludge can conserve fertilizer elements with a strong potential to recondition the soil and increase its fertility (Zhang, et al., 2013). Bayitse, et. al., (2014) reported that the sludge from cassava peels and manure is a good biofertilizer. The anaerobic digestion of cassava peels and cow dung slurry improved its value as fertilizer supplement because the available nitrogen and other substances increased in the produced sludge (Bayitse, et. al., 2014).

These results are a strong indication of a good quality biofertilizer from anaerobically digested sludge from cassava peels and cow dung. This was further confirmed when the biofertilizer was applied to soil used for maize plants cultivation. It was observed that the maize plants grown in the soil which contained the biofertilizer, grew much better than that from the soil without the biofertilizer. This result was similar to that earlier reported by Aisien et al., 2007 where the application of the digested sludge from cassava wastewater helped in improving plants growth. Also, Sawyer et al., (2017) reported that anaerobic co-digestion of cassava peels and cow waste generate energy like biogas and at the same time, the digested sludge from it can be used as fertilizer for agricultural applications. The sensory evaluation test carried out on the digested sludge (biofertilizer) after 40 days anaerobic digestion of cassava peels and cow dung shows that the biofertilizer odour level was extremely unobjectionable and this was an indication of significant reduction of odour after 40 days anaerobic digestion.

The result in Table 2 is in Mean ± SEM.

TABLE 2: The chemical composition of slurry and digested sludge from cassava peels and cow dung.

Parameters	Input Slurry	Output Digested Sludge	Percentage increase or decrease
Total Solids (%)	6.22 ± 0.42	2.86 ± 0.3	54.02
Volatile Acids (acetic acid mg/l)	735 ± 3.2	140 ± 2.2	80.95
Nitrogen (%)	0.45 ± 0.12	0.78 ± 0.2	75.00
Phosphorus (%)	0.92 ± 0.22	1.65 ± 0.27	79.35
Potassium (g/l)	6.46 ± 0.54	9.74 ± 0.4	50.77
Ammonia (g/l)	0.72 ± 0.15	0.31 ± 0.1	56.94
pH	5.8 ± 0.2	7.28 ± 0.3	2.52

## 4. CONCLUSIONS

The following conclusions can be drawn from this study:

- There were low biogas production/methane yield and slow onset of gas production at the beginning of the anaerobic digestion for the fresh cassava peels – cow dung mixed when compared with that of stale cassava peels – cow dung mixed.
- The cumulative biogas production after 40 days anaerobic digestion of stale cassava peels – cow dung mixed and fresh cassava peels – cow dung mixed were 104,961 cm<sup>3</sup> and 95,592 cm<sup>3</sup> respectively.
- There was no substantial increase in biogas production and methane yield for fresh cassava peels – cow dung mixed with NaOH and Ca(OH)<sub>2</sub> alkaline pretreatment without occasional pH adjustment. However, there was a significant improvement in biogas production and methane yield with the use of NH<sub>4</sub>Cl buffer pretreatment without any pH adjustment.
- The pH range (6.5 – 7.5) and temperature range (28 – 35°C) during the 40 days anaerobic digestion period were within the acceptable range for optimum biogas production and methane yield of 104,961 cm<sup>3</sup> and 62.3% respectively.
- The biofertilizer from the anaerobic digestion of cassava peels and cow dung sludge after 40 days digestion time was of good quality that improved the soil fertility and hence enhanced growth of the maize plants.

## REFERENCES

- Adelekan, B.A., Bamgboye, A.I. 2009. Comparison of biogas productivity of cassava peels mixed in selected ratios with major livestock waste types. *African Journal of Agricultural Research*.4 (7):571-577.
- Adeyanju, A. A. 2008. Effect of seeding of wood ash on biogas production using pig waste and cassava peels. *Journal of Engineering and Applied Sciences*, Vol. 3, No. 3, 242- 245, [Docsdrive.com/pdfs/medwelljournals/jeasci/2008/242-245.pdf](https://www.researchgate.net/publication/309124242).
- Ahmad, A.L., Ismail, S., Ibrahim, N., Bhatia, S. 2003. Removal of suspended solids and residual oil from palm oil mill effluent. *J. Chem. Tech. and Biotech.* 78 971-978.
- Aisien, F.A., Akakasiaka, U.F., Otoibhi, O.G., Aisien, E.T. 2007. Design and fabrication of a prototype biogas digester In: Ibhadode A.O. (Eds.), *Advances in Materials and Systems Technologies Trans TECH Publisher. Switzerland* pp. 527 – 532.
- Aisien, F.A.; Odafin, C.A., Aisien, E.T. 2007b. Application of cassava wastewater sludge as a liquid fertilizer. *Journal of Civil and Environmental Systems Engineering*, vol. 8, No. 1, pp. 31 – 39.
- Aisien, F.A., Aguye, M.D. and Aisien, E.T. 2010. Blending of ethanol from cassava wastewater with gasoline as a source of automobile fuel. *Electronic Journal of Environmental, Agricultural and Food Chemistry*, vol. 9,(8) pp. 445 – 450.
- Anaeto, M., Sawyerr, A.F., Alli, T.R., Tayo, G.O., Adeyeye, J.A. Olarinmoye, A.O. 2013. Cassava lead silage and cassava peel as dry season feed for West African dwarf sheep. *Global Journal of Science Frontier Research Agriculture and Veterinary Sciences*.13 (2).
- AOAC 1990. *Official Methods of Analysis of Assoc. of Analytical Chemistry*, 14th edn, Arlington, Virginia, 2209.
- Arowolo, A.A. and Adaja, J.I. 2012. Investigation of Manihot Esculenta and Manihot Duleis production in Nigeria: An Econometric Approach. *J. Appl. Sci. Environ.* 3:18-24.
- Bayitse, R.; Laryea, G.N.; Selormey, G.; Oduro, W.O.; Aggey, M.; Mansah, B.; Gustavsson, M. And Bjirre, A.B. 2014. Anaerobic co-digestion of cassava peels and manure: A technological approach for biogas generation and biofertilizer production – A feature article, *Journal of applied science and technology (JAST)*, vol. 19: No. 1 & 2, pp. 10 – 17.
- Ben, M.G. and Michael, E.I. 2018. Biogas production from farm waste (cassava peels and swine dung): Co-digestion and prospect on economic growth. *Res. Rev. J. Ecol., Environ. Sci.*, vol.6 issue 2, pp. 58 – 63.
- Buren, A.V. 1979. *A Chinese biogas manual. intermediate technology publications Ltd*, pp. 11-24.
- Buren, V. 1983. *A Chinese biogas manual. popularizing technology. Countryside intermediate technology Publications Ltd*.
- COP 21 2015. *Adaptation and resilience to climate change. 21st Conference of Parties on Climate Change, 30 November. to 11 December, Paris, France*.
- Cuzin, N., Labat M. 1992. Reduction of cyanide levels during anaerobic digestion of cassava. *Int. J. Food Sci. Technol.* 27:329-336.
- Deepanraj, B.; Sivasubramanian, V. and Jayaraj, S. 2014. Biogas generation through anaerobic digestion process research. A review *Journal of Chemistry and Environment*, 18 (5) pp. 80 – 93.
- Ezekoye V.A., Ezekoye, B.A. 2009. Characterization and storage of biogas produced from the anaerobic digestion of cow dung, spent grains/cow dung, and Cassava peels/rice husk. *Pac. J. Sci. Technol.*10 (2):898-904.
- FAO 2001. *Proceedings of The validation forum on the global cassava development strategy. Food and Agriculture Organization of the United Nations International Fund for Agricultural Development Rome, 2001. p. 65*.
- Gopinattan, C.; Himanshu, R. and Romilly, M.M. 2015. Cost-effective pretreatment of cassava peels for enhanced biogas production. *IOSR Journal of Environmental Science, Toxicology and Food Technology*, vol. 9, issue 9, pp. 21 – 25.
- Huiri, Z.; Yunjun, Y.; Liberti, F.; Bartocci, P. and Fantozzi, F. 2019. Feasibility analysis of an anaerobic digestion plant fed with canteen food waste. *Energy Conversion and Management*, vol. 180, pp. 938 – 948.
- Igbum, O.G.; Eloka-Eboka, A.C. and Adoga, S. 2019. Feasibility study of biogas energy generation from refuse dump in a community – based distribution in Nigeria. *International Journal of Low – Carbon Technologies*, vol. 14, issue 2, pp. 58 – 78.
- Igwe, N.J., 2014. Production of biogas from cassava and plantain peels blended with cow dung. *International Journal of Life Sciences Biotechnology and Pharma Research*, 3(4): 201-213
- Ilabaya, I.R., Asekham F.F., Ezugwu M.O., Eramhe A.A., Omofuma, F.E. 2010. Studies on biogas generation from Agricultural Waste; Analysis of the effects of alkaline on gas generation. *World Appl. Sci. J.* 9(5):537- 545.
- Ilori, M.O., Adebuseye, S.A., Lawal, A.K., Awotiwon, O. A. 2007. Production of biogas from banana and plantain peels. *Advances Environmental Biology*, Vol. 1, No. 1, 33-38, <http://www.the-free-library.com/production+of+biogas+from+banana+and+plantain+peels.-a0215720206>
- IITA -1 (<http://www.iita.org/cassava>, assessed 3/9/2013).
- Kongkiattikajorn J., Sornvorawea B. 2011. Comparative study of bioethanol production from cassava peels by monoculture and co-culture of yeast. *Kasetsart Journal (Natural. Science)*. 45:268-274.
- Kwasi – Effah, C. C., Obonor, A. I., Aisien, F.A. 2015. A Technical approach to balance the use of renewable and non-renewable energy sources.” *American Journal of Renewable and Sustainable Energy* 1, (3), 156- 165.
- ILRI. 2015. *Scaling the use of cassava peels as quality livestock feed in Africa. ILRI Research Proposal Summary. Nairobi, Kenya*
- McCarty, P. L, Smith, D 1987. Effect of hydrogen concentration on population distribution and kinetics in methanogenesis of Propionate Biotechnology Advance in Processing Municipal waste for Fuels and Chemicals. Antonopoulos New & Jersey, Noyes Data CO. Ofsofule, A.U., Uzodinma E.O. 2009. Biogas production from blends of cassava (Manihot utilisissima) peels with some animal wastes. *Int. J. Phys. Sci.* 4(7):398-402.
- Nkodi, T.M.; Taba, K.M.; Kayembe, S.; Mulaji, C. and Mihigo, S. 2016. Biogas production by co-digestion of cassava peels with urea. *IJSET* (5) : 3, pp. 139 – 141.
- Nkodi, T.M.; Kayembe, J.S.; Biey, M.E. and Taba, K.M. 2018. Comparative study of co-digestion of composted mixtures of cassava peels and coffee pulp with or without cow dung. *International Journal of Engineering Research and General Science*, vol. 6, issue 2, pp. 109 – 114.
- Mel, M.; Ihsan, S.I. and Setyobudi, R.H. 2015. Process improvement of biogas production from anaerobic co-digestion of cow dung and corn husk. *Procedia Chemistry*, 14. Pp. 91 – 100.

- Olanbiwoninu, A. A., Odunfa S.A. 2012. Enhancing the production of reducing sugars from cassava peels by pretreatment methods. *International Journal of Science and Technology*. 2(9):650-657.
- Olaniyan, A.M.; Olawale, T.T.; Alabi, K.P.; Adeleke, A.E. and Oyeniya, S.K. 2017. Design, construction and testing of a biogas reactor for production of biogas using cassava peel and cow dung as biomass. *Arid Zone Journal of Engineering, Technology and Environment*, vol. 13 (4) pp. 478 – 488.
- Olawale, O.E.; Oguntibeju, E.E. and Olawaseyi, J.B. 2017. Empirical analysis of energy potentials in co-substrates from cassava peels, cow dung and sawdust. *Proceeding of the world congress on July 5 – 7, London, U.K.*
- Onuorah, S.; Orji, M.I.; Okigbo, R. and Okeke, J. 2016. Co-digestion of livestock wastes for biogas production. *Bioengineering and Bioscience* 4 (3), pp. 42 – 49.
- Ozturk, M. 1991. Conversion of Acetate, Propionate and butyrate to methane under thermophilic condition in batch reactors” *Water research* 25(12):1509-1513.
- Sawyer, N. Trois, C., Workneh, T., Okudoh, V. 2017. Co-digestion for animal manure and cassava peels for biogas production in South Africa 9th International conference on advances in science, engineering, technology and waste management (ASETWM-17) Nov. 27-28, Parys, South Africa.
- Shah, F.A.; Mahmood, Q.; Rashid, N.; Pervez, A.; Raja, I.A. and Shah, M.M. 2015. Co-digestion, pretreatment and digester design for enhanced methanogenesis. *Renewable and Sustainable Energy Reviews*, 42, pp. 627 – 642.
- Smith, M. R., Lequerica, J. L. Hart, M. R. 1985. Inhibition of methanogenesis and carbon metabolism in *methanosarcina* sp. by cyanide. *J. Bacteriol.*, 162, pp. 67-71.
- Smith, K.; Cumby, T.; Lapworth, J.; Misselbrook, T. and Williams, A. 2007. Natural crusting of slurry storage as an abatement measure for ammonia emission on dairy farms. *Biosys. Eng.* 97, pp. 464 – 471.
- Ukpai, P. A., Nnabuchi, M. N. 2012. Comparative study of biogas production from cow dung, cowpea and cassava peeling using 45 litres biogas digester *Advances in Applied Science Research*, 3 (3):1864-1869.
- Wang, X., Yang G., Feng Y., Ren G., Han X. 2012. Optimizing feeding composition and carbon-nitrogen ratios for improved methane yield during anaerobic co-digestion of dairy, chicken manure and wheat straw. *Bioresour. Technol.* 120:78-83.
- Wantanee, A., Sureelak R. 2004. Laboratory scale experiments for biogas production from cassava tubers. *The Joint International Conference on “Sustainable Energy and Environment (SEE)”* 1 -3 December, Hua Hin, Thailand pp. 238-243.
- Zhang, T., Liu L., Song Z., Ren G., Feng Y., Han X., Yang G. 2013. Biogas production by co-digestion of goat manure with three crop residues. *PLoS ONE* 8(6): e66845. DOI:10.1371/journal.pone.0066845.



# ROLE OF BIOGENIC WASTE AND RESIDUES AS AN IMPORTANT BUILDING BLOCK TOWARDS A SUCCESSFUL ENERGY TRANSITION AND FUTURE BIOECONOMY – RESULTS OF A SITE ANALYSIS

Andrea Schüch<sup>1,\*</sup>, Jan Sprafke<sup>1</sup> and Michael Nelles<sup>1,2</sup>

<sup>1</sup> University of Rostock, Faculty of Agricultural and Environmental Sciences, Department of Waste and Resource Management, 18059 Rostock, Germany

<sup>2</sup> Deutsches Biomasseforschungszentrum gGmbH, 04347 Leipzig, Germany

## Article Info:

Received:  
15 July 2019  
Revised:  
10 February 2020  
Accepted:  
12 February 2020  
Available online:  
5 March 2020

## Keywords:

Biogenic waste and residues  
Bioenergy  
Energy transition  
Net stability  
Bioeconomy

## ABSTRACT

Renewable energies – especially wind and solar – have grown remarkably in recent years, but bioenergy is still the most important renewable resource worldwide and in Germany. In contrast to the situation in many other countries, bioenergy in Germany is often based on energy crops. As a result of changing political frameworks, the German bioenergy industry has to use alternative substrates as biogenic waste and residues and to implement more efficient utilization pathways. Biogenic waste and residues can cover in Germany 7 to 9% of the current total primary energy consumption. In the federal state of Mecklenburg-Western Pomerania, more electricity is produced than consumed. This means that the federal state exports electricity to other German regions or abroad, assuming grid bottlenecks do not prevent this. The share of fluctuating wind and solar power is still increasing. Without stabilization by coal power plants, the electrical network could be destabilized by those sources. The presented case study of Mecklenburg-Western Pomerania shows that there are opportunities to contribute to a stable network through the use of bioenergy. Besides the supply of electricity, thermal energy at different temperature levels, as well as fuels for transportation, are also provided by biomass. Around 22% of the annual energy consumption of the federal state could be covered by biogenic waste and residues (based on the technical fuel potential). The figure is currently 7.3%. This shows that there is room to extend bioenergy generation and the use of biogenic waste and residues in the bioeconomy without impacting food production.


## 1. INTRODUCTION

The world's population currently faces two fuel-related challenges: environmental degradation and resource scarcity. Environmental degradation includes global climate change, air toxicity, inadequate solid waste disposal, decreasing drinking water quality and the decline in insect populations. Every region of the world is affected but to different degrees. The global energy system is still dependent on fossil fuels and ranges from 32 to 100% in individual countries. Germany belongs to the group of countries with high fossil fuel dependency (>85%) along with China, India, Japan, the U.S. and Russia (Ediger 2019, BP 2019, Ediger 2007).

The energy transition, which includes the transition into a low-carbon economy, will only be possible with the decarbonization of the energy system (Ediger 2019). Multiple approaches have to be combined to be successful: (1) energy savings through greater efficiency, (2) increasing the

proportion of low-carbon-intensity fossil fuels such as gas, (3) increasing the proportion of renewables, and (4) carbon capture and storage technologies. The energy transition goes hand in hand with a transition of the fossil-based economy into a bioeconomy. The German renewable energy goals are ambitious, e.g. increasing the share of renewables to 65% by 2030 (related to the electricity supply, BMWi 2019).

Across the world and in Germany, renewable energies – especially wind and solar – have increased remarkably in recent decades. Globally, bioenergy is however still the most important renewable energy source. This may change in the future. Both worldwide and in Germany the bioenergy share, mainly from wood and energy crops, is around 7 to 9% (FNR (2019): 7.1% of the German primary energy consumption (PEC) in 2018, IEA (2017): 9% of global total primary energy supply in 2015). In the federal state of Mecklenburg-Western Po-

 \* Corresponding author:  
Andrea Schüch  
email: andrea.schuech@uni-rostock.de

merania, wind power has overtaken bioenergy (StatA MV 2017).

In contrast to the situation in many other countries, bioenergy in Germany is often based on energy crops. As a result of changing political frameworks, the bioenergy industry has to use alternative substrates such as biogenic waste and residues and to implement more efficient utilization pathways. But biogenic waste and residues are limited. At the same time, there is still unused potential – for example, one-third of the technical potential of waste biomass in Germany is still unused. By tapping the full potential, biogenic waste and residues could cover around 7 to 9% of the total PEC in Germany. Assuming decreased energy consumption, this share could increase to up to 15% (Brosowski et al. 2016).

The objective of sustainable integration of bioenergy into future global energy and bio-based economic system can only succeed if bioenergy is integrated as efficiently as possible, in a way that is environmentally sound and with the greatest possible economic benefits. Bioenergy, including that from biogenetic waste and residues, can contribute to this goal. Worldwide the demand for biomass will increase to meet the demand for material and energy (Piotrowski et al. 2015, Hoogwijk et al. 2005). The amount of biogenic waste and residues is also increasing. Seven billion people (in 2011) produce around 1.3 billion Mg dry matter (DM) organic waste per year and the world's population is still growing. Around one-third of this dry matter is food waste (0.51 billion Mg DM), since globally 30% of all food is wasted (Piotrowski et al. 2015, Schüch et al. 2017).

Globally and in Germany it seems to be clear that we have to explore the whole potential of biogenic waste and residues to cover our future needs. But to realize the available potential implementation at the local level is necessary. The advantages and limits of the available waste and residues for the energy transition and the bioeconomy are not well known at the federal state level. To determine the situation in Mecklenburg-Western Pomerania a site analysis was undertaken. The high biomass and renewable energy potential combined with low own energy demand from within the state make this area especially interesting. The aim of the study is to encourage developments that will make the state a pioneer in the field.

The objective of this study is to consider the role of biogenic waste and residues in the federal state of Mecklenburg-Western Pomerania for the energy transition and the bioeconomy. The paper will present selected results of site analysis and introduce technical solutions to how bioenergy plants could produce electricity (and heat) flexibly to stabilize local power grids and to contribute to the supply of renewable energy.

The objectives can be described as follows:

- i. To describe the importance of bioenergy and biogenic waste and residues in a renewable energy system and bioeconomy.
- ii. To compare the current status of bioenergy with the technical biomass fuel potential.
- iii. To calculate the potential of biogas plants in the study area for sector coupling, with a focus on biogas up-

grade and power-to-gas processes.

- iv. To assess the possible contribution of biogenic waste and residues for the energy transition and the bioeconomy in the study area.

## 2. MATERIAL AND METHODS

The available literature, reports and statistical data are analyzed to answer the set objectives. The study area is the federal state of Mecklenburg-Western Pomerania. For the site study, data were found in annual abstracts of energy statistics (StatA MV 2018 and 2017, BNetzA, EM MV 2018), annual waste management reports (LUNG 2018), a bioenergy potential report (AEE 2013) and the results of external analysis and our own based on surveys (Daniel-Gromke et al. 2017, Orth and Schüch 2018). The data were analyzed by means of Exel. German trends and developments were projected to the federal state using an allocation mechanism and local data.

### 2.1 Bioenergy in a renewable energy system

Fossil and biomass power plants (and combined heat and power (CHP) units) need to be optimized regarding their flexibility parameters to be able to integrate as much fluctuating renewable energy as possible and in that way maintain the stability of the electrical grid. Ancillary services can be categorized as primary, secondary or tertiary frequency control reserves (Hübel et al. 2018).

A wide variety of proven and future options are available for bioenergy generation. Biomass in the form of liquid, solid or gaseous energy carriers can be converted in a way that can fulfill the requirements of the different power products within the markets. The ability to store biomass and its derived energy carriers is an almost unique advantage compared to other renewable sources (Szarka et al. 2013).

Bioenergy, including that from biogenic waste and residues (Nelles et al. 2015), can provide the positive and negative electrical capacity to avoid the retaining of fossil energy sources in a more and more renewable energy system (Holzhammer et al. 2015, Mauky et al. 2014). The increasing share of fluctuating renewable energies such as wind and solar power needs to be balanced in a way that substitutes the most harmful fossil fuels (Holzhammer et al. 2013). Already today advanced biogas plants are able to meet this flexibility demand. A pilot project has shown that demand-oriented energy production is also possible for solid biomass conversion plants (Hoffstede 2013). About 50% of German biomass plants are able to provide energy in a flexible way (Szarka et al. 2013).

Biogas plants cover today in Germany about 4% of the gross electricity consumption. These plants as a future flexibility option (installed capacity of 1,500 MW, which corresponds to one-third of the current capacity) can decrease the surplus generation of renewables by about 8 to 10% compared to the reference scenario in the same period. (Lauer and Trähn 2017, FNR 2018)

Biomass-based fuels have a significant advantage over other renewable heat sources. One benefit is that by burning solid biomass, combustion temperatures of up to 500°C are common and even temperatures above 1,000°C

are possible when burning biomethane or hydrogen from power-to-gas processes.

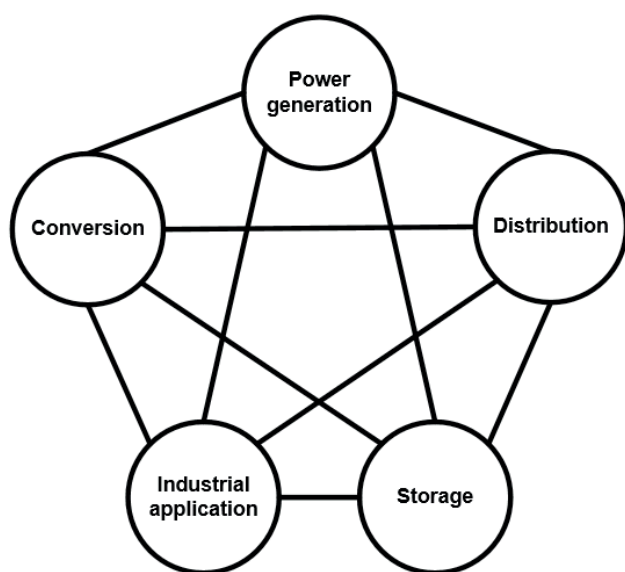
The interactions between the provision, storage, conversion, transport and use of energy are very complex (Figure 1). The use of and demand for thermal energy is very strongly influenced by the economic sector in which it is used. Companies with relatively similar products have a different energy demand than companies with changing production. Furthermore, a distinction is made between low temperature (<100°C), medium temperature (100–500°C) and high temperature (>500°C) levels. Exemplary technologies are cleaning, cooking, pasteurization, bleaching, drying, washing and pressing. The use of heat in industrial processes can furthermore contribute to sectoral coupling.

## 2.2 Role of biogenic waste and residues in the bioeconomy

Biogenic waste and raw materials are to be used even more efficiently in the green or bioeconomy (Nelles 2017). Current research focuses on integrated biorefinery concepts and the production of basic chemicals, specialized fibres or fillers, and biocomposites or chars based on biodegradable waste (Schüch et al. 2017). The (new) combination of technologies can lead to new or better products or enhance energy efficiency. Ding et al. (2017) describe for example the pretreatment of food waste by hydrothermal carbonization followed by two-stage anaerobic digestion.

The aim of a biorefinery concept is to produce high-value bioproducts by means of valorization. Several research and demonstration projects have been implemented and reported (e.g. Schüch et al. 2016, Cimpan et al. 2015, Rausen and Wagner 2017, Aichinger et al. 2015).

In the future, energy-efficient biowaste treatment plants are not only intended to safely fulfill their disposal and recycling function, but also to supply the electricity in line with demand and to link sectors such as transport and heat in an optimal way (Figure 2). Besides these new develop-



**FIGURE 1:** Interaction between provision, storage, conversion, transport and use of energy.

ments, traditional and proven technologies retain their importance (Schüch et al. 2017).

## 3. SITE ANALYSIS: FEDERAL STATE OF MECKLENBURG-WESTERN POMERANIA

Mecklenburg-Western Pomerania is located in the north of Germany on the Baltic Sea, bordering on Poland. With an average of 69 people per km<sup>2</sup> (45 in the countryside to 1,149 in the biggest city of the federal state), Mecklenburg-Western Pomerania is a low-populated state with migration from rural to urban areas (StatA MV 2018).

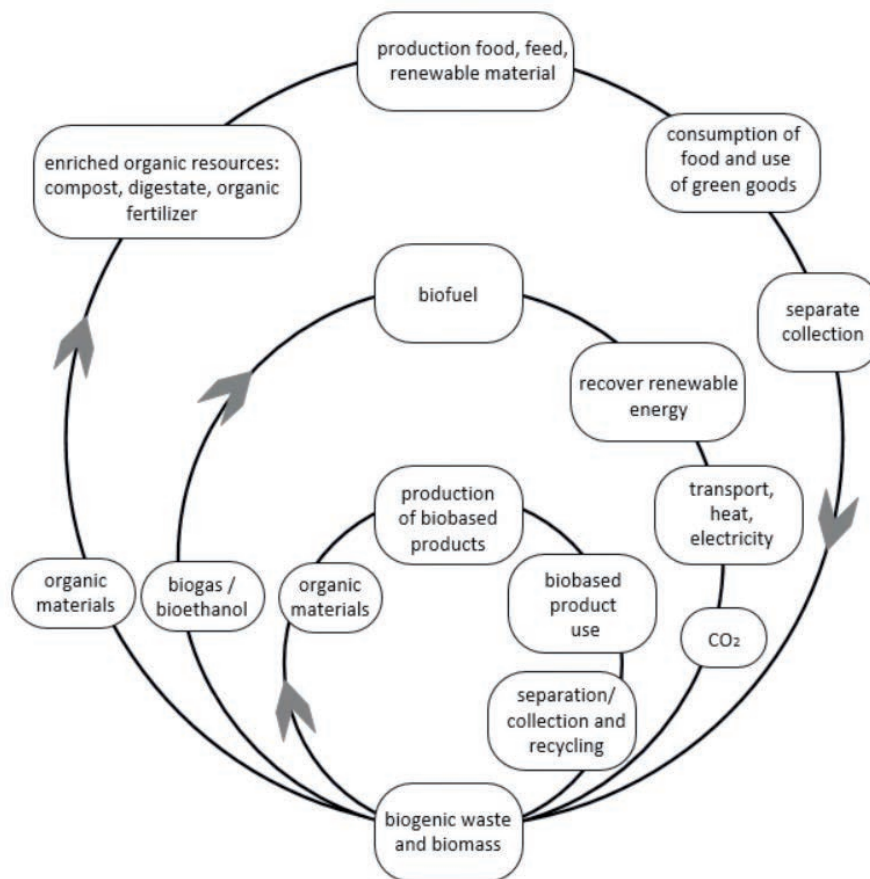
The demand centers for energy are strongly connected with population density and industry, in other words, and around the bigger cities as Rostock, Schwerin and Neubrandenburg and in coastal port towns. The federal-state is affected by demographic change, which influences living models, consumption and waste disposal structures.

Besides factors such as living standard, income and season, the site-specific creation of biowaste is connected to population density. Therefore the total potential of biowaste is low in the federal state. The separate collection of biowaste is not undertaken everywhere. In some regions, only green waste or garden waste is collected. In a nationwide comparison, the collected amount is relatively low. The annual German average amount of collected biowaste is 58 kg fresh mass (FM) per inhabitant (Kern et al. 2018) but in Mecklenburg-Western Pomerania only 29 kg (FM) (LUNG 2018). With the introduction of obligatory separate collection of biowaste nationwide the amount per capita increased slightly (e.g. from 2016 to 2017: +9.1%, LUNG 2018). In addition to the biowaste, per inhabitant 52 kg (FM) green waste was collected in the federal state (LUNG 2018). The separately collected bio- and green waste amounted to 131,022 Mg (FM) in 2017 (LUNG 2018). In comparison, the potential of agricultural residues and by-products especially for straw with around 1,070,600 Mg (TM), is much higher (AEE 2013).

The federal state has a technical biomass fuel potential of up to 31,000 GWh (AEE 2013). This corresponds to about 8% of the German potential. The highest potential was found for energy crops and forest biomass with 16,528 and 7,056 GWh/a respectively, followed by straw with 3,056 GWh/a (AEE 2013). According to this reference, the technical fuel potential of organic waste and residues amounts to 8,750 GWh/a. Therefore around 22% of the yearly energy consumption of the state could be covered by this source (in 2016 39,167 GWh energy was consumed, EM MV 2018).

### 3.1 Renewable energy sector

The geographic position of Mecklenburg-Western Pomerania makes the state especially suitable for wind power production. More than 60% (63.9% in 2015, 60.8% in 2016) of the generated electricity are renewable energies, 25.2% and 26.8% respectively are from hard coal and around 10% from fossil gases (EM MV 2018). Despite the adverse northern location with its relatively low solar radiation, in recent years the solar power sector has increased enormously (StatA MV 2017). The agrarian countryside with its high potential for biomass makes it especially suitable



**FIGURE 2:** Biogenic waste and biomass in the circular economy (author's figure after ECN 2019, adapted).

for bioenergy. Figure 3 shows the proportion of installed renewable energy capacity and net electricity production. Biomass, including biogenic waste and residues, contributes 25% to the federal renewable electricity production. Most were generated by using biogas or biomethane in co-generation (StatA MV 2017).

The biogas sector is well developed: 250 agricultural biogas plants produce 840 million Nm<sup>3</sup> biogas per annum. 542 biogas and biomethane CHP units are in operation. The total installed electrical capacity of these CHPs is 300 MW. Additionally, 15 biogas plants upgrade biogas into biomethane with a capacity of 135 million Nm<sup>3</sup>/a (StatA MV 2018, Daniel-Gromke et al. 2017). One biogas plant produces biogas from separately collected biowaste and uses this in cogeneration (capacity 18,000 Mg/a, Remondis 2019); one other uses the mechanically separated organic fraction from mixed municipal solid waste (OFMSW) and organic waste, capacity 40,000 Mg/a, Veolia 2019) and produces upgraded biogas. Besides this, a number of biogas plants use organic waste and residues from food production, agriculture, canteens and so on. Three of these upgrade the biogas into biomethane.

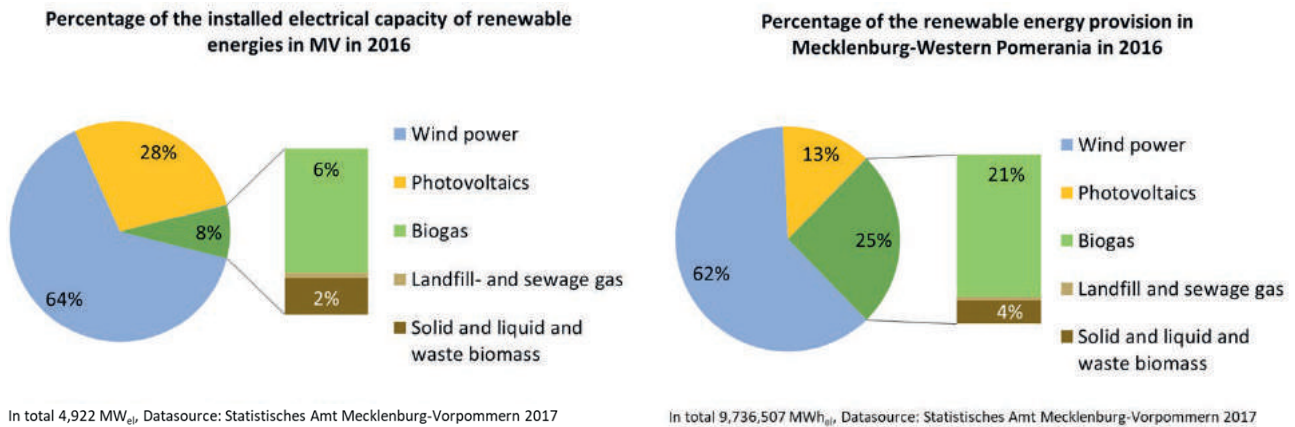
The electrical capacity of the plants that use solid and liquid biomass is 88 MW<sub>el</sub> (StatA MV 2017). Used biomass is mainly wood, waste wood and some plant oil. Biomass heat plants also use straw or dried grass from wetlands. Smaller thermal installations for biomass use, for instance, wood pellets or firewood.

In contrast, the installed electrical capacity of wind and photovoltaics is 3,310 and 1,426 MW respectively, which together is 72% of the total renewable capacity (StatA MV 2017).

The availability of the bioenergy plants is high: with a share of 8% of electrical capacity, 25% of the renewable net electricity was provided in 2016 (StatA MV 2017, Figure 3).

Total electricity consumption in Mecklenburg-Western Pomerania is around 6,800 GWh per year. In the state, more electricity is produced than consumed when considering the yearly balance. This means that the federal state exports electricity to other German regions or abroad. But this is not possible when the electrical network cannot transport electricity to demand centers as a result of network bottlenecks or low demand. Currently, this surplus energy is avoided by feed-in management measures (for electricity feed into the electrical grid) – producing plants are shut down for a time. This causes costs and valuable potential is lost. In the federal state the amount of loss was 317,570 MWh electricity in 2016 (StatA MV 2018). Figure 4 shows the distribution of renewable energy plants such as wind power and biogas plants as well as the location of electrical substations where the feed-in management measures took place.

The shut-down or curbed renewable energy plants are paid for the not produced electricity, which resulted in costs of €29,9 million in the year 2016 in the federal state (€372,7 million in Germany, BNetzA 2017). Germany wide, 93.5%



**FIGURE 3:** The proportion of renewable energy in the German federal state of Mecklenburg-Western Pomerania. Right: installed electrical capacity, left: net electricity production in 2016 (Source: StatA MV 2017).

of these costs could be attributed to wind power plants in 2016. Since the wind energy sector is growing faster than the net revision, this will cause problems in the future, especially in Mecklenburg-Western Pomerania. The energy transition can only be successful if resources are used as efficiently as possible. One solution to use surplus energy is sector coupling. The electricity could be used to produce hydrogen by electrolysis and used for transportation, industry or as energy storage. It is also possible to produce methane from the hydrogen. For this conversion, CO<sub>2</sub> is needed, which could easily be provided by bioenergy plants including waste treatment facilities. Biogas plants together with landfills and sewage sludge digestion plants in Mecklenburg-Western Pomerania could provide between 179 and 535 million m<sup>3</sup> CO<sub>2</sub> per year (Orth and Schüch 2018). Additionally, biomass heat (and power) plants produce biogenic CO<sub>2</sub>. Biomethane plants which separate the CO<sub>2</sub> from biogas can do this today already. For all these plants in the federal state, the capability of these CO<sub>2</sub> sources is estimated at 50 to 65 million m<sup>3</sup>/a.

### 3.2 Electricity feed-in

Not only is the amount of electricity supplied important for the site analysis, but also at which grid level it is fed. A distinction is made between high-voltage grids, high-voltage/medium-voltage grids, medium-voltage grids, medium-voltage/low-voltage grids and low-voltage grids. In Mecklenburg-Western Pomerania, biomass plants mainly feed into the medium-voltage grid, whereas plants with an installed (CHP) capacity of less than 100 kW<sub>el</sub> tend to feed into the low-voltage grid. Wind turbines, on the other hand, tend to feed their electricity at the medium and highest voltage levels. At the medium-voltage level, biomass, wind and solar plants feed-in electricity. Solar systems dominate the low-voltage level, at which few biomass plants and almost no wind turbines feed electricity (BNetzA 2017).

Important for future planning is also the spatial distribution of the plants. An accumulation of biogas and wind power plants can be found in the eastern part of the federal state as well as south of Rostock (Figure 4, Orth and Schüch 2018).

A calculation of the biogenic waste and residue share of the renewable electricity supply is difficult since statistical data are lacking and it was not possible to collect all information directly at the plants. But estimations could be made. Around 4% of the generated electricity comes from landfill, sewage gas CHP and liquid biofuels, and 21% from biogas and biomethane CHP units (based on StatA MV 2018). The majority of the biogas is produced in biogas plants using 76.7% (energy-related) energy crops and 23.3% biogenic residues such as animal feces, municipal bio- and green waste and residues from industry and agriculture. The number of waste digestion plants is low: in the study area, six of more than 250 biogas plants are waste digestion plants. The installed capacity ranges from 370 up to 2,000 kW<sub>el</sub>. For biomethane 82% (energy-related) energy crops are used and only 18% biogenic residues or waste (Daniel-Gromke et al. 2017). Based on this information and the statistical data on generated renewable electricity in 2016 (StatA MV 2018), the proportion of biogenic waste and residues of renewable electricity generation in the study area is estimated at 5.1%, of biobased electricity generation at nearly 20%, of total electricity generation at 3.4% and of total electricity consumption at 7.3%.

#### 3.2.1 Flexibility of biogas plant CHPs

Biogas plants, including waste digestion plants, are encouraged to generate energy in a demand-oriented manner. Different concepts are used, for example, the storage of biogas and CHP generation in times with higher market prices and low wind and solar power on the grid. This requires higher gas storage capacity and more CHP units (Schüch et al. 2017). One possibility to decrease the gas storage demand is flexible biogas production by means of adapted feeding strategies or the storage and selective supply of intermediates (Szarka et al. 2013). Biogas plants with on-site cogeneration or biomethane CHPs are able to offer ancillary services by operating reserves.

CHPs with biogas storage for several hours of operation is particularly suitable for securing the residual load for the daily compensation of fluctuating generation and consumption. For this purpose, the production is increased during peak load hours and the plant is operated according



**FIGURE 4:** Distribution of wind power, biogas plants and electrical substations with feed-in management measures in Mecklenburg-Western Pomerania in 2016 (Orth and Schüch 2018 based on OpenStreetMap).

to a timetable that is based on the prices on the spot market (FNR 2018).

To estimate the degree of flexibility for a demand-based power supply in the federal state of Mecklenburg-Western Pomerania, the ratio of installing to rated power and the presence of several CHPs are important. This however could not be determined in the project due to incomplete data. The use of the flexibility bonus (flex bonus, a special additional feed-in tariff of the German Renewable Energy Sources Act (EEG)) can be used as an indication of the possibility of flexible CHP operation. Through this bonus, the investment in additional CHP capacity can be partially refinanced. Experts assume that participation in the tendering model (replacing the former EEG tariffs) is hardly economically feasible without the use of the flexibility bonus. The main reason for this is that the EEG remuneration is lower and, at the same time, the financial burden of the necessary investments is higher (higher CHP capacity, storage, and repair of the stock). The use of the flexibility bonus is limited and has been reduced from 1,350 to 1,100 MW<sub>el</sub> installed capacity (Neumann 2018). In May 2017, the flex bonus had been used for 355.4 MW<sub>el</sub> nationwide, and as of December 2018 for 900.5 MW<sub>el</sub> (BNetzA register of facilities, as of 05/2017 and as of 12/2018). It was assumed that the flex bonus fee will be exhausted by summer 2019 (Neumann 2018).

Based on the installed capacity of biogas plants in Mecklenburg-Western Pomerania (268 MW<sub>el</sub>), the flex bonus was used for about 30% (78 MW<sub>el</sub>), whereby 49 biogas plants did not increase their capacity and 34 plants did increase their capacity (BNetzA, in the period from 08/2014 until the end of 12/2018). However, a statement on the rate of flexibilization cannot be drawn as the design performance of the biogas plants has not been published. Based on the data, however, it can be assumed that 30% of the biogas plant capacity or around 156 biogas plants can be operated flexibly (with on-site electricity generation, on the basis of an average of 500 kW<sub>el</sub> per plant).

The investigation of flexible operation of waste digestion plants is part of the Netz-Stabil project and is still in progress. Initial results show that flexibility options are available, but legislation and technical and economic barriers currently exist (Sprafke et al. 2019).

### 3.2.2 Flexibility of biomass power plants

Besides the production of heat and electrical energy, thermal power plants supply system stability to the electrical grid by providing ancillary services. Currently installed wind and photovoltaic generators are not able to supply primary control reserves. Alternative technologies such as large batteries are not yet available on the required scale. Studies by Hübel et al. (2018) show that flexibility improve-

ments at a reference hard coal power plant led to significant economic benefits compared to similar changes at a gas turbine power plant. In addition, specific improvements in cash flow can be calculated when future market price functions are used.

Biomass heat and power plants are working with similar technical principles, but usually at a lower scale than hard coal power plants. An important difference is that these plants are designed to supply a consumer (industry, district heat, etc.) with heat, which means they are driven by heat demand. Combined with heat storage and smart management of internal storage options these plants could provide electricity in a more flexible way than today, as confirmed in a pilot study by Hoffstede (2013).

### 3.3 Heat sector

#### 3.3.1 Heat from biogas CHP units

By far the largest number of biogas plants in Mecklenburg-Western Pomerania uses the generated biogas on-site in cogeneration. Demand-oriented biogas production and electricity generation is predominantly not implemented. In many plants, the generated heat is not fully utilized. This may be because appropriate heat sinks are lacking or the demand does not match the availability of the heat. The heat demand of the biogas plants is highest in winter, while the heat surplus is usually highest in the summer. Since households have the lowest heat demand in summer, the available heat can usually not be fully used when a district heat network is only fed by a biogas plant CHP.

In order to estimate the current heat utilization of biogas plants in the federal state, the heat production was calculated from the net electricity production. Average system data were used for this, according to an electrical efficiency of 28 to 47% and a thermal efficiency of 34 to 55% (KTBL 2013). After deducting the amount necessary to supply the fermenter heating, this results in the available heat from biogas plant cogeneration units in Mecklenburg-Western Pomerania amounting to approx. 1.5 million MWh<sub>th</sub> per year (Table 1). The net heat generation by power plants (owned by power utilities, industrial power plants and heating plants to supply >500 residential units) amounts to 3.9 million MWh<sub>th</sub> (2016), of which 2.5 million MWh is generated from natural gas (Stat. MV 2017). The available heat from biogas CHPs, therefore, corresponds to approximately 38% of the net heat production.

In Germany, 90% of the biogas plants use the available heat externally (Daniel-Gromke et al. 2017). If this were used to cover heat sinks, in Mecklenburg-Western Pomerania surplus heat from biogas CHPs could thus replace 35%

of the net heat generation (1.35 million MWh<sub>th</sub>/a). Currently, only 30% of biogas plants in Germany supply heating grids (Daniel-Gromke et al. 2017). Projected onto the federal state this would amount to about 0.33 million MWh<sub>th</sub> or about 8% of the net heat generation.

Electricity is also generated via CHP technology by using landfill and sewage gas, and heat can also be available here. Although landfills do not have their own heat demand, they are mostly far from heat sinks, which make it difficult to use. Due to the decrease in landfill gas and methane concentration (since 2005, no untreated waste may be deposited), the amount of electricity and heat is declining. Wastewater treatment plants often use the waste heat from electricity generation to cover various requirements of the plant, but also to supply district heating networks (e.g. WWT Grevesmühlen).

#### 3.3.2 Heat from biomass plants

In the heat sector, the share of renewables is around 20%, which is dominated by biomass (Orth and Schüch 2018). The potential of biomass residues and waste from municipals, industry, agriculture and forest is high. Especially straw, stalky biomass from wetland or landscape cultivation as well as manure from animal husbandry is not fully used. Woody biomass is in competition with the wood industry, but at the same time, large wood processing plants are using their own wood residues for heat provision (e.g. Holzcluster Wismar). Examples of the efficient use of waste wood also exist. For example, the heat and power plant in Hagenow (Biotherm Hagenow GmbH) provides all available heat for and district heat grid in an industrial site and recovers heat from the exhaust gas to dry (natural) wood chips to produce high-quality fuels with defined parameters (lower heating value, ash content).

#### 3.3.3 Biogas upgrade capacity and Power-to-Gas processes

One option is to decouple the biogas production and upgrade the biogas into biomethane. In Germany, this could be stored and transported easily via the natural gas grid. Furthermore, biomethane can replace natural gas in high-calorific industrial processes.

Limiting factors are the availability of the natural gas grid and the economic feasibility for small plants (<500 kW electrical equivalent capacity). So far this approach has only been economical for larger plants. In addition, a suitable natural gas pipeline must be available on-site. Research and development are being done to find applicable upgrade solutions with high efficiency, e.g. by using membranes (Park et al. 2017, Miltner et al. 2017).

The biogas upgrading capacity in Mecklenburg-Western Pomerania is currently 135 million Nm<sup>3</sup>/a (Daniel-Gromke et al. 2017). Three of the six waste digestion plants and additionally 15 agricultural biogas plants upgrade biogas into biomethane (Daniel-Gromke et al. 2017). According to Scholwin et al. (2015), approximately 10% of the installed capacity of biogas plants in Germany (with a minimum CHP capacity of 800 kW<sub>e</sub>) is suitable for a biogas upgrade: if more than 50% of the heat produced in cogeneration cannot be utilized and marketed, biogas upgrade under certain conditions is an economical alternative. Projected onto

**TABLE 1:** Assumptions for estimating the potential for external heat use from biogas, landfill and sewage gas CHP units in the federal state of Mecklenburg-Western Pomerania.

Plant type	Plants heat demand of the produced heat (KTBL 2013) [%]	Available heat for external use [MWh <sub>th</sub> ]
Biogas	28	1,502,266
Landfill gas	No demand	32,308
Sewage gas	28	11,631

the federal state, a capacity of about 26.8 MW<sub>el</sub> could be suitable for biogas upgrading (without biomethane CHP). Taking an average installed capacity of 500 kW<sub>el</sub> as a basis, this means that around 53 biogas plants may be suitable for biogas upgrade. In addition, there is still potential in the pooling of biogas plants that are not much further apart than 2 km. The analysis, to identify the potential in the federal state for that solution is not finished yet.

As stated in section 3.2, separated CO<sub>2</sub> can serve as a biogenic source for power-to-gas solutions. The total annual CO<sub>2</sub> potential of the biogas (including waste digestion plants), landfill and sewage gas plants in Mecklenburg-Western Pomerania is at least 390 million m<sup>3</sup> CO<sub>2</sub> and together with the biomethane plants around 440 million m<sup>3</sup> CO<sub>2</sub> (calculated from net electricity production, the reference year 2016, StatA MV 2017). With this amount of CO<sub>2</sub> it would be possible to provide approximately 153 to 456 million m<sup>3</sup> methane (methanation rate 85%). To produce hydrogen approximately 6.3 million to 7.1 million MWh<sub>el</sub> is needed. This means that the whole loss by feed-in management measures (317,570 MWh<sub>el</sub> in 2016) could be transferred into methane by biological or catalytic methanation.

### 3.4 Bioeconomy

Alongside the renewable energy industry and the health sector, agriculture is one of the most important economic sectors in the federal state of Mecklenburg-Western Pomerania. The percentage of agricultural areas is higher than the average in Germany (AEE 2013). The technical potential of residues from agriculture is high, especially of straw (technical potential 11,000 TJ/a) and manure from animal farming (technical potential 3,900 TJ/a) (AEE 2013). Besides the agriculture food processing industries as well as biofuel producing facilities are in operation and important employers locally. There is not much of a biobased industry, except the wood processing cluster in Wismar (Schüch et al. 2017). New pilot facilities have been established in the state such as Continental, which develops biobased tires (Holzhammer 2018). Altogether the potential to expand the bioeconomy in the federal state is high since a lot of space, biomass and renewable energy are available.

## 4. CONCLUSIONS

The energy transition goes hand in hand with a transition of the fossil-based economy into a bioeconomy. In the future, the circular economy will be strongly connected with the bioeconomy. The road to this "green economy" is a long one, but it is gaining more and more importance in politics, industry and research. To make the transition from traditional waste disposal to circular and green economy happen, awareness and the willingness of the population to support this development through a good waste separation is essential. Besides technology, economy and ecology, social aspects also need to be considered.

Waste segregation is a key requirement for high-quality recycling products. These more valuable products could contribute to economically feasible management concepts. Biodegradable waste can be a valuable resource

for energy generation and recycling. In many countries, its separate collection and high-quality utilization have been recognized as an opportunity for added value.

Mecklenburg-Western Pomerania has the potential to be an exporter of renewable energy, food, and biomaterial since the potential for generation is high. The technical fuel potential of biogenic waste and residues is lower than the total energy consumption but in the range of the electricity consumption of the study area. The currently achieved 493,658 MWh generated electricity from biogenic waste and residues represents only 5.6% of the technical fuel potential of organic waste and residues (8,750 GWh/a). Even when the cogenerated heat is considered, the scope for further exploitation is remarkable.

The main bioenergy plant stock consists of biogas plants that present a low flexibility rate. Only 30% of the installed electrical capacity uses a flex bonus. It is unlikely that plant operators are able to invest in additional CHP units to act in a more demand-oriented way. Therefore under the current framework, higher flexibility of the bioenergy plant stock cannot be expected. But activities of individual plant operators to improve the whole plant performance by installing additional CHPs and gas storage as well as improving the use of cogenerated heat in the study area are known by the authors. Since not many additional bioenergy plants are expected in the coming years, increasing installed capacity could be considered as growing the flexibility of the plant stock.

In the study area a number of biogas plants that use waste and residues as feedstock upgrade biogas into biomethane. This offers demand-oriented use in electricity, heat, mobility and industry sectors. Through the pooling of biogas plants, this option could be further developed for around 20% of the plants. Currently, surplus electricity is avoided by means of feed-in management. Producing plants are shut down, resulting in very high costs. Bioenergy plants generate climate-neutral CO<sub>2</sub>, which is needed in the future, e.g. for synthetic fuels or methanation. The potential of green CO<sub>2</sub> in the study area is high. The current surplus electricity from wind energy plants could be transferred into biomethane by the CO<sub>2</sub> of around 25 biogas plants (Orth and Schüch 2018).

The energy transition is only possible when the whole potential of wind, solar and bioenergy is explored. Further implementation means the installation of more renewable energy plants than are present today. This is an economic opportunity (jobs, regional added value) but also a challenge (exploitation of difficult waste substrates, logistics, infrastructure, and experienced personnel) and risk regarding nature protection (local nutrient surplus, emissions etc.). Altogether the energy transition and bioeconomy offer more opportunities than risks for the study area, but support from policymakers and a stable economic framework are needed to move forward with this development.

## REFERENCES

AEE, 2013. Potenzialatlas Bioenergie in den Bundesländern. [https://mediathek.fnr.de/media/downloadable/files/samples/a/e/aee\\_potenzialatlas\\_090114\\_2013\\_fnr.pdf](https://mediathek.fnr.de/media/downloadable/files/samples/a/e/aee_potenzialatlas_090114_2013_fnr.pdf), last website visit on 23.05.2019.



- Aichinger, P.; Kuprian, M.; Probst, M.; Insam, H.; Ebner, C., 2015: Demand-driven energy supply from stored biowaste for biomethanisation. *Bioresour. Technol.* 194, 389–393. <https://doi.org/10.1016/j.biortech.2015.06.147>
- BMWi 2019. Erneuerbare Energien in Zahlen - Nationale und internationale Entwicklung im Jahr 2018, Hrsg. Bundesministerium für Wirtschaft und Energie (BMWi), as of October 2019, [https://www.erneuerbare-energien.de/EE/Redaktion/DE/Downloads/Berichte/erneuerbare-energien-in-zahlen-2018.pdf?\\_\\_blob=publication-file&v=3](https://www.erneuerbare-energien.de/EE/Redaktion/DE/Downloads/Berichte/erneuerbare-energien-in-zahlen-2018.pdf?__blob=publication-file&v=3), last website visit on 27.11.2019.
- BNetzA, 2017. Bundesnetzagentur: Quartalsbericht zu Netz- und Systemsicherheitsmaßnahmen Viertes Quartal und Gesamtjahr 2016.
- BP, 2019. BP Statistical Review of World Energy 2019. <https://www.bp.com/content/dam/bp/business-sites/en/global/corporate/pdfs/energy-economics/statistical-review/bp-stats-review-2019-full-report.pdf>, last website visit on 15.11.2019.
- Brosowski, A.; Thrän, D.; Mantau, U.; Mahro, B.; Erdmann, G.; Adler, P.; Stinner, W.; Reinhold, G.; Hering, T.; Blanke, C., 2016. A review of biomass potential and current utilisation – Status quo for 93 biogenic wastes and residues in Germany. *Biomass and Bioenergy* 95, 257–272. <https://doi.org/10.1016/j.biombioe.2016.10.017>
- Cimpan, C.; Rothmann, M.; Hamelin, L.; Wenzel, H., 2015. Towards increased recycling of household waste: Documenting cascading effects and material efficiency of commingled recyclables and biowaste collection. *Journal of Environmental Management* 157, 69–83. DOI: 10.1016/j.jenvman.2015.04.008
- Daniel-Gromke, J.; Rensberg, N.; Denysenko, V.; Trommler, M.; Reinholz, T.; Völler, K.; Beil, M.; Beyrich, W., 2017. Anlagenbestand Biogas und Biomethan – Biogaserzeugung und –nutzung in Deutschland. Studie im Auftrag des Umweltbundesamtes, DBFZ Report Nr. 30 ISBN 978-3-946629-24-5.
- Ding, L.; Cheng, J.; Qiao, D.; Yue, L.; Li, Y.; Zhou, J.; Cen, K., 2017. Investigating hydrothermal pretreatment of food waste for two-stage fermentative hydrogen and methane co-production. *Bioresour. Technol.* 241, 491–499. <https://doi.org/10.1016/j.biortech.2017.05.114>
- ECN, 2019. Biowaste in the Circular Economy. EUROPEAN COMPOST NETWORK, <https://www.compostnetwork.info/policy/circular-economy/>, last website visit on 23.05.2019.
- Ediger, V.Ş.; Hoşgör, E.; Sürmeli, A.N.; Tatdil, H. 2007. Fossil Fuel Sustainability Index: An application of resource management. *Energy Policy* 2007; 35(5), 2969–2977
- Ediger, V. Ş., 2019. An integrated review and analysis of multi-energy transition from fossil fuels to renewables. *Energy Procedia* 156, 2-6. <https://doi.org/10.1016/j.egypro.2018.11.073>
- EM MV, 2018. Energie- und CO<sub>2</sub>-Bericht 2017 – 2018 mit Energiebilanz und Bilanz energiebedingter CO<sub>2</sub>-Emissionen 2015 und 2016, Ministerium für Energie, Infrastruktur und Digitalisierung Mecklenburg-Vorpommern (Hrsg.), <https://www.regierung-mv.de/Landesregierung/em/Service/Publikationen/?id=18721&processor=veroeff>, last download 23.05.2019.
- FNR, 2019. BASISDATEN BIOENERGIE DEUTSCHLAND 2018, Fachagentur Nachwachsende Rohstoffe e.V. (FNR), [http://www.fnr.de/fileadmin/allgemein/pdf/broschueren/Broschuere\\_Basisdaten\\_Bioenergie\\_2018\\_web.pdf](http://www.fnr.de/fileadmin/allgemein/pdf/broschueren/Broschuere_Basisdaten_Bioenergie_2018_web.pdf), last website visit on 15.11.2019.
- FNR, 2018. Flexibilisierung von Biogasanlagen. Fachagentur Nachwachsende Rohstoffe e. V. (Hrsg.), [https://fnr.de/fileadmin/allgemein/pdf/broschueren/Broschuere\\_Flexibilisierung\\_Biogas\\_Web.pdf](https://fnr.de/fileadmin/allgemein/pdf/broschueren/Broschuere_Flexibilisierung_Biogas_Web.pdf), last download 23.05.2019.
- Hoffstede, U., 2013. FlexHKW Flexibilisierung des Betriebes von Heizkraftwerken. In: Konferenzreader 5. Statuskonferenz "Energetische Biomassenutzung", 14./15. November 2013 in Leipzig. Leipzig: DBFZ, 2013, pp. 496499
- Holzhammer, A., 2018. Russischer Löwenzahn als Lieferant für Naturkautschuk. *Agrarheute* 27.12.2018, <https://www.agrarheute.com/technik/traktoren/reifen-continental-loewenzahn-550458>, last website visit on 19.11.2019.
- Holzhammer, U.; Nelles, M.; Scholwin, F., 2013. Auswirkungen der flexiblen Stromproduktion aus Biogas auf den konventionellen Kraftwerkspark und dessen CO<sub>2</sub>-Emissionen, In: Kern, M.; Raussen, T. (Hrsg.): Optimierte Erfassung und Verwertung von Bioabfall, Reihe Witzenhausen-Institut, Neues aus Forschung und Praxis, S. 145–167, Dezember 2013, ISBN 3-928673-65-3.
- Holzhammer, U.; Stelzer, M.; Nelles, M.; Scholwin, F., 2015. Die neue Flexibilität der Stromwirtschaft und die zukünftige Rolle der Abfallwirtschaft, In: Erich-Schmidt-Verlag (Hrsg.): Müll und Abfall, 02.15, S. 79-89, ISBN 978-3-503-12493-0
- Hoogwijk, M.; Faaij, A.; Eickhout, B.; Vries, B. de; Turkenburg, W., 2005. Potential of biomass energy out to 2100, for four IPCC SRES land-use scenarios. *Biomass and Bioenergy* 29, 225–257.
- Hübel, M.; Prause, J.; Gierow, C.; Holtz, D.; Wittenburg, R.; Hassel, E., 2018. Evaluation of Flexibility Optimization for Thermal Power Plants, ASME Power and Energy Conversion Conference, 2018, Orlando, USA.
- IEA, 2017. Technology Roadmap - Delivering Sustainable Bioenergy.
- Kern, M.; Siepenkothen, H.-J.; Turk, T. 2018. Erfassung und Qualität von haushaltstämmigen Bioabfällen. 12. Biomasseforum "Neue Perspektiven für die Bioabfallwirtschaft", ISBN 3-928673-77-7, 53-68.
- Lauer and Trähn, D., 2017. Biogas plants and surplus generation: Cost driver or reducer in the future German electricity system? *Energy Policy* 109, 324-336. <http://dx.doi.org/10.1016/j.enpol.2017.07.016>
- LUNG, 2018. Daten zur Abfallwirtschaft. Landesamt für Umwelt, Naturschutz und Geologie Mecklenburg-Vorpommern (Hrsg.). [https://www.lung.mv-regierung.de/dateien/dza\\_2017.pdf](https://www.lung.mv-regierung.de/dateien/dza_2017.pdf), last website visit on 23.05.2019.
- Mauky, E.; Jacobi, H.F.; Liebetrau, J.; Nelles, M., 2014. Flexible biogas production for demand-driven energy supply – Feeding strategies and types of substrates. *Bioresour. Technol.* 178, 262-269, <https://doi.org/10.1016/j.biortech.2014.08.123>
- Miltner, M.; Makaruk, A.; Harasek, M., 2017. Review on available biogas upgrading technologies and innovations towards advanced solutions. *Journal of Cleaner Production* 161, 1329–1337. DOI: 10.1016/j.jclepro.2017.06.045
- Raussen, T.; Wagner, J.: EEG 2017 in der abfallwirtschaftlichen Praxis – Chancen für Bio- und EEG 2017 in der abfallwirtschaftlichen Praxis – Chancen für Bio- und Grüngutverwertungsanlagen. Müll und Abfall 7-2017, 328–334. <https://www.muellundabfall.de/MA.07.2017.328>
- Remondis, 2019. SAS gewinnt klimafreundlichen Strom aus Bioabfällen, <https://www.remondis-aktuell.de/012015/recycling/mit-energie-fuer-schwerin/>, last website visit on 23.05.2019.
- Schüch, A.; Morscheck, G.; Lemke, A.; Nelles, M., 2016. Bio-waste Recycling in Germany – Further Challenges. *Procedia Environmental Sciences* 35, 308–318. <https://doi.org/10.1016/j.proenv.2016.07.011>
- Schüch, A.; Morscheck, G.; Nelles, M. 2017. Technological Options for Biogenic Waste and Residues – Overview of Current Solutions and Developments. In: Ghosh, S. K.: 7th International Conference on Solid Waste Management. (Ed.): Global Waste Management: Proceedings of the 7th IconSWM 2017, 1029 - 1044.
- Schüch, A.; Nelles, M.; Nassour, A., 2017. Nachhaltige energetische Nutzung biogener Ressourcen durch industrielle Synergien. In: Nelles, M. (Hrsg.) 11. Rostocker Bioenergieforum: Am 22. und 23. Juni 2017 an der Universität Rostock: Tagungsband. Rostock: Professur Abfall- und Stoffstromwirtschaft Agrar- und Umweltwissenschaftliche Fakultät Universität. ISBN: 978-3-86009-455-6. S. 363–371.
- Sprafke, J.; Engler, N.; Nelles, M.; Schüch, A. Bioabfallvergärung – Prozessoptimierung durch Substrat-management. In: Nelles, M.: 13. Rostocker Bioenergieforum. Rostock, 2018. ISBN 978-3-86009-487-7, 135 - 142.
- StatA MV (2017): Statistisches Jahrbuch 2017, StatA MV, 19 Energie
- StatA MV (2018): Statistisches Jahrbuch 2018 (Kennziffer: Z011 2018 00), ISBN-13 978-3-9316-54-34-4.
- StatA MV (2019): Statistisches Jahrbuch 2019, StatA MV, 19 Energie
- Szarka, N.; Scholwin, F.; Trommler, M.; Jacobi, H. F.; Eichhorn, M.; Ortwain, A.; Thrän, D., 2013. A novel role for bioenergy: A flexible, demand-oriented power supply. *Energy* 61, 18-26, <https://doi.org/10.1016/j.energy.2012.12.053>
- Orth, M.; Schüch, A. (2018): Die Rolle der Bioenergie bei der Sektorenkopplung in MV. In: Nelles, M.: 12. Rostocker Bioenergieforum. Rostock, 2018. ISBN 978-3-86009-473-0, 35 - 47.
- Park, A.; Kim, Y. M.; Kim, J. F.; Lee, P. S.; Cho, Y. H.; Park, H. S., 2017. Biogas upgrading using membrane contactor process. Pressure-cascaded stripping configuration. *Separation and Purification Technology* 183, 358–365. DOI: 10.1016/j.seppur.2017.03.006
- Piotrowski, S.; Carus, M.; Essel, R. (2015): Global bioeconomy in the conflict between biomass supply and demand. Hürth (7). In nova paper on bio-based economy.
- Veolia, 2019. Teilstromvergärungsanlage Rostock, <https://www.veolia.de/teilstromvergaerungsanlage-rostock>, last website visit on 23.05.2019.

# USE OF ALTERNATIVE COVER MATERIALS TO CONTROL SURFACE EMISSIONS (H<sub>2</sub>S AND VOCs) AT AN ENGINEERED LANDFILL

Yann Le Bihan <sup>1,\*</sup>, David Loranger-King <sup>2</sup>, Nicolas Turgeon <sup>1</sup>, Nadine Pouliot <sup>3</sup>, Nicolas Moreau <sup>4</sup>, Daniel Deschênes <sup>4</sup> and Guy Rivard <sup>5</sup>

<sup>1</sup> CRIQ, EIE, 333 Franquet street, Quebec G1P 4C7, Canada

<sup>2</sup> Mrc de Bellechasse, Saint-Lazare-de-Bellechasse, Quebec, Canada

<sup>3</sup> Ville de Québec - Service des projets industriels et de la valorisation, Quebec, Canada

<sup>4</sup> EnGlobe Corp - Centres régionaux de traitement de sols et de la biomasse, Quebec, Canada

<sup>5</sup> AIM Éco-Centre, Saint-Augustin-de-Desmaures, Quebec, Canada

## Article Info:

Received:

8 July 2019

Revised:

14 January 2020

Accepted:

4 February 2020

Available online:

5 March 2020

## Keywords:

Sanitary landfill sites

daily cover

incineration

bottom ash,

concrete residues

gypsum

H<sub>2</sub>S

Odors

## ABSTRACT

Between 2010 and 2015, the Bellechasse Regional County Municipality (Bellechasse RCM) was affected by particularly noxious odors issuing from its Municipal Solid Waste Landfill (Bellechasse RCM MSWL) in Armagh, Canada. A study carried out in 2015-2016 by Centre de recherche industrielle du Québec (CRIQ) confirmed that it was still possible for hydrogen sulfide (H<sub>2</sub>S) emissions to cause odor issues in and around the site. The experimental project carried out by CRIQ in cooperation with Bellechasse RCM, Englobe, Quebec City and the Regroupement des récupérateurs et des recycleurs de matériaux de construction et de démolition du Québec (represented by AIM Éco-centre) made it possible to test three (3) different industrial residue as an alternative cover materials on site and study how they controlled H<sub>2</sub>S emissions, volatile organic compounds (VOCs) and odors at the Bellechasse RCM's landfill. The site was monitored from November 2016 to September 2017 to confirm the effectiveness of alternative biofiltration cover materials (soil + compost), domestic waste incineration bottom ash and 0 to 2.5-inch concrete residues and to compare the results with the sand cover currently used as the cover material. Effectiveness was determined by measuring the Area Source Emission Rate (ASER) with a 3 m x 3 m static flux chamber developed for the project. Methane measurements were concomitantly taken to confirm that the biogas could escape through the cover materials. The monitoring results made it possible to demonstrate that domestic waste incineration bottom ash as well as 0-2.5 in. concrete received the highest load of H<sub>2</sub>S and showed an H<sub>2</sub>S capture performance of greater than 83%. For volatile organic compounds, materials such as 0-2.5 in. concrete and the alternative biofiltration cover materials were most effective for capture (greater than 73%) for the highest loads. The lowest content of CH<sub>4</sub> after covering was measured for the alternative cover materials. The site where the incineration bottom ash was used managed to decrease odors by ±200 odor units. Overall, we have demonstrated in this project, the capacity of different alternative cover materials under real condition for the control of gas emissions from landfill.

## 1. INTRODUCTION

The control of hydrogen sulfide (H<sub>2</sub>S), a toxic, foul-smelling gas (rotten egg odor), remains a significant environmental challenge for several industrial and municipal sectors including landfills. The primary sources of sulfur compounds in landfills that generate H<sub>2</sub>S include gypsum residues (CaSO<sub>4</sub>), the sulfur contained in organic matter (food and paper), and biosolids (sludge from waste water treatment plants). The residues from gypsum panels, frequently used

in the construction of interior walls because of their high degree of fire resistance, undoubtedly constitute one of the most significant sources of sulfur compounds, particularly in construction, renovation, and demolition (CRD) landfills. The production of H<sub>2</sub>S from buried gypsum residues has been studied by a number of researchers, including Xu et al. (2010) and Fairweather and Balaz (1998).

The main technologies currently available for the treatment of H<sub>2</sub>S rely on the principles of absorption (chemical scrubbing), adsorption (activated charcoal), or biological



\* Corresponding author:  
Yann Le Bihan  
email: yann.lebihan@criq.qc.ca



processes (sulfo-oxidant microorganisms). Although the effectiveness of these so-called “conventional” technologies have largely been demonstrated in an industrial context for several years (Davis, 2000), their primary disadvantage is related to operating costs (chemical products, adsorbents, packing, etc.), which can be significant, or even prohibitive, depending on the load to be treated. This is what is currently driving a number of R&D teams to identify and test different treatment approaches based on industrial ecology; in other words, the identification of innovative and sustainable outlets for the use and valorization of industrial residues (Sarperi et al., 2014, Starr et al., 2012).

For that matter, scientific studies indicate that some materials considered as residues are quite capable of removing H<sub>2</sub>S and other foul-smelling gaseous contaminants. For example, incineration ash has been used in several studies, and the results indicate that these materials have a significant affinity for certain sulfur compounds and for CO<sub>2</sub> (Mostbauer et al., 2012; Timoveanu, 2004; CRIQ, 2016).

The use of off-specification compost has also been widely documented with regard to the biological treatment of hydrogen sulfide using biofilters (Yang and Allen, 1994; Syed et al., 2006). A study by Xu et al. (2010) identifies several types of material as alternative cover materials, and the results they obtained indicate that the H<sub>2</sub>S capture performance is significantly better with materials such as compost, fine concrete residues and soil amended with lime. Plaza et al. (2007) also used a mix of hydrated lime and sandy soil, as well as concrete residues, as covering in laboratory tests. The best performance for H<sub>2</sub>S removal was obtained with concrete chips (< 2.5 cm) and sandy soil containing hydrated lime (5% w/w).

When considering the option of using alternative cover materials to replace the sand currently in use as daily cover, the Bellechasse Regional County Municipality (Bellechasse RCM), which was grappling with an H<sub>2</sub>S odor problem at its engineered landfill, decided to launch an on-site, proof-of-concept project at its landfill to test three (3) different cover materials.

The originality of the project lies in the use of a large static flow chamber for monitoring H<sub>2</sub>S emissions from a landfill over a period of one year. The use of a static flow chamber was performed by Capena et al 2013, Cabral et al 2010 for CH<sub>4</sub> emission or COV emission. To our knowledge, there are little information regarding the use of a static flow chamber for H<sub>2</sub>S emissions.

To measure gas emissions, a large static flux chamber was used as gas emissions can not be accurately assessed with a small chambers (Geck et al 2016a, 2016b). The typical small chamber is significantly smaller than 1 m<sup>2</sup>. Thus, chamber measurements are prone to missing emissions if emissive areas are larger than the base area of these chambers. In addition, it has been reported that emission level are underestimate while using a small chamber especially when the advective component of the flux is dominant (Pilhatie et al 2013). Other studies have shown that static flux chamber also underestimated gas emission and to avoid this underestimation, gas flux chamber should be equipped with at least one fan and a vent

tube to increase mixing and reduce pressure propagation (Juszczak et al 2009).

The project goals described in this article therefore aim to present the main results concerning the control of H<sub>2</sub>S emissions, volatile organic compounds (VOCs), and odors obtained from three (3) different alternative cover materials and to compare their performance with the current cover material (sand). The project took place at Bellechasse RCM landfill in Armagh (Québec, Canada) during the period between November 2016 and September 2017.

## 2. MATERIALS AND METHODS

### 2.1 Description of the landfill site

The Bellechasse RCM Municipal solid waste landfill MSWL covers a surface area of 15 hectares, representing an operating lifetime of about 40 years and a total capacity of 1,444,200 m<sup>3</sup>. All of the MSWL's cells have a double layer of protective membrane, with treatment of leachate and biogas as required by current regulations. According to the current agreement, 33 municipalities are served by the current site. Remedial work aiming to control landfill gases emitted by the closed cells, which had been permanently covered, was carried out in summer 2012. Thus, four (4) passive waste biogas burners were installed and put into operation in August of the same year.

### 2.2 Description of the static flux chamber (SFC)

A 3 m x 3 m static flux chamber (SFC) was developed in order to carry out monitoring in the field. The SFC, which covers a wide surface, has the advantage of measuring emission rates more quickly. The development of the static flux chamber was inspired by the work of Geck et al. (2015). These authors used a 5 m x 5 m flux chamber to measure CH<sub>4</sub> emissions at a landfill. In our case, and for easier handling, a reduced-size 3 m x 3 m chamber was considered to be transportable by two (2) people. The chamber was assembled using a molded aluminum structure whose top was covered with Coroplast polypropylene plastic, and the sides with Flexfoil-type insulating material. These materials are known to have low VOC emissions. Five-meter-long (5 m) Teflon pipes placed at four (4) locations in the chamber enable collection of the gases. Two (2) battery-powered fans (1.5-1.6 m/sec@30 cm) provided air circulation in the chamber. The chamber is shown in Figure 1.

The validation stage for the static flux chamber (SFC) was carried out using an H<sub>2</sub>S standard reference gas in concentrations of 1.98, 8.5, and 100 pm with a flow rate of 0.1 to 10 L/min. The Area Source Emission Rate (ASER) measured for H<sub>2</sub>S is calculated according to the following equation:

$$\text{Measured ASER} = \frac{V}{A} \times \frac{dC}{dT} \quad (1)$$

Where:

dC/dT = The variation in gas concentration as a function of time in the SFC (µg/m<sup>3</sup>.h or µl/m<sup>3</sup>.h). This variation must have an increasing slope with a significant coefficient of determination in order for the ASER to be calculated.

V=Volume of the chamber=3.0294 m<sup>3</sup>;



**FIGURE 1:** Appearance of the static flux chamber (3 m x 3 m).

A=Surface area of the chamber=9.18 m<sup>2</sup>;  
Factor V/A=0.33 m.

ASER measured using the chamber during validation or in the field was calculated using the approach described by Eun et al. (2007) and Green et al. (2010). The measurements of gas concentrations were collected immediately after the SFC was closed (time = 0) and every 30 seconds thereafter for 10 to 20 minutes. The gas flow (H<sub>2</sub>S or VOC) was determined by plotting the gas concentration (C) in relation to elapsed time (t). The slope of the adjusted straight line (dC/dT) was determined by a regression, and a non-zero flow was only noted if there was a significant coefficient of determination (T test) with a 95% confidence interval (p < 0.05). If no significant correlation was observed, a flow of zero was recorded. ASER measured in the field is calculated according to Equation 1.

During the validation stage, it was possible to compare the measured ASER and the theoretical ASER calculated based on the flow rate and concentration of the standard reference gas. This approach was proposed by Green et al., 2010. The linear slope measured for dC/dT was considered to be valid if the coefficient of determination was significant at a threshold of 0.05 (T-test). Otherwise (with a decreasing or no significant slope), the emissions rate was considered to be zero.

During a series of experimental measurements in the field, the general operations of the components were verified. This verification aimed to ensure:

- the flowrate of the fans, with validation using a Kestrel 1000 anemometer from 0.3 to 40 m/sec on the morn-

ing of any monitoring day,

- the operation of the fans (visual verification of blade rotation) between each measurement;
- the absence of condensation in the sampling pipes (visual verification);
- the seal between the edges of the chamber and the ground, primarily on the windy side.

### 2.3 Description of cover materials used

The four (4) cover materials were supplied by the project's collaborators. The City of Québec supplied the Municipal Solid Waste Incinerator Bottom Ash (IBA); Englobe provided a mix of soil + compost called the alternative bio-filtration cover material (ABCM); 3RMCDQ (represented by AIM Eco-centre) provided the chipped concrete residues (0-2.5 inches); and finally, the current cover material (control), the sand, was supplied by the Bellechasse RCM.

The first step before field test has consisted in characterizing the three (3) alternative covering materials with regard to hydraulic conductivity and grain size. All alternative cover materials were sampled from containers at eight (8) different locations. Four subsamples were collected at ten (10) cm depth and four (4) others at 30 cm depth. To be used as a daily recovering materials, the materials must meet the criteria described in paragraph 42 of the "Règlement sur l'enfouissement et l'incinération de matières résiduelles" (Gouvernement du Québec 2016). The requirements of this regulation are based on the minimum hydraulic conductivity of  $1 \times 10^{-4}$  cm / s and the material must have less than 20% by weight of particles with a diameter equal to or less than 0,08 mm.

Other complementary test on all materials have been done including acid leaching tests as described by SPLP, EPA 1312 to simulate acid rain were carried out (CEAQ2012). The concentration of heavy metals, phenolic compounds and VOCs have been measured on the leachate (result not shown).

A volume of approximately 10 m<sup>3</sup> of each material was transported to the site to carry out the tests over a 5 m x 5 m area. No top soil was added because the effectiveness of the recovering materials alone have been measured.

As shown at Figure 2, the surfaces were cleaned of the plant layer and leveled. Subsequently, baseline emission rates were measured using the 3m x 3m static flow chamber for each of the test area. Table 1 present the characterization of the cover materials.

## 2.4 Analysis of gases and odors

The gas emission rates were measured using the specific devices shown in Table 2.

On each day of analysis, field blanks were produced for the H<sub>2</sub>S, VOC, and CH<sub>4</sub> measurements on the access path near the test site.

### 2.4.1 Measurement of H<sub>2</sub>S

Hydrogen sulfide (H<sub>2</sub>S) was measured using two (2) methods. The first, a one-off approach, was carried out during the localization of the emissions zones. This method provides a qualitative approach to determine whether H<sub>2</sub>S has been emitted locally in order to position the test banks.

For the measurement of the initial surface emission rate and for regular monitoring, the 3 m x 3 m static flux chamber (SFC) was used to analyze the concentration of H<sub>2</sub>S every 30 seconds using a JEROME® brand portable hydrogen sulfide (H<sub>2</sub>S) analyzer, model 631-X. This frequency corresponds to the device's maximum rate of analysis. The device can measure from 0.003 ppm to 50 ppm. The verification of the standard reference was carried out in October and November 2016 and March and July 2017 using

**TABLE 1:** Description of cover materials.

Material	Installed thickness (m)	Volume of material covering 1 m <sup>2</sup> (m <sup>3</sup> )	Dry mass density (kg/m <sup>3</sup> )	Dry mass of material covering 1 m <sup>2</sup> (kg)
Incinerator bottom ash (IBA)	0,1	0,1	1 469	147
0-2.5 cm concrete residues	0,1	0,1	1 480	148
Alternative biofiltration cover material (ABCM)	0,15	0,15	1 675	251
Control sand	0,2	0,2	1 634	327



**FIGURE 2:** Photos showing the cleaning of the surface (top left photo), the measurement of initial ASER (top right photo), and the final appearance after the installation of the cover materials.

**TABLE 2:** Gas measurement devices used in this project.

Gas	Measurement device	Detection limit	Pumping capacity (ml/min)
H <sub>2</sub> S	Jerome 631 X #77830604	0,003 ppmv	150
VOC <sub>total</sub>	PBRae 3000	1 ppbv	500
CH <sub>4</sub>	20L Tedlar sampling bag single-point-in-time lab analysis Gasmeter DX4015 FTIR	1 ppmv	4 000
Odor	30L Nalophan sampling bag in triplicate with external dynamic olfactometry analysis (EN 13725:2003).	Lab blank <13 odor units	4 000

three standard reference gases containing a representative concentration range of the contaminant, namely hydrogen sulfide (H<sub>2</sub>S).

#### 2.4.2 Measurement of VOCs

VOCs were sampled in a similar fashion to the H<sub>2</sub>S measurement. For determining the initial surface emission rate and for regular monitoring, the 3 m x 3 m SFC was used to measure and analyze the VOC concentration every 30 seconds using a Model 3000 ppbRAE type portable device. This device's detection limit ranges from 1 ppb to 10,000 ppm. Before measuring VOCs, the chamber was ventilated in order to eliminate gases accumulated inside during the previous measurements. This ventilation was carried out by lifting the chamber up and down five (5) times in order to expel the gaseous mix accumulated in the enclosure.

#### 2.4.3 Measurement of methane

Methane was measured using a one-off approach between the measurement of the H<sub>2</sub>S and the VOCs under the SFC. This measurement was intended to detect biogas emissions through the layers of tested materials. Since methane is a gas that does not dissolve in water, it can indicate the presence of real biogas emissions through the cover materials. The use of a sealed cover material could, for example, prevent the biogas from diffusing through the material, which would give a zero result for gas analysis (H<sub>2</sub>S and VOCs). In this case, the significant presence of methane indicates real biogas emissions through the filling material.

The sample was taken on site using a vacuum chamber (Lung) and Flexfoil PLUS® bags (20 liters). The gas was collected using a GilAir Plus type pump adjusted to a flow rate of 4L/min.

Subsequently, the samples were analyzed in the laboratory within 24 hours. The concentration of CH<sub>4</sub> was evaluated using a Gasmeter DX 4015 FTIR gas analyzer. This device's detection limit is 1 ppm. The device was calibrated every six (6) months, in the months of November and May. A laboratory blank was also measured, as was a field blank.

#### 2.4.4 Measurement of odors

For the olfactometric analyses (odors), gas samples were collected in triplicate using a lung-type extraction system under vacuum and 30-liter Nalophan™ bags under the SFC. The samples were then sent to an external olfactory evaluation lab (Consumaj Experts Conseils), where they were analyzed using a dynamic olfactometer in compliance with the NF EN 13725:2003 standard within 24 hours. During transport and storage, the samples were

maintained at ambient temperature (~ 20°C) and were not exposed to light. The results are given in odor units per meter cubed of air (O.U./Nm<sup>3</sup>). The analysis of odors was carried out at the beginning of the project during the initial measurements, before covering by the test materials, and at the end of monitoring.

## 3. RESULTS AND DISCUSSION

### 3.1 Validation of the static flux chamber (SFC)

The 3 m x 3 m SFC developed by CRIQ was validated using field tests. Different concentrations of standard reference H<sub>2</sub>S gas were used, at 1.98, 8.5, and 100 ppm with flow rates varying from 0.1 to 10L/min. These conditions made it possible to generate theoretical ASERs varying from 1.93 to 2055 µg of H<sub>2</sub>S/m<sup>2</sup>/h covering the range of measurements collected during an earlier study in the field

To calculate the theoretical ASERs of H<sub>2</sub>S during the validation of the SFC using standard reference gases, the following equation was used:

$$\text{Calculated ASER} = \frac{\text{Injected gas flow rate (m}^3/\text{h)} \times \text{Concentration H}_2\text{S (ug/m}^3\text{)}}{A} \quad (2)$$

Where:

A = surface of the SFC, namely 9.18 m<sup>2</sup>.

An example of the measurement of H<sub>2</sub>S ASER in the 3m x 3m chamber is presented in Figure 3. It represents a validation test carried out with an H<sub>2</sub>S standard reference gas at 105 ppm injected at a flow rate of 0.1L/min. The ASER value measured here is calculated using Equation 1.

Using the data presented in Figure 3 and the measure of the slope, the measured ASER was calculated using Equation 1 and compared with the theoretical ASER calculated based on the gas flow rate and the concentration of standard reference gas injected into the static flux chamber.

For the laboratory tests, the relationship between the theoretical ASER values and the measured ASER values is presented in Figure 4. In this figure, all of the theoretical ASER values calculated based on concentrations of standard reference gas and specific flow rates (Equation 2) have been plotted as a function of the ASER value measured in the chamber, according to Equation 1.

The correlation between the two parameters is significant. Thus, from the ASER measured using the SFC and the correlation obtained in Figure 4, a corrected ASER can be calculated using a correction factor (Eq. 3).

$$\text{Corrected ASER} = 1.263 \times \text{ASER (measured eq.1)} + 13.59 \quad (3)$$

During field tests of H<sub>2</sub>S emissions, Equation 3 was

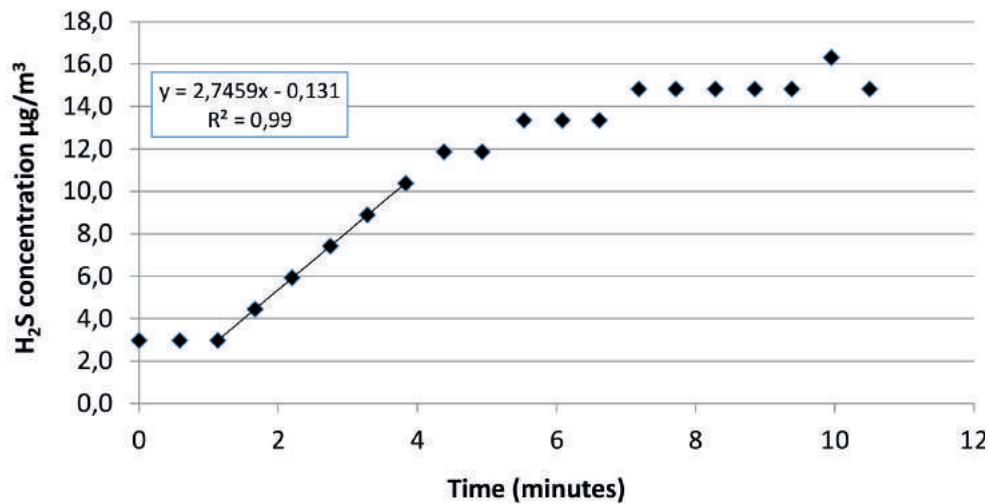


FIGURE 3: Validation tests of the SFC using an H<sub>2</sub>S standard reference gas at 105 ppm and a flow rate of 0.1L/min.

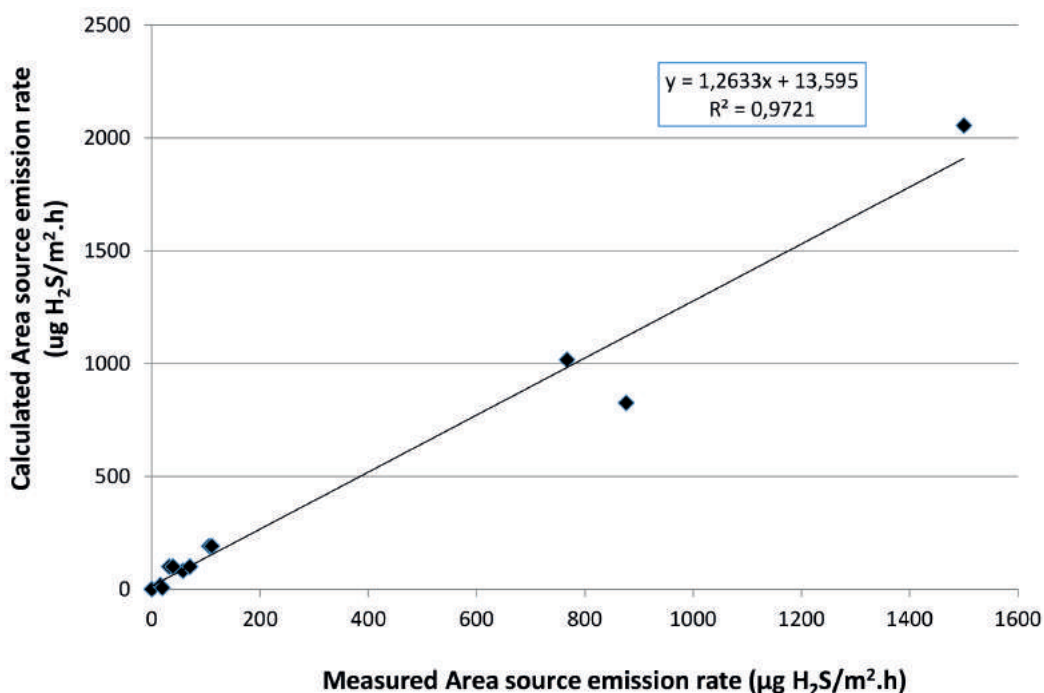


FIGURE 4: Relationship between calculated ASER (standard reference gas with controlled flow rate - Equation (2)) and ASER measured using the 3m x 3m chamber - Equation (1)).

used to calculate corrected ASER. Because of time constraints, the correlation presented in Figure 3 was not carried out with VOCs. Given this, the measured ASER values for VOCs were calculated directly from Equation 1 without any correction.

### 3.2 Monitoring of gaseous emissions from different cover materials

The removal effectiveness performance during field tests are presented in Figures 5 and 6. These figures make it possible to compare the different materials used for capturing H<sub>2</sub>S and VOCs during the study period. Since the initial ASER, and therefore the load applied to the cover mate-

rials, differs from site to site, this graphical approach makes it possible to compare performance between sites. The dotted line presents a material able to capture 100% of the applied load. The more effective a material, the more the points approach the dotted line, indicating 100% efficiency.

The gas load applied was defined as follows:

$$\begin{aligned}
 \text{Gaseous load applied } L_t &= \\
 &= \frac{(\text{Initial ASER} \times 24\text{h} \times \text{number of days of monitoring})}{1,000 \times \text{mass of the dry material per } 1 \text{ m}^2} \quad (4)
 \end{aligned}$$

Where:

The gas load applied (mg H<sub>2</sub>S/kg material or ml VOC/kg dry material);  
Initial ASER (µg H<sub>2</sub>S/m<sup>2</sup>.h);

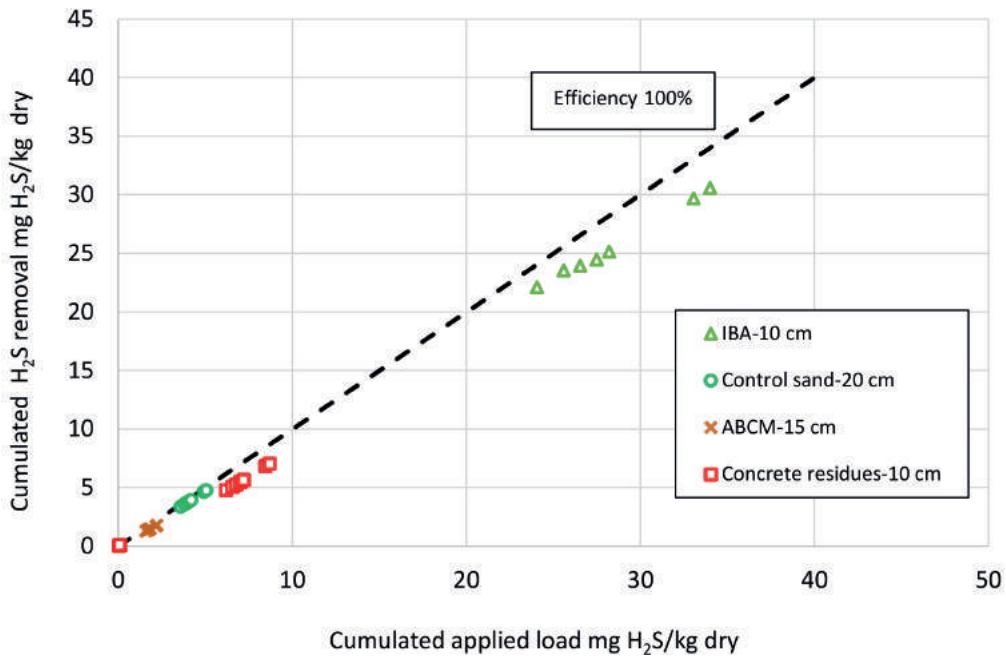


FIGURE 5: Relationship between the applied load of H<sub>2</sub>S (eq. 4) and the cumulative captured load (eq. 6) during field tests for different cover materials.

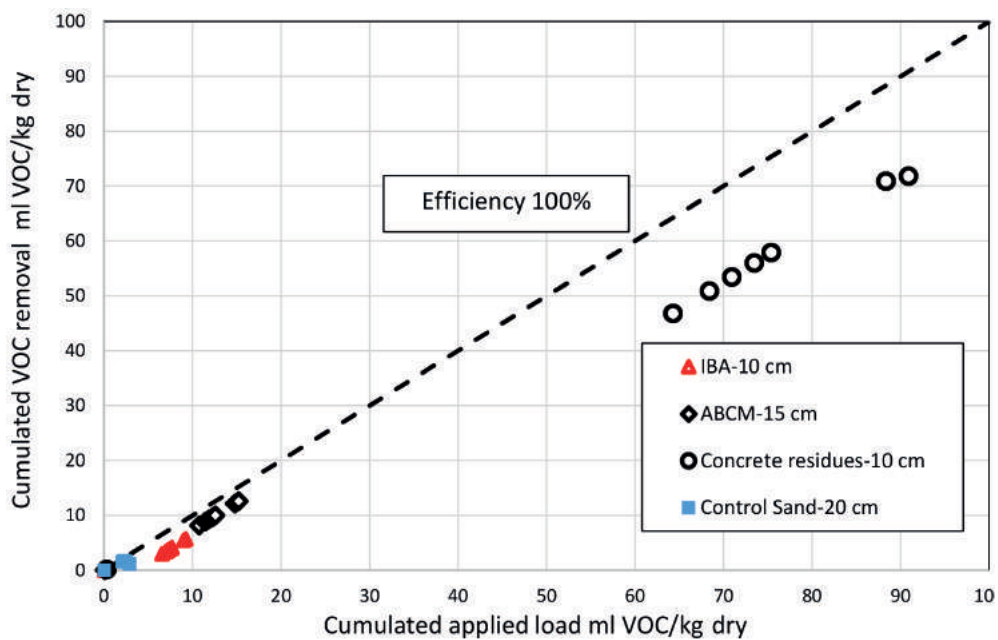


FIGURE 6: Relationship between the applied load of VOC (eq. 4) and the cumulative captured load (eq. 6) during field tests for different cover materials.

1,000 = conversion factor for  $\mu\text{g}$  to  $\text{mg}$ .

The factor used to evaluate the performance of the cover materials is referred to as “cumulative load removed by the material.” This value corresponds to the difference between the initial ASER, which is constantly generated under the material, and the ASER emitted or measured during monitoring. In sum, the material receives emissions of gaseous pollutants such as H<sub>2</sub>S and VOCs constantly, and some passes through to be released constantly (emitted

ASER). The fraction of ASER emitted was measured in the field eight (8) times during a 286-day monitoring period. From these ASERs, the loads were calculated by taking the difference between the initial load and the emitted load (Equation 5); it is therefore possible to estimate the quantity of pollutants retained by the material at a time T.

$$\begin{aligned}
 \text{Gaseous load emitted} &= \\
 &= \frac{(\int_0^t \text{ASER emitted} \times 24h)}{1,000 \times \text{mass of the dry material per } 1 \text{ m}^2} \quad (5)
 \end{aligned}$$



Where:

gaseous load emitted (mg H<sub>2</sub>S/kg material or ml VOC/kg dry material);

Emitted ASER (μg H<sub>2</sub>S/m<sup>2</sup>.h). The ASERs emitted at a time T are estimated by linear extrapolation between two (2) measured ASERs;

1,000 = conversion factor for μg to mg.

Thus, the performance of the material expressed in the form of the cumulative captured load is written according to Equation 6 as follows:

$$\text{Cumulative removed load} = \text{Applied gaseous load}_t \text{ (eq.4)} + \text{Gaseous load emitted}_t \text{ (eq.5)} \quad (6)$$

According to the results presented in Figure 5, the bench test using the IBA as well as the 0-2.5 in. concrete received the highest load of H<sub>2</sub>S and showed the best H<sub>2</sub>S removal performance, greater than 83%. The Sand control material as well as the 15 cm ABCM also showed good capture performance, but for lower loads of H<sub>2</sub>S. Taking these lower loads into account, it is difficult to draw a conclusion about their effectiveness for higher loads. For VOCs (Figure 6), the materials such as Concrete and ABCM showed better capture effectiveness (> 73%) for higher loads.

The different materials tested here have already been subjected to a variety of scientific studies, which demonstrated their capacity for removing H<sub>2</sub>S and other foul-smelling gaseous contaminants. For example, MSWI bottom ash, because it is alkaline, was used in several studies, and the results indicate that this material would have a strong affinity for certain sulfur compounds and for CO<sub>2</sub> (Mostbauer et al., 2012; Tirnovanu, 2004; Turgeon et al., 2017).

The use of compost has also been widely studied with regard to the biological treatment of hydrogen sulfide using biofilters (Yang and Allen, 1994; Syed et al., 2006). The study by Xu et al. (2010) evaluated several types of materials as alternative covers including sandy soil, compost, fine concrete residues (79.6% < 2 mm), and mixes of lime with sandy soil with different proportions by weight. The results they obtained indicate that H<sub>2</sub>S capture performance is significantly better with materials such as compost, fine concrete residues and soil amended with lime. Plaza et al. (2007) also used a mix of hydrated lime and sandy soil, as well as concrete residues, as covering in laboratory tests. In this study, the best performance for H<sub>2</sub>S removal was obtained with concrete chips (< 2.5 cm) and sandy soil containing hydrated lime (5% w/w). In this case, alkaline materials such as incineration bottom ash and concrete residues seem more effective for the abatement of H<sub>2</sub>S. That said, for ABCM, the low applied loads did not allow us to draw a conclusion about the material's purifying capacity.

For VOCs, treatment usually involves microbial activity, and the use of composts or other organic materials is widely documented in the scientific literature (Chou et Cheng 1997, Liu et al 2009).

The results of one-off measurements of CH<sub>4</sub> are presented in Table 3. These measurements were taken once the analyses of H<sub>2</sub>S were complete and made it possible to detect the presence of biogas diffusing through the cover materials. CH<sub>4</sub> is poorly water soluble and adsorbable, and

its biodegradation using methanotrophic bacteria can be relatively quick, but requires specific environmental conditions (CRIQ, 2015). Aerobic conditions, warm temperatures, and nitrogen and phosphate-based nutrients are all conditions that can be found in the ABCM mix.

The olfactometric results are presented in Table 4. The odor units indicate the number of times that the sample had to be diluted before 50% of the judging panel could perceive the odor. The hedonic quality of the odor was not evaluated in the expression of odor units. A high number indicates a gas that requires a high degree of dilution before being perceived by 50% of the judging panel, regardless of whether the odor was pleasant or foul. The gas collected from the platform covered with IBA was odorous with an average of 360 OU/Nm<sup>3</sup>. An abatement of around 200 OU/Nm<sup>3</sup> is nevertheless observed with this material, since at first the collected gas registered 564 OU/Nm<sup>3</sup>. Since the odor of IBA resembles that of fresh concrete, it is normal to perceive this odor being released by the material at the end of the project. As has already mentioned, the elevated OU/Nm<sup>3</sup> value does not represent the quality of the odor, but rather its intensity.

In the case of ABCM, the odor levels of the collected gas at the beginning and end of the project were relatively low (32 and 28 OU/Nm<sup>3</sup>). For the control sand, the gas collected at the end of the project was more odorous than at the beginning (26 and 81 OU/Nm<sup>3</sup>).

## 4. CONCLUSIONS

This experimental project took place from autumn 2016 to the end of summer 2017. Tests to monitor the performance of different cover materials were carried out at the BELLECHASSE RCM Engineered landfill in Armagh (Québec, Canada). The field tests aimed to confirm the effectiveness of alternative biofiltration cover materials (ABCM), MSW incineration bottom ash (IBA), and 0-2.5

TABLE 3: One-off measurement of CH<sub>4</sub> in the static flux chamber.

Material	One-off measurement of CH <sub>4</sub> concentration (ppmv)	
	Before covering	After covering
20 cm control sand	455	366
10 cm IBA	132	71
10 cm concrete (0-2.5 inches)	61	66
15 cm ABCM	51	22
Field blank	ND	6

TABLE 4: Olfactometric monitoring of emissions in the static flux chamber.

Material	Measurement of Odor units (U.O./Nm <sup>3</sup> of air) Average ± standard deviation (n=3 obs)	
	Before covering	After covering
20 cm control sand	26 ± 4	81 ± 3
10 cm IBA	564 ± 45	360 ± 60
10 cm concrete (0-2.5)	246 ± 28	ND
15 cm ABCM	32 ± 2	28 ± 5

inch concrete residues and to compare the results with the sand currently used as the cover material. The effectiveness of these materials specifically evaluated their ability to reduce emissions of H<sub>2</sub>S and VOCs. Effectiveness was determined by measuring the Area source emission rate (ASER) with a 3 m x 3 m measuring chamber developed for this project. Methane measurements were concomitantly taken to confirm that the biogas could escape through the cover materials. Olfactometric analysis were also carried out at the beginning and end of the project to evaluate the abatement of odors by all cover materials.

The results of the characterization made it possible to verify that the bench test with IBA and the 0-2.5 in. concrete received the largest load of H<sub>2</sub>S and showed H<sub>2</sub>S capture performance of greater than 83%. For VOCs, the materials such as 0-2.5 in. concrete and ABCM showed the best capture effectiveness, greater than 73%, for the highest loads. Lower loads of CH<sub>4</sub> after covering were measured on the bench test using the alternative biofiltration cover materials. For odor monitoring, the bench test using the IBA succeeded in decreasing odors by ±200 OU/Nm<sup>3</sup>.

Overall, we have demonstrated in this project, the capacity of different alternative cover materials under real condition for the control of gas emissions from landfill. However, field tests always involve the unexpected and can generate results affected by climate and environmental conditions that are more thoroughly controlled in laboratory tests.

## ACKNOWLEDGEMENTS

The authors would like to thank the Ministère de l'Économie et de l'Innovation-Québec, the Bellechase RCM, Englobe, the City of Québec, and the 3RMCDQ (represented by AIM Éco-centre) for their financial support and technical participation in this project

## REFERENCES

- Cabral, A. R., Capanema, M. A., Gebert, J., Moreira, J. F., & Jugnia, L. B. (2010). Quantifying microbial methane oxidation efficiencies in two experimental landfill biocovers using stable isotopes. *Water, Air, & Soil Pollution*, 209(1-4), 157-172
- Capanema, M. A., Ndanga, E., Lakhout, A., & Cabral, A. R. (2013). Methane oxidation efficiencies of a 6-year-old experimental landfill biocover. In *Proceedings Sardinia 2013, Fourteenth International Waste Management and Landfill Symposium S. Margherita di Pula, Cagliari, Italy*; 30 September-4 October 2013.
- CEAQ (2012) Centre d'expertise en analyse environnementale du Québec (2012). Protocole de lixiviation pour les espèces inorganiques, MA. 100 – Lix.com.1.1, Rév. 1, Ministère du Développement durable, de l'Environnement, de la Faune et des Parcs du Québec, 2012, 17 p.
- Chou, M. S., & Cheng, W. H. 1997. Screening of biofiltering material for VOC treatment. *Journal of the Air & Waste Management Association*, 47(6), 674-681.
- CRIQ 2015. Développement d'un inoculum méthanotrophe. Dossier CRIQ no PE46357, Rapport final, 28 pages
- CRIQ 2016. Étude du mâchefer de l'incinérateur de la Ville de Québec envers l'élimination du sulfure d'hydrogène (H<sub>2</sub>S). Dossier CRIQ no PE50122, rapport final, 27 pages.
- Davis, W. T., 2000. *Air Pollution Engineering Manual*. 2nd Ed., AWMA, Wiley Interscience.
- Eun, S., Reinhart, D. R., Cooper, C. D., Townsend, T. G., & Faour, A. 2007. Hydrogen sulfide flux measurements from construction and demolition debris (C&D) landfills. *Waste Management*, 27(2), 220-227.
- Fairweather, R. J., Barlaz, M. A. 1998. Hydrogen sulfide production during decomposition of landfill inputs, *Journal of Environmental Engineering ASCE*, 124, 353-361.
- Geck, C., Scharff, H., Pfeiffer & J. Gebert 2015. Validation of a Simple Model to Predict Efficiencies of methane Oxidation systems. *Proceedings Sardinia 2015. Fifteenth International Waste Management and Landfill Symposium S. Margherita di Pula, Cagliari, Italy*; 5 – 9 October 2015.
- Geck, C., Röwer, I. U., Kleinschmidt, V., Scharff, H., & Gebert, J. (2016a). Design, validation and implementation of a novel accumulation chamber system for the quantification of CH<sub>4</sub> and CO<sub>2</sub> emissions from landfills. Technical Report
- Geck, C., Scharff, H., Pfeiffer, E. M., & Gebert, J. (2016b). Validation of a simple model to predict the performance of methane oxidation systems, using field data from a large scale biocover test field. *Waste management*, 56, 280-289.
- Gouvernement du Québec (2012). Règlement sur l'enfouissement et l'incinération de matières résiduelles. Québec, Canada.[En ligne] <http://www2. Publications du quebec. gov. qc. ca/dynamicSearch/telecharge. php>.
- Green, R. B., Hater, G. R., Thoma, E. D., DeWees, J., Rella, C. W., Crosson, E. R., & Swan, N. 2010. Methane emissions measured at two California landfills by OTM-10 and an acetylene tracer method. In *Proceedings of the Global Waste Management Symposium 2010* (pp. 3-6).
- Juszcak, R., Pihlatie, M., Christiansen, J. R., Giebels, M., Schreiber, P., Aaltonen, H., ... & Urbaniak, M. (2009, April). Effect of headspace mixing in static chambers and sampling protocol on calculated CH<sub>4</sub> fluxes from soils. In *EGU General Assembly Conference Abstracts* (Vol. 11, p. 9715).
- Mostbauer, P., Olivieri, T., Lombardi, L., & Paradisi, A. 2012. Pilot-scale upgrading of landfill gas and sequestration of CO<sub>2</sub> by MSWI bottom ash. In *Ash 2012 Conference*, January (pp. 25-27).
- NF EN 13725 Standard, B. 2003. Air quality—Determination of odour concentration by dynamic olfactometry. BS EN, 13725, 2003.
- Pihlatie Mari K., Jesper Riis Christiansen, Hermann Aaltonen, Janne F.J. Korhonen, Annika Nordbo, Terhi Rasilo, Giuseppe Benanti, Michael Giebels, Mohamed Helmy, Jatta Sheehy, Stephanie Jones, Radoslaw Juszcak, Roland Klefoth, Raquel Lobo-do-Vale, Ana Paula Rosa, Peter Schreiber, Dominique Serça, Sara Vicca, Benjamin Wolf, Jukka Pumpanen, (2013). Comparison of static chambers to measure CH<sub>4</sub> emissions from soils. *Agricultural and forest meteorology*, 171, 124-136.
- Plaza, C., Xu, Q., Townsend, T., Bitton, G., & Booth, M. 2007. Evaluation of alternative landfill cover soils for attenuating hydrogen sulfide from construction and demolition (C&D) debris landfills. *Journal of Environmental Management*, 84(3), 314-322.
- Liu, Q., Li, M., Chen, R., Li, Z., Qian, G., An, T., Fu, J & Sheng, G. 2009. Biofiltration treatment of odors from municipal solid waste treatment plants. *Waste Management*, 29(7), 2051-2058.
- Sarperi, L., Surbrenat, A., Kerihuel, A., & Chazarenc, F. 2014. The use of an industrial by-product as a sorbent to remove CO<sub>2</sub> and H<sub>2</sub>S from biogas. *Journal of Environmental Chemical Engineering*, 2(2), 1207-1213.
- Starr, K., Gabarrell, X. & Villalba G., 2012. Life cycle assessment of biogas upgrading technologies, *Waste Management*, Elsevier, 32, pp. 991-999.
- Syed, M., Soreanu, G., Falletta, P. & Béland, M. 2006. Removal of hydrogen sulfide from gas streams using biological processes-A review. *Canadian Biosystems Engineering*, 48, 2.
- Tirnoveau, D. R. 2004. Étude des propriétés épuratoires des mâche-fers d'incinération d'ordures ménagères et de leur mise en œuvre (Doctoral dissertation, Université de Limoges).
- Turgeon, N., Le Bihan, Y., Savard, S., D'Aoust, M., Fournier, M., & Sénéchal, D. 2017. Utilisation de mâchefer d'incinération de déchets solides municipaux pour l'élimination du sulfure d'hydrogène: Un exemple d'écologie industrielle. *Vecteur Environnement*, 50(4), 40-47.
- Xu, Q., Townsend, T., & Reinhart, D. 2010. Attenuation of hydrogen sulfide at construction and demolition debris landfills using alternative cover materials. *Waste Management*, 30(4), 660-666.
- Yang, Y. & Allen, E. R. 1994. Biofiltration control of hydrogen sulfide 1. Design and operational parameters. *Air & Waste*, 44(7), 863-868.

# DETECTION AND ANALYSIS OF METHANE EMISSIONS FROM A LANDFILL USING UNMANNED AERIAL DRONE SYSTEMS AND SEMICONDUCTOR SENSORS

Ignas Daugela<sup>1</sup>, Jurate Suziedelyte Visockiene<sup>1,\*</sup> and Jurate Kumpiene<sup>2</sup>

<sup>1</sup> Department of Geodesy and Cadastre, Vilnius Gediminas Technical University, Vilnius 10223, Lithuania

<sup>2</sup> Waste Science and Technology, Luleå University of Technology, 97187 Luleå, Sweden

## Article Info:

Received:  
26 November 2019  
Revised:  
11 February 2020  
Accepted:  
28 February 2020  
Available online:  
8 May 2020

## Keywords:

Landfill  
UADS  
RGB  
TIR  
NIR

## ABSTRACT

Landfill operators must collect data on the topography of their landfills, their biological and hydrological characteristics, and local meteorological conditions. These data can be collected by satellite, using Unmanned Aerial Vehicles (UAVs), or by traditional methods such as static flux chambers or modelling. They serve as the basis for landfill monitoring, including the identification and measurement of methane (CH<sub>4</sub>) gas emissions. Here, we present an approach for landfill mapping using sensor data from unmanned aerial drone systems (UADS) based on DJI Matrice 200 UAVs with Zenmuse X4S sensors and Trimble UX5 UAVs with Sony NEX-5R sensors. RGB (Red, Green, Blue) and near infrared (NIR) data from these sensors were processed using a Geographic Information System (GIS) to generate orthoimages, digital elevation models (DEMs), and normalized difference vegetation index (NDVI) maps. These were then used to evaluate changes in the surface structure and topography of the study area (Kariotiskes landfill, Lithuania). The NDVI maps were used to identify areas of sparse vegetation cover that may indicate localized CH<sub>4</sub> emissions. Surface temperature maps based on thermal infrared (TIR) images were then prepared for analysis of these problematic areas. Finally, the presence of CH<sub>4</sub> in these areas was investigated using a prototype lightweight gas sensor array. The structure of the Kariotiskes landfill site remained unchanged over three years, but there is evidence of possible CH<sub>4</sub> gas influence at the landfill cover's surface. The combination of UADS-mounted imaging systems and the prototype gas sensor array enabled rapid analysis of emission hotspots and of landfill topography.

## 1. INTRODUCTION

European landfill operators are obliged to collect, treat, and use landfill gas (LFG) in landfills receiving biodegradable waste, and to monitor fugitive emissions. Modern European landfills have nearly impermeable top covers and LFG collection systems to reduce the amount of LFG escaping to the atmosphere. Nevertheless, localized uncontrolled LFG emissions occur frequently, which can contribute significantly to the global flux of greenhouse gases into the atmosphere. A top cover can effectively minimize CH<sub>4</sub> emissions by promoting microbial CH<sub>4</sub> oxidation (Stern et al., 2007, Thomasen et al., 2019; Fredenslund et al., 2019). Therefore, if spots with high CH<sub>4</sub> emissions could be localized, it may be possible to take remedial action by stimulating CH<sub>4</sub>-oxidizing bacteria (Scheutz et al., 2017). Such localized high emission spots can account for as much as 50-75% of LFG emissions from modern landfills, but they are transient; their temporal and spatial distributions vary

widely (e.g. Scheutz et al., 2003, 2008, Ishigaki et al., 2005, Spokas and Bogner, 2011, Xu et al., 2014, Lando et al., 2017). Effective monitoring systems are required to detect, quantify, and control such releases of LFG into the atmosphere.

Recent advances in the development of Remotely Piloted Aircraft Systems (RPAS) have expanded the applications of Unmanned Aerial Vehicles/Systems (UAV/UAS) in environmental research, enabling their use to detect potential CH<sub>4</sub> release spots. Localized gas emissions from landfill sites can be identified and monitored by analyzing Remote Sensing (RS) data acquired using UAVs with mounted cameras and sensors (Abichou et al., 2006, USEPA, 2006, De la Cruz et al., 2016, Innocenti et al., 2017, Bourn et al., 2019, Fjelsted et al., 2019; Allen et al., 2019).

Digital ground models (DGM), also known as digital elevation models (DEMs), are prepared using RS data, which may be integrated into a GIS along with data on indicators

\* Corresponding author:  
Jurate Suziedelyte Visockiene  
email: jurate.visockiene@vgtu.lt

of environmental conditions (Manzo et al., 2017). High resolution 3D surface models can then be prepared to detect and characterize events such as landslides, to evaluate the area affected, and to estimate the volumes and displacement rates of land masses (Tanteri et al., 2017, Daugela et al., 2018). This can enable rapid detection of surface deformations at landfill sites, which is important because cover stability is essential for preventing uncontrolled LFG emissions. Settlement and surface deformations may occur over time, disrupting the liner and forming cracks in the cover system, leading to the formation of localized CH<sub>4</sub> release spots (e.g. El-Fadel and Khoury, 2000).

Because methane oxidation is exothermic, LFG escape spots exhibit elevated surface temperatures. Even if no oxidation occurs, temperatures inside a landfill can be substantially higher than in the surroundings, and LFG seeping through the cover will allow some of this heat to rise. Therefore, surface temperature measurement using thermal infrared (TIR) cameras can help reveal spots of uncontrolled LFG emission. Previous efforts to detect LFG escape spots at landfill sites using TIR imaging have yielded mixed results, primarily due to the limitations of current techniques (e.g. Desideri et al., 2007, Battaglini et al., 2013, Capodici et al., 2015, Fjelsted et al., 2019). It may therefore be necessary to combine TIR data with additional measurements to accurately monitor uncontrolled LFG emissions.

TIR cameras with infrared thermography imaging sensors can be used to detect temperature differences between released gases and the background atmosphere, and to identify those gases. Like many compounds, CH<sub>4</sub> has absorption and emission bands in the infrared (IR) range, so imaging with multispectral IR cameras can enable identification of CH<sub>4</sub> concentrations above 5% as well as detection of temperature differences of as little as 2.6 K (Kastek et al., 2009). Some authors have suggested that UAV platforms could be equipped with temperature/humidity sensors together with an on-board high-precision near-infrared (NIR) CO<sub>2</sub> sensor (Allen et al., 2019) to increase the reliability of LFG detection. NIR sensors, which rely on photonic crystals that create an optical absorption path, were initially used to identify and measure gases in laboratory settings (Kamieniak et al., 2015). The technology has been further developed for field use, enabling NIR cameras to be mounted on UAVs and used for aerial imaging of e.g. vegetation.

Vegetation on a landfill's top cover may affect and be affected by LFG emissions, and irregularities in vegetation cover could indicate the presence of problematic spots. Plant roots can form channels and macropores in soil that facilitate O<sub>2</sub> diffusion and CH<sub>4</sub> supply to bacteria, stimulating CH<sub>4</sub> oxidation (Abichou et al., 2015, Ndanga et al., 2015). If the soil moisture content is sufficiently high, plant roots may also provide a favorable environment for CH<sub>4</sub>-oxidizing bacteria (Feng et al., 2017), which play a key role in reducing CH<sub>4</sub> emissions from landfills. LFG in the root zone can cause O<sub>2</sub> deficiency and asphyxia in plants. Although CH<sub>4</sub> in the root zone has no major effect on plants (Arif and Verstraete, 1995), CO<sub>2</sub> concentrations above 20% are phytotoxic even if sufficient O<sub>2</sub> is present (Gendebien et al., 1992). Some species are more tolerant than others and

are affected by escaping LFG differently, so plant density and species richness can be utilized as indicators of LFG emissions (Maurice et al., 1995). But time-efficient observations are only possible by digital imaging. The biophysical and physiological characteristics of vegetation using digital imagery has been modelled since the technology became available (Zhang et al., 2009, Thenkabail, 2015). Many of these studies involve the use of vegetation indices and the application of complex mathematical equations to image bands to measure the relative greenness of image features. A notable graphical indicator of plant greenness is the normalized difference vegetation index (NDVI) (Bhandari and Kumar 2012, Gandhi et al., 2015). NDVI is widely used in RS to detect and quantify healthy vegetation cover and has been tested in landfill monitoring (Yang et al., 2008; Mohamood et al., 2016).

Multiple techniques are available for CH<sub>4</sub> monitoring and their combinations have been applied to improve location and quantification of CH<sub>4</sub> landfill emissions (Fjelsted et al., 2019; Mønster et al., 2019). Combined analysis of changes in landfill surface topography, temperature, and vegetation cover could enable fast and reliable hotspot detection if complemented with quantitative CH<sub>4</sub> measurements. However, the size and weight of high precision CH<sub>4</sub> measuring instruments preclude their use on UAVs. Direct measurements of LFG emissions at the landfill surface are challenging due to their spatial and temporal variability and also because of the technical limitations and commercial unavailability of existing measurement techniques (Mønster et al., 2019; Hildmann and Kovacs, 2019). The large areas and complex topography of landfills further complicates the application of traditional direct measurement methods such as flux chambers (e.g. Scheutz et al., 2003, 2008, 2011, Gebert and Gröngroft, 2006) or walkover surveys with portable analyzers (Lando et al., 2017). It would therefore be desirable to adapt small and inexpensive sensors developed for other applications (e.g. gas leak detectors) for use at landfills. The main barrier to using such sensors to quantify LFG emissions is interference due to atmospheric conditions. Since changes in landfill surface topography, temperature, or vegetation cover are frequently but not necessarily associated with LFG emissions, it would be sensible to only use CH<sub>4</sub> sensors to validate the identified potential hotspots by confirming the occurrence of CH<sub>4</sub> emissions.

The aim of this study was to develop a cost-effective landfill site analysis method that could integrate various benefits of an unmanned aerial drone system (UADS) 1) to remotely localize CH<sub>4</sub> emission spots at a closed landfill site by evaluating changes in surface structure and topography, thermal maps, and vegetation cover indices based on RGB, NIR, and TIR imaging data; and 2) to detect the presence of CH<sub>4</sub> and CO<sub>2</sub> in those spots using gas sensors that may be suitable for future mounting on UADS.

## 2. MATERIALS AND METHODS

### 2.1 Study area

The study object was Kariotiskes landfill, located in Trakai district, 25 km from Lithuania's capital city, Vilnius

at 54.716111°, 24.959167° in WGS84 coordinate system. This landfill has been used for unsorted municipal solid waste disposal since 1987.

About 3 mln. m<sup>3</sup> of waste was landfilled over 20 years in a 27.6 ha area. A 0.5 m thick clay layer and a high-density polyethylene geomembrane comprise the landfill bottom liner. The landfill has a leachate collection system that transfers the leachate to a wastewater treatment plant for treatment. Groundwater monitoring wells are installed around the landfill: four in the direction of groundwater flow and one against the flow.

The Kariotiskes landfill was closed in 2008 in accordance with EU regulations on landfill closure. A cover consisting of a drainage layer, a protective liner and a vegetation layer was placed above the landfill. Gas extraction wells and a gas collection system were installed in 2010, and a power plant was built to convert the LFG into electricity. During the gas extraction, testing the composition of the collected gas samples was performed by C.A.U. analytical laboratory (Germany). The proportions of the major components were as follows: 57% CH<sub>4</sub>, 30% CO<sub>2</sub>, 12% N<sub>2</sub>, 1% other gases.

A RS methodology was used for object analyses and to extract information from the acquired (RGB, NIR, TIR) imaging data. These processes involve many different algorithms and can be used to acquire meaningful information from images (Prasad et al. 2015; Yuan et al., 2019), which may be acquired using a satellite system or a UADS platform equipped with various sensors.

## 2.2 The UADS platform and data

The Kariotiskes landfill imaging done with two types of UADS: a commercial UAV DJI Matrice 200 quadcopter and Trimble UX5 Aerial Imaging Rover. DJI Matrice 200 quadcopter with Zenmuse X4S sensors (spectral configurations RGB and TIR) was used for imaging in 2018. This UAV weighs 4.53 kg, with unfolded dimensions of 887×880×378 mm. Its maximum payload is 6.14 kg. For navigation and control, the UAV was equipped with a Global Positioning System (GPS) receiver, a basic inertial system, and distance sensors. Its hovering accuracy in special

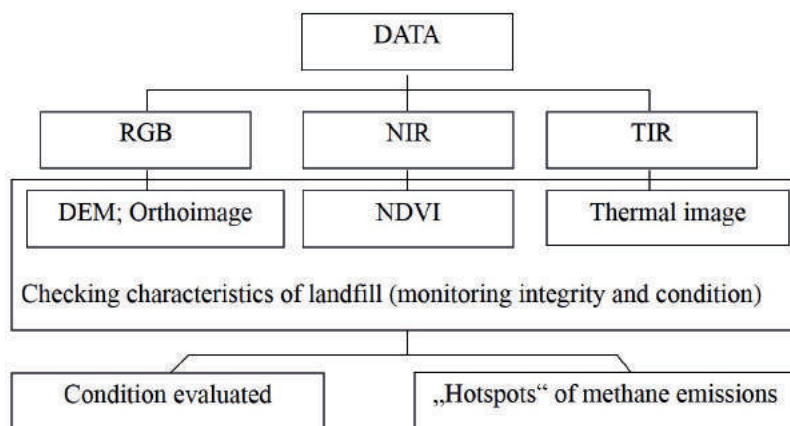
P-mode with good GPS reception and the Downward Vision System (DVS) enabled was ± 0.1-0.5 m vertically and ± 0.3 m-1.5 m horizontally. The Zenmuse X4S camera used in the DJI Matrice 200 weight is only 253 g, it could be flight under 35 minutes (RGB imaging) and 28 minutes (TIR imaging) and have the Controllable Range.

Trimble UX5 UAV equipped with a Sony mirrorless NEX-5R digital camera (spectral configurations RGB and NIR). At a flying height of 150 m, the Trimble UX5 achieves a Ground Sampling Distance (GSD) of 4.8 cm. It can also achieve a GSD of 2.4 cm when flying at altitudes as low as 75 m above ground level (AGL). Operation at such low altitudes requires faster shutter speeds on the camera to prevent forward motion blur. The Sony NEX-5R camera used in the Trimble UX5 is capable of using the higher ISO values necessary to compensate for the darkness resulting from such high shutter speeds while maintaining acceptable levels of noise for photogrammetric applications (Cosyn and Miller, 2013). The Trimble Access Aerial Imaging application can be used for mission planning in the office or at a Ground Control Station (GCS). The user defines the project area and avoidance zones by drawing them over an industry-standard map interface and also specifies the flight height AGL, GSD, and desired image overlap. Trimble Access then calculates the number of flights, flight pattern, and duration of flight(s) needed to meet the user's specifications. After locations for take-off and landing have been selected, the UADS is taken to the field to perform the flights (Cosyn and Miller, 2013).

Figure 1 summarizes the types of raw data acquired in this study, the products (3D models, maps, and images) generated from UAV data, and the uses of these products.

Table 1 presents information on the flights that were undertaken during this work, the number of images captured, and the spatial resolution of the images for three sensor types. The spatial resolution is defined based on the number of pixels used to construct the images. All images were acquired during spring (usually around May) in 2015, 2016, or 2018.

High spatial resolution (Table 1) RGB images were obtained using DJI Matrice 200 and Trimble UX5 UAVs in the



**FIGURE 1:** Data types used in this study; the images, maps, and models generated by processing the acquired data; and the use of these images, maps, and models to analyze methane emissions.

**TABLE 1:** Flight characteristics.

Sensor	Spatial resolution (m)	Number of images	Flight height (m)	Flight time (min)	Image series time (year)	Processing software
RGB	0.14	40	470	5	2015	TBC *
	0.04	419	140	21	2016	TBC
	0.13	333	70	10	2018	UAS Master
TIR	various	22	various	-	2018	-
NIR	0.02	686	77	22	2018	TBC

\* TBC - the Trimble Business Center Software Photogrammetry Module

years 2015, 2016 and 2018. Flights were performed at a range of altitudes, resulting in the acquisition of 40 images in 2015, 419 images in 2016, and 333 images in 2018. The RGB data acquired in 2015 and 2016 are equivalent to the ground spatial distance (GSD) values for the orthoimages and colored surface models generated by processing this RGB data. The quality of an image depends on the subject's characteristics, camera optics (sensor resolution), and atmospheric conditions at the moment of shooting. The photographic images were processed using photogrammetric methods (Förstner and Wrobel, 2016) involving (i) determination of inner orientation; (ii) determination of relative orientation (triangulation); (iii) photogrammetric (3D) model creation; and (iv) integration of ground control points and absolute orientation (projective transformation) to generate a new 3D point cloud (DEM) or orthoimage.

Vegetation and cover observations results were generated using Trimble UX5 UAV data acquired in 2018. The NIR sensor (a Sony mirrorless NEX-5R camera) was used to capture two colored bands and one NIR band. The spatial resolution of the NIR images was 0.02 m, i.e. each pixel corresponded to an area of  $1.9 \times 1.9$  cm on the ground. Vegetation cover levels were assessed by computing per-pixel NDVI values based on the NIR data. NDVI values can range from +1.0 to -1.0. Low values (0.1 or less) correspond to areas of barren rock, sand, or snow; moderate values (0.2 to 0.5) correspond to sparse vegetation such as shrubs, grasslands, or senescing crops; and high values (0.6 to 0.9) correspond to dense vegetation (temperate and tropical forests or fully grown crops) (Remote Sensing Phenology, 2018; NASA, 2018). NIR imaging data were used to create thematic NDVI maps via the work steps (algorithm) outlined in Table 1 of supplementary material.

The NDVI values were calculated and assigned to orthoimage pixels based on absolute position using the local coordinate system (LKS94). The NDVI is computed using the Eq. (1) below (Xie et. al. 2008, NASA, 2018, Remote, 2018):

$$NDVI = (NIR-RED)/(NIR+RED) \quad (1)$$

where NIR and RED denote the intensity of the near infrared and red bands, respectively.

Orthoimages and point clouds were generated using the TBC software and colored using NirGB (eCognition software).

TIR images were collected with a UADS DJI Matrice 200 with Zenmuse XT sensor (8-9.2µm). The sensor's output was processed using an on-board computer and immedi-

ately converted into radiant temperatures, so the resulting image information consisted of a single band. Before use, the sensor was calibrated in a laboratory environment and a sensor certificate was obtained. The processed images show the minimum and maximum temperature of each frame pixel; the pixels with the highest temperature within a frame were identified in real time. The images were also tagged with the UAV's GPS position and heading at the time of acquisition for geo-referencing. Finally, to generate a visual representation of the imaging data, ortho-rectification was performed and a color-thematic map was applied based on the pixel values. The color mapping was chosen to highlight the features most relevant to the analysis (i.e. the spatial variation of stream temperatures) and the interpretation of problematic areas.

### 2.3 Concentration screenings by walk-overs

Areas identified as potential CH<sub>4</sub> release hotspots were investigated using a newly constructed prototype device with semiconductor-based sensors to measure changes in CH<sub>4</sub> levels and detect unusually high (>21%) levels of CO<sub>2</sub> relative to background gases. The prototype was created from inexpensive parts that are readily available via web portals such as [www.adafruit.com](http://www.adafruit.com) or [www.aliexpress.com](http://www.aliexpress.com). These parts include a 2-line LCD display unit with an I2C interface for showing real-time values, a Real Time Clock (RTC) module with a micro SD card reader for storing readings with current time and relative session time stamp, and a Bluetooth module for sending real-time data to a mobile device (e.g. a mobile phone or laptop). Readings and communications are processed by an Arduino Uno microcontroller fitted with a DHT22 temperature and specific humidity sensor capable of measuring humidities between 0 and 100% (accuracy: 2-5%) and temperatures between -40 and 80°C (accuracy: ± 0.5°C) at a maximum sampling rate of 0.5 Hz (once every 2 seconds). The gas sensing array comprises 3 Arduino modules (MQ2, MQ4, and MQ135). Each sensors (models) have different sensitivity in terms of readings (values). It can be altered by changing circuit. Each sensor can be damaged while exposed to extreme conditions over prolonged time. Other than that, it is easily exchanged and can be recalibrated quickly as well as upgraded to newer version or model with better characteristics (even factory pre-calibrated). This study is based on testing methods, so before going into field it was verified in laboratory. The MQ2 module is sensitive to CH<sub>4</sub>, C<sub>3</sub>H<sub>8</sub>, and C<sub>4</sub>H<sub>10</sub>; MQ4 is sensitive to CH<sub>4</sub>; and MQ135 is sensitive to CO<sub>2</sub>, C<sub>6</sub>H<sub>6</sub>, NH<sub>3</sub>, and NO<sub>x</sub>. These sensors are mainly used

as “air quality” sensors in various industrial and household appliances and are sensitive to deviations from the composition of the common unpolluted air mixture. Each sensor’s output was recorded on a micro SD card once per second as plain text, enabling import into tables or databases for further processing. The sensor data were also used to generate plots of measurements over time and scatter plots. The most important sensor in this work was the MQ4 module because its SnO<sub>2</sub> sensing layer is designed to specifically detect CH<sub>4</sub> while suppressing noise due to alcohol, flame fumes, and cigarette smoke. The more CH<sub>4</sub> in the air flow around this module, the higher its output voltage (which is capped at 5000 mV by the microcontroller’s specifications). The device was coupled to a Spectra Precision SP60 Global Navigation Satellite System (GNSS) receiver to accurately record its location.

The prototype gas sensing device calibration was done in laboratory environment. For tests, a sealed non-diffusing gas collection bag was used. Air from the bag was evacuated using an air compressor before the test. After the electronic parts warmed up (constant readings achieved) a controlled amount of gases was injected through a system of valves using a glass syringe. Calibration gases were obtained from AGA Gas AB. A table of five points with increasing known amounts of CH<sub>4</sub> and other gases was made. Each concentration was compared to electronic value obtained by averaging several 300 sec readings. Three similar tests were conducted with different concentrations of CH<sub>4</sub> and background gases. The results for CH<sub>4</sub> are presented in the Figure 1 of supplementary material, regression equation was derived and with r squared of 0.9998 calculated for MQ4 sensor.

Field measurements were conducted by holding the device 25 cm above the ground surface (Figure 2), i.e. the gas-sensing array was not mounted on the drone when measuring in the study landfill (although such possibility was tested elsewhere). The maps were used to measure

gas concentrations in localized areas. The prototype device was calibrated against CH<sub>4</sub> and CO<sub>2</sub> in the laboratory to verify that its sensors respond proportionally to these gases.

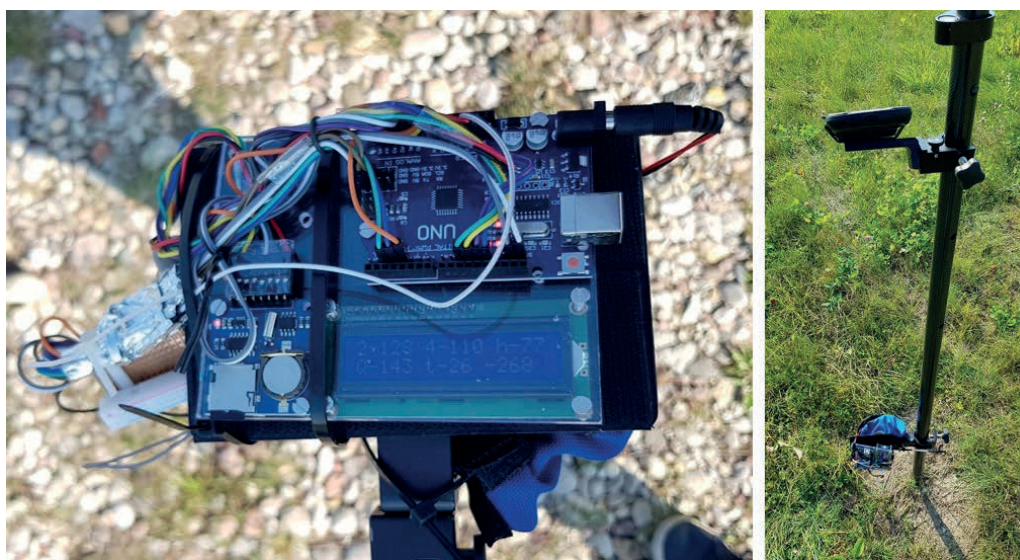
The microcontroller calculates changes in the relative abundance of the gases its sensors detect in real-time in the field. The raw sensor data are recorded together with real-time clock and geographic position data, facilitating data processing and cleaning.

### 3. RESULTS AND DISCUSSION

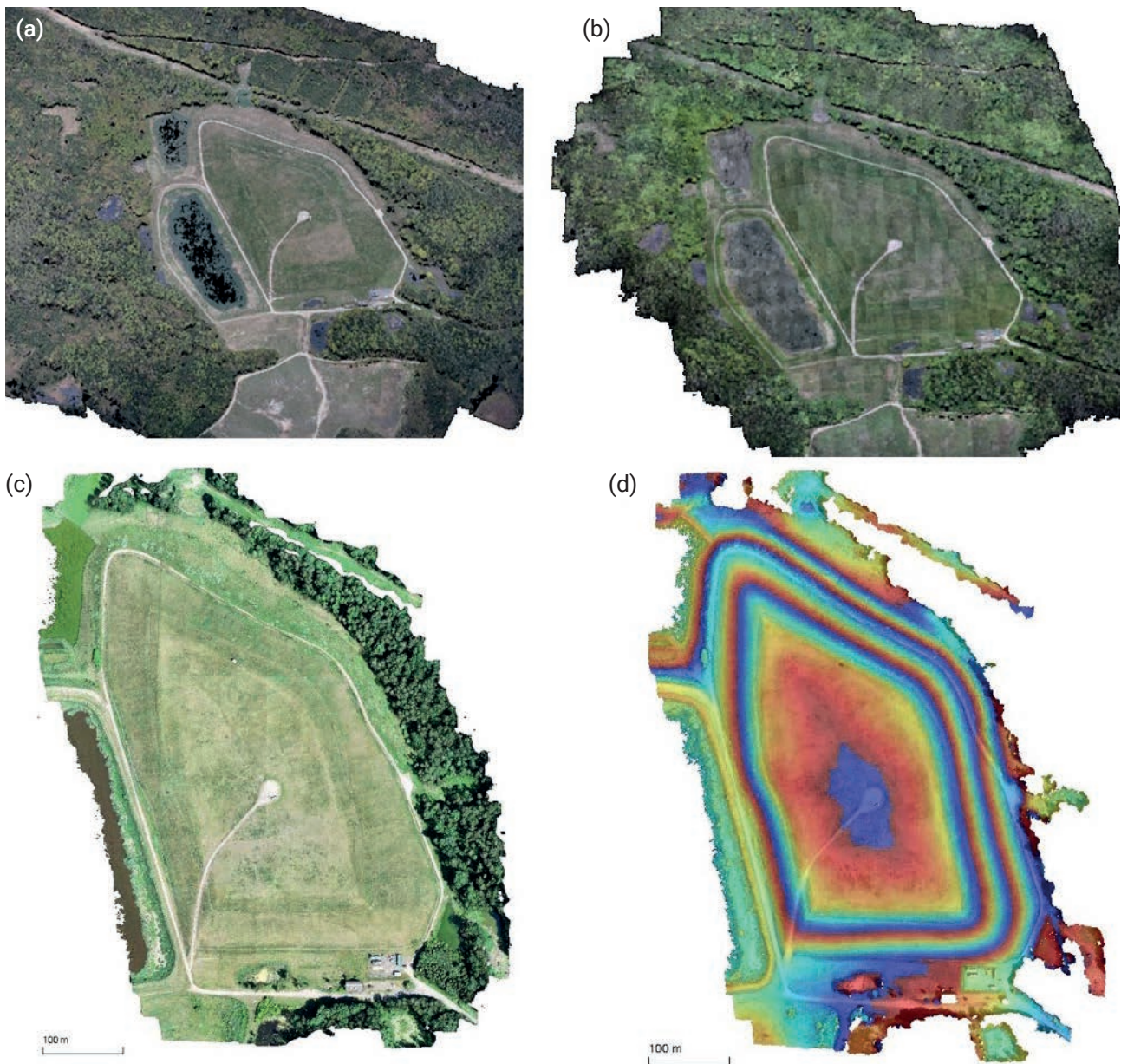
The first part of this section described the result changes of landfill surface structure and topography. After that, it is presented vegetation and thermal imaging and result of methane and carbon dioxide measurement.

#### 3.1 Landfill surface structure and topography

While the details of the orthoimages differ, the vegetation cover at the site clearly improved over time, becoming greener and denser. Figure 3 (a) and (b) show 3D surface models based on RGB data acquired in 2015 and 2016, which have very similar appearances. In particular, there are no appreciable differences in the size or distribution of vegetation-covered spots. All flights were performed on moderately sunny days with low wind speeds and no precipitation. A more powerful UAV and more sophisticated software were used in 2018, enabling better feature matching, structure from motion photogrammetry, and classic aerial triangulation blunder detection. Triangulation was performed based on the 10823 automatically collected tie-points in the 333 RGB sensor images. The data were processed in 10 min 41 s, and a natural-colored point cloud was generated, yielding the 0.14 m GSD orthoimage shown in Figure 3 (c) (Daugela et al., 2018). The point cloud was also used to generate the DEM shown in Figure 3 (d), which is colored by elevation; the colors repeat at elevation intervals of 10m, starting from blue. The highest point in the site



**FIGURE 2:** Close-up of the prototype gas sensing device (left) and the device affixed to a pole, 25 cm above ground level, to perform a gas measurement (right).



**FIGURE 3:** 3D surface models of Kariotiskes landfill in a) 2015; b) 2016; c) 2018 and d) Digital elevation model based on the 2018 3D model.

(altitude: 161.8 m) is the small blue area in the center of the image; its altitude was used as the origin height. To identify changes in the site's visible surface level and structure over time, transparent orthoimages based on data acquired in 2015, 2016, and 2018 were superimposed on one-another (see Figure 4).

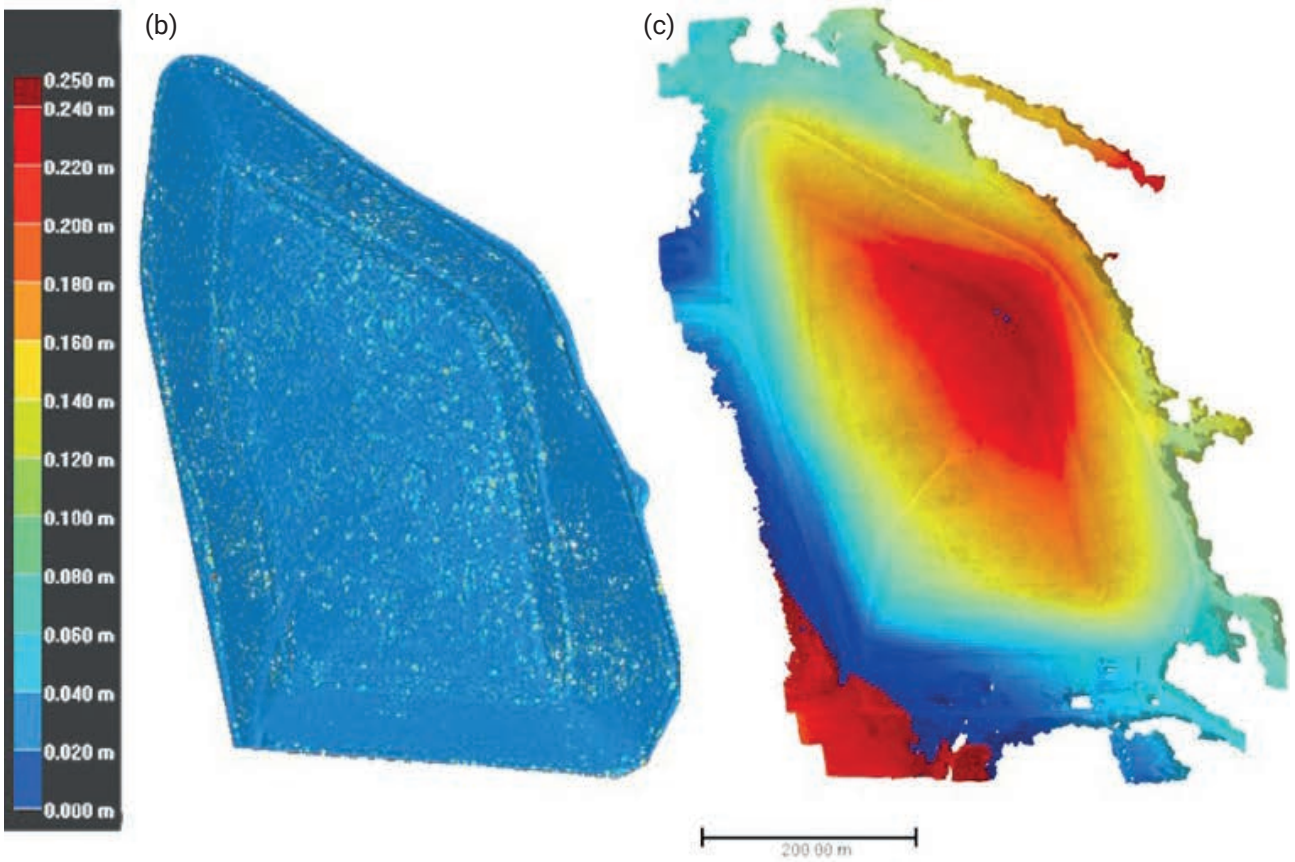
The coloration of the orthoimages makes it difficult to identify small changes in color (and thus small changes in surface height or structure). Therefore, to better detect changes in relief, automated change detection based on distances between digital surfaces was performed using the Trimble RealWorks program.

RGB information was compared by interpolating Z (height) values between the years 2015 and 2018, yielding the results shown in Figure 4 (b). Surfaces were matched

with an average error of 39 mm between points in most cases, so the measurement error was minimal. The deviation in the Z distance (height) between 2018 and 2015 was within 2 cm for most points, with no areas showing markedly larger deviations (see Figure 4 (c)). The processed RGB images for the period 2015-2018 showed that the landfill's surface structure and topography had not changed. This suggests that the protective top cover's integrity has not been reduced by processes such as settling and that the cover should therefore still be functioning well.

Remedial efforts to mitigate localized fugitive CH<sub>4</sub> emissions ideally require fast, cost-efficient, and user-friendly methods for hotspot localization. RGB photo-images, such as those taken in this study, are easily converted into orthoimages and DEM results, which can then be used to detect





**FIGURE 4:** Results: a) layered RGB orthoimage based on data acquired in 2015, 2016, and 2018; b) change in elevation between 2015 and 2018; c) elevation model based on RGB data from 2018.

changes in landfill topography annually or on demand. It took only 5-21 minutes to collect imaging data covering the entire area of the landfill site (which extends over about 30 ha). RGB data recommended around 5 cm GSD, as well as NIR (2 cm GSD was too dense, too heavy for effective calculations). No detectable changes in topography and surface structure were identified at the site over the three-year study period. This indicates that the landfill, which was covered about ten years before the study began, was mechanically stable and that no settlement or surface deformation that could damage the cover structure occurred during the study period.

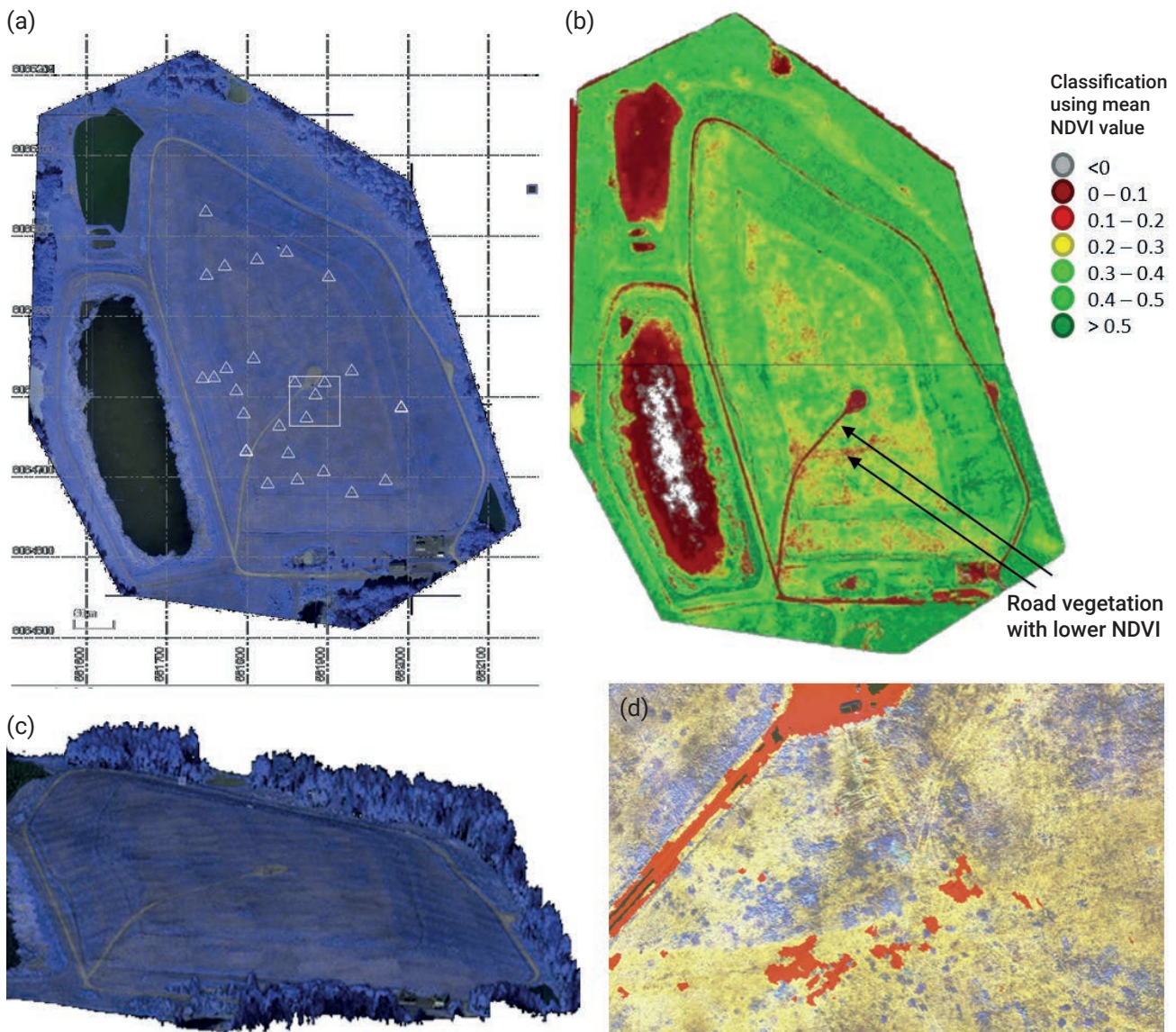
### 3.2 Vegetation and Thermal imaging

Figure 5 (a) shows an NIR-based orthoimage of the landfill in which identifiable protruding pipes belonging to the LFG recovery system's wells are indicated by triangles.

A 3D surface model based on the NIR point cloud is

shown in Figure 5 (b), and an NDVI map of the studied area based on the NIR data is shown in Figure 5 (c). Areas with NDVI values of 0.1-0.2 (shown in red) may contain vegetation experiencing water stress due to LFG exposure. Automated Object Based Image Analysis (OBIA) was used to create a thematic map in which these problematic areas are highlighted in red (Figure 5 (c)). In this process, each pixel's NDVI value was calculated based on its red and NIR intensities. These values were then used to generate cells, which were grouped to represent distinct objects, each of which was then analyzed. Objects with NDVI values below 0.2 were identified as potentially problematic areas and colored in red. They were then exported as polygons in shape files (geodatabase), while the thematic layers were combined to create an oriented geoTIFF image.

Analysis of NIR imaging data revealed several spots on the landfill surface that had low NDVI values (i.e. areas with little greenness or dried up vegetation). Moreover,



**FIGURE 5:** NIR imaging of the landfill surface: a) NIR orthoimage with triangles indicating identifiable LFG recovery pipes; b) 3D surface model derived from NIR point cloud; c) NDVI map; d) Thematic map with problematic areas of low NDVI highlighted in red.

TIR imaging revealed that many of these areas also had slightly elevated surface temperatures. The co-occurrence of these findings (which individually are not necessarily sufficient to identify potential areas of concern) enabled fast (22 min flight time plus data processing) and relatively easy identification of potentially problematic areas. Thermal images could also be combined to cover all area in one orthophotograph and done only when surface is cold (for anomalies to stand out).

Stronger voltage signals were observed upon testing with a prototype microcontroller-based gas sensor array at some spots, indicating elevated methane concentrations relative to the surroundings.

TIR images were generated from data acquired using the DJI Matrice 200 UAV in 2018. Images were acquired in areas found to have unusually low NDVI values to determine whether their temperatures differed from those of their surroundings (Figure 6, purple colour). The cells of the grayscale images were colored according to their measured temperatures and the temperature data were prepared for analysis to identify correlations.

### 3.3 Methane and carbon dioxide measurement

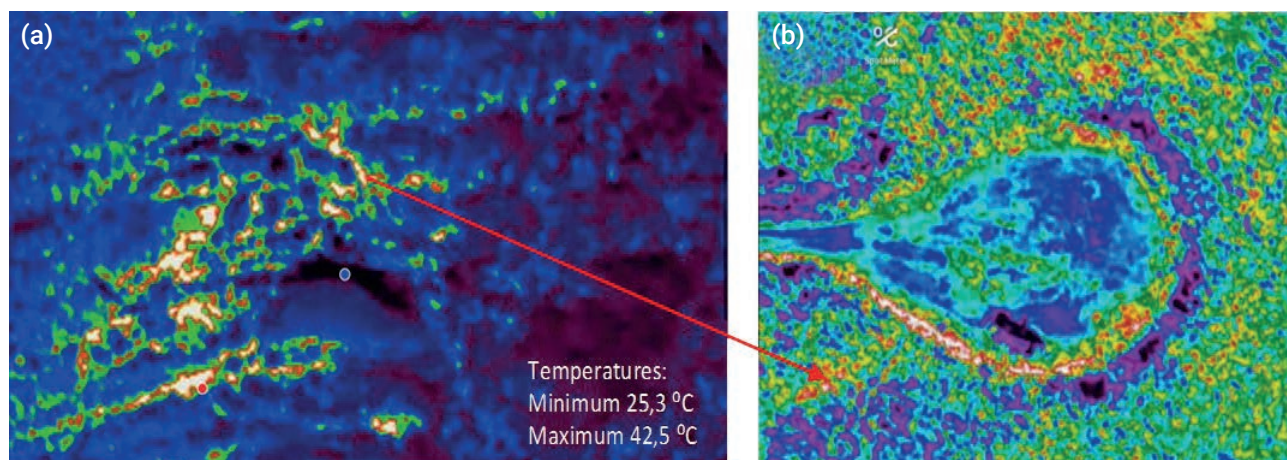
The prototype device containing the semiconductor sensors was used to determine the levels of CH<sub>4</sub> and CO<sub>2</sub> in the air above the previously identified problematic areas of the landfill. The readings of each gas sensor in millivolts are presented in Figure 7, which shows uncorrected and uncalibrated values measured when walking around the Kariotiskes landfill site (see the Figure 2 in the Supplementary Material).

Measurements acquired with the MQ2 and MQ135 sensor modules are shown in blue and green, respectively (Figure 7). The green line can be interpreted as a measure of air pollution; a high voltage from the MQ135 sensor typically indicates comparatively high CO<sub>2</sub> levels and low O<sub>2</sub> levels. The MQ2 sensor (blue) responds to CH<sub>4</sub> and CO<sub>2</sub> with similar strength and is sensitive to all explosive gases. MQ4 sensor's high voltages from 500 to 760 mV (and thus possible higher gas levels) were observed during the

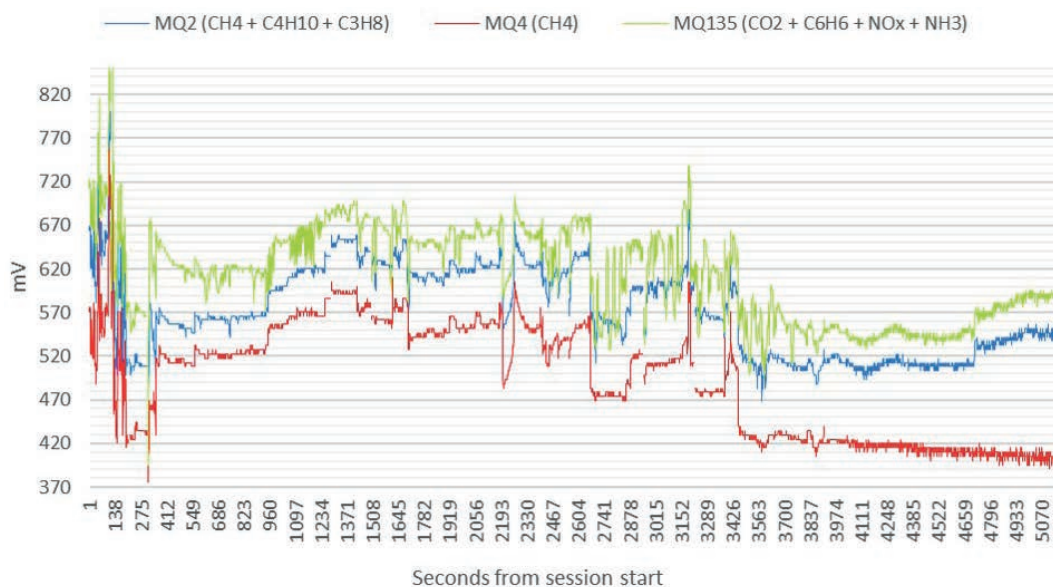
first 200 or so seconds of the sampling period because the device was initially placed in the vicinity of a gas collection well. The sudden decrease in voltage at the end of this period could be due to an increase in wind speed and/or changes in temperature and humidity. The increase in voltage from 530 to 610 mV between 950 and 1400 seconds occurred when the device was moved to the site's northern slope, in locations found to have much less vegetation cover than the rest of the site based on NDVI analysis. The middle section of the graph shows measurements made at various places at the top of the hill (in the central area of the site). The section from roughly 3500 seconds onwards shows measurements made at various places in the southern part of the Kariotiskes landfill. The low readings from 390 to 440 mV in this region are likely due to dispersal of the measured gases by wind. In addition, these measurements were conducted at around mid-day, when the temperature was around 8°C higher and the specific humidity around 26% lower than they were when the first measurements were conducted. Device as it is described should be used for qualitative detection, not aiming to detect exact quantities, but speeding process of finding spots where precise measurements of quantity is needed. To get most out of such sensors: temperature should be chosen similar to the calibration and factory recommended (in our case around 22°C); wind should not be strong or housing with constant internal flow made; strong gradient in humidity should be avoided, if changes not compensated by real time or post-processing algorithm.

If these sensors found to be not suitable for some particular measurements in landfill sites, then they can be changed into newer or with better characteristics easily, in most cases without much altering the code or circuit and some might be found factory pre-calibrated.

While the prototype device is not yet capable of quantitative gas concentration measurement, the results clearly show that combining drone-based infrared imaging with simple gas detection sensors could give landfill operators useful and cost-efficient tools for rapidly identifying local-



**FIGURE 6:** Thermal images from the TIR sensor. Pixels are colored according to their temperature values; the color scale goes from red (high temperature) to violet (low temperature). a) a point of interest imaged from an altitude of 31 m; b) a larger area imaged from an altitude of 122 m.



**FIGURE 7:** Voltage signals generated by the semiconducting CO<sub>2</sub> and CH<sub>4</sub> sensors above the identified problematic areas of the landfill surface as functions of time.

ized CH<sub>4</sub> emissions. The power of techniques used is likely to increase in future as software and UAVs become more capable: the use of an improved UAV and more sophisticated desktop software in 2018 allowed better results to be achieved in less time than was required in 2015 and 2016. Additionally, the cost of the equipment and software necessary for imaging could be reduced up to 2.5-fold in cases where RGB data with a mediocre spatial resolution would be adequate. This method (with low cost gas sensor) has shortage of exactly identifying gas type, as mostly it reacts to several gases and is only more sensitive to one of them. Although it can be calibrated more accurately to one specific gas, it must be used in known environment in order to rely on results. In case of landfill sites, any kind of gases detected by these sensors are unwanted. False positive is possible because of meteorological conditions and construction of form factor. False negatives have almost zero chance when performing qualitative detection, while a bigger chance of false negatives is possible in quantitative detection if instrument is calibrated incorrectly or used in strongly different environmental conditions than those at calibration.

Further, to improve results, measurements of temperature and humidity with fixed amount of CH<sub>4</sub> will be conducted in the future and calibration for these two parameters are planned, which will be taken into account by the real time CH<sub>4</sub> measurement algorithm.

Another factor influencing reading values is power source. It must be redesigned, to be stable at least to 0.1 mV and separated from electronical sensing parts. This way it will not be a source of error for calibration and field measurements or influence precision of repeated field measurements. All parts must be tested by experienced electrician and if found according to specification and sufficient for device, then not changed or altered, otherwise the whole device needs to be recalibrated in laboratory. Sensor fusion techniques can be applied while more exper-

iments conducted with this prototype, as well as machine learning algorithms could improve or change common calibration routine.

#### 4. CONCLUSIONS

The use of a prototype microcontroller-based gas sensor array, that is suitable for future mounting on UADS, together with imaging systems mounted on unmanned aerial drones enabled remote localization of potential CH<sub>4</sub> emission hotspots at the closed Kariotiskes landfill site. Although the site's surface structure and topography remained unchanged over the three-year study period, analysis of surface temperatures and vegetation cover based on RGB, NIR, and TIR imaging data revealed several spots of interest. Testing with the gas sensor array confirmed the possible presence of elevated CH<sub>4</sub> concentrations in these spots. The combination of thermal and vegetation imaging using infrared cameras with commercially available gas sensors thus offers a relatively simple and inexpensive way to rapidly identify CH<sub>4</sub> release hotspots in closed landfill sites. Although the developed gas-sensing array was used in this study as a handheld instrument, it has a full potential to be mounted on the drone for remote measurements. This approach should be affordable for landfill operators and, with further development, could be used to quantify fugitive CH<sub>4</sub> emissions over an entire landfill surface.

#### ACKNOWLEDGEMENTS

The authors thank the employees of the Vilnius County Waste Management Center for allowing them to carry out their research work at the Kariotiskes landfill.

#### CONFLICT OF INTEREST

The author declares that there is no conflict of interests regarding the publication of this paper.

## REFERENCES

- Abichou, T., Kormi, T., Yuan, L., Johnson, T., Francisco, E., 2015. Modeling the effects of vegetation on methane oxidation and emissions through soil landfill final covers across different climates. *Journal of Waste Manage* 36, 230-240. <https://doi.org/10.1016/j.wasman.2014.11.002>.
- Abichou, T., Powelson, D., Chanton, J., Escoriza, S., 2006. Characterization of methane flux and oxidation at a solid waste landfill. *Journal of Environmental Engineering* 132, 220-228. [https://doi.org/10.1061/\(ASCE\)0733-9372\(2006\)132:2\(220\)](https://doi.org/10.1061/(ASCE)0733-9372(2006)132:2(220)).
- Allen, G., Hollingsworth, P., Kabbabe, K., Pitt, J.R., Mead, S.I., Robers, G., Bount, M., Shallcross, D.E., Percival, C.J., 2019. The development and trial of an uncrossed aerial system for the measurement of methane flux from landfill and greenhouse gas emission hotspots. *Journal of Waste Manage* 87, 883-892. <https://doi.org/10.1016/j.wasman.2017.12.024>.
- Arif, M.A.S., Verstraete, W., 1995. Methane dosage to soil and its effect on plant growth. *World J Microbiol Biotechnol* 11(5), 529-35. <https://doi.org/10.1007/BF00286368>.
- Battaglini, R., Raco, B., Scozzari, A., 2013. Effective monitoring of landfills: flux measurements and thermography enhance efficiency and reduce environmental impact. *J. Geophys. Eng.* 10, 64002. <https://doi.org/10.1088/1742-2132/10/6/064002>.
- Bhandari, A.K., Kumar, A., 2012. Feature extraction using normalized difference vegetation index (NDVI): A Case Study of Jabalpur City. *Proceedings of Communication, Computing & Security. Proc. Technol.* 6, 612- 621.
- Bourn, M., Robinson, R., Innocenti, F., Scheutz, C., 2019. Regulating landfills using measured methane emissions: An English perspective. *Journal of Waste Manage* 87, 860-869. <https://doi.org/10.1016/J.WASMAN.2018.06.032>.
- Capodici, M., Ciraolo, G., Trapani, D.D.I., Viviani, G., 2015. Remote sensing analysis coupled to field measurements for the evaluation of methane emissions from a landfill site: a case study. In: *Proceedings Sardinia 2015, Fifteenth International Waste Management and Landfill Symposium*.
- Christensen, T. H., Cossu, R., Stegmann, R., 1996. Landfilling of Waste. Biogas, in: Christensen, T.H., Cossu, R., Stegmann, R. (Eds), New York, 860.
- Cosyn, P., Miller, R., 2013. Trimble UX5 aerial imaging solution. A new standard in accuracy, robustness and performance for photogrammetric aerial mapping, in: Trimble Navigation Limited, Westminster, USA.
- Daugela, I., Suziedelyte Visockiene, J., Aksamitauskas, Č.V., 2018. RPAS and GIS for landfill analysis. Tenth Conference on Interdisciplinary Problems in Environmental Protection and Engineering EKO-DOK 2018, Centrum Zdrowia i Wypoczynku Nowy Zdrój, Polanica-Zdrój, 16-18 April 2018.
- De la Cruz, F.B., Green, R.B., Hater, G.R., Chanton, J.P., Thoma, E.D., Harvey, T.A., Barlaz, M.A., 2016. Comparison of field measurements to methane emissions models at a new landfill. *Environ. Sci. Technol.* 50, 9432-9441. <https://doi.org/10.1021/acs.est.6b00415>.
- Desideri, U., Leonardi, D., Proietti, S., 2007. Application of infrared thermography to study behaviour of biogas captation wells. In: *Proceedings Sardinia 2007, Eleventh International Waste Management and Landfill Symposium*.
- Environmental Protection Agency, 2000. Landfill manuals. Landfill site design. Wexford, Ireland. [https://www.epa.ie/pubs/advice/waste/waste/EPA\\_landfill\\_site\\_design\\_guide.pdf](https://www.epa.ie/pubs/advice/waste/waste/EPA_landfill_site_design_guide.pdf) (accessed 25 February 2019).
- El-Fadel, M., Houry, R., 2000. Modeling settlement in MSW landfills: a critical review. *Crit Rev Environ Sci Technol.* 30, 327-361.
- Feng, S, Leung, A.K., Ng, C.W.W., Liu, H.W., 2017. Theoretical analysis of coupled effects of microbe and root architecture on methane oxidation in vegetated landfill covers. *Sci Total Environ.* 599-600, 1954-1964.
- Fjelsted, L., Christensen, A.G., Larsen, J. E. Kjeldsen, P., Scheutz, C., 2019. Assessment of a landfill methane emission screening method using an unmanned aerial vehicle mounted thermal infrared camera – A field study. *Journal of Waste Manage* 87, 893-904. <https://doi.org/10.1016/J.WASMAN.2018.05.031>.
- Fredenslund, A. M., Mønster, J., Kjeldsen, P., Scheutz, Ch., 2019. Development and implementation of a screening method to categorize the greenhouse gas mitigation potential of 91 landfills. *Journal of Waste Manage* 87, 915-923. <https://doi.org/10.1016/j.wasman.2018.03.0050956-053X/>.
- Förstner, W., Wrobel, B.P., 2016. Photogrammetric Computer Vision. Statistics, Geometry, Orientation and Reconstruction. Ebook, ISBN 978-3-319-11550-4.
- Gandhi, G.M., Parthiban, S., Thummalu, N., Cristy, A., 2015. NDVI: vegetation change detection using remote sensing and GIS – A Case Study of Vellore Distric. *Procedia Comput. Sci.* 57, 1199-1210.
- Gebert, J., Groengroeft, A., 2006. Passive landfill gas emission – influence of atmospheric pressure and implications for the operation of methane-oxidising biofilters. *Waste Manage* 26, 245-251. <https://doi.org/10.1016/J.WASMAN.2005.01.022>.
- Gendebien, A., Pauwels, M., Constant, M., Ledrut-Damanet, M.J., Nyns, E.J., Fabry, R., Ferrero, G.L., Willumsen, H.C., Butson, J., 1992. Landfill gas from environment to energy (EUR-14017/1). Commission of the European Communities (CEC).
- Hildmann, H., Kovacs, E., 2019. Review: Using Unmanned Aerial Vehicles (UAVs) as Mobile Sensing Platforms (MSPs) for Disaster Response, Civil Security and Public Safe. *Drones* 3, 59. <https://doi.org/10.3390/drones3030059>.
- Innocenti, F., Robinson, R., Gardiner, T., Finlayson, A., Connor, A., 2017. Differential absorption lidar (DIAL) measurements of landfill methane emissions. *Remote Sens.* 9, 953.
- Ishigaki, T., Yamada, M., Nagamori, M., Ono, Y., Inoue, Y., 2005. Estimation of methane emission from whole waste landfill site using correlation between flux and ground temperatures. *Environ. Geol.* 48, 845-853. <https://doi.org/10.3390/RS9090953>.
- Kamieniak, J., Randviir, E.P., Banks, C.E., 2015. The latest developments in the analytical sensing of methane. *Trends Analyt Chem.* 73, 146-157.
- Kastek, M., Sosnowski, T., Orzanowski, T., Kopczyński, K., Kwaśny, M., 2009. Multispectral gas detection method. *WIT Trans. Ecol. Envir.* 123, 227-236. <https://doi.org/10.2495/AIR09021>.
- Lando, A.T., Nakayama, H., Shimaoka, T., 2017. Application of portable gas detector in point and scanning method to estimate spatial distribution of methane emission in landfill. *Waste Manage.* 59, 255-266. <https://doi.org/10.1016/J.WASMAN.2016.10.033>.
- Mahmood, K., Batool, S. A., Chaudhry, M. N. 2016. Studying bio-thermal effects at and around MSW dumps using Satellite Remote Sensing and GIS. *Waste Manage.* 55, 118-128.
- Manzo, C., Mei, A., Zampetti, E., Bassani, C., Paciucci, L., Manetti, P., 2017. Top-down approach from satellite to terrestrial rover application for environmental monitoring of landfills. *J. Sci. Total Environ.* 584-585, 1333-1348. <https://doi.org/10.1016/J.SCITOTENV.2017.01.033>.
- Maurice, C., Bergman, A., Ecke, H., Lagerkvist, A., 1995. Vegetation as a biological indicator for landfill gas emissions: initial investigations. In: *Proceedings: Sardinia 1995, Fifth International Landfill Symposium*.
- Mønster, J., Kjeldsen, P., Scheutz, C., 2019. Methodologies for measuring fugitive methane emissions from landfills – a review. *Waste Manage*, <https://doi.org/10.1016/J.WASMAN.2018.12.047>.
- Ndanga, T.M., Bradley, R.L., Cabral, A.R., 2015. Does vegetation affect the methane oxidation efficiency of passive biosystems? *Waste Manage*, 38, 240-249.
- NASA, 2018. Normalized Difference Vegetation Index (NDVI). Retrieved from The Earth Observatory: [http://earthobservatory.nasa.gov/Features/MeasuringVegetation/measuring\\_vegetation\\_2.php](http://earthobservatory.nasa.gov/Features/MeasuringVegetation/measuring_vegetation_2.php) (accessed 25 February 2019).
- Remote Sensing Phenology, 2018. NDVI – the foundation. Retrieved from USGS: [https://phenology.cr.usgs.gov/ndvi\\_foundation.php](https://phenology.cr.usgs.gov/ndvi_foundation.php) (accessed 25 February 2019).
- Scheutz, C., Cassini, F., De Schoenmaeker, Jan, Kjeldsen, P., 2017. Mitigation of methane emissions in a pilot-scale biocover system at the AV Miljø Landfill, Denmark: 2. Methane oxidation. *Waste Manage* 63, 203-212.
- Scheutz, C., Fredenslund, A.M., Nedenskov, J., Samuelsson, J., Kjeldsen, P., 2011. Gas production, composition and emission at a modern disposal site receiving waste with a low organic content. *Waste Manage* 31, 946-955.
- Scheutz, C., Bogner, J., Chanton, J.P., Blake, D., Morcet, M., Aran, C., Kjeldsen, P., 2008. Atmospheric emissions and attenuation of non-methane organic compounds in cover soils at a French landfill. *Waste Manage* 28, 1892-1908.
- Scheutz, C., Bogner, J., Chanton, J., Blake, D., Morcet, M., Kjeldsen, P., 2003. Comparative oxidation and net emissions of methane and selected nonmethane organic compounds in landfill cover soils. *Environ. Sci. Technol.* 37, 5150-5158.

- Spokas, K., Bogner, J., 2011. Limits and dynamics of methane oxidation in landfill cover soils. *Waste Manage.* 31, 823–832. <https://doi.org/10.1016/j.wasman.2009.12.018>.
- Stern, J. C., Chanton, J., Abichou, T., Powelson, D., Yuan, L., Escoriza, S., Bogner, J., 2007. Use of a biologically active cover to reduce landfill methane emissions and enhance methane oxidation. *Waste Manage* 27, 248-1258.
- Tanteri, L., Rossi, G., Tofani, V., Vannocci, P., Moretti, S. and Casagli, N., 2017. Multitemporal UAV survey for mass movement detection and monitoring. In: *Workshop on World Landslide Forum*. Springer, Cham.
- Thenkabail, P.S., 2015. Remotely Sensed Data Characterization, Classification, and Accuracies. *Remote Sensing Handbook*. First ed. CRC Press. Boca Raton.
- Thomasen, T.B., Scheutz, C., Kjeldsen, P., 2019. Treatment of landfill gas with low methane content by biocover systems. *Waste Manage* 84, 29-37.
- USEPA, 2006. EPA Test Method (OTM 10), <http://www.epa.gov/ttn/emc/prelim/otm10.pdf> (accessed June 2018).
- Xu, L., Lin, X., Amen, J., Welding, K., McDermitt, D., 2014. Impact of changes in barometric pressure on landfill methane emission. *Global Biogeochem. Cy.* 28, 679–695. <https://doi.org/10.1002/2013GB004571>.
- Xie, Y., Sha, Z., Yu, M., 2008. Remote sensing imagery in vegetation mapping: review. *Plant Ecol.* 1, 9-23.
- Zhang, H., Hu, H., Yao, X., Zheng, K., Gan, Y., 2009. Estimation of above-ground biomass using HJ-1 hyperspectral images in Hangzhou Bay, China. In: *International Conference on Information, Engineering and Computer Science*. <https://doi.org/10.1109/ICIECS.2009.5364800>.
- Yuan, H., Xiao, Ch., Zhan, W., Wang, Y., Shi, Ch., Ye, H., Jiang, K., ChunhuiZhou, Z., Wen, Y., Li, Q. 2019. Target Detection, Positioning and Tracking Using New UAV Gas Sensor Systems: Simulation and Analysis. *Journal of Intelligent & Robotic Systems* 94, 871–882. <https://doi.org/10.1007/s10846-018-0909-2>.

# LANDFILL AIR POLLUTION BY ULTRAFINE AND MICROPARTICLES IN CASE OF DRY AND WINDLESS WEATHER CONDITIONS

Emília Hroncová \*, Juraj Ladomerský and Denisa Ladomerská

European Science and Research Institute, Hlinku 29, 960 01 Zvolen, Slovakia

## Article Info:

Received:  
2 August 2019  
Revised:  
23 January 2020  
Accepted:  
4 February 2020  
Available online:  
5 March 2020

## Keywords:

Landfill  
Air pollution  
Ultrafine particles  
Microparticles  
Windless weather

## ABSTRACT

In the present article we give the results for ultra-fine particles and microparticles at a landfill of municipal waste, taking into consideration various factors. The landfill is a large-scale source of dust. There is little knowledge in terms of fractional composition of dust particles. We have performed concentration measurements of the number of ultrafine (10 to 100 nm) and microparticles (0.1 to 10  $\mu\text{m}$ ) in the field conditions of the municipal waste landfill using the TSI Technique (Optical particle sizer 3330 and Nanoscan SMPS nanoparticle sizer 3910). The particle number concentration in the atmosphere in case of dry and windless weather conditions at the landfill was in the range of about 2,500 to 5,500 of ultrafine particles per  $\text{cm}^3$ . The mass concentrations of the microparticles was in the range of 29 to 163  $\mu\text{g}\cdot\text{m}^{-3}$  (assuming  $\rho=1 \text{ g}\cdot\text{cm}^{-3}$ ). There was an evident trend of increase of concentration of the ultrafine particles and microparticles in the lower location of the landfill occurring in the case of dry and windless weather conditions. The surprising finding was that passing haulage vehicles and in particular the operation of the compactor increase the mass concentration of microparticles, but they do not increase the concentration of the number of microparticles or even of ultrafine particles.

## 1. INTRODUCTION

The field of air pollution control has seen an intensive process of awareness-raising regarding the seriousness of air pollution caused by particles as well as measures to reduce it. It is considered that air pollution by particles shortens life expectancy. According to the methodology of the World Health Organization WHO, 400 people die in Slovakia every year due to urban high mean concentration of  $\text{PM}_{10}$  particles  $31 \mu\text{g}\cdot\text{m}^{-3}$  (Country profiles of Environmental Burden of Disease - Slovakia, 2009). In the Czech Republic it is 1,700 deaths per year (Country profiles of Environmental Burden of Disease - Czech Republic, 2009).

The European Commission continuously reports violations of air quality standards, and points out that air pollution by  $\text{PM}_{2.5}$  particles claimed 436,000 lives in 28 EU countries in 2013 (Crisp, 2017). These findings are of key importance for the waste management domain, as almost all its activities produce particles of various sizes, which subsequently become airborne. Many waste management activities are performed outdoors or in large factories with their doors open, and become the source of diffuse or fugitive emissions.

It is generally known that mineral particles with an aerodynamic diameter of  $> 30 \mu\text{m}$  are subject to deposition ranging up to 100 metres from the source, particles with

a diameter 30-10  $\mu\text{m}$  from 250-500 metres, but particles smaller than  $< 10 \mu\text{m}$  can be deposited as far as 1 kilometre. Particles  $< 2.5 \mu\text{m}$  practically do not settle or deposit. However, it is interesting that the dispersion rate of ultrafine particles  $< 100 \text{ nm}$  is much slower than the dispersion rate of gases. Particles of organic substances have lower density and thus deposit at a lower rate.

The most common mechanical processes of waste management such as grinding, shredding and separation of fractions are sources of aerosols and bioaerosols. Bioaerosols are solid airborne particles carrying microorganisms or their fragments. A serious bioaerosol contamination risk may occur as a result of long-term storage of waste containing even a small amount of organic material.

Landfilling is a typical activity of waste management and it is the main source of diffuse emissions. It is considered that all works on the landfill especially truck traffic and operation of a compactor, unloading of waste and compacting it (dumping and spreading of waste by compactor), manipulation of the daily cover, wind erosion, burning of landfill gas, is the source of emissions of microparticles and maybe of ultrafine particles. The size of the active face of the landfill is also very important. Workers at a landfill site may be exposed to high concentrations of aerosols, which contain various mineral and organic fibres, bioaer-



\* Corresponding author:  
Emília Hroncová  
email: emilia.hroncova@gmail.com



osols, crystalline SiO<sub>2</sub>, metals etc. The amount of wind-blown particles from a landfill depends on the wind speed, weather (drought spells, rain, snow cover), the surface conditions of the roads connecting individual deposits of waste at the landfill as well as the landfill itself and the size of the particles on its surface.

Landfills of waste are particularly interesting as a source of energy, as well as from the point of view of global climate change and emissions of various gaseous pollutants (EPA, 2008; US EPA, 2015; Chalvatzaki, Lazaridis 2010). Landfills of waste are studied in a lesser extent as a source of microparticles and ultrafine particles and their dispersion into the environment is studied even less. The lowest emissions of the particles on the surface of a landfill can be observed on a wet surface or during rain. Therefore, wetting the surface can be used as a secondary measure to alleviate pollution during dry and windy weather conditions. Daily cover is also of high importance at a landfill. There is even a patented procedure to reduce dustiness at the site by spraying the surface by concentrated solution of boric acid or a diluted solution of polyethylene glycol and boric acid (Keith K. McDamel, 1987).

It is quite difficult to carry out medical studies concerning people working at landfills or the population living in their vicinity, but also other related waste management activities due to numerous exposition channels of harmful pollutants and toxicological diversity (WHO - Europe, 2007). Prior studies addressing waste management discuss almost exclusively PM<sub>10</sub> and PM<sub>2.5</sub> particles although ultrafine particles can be much more detrimental (Macklin et al., 2011).

Nowadays, waste management within the EU often uses e.g. composting or mechanical-biological waste treatment, which are generally considered to be nature-friendly activities (COM, 2008). Such activities are finding their way to landfills too. However, establishing and ventilation of compost heaps as well as finalising of the composting process and subsequent sifting of compost turns the composter into a source of bioaerosols. The workers may be exposed to high concentration of aerosols and bioaerosols when performing their activities at a compost site. The production of microbial aerosols by urban sewage treatment plants may have wide hygienic implications which call for careful evaluation: exposure to such aerosols may in fact represent a health hazard for plant workers and nearby residents alike (Carducci et al., 2000).

The scientific knowledge about the impact of ultrafine particles (UFPs) on human health (cardiovascular system, respiratory diseases) is not so extensive as it is in the case of PM<sub>10</sub> and PM<sub>2.5</sub> particles. Furthermore, there is no database of the sources of these particles in the working environment. Even less information is available on the impact of higher concentrations of airborne UFPs and no limits have been defined yet. Therefore, the measurement of the concentration of particles is an important tool with respect to introducing measures to curb dustiness and evaluate their effectiveness.

This paper aims to analyse the quality of air from the perspective of its pollution by ultrafine particles and microparticles at a selected municipal waste landfill. The measure-

ment was performed in stable, dry and calm weather, when air quality is not influenced by wind erosion and dispersed wind-blown particles. Even under the mentioned conditions it is important to compare the concentrations of the number and size distribution of UFPs or weight concentrations of microparticles with the background concentration in the vicinity of the landfill. It is not known yet whether the landfill can permanently increase the level of ultrafine particles and microparticles in the nearby villages (2 to 4 km), and whether it poses any risks for the population. The results obtained, together with next measurements of downwind concentrations of the aforementioned particles at a wind speed over 6 m.s<sup>-1</sup> (planned next measurements), will confirm suitability of the landfill technology, or indicate a need to introduce further measures to achieve their reduction.

The relative significance of air pollution by particles is different for each waste management facility. It depends on its type, size, duration of its operation as well as the nature of its waste. Furthermore, there are a number of external factors which affect its emitting and dispersion such as meteorological conditions especially rainfall and wind force. Topography can also play a role as to whether waste management operations are performed inside buildings or outdoors. Each landfill is unique with respect to age, quantity and type of waste contained, daily cover, adherence to working processes, local meteorology, hydrogeology, and engineering control of leachate and landfill gas and monitoring.

## 2. MATERIALS AND METHODS

### 2.1 Site selection and measurement conditions

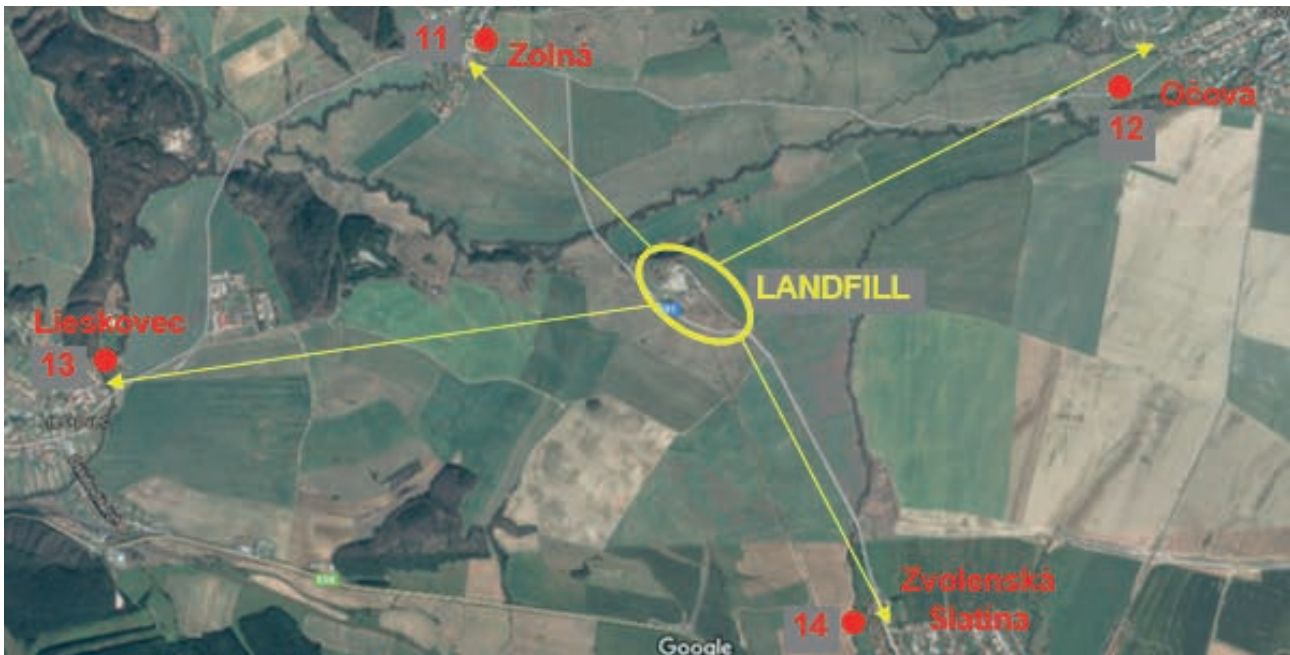
The measurements of air pollution were performed at a typical municipal waste landfill site in Central Slovakia. The landfill site is used to dispose of non-hazardous waste within the meaning of the Decree of the Ministry of the Environment No. 371/2015 Coll. The landfill is able to manage more than 10 tonnes per day with a total capacity of more than 25,000 tonnes, the volumetric capacity of the landfill is 264,401 m<sup>3</sup> and its surface area is 12,300 m<sup>2</sup>. A compost site for biological waste (open windrow heaps) was established on part of the site of a former landfill.

The closest municipality is located 2 km, to the northwest (measured from the centre of the landfill), the other is situated 2 km northwest, the third is 3 km away to the northeast, and the fourth village is 4 km to the southwest of the landfill (Figure 1).

The measurement was conducted at the landfill on a single day. A period of dry and hot windless weather (temperature 22-30°C wind speed below 1 m.s<sup>-1</sup>) was selected to obtain accurate information on the lowest pollution rate in the vicinity of the landfill. Ultrafine particles and microparticles are not dispersed in this weather, if we do not consider rain conditions. Measurements were carried out in the period of stable weather, minimally five windless days without rain in a row.

Sampling sites were situated at critical locations where the movement of the workers and machinery is concentrated, including trucks, dumping and spreading of waste by excavator and compactor over a currently used landfill cell as well as compacting. Figure 2 shows the plan of the ac-





**FIGURE 1:** Map of broader relations with the sampling sites outside the landfill site (Sampling sites: No. 11 Zolná, No. 12 Očová, No. 13 Lieskovec, No. 14 Zvolenská Slatina).

tive zone at the landfill site with the sampling sites marked. Not all the airborne or deposited particulate matter around the landfill site will be caused by the facility itself. Therefore, additional sampling sites were designated outside the landfill in the direction towards the individual municipalities. The map of sampling sites outside the landfill site towards surrounding villages is shown in Figure 2.

**Sampling sites:**

- N° 1 - Truck scale for weighing loaded and unloaded vehicles after dumping the waste (no passing through);
- N° 2 - Truck scale (6 vehicles can pass through);
- N° 3 - Under the landfill at a direct distance of approximately 40 m from the compactor (when in operation) and 13 metres below the top of the site;
- N° 4 - Under the landfill, direct distance of 30 m from the compactor (when in operation) and 13 metres below the top of the site;
- N° 5 - In immediate proximity to the operating compactor;
- N° 6 - 2 m below the top of the landfill site (with compactor in operation);
- N° 7 - 2 m below the top of the landfill site (with compactor in operation) and 2 vehicles can pass through;
- N° 8 - At the top of the landfill site (compactor in operation);
- N° 9 - At the top of the landfill site (compactor out of operation) 15 m away from the compactor;
- N° 10 - The compost site (under the landfill, direct distance 120 m from the compactor (when in operation) and 15 metres below the top of the site.

Two parallel 10-minute long measurements were taken with 1-minute sampling interval at each sampling site. The interval between parallel measurements min. 2 h. Mean values were calculated from these minute values.

**2.2 Methods for determining the concentration of ultrafine particles and microparticles**

Particles ranging between 10 nm to 10 µm were analysed by means of two analysers manufactured by TSI Incorporated, Minnesota USA. They were NanoScan SMPS Model 3910 (portable separator and particle counter with size magnitude from 10 to 350 nm) and Optical Particle Sizer Model 3330 (portable separator and particle counter with size magnitude 0.3-10 µm). The air samples were taken 1.5 m above the ground.

**2.2.1 NanoScan SMPS Model 3910, TSI**

The principle is to determine the particle number of



**FIGURE 2:** Layout of the landfill site with the sampling sites marked.

specific sizes contained in a given air sample. The particles are electrically charged and afterwards separated in an electrical field based on their size and electric charge. Eventually, a computer evaluates the particle count for each fraction. The device is equipped with a pre-conditioner, which removes larger particles (particles larger than 420 nm). Finer particles are charged by corona discharge, then they enter the size selector where they are separated into thirteen channels based on their size and finally they are counted in the isopropanol-based particle counter. The measurable concentration of particles in the aerosol is up to  $10^6$  particles. $\text{cm}^{-3}$ , accuracy 1 particle. $\text{cm}^{-3}$ . Sampling time is 1 second and the airflow through the device is minimum 1 l. $\text{min}^{-1}$ .

### 2.2.2 Optical Particle Sizer Model 3330, TSI

A sample of examined air is sucked directly into an optical chamber where it passes through a light beam. Size resolution is based on the principle of light scattering. The sample then passes through a chamber equipped with a filter for measuring PM weight by gravimetric method or for the purposes of other chemical or microscopic analyses. The size range of identified particles is 0.3-10  $\mu\text{m}$ . in at least 13 size channels. The minimum measurement range: mass concentration 0.001-275,000  $\mu\text{g}.\text{m}^{-3}$ , particle concentration range 1-3,000 particles. $\text{cm}^{-3}$ , 1 particle. $\text{cm}^{-3}$ , size resolution < 5% at 0.5  $\mu\text{m}$ . Sampling time is 1 s and gas flow rate is min. 1 l. $\text{min}^{-1}$ .

Concentrations of ultrafine particles ranging from 10 to

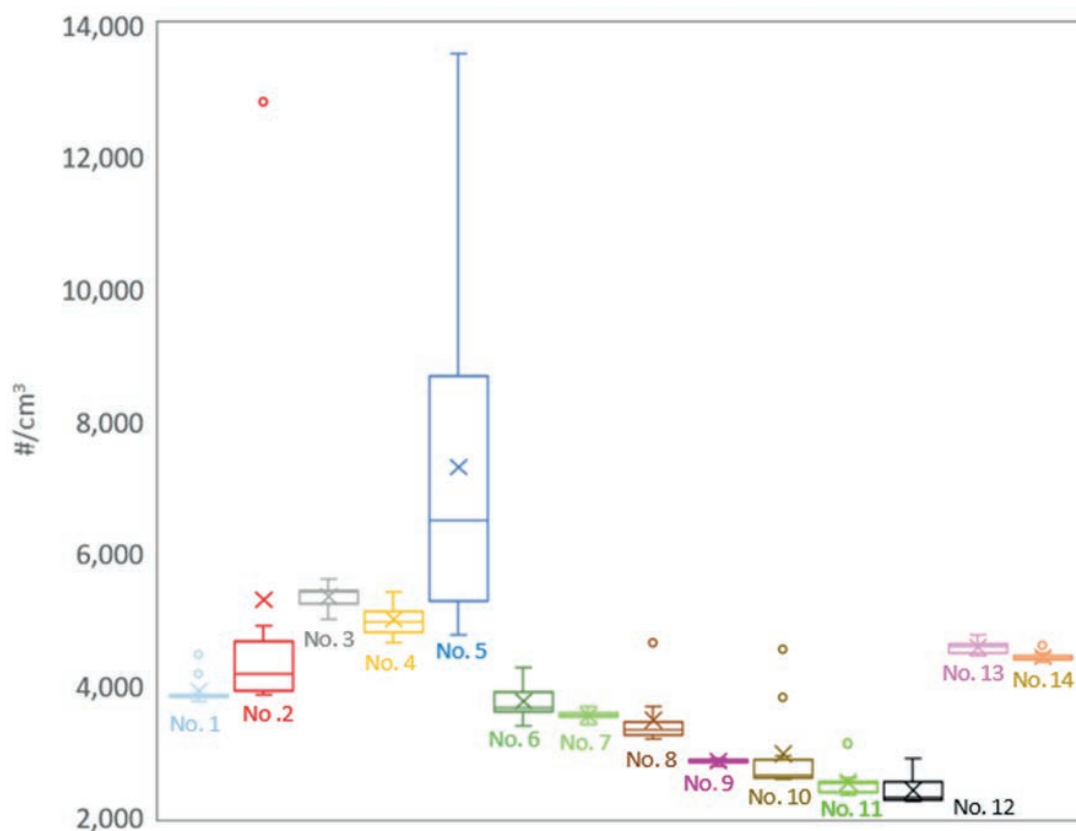
100 nm and from 100 to 300 nm were obtained from NanoScan SMPS Model 3910, and the values for the range 100-300 nm, assigned to microparticles, were provided by Optical Particle Sizer Model 3330.

## 3. RESULTS AND DISCUSSION

Operations at a landfill site take place over a large area (hectares) throughout the year, but a compactor covers a rather smaller area (hundreds of  $\text{m}^2$ ) per day. The measurement results of ultrafine particle concentration are shown in Figure. 3.

There is still not sufficient knowledge of ultrafine particles especially because for decades research has been based on measurements of mass concentration. Therefore, no limits for airborne ultrafine particles have been defined. Their mass is much smaller than  $\text{PM}_{10}$  and  $\text{PM}_{2.5}$ , so the particle number concentration has the highest evidential value. Air with ultrafine particle concentration less than approximately 4,000 per  $\text{cm}^3$  is considered clean (Morawska et al. 2009, Hama et al., 2015). Typical urban background UFP concentration is 10,760 particles. $\text{cm}^{-3}$  (Morawska et al. 2008).

As there are no limits for ultrafine particles in place, it is important to know the concentration of the particles in question at the exposed sites. Furthermore, it is important whether the particles are dispersed in the vicinity of the operation and whether there is a link between activities performed at the site and the potential concentration maximum. The data in Figure 3 demonstrate that even in calm-



**FIGURE 3:** Boxplots of ultrafine particle number concentrations at the waste facility and its surroundings; x-axis No of sampling site and y-axis is particle number concentration.

weather there are low particle number concentrations with the exception of the landfill site sampling sites No. 2-5.

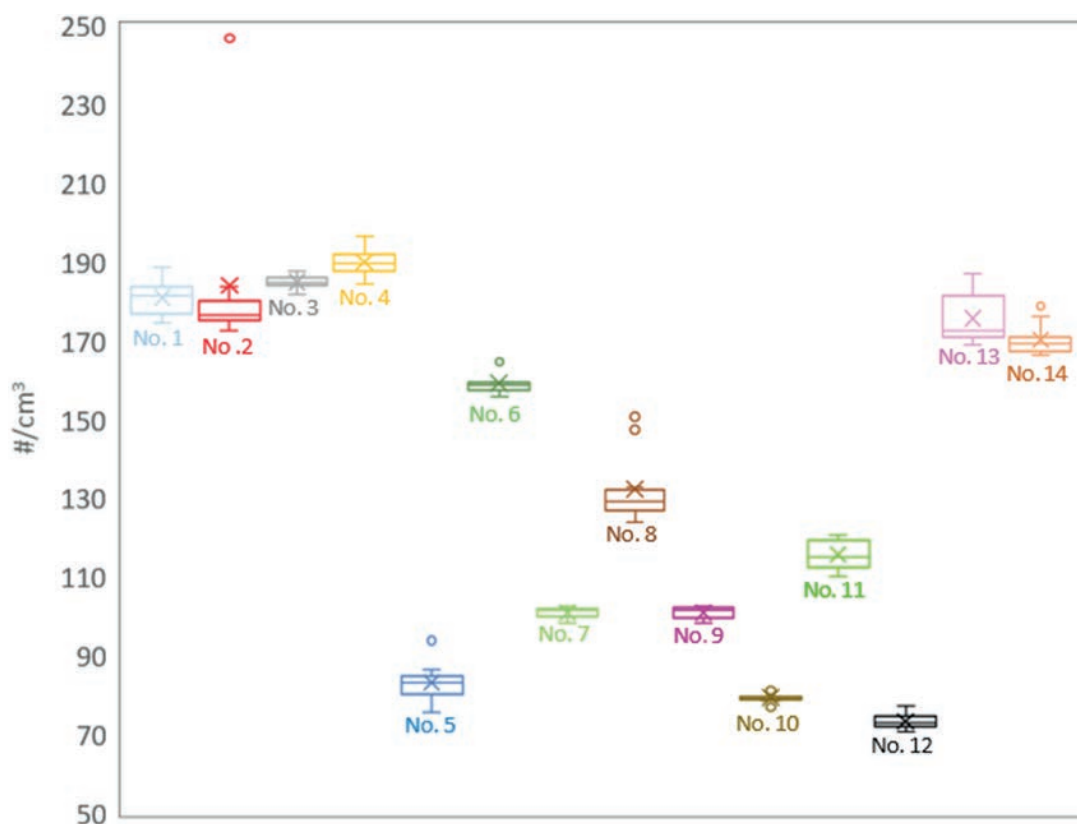
Figure 3 shows two sampling sites (No 2 and 5), which differ from the others regarding ultrafine particle number concentrations. Sampling site No. 2 was located right next to the scale for weighing full and empty trucks. 6 trucks passed through over a period of 20 minutes, which was manifested in a short surge in the particle number concentration. The concentrations differed considerably at the same location sampling site No. 1 when there were no vehicles in operation. The operation of a compactor exhibited a similar effect. The highest concentrations ranging with max 13,558, were recorded in its immediate proximity (No. 5), but at the distance of 15 m from the compactor (No. 6, 7 and 8) the concentrations were much lower from 3,190 to 4,640. A brief interruption of its operation caused an even further drop in the concentrations (No. 9). In general, these data suggest that even in calm weather, ultrafine particle number concentrations decreased considerably with increasing distance from the source. This trend is confirmed by the measurement results obtained at the sampling site No. 10 and outside the facility at sites 11 and 12. The exception is sampling site No.13 and partly No. 14. In the first case, the air pollution can be generated by large sources from a nearby industrial area ca 3.6 km away (energy production from biomass, production of chipboards, pyrolysis of waste, plastic etc.). The slightly higher concentration at the sampling site No. 14 in comparison with No. 11 and 12 may be partly due to the same industrial area or heavy

truck traffic through the village of Zvolenská Slatina.

Another interesting fact is that the lowest-lying sections of the waste facility (sampling sites No. 3 and 4) exhibited high ultrafine particle number concentrations and they drop at the highest points of the landfill. It may mean that dispersion of the particles was less intensive in the lower layers, which may be related to long-lasting insufficient air circulation in these leeward parts of the landfill.

The surprising finding was that passing haulage vehicles and in particular the operation of the compactor increase the mass concentration of microparticles, but they do not increase the concentration of the number of microparticles in 0.3-10  $\mu\text{m}$  (Figure 4) or even of ultrafine particles. It is mechanical generation of microparticles. Compactor pulverises the surface of landfill and ejects coarse particles to the air much more in comparison with the period when only trucks travel to offload garbage in the landfill cell. That confirms the results of the authors Chalvatzaki et al. (2015), who found out at the background area the percentage contributions of fine ( $\text{PM}_{2.1}$ ) and coarse particles ( $\text{PM}_{10-2.1}$ ) to  $\text{PM}_{10}$  31 and 69%, respectively, while at the outdoor weighing facility on the landfill, they were 6 and 94%, respectively.

Particle size distribution represents data important for examining how various sources of pollution influence particle number concentration at a specific location. Figure 5 shows the particle size distribution. These relations demonstrate that movement of vehicles as well as the operation of a compactor in the vicinity of the sampling site is



**FIGURE 4:** Boxplots of microparticle (0.3-10  $\mu\text{m}$ ) number concentrations at the waste facility and its surroundings; x-axis No of sampling site and y-axis is particle number concentration.

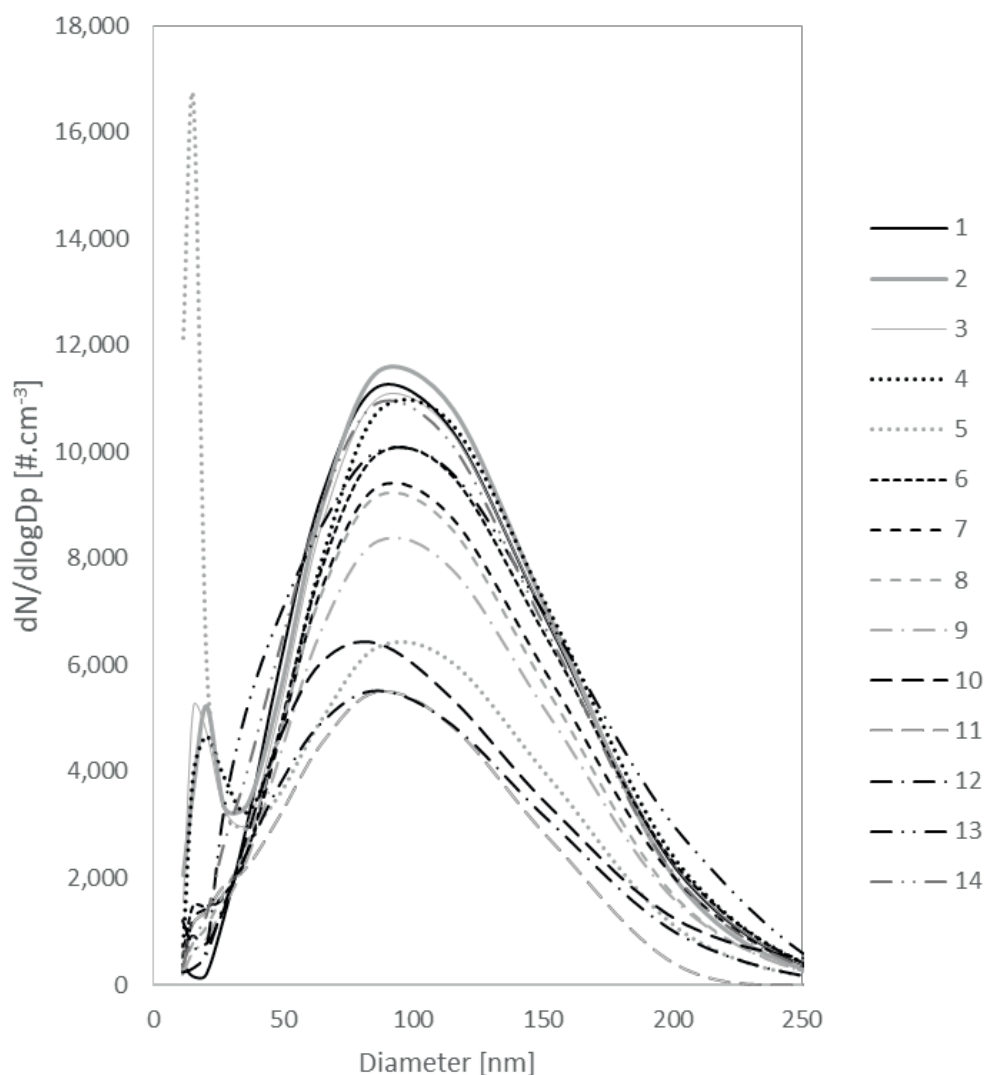
manifested in a bimodal distribution; in other cases there is a unimodal distribution at the landfill site. Particle size distribution at the sampling site No. 3 and 4 implies that there is poor air circulation in the lowest-lying leeward sections of the waste facility. This prevented faster diffusion of the finest fractions of ultrafine particles. This is also reflected in the fact that the correlation is bimodal.

An additional piece of data is the surface area, which may influence the level of risk to human health. The surface area concentration [ $\mu\text{m}^2.\text{cm}^{-3}$ ] is important in toxicology studies. Further information on the impacts of waste management activities on air pollution can be obtained from the proportion of ultrafine particles in the total particle number ranging from 10 nm - 10  $\mu\text{m}$ . Finally, from a relative perspective, the microparticle mass concentration can provide a full picture of the pollution. The aforementioned data are in Table 1.

The movement of vehicles was found to be the most significant factor with respect to the surface area concentration with the values of 100  $\mu\text{m}^2.\text{cm}^{-3}$  at sampling site No.

2, while the lowest measured value did not exceed 30 in case of the sampling sites 11 and 12. It should be taken into account that the value was only 39  $\mu\text{m}^2.\text{cm}^{-3}$ . Conversely, the proximity of the compactor at sampling site No. 5, the proportion of ultrafine particles amounted to 83.6%. The most evident impact of the compactor was observed when measuring the mass concentration of microparticles at 187  $\mu\text{g}.\text{m}^{-3}$ .

The most representative attribute of microparticles is their mass concentration. The measurement devices do not determine actual values of the mass concentration, but yield data provided the particle density is 1  $\text{g}.\text{cm}^{-3}$ . This value was used due to a lack of knowledge concerning more precise value of density of microparticles. The analysed relationships are not changed by using this value. Based on Table 1, it can be assumed that in some cases the microparticle mass concentrations will exceed the limits for outdoor areas of 50  $\mu\text{g}.\text{m}^{-3}$  (for  $\text{PM}_{10}$ ). Similarly, in other cases it was observed that  $\text{PM}_{10}$  concentrations were above this limit with values up to 275  $\mu\text{g}.\text{m}^{-3}$  (Chalvatzaki et



**FIGURE 5:** Particle size distribution for fourteen sampling sites; x-axis – particle diameter  $D_p$ , y-axis – particle number concentration  $dN/d\log D_p$ .

**TABLE 1:** Discharge conditions set by Severn Trent Water Limited on 14th August 2014, for wastewaters being discharged into the Upper Cole Valley Sewer.

Sampling site%	$\Delta$ UFPs $\mu\text{m}^2/\text{cm}^3$	N** $\mu\text{g}/\text{m}^3$	M*	
No. 1	Truck scale for weighing loaded and unloaded vehicles after dumping the waste (no passing through)	60.6	55.7	46.4
No. 2	Truck scale (6 vehicles can pass through)	66.5	57.7	44.3
No. 3	Under the landfill at a direct distance of approximately 40 m from the compactor (when in operation) and 13 metres below the top of the site	67.7	55.6	46.1
No. 4	Under the landfill, direct distance of 30 m from the compactor (when in operation) and 13 metres below the top of the site	65.6	53.4	50.2
No. 5	In immediate proximity to the operating compactor	83.6	39.1	187.3
No. 6	2m below the top of the landfill site (with compactor in operation)	61.2	48.8	36.4
No. 7	2m below the top of the landfill site (with compactor in operation) and 2 vehicles can pass through	62.1	46.2	106.3
No. 8	At the top of the landfill site (compactor in operation) 15 m away from the compactor	62.8	45.7	162.3
No. 9	At the top of the landfill site (compactor out of operation) 15 m away from the compactor	62.6	38.7	29.0
No. 10	The compost site (under the landfill, direct distance 120 m from the compactor (when in operation) and 15 metres below the top of the site	68.8	35.3	67.7
No. 11	Zolná	69.9	28.7	7.8
No. 12	Očová	67.4	29.7	25.0
No. 13	Lieskovec	64.5	56.2	25.9
No. 14	Zvolenská Slatina	64.2	56.2	26.2

N\*\* (range 10 - 100 nm), M\* (range 0,1 - 10  $\mu\text{m}$ )

al., 2015). This value is to a significant extent the result of the movement of vehicles near the sampling site.

Higher levels of daily and annual mean  $\text{PM}_{10}$  concentrations are associated with an increase in mortality and lung function impairment. The recommended maximum value, as stated in the WHO Guideline Values from 2006 for acceptable health risks and short-term effects of  $\text{PM}_{10}$ , obtained from mean 24-hour interval concentrations, is  $50 \mu\text{g}\cdot\text{m}^{-3}$ . As for long-term effects, the recommended value is much lower and should not surpass  $20 \mu\text{g}\cdot\text{m}^{-3}$ . Exceeding of these concentrations heightens the risk of mortality, e.g. annual average concentration of  $70 \mu\text{g}\cdot\text{m}^{-3}$  can raise such risk by 15%.

The limits for mass concentration  $\text{PM}_{10}$  and  $\text{PM}_{2.5}$  particles applied in Slovakia are equally strict. According to the Government Decree No. 244/2016 Coll. on air quality as amended, the daily limit for  $\text{PM}_{10}$  is  $50 \mu\text{g}\cdot\text{m}^{-3}$  and the upper and lower threshold value of  $35 \mu\text{g}\cdot\text{m}^{-3}$  and  $25 \mu\text{g}\cdot\text{m}^{-3}$  respectively should not be exceeded more than 35 times per year. The daily limit for  $\text{PM}_{2.5}$  is not specified. The annual average for  $\text{PM}_{10}$  is  $40 \mu\text{g}\cdot\text{m}^{-3}$  and for  $\text{PM}_{2.5}$  is  $20 \mu\text{g}\cdot\text{m}^{-3}$ .

The results of the measurement point to "diffusivity" ultrafine particles and microparticles from landfill site to rural area in case of dry and windless weather conditions. Measured UFPs and MP at varying distances and in different wind directions from the landfill (at the boundary line, 2-4 km or more from the boundary line, see Figure 1) are labelled as background concentrations. It is reasonable to expect during long-term stable weather that concentrations of UFPs and MP would decrease with increasing distance from the landfill; in most cases where both were measured, they did. Where this did not happen, an external source is

suspected. But no correlation was observed between the measurements at the landfill and the background sites when located 7 km away from a landfill (Chalvatzaki et al., 2010).

Interesting findings by (Chalvatzaki et al., 2015) reveal that the percentage contributions of road and wind-blown dust to the  $\text{PM}_{10}$  concentrations on weekdays were near the unpaved road equal to 76 and 1%, respectively. The influence of the background concentration is estimated at close to 23%. Thus, contribution of wind-blown dust to the  $\text{PM}_{10}$  concentrations directly at the landfill is very modest, but the speed and force of wind represent the most significant factors in terms of particle distribution towards the adjacent villages.

Humans perceive the air near a landfill site as rather dusty. It may be caused by irritation of respiratory system by coarse particles ( $>10 \mu\text{m}$ ) in aerosol: The coarse aerosol, however, does not have adverse health effects. Conversely, finer particles ( $<10 \mu\text{m}$ ) penetrate deeper parts of the respiratory tract. It is likely that people do not perceive higher concentrations of ultrafine particles, which can be harmful for human health, as excessive air pollution. This even more stresses the seriousness of ultrafine particulate air pollution. The findings by Ray et al. (2005), demonstrate higher incidence of respiratory symptoms, airway inflammations, lung function impairment and a number of different health problems of people working in the waste disposal field.

#### 4. CONCLUSIONS

Measurements of the concentration of ultrafine particles (10-100 nm) and microparticles (0.1-10  $\mu\text{m}$ ) were

performed at a municipal solid waste landfill in long-term stable dry, windless weather (only short-term fluctuations in wind speed with  $v < 1 \text{ m}\cdot\text{s}^{-1}$ ). This way we obtained data on the lowest particulate concentrations at the landfill and its surrounding area.

During windless weather conditions, there are relatively low concentrations of ultrafine particles in the air also at the landfill site and in most of cases they range from 2,500 to 5,000 particles per  $\text{cm}^3$ . The concentrations may rise rapidly up to 14,000 particles per  $\text{cm}^3$  only in the close proximity of an operating compactor or waste collection vehicles transporting the waste to the landfill.

The measurement results suggest that even in calm weather ultrafine particle number concentrations decreased considerably with increasing distance from the source. In terms of health risks, the compactor operator seems to be the most vulnerable individual working at the landfill site.

The results can be generalised to all landfills with untreated municipal waste. Particulate dispersion is minimal in these conditions and the operation of a compactor at a landfill does not affect the concentration of UFPs and MP in the surrounding areas of the waste site. In the next stages of the study, the measurements will be performed again in dry weather, at different wind speeds and in four directions towards the closest villages situated 2 to 4 km away from the landfill. This should enable definition of the contribution of the landfill to the overall air pollution by ultrafine particles and microparticles in the adjacent villages.

## ACKNOWLEDGMENTS

This research was supported by the Slovak Grant Agency VEGA under contract No. VEGA 1/0547/15 "Experimental measurement and modelling of fugitive emissions" and KEGA under contract No. 030UMB-4/2017 "Educational Centre for Integrated Safety".

## REFERENCES

Carducci A., Tozzi E., Rubulotta E., Casini B., Cantiani L., Rovini E., Muscillo M., Pacini R. (2000). Assessing airborne biological hazard from urban wastewater treatment. *Water Research* 34, 1173–1178. doi:10.1016/S0043-1354(99)00264-X

COM (2008). Green Paper on the management of bio-waste in the European Union. Brussels.

Country profiles of Environmental Burden of Disease - Czech Republic (2009). Public Health and the Environment Geneva. Geneva. [https://www.who.int/quantifying\\_ehimpacts/national/countryprofile/czechrepublic.pdf](https://www.who.int/quantifying_ehimpacts/national/countryprofile/czechrepublic.pdf)

Country profiles of Environmental Burden of Disease - Slovakia (2009). Public Health and the Environment, Geneva. Geneva. [http://www.who.int/quantifying\\_ehimpacts/national/countryprofile/slovakia.pdf?ua=1](http://www.who.int/quantifying_ehimpacts/national/countryprofile/slovakia.pdf?ua=1)

Chalvatzaki E., Glytsos T., Lazaridis M. (2015). A methodology for the determination of fugitive dust emissions from landfill sites. *International Journal of Environmental Health Research* 3123, 1–19. doi:10.1080/09603123.2014.989491.

Chalvatzaki E., Lazaridis M. (2010). Estimation of greenhouse gas emissions from landfills: Application to the akrotiri landfill site (CHANIA, GREECE). *Global NEST Journal* 12(1), 108-116.

Chalvatzaki E., Kopanakis I., Kontaksakis M., Glytsos T., Kalogerakis, N. Lazaridis M. (2010). Measurements of particulate matter concentrations at a landfill site (Crete, Greece). *Waste Management* 30, 2058–2064. doi:10.1016/j.wasman.2010.05.025.

Crisp J. (2017). 23 EU countries are breaking European air quality laws. 7.2.2017. Dostupné na: [www.EurActiv.com](http://www.EurActiv.com)

EPA (2008). Background Information Document for Updating AP42 Section 2.4 for Estimating Emissions from Municipal Solid Waste Landfills. EPA/600/R-08-116 September 2008.

Hama S.M., Monks P.S., Cordell, R.L. Monitoring of Ultrafine Particle Number Concentration and Other Traffic-related Air Pollutants at One Urban Background Site in Leicester, over The Course of a Year. [http://www.nanoparticles.ch/archive/2015\\_Hama\\_PO.pdf](http://www.nanoparticles.ch/archive/2015_Hama_PO.pdf)

US EPA (2015). Emission Guidelines, Compliance Times, and Standards of Performance for Municipal Solid Waste Landfills; US EPA. Federal Register 80(166), August 27, 2015, Proposed Rules.

Keith K. McDamel (1987). High concentration boric acid squalidification process. Patent 4,664,895.

Macklin Y., Kibble A., Pollitt F. (2011). Impact on Health of Emissions from Landfill Sites: Advice from the Health Protection Agency, Health Protection Agency.

Morawska L., Ling X., Jayaratne R. (2009). Nano and ultrafine particle number concentrations in different environments: application towards air quality regulations. In 19th International Clean Air and Environment Conference, 6-9 September 2009, Perth Convention Exhibition Centre, Perth, WA. This file was downloaded from: <https://eprints.qut.edu.au/75159/>.

Morawska L., Ristovski Z., Jayaratne ER et al. (2008). Ambient nano and ultrafine particles from motor vehicle emissions: characteristics, ambient processing and implications on human exposure. *Atmos Environ*; 42: 8113–38.

Ray M.R., Roychoudhury, S., Mukherjee, G., Roy, S., Lahiri, T. (2005). Respiratory and general health impairments of workers employed in a municipal solid waste disposal at an open landfill site in Delhi. *International Journal of Hygiene and Environmental Health* 208, 255–262. doi:10.1016/j.ijheh.2005.02.001

WHO - Europe (2007). Population health and waste management: scientific data and policy options. Report of a WHO workshop, Rome, Italy 29-30 March 2007, World Health Organization.

# THE ELEVATED TEMPERATURE AND GAS COMPONENT WITHIN AN OPERATING SEMI-AEROBIC LANDFILL

Vu Quang Huy \*, Yukihiro Kohata and Hideki Yoshida

Course of Civil Engineering, Muroran Institute of Technology, 27-1 Mizumoto-cho, Muroran, Hokkaido, 050-8585, Japan

## Article Info:

Received:  
19 October 2019  
Revised:  
17 February 2020  
Accepted:  
11 March 2020  
Available online:  
8 May 2020

## Keywords:

Semi-aerobic landfill  
Aerobization  
Landfill gas temperature  
Landfill gas component

## ABSTRACT

The semi-aerobic landfill concept, which is based on passive aeration, is the compulsory standard for planning new landfill projects in Japan. The semi-aerobic landfill concept is also applied in several other countries because of its low construction and operating costs. The landfill gas (LFG) component and the LFG temperature are the main indicators of the aerobization of semi-aerobic landfills. Analysis of LFG, its concentration, and its temperature can be easily carried out on-site to evaluate the passive aeration of an operating semi-aerobic landfill. Therefore, this study observed LFG temperatures and LFG components to assess the partial aerobization within an operating semi-aerobic landfill. The observational data revealed that the methane ( $\text{CH}_4$ ) gas concentration of most of the main LFG venting pipes (VPs) was below 15%. The aerobic condition happened effectively surrounding the main LFGVP M2 because over the observation period, the ratio of  $\text{CH}_4$  to  $\text{CO}_2$  was less than 1.0. The highest gas temperature was above  $60^\circ\text{C}$  within the main LFGVP M2, and there was a trend of high temperatures above  $40^\circ\text{C}$  for more than 5 years before the temperature declined to  $20^\circ\text{C}$  in the most recent observation. The high LFG temperatures were recorded in the winter months due to the buoyancy effect. High temperature and the  $\text{CH}_4/\text{CO}_2$  ratio less than 1.0 potentially representing good indicators showed that aerobic decomposition is becoming dominant. The study showed clearly that the aerobic biodegradation performance in this semi-aerobic landfill is extremely good.

## 1. INTRODUCTION

Landfilling technology continues to be one of the main methods used in future modern municipal solid waste (MSW) strategies (Cossu, 2012), particularly in developing countries, because of low construction and operation costs as compared to other technologies. It is a necessary and unavoidable step in closing the material cycle (Cossu, 2009; Cossu et al., 2016). At present, there are 4 types of main landfilling concepts: anaerobic, aerobic, semi-aerobic, and hybrid. Each type has its own advantages and disadvantages. The choice of a specific type depends on many factors (i.e., cost, regulations, climate, waste characteristics). Also, the goals of waste treatment (i.e., energy recovery, increasing the waste stabilization) play a role in landfill type selection (Grossule et al., 2018). One of the biggest challenges of landfilling technology is to maintain the performance of a landfill as its initial design purposes to minimize the risks to the surrounding environment. A good design, together with an appropriate operation mode, will reduce significantly the negative impacts on the environment and public health (Hrad et al., 2013; Stegmann and Ritzkowski, 2007).

The rapid development of science and technology during the last decades helped researchers to propose the "sustainable landfill" concept (Antonis and Haris, 2009; Cossu, 2005) with the aim of (1) reducing waste volume, (2) accelerating the stabilization of waste, (3) minimizing landfill gas production which leads to greenhouse effect, (4) rapid biogas production, and (5) decreasing the leachate organic load. In 2002, a special Task Group of International Waste Working Group (IWWG) was established to achieve these targets through a project named "Landfill Aeration". By means of the research projects all over the world, researchers realized that aerobic conditions process faster the waste degradation and reduce more significantly emissions than the anaerobic environment. Besides, the "Landfill Aeration" project has paved the way for the recovery of valuable resources through landfill mining. Therefore, in recent years, in situ landfill aeration projects have received much attention. It has been considered as a useful tool for the sustainable conversion of conventional anaerobic landfills into a biologically stabilized state. It has also shown a minimized emission potential (Ritzkowski and Stegmann, 2012).



Many years ago, in some places in America, Europe and Japan the air and moisture have been added into a landfill to create the optimized aerobic conditions which help aerobic microorganisms degrade biodegradable organic matter. The concept of semi-aerobic landfill might be the oldest method for landfill aeration.

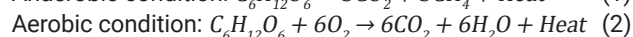
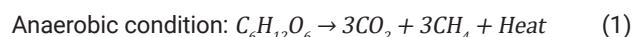
The semi-aerobic landfill concept is based on passive aeration. This concept was developed in 1975 by researchers at Fukuoka University, Japan, when it was given the name semi-aerobic landfill. In semi-aerobic landfills, waste is aerated naturally by atmospheric air via a network of horizontal leachate collection pipes (LCPs) connected to vertical landfill gas (LFG) venting pipes (VPs). The outlet of the main LCP in the leachate pond is always open. Air is drawn into the main LCP due to a buoyancy effect, and the LFG is discharged into the atmosphere (Matsufuji and Tachifuji, 2007). Because of both the limited strength of the passive aeration induced by natural ventilation and anaerobic zones remaining inside the semi-aerobic landfill, the process of biological stabilization occurs more slowly in semi-aerobic landfill than that in actively aerated landfill. For this reason, semi-aerobic landfill has partial aeration around the wells and pipes.

Although numerous studies have focused on the semi-aerobic landfill concept (Ahmadifar et al., 2016; Cosu et al., 2016; Grossule and Lavagnolo, 2017; Hanashima et al., 1981; Hirata et al., 2012; Huang et al., 2008; Matsuto et al., 2015; Morello et al., 2017; Ritzkowski et al., 2006; Shimaoka et al., 2000; Theng et al., 2005; Wu et al., 2017; Yang et al., 2012), most of them were conducted using a lysimeter either in a laboratory or at pilot scale. Those demonstrated significant achievements of the semi-aerobic landfill concept, including (1) accelerating the biodegradation of organic matter, (2) improving leachate quality, (3) reducing methane (CH<sub>4</sub>) gas emission, and (4) entailing lower construction and maintenance costs (Ishigaki et al., 2011). The current study has been carried out over many years to monitor and evaluate the aerobization within a full-scale operational semi-aerobic landfill based on measurements of the LFG temperature and concentration.

LFG temperature is regarded as a good index for assessing the decomposition of biodegradable waste. Both aerobic and anaerobic decomposition processes generate heat (see Equations 1 and 2). Rees (1980) measured a temperature range of 40°C-45°C in a waste layer that was 4 m thick. High temperatures, in the range of 60°C-90°C, have also been measured in other parts of the world (Bouazza et al., 2011; Yesiller et al., 2015, 2011; Yoshida and Rowe, 2003). Moreover, several studies have been aimed at determining the heat generation value through theoretical analyses of biochemical decomposition of waste. Pirt (1978) and Rees (1980) reported a heat generation value of 632 kJ/kg glucose for anaerobic digestion. Cooney et al. (1969) reported a heat generation value of approximately 110 kcal/mol oxygen (O<sub>2</sub>) (15,400 kJ/kg glucose) for aerobic digestion. Thus, it is clear that aerobic decomposition generates a larger amount of heat from waste decomposition than does anaerobic decomposition.

In practice, LFG is considered to be a mixture of the gases CH<sub>4</sub>, carbon dioxide (CO<sub>2</sub>), O<sub>2</sub>, and nitrogen (N<sub>2</sub>). LFG

is composed 45% to 60% methane and 40% to 60% carbon dioxide (ATSDR, 2001). In conventional sanitary anaerobic landfills operating under normal conditions, the ratio is typically from 0.8 to 1.4 (Benson, 2017). Theoretically, if the ratio of CH<sub>4</sub> to CO<sub>2</sub> is either greater than or equal to 1 (from Equation 1), the anaerobic condition predominates (Barlaz et al., 2010; Jafari et al., 2017; Martin et al., 2013). Thus, it can be derived that if the CH<sub>4</sub>/CO<sub>2</sub> ratio is less than 0.8, anaerobic and aerobic conditions are coexisting simultaneously within the landfill. Matsufuji et al. (1996) created a semi-aerobic landfill model in a lysimeter and found the CH<sub>4</sub>/CO<sub>2</sub> ratio to be 1.0. IPCC (2006) calculated the ratio to be 0.33 by using default values. Kim et al. (2010) measured the ratio at 1.0 in a closed landfill site that had been undergoing remediation to accelerate landfill stabilization through installing numerous passive LFGVPs that were not connected to the LCPs. Yang et al. (2012) found the CH<sub>4</sub>/CO<sub>2</sub> ratios for anaerobic landfills and semi-aerobic landfills to be 1.9 and 0.8, respectively. Zhang and Matsuto (2013) reported a CH<sub>4</sub>/CO<sub>2</sub> ratio between 1.0 and 1.5 for a semi-aerobic landfill site that was not being operated correctly. Jeong et al. (2015) measured LFG from VPs in five semi-aerobic landfills in South Korea. However, the ends of LCPs in all five landfill sites were closed, and the CH<sub>4</sub>/CO<sub>2</sub> ratio ranged from 1.08 to 1.46, averaging 1.30. Thus, a CH<sub>4</sub>/CO<sub>2</sub> ratio below 1.5 might be an indicator of landfills with a semi-aerobic design. The reactions in aerobic and anaerobic decomposing processes are shown in a simplified way as follows:



The CH<sub>4</sub>/CO<sub>2</sub> ratio is regarded as an indicator for evaluating the proportions of anaerobic decomposition and aerobic decomposition. Semi-aerobic landfill is a partial aerobization system because passive aeration works only around LFGVPs and LCPs, and there is limited penetration of O<sub>2</sub> into waste mass.

## 2. DESCRIPTION OF THE SURVEYED LANDFILL

### 2.1 General description

This semi-aerobic landfill site is located in the northern part of Hokkaido, Japan (Figure 1). It has been designed following the canyon/depression method, and the waste is filled in multiple lifts (sandwiched method). The area of the landfill is 12.3 ha, and its volume is expected to reach 1,840,000 m<sup>3</sup> over a 27-year period (2003-2030). Each waste type, such as mixed waste, incombustible waste, bottom ash, and fly ash, is placed into the site in different lifts. The operation began in 2003 and is expected to proceed until 2030.

The overall landfill design involves the installation of 73 LFGVPs, classified into three different types, including 9 main gas VPs (M), 59 branch gas VPs (B), and 5 monitoring gas VPs (MH).

Figure 2 shows a typical landfill gas venting pipe in the landfill site. The LFGVP arrangement consists of a 200 mm high-density polyethylene pipe surrounded by a vertical





**FIGURE 1:** Aerial view of the operating semi-aerobic landfill in the northern part of Hokkaido, Japan (in 2003).

gravel layer measuring  $1,200 \times 1,000$  mm. The VP is perforated along its length with small holes measuring 5-10 mm in diameter. The average diameter of the gravel (stone) is 15-20 cm. Wire netting is used to support and embed the vertical gravel layer. The purpose of surrounding the VP with this vertical gravel layer is to (1) protect the VP from deformation due to waste compaction and other external forces, (2) reduce clogging of the perforations on the body of the VP, (3) enable the leachate head to quickly, and (4) create another pathway for ambient air to penetrate waste layers.

Apart from the monitoring LFGVPs, which are not connected to the LCP network, all the LFGVPs (e.g., main LFGVPs and branch LFGVPs) are connected to the LCPs to take the air flow into the waste layers. Currently, 53 of 73 LFGVPs have been installed, including 9 main LFGVPs, 39 branch LFGVPs, and 5 monitoring LFGVPs (Figure 3). The unique structure of the semi-aerobic landfill generates passive aeration because its mechanism is based entirely on the buoyancy effect resulting from the temperature differ-

ence between the waste mass and the outside air. Thus, a negative pressure siphoning effect is created to draw air into the pipes, and air penetrates the waste mass (Matsufuji and Tachifuji, 2007).

The leachate is collected via an LCP network at the bottom of the landfill and is conveyed to the leachate pond (Figure 1). The diameters of the main LCP and branch LCP are 700 and 400 mm, respectively. The average leachate discharge is  $600 \text{ m}^3/\text{day}$ , and the volume of the leachate pond is  $12,700 \text{ m}^3$ . As for the water quality of the leachate, the suspended solids' concentration is less than  $890 \text{ mg/L}$ , and the biochemical  $\text{O}_2$  demand is less than  $1,900 \text{ mg/L}$ . As mentioned above, in addition to collecting leachate, LCPs convey air into the waste layers. Therefore, the main end of an LCP is always open to the atmosphere.

To date, 53 LFGVPs have been installed in the landfill site. Some of these LFGVPs were built when the landfilling began, whereas others have been installed more recently. Currently, the landfill site is divided into two zones: A and B.



**FIGURE 2:** A typical landfill gas venting pipe.

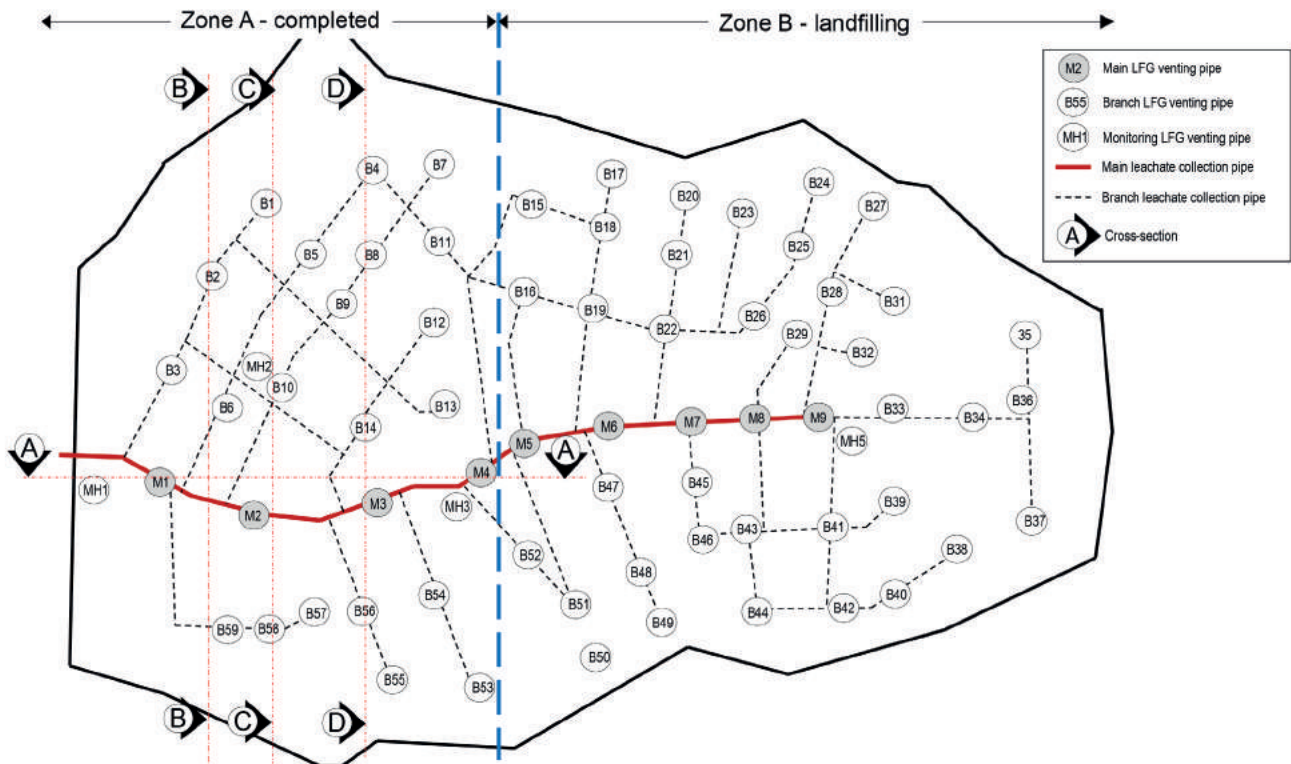
In Zone A, the landfilling operation was completed in 2010 (Figure 3). By 2014, the volume of waste deposited was 730,550 m<sup>3</sup>. Zone A contains 28 LFGVPs (4 main LFGVPs, 21 branch LFGVPs, and 3 monitoring LFGVPs), and the waste mass has reached the designed height. The heights

of the waste at the main gas VPs M1, M2, M3, and M4 are 17.6, 26.6, 30.8, and 33.0 m, respectively. Waste is still being placed in Zone B. Consequently, our analysis focuses on the LFGVPs in Zone A. Figure 4 is the cross-section through some LFGVPs in Zone A and depicts the waste layers buried from before 2005 to 2014. It should be noted that, before 2005, the landfill accepted organic waste because the city's incineration plant could not accept all combustible wastes. However, since 2005, the landfill has accepted only incombustible waste, bottom ash, and fly ash.

Ideally, we should consider all the LFGVPs in Zone A. However, we focus only on measuring the LFG temperature and concentration to identify whether aerobization is occurring within the semi-aerobic landfill. Therefore, the LFGVPs installed in cells containing only bottom ash and fly ash are not considered in this analysis. The monitoring LFGVPs are also not considered in this study because the bottom of these LFGVPs are not connected to the LCPs network and the positions of these LFGVPs are so close to the main LFGVPs or LCPs (i.e., MH2, MH3), the performance of monitoring LFGVPs can be affected by the main LFGVPs.

### 3. METHODS

As shown in Figure 5, the temperature was measured using a thermocouple recorder (Graphtec GL200A, measurement range of thermocouple type T), and the gas component was measured using a portable LFG analyzer (Geotech GA5000, Portable Landfill Gas Analyzer). The analyzer was equipped with a pump working at a sampling rate of 550 mL/min. Typically, a gas sampling tube and a thermom-



**FIGURE 3:** The layout of landfill gas venting pipes and the leachate collection system in the surveyed operating semi-aerobic landfill.

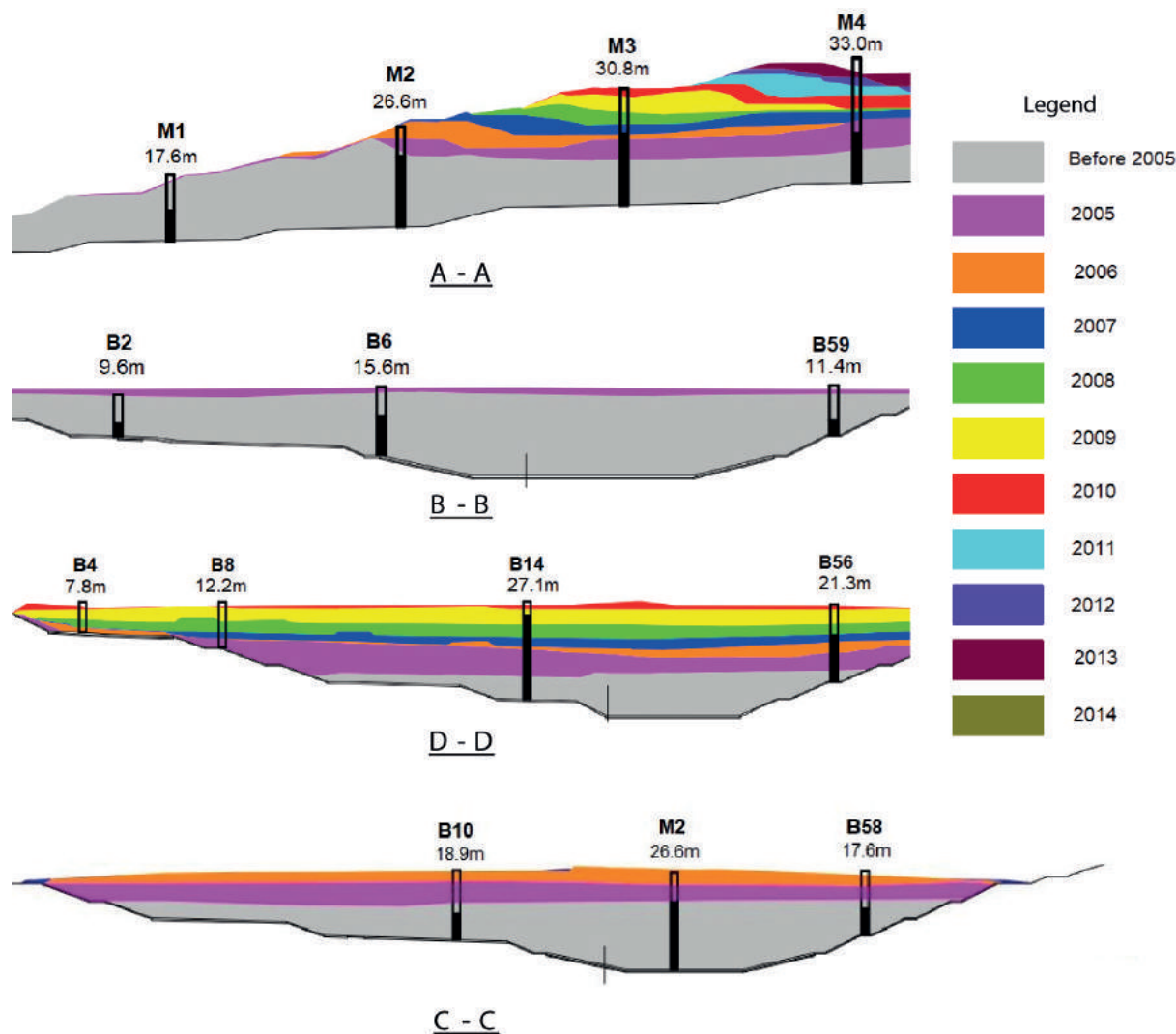


FIGURE 4: Cross-section of waste layers through the landfill gas venting pipes.

eter sensor were lowered into LFGVPs to sample the air at 1-m-depth intervals from ground level, and measurements were recorded after 90 s of sampling. Three different gases – CH<sub>4</sub>, CO<sub>2</sub>, and O<sub>2</sub> – were detected occurring simultaneously. The N<sub>2</sub> content was determined from the balance of CH<sub>4</sub>, CO<sub>2</sub>, and O<sub>2</sub>. The accuracy of the measurement after calibration for CH<sub>4</sub>, CO<sub>2</sub>, and O<sub>2</sub> was ±0.5%, ±0.5%, and ±1%, respectively.

Since 2006, gas temperatures and gas component data have been measured in waste layers aged from 2 years to >11 years. There are movements of air and gases in the gas wells, and the temperatures measured may not fully represent the adjacent waste mass temperatures at a given measurement location. Nevertheless, due to employing a consistent measurement method, these temperature measurements are representative of temperature trends and variations in temperatures due to changing decomposition conditions in the waste mass and have been used in the analysis presented herein (Yesiller et al., 2011).

Carbon monoxide (CO) concentration was also measured by the Portable Landfill Gas Analyzer. The CO concen-

tration was below 30 ppm. Therefore, the concern about the potential for subsurface combustion was not significant in this study (FEMA, 2002).

## 4. RESULTS AND DISCUSSION

### 4.1 Spatial distribution of LFG

Figure 6(a) describes the main LFG components, including CH<sub>4</sub>, CO<sub>2</sub>, O<sub>2</sub>, and N<sub>2</sub>, at the exit of LFGVPs surveyed on September 2013. It can be seen that the CH<sub>4</sub> concentration at the exit of the surveyed LFGVPs is below 10% (blue color), apart from the case of the branch LFGVP B10 (24.4%). Figure 6(b) shows the range of CH<sub>4</sub> concentrations at the exits of the surveyed LFGVPs. Here, we rank the CH<sub>4</sub> concentration using four colors: green represents a CH<sub>4</sub> concentration either less than or equal to 5%, blue represents a concentration greater than 5% and either less than or equal to 10%, yellow represents a concentration greater than 10% and either less than or equal to 20%, and red represents a concentration greater than 20%. Most of the main LFGVPs (M1, M2, M3, and M4) have a CH<sub>4</sub> concentration below 10%, whereas the CH<sub>4</sub> concentration of

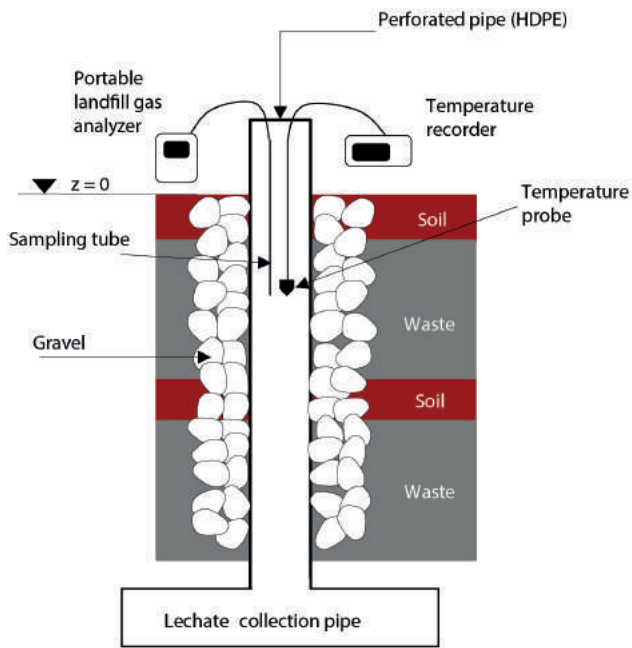


FIGURE 5: LFG temperature and LFG component sampling.

branch LFGVPs ranges from 1.4% (B12) to 24.4% (B10). The ranking map of CH<sub>4</sub> concentration [Figure 6(b)] shows that most of the LFGVPs with high CH<sub>4</sub> concentration are branch LFGVPs (B6, B9, B10, and B13). This could be due to

the branch LFGVPs are far away from the main LCP; the air flow is difficult to move to these branch LFGVPs through the main LCP at the bottom of the landfill.

## 4.2 Influence of the type of gas VPs on LFG concentration and temperature

### 4.2.1 The main gas VP M2

Zone A (landfilling completed) contains four main LFGVPs: M1, M2, M3, and M4. Our analysis focuses on the main gas VP M2, where the height of the organic waste (approximately 20 m) was the largest in the landfill site (see Figure 4).

Figure 7 shows the LFG concentration and temperature and the CH<sub>4</sub>/CO<sub>2</sub> ratio at the exit of the main LFGVP M2. The air temperature fluctuated from -20°C in winter to 25°C in summer. Though the air temperature was always below 0°C in the winter months, the high-temperature trend of LFG remained at >40°C for more than 5 years before declining to 20°C in the most recent observation. This means that there was a continuous active aerobic condition around this LFGVP. Over the observation period, the CH<sub>4</sub>/CO<sub>2</sub> ratio was below 1.0 (from 0.34 to 1.04). This shows that aerobization was active in this LFGVP, and the aerobic condition became dominant. The trend of this ratio increased slightly from the 1,200th day to the 2,450th day (from 2006 to January 2010) from the commencement of the landfilling operation and then declined gradually to less

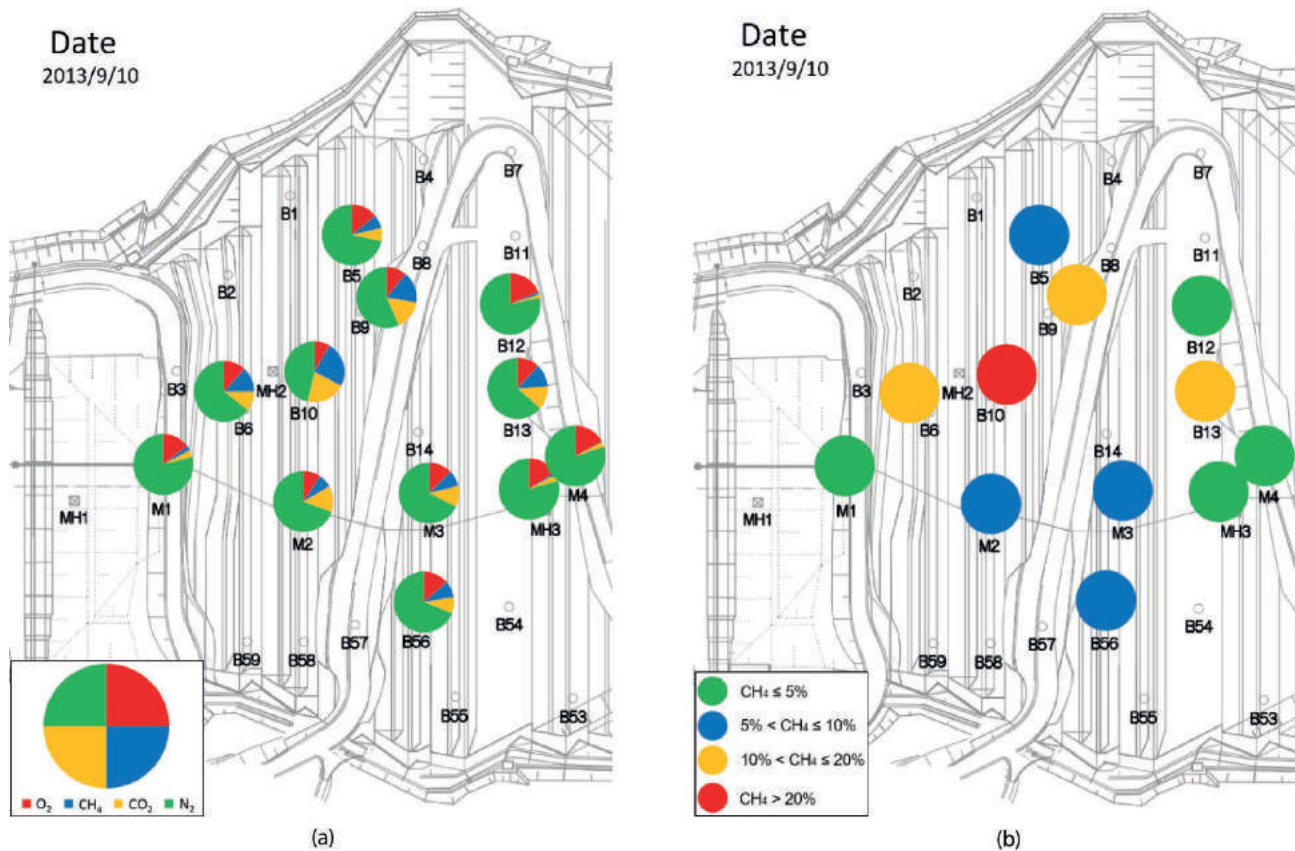


FIGURE 6: (a) Gas components and (b) ranking map of CH<sub>4</sub> concentration at the exit of surveyed landfill gas venting pipes (Zone A) on September 10, 2013.

than 0.5 by the 3,800th day (February 2014). The CH<sub>4</sub> concentration at the exit ranged from 5% to 15%. The CH<sub>4</sub> concentration increased slightly, from 7% to 15%, in the early observation and then decreased gradually to 5%.

The findings reveal that, during the 7 years from December 2006 (3 years after the landfilling operation commenced) to February 2014, the CH<sub>4</sub> concentration of the LFGVP M2 varied from ~7% to ~15% from December 2006 to August 2010 and then declined gradually. This decline may have been due to the gradual disappearance of organic waste. Obviously, the trend of reduction of LFG temperature, CH<sub>4</sub> concentration, and the CH<sub>4</sub>/CO<sub>2</sub> ratio may be useful indicators of the landfill stabilizing.

As the CH<sub>4</sub> concentration data were recorded only at the exits of LFGVPs, the measured CH<sub>4</sub> content could be diluted by air. However, even when we measured the CH<sub>4</sub> and O<sub>2</sub> concentrations since 2010 along the depths of the LFGVP M2, the CH<sub>4</sub> concentration of this LFGVP was always less 20% from 2010 to 2013, and it then declined to below 10% in 2014 (Figure 8(a)).

The CH<sub>4</sub> concentrations were always below 20% at all depths, whereas the O<sub>2</sub> concentrations ranged from ~1% to ~15%. The waste mass at the LFGVP M2 reached the designed elevation of 211 m in 2008. Most of the measurements were obtained in winter (January and February), and the surface of the landfill was covered with a thick lay-

er of snow (the average annual snowfall is around 0.8 m). This meant that it was impossible for air to migrate into the landfill body through the soil cover layers. However, the O<sub>2</sub> concentrations inside the VP fluctuated around 8-15%. During the summer and autumn months (August, September, and October), when there was no snow, the O<sub>2</sub> concentrations dropped to below 5%, and the CH<sub>4</sub> concentrations increased to 20% (Figure 8(a,b)). Such phenomena proved that the semi-aerobic mechanism was functioning. O<sub>2</sub> is supplied into the waste mass from the LCPs at the bottom due to the buoyancy effect, which is a product of the temperature difference between the inside and outside of the landfill, and then it migrates to the waste layers near the LFGVPs. The more the temperature difference increases, the greater the amount of O<sub>2</sub> drawn into the pipe network. As a result, aerobization happens strongly at the waste layers close to the LFGVPs.

The aim of semi-aerobic landfill is to promote aerobic biodegradation of organic wastes within the landfill. To assess the aerobization of the semi-aerobic landfill, LFG temperatures of LFGVPs should be measured. Figure 8(c) depicts the LFG temperature profiles of the main LFGVP M2. The LFG temperatures have been monitored since 2010 (7 years after the landfilling operation commenced).

The main LFGVP M2 showed the highest gas temperature of all the LFGVPs installed in the landfill area. The high-

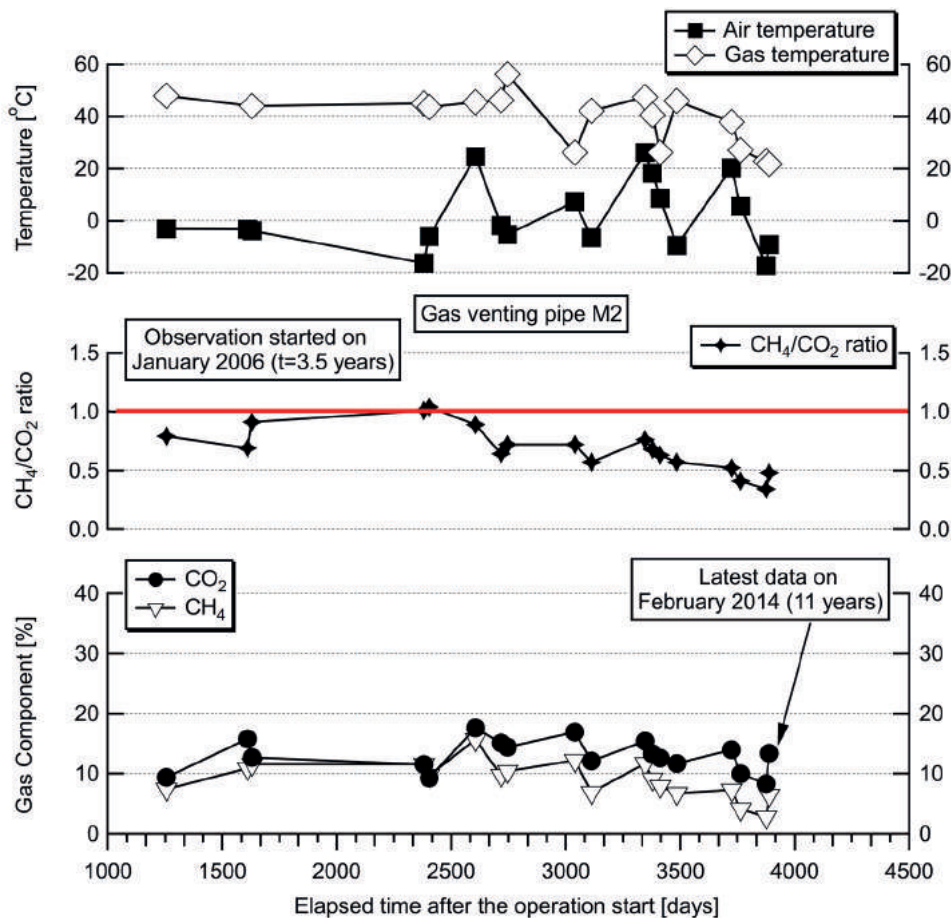
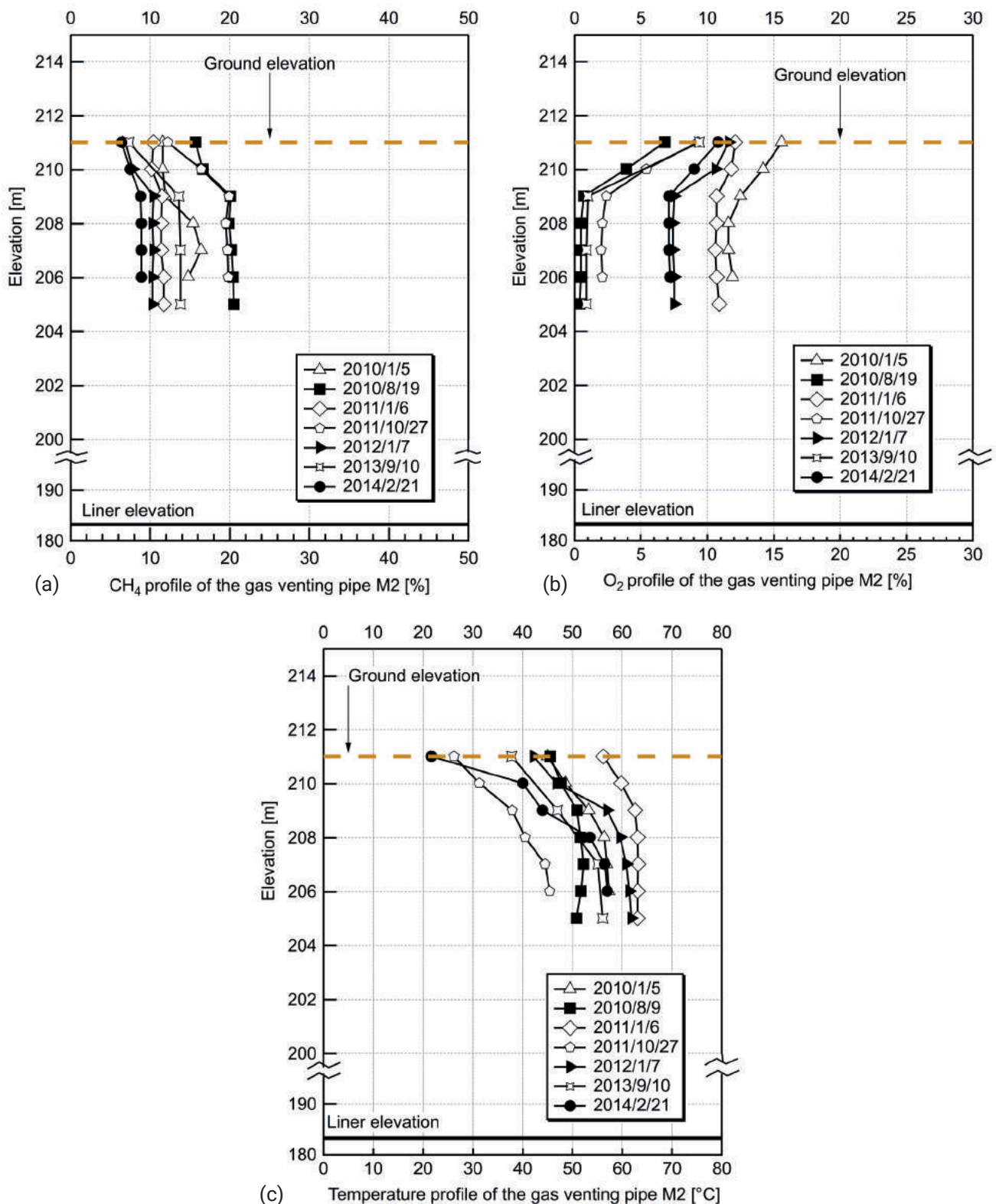


FIGURE 7: Landfill gas concentration and temperature and the CH<sub>4</sub>/CO<sub>2</sub> ratio at the exit of the main landfill gas venting pipe M2.



**FIGURE 8:** (a) CH<sub>4</sub> concentration profile of the main landfill gas venting pipe M1; (b) O<sub>2</sub> concentration profile of the main landfill gas venting pipe M2; (c) Temperature profile of the main LFG venting pipe M2.

est temperature recorded was 63.2°C at -4 m depth in January 2011, and the high-temperature trend continued until 2014. Figure 8(c) also indicates the elevated temperature of above 40°C from January 2010 to 2014. The high temperatures were observed particularly in early January and

February. At that time, it was winter at the study site, and the average daily ambient temperature was from -20°C to -5°C. The temperature difference between the inside and outside of the LFGVP was greater than 60°C (Figure 7). This affirms that the driving force of air flow in the semi-aerobic

landfill increases in winter. Yanase et al. (2010) measured the rate of air flow into the LCP for 1 year and found a high flow rate in winter and no air flow in summer. That explains why our measurements recorded high temperatures in the landfill over the observation period.

#### 4.2.2 The branch gas VP B10

The branch LFGVP B10 is located near the main LFGVP M2. At this location, the height of the waste layers, including organic waste, was ~10 m. However, the average CH<sub>4</sub> concentration of this branch LFGVP was highest (18.9%) among the surveyed LFGVPs.

Figure 9 shows that the gas temperatures at the exits were affected by air temperatures. The LFG temperatures ranged from 7.1°C to 32.4°C. Meanwhile, the CH<sub>4</sub> concentrations ranged from 15% to 38% at the exit during 2,000 days (approximately 6 years) before declining to 0% at the most recent observation. Clearly, the CH<sub>4</sub> concentration of the branch LFGVP B10 was 2–3 times higher than that of the main LFGVP M2 (see Figures 6, 7, and 12).

The ratio of CH<sub>4</sub>/CO<sub>2</sub> ranged from 0.8 to 1.2 for 6 years before decreasing to 0. The fact that the LFG concentration was 0 in the most recent observation could be due to the disappearance of organic waste. In this case, the anaerobic condition could become more dominant than the aerobic condition.

Figure 10(a,b) shows the CH<sub>4</sub> and O<sub>2</sub> concentration profiles of the branch LFGVP B10. The CH<sub>4</sub> concentrations

ranged from 20% to 45%, whereas the O<sub>2</sub> concentrations ranged, approximately, from 0% to 10%. Apart from the measurement obtained in August 2010, the O<sub>2</sub> concentration reached 0% and the CH<sub>4</sub> concentration reached 45%. In other measurements, the CH<sub>4</sub> concentration fluctuated from 20% to 38%, whereas the O<sub>2</sub> concentration ranged from 3% to 10%, and the temperature ranged from 10°C to 30°C [Figure 10(c)]. These indicators reveal that the anaerobic condition became dominant.

Figure 10(c) depicts the temperature profile of the branch LFGVP B10. The highest temperature was 40°C at 0 m depth (at ground elevation) in September 2012, and a high-temperature trend was recorded in August 2010, when the gas temperature ranged from 22°C to 32°C, with the highest value being at ground level. In general, the shape of the gas temperature line of this LFGVP was different from the shape of the temperature line of the LFGVP M2 (see Figure 8). In this case, as the O<sub>2</sub> concentration remained between 3% and 10% inside the LFGVP [Figure 10(b)], it may be that the organic wastes near the LFGVP were exhausted and the CH<sub>4</sub> moved to the LFGVP from distant areas where anaerobic conditions existed.

#### 4.2.3 The average values of the gas temperature, CH<sub>4</sub> concentration and the ratio of CH<sub>4</sub>/CO<sub>2</sub>

Figure 11 shows the average values of the gas temperatures, the CH<sub>4</sub> concentrations, and the CH<sub>4</sub>/CO<sub>2</sub> ratios at the exits of the surveyed LFGVPs (from December 2006 to

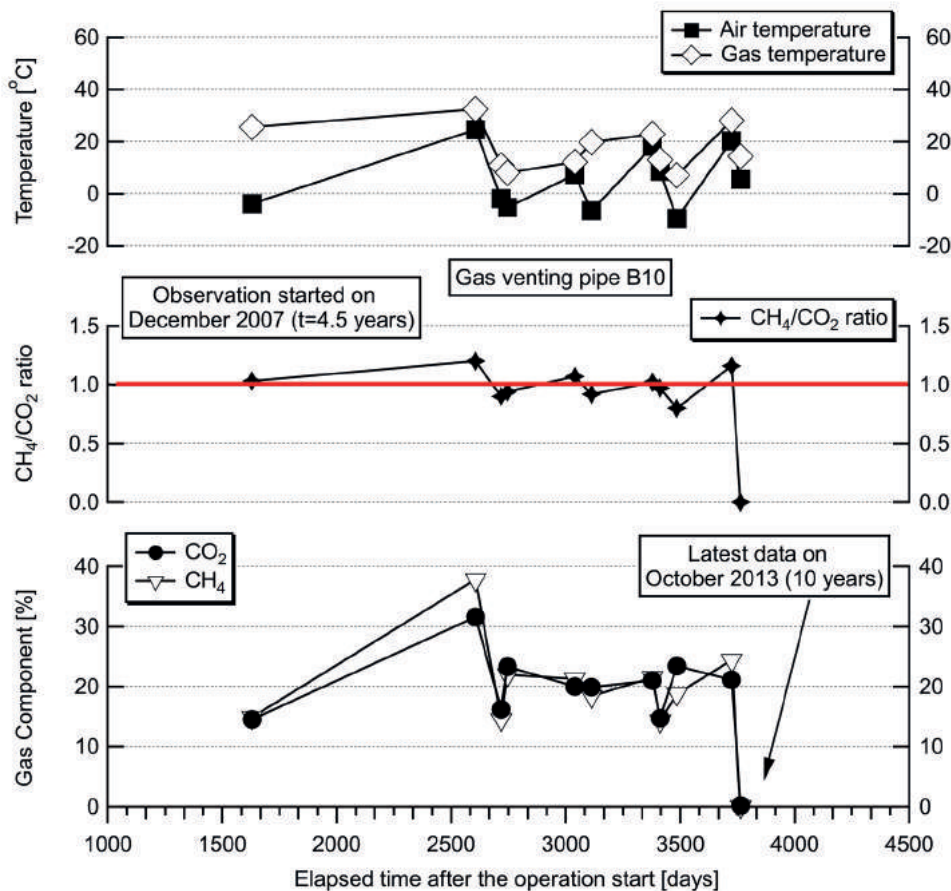
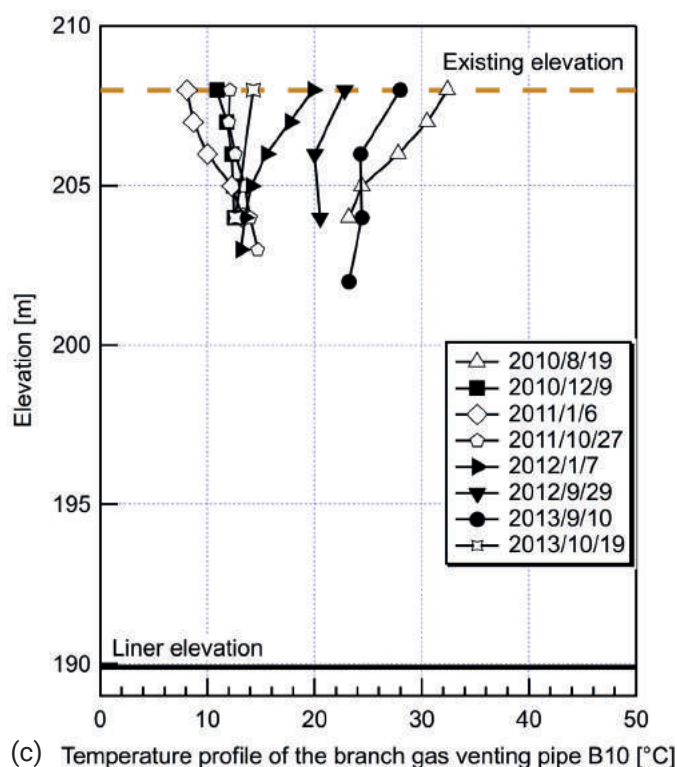
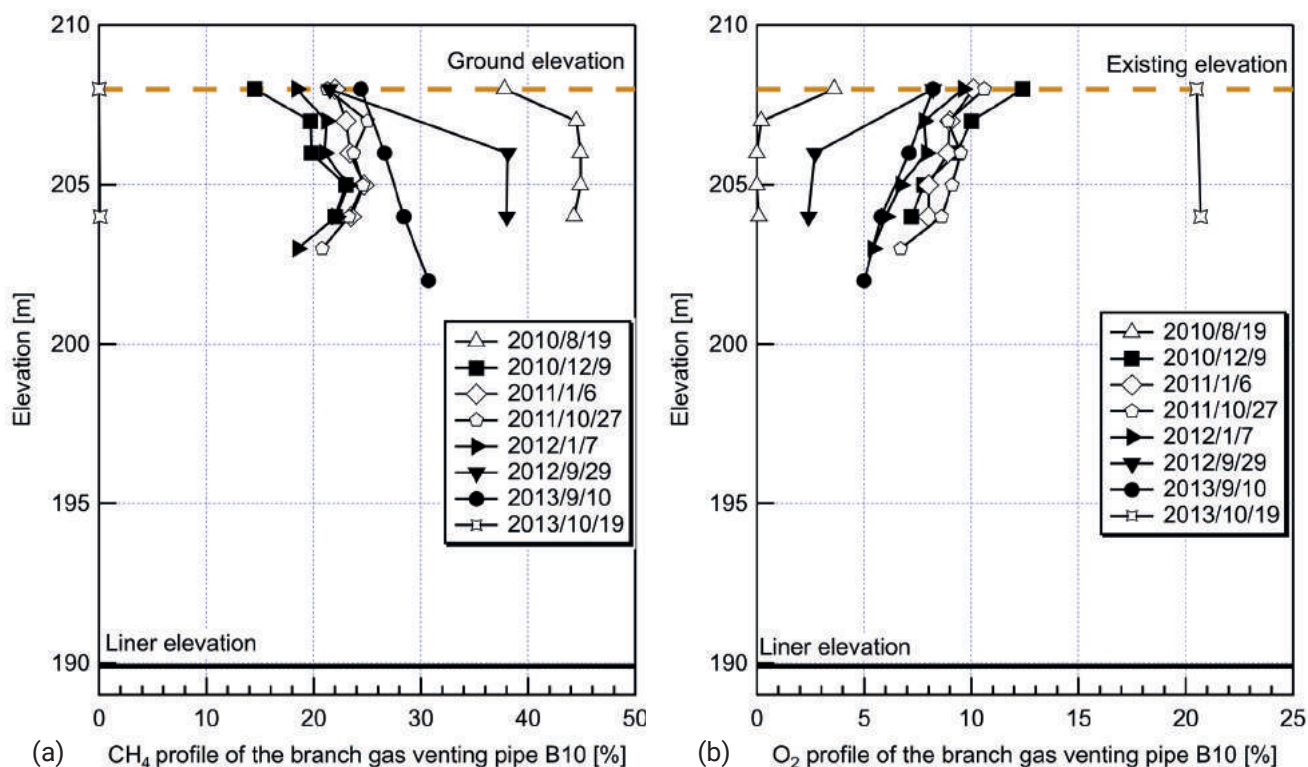


FIGURE 9: Landfill gas concentration and temperature and the CH<sub>4</sub>/CO<sub>2</sub> ratio at the exit of the branch landfill gas venting pipe B10.



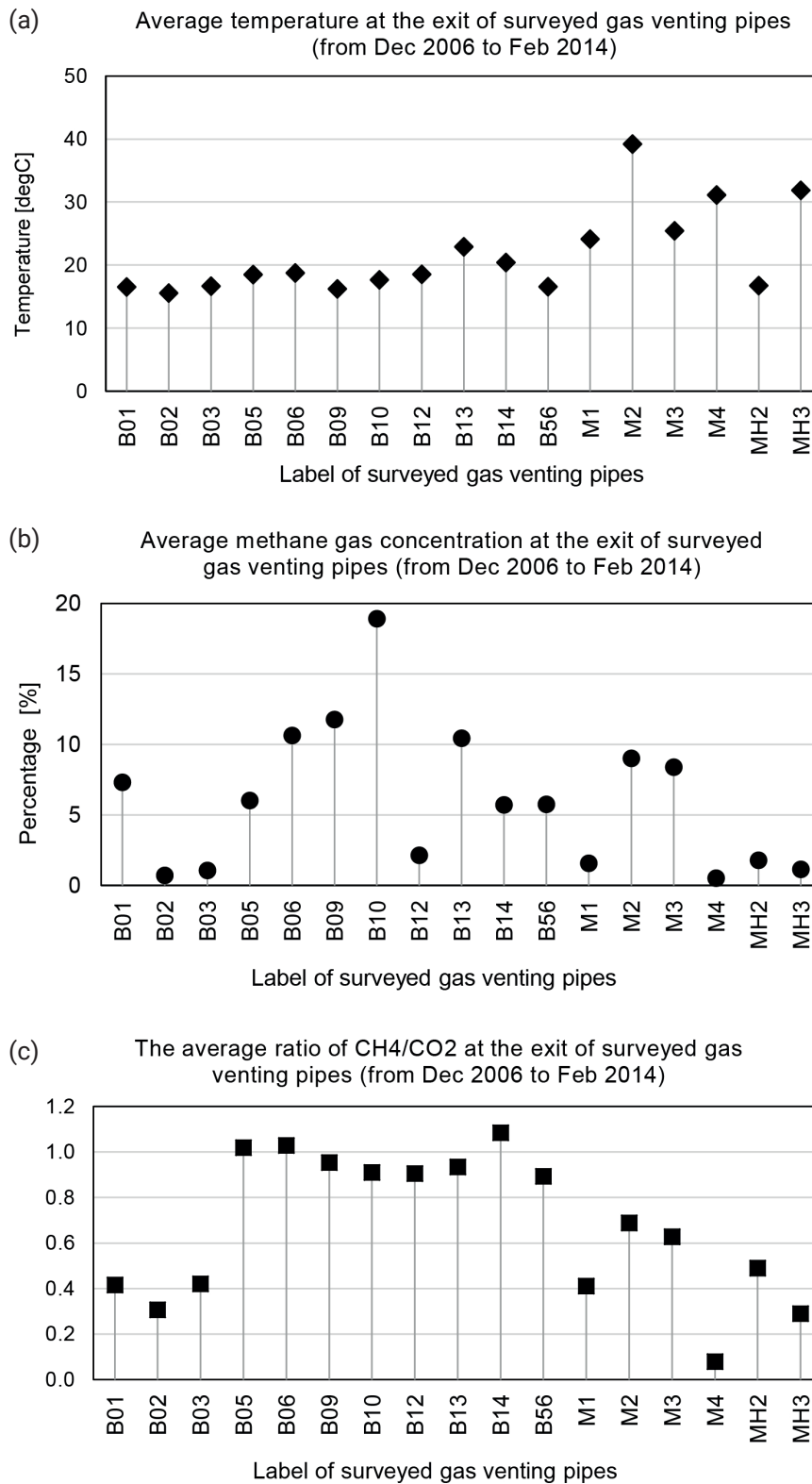
**FIGURE 10:** (a) CH<sub>4</sub> concentration profile of the branch landfill gas venting pipe B10; (b) O<sub>2</sub> concentration profile of the branch landfill gas venting pipe B10; (c) Temperature profile of the branch landfill gas venting pipe B10.

February 2014). The average LFG temperatures of the main LFGVPs (M1, M2, M3, and M4) were higher than those of the branch LFGVPs. The average CH<sub>4</sub> concentrations of the main LFGVPs were below 10%. In particular, the CH<sub>4</sub>/CO<sub>2</sub> ratios of the main LFGVPs were below 0.8, whereas the CH<sub>4</sub>/

CO<sub>2</sub> ratios of the branch LFGVPs ranged from 0.9 to 1.1. This means that there was more effective aerobic biodegradation at the main LFGVPs than that at the branch LFGVPs.

Although the branch LFGVPs B1, B2, and B3 showed average CH<sub>4</sub>/CO<sub>2</sub> ratios of below 0.4 and average CH<sub>4</sub>





**FIGURE 11:** The average values of (a) the gas temperature and (b) CH<sub>4</sub> concentrations and (c) the CH<sub>4</sub>/CO<sub>2</sub> ratio at the exit of the surveyed landfill gas venting pipes during the period from December 2006 to February 2014.

concentrations below 7%, the average LFG temperatures were below 20°C. Thus, it may be that the anaerobic condition was still dominant. Another reason could be due to the amount of organic matter within the waste mass exhausted.

## 5. CONCLUSIONS

In this study, we surveyed several important indicators, including the LFG temperature and concentration and ratio of CH<sub>4</sub> to CO<sub>2</sub>, of an operating semi-aerobic landfill at full

scale. Our observations indicated that the passive aeration happened effectively. The aerobic condition occurred around the main LFGVPs. The highest LFG temperature was over 60°C and remained above 40°C for over 5 years. The average CH<sub>4</sub> concentrations were below 15%. These above analyses also showed that high temperature and the CH<sub>4</sub>/CO<sub>2</sub> ratio less than 1.0 potentially are useful indicators of the type of landfill processes. They can help landfill operators realize the predominance of aerobic biodegradation within the landfill. Oxygen (O<sub>2</sub>) is supplied naturally into the waste mass without the need for a blower, promoting aerobization within the landfill through the buoyancy effect. This leads to reducing significantly the costs of construction and operation. The aerobic biodegradation performance of the branch LFGVPs was not as efficient as the main LFGVPs.

Although our study focuses only on the analysis of LFG components and LFG temperatures, these are useful indicators that can be measured easily on-site to identify the aerobic condition of operating semi-aerobic landfills. Besides analyzing the leachate quality, monitoring the LFG concentration and temperature periodically is required to detect the sudden rise in CH<sub>4</sub> concentrations in semi-aerobic landfills. This monitoring should play a key role in evaluating the passive aeration performance of semi-aerobic landfills.

This paper is the first step in a series of our researches. We will develop the research in further works by conducting the coupling analysis. Next steps, the numerical simulations will be used for modeling the gas production, temperature distribution, gas concentrations and we will compare the numerical simulations with the real data and evaluate the gas and heat transport phenomena within the semi-aerobic landfill.

## ACKNOWLEDGMENTS

The authors would like to thank the Asahikawa Municipality Government and the Yoshino semi-aerobic landfill operation management team for their valuable supports.

## REFERENCES

Ahmadifar, M., Sartaj, M., Abdallah, M., 2016. Investigating the performance of aerobic, semi-aerobic, and anaerobic bioreactor landfills for MSW management in developing countries. *J Mater Cycles Waste Manag* 18, 703–714. <https://doi.org/10.1007/s10163-015-0372-0>

Antonis, M., Haris, K., 2009. The concept of sustainable landfills. Presented at the 2009 World Waste Congress, Lisbon.

ATSDR, 2001. Chapter 2: Landfill Gas Basics. *Landfill Gas Primer, an Overview for Environmental Health Professionals*, pp. 3–14.

Barlaz, M.A., Bryan, F.S., Francis, L.D.L.R.I., 2010. Anaerobic Biodegradation of Solid Waste, in: *Environmental Microbiology*, 2nd Ed. Wiley-Blackwell, Hoboken, New Jersey, pp. 281–300.

Benson, C.H., 2017. Characteristics of Gas and Leachate at an Elevated Temperature Landfill, in: *Geotechnical Frontiers 2017*. Presented at the Geotechnical Frontiers 2017, American Society of Civil Engineers, Orlando, Florida, pp. 313–322. <https://doi.org/10.1061/9780784480434.034>

Bouazza, A., Nahlawi, H., Aylward, M., 2011. In Situ Temperature Monitoring in an Organic-Waste Landfill Cell. *J. Geotech. Geoenviron. Eng.* 137, 1286–1289. [https://doi.org/10.1061/\(ASCE\)GT.1943-5606.0000533](https://doi.org/10.1061/(ASCE)GT.1943-5606.0000533)

Cooney, C.L., Wang, D.I.C., Mateles, R.I., 1969. Measurement of heat evolution and correlation with oxygen consumption during microbial growth. *Biotechnol. Bioeng.* 11, 269–281. <https://doi.org/10.1002/bit.260110302>

Cossu, R., 2012. The environmentally sustainable geological repository: The modern role of landfilling. *Waste Management* 32, 243–244. <https://doi.org/10.1016/j.wasman.2011.11.005>

Cossu, R., 2009. From triangles to cycles. *Waste Management* 29, 2915–2917. <https://doi.org/10.1016/j.wasman.2009.09.002>

Cossu, R., 2005. The Sustainable Landfilling Concept, in: *Proceedings Sardinia 2005*. Presented at the Tenth International Waste Management and Landfill Symposium, 3-7 October 2005, S. Margherita di Pula, Cagliari, Italy, p. 9.

Cossu, R., Morello, L., Raga, R., Cerminara, G., 2016. Biogas production enhancement using semi-aerobic pre-aeration in a hybrid bioreactor landfill. *Waste Management* 55, 83–92. <https://doi.org/10.1016/j.wasman.2015.10.025>

FEMA, 2002. Landfill Fires Their Magnitude, Characteristics, and Mitigation. <https://www.usfa.dhs.gov/downloads/pdf/publications/fa-225.pdf>

Grossule, V., Lavagnolo, M.C., 2017. Innovative Semi-aerobic Landfill Management in Tropical Countries, in: *Proceedings Sardinia 2017*. Presented at the Sixteenth International Waste Management and Landfill Symposium, 2 - 6 October 2017, CISA, S. Margherita di Pula, Cagliari, Italy, p. 14.

Grossule, V., Morello, L., Cossu, R., Lavagnolo, M.C., 2018. Bioreactor Landfills: Comparison and kinetics of the Different Systems. *DETRITUS - Multidisciplinary Journal for Waste Resources & Residues* 03, 100–113. <https://doi.org/10.31025/2611-4135/2018.13703>

Hanashima, M., Yamasaki, K., Kuroki, T., Onishi, K., 1981. Heat and gas flow analysis in semiaerobic landfill. *Journal of the Environmental Engineering Division* 107, 1–9.

Hirata, O., Matsufuji, Y., Tachifuji, A., Yanase, R., 2012. Waste stabilization mechanism by a recirculatory semi-aerobic landfill with the aeration system. *J Mater Cycles Waste Manag* 14, 47–51. <https://doi.org/10.1007/s10163-011-0036-7>

Hrad, M., Gamperling, O., Huber-Humer, M., 2013. Comparison between lab- and full-scale applications of in situ aeration of an old landfill and assessment of long-term emission development after completion. *Waste Management* 33, 2061–2073. <https://doi.org/10.1016/j.wasman.2013.01.027>

Huang, Q., Yang, Y., Pang, X., Wang, Q., 2008. Evolution on qualities of leachate and landfill gas in the semi-aerobic landfill. *Journal of Environmental Sciences* 20, 499–504. [https://doi.org/10.1016/S1001-0742\(08\)62086-0](https://doi.org/10.1016/S1001-0742(08)62086-0)

IPCC, 2006. IPCC guidelines for national greenhouse gas inventories. Prepared by Intergovernmental Panel on Climate Change (IPCC).

Ishigaki, T., Hirata, O., Oda, T., Wangyao, K., Chiemchaisri, C., Towprayoon, S., Lee, D.-H., Yamada, M., 2011. Greenhouse Gas Emission from Solid Waste Disposal Sites in Asia, in: *Integrated Waste Management*. InTech.

Jafari, N.H., Stark, T.D., Thalhamer, T., 2017. Spatial and temporal characteristics of elevated temperatures in municipal solid waste landfills. *Waste Management* 59, 286–301. <https://doi.org/10.1016/j.wasman.2016.10.052>

Jeong, S., Nam, A., Yi, S.-M., Kim, J.Y., 2015. Field assessment of semi-aerobic condition and the methane correction factor for the semi-aerobic landfills provided by IPCC guidelines. *Waste Management* 36, 197–203. <https://doi.org/10.1016/j.wasman.2014.10.020>

Kim, H.-J., Yoshida, H., Matsuto, T., Tojo, Y., Matsuo, T., 2010. Air and landfill gas movement through passive gas vents installed in closed landfills. *Waste Management* 30, 465–472. <https://doi.org/10.1016/j.wasman.2009.10.005>

Martin, J.W., Stark, T.D., Thalhamer, T., Gerbas-Graf, G.T., Gortner, R.E., 2013. Detection of Aluminum Waste Reactions and Waste Fires. *J. Hazard. Toxic Radioact. Waste* 17, 164–174. [https://doi.org/10.1061/\(ASCE\)HZ.2153-5515.0000171](https://doi.org/10.1061/(ASCE)HZ.2153-5515.0000171)

Matsufuji, Y., Kobayashi, H., Tanaka, A., Ando, S., Kawabata, T., Hanashima, M., 1996. Generation of greenhouse effect gases by different landfill types and methane gas control, in: *Proceedings of 7th ISWA International Congress and Exhibition*, Yokohama, Japan. Yokohama, Japan, pp. 230–237.

Matsufuji, Y., Tachifuji, A., 2007. The history and status of semi-aerobic landfills in Japan and Malaysia, in: *Landfill Aeration, IWWG Monograph*. CISA, pp. 109–116.

- Matsuto, T., Zhang, X., Matsuo, T., Yamada, S., 2015. Onsite survey on the mechanism of passive aeration and air flow path in a semi-aerobic landfill. *Waste Management* 36, 204–212. <https://doi.org/10.1016/j.wasman.2014.11.007>
- Morello, L., Raga, R., Lavagnolo, M.C., Pivato, A., Ali, M., Yue, D., Cossu, R., 2017. The S.An.A.® concept: Semi-aerobic, Anaerobic, Aerated bioreactor landfill. *Waste Management* 67, 193–202. <https://doi.org/10.1016/j.wasman.2017.05.006>
- Pirt, S.J., 1978. Aerobic and anaerobic microbial digestion in waste reclamation. *Journal of Applied Chemistry and Biotechnology* 28, 232–236.
- Rees, J.F., 1980. Optimisation of methane production and refuse decomposition in landfills by temperature control. *J. Chem. Technol. Biotechnol.* 30, 458–465. <https://doi.org/10.1002/jctb.503300158>
- Ritzkowski, M., Heyer, K.-U., Stegmann, R., 2006. Fundamental processes and implications during in situ aeration of old landfills. *Waste Management* 26, 356–372. <https://doi.org/10.1016/j.wasman.2005.11.009>
- Ritzkowski, M., Stegmann, R., 2012. Landfill aeration worldwide: Concepts, indications and findings. *Waste Management* 32, 1411–1419. <https://doi.org/10.1016/j.wasman.2012.02.020>
- Shimaoka, T., Matsufuji, Y., Hanashima, M., 2000. Characteristic and Mechanism of Semi-Aerobic Landfill on Stabilization of Solid Waste. Presented at the Intercontinental Landfill Research Symposium.
- Stegmann, R., Ritzkowski, M., 2007. Landfill Aeration, IWWG Monograph. CISA.
- Theng, L.C., Matsufuji, Y., Hassan, M.N., 2005. Implementation of the semi-aerobic landfill system (Fukuoka method) in developing countries: A Malaysia cost analysis. *Waste Management* 25, 702–711. <https://doi.org/10.1016/j.wasman.2005.01.008>
- Wu, X., Yue, B., Huang, Q., Wang, Q., Lin, Y., Zhang, W., Yan, Z., 2017. Spatio-temporal variation of landfill gas in pilot-scale semi-aerobic and anaerobic landfills over 5 years. *Journal of Environmental Sciences* 54, 288–297. <https://doi.org/10.1016/j.jes.2016.09.015>
- Yanase, R., Matsufuji, Y., Michihiro, S., Tashiro, T., Shigeo, N., 2010. Study of the air inflow velocity in the semi aerobic landfill site (in Japanese), in: Proceedings of the 21th Annual Conference of the Japan Society of Material Cycles and Waste Management. <https://doi.org/10.14912/jsmcwm.21.0.260.0>
- Yang, Yangfei, Yue, B., Yang, Yu, Huang, Q., 2012. Influence of semi-aerobic and anaerobic landfill operation with leachate recirculation on stabilization processes. *Waste Manag Res* 30, 255–265. <https://doi.org/10.1177/0734242X11413328>
- Yesiller, N., Hanson, J.L., Yee, E.H., 2015. Waste heat generation: A comprehensive review. *Waste Management* 42, 166–179. <https://doi.org/10.1016/j.wasman.2015.04.004>
- Yesiller, N., Hanson, J.L., Yoshida, H., 2011. Landfill Temperatures under Variable Decomposition Conditions, in: *Geo-Frontiers 2011*. Presented at the Geo-Frontiers Congress 2011, American Society of Civil Engineers, Dallas, Texas, United States, pp. 1055–1065. [https://doi.org/10.1061/41165\(397\)108](https://doi.org/10.1061/41165(397)108)
- Yoshida, H., Rowe, R.K., 2003. Consideration of Landfill Liner Temperature, in: *Proceedings Sardinia 2003*, Presented at the Ninth International Waste Management and Landfill Symposium, 6-10 October, CISA, Environmental Sanitary Engineering Centre, Italy, S. Margherita di Pula, Cagliari, Italy.
- Zhang, X., Matsuto, T., 2013. Assessment of internal condition of waste in a roofed landfill. *Waste Management* 33, 102–108. <https://doi.org/10.1016/j.wasman.2012.08.008>

# OPTIMISED MANAGEMENT OF SEMI-AEROBIC LANDFILLING UNDER TROPICAL WET-DRY CONDITIONS

Valentina Grossule \* and Maria Cristina Lavagnolo

DICEA, Department of Civil, Architectural and Environmental Engineering, University of Padova. Via Marzolo 9, 35131 Padova, Italy

## Article Info:

Received:  
19 September 2019  
Revised:  
22 December 2020  
Accepted:  
21 January 2020  
Available online:  
5 March 2020

## Keywords:

Developing countries  
Semi-aerobic landfill  
Tropical climate  
Sustainable landfill  
Landfill bioreactor

## ABSTRACT

The processes involved in semi-aerobic landfills are heavily influenced by local climate conditions and waste composition. In particular, when considering rainfall seasonality in a tropical climate, the lack of moisture during the dry season and heavy rainfalls during the wet season may negatively affect biodegradation processes and landfill emissions. The aim of the present study was to investigate the performance of semi-aerobic landfill under tropical dry-wet climate conditions and to assess the potential benefits afforded by appropriate management of water input when operating the landfill by overlaying a new layer of waste in each climate season. Six lab-scale lysimeters were operated in two phases to reproduce, on two subsequent waste layers, a sequence of dry and wet tropical seasons: two with an initial dry phase, two with an initial dry phase under controlled watering and two with an initial wet phase, during which leachate was stored to allow recirculation during the subsequent dry phase. In each pair of lysimeters one was filled with low putrescible content waste and the other with high putrescible content waste. Although appropriate management of water input significantly improved landfill performance under dry climate conditions, the overlaying of a new layer of waste in each climate season played a fundamental role in ensuring good stabilisation over the one year simulation period; following stabilisation, the landfill bottom layer acts as an internal attenuating biological filter. In particular, under initial dry conditions, final BOD COD and ammonia values detected were below 20mgO<sub>2</sub>/L, 200mgO<sub>2</sub>/L, and 30mgN/L, respectively.

## 1. INTRODUCTION

The role of landfilling in modern waste management strategies is based on two concepts: environmental sustainability and sinking of elements (Cossu and Stegmann, 2018). Sustainability can be achieved by means of a combination of different technologies, including semi-aerobic landfilling. Semi-aerobic landfill is considered a cost-effective technology with huge application potential in Developing Countries (DCs), where the technical and economic resources are limited. This method is based on a specific design, which promotes the passive natural aeration of waste mass through a temperature difference present between landfill waste mass and external ambient. The design is aimed at reproducing an aerobic environment within the waste mass accelerating stabilisation, whilst avoiding typical operational costs linked to air injection/biogas management. The achievable benefits of semi-aerobic landfilling have been confirmed by several studies (i.a. Grossule et al., 2018; Ahmadifar et al., 2016; Aziz et al., 2010) and include: improvement of carbon and nitrogen degradation rate due to the aerobic processes, reduction of methane

generation and increased carbon gasification rate. Several full-scale semi-aerobic landfills are operating throughout the world, both in industrialised (e.g. Japan, Italy) and developing countries (China, Iran, Malaysia, Pakistan, Samoa, Vietnam) (Matsufuji et al., 2018), however controversial issues relating to leachate generation and management have been raised when operating under tropical climate conditions (Kortegast et al., 2007; Malek and Shaaban, 2008).

Landfill stabilisation in fact is heavily influenced by specific local climate conditions and composition of landfilled waste. The key factors controlling the stabilisation processes in a semi-aerobic landfill are water availability and putrescible organic content of landfilled waste, which may fluctuate considerably according to geographical position and socio-economic condition (Grossule and Lavagnolo, 2019). Water availability is fundamental for the biodegradation processes to promote the removal of soluble non-degradable contaminants; however, excessive water availability interferes with advective air flow promoting anaerobic processes. The putrescible fraction in waste is responsible for the main environmental impacts deriving

\* Corresponding author:  
Valentina Grossule  
email: valentina.grossule@phd.unipd.it

from landfilling (methane and CO<sub>2</sub> emissions, emissions of carbon and nitrogen contaminants in leachate, odours, risks of fires, etc.). Impacts are mitigated through the promotion of aerobic stabilisation processes in semi-aerobic landfill, although high putrescible waste content may potentially reduce the advective circulation of air, enhancing anaerobic processes and negatively influencing the quality of the gas released into the atmosphere.

A previous study (Grossule and Lavagnolo, 2019) investigated the stabilization performance of semi-aerobic landfill under conditions of different water availability and putrescible waste content.

The results of the study demonstrated that low water availability limits biodegradation processes in the presence of low putrescible content waste, while high water availability and high putrescible content waste results in anaerobic processes negatively affecting the quality of biogas and leachate emissions. Proper management of water input proved to be an effective solution in improving landfill performance.

Tropical climate, which affects the majority of DCs, poses significant challenges for a proper semi-aerobic landfill management, alternating extreme rainfall conditions. In particular, according to the Kopper Geiger climate classification, the specific Savanna tropical climate (Aw), which represents the second most diffuse climate worldwide, is characterized by alternating dry (little or no precipitation) and wet seasons (heavy precipitations) (Chen and Chen, 2013; Kottek et al., 2006).

To overcome the negative impacts of rainfall seasonality on semi-aerobic landfill performance, Lavagnolo et al. (2018) proposed a dual-step management consisting in the storage of excess leachate during the wet season, and subsequent recirculation during the dry season to enhance biodegradation activity and perform an in-situ leachate treatment. Compared with anaerobic conditions, the results obtained were extremely positive leading to a more rapid and intense biological stabilisation of the waste mass.

The goal of this study was to investigate, using lab scale lysimeters, performance of a semi-aerobic landfill under tropical wet and dry climate conditions and to assess the potential benefits afforded by appropriate management of water input when operating the landfill by overlaying a new layer of waste in each climate season. In particular, given the relevance of water availability, the initial phase of the semi-aerobic landfill related to the specific climate season (wet or dry) was specifically considered.

The following three paradigmatic conditions were studied:

- Initial phase during the dry season, without any external water addition;
- Initial phase during the dry season, with controlled water addition;
- Initial phase during the wet season, with storage of leachate for subsequent recirculation during the dry phase.

These initial conditions are identical to those adopted in a previous study by the same Authors (Grossule and Lavagnolo, 2019).

The paper aims to provide an answer to the following

question: "How would alternate landfilling phases under different climatic conditions (wet-dry), with and without proper water input control, influence the landfill behaviour in terms of stabilisation, long-term emissions of leachate and biogas, and general operational issues?".

## 2. MATERIALS AND METHODS

### 2.1 Research program

Six lab-scale lysimeters were operated in two phases to reproduce, on two subsequent waste layers, a sequence of dry and wet tropical seasons: two with an initial dry phase (D), two with an initial dry phase under controlled watering (D') and two with an initial wet phase, during which leachate was stored to allow for subsequent recirculation during the dry phase (W). In each pair of lysimeters one was filled with low putrescible content waste (LP) and the other with high putrescible content waste (HP). Following the initial phase, represented by the results reported previously by the same Authors (Grossule and Lavagnolo, 2019), a second phase was simulated by adding to the previously used lysimeters a second layer of fresh waste under alternating climate conditions.

The research programme is graphically illustrated in Figure 1.

### 2.2 Waste samples

Two different types of waste were tested, reproducing Municipal Solid Waste (MSW) with Low Putrescible (LP) and High Putrescible (HP) content. LP waste, yielding a 9% wet weight of kitchen wastes, consisted in residual waste from MSW source segregation and separate collection, and it was sampled at the gate of the Legnago (Verona, North Italy) waste treatment facilities. HP waste was obtained by mixing LP waste with source segregated kitchen waste in order to achieve a 50% w/w ratio. Kitchen waste was sampled at the gate of Sesa (Padova, North Italy) composting plant.

The composition of the waste used in the two different experimental phases and the main analytical parameters are reported in Table 1.

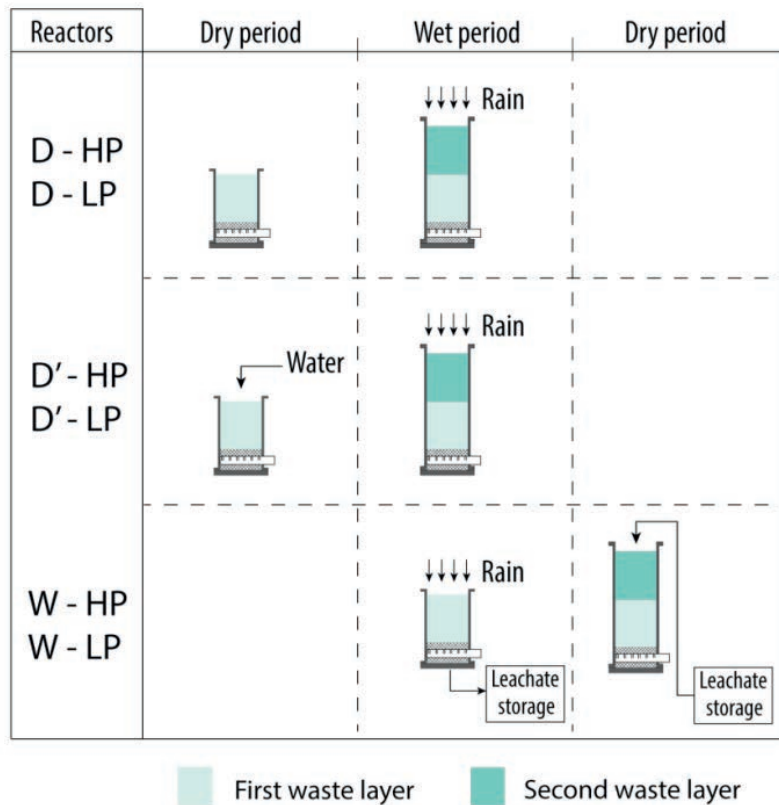
### 2.3 Equipment

The experiment was carried out using six cylindrical Plexiglass lysimeters (1.0 m height, inner diameter of 40 cm). Each column was equipped at the bottom with a slotted pipe (8 cm diameter), open to the air.

A 20 cm layer of gravel (size 16-32 mm) was placed at the bottom of lysimeters to allow leachate drainage and facilitate air circulation. Gas sampling valves were fitted laterally, while leachate was collected at the bottom of each column. Columns were thermally insulated by a coating system made of polyethylene. Temperatures in each column were monitored by means of thermocouples (Thermo Systems TS100).

A perforated plate placed at the top of each column allowed uniform water irrigation.

Following operations for the first phase (Grossule and Lavagnolo, 2019), columns were lengthened by flanging an additional cylinder section in order to perform the second phase (Figure 2).



**FIGURE 1:** Research programme. (According to the first simulated season: D=Dry conditions, D'=Dry conditions with controlled watering, W=Wet conditions. According to tested waste type: HP= High putrescible content waste; LP=Low putrescible content waste).

Reactors were operated in a thermally controlled room.

## 2.4 Methodology

The experiment lasted approximately 6 months, divided into two subsequent phases (0-108th day and 109-216th day), to reproduce, by controlling the Liquid/Solid ratio, one year landfill operation in around six months. The lab scale

operative conditions (temperature, waste granulometry, density, height of the waste layer, etc.) assure accelerated processes compared to the full scale.

Six lysimeters were operated, each reproducing both a dry and a wet tropical season: two with an initial dry phase (D), two with an initial dry phase under controlled watering (D') and two with an initial a wet phase, with storage of

**TABLE 1:** Composition of the different types of waste (LP, HP) tested during the first and second phases. (LP= Low Putrescible waste, HP=High Putrescible waste).

		First phase		Second phase	
		LP	HP	LP	HP
Categories	Paper and paperboard (%)	19.9	11.0	17.9	9.9
	Plastics (%)	17.5	9.6	17.4	9.6
	Metals (%)	1.9	1.1	1.8	1.0
	Aggregates (%)	9.6	5.3	14.1	7.8
	Textiles (%)	2.1	1.2	1.8	1.0
	Glass and inerts (%)	8.9	4.9	8.1	4.5
	Kitchen residues (%)	9.2	50.0	9.4	50.0
	Green and wooden materials (%)	3.1	1.7	2.4	1.4
	Under-sieve (20 mm) (%)	27.7	15.3	27.0	14.9
Characterization	Waste mass (kg)	27	27	27	27
	TS (%)	56.9	39.5	56.3	37.9
	VS (%TS)	72.7	84.4	70.5	74.5
	TOC (%TS)	34.5	40.3	30.2	35.4
	RI <sub>4</sub> (mgO <sub>2</sub> /gTS)	38.4	93.3	26.7	6.4

leachate for subsequent recirculation during the dry phase (W). In each pair of lysimeters one was filled with low putrescible content waste (LP) and the other with high putrescible content waste (HP).

The columns were filled with 27 kg waste at the beginning of the first phase, with addition of a further 27 kg at the beginning of the second phase. An approximate initial compaction of 0.5 kg/L was achieved. A 5 cm layer of gravel was placed on top of both waste layers to ensure uniform water irrigation.

Environmental temperature values in the testing room were varied and maintained between 18°C and 30°C to reproduce the night/day cycle, producing a significant influence on the temperature gradient between the waste mass and the external ambient temperature, and thus natural air circulation.

During the wet phase a distilled water input of 3 L/d was adopted in all columns to simulate rainfall and reproduce water infiltration corresponding to a yearly mean precipitation of 1400 mm. This corresponded to a liquid to solids ratio (L/S) of 20.5 and 14.4 L/kgTS in columns with HP waste and LP waste, respectively. During the dry phase, no water was added to D columns, reproducing dry climate conditions. Conversely, in D' and W columns a hydraulic load of 0.25 L/d was added during the dry phase to reproduce optimal water availability for biodegradation, achieving a final L/S ratio of 2.2 and 1.6 L/kgTS in columns with HP waste and LP waste, respectively, as suggested by Lavagnolo et al. (2018). Hydraulic load was achieved by means of water irrigation in D' columns, and by recirculating leachate stored during the wet phase, in W columns.

During the experimental test, solid, liquid, and gas samples were analysed according to International Standard Methods. Biogas concentrations of CO<sub>2</sub>, CH<sub>4</sub> and O<sub>2</sub> were

monitored daily using an Eco-Control LFG20 analyser.

At the beginning and end of both phases, waste was sampled from each reactor (approx. 100g, from the top at the end of first phase and by emptying the lysimeters at the end of the second phase). The following parameters were measured: 4-day Respirometric Index (RI4), Total Carbon (TC), Total Organic Carbon (TOC), Total Kjeldahl Nitrogen (TKN), TS and VS. TC and TOC on solid samples were determined using a TOC-VCSN Shimadzu Analyzer. RI4 was measured using a SaproMat respirometer (H+P Labortechnik, Germany).

pH, alkalinity, TS and VS, volatile fatty acids (VFA), chemical oxygen demand (COD), TC and TOC, five-day biochemical oxygen demand (BOD5), nitrogen compounds (TKN, ammonia, nitrate, nitrite) and chlorides, were regularly analysed in leachates (once/twice weekly).

### 3. RESULTS AND DISCUSSION

#### 3.1 Temperatures

Figure 3 illustrates the temperature values and water availability over time for all tested columns, referred to the fresh waste layers in the two experimental phases.

Water availability can be defined as follows (1):

$$wa = ew + L/S = u \cdot (\text{kg waste}) / (\text{kg TS}) + L/S \quad (1)$$

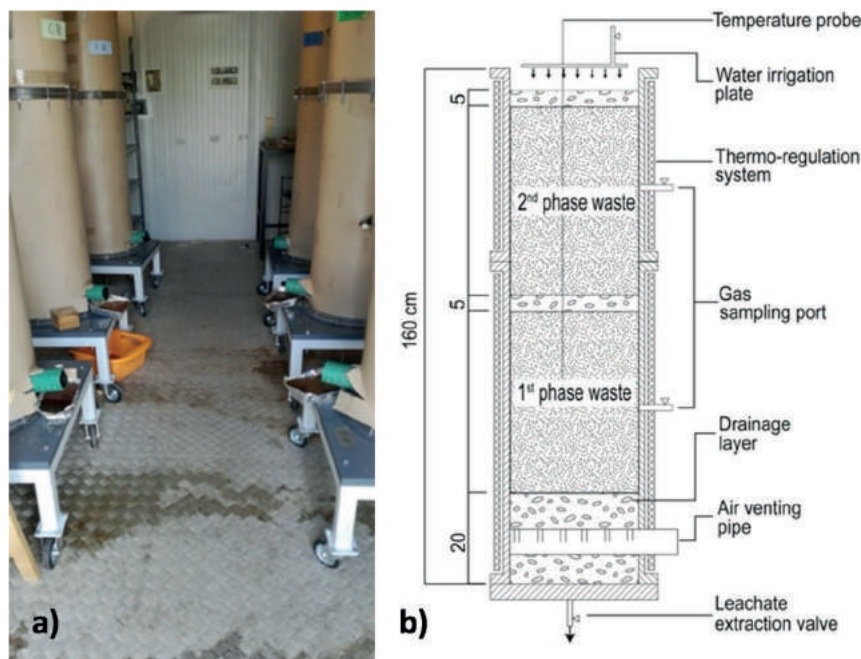
Where:

wa: water availability (kgH<sub>2</sub>O/kg TS)

ew: endogenous water (kgH<sub>2</sub>O/kg TS) =  $u \cdot (\text{kg waste}) / (\text{kg TS})$

L/S: liquid (input water) over solid ratio (kgH<sub>2</sub>O/kg TS) in a given time.

u: moisture in waste to be landfilled (kgH<sub>2</sub>O/kgwaste).



**FIGURE 2:** Set up of the semi-aerobic landfilling reactors (a) and constructive details of the individual reactors (b). The lengthening of columns to enable conduction of the second research phase is indicated.

Generally, in all test columns temperature values were in line with the degradation processes, registering higher values at the start, which gradually decreased over time.

Temperatures were generally higher in columns containing low putrescible waste (LP) under dry climate conditions. The highest values (58°C) were observed in the first phase in the D-LP Column (Low putrescible under dry conditions) and in the second phase in the W-LP column in the new layer added under dry conditions.

The results obtained suggested that the higher the water availability (endogenous waste moisture + water input), the lower the temperatures. In particular, high water availability results in heat loss in water evaporation and in prevailing of anaerobic processes, with slower exothermic reactions compared to the aerobic processes. It is confirmed by the quality of the biogas (Figure 4): increased water availability due to excess external addition of water negatively influenced natural air advection, resulting in reduced aerobic oxidative processes, and consequently lower temperature values. During the first phase, temperature values remained higher than ambient values over a lengthier period of time compared to the second phase. This should be ascribed to the different putrescible content of the waste (RI4 values in HP columns were 93 and 63 mgO<sub>2</sub>/gTS for the 1st and 2nd phase, respectively, while for LP were 38 and 27 mgO<sub>2</sub>/gTS).

### 3.2 Landfill Gas (LFG) composition

Volumetric percentages of the most significant LFG components (CH<sub>4</sub>, CO<sub>2</sub> and O<sub>2</sub>) are represented in the

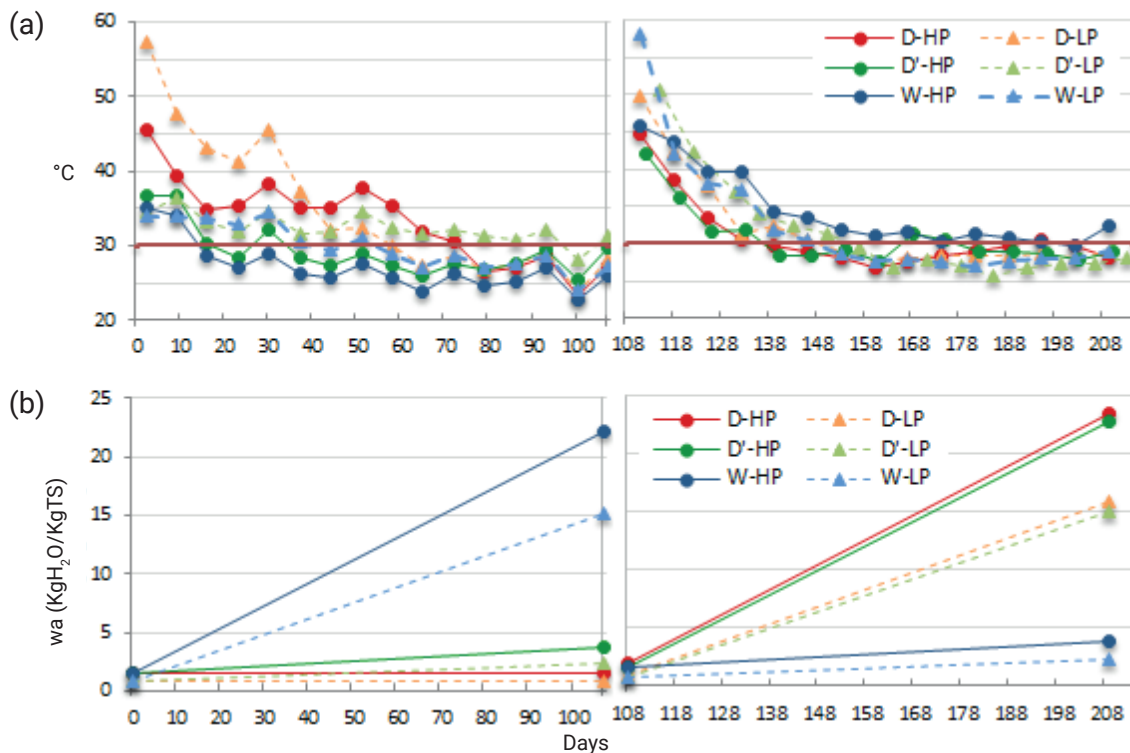
stacked area chart in Figure 4, together with stability values measured at the beginning and end of each individual phase.

At the beginning of all individual phases, aerobic conditions elicited rapid degradation of the readily-biodegradable fractions, depletion of oxygen (<5%) and a consequent high production of CO<sub>2</sub>.

During the first phase gas composition, decrease in CO<sub>2</sub> concentrations and final waste stability (RI4 values) were driven by waste type and water availability. In particular, the combination of high putrescible waste and high water availability resulted in anaerobic effects and limited waste stabilisation (D'-HP, W-HP), while low putrescible waste and high water availability resulted in flushing effect and promoted high contaminant mobility (W-LP); low water availability halted the biodegradation processes (D-LP).

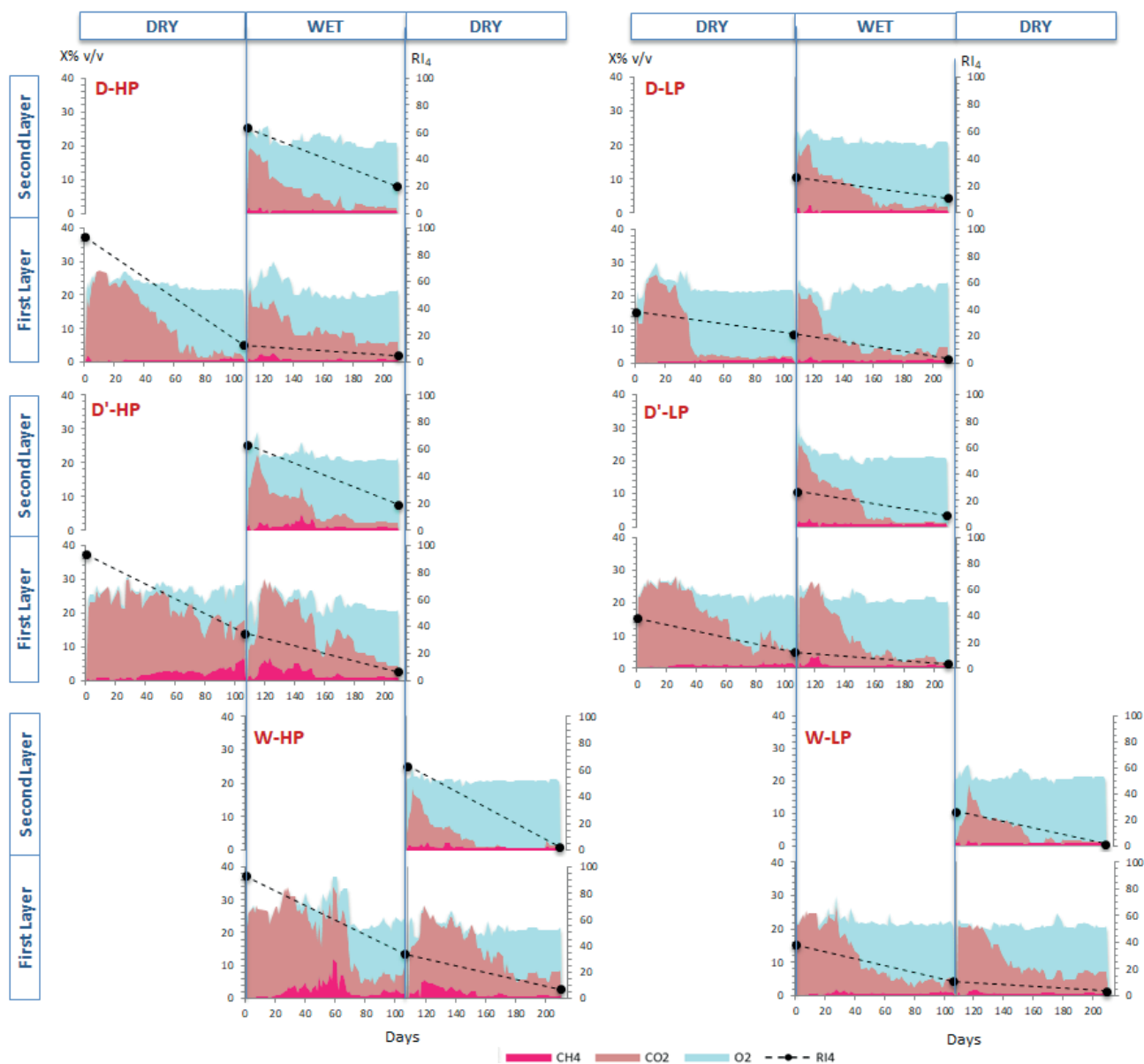
Proper water availability management and the proportioning of endogenous water (naturally present in putrescible fraction) and water input, significantly improved landfill performance (D'-LP, D-HP).

During the second phase, water input (simulated rainfall infiltration for D and D' columns; leachate recirculation for W column) moved the soluble putrescibles from the fresh waste layer to the bottom layer, provoking rising concentrations of CO<sub>2</sub> and decreasing RI4 values in the bottom layer. RI4 values remained constantly below 12 mgO<sub>2</sub>/g TS and the lowest values (6-7 mgO<sub>2</sub>/g TS) were observed for all LP columns and for the column with High Putrescible waste under dry climatic conditions (D-LP). This suggested that during the 2nd phase the first layer in all columns com-



**FIGURE 3:** Temperature values (a) and water availability (b) in the layers of fresh waste in the first and second phase for all testing columns. The highest environmental temperature is illustrated in the temperature chart with a red line (30°C) (D=Dry conditions, D'=Dry conditions with controlled watering; W=Wet conditions, HP=Waste with high putrescible content; LP=Waste with low putrescible content).





**FIGURE 4:** Landfill gas (LFG) composition (Stacked area chart) and waste stabilisation in the lysimeters, over testing time. (X% v/v: volumetric gas fractions; RI4: 4 days Respirometric Index, mgO<sub>2</sub>/kgTS). Nitrogen gas is not represented. RI4 values are only referred to the beginning and end of each individual phase; the line connecting these values is only indicative to facilitate reading. (D=Dry conditions, D'=Dry conditions with controlled watering; W=Wet conditions, HP=Waste with high putrescible content; LP=Waste with low putrescible content).

pleted the stabilisation processes and became a bottom layer, acting as a sort of internal Biological Filter for leachate from the new layer of fresh waste. On the other hand, the second waste layer (fresh waste) achieved good stabilisation values, below 20 mgO<sub>2</sub>/g TS, which was particularly low in W columns under controlled water input, with values around 3 mgO<sub>2</sub>/g TS compared to D and D' columns under wet conditions.

In general, input of excess water results in initial saturated condition which limits air circulation and promotes anaerobic processes witnessed by an increase in CH<sub>4</sub> concentration (particularly in case of high putrescible waste); later on the flushing effect reduces the presence of putrescible in the waste mass, allowing consequently an increase in the oxygen concentration.

Methane generation occurred mainly with HP waste, particularly in the presence of high water availability, achieving the highest methane concentrations (up to 10%) in W-HP column during the first wet phase.

### 3.3 Leachate quality and quantity

In all columns during the 2nd phase leachate generation ranged between 70-80%(wa), with the exception of the column with leachate recirculation and high putrescible waste (W-HP) where over 100%(wa) was reached.

Leachate produced during the 2nd phase was collected from the bottom of the columns and analysed. The results were compared with those obtained in the first phase.

COD and BOD concentrations in leachate during the test period are illustrated in the stacked area chart of Fig-

ure 5, jointly with BOD/COD ratio trend, while Total Organic Carbon (TOC), Volatile fatty acids (VFA) are represented in Figure 6.

The above-mentioned Biological Filter effect of the bottom layer during second phase is clearly evident from the behaviour of all parameters. In particular, the concentrations achieved for all parameters during the wet phase were much lower in D and D' columns (during the second phase) compared to those achieved in W columns, in which the wet phase coincided with the first phase. The same considerations are valid for the dry phase, when not considering D columns in which no/limited leachate generation occurred. Final BOD values in leachate were comprised between 5-20 mg/L, while COD values were around 200 mg/l. Only in W columns, BOD and COD values after 200 days, were respectively 20 and 790 mg/L in W-HP and 5 and 510mg/L in W-LP, corresponding to negligible values from an environmental point of view (D.G.R. 2461/14, reference legislation).

Similar behaviour was displayed by TOC, which remained around 50-60 mg/l in all columns, with the exception of W columns. In particular, 280 and 200 mgC/L were detected in columns with High putrescible and Low putrescible waste, respectively.

The ratio of VFA/TOC in the second phase remained generally low, averaging around 0.1-0.5 mg CH<sub>3</sub>COOH/mg C (Figure 7a). This aspect, together with the evident stabil-

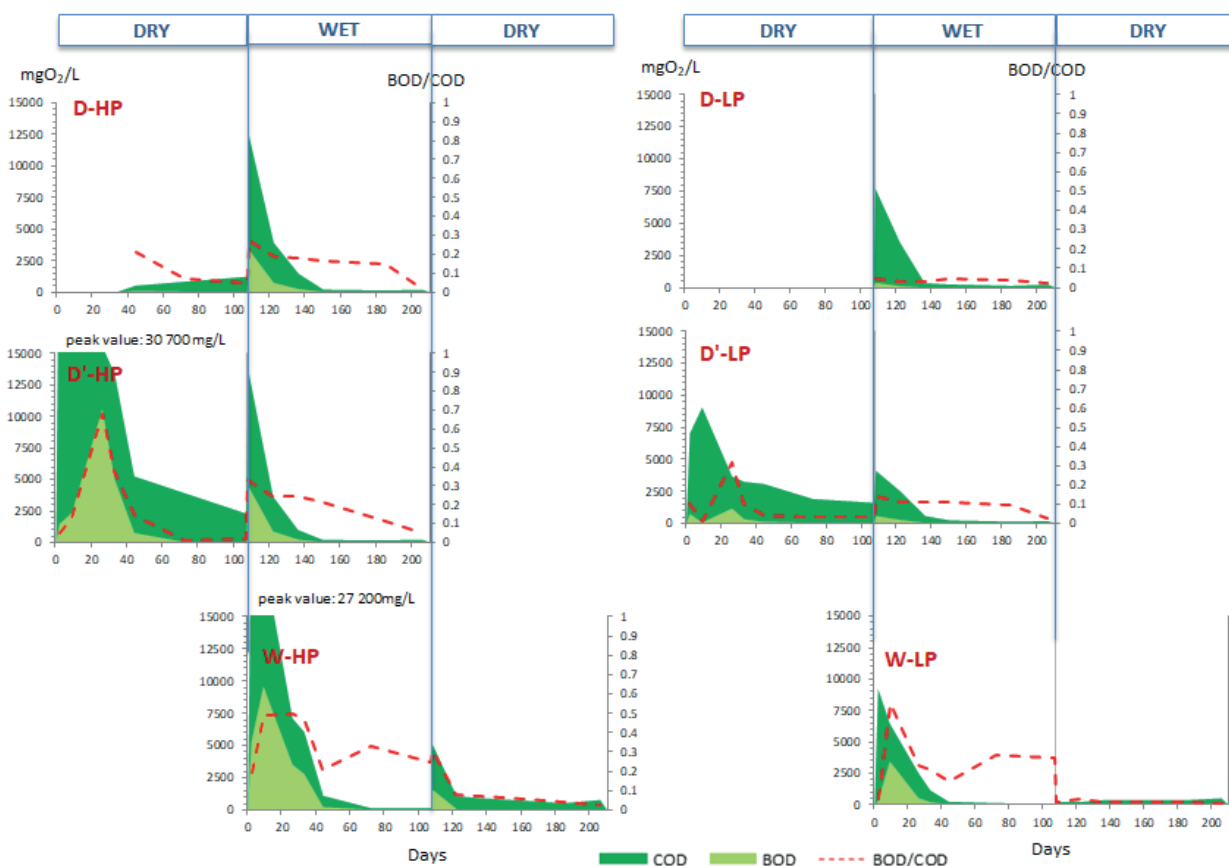
ity of pH over time (pH values around 7.7, see Figure 7b), highlighted the role carried out by stabilised waste in the bottom layer during the second phase.

The Biological Filter effect on the contrary was less evident with regard to nitrogen transformation, particularly during the wet phase. In this case, wet conditions in the second phase reduced air circulation, thus decreasing nitrogen oxidation, while the watering of columns promoted hydrolysis of Organic nitrogen and flushing of Ammonia Nitrogen. Final TKN concentrations ranged between 10 and 30 mg/l, with the exception of W-HP where a concentration of 80 mg/L was found. The behaviour of the different nitrogen compounds throughout the two climate phases tested is represented in Figure 8.

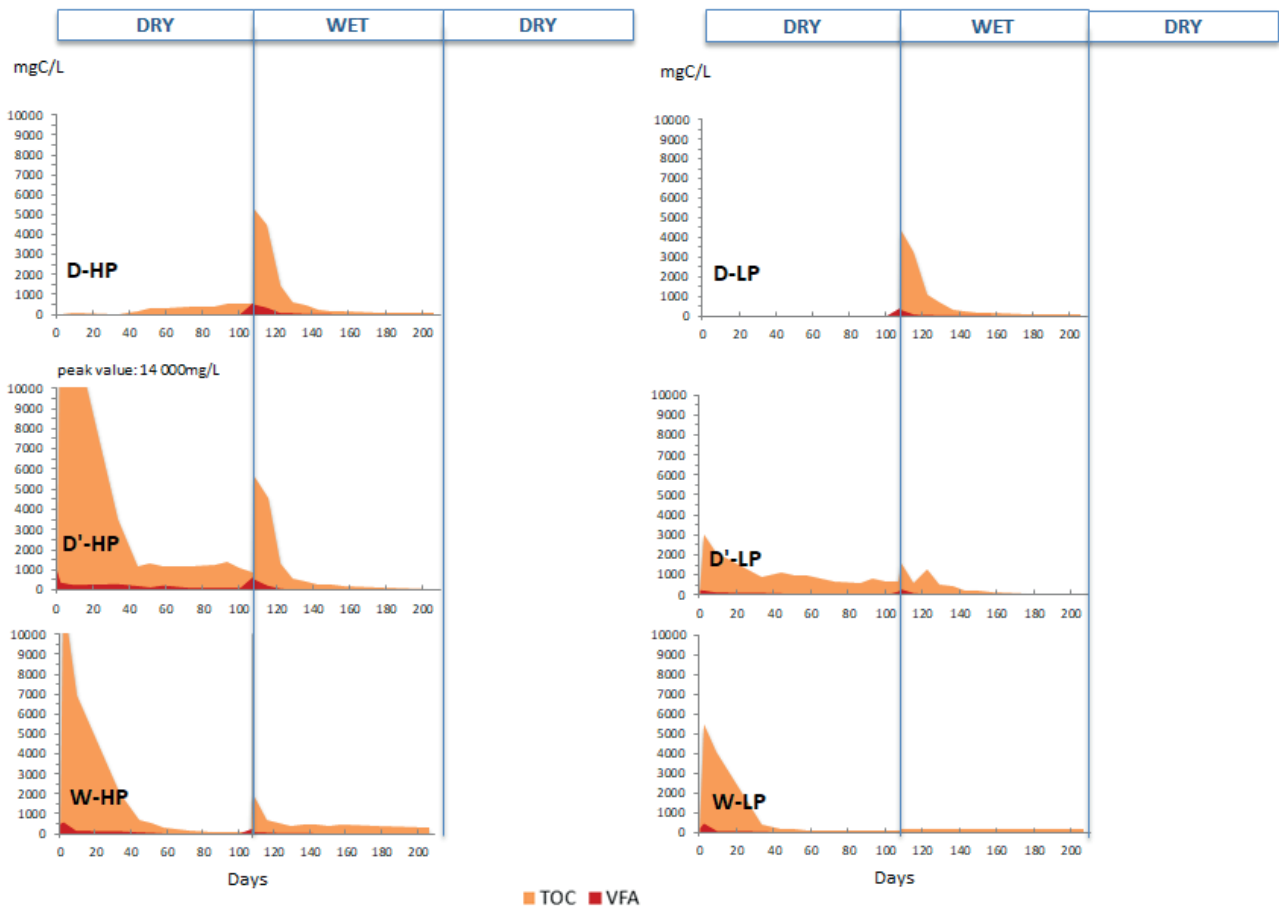
#### 4. CONCLUSIONS

Based on the above reported results the following conclusive remarks can be drawn:

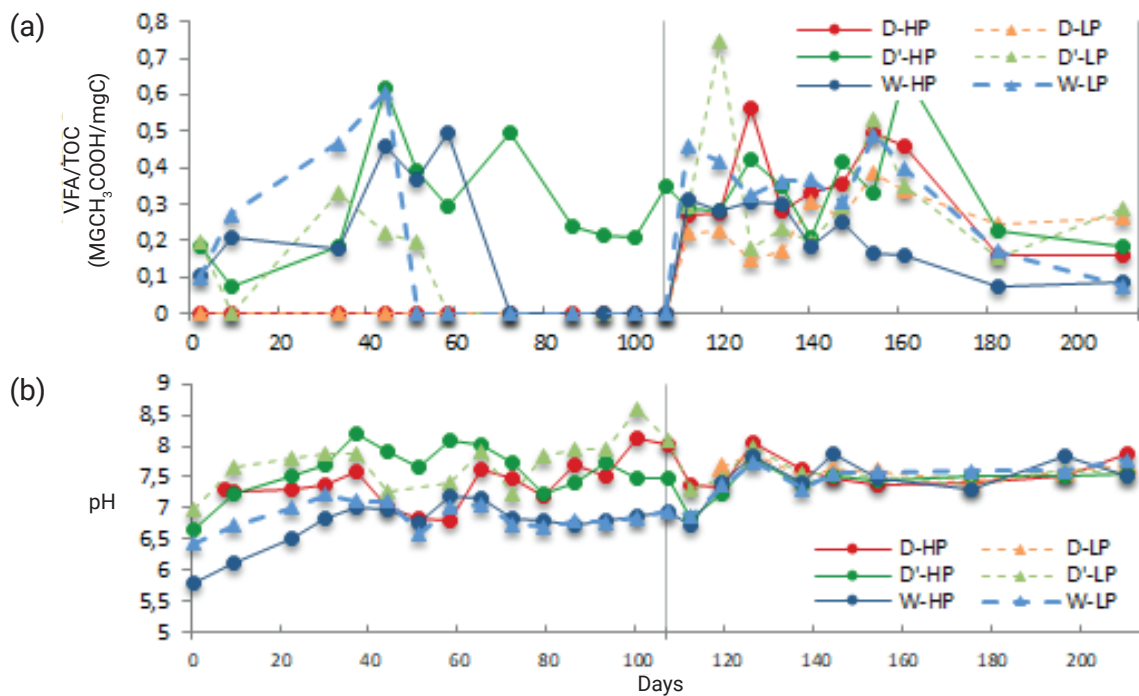
- Semi-aerobic landfilling might be heavily influenced by tropical wet-dry climate, due to the influence produced by water availability and different putrescible content of waste on natural advective air circulation. A consistently balanced availability of water, both in terms of endogenous water naturally present in the putrescible fraction, and external water input (rainfall, leachate recirculation), is fundamental in promoting good natu-



**FIGURE 5:** BOD/COD ratio, BOD and COD concentrations in leachate (overlapped area chart) vs. testing time, for the different lysimeters. D=Dry conditions, D'=Dry conditions with controlled watering; W=Wet conditions, HP=Waste with high putrescible content; LP=Waste with low putrescible content.



**FIGURE 6:** pH, VFA and TOC concentrations in leachate (overlapped area chart) vs. testing time, for the different lysimeters. D=Dry conditions, D'=Dry conditions with controlled watering; W=Wet conditions, HP=Waste with high putrescible content; LP=Waste with low putrescible content.



**FIGURE 7:** VFA/TOC ratios (a) and pH values (b) measured over time in leachate collected at the bottom of all test columns during the first and second climate phases.

ral air circulation while supporting aerobic degradation processes during the dry phase;

- When implementing semi-aerobic landfill under tropical dry-wet climate conditions, the overlaying of a new layer of waste in each climate season plays a fundamental role in ensuring good stabilisation. In particular, alternation of new waste layers together with rainfall seasonality, maintaining constant operational conditions throughout the entire climate season (wet or dry) for each individual layer will contribute towards enhancing stabilisation of the landfill bottom layer, which behaves as an internal attenuating biological filter for leachate produced during subsequent phases;
- during the wet season flushing effect, in terms of mobility of contaminants, and anaerobic processes prevail over semi-aerobic conditions limiting natural air circulation, particularly in case of high putrescible waste;
- during the dry season, by ensuring a constantly balanced water availability through proportioning of putrescible waste content and external water addition, the circulation of natural air can be conveniently maintained.

In conclusion, a semi-aerobic landfill operated under wet-dry climate conditions in tropical areas can be managed as a hybrid reactor, aerated throughout the dry sea-

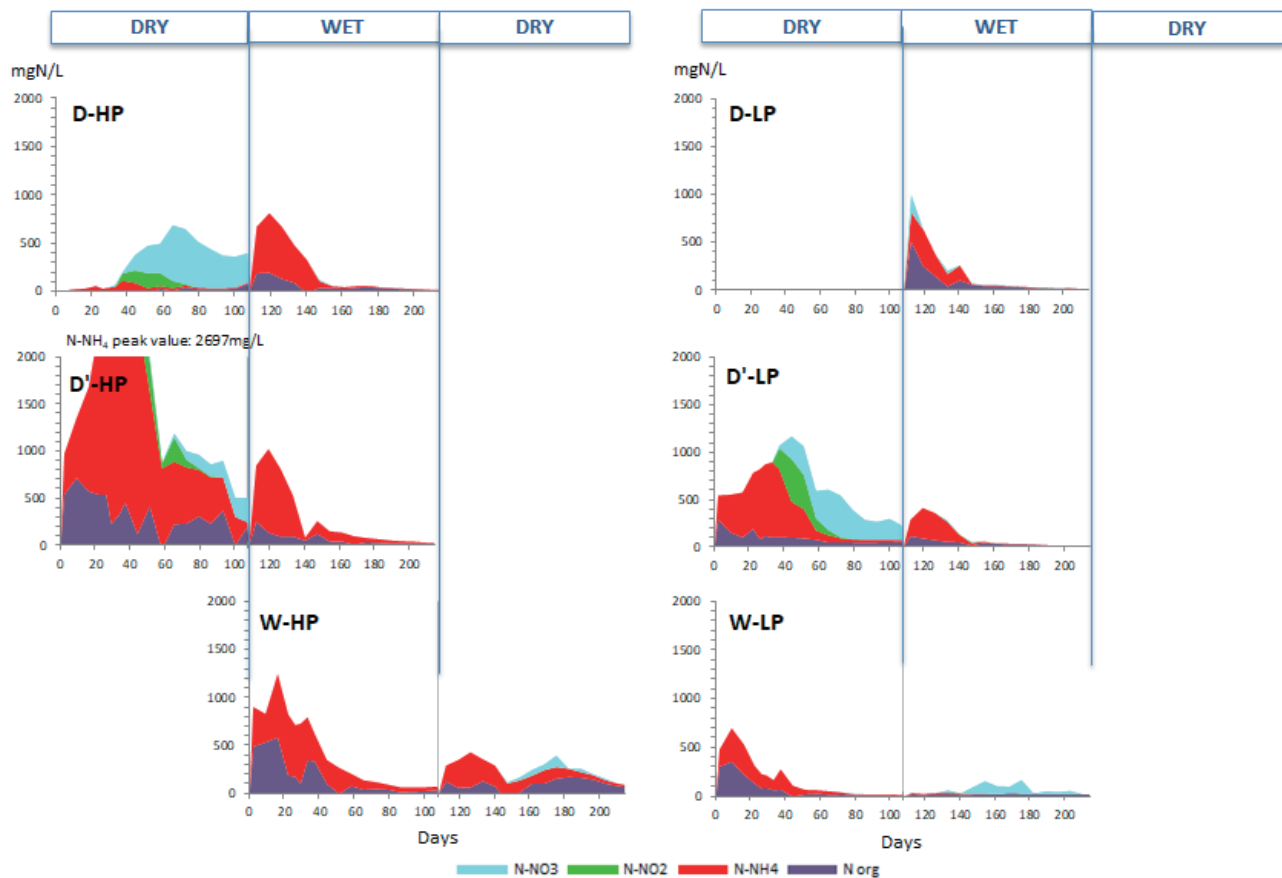
son and flushed in anaerobic conditions in the wet season.

However, the positive results obtained in this preliminary investigation should be confirmed by further pilot studies in order to identify and define appropriate design parameters.

Finally an important full-scale operative issue should be carefully considered and controlled. Under tropical climate conditions a huge amount of leachate might be generated as a consequence of excessive rain infiltration in the wet season. The accumulation of large amount of leachate might negatively affect the convective circulation of air, so reducing the efficiency of semi-aerobic landfilling. Problems like this have been already reported in literature (Cossu, 2019; Kortegas et al., 2007; Malek and Shaaban, 2008). This problem can be controlled by assuring well drained conditions of the waste mass (no use of low permeable material as daily top cover, drainage systems at the different waste layers, regular collection of leachate) and by adopting landfill top covers which reduce the rain infiltration.

## REFERENCES

Ahmadifar, M., Sartaj, M., Abdallah, M., 2016. Investigating the performance of aerobic, semi-aerobic, and anaerobic bioreactor landfills for MSW management in developing countries. *J. Mater. Cycles Waste Manag.* 18, 703–714. DOI:10.1007/s10163-015-0372-0



**FIGURE 8:** N-NH<sub>4</sub><sup>+</sup>, N organic, NO<sub>2</sub>, NO<sub>3</sub> concentrations in leachate (Stacked area chart) vs. testing time measured for each individual lysimeter, for the two (1<sup>st</sup> and 2<sup>nd</sup>) different climate phases. (D=Dry conditions, D'=Dry conditions with controlled watering; W=Wet conditions, HP=Waste with high putrescible content; LP=Waste with low putrescible content).

- Aziz, S.Q., Aziz, H.A., Yusoff, M.S., Bashir, M.J.K., Umar, M., 2010. Leachate characterization in semi-aerobic and anaerobic sanitary landfills: A comparative study. *J. Environ. Manage.* 91, 2608–2614. DOI:10.1016/j.jenvman.2010.07.042
- Chen, D., and Chen, H.W., 2013. Using the Köppen classification to quantify climate variation and change: An example for 1901–2010. *Environmental Development* 6(1): 69–79. DOI: 10.1016/j.envdev.2013.03.007.
- Cossu, R., 2019. Full-scale Operation of the Sassari Landfill. Problems in Semi-aerobic Operation. Personal communication.
- Cossu, R., Stegmann, R., 2018. *Solid Waste Landfilling, Concepts, Processes, Technology*. Elsevier, ISBN: 9780128183366.
- D.G.R. 2461/14 – Delibera Giunta Regionale n 2461, 2014. Linee guida per la progettazione e gestione sostenibile delle discariche. *Bollettino Ufficiale Regione Lombardia*, n.41 (10/10/2014).
- Grossule, V., Lavagnolo, M.C., 2019. Lab tests on semi-aerobic landfilling of MSW under varying conditions of water availability and putrescible waste content. Submitted to *Journal of Environmental Management*.
- Grossule, V., Morello, L., Cossu, R., Lavagnolo, M.C., 2018. Bioreactor landfills : comparison and kinetics of the different systems, *Detritus*, 03, 100–113, DOI: 10.31025/2611-4135/2018.13703.
- Kortegast, A., Richards, B.A., Yong, S., Chock, E.T., Bryce, A., Eldridge, S., Robinson, H., Carville, M., 2007. Leachate generation and treatment at the bukit tagar landfill, Malaysia. In: Paper presented to Sardinia 2007, the Eleventh International Waste Management and Landfill Symposium, S. Margherita di Pula. Cagliari, Italy, 1-5 October 2007.
- Kottek, M., Grieser, J., Beck, C., Rudolf, B., Rubel, F., 2006. World map of the Köppen-Geiger climate classification updated. *Meteorologische Zeitschrift* 15(3): 259–263. DOI: 10.1127/0941-2948/2006/0130.
- Lavagnolo, M.C., Grossule, V., Raga, R., 2018. Innovative dual-step management of semi-aerobic landfill in a tropical climate. *Waste Manag.* 1–10. DOI:10.1016/j.wasman.2018.01.017
- Matsufuji, Y., Tanaka, A., Cossu, R., 2018. Semiaerobic landfilling. In Cossu, R., Stegmann, R. *Solid Waste Landfilling, Concepts, Processes, Technology*. Elsevier, 2018, ISBN: 9780128183366.
- Malek, M.I., Shaaban, M.G., 2008. *Landfill Common Method and Practices of Solid Waste Disposal in Malaysia*. ISWA World Congress.

# TECHNO-ECONOMIC EVALUATION OF LANDFILL LEACHATE TREATMENT BY HYBRID LIME APPLICATION AND NANOFILTRATION PROCESS

Ronei de Almeida \*, Fábio de Almeida Oroski and Juacyara Carbonelli Campos

School of Chemistry, Federal University of Rio de Janeiro, 149 Athos da Silveira Ramos Avenue, room E206, 21941-909, Rio de Janeiro, Brazil

## Article Info:

Received:  
8 June 2019  
Revised:  
15 December 2019  
Accepted:  
13 January 2020  
Available online:  
29 January 2020

## Keywords:

Leachate  
Lime  
Air stripping  
Nanofiltration  
Hybrid process  
Cost estimation

## ABSTRACT

Leachate treatment is a major issue in the context of landfill management since solutions have not been yet developed, resulting in more satisfactory technical and economic results concerning leachate treatment. In this paper, the technical and economic factors concerning lime application and nanofiltration for the treatment of leachate from the Seropédica landfill (Rio de Janeiro State, Brazil) were evaluated. The results indicate that the application of 30 g lime L<sup>-1</sup>, under optimum conditions, followed by air stripping, was able to place the effluent within the ammonia nitrogen discharge standard imposed by local legislation. The use of nanofiltration produced a clear and colorless permeate and has proved to be very effective at removing all pollutants. Regarding cost estimates, considering a means leachate generation flow of 1000 m<sup>3</sup>, recovery of 60% and average permeate flux of 12 L m<sup>-2</sup> h<sup>-1</sup>. The total cost per m<sup>3</sup> of treated effluent was estimated in two scenarios, using different types of membrane and therefore different membrane costs per m<sup>2</sup>. Considering that the landfill would operate for 25 years and after closing, the leachate treatment station would maintain its activities for another 15 years, totaling 40 years, the cost to treat leachate would be of US\$ 10.54 and US\$ 11.33 m<sup>-3</sup>. In both evaluated scenarios, with regard to process operation costs, the percentage value relative to membrane exchange was emphasized. It is noteworthy that, a treated effluent at a lower cost to that currently presented by the landfill was obtained through the applied hybrid process.

## 1. INTRODUCTION

Considering the high concentration of pollutants and varying composition influenced by the type of waste, landfill age, and geological conditions, leachate treatment is undeniably one of the most challenging tasks in municipal solid waste management (Kjeldsen et al., 2002; Zhang et al., 2019). Landfill leachate contains high loads of organic matter, inorganic salts (sulfates, carbonates, and sodium chloride), ammonia, and halogenated and heavy metals that must be treated before being released into the environment (Kjeldsen et al., 2002). According to the literature, critical parameters for most landfills are chemical oxygen demand and ammoniacal nitrogen (NH<sub>3</sub>-N) (Ehrig and Robinson, 2010). Although many methods may apply, the most appropriate leachate treatment choice will depend on its features, technical applicability, cost-effectiveness, and other factors related to the quality requirements of the effluents.

Main classification of the technical solution and

technology classification for leachate management and treatment on the site or at the leachate treatment plant could be divided into following groups: leachate treatment on the site or transfer to the central wastewater treatment plant (leachate lagoons and recirculation into the landfill body or at the surface, combined leachate with the domestic sewage system and treatment at the wastewater treatment plant), biological processes (different combination of the aerobic and anaerobic processes), physicochemical processes (chemical oxidation, adsorption on activated carbon, chemical precipitation, coagulation-flocculation, air stripping) and membrane processes (main reverse osmosis and nanofiltration) (Ehrig and Robinson, 2010; Schiopu et al., 2012; Serdarevic, 2018; Yao, 2013). The conventional biological process could be effective for the removal of organic biodegradable substances, suspended solids and nutrients (Metcalf et al., 2003; Zhao and Zyyang, 2019). With time, the major presence of refractory compounds (mainly humic and fulvic acids) contribute to limit

\* Corresponding author:  
Ronei de Almeida  
email: ronei@eq.ufrj.br

the process's effectiveness (Rodrigues et al., 2009; Talalaj et al., 2019). Therefore, for the removal of recalcitrant compounds, advanced treatment processes such as physico-chemical and membrane technologies are required (Renou et al., 2008; Talalaj et al., 2019; Zawierucha et al., 2013).

Coagulation-flocculation may be used successfully in treating stabilized and old landfill leachates. It is widely used as a pre-treatment, prior to biological or nanofiltration step, or as a final polishing treatment step in order to remove non-biodegradable organic matter (Amaral et al. 2016; Amokrane et al., 1997; Amor et al., 2015). On the other hand, one option for reducing  $\text{NH}_3\text{-N}$  concentrations is the stripping of ammonia gas. At raised pH values or temperatures, an increased proportion of the total ammoniacal-N (ammonium + ammonia) is present as gaseous ammonia (Campos et al., 2013; Metcalf et al., 2003). During intensive contact with gases (e.g. with air) concentrations of dissolved ammonia gas adjust to an equilibrium between liquid and gaseous phases. Using this effect ammonia can be stripped from the liquid within the gas stream (Ehring and Robinson, 2010; Metcalf et al., 2003). Pretreatment by lime application, therefore, appears as a promising approach by combining the coagulation-flocculation process and favoring the raised of the pH of the leachate favoring, subsequently, the  $\text{NH}_3\text{-N}$  stripping by airflow.

In the last decades, nanofiltration (NF) has been widely used in landfill leachate treatment (Zhao and Zyyang, 2019). The advantage of using NF membrane is that its request for lower operating pressures and energy consumption ( $10 \text{ kWh m}^{-3}$ ), has higher fluxes than reverse osmosis (RO) membranes, better retention than an ultrafiltration (UF) membrane, high rejection of polyvalent ions and organic with molecular weight above 300 Da, relatively low investment and has low operational and maintenance costs. Moreover, due to its unique properties as compared to UF and RO membranes, the NF membrane has an important advantage that is the ability to remove recalcitrant organic compounds and heavy metals in leachate (Kwon et al., 2008; Chaudhari and Murthy, 2010).

The costs for treatment of leachate vary from simpler processes such as co-treatment with sewage (about  $18\text{-}27 \text{ € m}^{-3}$ ) to more sophisticated technologies such as reverse osmosis ( $15\text{-}40 \text{ € m}^{-3}$ ) (Calabro et al., 2018; Robinson, 2005). Brazilian researchers have highlighted the need to use efficient and economically viable technologies for the treatment of leachate in Brazilian landfills (Amaral et al., 2015; Amaral et al., 2016; De Almeida et al., 2019). However, to the best of our knowledge, the most advanced leachate treatment technologies are not feasible in most of the municipalities due to, for instance, the high cost of implementation and maintenance, and the volumes of leachate to be treated. Consequently, municipalities are required to implement treatment processes that are incompatible with the characteristics of the leachate, resulting in a treated effluent on disagreement with established disposal legislation. In this context, the objective of the present study is, therefore, to evaluate the technical and economic factors concerning hybrid lime application and nanofiltration treatment of leachate from the Seropédica landfill, located in Rio de Janeiro State (Brazil).

## 2. MATERIALS AND METHODS

### 2.1 Leachate characterization

The leachate utilized for the experiments was provided by the COMLURB (Municipal Urban Cleaning Company, Rio de Janeiro city) of the Seropédica landfill, located in Rio de Janeiro – Brazil, in September 2017. The Seropédica landfill received in recent years approximately 10000 tonnes per day of waste and currently generates  $1000 \text{ m}^3$  leachate per day.

The characterization of the leachate was based on the following parameters and methods recommended by American Public Health Association (APHA, 2012): potential of hydrogen (pH), Chemical Oxygen Demand - COD (5220-D), ammonium nitrogen -  $\text{NH}_3\text{-N}$  (4500-E), true-color (2120-C) chloride-Cl<sup>-</sup> (4500-Cl<sup>-</sup>), conductivity, turbidity, and absorbance at 254 nm (5910-B), it provides an indication of the content of aromatic organic matter and humic substances (APHA, 2012). The concentration of humic substances (humic and fulvic acids) were determined by the modified spectrophotometric/colorimetric method, based on the binding of toluidine blue dye (TB) with humic acid molecules to produce a dye-humic acids complex that causes the decrease in absorbance at 603 nm (Lima et al., 2017).

### 2.2 Leachate treatment

#### 2.2.1 Lime application

Jar tests were conducted to determine the optimum dosage of lime to be used before the final step of treatment by nanofiltration. The lime was added as "lime milk" (at  $200 \text{ g L}^{-1}$  of lime), in 500 mL beakers and its concentration after addition ranged from  $10$  to  $50 \text{ g L}^{-1}$ . After the lime had been added, coagulation-flocculation (C-F) was achieved by rapid stirring ( $150 \text{ rpm}$ ) for 1 min followed by slow stirring ( $50 \text{ rpm}$ ) for 30 min. The suspension was, then, allowed to settle for 30 min. The operational condition stirring employed in C-F was based on reports in the literature (Aziz et al., 2007; Lima et al., 2017; Renou et al., 2008; Renou et al., 2009). At the end of the decantation step, samples of supernatant phases were collected to be analyzed.

At optimum lime dose, the sobrenadant was aerated through an air compressor (Boyu S-500A model) at a flow rate of  $1.33 \text{ L of air min}^{-1}$  per liter of effluent. In a period of 12h, samples were collected every 1 h to evaluate the COD and  $\text{NH}_3\text{-N}$  concentration of the effluent and after 24h, the same parameters were analyzed. The operational condition of the air stripping was based on reports described by Campos et al. (2013).

The removal efficiency ( $E(\%)$ ) of the pollution parameters was defined by Equation 1.

$$E(\%) = 100 \times ((C_0 - C) / C_0) \quad (1)$$

Where,  $C_0$  is the concentration of the pollution parameter of raw leachate and  $C$ , the concentration of the pollution parameter of treated effluent.

#### 2.2.2 Nanofiltration

Nanofiltration (NF) was performed using a bench-scale filtration module. The experimental system consisted of a heated feed tank, a membrane module, a pressure gauge,

a recirculation pump (B-01), flow meters (FI-01 and FI-02), flow control valves in the feed (V-1), permeate (V-3, V-4) and concentrate streams (V-2) (Figure 1). The system has a capacity of 5.0 L, an effective circular membrane area of 77.7 cm<sup>2</sup>, the material of construction of 316 stainless steel cells (PAM Selective Membranes Inc.).

The leachate was tested with two polymer membrane models: SR100, consisting of polyamide and nominal retention of 200 Da and NP030, consisting of polyethersulfone and nominal retention of 400 Da. Previously, permeate flux (J, L m<sup>-2</sup> h<sup>-1</sup>) measurements were performed as a function of the operating pressure (7 and 8 bar) and the recirculation flow rate (30, 60, 90 120 L h<sup>-1</sup>). Subsequently, under ideal conditions of operation, the system was fed with 3.0 liters of leachate pretreated by the physicochemical process. The operating conditions have been defined by the system's technical constraints.

The volume reduction factor (VRF) was used to describe the extent of concentration in the NF unit during filtration. VRF was calculated using Equation 2.

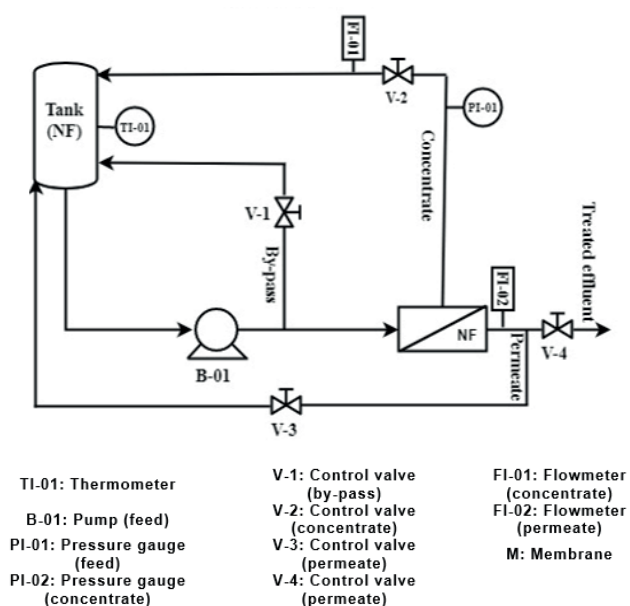
$$VRF = V_f / V_c \quad (2)$$

Where V<sub>f</sub> and V<sub>c</sub> are the initial volumes of the NF feed and the volume of NF concentrate produced, respectively, both measured in L.

During testing, the valves V-2 and V-4 remained opened, valve V-3 was closed and the feed flow rate and pressure were controlled by the frequency inverter connected to the pump B-01 and through the valve V-1. The permeate was collected and conditioned at 4°C. At the end of the filtration step, samples of permeate were collected to be analyzed. All the experiments were performed in triplicate.

### 2.2.3 Hybrid process

After the establishment of the ideal operating conditions of the lime application and nanofiltration process, the



**FIGURE 1:** Schematic diagram of the nanofiltration experimental setup.

hybrid treatment proposed in this study was operated in order to jointly evaluate the removal efficiency of the liquid effluent pollution parameters described in item 2.1.

### 2.3 Cost estimation

The cost estimation was performed based on the results obtained in the tests in filtration module and extrapolated to a real system with pre-defined leachate treatment flow, being represented, in this work, by the capital expenditure (CAPEX), by the operational expenditure (OPEX) and total cost (TC) normalized per unit volume of treated leachate. For preliminary estimation of costs of the hybrid process, the following considerations were made:

- The value of the capital cost of the lime treatment process was estimated from the study presented by Silva et al. (2011). The authors estimated the cost of implantation of the lime application process, considering the implantation of tanks, pumps, blowers, valves and pipes, civil construction and a feed flow of 1000 m<sup>3</sup>.day<sup>-1</sup>, as proposed in this work;
- Treatment and final disposal of the sludge and the concentrate generated in the process were not considered since these wastes can be disposed of in the landfill itself without additional costs for the leachate treatment plant;
- The leachate treatment plant would operate 365 days a year and would be out of operation only during periods of routine maintenance, chemical cleaning and integrity testing (Guerra and Pellegrino, 2012);
- The nanofiltration process plant would operate with 60% efficiency (Amaral et al., 2016);
- The membrane spiral modules used would be 1.016 m long, 0.2 m in diameter and 40 m<sup>2</sup> in working area (Baker, 2012);
- The preliminary cost of the process was estimated considering the cost of the m<sup>2</sup> of the polymer membrane of US\$ 40.00 (Baker, 2012; Guerra and Pellegrino, 2012) and US\$ 180.00 (Amaral et al., 2016).

CAPEX was determined by adding up the acquisition costs of the membrane modules, housing, valves, pipes and instrumentation that constitute a permeation unit (Salehi et al., 2014; Singh and Cheryan, 1998). The startup cost which is the amount of capital required to start the operation, corresponding to 8% of fixed investment, was also considered as an investment cost.

For the composition of OPEX, the costs of energy consumption for the operation of the nanofiltration system, investment depreciation, membrane exchange, maintenance, hand labor, and membrane regeneration were included (Singh and Cheryan, 1998). The energy consumption was estimated at 20.7 kW (496.8 kWh, given continuous for 24 h day<sup>-1</sup> operations) with 0.5 kW used to coagulation-flocculation, 1.5 kW to aeration during air stripping, 3.7 kW to sludge recirculation and 15 kW for NF system. For the maintenance cost, a value of 5% of the initial investment associated with preventive and corrective maintenance of the membrane was considered. As an estimated cost of chemicals used to clean the membranes, a value of 2% of



the initial investment was considered (Amaral et al., 2016).

The TC per unit volume of treated leachate was obtained by Equation 3, which accounts for the OPEX normalized by annual volume of treated effluent and the CAPEX normalized by volume of treated effluent added annually to the time, in years, of operation of the nanofiltration process, determined by means of Equation 4.

$$TC = R_{CAPEX} + OPEX/V_T \quad (3)$$

$$R_{CAPEX} = CAPEX/V_T \cdot n \quad (4)$$

Where,

$R_{CAPEX}$ : normalized capital cost per volume of treated effluent (US\$ m<sup>-3</sup>);  $n$ : operating period of the leachate treatment plant considered in years;  $V_T$ : total volume of treated effluent (m<sup>3</sup>).

### 3. RESULTS AND DISCUSSION

#### 3.1 Leachate characterization

Table 1 shows the values of the parameters obtained in the characterization of the raw leachate used in this study.

Leachate samples were slightly alkaline with dark color, eventually brown, and showed a high concentration of ammoniacal nitrogen (1512±239 mg L<sup>-1</sup>). The presence of NH<sub>3</sub>-N in landfill leachates represents a risk of surface and groundwater pollution. Dregs with a high concentration of ammoniacal nitrogen released into water bodies without previous treatment can cause eutrophication, depletion of dissolved oxygen and toxic effects on aquatic fauna (Metcalfe et al., 2003; Postacchinine et al. 2018).

The HS/COD (0.32) ratio also supports the assumption that the leachate has a high concentration of recalcitrant organic compounds (Lima et al., 2017), so the conventional treatments have limited efficiency when used to treat the leachate. Moreover, the ratio between biodegradable COD and NH<sub>3</sub>-N should be greater than four for the completion of the nitrate denitrification in biological processes (Talaj and Biedka, 2015). This effluent is also characterized

**TABLE 1:** Parameters obtained in the characterization of the raw leachate (n=10).

Parameters	Min	Max	Average±σ <sub>M</sub>	σ
pH	7.7	8.2	8.0±0.1	0.1
COD (mg L <sup>-1</sup> )	4330	4690	4522±28	90
HS (mg L <sup>-1</sup> )	1238	1678	1466±151	120
NH <sub>3</sub> -N (mg L <sup>-1</sup> )	1150	1851	1512±76	239
Abs 254 nm	26.29	27.01	26.70±0.03	0.10
True color (mg Pt-Co L <sup>-1</sup> )	5560	7640	6391±190	602
Conductivity (mS cm <sup>-1</sup> )	15	20	19±1	4
Turbidity (NTU)	110	120	110±5	15
Cl <sup>-</sup>	890	1327	887±90	67

$$\sigma = \sqrt{\frac{\sum_{i=1}^n (M-M_i)^2}{n-1}}; \sigma_M = \frac{\sigma}{\sqrt{n}}$$

σ = standard deviation; M = test value; = average value; n = number of tests; σ<sub>M</sub> = standard deviation of the mean

pH: potential of hydrogen; COD: Chemical Oxygen Demand; HS: Humic Substance; Abs 254 nm: Absorbance at 254 nm; NH<sub>3</sub>-N: ammoniacal nitrogen; Cl<sup>-</sup>: Chloride.

by a very high content in dissolved salts, notably chlorides (887±67 mg L<sup>-1</sup>) and conductivity (19±4 Ms cm<sup>-1</sup>).

Ahmed and Christopher (2012) reported that the composition of leachate and the concentrations of contaminants are influenced by the type of waste deposited and the age of the landfill. In this case, high concentrations of recalcitrant organic matter and NH<sub>3</sub>-N may be justified as a result of the characteristics of the waste deposited in the landfill and consequence of the biological degradation of amino acids and other organic nitrogen compounds.

#### 3.2 Leachate treatment

##### 3.2.1 Lime application

The coagulation-flocculation process was performed to reduce the concentration of recalcitrant organic matter (humic substances). This stage was a pretreatment of the effluent, conditioning the leachate for the subsequent process of air stripping and nanofiltration. The results of the assays performed at concentrations of 10 to 50 g L<sup>-1</sup> lime, 1 min rapid mixing at 150 rpm, 30 min slow mixing at 50 rpm and decanting for 30 minutes are shown in Table 2.

As can be observed, larger COD removal was obtained in a concentration of 40 g L<sup>-1</sup> of lime (56%), while the highest percentage of HS removal was obtained in a concentration of 30 g lime L<sup>-1</sup> (42%). Comparatively, in this last coagulant concentration, considering the standard deviation, the percentage of COD removal (48%) was close to that obtained in higher concentrations of lime. Additionally, this lime concentration also corresponded to the lowest conductivity value obtained for the treated effluent (13±1 mS cm<sup>-1</sup>).

According to Renou et al. (2009), lime addition seems to have various effects on leachate. The lime pretreatment induces the leachate decarbonation, which has a strong effect on its inorganic fraction. While lime is being added, the carbonate ions precipitate massively and it results in a decrease in conductivity. Conductivity decreases until the carbonate concentration becomes limiting and prevents the solubility limit of this salt from being exceeded. At this point, the lime dose is considered optimum (within the assessed range) and corresponds to a maximum reduction of conductivity.

According to Lima et al. (2017), physical-chemical treatments show satisfactory results in terms of the removal of recalcitrant compounds (mainly monitored by color and absorbance at 254 nm) present in the leachate samples. Although lime application has been traditionally used to overcome temporary water hardness by a decarbonating process, a number of studies have been effective to remove some organic molecules of high molecular weight such as humic and fulvic acids (Amaral et al., 2015; Chen et al., 2017; El-Gohary et al., 2013; Renou et al., 2009). However, in general, the introduction of chemical agents leads to an increase in the concentration of salts in the effluent, therefore, the further treatment process is needed.

In the optimum concentration of lime (30 g L<sup>-1</sup>), the removal of NH<sub>3</sub>-N and COD was evaluated under the conditions described in item 2.2.1. Figure 2 shows the concen-

**TABLE 2:** Parameters obtained for determination of the optimum lime concentration for the coagulation-flocculation process in the concentration of 10 to 50 g lime L<sup>-1</sup>, rapid mixing of 1 min at 150 rpm, slow mixing for 30 min at 50 rpm and decantation by 30 min (n=3).

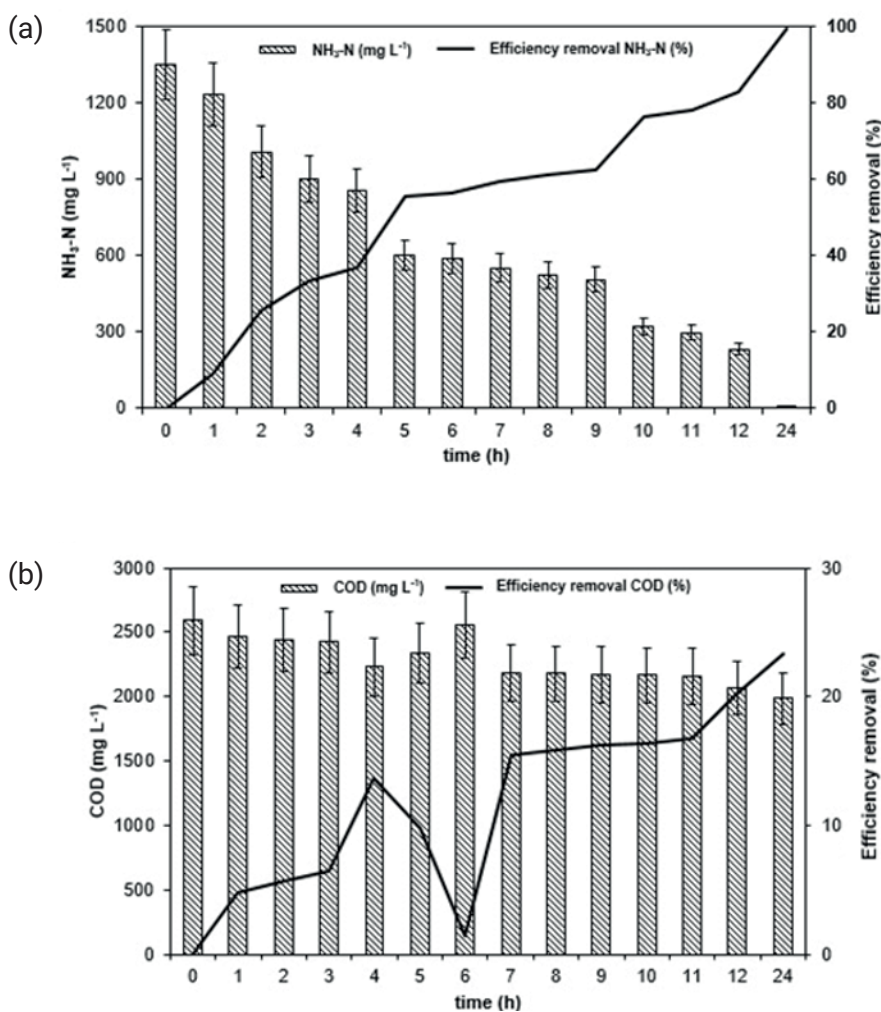
Parameters									
Lime (g.L <sup>-1</sup> )	pH	COD (mg L <sup>-1</sup> )	HS (mg L <sup>-1</sup> )	ABS 254 nm	NH <sub>3</sub> -N (mg L <sup>-1</sup> )	True color (mg Pt-Co L <sup>-1</sup> )	Conductivity (mS cm <sup>-1</sup> )	Cl <sup>-</sup> (mg L <sup>-1</sup> )	Turbidity (NTU)
Raw leachate	8.0±0.1	4522±452	1466±151	26.70±0.03	1512±148	6391±640	19±2	887±80	110±12
10	8.0±0.1	3165±315	1180±120	22.30±0.02	1120±119	5875±588	16±2	766±77	105±11
20	8.5±0.1	3210±320	1298±130	18.87±0.02	1098±101	5760±576	16±2	754±75	87±9
30	9.1±0.1	2344±240	855±87	13.78±0.01	1310±126	1560±140	13±1	562±56	54±5
40	9.6±0.1	1995±200	990±101	15.60±0.02	996±93	2230±230	15±2	495±50	48±5
50	9.8±0.1	3220±321	1005±110	10.57±0.01	1078±101	995±100	19±2	568±61	52±5

trations of NH<sub>3</sub>-N, COD and the respective percentages of removal efficiency along the air stripping process.

It is important to stress that, the airflow entrainment process in the operating conditions of 1.33 L air min<sup>-1</sup> per liter of effluent and 24h hydraulic retention time showed a removal efficiency of about 99% of ammoniacal nitrogen. The final NH<sub>3</sub>-N concentration of the effluent was approximately 9.8±1.0 mg L<sup>-1</sup>. According to Campos et al. (2013), when evaluating the removal of ammoniacal nitrogen from

landfill leachate through the treatment with lime, as the alkalinity of the effluent decreases, there is a decrease in the concentration of ammoniacal nitrogen, due to the previous removal of CO<sub>2</sub>, which consequently favors the removal of NH<sub>3</sub>-N by stripping.

El-Gohary et al. (2013) carried out a study that evaluated the removal of ammoniacal nitrogen from landfill leachate by air stripping. Percent removal efficiency values of 94.5% were obtained after 24 h of stripping. The pH of



**FIGURE 2:** Concentration and efficiency of removal of NH<sub>3</sub>-N (a) and COD (b) as a function of the time of operation of the air stripping process (1.33 L min<sup>-1</sup> per liter, 24h retention time).

the effluent at the end of the experiments was equal to 11. According to the authors, after 6 h of air stripping, it was possible to observe a linear increase in the pH of the leachate (9-10) and at a hydraulic time of more than 6 h, a significant increase in the percentage values of  $\text{NH}_3\text{-N}$  removal. Thus, the authors concluded that 6 h of air stripping was sufficient to remove ammoniacal nitrogen from the leachate in considerable percentage terms of removal efficiency. On the other hand, in a study performed by Amaral et al. (2016), pretreatment by air stripping at 10 m<sup>3</sup> reactor fed with raw leachate and hydraulic retention time of 48 h, conducted at the natural pH (8.1), removed 65% of  $\text{NH}_3\text{-N}$  present in the leachate.

An issue related to air stripping is that the ammonia passes to the gas phase, so the process must contain a collection system. Liu et al. (2014) presented an ammonia recovery efficiency to 80%, using a solution of sulfuric acid (1 mol L<sup>-1</sup>). The authors comment that this solution can be used as a source of nitrogen for the manufacture of compounds that can be used as soil conditioning.

Additionally, in this study, it was decided to carry out an evaluation of the COD along with the air stripping, although this technology is not mentioned in the literature as the most appropriate for the removal of organic matter from the effluent. However, it was still observed that during the process, the COD concentration was reduced from 2590±250 to 1987±190 mg L<sup>-1</sup>, about 23% removal efficiency. This percentage reduction in COD can be attributed to the fact that, during the aeration process of the effluent, colloid particles still present in the leachate are agglutinated and in a subsequent sedimentation process, this organic material is possibly removed (De Almeida et al., 2019).

It is worth noting that coagulant addition increased the particle size of suspended material. This, in turn, enhances the settling of suspended matter due to coagulation. Con-

sequently, this will affect the removal of COD (Ismail et al., 2012). However, in time 6h was observed a sharp decrease in COD removal efficiency. This may be justified due to the presence of suspended solids in the analyzed sample. One way to minimize possible measurement errors would be to perform sample filtration and quantify the filtered effluent COD (Golob et al., 2005).

### 3.2.2 Nanofiltration

Initially, for the two membranes used (SR100 and NP030), the permeate flux was evaluated with time, returning the permeate stream to the feed tank, at pressures of 7 and 8 bar, at a recirculation flow rate of 120 L h<sup>-1</sup>. The results are shown in Figure 3.

By the analysis of the permeate fluxes obtained during the filtration process of the membranes SR100 and NP030, it was verified that the permeated flux, in the two pressures evaluated, is higher in the NP030 membrane, this can be explained by comparing the nominal retention of the membranes, 200 Da for membrane SR100 and 400 Da for NP030. Sir et al. (2012) points out that the continuous decrease of the permeate flux along the membrane separation processes is also associated with other phenomena, such as the adsorption of humic and fulvic acids on the surface of the membrane, which can cause fouling of the membrane and lead to extremely low permeate fluxes, making the process unfeasible.

At the pressure of 7 bar, in the recycle flow rate evaluated, the permeate flux of the SR100 membrane oscillated between 11.6 and 10.3 L m<sup>-2</sup> h<sup>-1</sup>, whereas for the NP030 membrane, this value was 16.0 at 15.7 L m<sup>-2</sup> h<sup>-1</sup>. At higher pressure, the range of values was 13.5-12.9 L m<sup>-2</sup> h<sup>-1</sup> (SR100) and 17.4-16.1 L m<sup>-2</sup> h<sup>-1</sup> (NP030).

Subsequently, the permeate flux was evaluated as a function of the recirculation flow, at pressures of 7 and 8

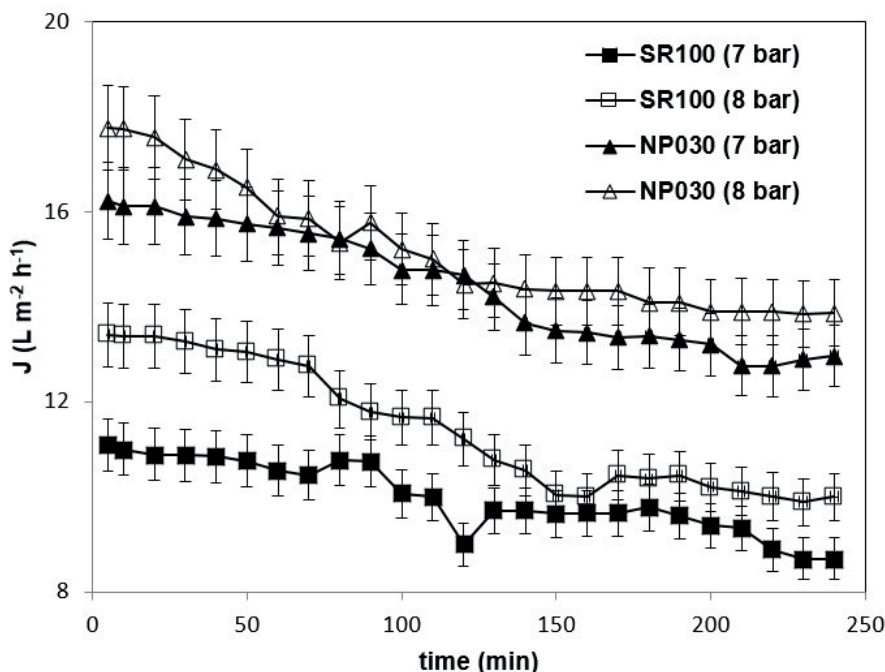


FIGURE 3: Monitoring of the permeate flux during the nanofiltration process with membranes SR100 and NP030, at 7 and 8 bar pressure.

bar, after 1 h of system operation. Figure 4 shows the permeate flux values obtained in the filtration process with the membranes SR100 and NP030 at 7 and 8 bar at 30, 60, 90 and 120 L h<sup>-1</sup> recirculation flow rates.

In the NF process of this study, not only for the SR100 membrane, as for the NP030 membrane, the variation of the recirculation flow rate of the system had little influence on the permeate flux values obtained. Tavares and Brião (2012) evaluated the effect of pressure and tangential velocity on the permeate flux in a spiral-type filtration system and observed that the higher the pressure and the tangential velocity of the system, greater the permeate flux. It was observed that in this work, probably due to the high range of the recirculation flow rate of the system, little influence was exerted on the values of tangential velocities and, consequently, the variation of the permeate value of the process was negligible. Probably, in a range of variation of the recirculation flow smaller, there will be a greater impact on the values of the tangential velocities and consequently of the permeate flux.

Finally, the membrane separation process was batch operated, where the permeate stream was collected until a determined VRF defined in this study as 2.5, operated for about 8 h at a pressure of 8 bar, the pressure of NF step was maintained at 8 bar due to the system's technical constraints, and a recirculation flow rate of 30 L h<sup>-1</sup>. Figure 5 shows the permeated flow as a function of the VRF.

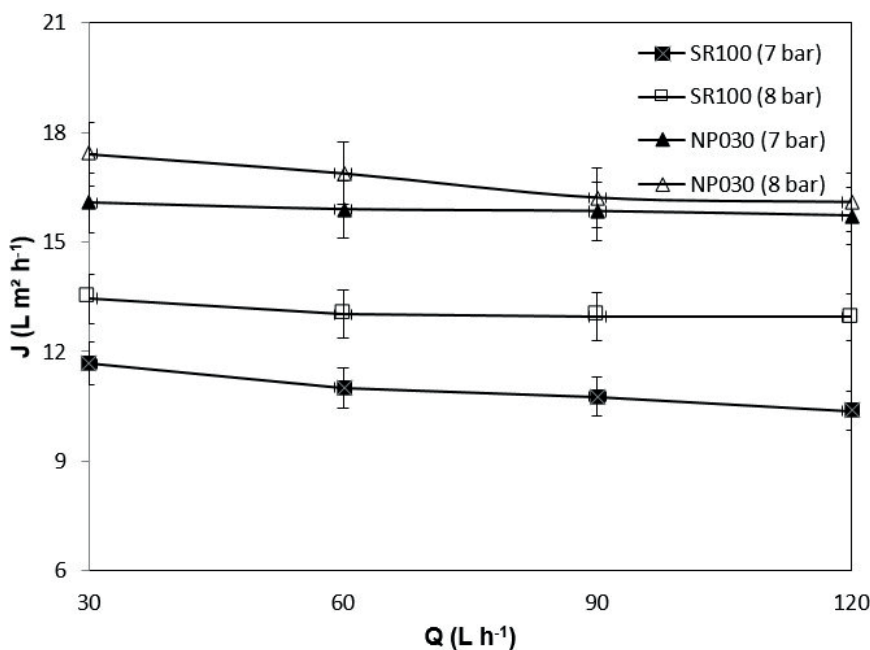
It was observed that, during the filtration process, up to 60% yield, the permeate flux of the nanofiltration process with the SR100 membrane presented a 33% reduction, while for the NP030 membrane the permeate flux drop was 25% approximately. Membrane fouling phenomena can be investigated by monitoring the water permeability (Cingolani et al., 2018). The membrane permeability varied throughout the process, between 1.58-1.23 L m<sup>-2</sup> h<sup>-1</sup> bar<sup>-1</sup> (SR100)

and 2.33-1.95 L m<sup>-2</sup> h<sup>-1</sup> bar<sup>-1</sup> due to the degree of membrane fouling during the continuous operation. The initial hydraulic permeability of the membrane (new membrane) was 1.70 (SR100) and 2.38 L m<sup>-2</sup> h<sup>-1</sup> bar<sup>-1</sup> (NP030). A cleaning process could be applied to try to recover the permeate flux of the NF and to minimize the fouling of the membranes (Rukapan et al., 2012).

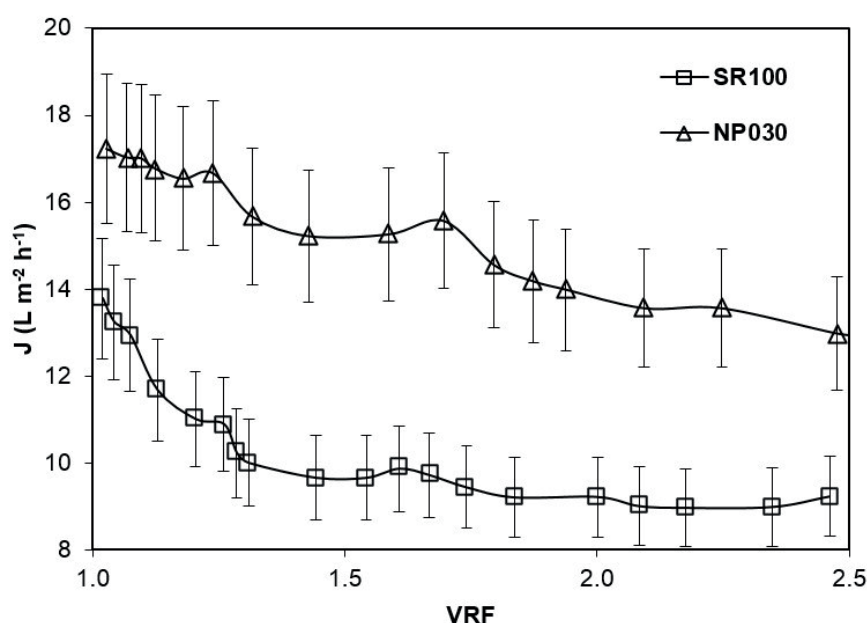
Table 3 presents the values of the parameters of pretreated leachate and effluent after the application of the NF under operational conditions defined.

The concentration of HS was considerably reduced and their final value corresponded to a reduction of 90% and 87% of the concentration present in the pretreated leachate, given the filtration process with membranes SR100 and NP030, respectively.

According to Baker (2012), the nanofiltration process is inefficient in the removal of salts, since it is able to retain molecular species with molar mass varying between 500 and 2000 Da, even though, it was observed percentages of removal of Cl<sup>-</sup> higher than 40% after the NF. Amaral et al. (2015) reported chloride removal percentages of 84% and 90% of conductivity after the application of NF. Baker (2012) points out that chloride is a monovalent anion, and the removal of this type of ion is not characteristic of the nanofiltration membrane. However, its removal can occur due to the precipitation of chloride ions in the membrane, or even by the transport of ions, in order to maintain the membrane electroneutrality. In complex aqueous matrices, such as effluents, the presence of a wide variety of ions also presents a wide variety of complex interactions. In order to maintain the electroneutrality, other ions are also retained or otherwise forced through the membrane, depending on the ionic forces involved (Amaral et al., 2015; Renou et al., 2008).



**FIGURE 4:** Permeate flux obtained in the filtration process with membranes SR100 and NP030 at 7 and 8 bar in recirculation flows of 30, 60, 90 and 120 L h<sup>-1</sup>.



**FIGURE 5:** Variation of the permeate flux as a function of the VRF of the nanofiltration process (Operating pressure of 8 bar, recirculation flow of 30 L h<sup>-1</sup> and 5 h of operation).

### 3.3 Hybrid process

Table 4 shows the results of the parameters of raw leachate, treated leachate in optimum lime concentration (30 g L<sup>-1</sup>), air stripping (1.33 L air.min<sup>-1</sup> per liter effluent and time 24h hydraulic retention) and nanofiltration with SR100 and NP030 membranes (8 bar operating pressure and 30 L h<sup>-1</sup> recirculation flow).

The application of lime was efficient in the removal of recalcitrant organic matter, true-color, and NH<sub>3</sub>-N. The concentration of COD, HS, and the true color was reduced to concentrations of 2258±232 mg L<sup>-1</sup>, 821±80 mg L<sup>-1</sup> and 1290±107 mg Pt-Co L<sup>-1</sup>, respectively. The concentration of NH<sub>3</sub>-N, through the proposed pretreatment, was reduced to a concentration compatible with the disposal limit established by local legislation.

In addition, it was observed that the application of the

NF process, after the physicochemical treatment, was efficient as a complementary step to remove the effluent pollution parameters. The combined treatment process with the SR100 membrane showed percentage removals of COD, SH, ABS 254 nm, true-color and ammoniacal nitrogen of 96%, 94%, 89%, 99%, and 99%, respectively. On the other hand, with the NF030 membrane, removal percentages were 94%, 93%, 89%, 98%, and 99%, respectively, for the same parameters. These results are comparable with Smol and Włodarczyk-Makula (2016) that studied an integrated system of coagulation-NF/RO.

### 3.4 Economical aspect

Regarding cost estimates for the process, the information obtained from the experimental units was used to carry out an initial survey of the project variables and

**TABLE 3:** Physico-chemical parameters of pretreated leachate and effluent after the application of the nanofiltration (n=3).

Parameters	Pre-treated leachate			Nanofiltration					
	Min	Max	Average±σ	SR100			NP030		
				Min	Max	Average±σ	Min	Max	Average±σ
pH	10.7	11.5	11.1±0.1	7.8	8.3	8.0±0.1	7.9	8.2	8.1±0.1
COD (mg L <sup>-1</sup> )	2116	2368	2258±226	174	205	193±19	220	278	249±25
HS (mg L <sup>-1</sup> )	782	866	821±80	75	98	84±8	95	121	109±10
Abs 254 nm	12.98	13.38	13.25±0.20	2.46	3.44	2.88±0.10	2.55	3.07	2.87±0.10
NH <sub>3</sub> -N (mg L <sup>-1</sup> )	10.9	18.5	14.8±1.0	7.9	10.2	8.9±1.0	5.6	12.5	9.4±0.9
True color (mg Pt-Co L <sup>-1</sup> )	1120	1340	1290±121	67	97	83±8	110	135	122±12
Cl <sup>-</sup> (mg L <sup>-1</sup> )	523	632	585±55	225	371	298±27	302	343	318±29
Conductivity (mS cm <sup>-1</sup> )	12	13	13±1	6	7	7±1	9	10	9±1
Turbidity (NTU)	36	45	39±4	0.25	0.56	0.40±0.10	0.50	1.10	0.77±0.10

**TABLE 4:** Parameters of raw leachate, lime application (30 g L<sup>-1</sup>), air stripping (1.33 L air min<sup>-1</sup> per liter of effluent and 24-hour hydraulic retention time) and NF with the membranes SR100 and NP030 (8 bar operating pressure and 30 L h<sup>-1</sup> recirculation flow) (n=3).

Parameters	Raw leachate			C-F/Air Stripping Lime (30 g L <sup>-1</sup> )			Nanofiltration						Brazilian legislation
	Min	Max	Average ± σ	Min	Max	Average ± σ	SR100			NP030			
							Min	Max	Average ± σ	Min	Max	Average ± σ	
pH	7.7	8,2	8.0±0.1	10.7	11.5	11.1±0.1	7.8	8.3	8.0±0.1	8.0	8.3	8.1±0.1	5 - 9
COD (mg.L <sup>-1</sup> )	4330	4690	4522±90	2116	2368	2258±232	174	205	193±21	220	278	249±22	250
HS (mg.L <sup>-1</sup> )	1233	1543	1466±120	782	866	821±80	75	98	84±9	95	121	109±11	-
ABS 254 nm	26.29	27.01	26.70±0.10	12.98	13.38	13.25±1	2.46	3.44	2.88±0.55	2.55	3.07	2.87±1	-
NH <sub>3</sub> -N (mg L <sup>-1</sup> )	1150	1851	1512±139	10.9	18.5	14,8±0.8	7.9	10.2	8.9±1	5,6	12.5	9.4±1	20
True color (mg Pt-Co L <sup>-1</sup> )	5560	7640	6391±602	1120	1430	1290±107	67	97	83±7	110	135	122±14	-
Cl <sup>-</sup> (mg L <sup>-1</sup> )	890	1327	887±67	523	632	585±55	225	371	298±30	302	343	318±33	-
Conductivity (mS cm <sup>-1</sup> )	14,57	20.45	19±4	12.48	12.57	12.53±1	6.34	7.21	6.85±0.7	9.00	9.32	9.18±1	-
Turbidity (NTU)	110	120	110±15	36	45	39±2	0.25	0.56	0.40±0.05	0.50	1.10	0.77±0.08	-

subsequent assessment of leachate treatment costs. Considering a means leachate generation flow of 1000 m<sup>3</sup>, nanofiltration process recovery efficiency of 60% and average permeate flux of 12 L m<sup>-2</sup> h<sup>-1</sup>, the total cost per m<sup>3</sup> of treated effluent was estimated in two scenarios, in which different membrane m<sup>2</sup> prices of the used in the filtration process were considered.

The CAPEX of the leachate treatment system was US\$ 5.618.661,80 considering the cost of the polymer membrane of US\$ 40 m<sup>2</sup> presented by Baker (2012); Guerra and Pellegrino (2012), and US\$ 6.289.481,30 in the scenario in which the cost of m<sup>2</sup> of membrane was US\$ 180, as pointed out by Amaral et al. (2016). It stands out, the proposed treatment does not present any biological processes, which in addition to increasing the costs of treatment of leachate, is inefficient in the treatment of effluents with a high concentration of recalcitrant organic matter. In addition, NF meets a growing demand in the area of leachate treatment – decentralized treatment plants – that is, land and construction costs are reduced, since membrane processes are compact systems and can be arranged in mobile structures, representing a reduction in the CAPEX.

Figure 6 shows the relative composition, in percentage, of CAPEX (a, b) and OPEX (c, d), considering the cost of the membrane m<sup>2</sup> presented by Baker (2004); Guerra and Pellegrino (2012) (a and c) and Amaral et al. (2016) (b and d), respectively.

CAPEX has highlighted the expenses with an installed system, which accounts for the acquisition of equipment, valves, pipes, and instrumentation. It should be noted that these costs are related to the m<sup>2</sup> of the membrane used in the NF process. Regarding the OPEX, the percentage value related to the exchange of membranes stands out, 41.5% (Figure 7.c) and 39.2% (Figure 7.d). Operating expenses are incurred over the life of the project and include a variable component that can be managed continuously, thus it is evident that good operational practices throughout the

useful life of the leachate treatment plant, such as periodic cleaning of membranes, may reduce operating costs and make the proposed treatment process more economically attractive.

Figure 7 shows the total cost values per m<sup>3</sup> of treated leachate for different periods of operation of the treatment plant.

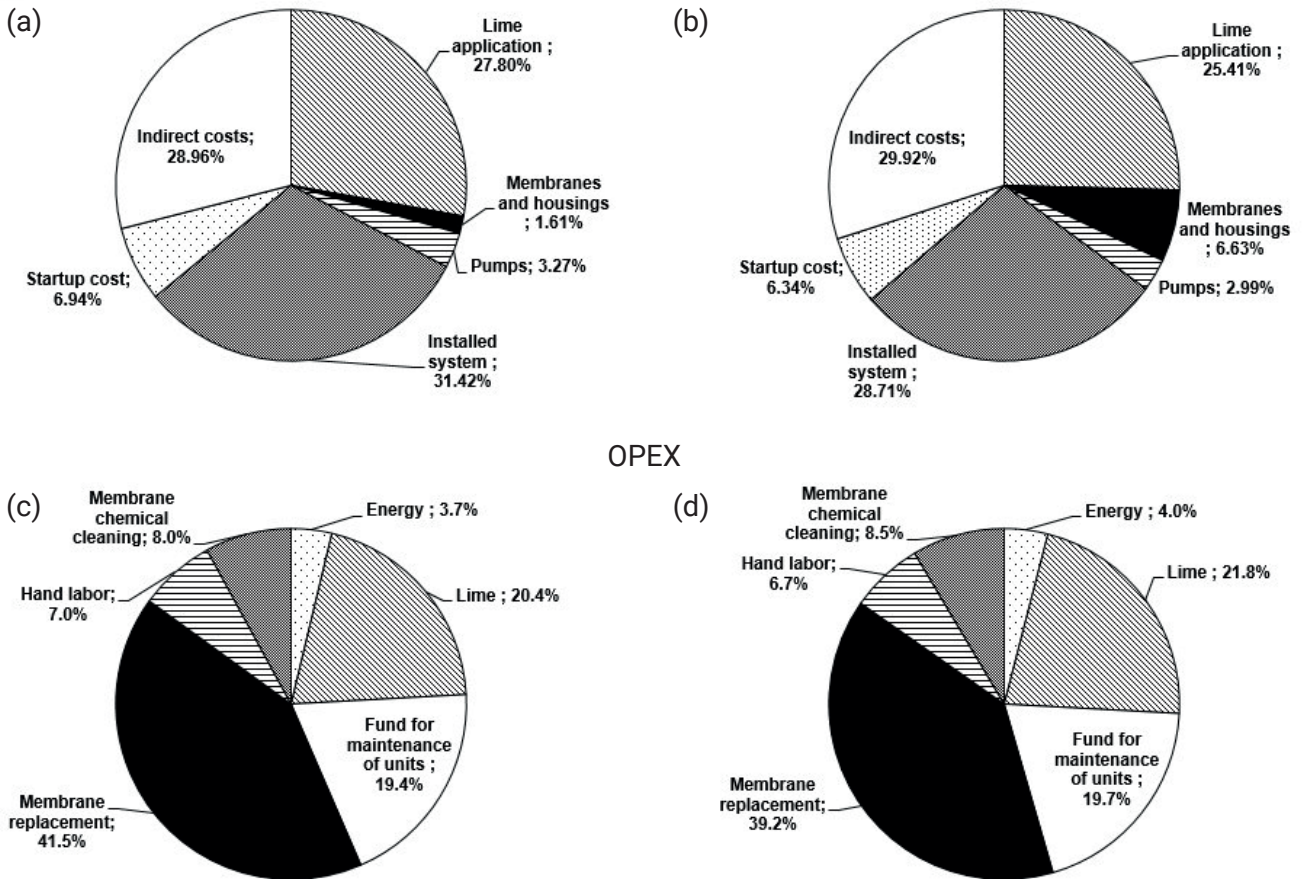
Considering that the landfill would operate for 25 years and after closure, the leachate treatment plant would maintain its activities for another 15 years, over a period of 40 years, the total cost to treat the m<sup>3</sup> of leachate would be US\$ 10.54 (scenario a) and US\$ 11.33 (scenario b).

Regarding of leachate treatment in Brazil, considerable efforts have been made to implement efficient technologies for the removal of pollutants and achieve compliance with the standards established by environmental legislation (Costa et al., 2019). Also, it is important to note that the selection of the most suitable treatment technology for landfill leachate depends on the quality and quantity of leachate, age of landfill, plant flexibility and operation conditions (Talalaj et al., 2019). Economic parameters also play an important role in this decision-making process.

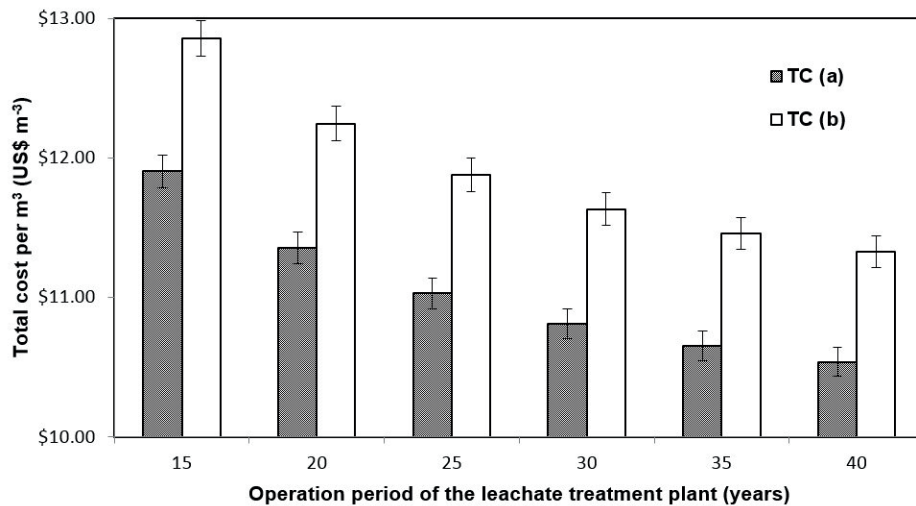
## 4. CONCLUSIONS

Due to the complexity of landfill leachate, to provide a treated effluent that can be discharged into natural water streams is not achievable using a single technique but a combination of different processes is required. In this study, the combined process allowed the production of a clear and colorless permeate and has proved to be very effective at removing all pollutants. The total cost to treat the leachate ranged from 10,5 to US\$ 12,80. Regarding cost estimates for the process, it was verified that a treated effluent at a lower cost to that currently presented by the Sero-pédica landfill was obtained through the applied treatment. In addition, it was assumed that it would be possible to abrogate the biological processes currently employed at the

## CAPEX



**FIGURE 6:** Relative composition, in percentage, of CAPEX (a, b) and OPEX (c, d). (a and c) Baker (2012); Guerra and Pellegrino (2012) membrane price; (b and d) Amaral et al. (2012) membrane price.



**FIGURE 7:** Total cost per m<sup>3</sup> of treated leachate for different periods of operation of the nanofiltration treatment.

leachate treatment plant, using the proposed system under the conditions established. Future investigations should focus on the recovery of permeate flux of nanofiltration, minimizing the fouling of membranes and the destination of the sludge lime application and membrane concentrate.

## ACKNOWLEDGMENTS

The authors would like to thank Municipal Urban Cleaning Company (Rio de Janeiro city) for sending samples of leachates and also to express their gratitude to Brazilian National Council for Scientific and Technological Develop-

ment (CNPq) (process 147737/2016-8) and Foundation for Research Support of the State of Rio de Janeiro (Faperj) (reference E-26/202.923/2018) for the financial support.

## REFERENCES

- Ahmed, F. N. and Christopher Q. (2012). Treatment of landfill leachate using membrane bioreactors: A review. *Desalination*, 287, 41-54. <https://doi.org/10.1016/j.desal.2011.12.012>
- Amaral M. C. S., Pereira H. V., Nani E. and Lange L. C. (2015). Treatment of landfill leachate by hybrid precipitation/microfiltration/nanofiltration process. *Water Sci Technol*, 72.2, 269-276. <https://doi.org/10.2166/wst.2015.218>
- Amaral, M. C. S., Moravia, W. G., Lange, L. C., Rico, M. R., Magalhães, N. C., Ricci, B. C., Reis, B. G. (2016). Pilot aerobic membrane bioreactor and nanofiltration for municipal landfill leachate treatment. *J. Environ. Sci. Health, Part A*, 51:8, 640-649. <https://doi.org/10.1080/10934529.2016.1159874>
- Amokrane, A., Comel, C., Veron, J. (1997). Landfill leachate pretreatment by coagulation-flocculation. *Water Res.*, 31, 2775-2782. [https://doi.org/10.1016/S0043-1354\(97\)00147-4](https://doi.org/10.1016/S0043-1354(97)00147-4)
- Amor, C., De Torres-Socias, E., Peres, J. A., Maldonado, M. I., Oller, I., Malato, S., Lucas, M. S. (2015). Mature landfill leachate treatment by coagulation/flocculation combined with Fenton and solar Photo-Fenton processes. *J. Hazard. Mater.*, 286, 261-268. <https://doi.org/10.1016/j.jhazmat.2014.12.036>
- APHA/ AWWA/ WEF. Standard Methods for the Examination of Water and Wastewater, 22nd. USA, APHA, 2012.
- Aziz, H. A., Alias, S., Adlan, M. N., Faridah, Asaari, A. H., Zahari, M. S. (2007). Color removal from landfill leachate by coagulation and flocculation processes. *Bioresour. Technol.*, 98, 218-220. <https://doi.org/10.1016/j.biortech.2005.11.013>
- Baker R. W. (2012). *Membrane Technology and Applications*. John Wiley & Sons, United Kingdom, 3rd ed., 575 p.
- Calabrò, P. S., Gentili, E., Meoni, C., ORSI, S., Komilis, D. (2018). Effect of the recirculation of a reverse osmosis concentrate on leachate generation: A case study in an Italian landfill. *Waste Manage.* 76, 643-651. <https://doi.org/10.1016/j.wasman.2018.03.007>
- Campos, J. C., Moura, D., Costa, A. P., Yokoyama, L., Araujo, F. V. F., Cammarota, M. C. (2013). Evaluation of pH, alkalinity and temperature during air stripping process for ammonia removal from landfill leachate. *J. Environ. Sci. Health., Part A*, 48, 1105-1113. <https://doi.org/10.1080/10934529.2013.774658>
- Chaudhari L. B. and Murthy Z. V. P. (2010). Treatment of landfill leachates by nanofiltration. *J Environ Manage.*, 91, 1209-1217. <https://doi.org/10.1016/j.jenvman.2010.01.007>
- Chen G., Grasel, P., Millington, G., Hallas J., Ahmad H., Tawfiq, K., 2017. Chloride removal from landfill leachate by the ultra-high lime with aluminum process. *J Urban Environ Eng* 11:1, 3-8. <https://doi.org/10.4090/juee.2017.v11n1.003008>
- Cingolani, D., Fatone, F., Frison, N., Spinelli M., Eusebi A. L. (2018). Pilot-scale multi-stage reverse osmosis (DT-RO) for water recovery from landfill leachate. *Waste Manage.*, 76, 566-574. <https://doi.org/10.1016/j.wasman.2018.03.014>
- Costa A. M., Alfaia R. G. S. and Campos J. C. (2019). Landfill leachate treatment in Brazil – An overview. *J Environ Manage*, 232, 110-116. <https://doi.org/10.1016/j.jenvman.2018.11.006>
- De Almeida, R., Costa, A. M., Oroski, F. A., Campos, J. C. (2019). Evaluation of coagulation-flocculation and nanofiltration processes in landfill leachate treatment. *J. Environ. Sci. Health., Part A* 54(11), 1091-1098. doi: 10.1080/10934529.2019.1631093
- Ehrig, H.-J., & Robinson, H., 2010. Landfilling: Leachate Treatment. *Solid Waste Technology & Management*, 858-897. <https://doi.org/10.1002/9780470666883.ch54>
- El-Gohary, F.A., Khater, M., Gamal Kamel, M. (2013). Pretreatment of landfill leachate by ammonia stripping. *J. Appl. Sci. Res.*, 9, 3905-3913.
- Golob, V., Vinder, A., Simonic, M. (2005). Efficiency of the coagulation/flocculation method for the treatment of dyebath effluents. *Dyes and Pigments*, 67(2), 93-97. doi:10.1016/j.dyepig.2004.11.003
- Guerra K. and Pellegrino J. (2012). Investigation of Low-Pressure Membrane Performance, Cleaning, and Economics Using a Techno-Economic Modeling Approach. U.S. Department of Interior, 127.
- Ismail, I. M., Fawzy, A. S., Abdel-Monem, N. M., Mahmoud, M. H., El-Halwany, M. A. (2012). Combined coagulation flocculation pre treatment unit for municipal wastewater. *Journal of Advanced Research*, 3(4), 331-336. doi:10.1016/j.jare.2011.10.004
- Lima L. S. M. S., Almeida R., Quintaes B. R., Bila D. M. and Campos J. C. (2017). Evaluation of humic substances removal from leachates originating from solid waste landfills in Rio de Janeiro State, Brazil. *J. Environ. Sci. Health, Part A*, 52, 828-836. <https://doi.org/10.1080/10934529.2017.1312182>
- Liu Z., Wu W., Shi P., Guo J. and Cheng J. (2015). Characterization of dissolved organic matter in landfill leachate during the combined treatment process of air stripping, Fenton, SBR and coagulation. *Waste Manage.*, 41, 111-118. <https://doi.org/10.1016/j.wasman.2015.03.044>
- Liu, B., Giannis, A., Zhang, J., Chang, V. W.-C., & Wang, J.-Y. (2014). Air stripping process for ammonia recovery from source-separated urine: modeling and optimization. *J. Chem. Technol. Biotechnol.*, 90 (12), 2208-2217. <https://doi.org/10.1002/jctb.4535>
- Metcalfe, E., Eddy, H., Tchobanoglous, G., Burton, F.L., Stensel, H.D. (2003). *Wastewater Engineering: Treatment and Reuse*, fourth ed. McGraw-Hill. [https://doi.org/10.1016/0309-1708\(80\)90067e6](https://doi.org/10.1016/0309-1708(80)90067e6).
- Postacchini L., Ciarapica, F. E., Bilivacqua, M. (2018). Environmental assessment of a landfill leachate treatment plant: Impacts and research for more sustainable chemical alternatives. *J Clean Prod.*, 183, 1021-1033. <https://doi.org/10.1016/j.jclepro.2018.02.219>
- Renou S., Poulain S., Givaudan J. G. and Moulin P. (2008). Treatment process adapted to stabilized leachates: Lime precipitation–pre-filtration–reverse osmosis. *J. Membr. Sci.* 313, 9-22. <https://doi.org/10.1016/j.memsci.2007.11.023>
- Renou, S., Poulain S., Givaudan J.G., Sahut, C., Moulin P. (2009). Lime treatment of stabilized leachates. *Water Sci. Technol.*, 59:4, 673-685. <https://doi.org/10.2166/wst.2009.014>
- Robinson, A.H., 2005. Landfill Leachate Treatment, 6-12.
- Rodrigues, F. S. F., Bila, D. M., Campos, J. C., Sant'anna Jr, G. L., Dezotti M., 2009. Sequential treatment of an old-landfill leachate. *Int. J. Environ. Waste Manage.* 4, 445-456. <https://doi.org/10.1504/IJEW.2009.027408>
- Rukapan, W., Khananthai, B., Chiemchaisri, C., Chiemchaisri, W., 2012. Short- and long-term fouling characteristics of reverse osmosis membrane at full scale leachate treatment plant. *Water Sci. Technol.* 65 (1), 127-134. <https://doi.org/10.2166/wst.2011.844>
- Salehi E., Madaeni S. S., Shamsabadi A. A. and Laki S., 2014. Applicability of ceramic membrane filters in the pretreatment of coke-contaminated petrochemical wastewater: Economic feasibility study. *Cerami Inte.* 40, 4805-4810. <https://doi.org/10.1016/j.ceramint.2013.09.029>
- Schiopu A. M., Piuleac G. C., Cojocar C., Apostol I., Mămăligă I. and Gavrilescu M. (2012). Reducing environmental risk of landfills: leachate treatment by reverse osmosis. *Environ. Eng. Manage. j.* 11, 2319-2331. doi:10.30638/eemj.2012.286
- Serdarevic, A. (2018). Landfill Leachate Management – Control and Treatment. *Advanced Technologies, Systems, and Applications II, Lecture Notes in Networks and Systems* 28, [https://doi.org/10.1007/978-3-319-71321-2\\_54](https://doi.org/10.1007/978-3-319-71321-2_54)
- Silva, L.C., Reis, H. S., Afonso, B. W. Avaliação econômica de diferentes processos para remoção de amônia de lixiviados de aterros sanitários. Trabalho de Conclusão de Curso em Engenharia Química. 2011. 79 f. Escola de Química, UFRJ, RJ, 2011. (In Portuguese).
- Singh N. and Cheryan M. (1998). Process Design and Economic Analysis of a Ceramic Membrane System for Microfiltration of Corn Starch Hydrolysate. *J Food Eng.* 38, 57-67. [https://doi.org/10.1016/S0260-8774\(98\)00103-4](https://doi.org/10.1016/S0260-8774(98)00103-4)
- Sir M., Podhola M., Patocka T., Honzajkova Z., Kocurek P., Kubal M. and Kuras M. (2012). The effect of humic acids on the reverse osmosis treatment of hazardous landfill leachate. *J Hazard Mater.*, 207-208, 86-90. <https://doi.org/10.1016/j.jhazmat.2011.08.079>
- Smol, M., Włodarczyk-Makula, M. (2016). Effectiveness in the removal of organic compounds from municipal landfill leachate in integrated membrane systems: coagulation – NF/RO. *Polycycl. Aromat. Compd.*, 37, 456-474. <https://doi.org/10.1080/10406638.2016.1138971>
- Talalaj, I. A. and Biedka, P. (2015). Impact of concentrated leachate recirculation on effectiveness of leachate treatment by reverse osmosis. *Ecol. Eng.*, 85, 185-192. <http://dx.doi.org/10.1016/j.ecoeng.2015.10.002>
- Talalaj, I. A., Biedka, P., Bartkowska I. (2019). Treatment of landfill leachates with biological pretreatments and reverse osmosis. *Environmental Chemistry Letters*. <https://doi.org/10.1007/s10311-019-00860-6>



- Tavares C. R. G. and Brião V. B. (2012). Ultrafiltration of effluents from a dairy industry for nutrient recovery: effect of pressure and tangential velocity. *J. Food Technol.*, 15:4, 352-362. <http://dx.doi.org/10.1590/S1981-67232012005000028>
- Yao, P. (2013). Perspectives on technology for landfill leachate treatment. *Arabian J. Chem.* <http://dx.doi.org/10.1016/j.arab-jc.2013.09.031>
- Youcai, Z., & Ziyang, L. (2017). General Structure of Sanitary Landfill. *Pollution Control and Resource Recovery*, 1–10. <https://doi.org/10.1016/b978-0-12-811867-2.00001-7>
- Zawierucha I., Kozłowski C., Malina G. (2013). Removal of toxic metal ions from landfill leachate by complementary sorption and transport across polymer inclusion membranes. *Waste Manage.* 33, 2129-2136. <https://doi.org/10.1016/j.wasman.2012.12.015>
- Zhang L., Lavagnolo M. C., Baid H., Pivato A., Raga R., Yue D. (2019). Environmental and economic assessment of leachate concentrate treatment technologies using analytic hierarchy process. *Resour Conserv Recy.*, 141, 474-480. <https://doi.org/10.1016/j.resconrec.2018.11.007>

# TREATMENT OF LANDFILL LEACHATE AT A REMOTE CLOSED LANDFILL SITE ON THE ISLE OF WIGHT

Tim Robinson \*

Phoenix Engineering, Phoenix House, Scarne Mill Industrial Estate, Launceston, Cornwall, PL15 9GL, United Kingdom

## Article Info:

Received:  
1 November 2019  
Revised:  
5 March 2020  
Accepted:  
11 March 2020  
Available online:  
30 March 2020

## Keywords:

Biological treatment  
Landfill leachate  
Leachate treatment  
Nitrification  
Wastewater treatment

## ABSTRACT

Safe treatment and disposal of leachates is an important issue at many old landfill sites, where the ingress of rainfall or groundwater is a significant issue requiring consideration. Such leachates may typically be relatively weak, but flows are often characterised by large seasonal variations, in response to winter rainfall. This paper compiles and presents long-term data from a case study on the Isle of Wight, UK. This paper highlights how a successful treatability trial using representative leachates can help predict the effectiveness of a large-scale treatment plant when treating landfill leachates biologically. Bleakdown leachate treatment plant effectively removes all concentrations of ammoniacal-N within the weak leachate generated by the site, ensuring that the discharge consent set by the Environment Agency is achieved consistently. The site is completely unmanned and remote, where monitoring technicians are only required to attend site twice per month in order to assess the success of the biological process. Through an online SCADA control system, operation of the treatment plant can be monitored and controlled remotely, trends in results can be observed, and daily data and treatment records downloaded. This treatment plant is an example of how leachate from old closed landfills can be effectively managed, with very low costs of operation, maintenance and site attendance. This paper presents comprehensive analytical and volumetric treatment data from the Bleakdown LTP, before presenting practical steps that would enable this success to be replicated at similar remote closed landfill sites.

## 1. INTRODUCTION

The Bleakdown landfill site is located approximately 7km south of Newport, on the Isle of Wight. The site comprises an infilled sand and gravel pit, which received inputs of domestic, commercial, and non-hazardous industrial wastes, as well as inert, construction and demolition wastes, between 1977 and 1998. There was no engineered lining of the base, and the site was designed to operate on the “dilute and disperse” principle that was widely adopted at that time. There are three locations where leachates are currently being intercepted and collected at the Bleakdown site. Leachate quality is surprisingly consistent at each location, showing relatively small seasonal variations in strength.

It is primarily the dilute nature of the Bleakdown leachate that distinguishes this case study from more typical leachate treatment projects. The weaker characteristics of the leachate at Bleakdown compared to other landfill sites are considered throughout the report, particularly when discussing the different blends of leachate that were sampled through the Bleakdown treatability trials initially, before

samples were regularly taken after the full-scale treatment plant was commissioned.

Because of the implications for the sustainability of the biomass within the treatment process, it is very important to highlight the low ratio of ammoniacal-N ( $\text{NH}_4\text{-N}$ ) when compared to the combined iron (Fe) and calcium (Ca) concentrations. Due to the low potential for biological sludge growth, it was important to highlight to the client that occasional supplementation of biological sludge may well be required by the treatment process – this is often most beneficial on an annual basis, before wetter winter months.

Later in this paper, the anticipated sludge biomass growth rate will be considered using the information displayed in Table 1, in order to highlight such requirements.

Based on the results obtained from an extended leachate treatability trial performed during December 2015, it was concluded that a well-designed, but relatively simple SBR aerobic biological leachate treatment plant could readily and reliably achieve complete degradation of all biodegradable COD, and full nitrification of all ammoniacal-N, to produce an effluent suitable for direct discharge into a small local surface watercourse. During June 2017, Phoe-



nix completely redesigned and refurbished an existing but ineffective treatment plant at Bleakdown, making several significant changes to the process and plant components, in order to provide consistent leachate treatment.

Plate 1 depicts the re-furbished leachate treatment plant following installation during June/July 2017. The three main tanks can be seen in the photograph below; the pre-existing Raw Leachate Balancing Tank (RLBT), the Treated Leachate Balancing Tank (TLBT), and the newly installed glass/epoxy fused steel tank that is operated as a modified Sequencing Batch Reactor (SBR), providing full nitrification of the leachate requiring treatment.

## 2. PREVIOUS OPERATION OF THE TREATMENT PLANT

The pre-existing leachate treatment plant at Bleakdown Landfill Site was not able to treat volumes of leachate being generated at the site either reliably or consistently, to achieve required discharge standards. This was partly because the plant was originally designed to treat only small volumes of leachates from the minor collection chambers at DP1 and DP2, rather than the newer leachate Sump which now produces increased volumes of stronger leachate.

The Sump collection point comprises a 1.2m diameter sump which had been installed within a recently improved and cleaned out perimeter ditch, running from SW to NE towards the eastern boundary of the site. The sump contains an electric pump, which operates between high and low-level float switches, and pumps leachate in a westerly direction, through a 2-way electric solenoid valve that is able to divert sump leachate either to the leachate treatment plant, or for irrigation through a single pipeline. Plate 2 depicts the general location of the Sump and ditch at Bleakdown.

Pumping Chambers DP1 and DP2, are located along the eastern perimeter of the landfill, DP1 to the north end of the site, about 60m SE of the leachate treatment plant, and DP2 nearly 300m further south along the eastern boundary, just to the east of the main sump.

Each location represents a collection location for diluted leachates collected by various gravel-filled trenches/French drains constructed along the eastern boundary of the landfill. These intercept surface breakouts of leachate, which probably represent perched water tables above the underlying clay layer at the base of landfilled wastes. Each chamber contains an electric pump, controlled by high and low-level float switches, which pumps leachate from within it to the leachate treatment plant, via connections into the pipeline mentioned earlier, that also pumps leachate from the Sump to the leachate treatment plant. Plates 3A and 3B show the DP1 and DP2 locations respectively.

Plate 4 displays the original layout of the treatment plant, where three tanks were used to collect and store leachate from only DP1 and DP2, before this was discharged to the local stream.

Figure 1 displays an aerial schematic of the landfill site, highlighting the three leachate pumping locations and also the location of the leachate treatment plant towards the North of the site. The leachate pumping lines from each collection location are also highlighted, where DP2 and the Sump location share a pipeline.

In the absence of any historic data for concentrations of ammoniacal-N in the blended leachate being treated, or any data for concentrations of nitrate-N or nitrite-N in treated leachate being discharged, it was difficult to know precisely the extent to which the previous plant was receiving or treating ammoniacal-N in the leachate. Nevertheless, during a period from September to Novem-



**PLATE 1:** Aerial photograph of the Bleakdown landfill leachate treatment plant (LTP), showing the control building, RLBT, TLBT, and new glass/epoxy fused steel SBR tank (left to right).



**PLATE 2:** General view of the more recently installed leachate collection point at the Sump on the Bleakdown landfill site.



**PLATE 3:** (a) Sampling performed at DP1; (b) Routine sampling work at DP2.

ber 2014, when higher concentrations of ammoniacal-N in leachate collected at the Sump to the South East of the site were included in the raw leachate blend, treatment was clearly unsuccessful, with nearly 20 mg/l of ammoniacal-N found in the treated leachate failing the discharge consent significantly (an Environment Agency discharge consent had previously been set at 5 mg/l). It was concluded that this was due to an inadequate treatment plant process design.

Average annual rainfall at Bleakdown during the six years prior to Phoenix's involvement in 2015 had been about 940mm. Over the 10 hectares of the completed land-

fill site, it was therefore calculated that on average, about 94,000m<sup>3</sup> of rain had fallen per year. By the end of 2015, it appeared likely that about 10,000m<sup>3</sup> of leachate may have been collected in total from DP1, DP2 and the Sump, representing just over 10 per cent of incident rainfall. This volume is more than twice that collected in 2014, and more than three times that extracted during 2013. It was therefore clear that during recent years, and possibly all previous years, significant volumes of leachate had been generated, and were either accumulated within wastes, or (more likely) were leaving the site and being attenuated and diluted to an uncertain degree.



**PLATE 4:** The Bleakdown landfill leachate treatment plant (LTP) in July 2016, prior to refurbishment work.

For more than 12 months, from summer 2014, the significantly stronger leachate from the Sump location (making up the majority of all leachate being generated at Bleakdown) had therefore been excluded from treatment and was being spray irrigated onto the “restored” landfill surface (see Figure 1). At the time, it appeared likely that most of this leachate was simply infiltrating into wastes, and was being represented by significantly increasing overall rates of leachate generation. What was certain is that, having collected leachates from DP1, DP2 and the main Sump, it was going to be far better for all of the leachate to be treated reliably and discharged safely off-site in compliance with the discharge consent, rather than being reintroduced back into wastes through the cap, to reappear as increased leachate generation rates.

Since autumn 2014, weakest leachates from DP2 (mean ammoniacal-N of 2.2 mg/l) comprised most of the leachate being passed through the pre-existing on-site treatment plant. This is the primary reason why “treated” leachate had historically consistently met the discharge consent value of 5 mg/l for ammoniacal-N, although actually receiving minimal treatment.

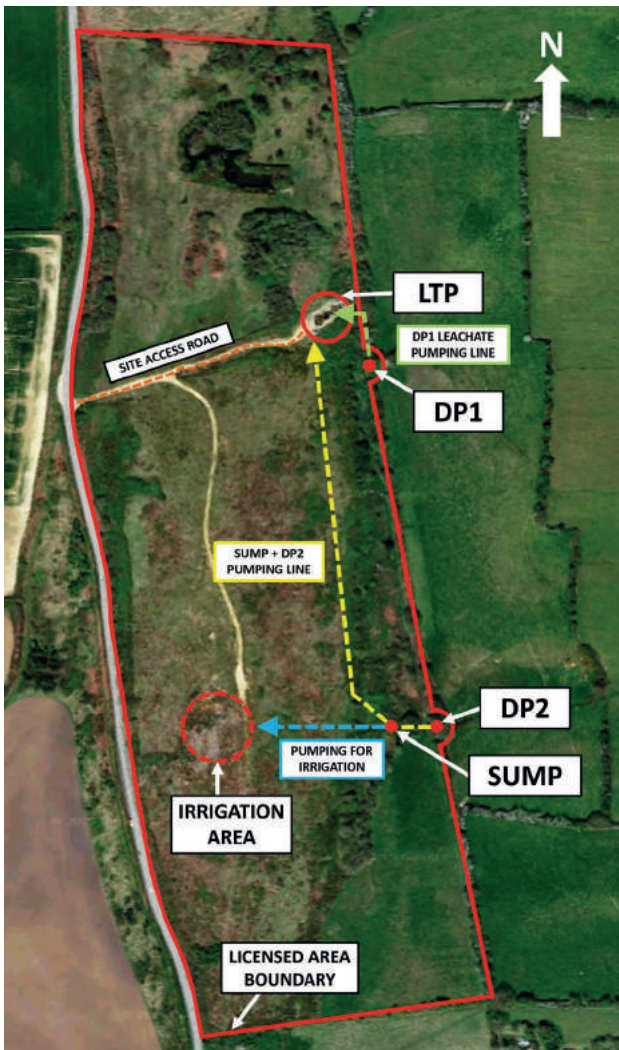
From leachate flow data collected during 2015, it appeared that a full-scale plant at Bleakdown would be required to treat leachates at rates of up to 50 or 60m<sup>3</sup>/d

depending on seasonal rainfall variations, whilst average annual rates of 25 or 30m<sup>3</sup>/d could be expected.

Phoenix considered all options for making use of the existing treatment plant infrastructure, as far as this was possible, to minimise costs of a new plant with an appropriate and modified process design. This upgraded treatment system would need to be completely automated, with full remote internet access enabling remote monitoring, operation and observation for this remote and unmanned site. The preferred and recommended option was that a new SBR tank be constructed to replace one of the pre-existing tanks on the existing concrete slab of the LTP. The other existing tanks were re-used as raw leachate balancing and feed tanks, as part of the new treatment process.

### 3. SITE INVESTIGATIONS AND TREATABILITY TRIALS

Before a new leachate treatment plant design could be constructed and commissioned at Bleakdown, detailed site investigations were necessary, in addition to the completion of thorough treatment trials on representative Bleakdown leachates. These site investigations and treatability trials were performed during late 2015 and early 2016.



**FIGURE 1:** Satellite image of the Bleakdown landfill site and leachate treatment plant (LTP).

### 3.1 Site investigations and reporting

Preliminary site investigations revealed that there was no engineered lining of the base of the Bleakdown landfill site, and that the site was designed to operate on the “dilute and disperse” principle that was widely adopted at that time (e.g. see UK Department of the Environment, “Cooperative Programme of Research on the Behaviour of Hazardous Wastes in Landfill Sites: Policy Review Committee Final Report”, April 1978). Nevertheless, sands and gravels were reportedly extracted down to the top of an underlying clay layer, which had been shown to exist in several areas of the site, and locally enables relatively diluted leachates to emerge around the site perimeter in some locations, particularly along its eastern boundary.

The landfill site runs north to south, is approximately 550m long and 230m wide, and has an approximate total surface area of about 9 or 10 hectares, over which wastes are typically up to 10m deep. The highest point on the completed landfill surface is at an elevation of about 86m AOD.

The site’s Environmental Permit requires the site owners to submit an annual Environmental Monitoring Report,

which details results that include monitoring of leachates and surface waters at the site.

### 3.2 Treatability trials

It was considered that a well-designed and relatively simple on-site plant could readily treat all leachates generated at Bleakdown, reliably and robustly. In order to demonstrate this, pilot-scale treatment trials were therefore undertaken on a representative blend of Bleakdown leachates (80% from the Sump, 10% each from DP1 and DP2), which contained just over 20 mg/l of ammoniacal-N:

Sampling location	Proportion of leachate included
SUMP	80%
DP 1	10%
DP 2	10%

Treatment during the trials was accomplished at mean hydraulic retention times of 1 day or less, using a relatively simple process design, consisting of a modified Sequencing Batch Reactor (SBR) with 8-hour and then 6-hour cycles, as Phoenix have installed at many similar sites. Those trials were operated at temperatures of between 12°C and 14°C, which appeared realistic, based on experience at similar installations.

Leachate for use in the trials was collected from Bleakdown Landfill, on 20<sup>th</sup> and 21<sup>st</sup> October 2015, from each of the 3 discharge locations along the Western perimeter of the site, including the Sump and Discharge Points DP1 and DP2.

A total of 1,200 litres of leachate was collected in measured volumes, to be blended together for use as feedstock for the treatment trials. Leachate was transported to Phoenix’s leachate laboratory in Launceston, Cornwall, where it was stored in a sealed container during the trials.

By mixing calculated proportions of leachate from each individual location, a representative blend of Bleakdown leachate was produced, to be used in Stage One, and then in Stage Two, of the treatment trials. The blended proportions of leachate from each of the three locations, making up the leachate feed for each stage of the trials, are summarised below.

These proportions were estimated prior to detailed examination of actual pumping data, and based on broad information. However, when such examination was completed and reported, it was clear that the blend of leachates used as feedstock for the treatability trials was entirely typical of the quality of leachate that an on-site plant would probably be required to treat for extended periods (see Table 1).

The Bleakdown treatability trials were seeded using 75 litres of mixed liquor, from biological sludge that had been collected and transported from Small Dole Leachate Treatment Plant near to Shoreham-on-Sea, on 22<sup>nd</sup> October 2015. Because that sludge had been well acclimatised to similar leachate, relatively rapid establishment of successful treatment was anticipated for the new leachate feed. The initial mixed liquor that was aerated before the start of the trials, contained 12,300 mg/l suspended solids, but af-

**TABLE 1:** Leachate blend quality used for the representative treatability trials on Bleakdown leachate.

Sample ID	Leachate blend	Day 11 leachate feed	Day 15 leachate feed
Sampled Date	21/10/2015	06/11/2015	10/11/2015
COD, unfiltered	92.1	85.7	80.7
BOD, unfiltered	-	28	-
Total Organic Carbon	29.1	30.8	36.3
conductivity ( $\mu\text{S}/\text{cm}$ )	-	1,170	-
ammoniacal-N	16.7	17.8	15.7
nitrate-N	1.52	2.16	3.83
nitrite-N	0.051	0.51	0.565
alkalinity (as $\text{CaCO}_3$ )	500	530	520
Total Oxidised Nitrogen	-	2.67	-
pH-value	-	8.23	-
chloride	108	124	120
sulphate	-	21.2	-
phosphate as P	-	<0.05	-
sodium	69.9	89.3	74.8
magnesium	-	25.6	-
potassium	-	30.8	-
calcium	-	149	-
chromium	-	3.14	-
iron	8.81	-	-
nickel	-	5.53	-
copper	-	<4	-
zinc	-	5.58	-
cadmium	-	<0.5	-
lead	-	<0.5	-
arsenic	-	2.54	-
mercury	-	<0.02	-
manganese	-	184	-
selenium	-	4.88	-

Notes: All results in mg/l, except pH-value, conductivity ( $\mu\text{S}/\text{cm}$ ) and heavy metals (in  $\mu\text{g}/\text{l}$ ); Alkalinity as  $\text{CaCO}_3$ ; - = No Result; Analyses by ALS Ltd, Chester Laboratory.

ter desludging to a desired concentration, suspended solids within the aerated reactor remained fairly consistent at about 5,000 mg/l (375 grams total solids), from Day 5 until the end of the trials.

Concentrations of solids in mixed liquor within the aerobic reactor were tested for suspended solids (SS) every two or three days during the entire trial, and results were both replicable and consistent. In addition, samples were taken twice each week and submitted to ALS Laboratories for determination of both suspended solids (SS) and volatile suspended solids (VSS). The ALS results were also consistent and considered to be reliable. The sludge settled well and effluent clarified very well throughout the trial.

In full-scale leachate treatment plants treating strong

and undiluted leachates from recently-emplaced wastes (e.g. 2,000mg/l of ammoniacal-N), mixed liquor would typically contain a ratio of VSS:SS of about 70 or 80 per cent. However, in leachates from old closed landfills, such as Small Dole and also Bleakdown, which contain significant concentrations of iron and calcium, greater levels of inorganic compounds in sludge, typically mean sludges contain only 20 or 25 per cent of VSS, as was the case for seed sludge collected and used in these trials.

Unlike SBR processes treating stronger leachates with high concentrations of ammoniacal-N (>1,000 mg/l), where sludge growth and accumulation is common, it would probably not be necessary to allow for desludging of the full-scale SBR system at Bleakdown. In contrast, it would be likely that occasional further additions of biological sludge would occasionally be necessary.

By interpreting results presented in Table 1, the low ratio of ammoniacal-N to inorganic iron and calcium solids can be highlighted quantitatively. A mean ammoniacal-N concentration of 16.7 mg/l can be compared to the combined inorganic solids concentrations of iron (8.81 mg/l) and calcium (149 mg/l), which equates to a ratio of approximately 1:9.3. This ratio highlights an extremely low concentration of ammoniacal-N when compared to inorganic solids. In addition to this ratio, the low BOD of 28 mg/l within the leachate emphasises the potential requirement for occasional deliveries of fresh biological sludge, alongside possible accumulation of inorganic solids within the SBR.

Figure 2 presents data for suspended solids (SS) and volatile suspended solids (VSS) concentrations during the treatability trials. This figure highlights that although both SS and VSS did reduce during the first five days of the trial, consistent concentrations were met, which stabilised until the end of the trial. From these results it was concluded that, on a larger scale, the same phenomenon would be achieved, whereby a lower suspended solids and volatile suspended solids concentration could be maintained and effectively provide treatment over extended periods of up to 18 months (see Figure 17 presented later).

As anticipated, because the ratio of alkalinity to ammoniacal-N in raw leachate being treated was about 30:1 (530mg/l: 18mg/l), pH-values remained consistent throughout the trial, meaning no additions of external alkalinity as sodium bicarbonate were required (see Figure 7 later). This is typical of leachates from older closed landfills, and considerably simplified design for on-site treatment of leachate at Bleakdown.

Figure 3 presents data for volumes of the Bleakdown leachate blend that were treated each day during Stage 1 and Stage 2 of the trials. Treatment began on the basis of three complete SBR cycles per day, of 8 hours each. At the end of Day 11, the operating system was modified so that four treatment cycles were fitted into 24 hours, which overcame hydraulic constraints imposed by the volume of treated leachate which could be decanted in any given cycle, and enabled significantly more leachate to be treated by the SBR setup. Figure 4 expresses these data as mean daily Hydraulic Retention Time (HRT) being achieved.

The treatment unit rapidly achieved flow rates in excess of 40 litres of leachate feed per day from the start of the tri-

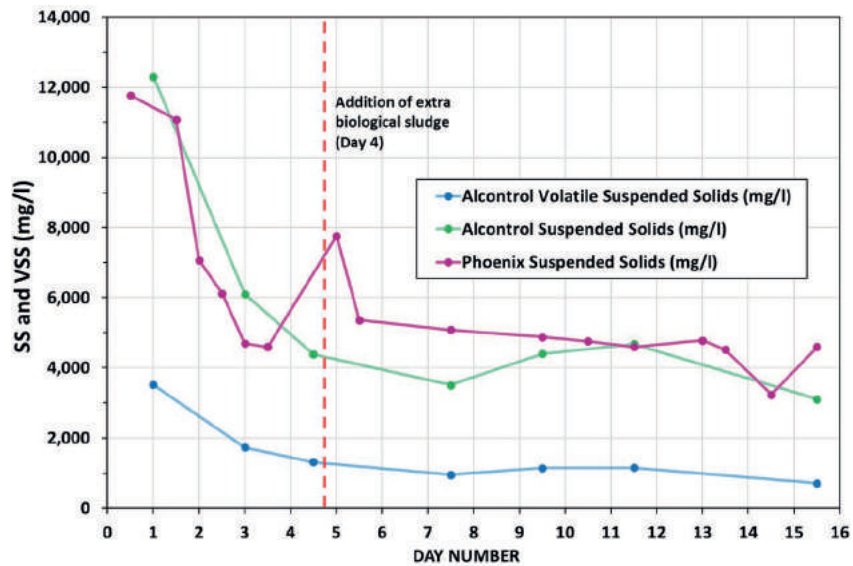


FIGURE 2: Concentrations of Suspended Solids and Volatile Suspended Solids during the treatability trials.

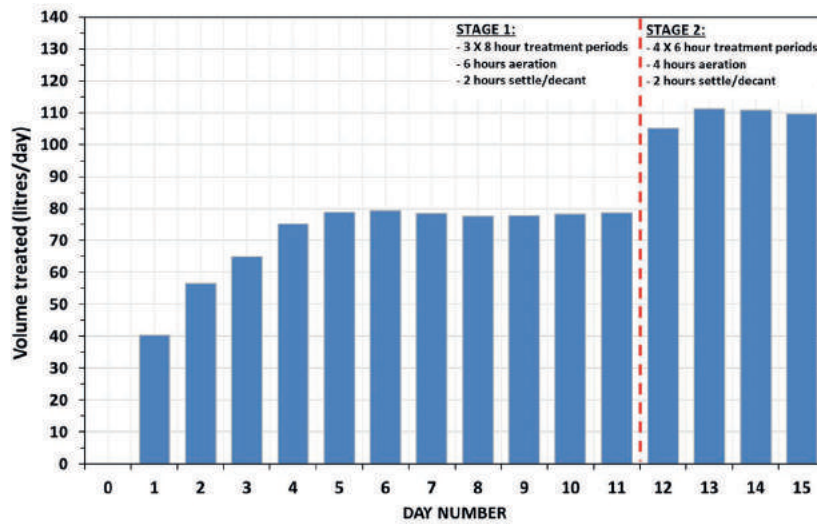


FIGURE 3: Volumes of leachate (litres) treated each day during the trials, days 0 to 15.

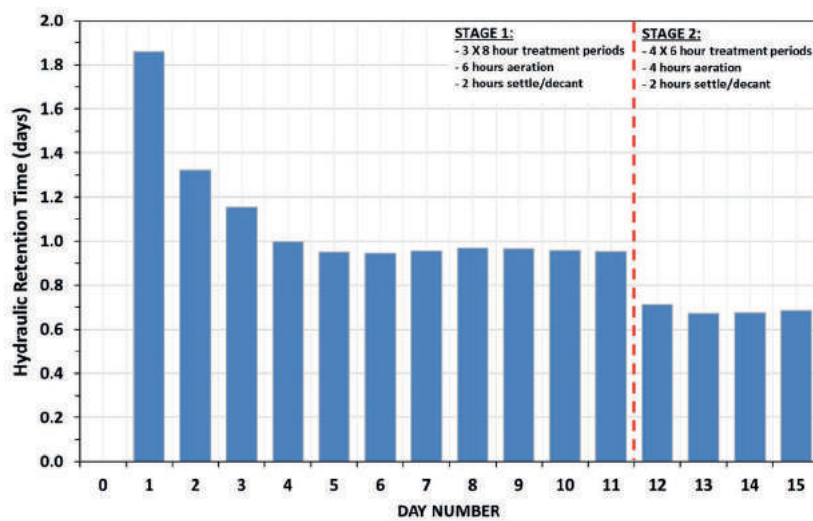


FIGURE 4: Mean Hydraulic Retention Time (days) during the trials, days 0 to 15.



al, rising to exceed 75 litres per day within four days (mean HRT 1.33 days). From Day 4, more than 75 litres of leachate was treated on a daily basis, with an average daily volume of 78.0 litres fed from Day 4 until Day 11 (representing a mean HRT of 0.96 days). By Day 11 nearly 800 litres (785.7) of leachate had been treated in total, at an overall mean HRT of 1.09 days. The stability and consistency with which the trials operated is evident from all results and figures.

During Stage 2 of the trials, from Days 12 to 15, an additional 436.9 litres of leachate was fed and treated, with a mean daily feed volume of 109.2 litres achieved. At this point the mean Hydraulic Retention Time achieved was substantially below one day (mean HRT of 0.69 days).

Overall, 1222.6 litres of leachate were treated at mean rate of 81.5 litres per day, representing an overall mean hydraulic retention time (HRT) of 0.92 days. However, following the initial three days of increasing the leachate feed, the mean treatment rate was actually 88.4 litres per day (Mean HRT of 0.85 Days) during the final 12 days of the trial before leachate feed ran out. Treatment was stable at a mean HRT of less than 0.7 days during the last 4 days.

The treatment process adopted involved a relatively straightforward process design, comprising a modified Sequencing Batch Reactor (SBR) operated with cycle durations of initially 8 hours, and then 6 hours during the last 4 days of the trials. Leachate was treated at rates of up to 110 litres per day, in a reactor having a minimum hydraulic volume of 75 litres, achieving a minimum mean hydraulic retention time (HRT) of down to 0.7 days.

The trials were carried out for a total of 15 days, during which complete, precise and consistent treatment of leachate was maintained, with essentially full removal of ammoniacal-N (>98.5%) by complete nitrification at all times. Figure 5 highlights successful nitrification of ammoniacal-N throughout the trials, where ammoniacal-N is removed whilst Nitrate-N is released.

Figure 6 shows that removal of degradable COD was minimal (~10%), however, with such a low initial COD concentration of ~85 mg/l, it was not necessary to remove significant amounts. In addition to this, COD was not listed as a parameter that required particular attention on the discharge consent set by the Environment Agency (see Table 2).

Very accurate data were obtained for alkalinity balance, which confirmed that it would not be necessary to add external alkalinity during treatment of the leachate, and considerably simplified design of the full-scale treatment plant. Figure 7 shows that pH-value was maintained between 8.1 and 8.5 throughout the treatability trials. Because nitrification is an acid-generating process, in some cases it is necessary to add an alkali to the treatment process in order to raise the pH. However, in this instance the leachate provided sufficient alkalinity to buffer any impact of nitrification on pH-values within the reactor. This is common to the treatment of most weak leachates.

Throughout the treatability trial, the effluent clarified well, which provided an effluent containing low levels of suspended solids throughout the trial. This was an important factor when designing the full-scale treatment plant, because it showed that an effluent containing few solids would be discharged into a small, local watercourse.

The trials confirmed that a well-designed, modified SBR leachate treatment plant at Bleakdown would work reliably and consistently, and would require a treatment reactor with a mean Hydraulic Retention Time of less than 1 day. The next stage was therefore to design how this treatment process could be provided at full-scale, making best use of existing infrastructure from the previous plant. It was clear that a relatively small plant, based on the process design that had been tested during the trials could be developed for relatively low cost at Bleakdown.

## 4. SITE REPORTING AND DETAILED DESIGN

The refurbished leachate treatment plant (LTP) at Bleakdown Landfill was designed, constructed and commissioned as an aerobic biological suspended growth plant (Modified Sequence Batch Reactor SBR) during summer 2017. The treatment process adopted was one of biological nitrification. The design was based on information obtained during the comprehensive laboratory treatability trial.

The process design parameters used were adopted from the discharge permit, as outlined by the Environment Agency. These design parameters and loading concentrations are presented in Table 2.

As highlighted previously, leachates are generated from three locations at Bleakdown Landfill, which are termed "Sump", "DP1", and "DP2". At each of these three locations there was a pre-existing pump and pipeline leading to the refurbished leachate treatment plant. Leachate collected at these three points was to be pumped via the existing pumps and pipelines to the refurbished LTP, where it would be aerobically treated. Using the three existing leachate collection locations across the site, the new system is able to manage the incoming blend of leachate, by pumping this volume to a holding Raw Leachate Balancing Tank (RLBT) at the LTP.

Existing raw leachate collection systems and pipework were in good working order along the boundary of the existing reinforced concrete base, and no additional work was required, other than connection and integration into the new control system.

The new SBR comprises a circular glass/epoxy fused steel tank, with a nominal working volume of 122m<sup>3</sup> (Tank ID 7800mm, Height 3060mm). The top liquid depth is 2560mm and the bottom liquid depth is 2240mm.

Figure 8 depicts the original process flow diagram that was outlined during the initial design phase of the new leachate treatment plant at Bleakdown, where leachate is received by the RLBT, before being fed into the SBR in controlled doses.

## 5. CONSTRUCTION AND COMMISSIONING

In order to install the new SBR reactor, a reinforced concrete base was constructed on top of the existing concrete foundations. The glass/epoxy coated steel tank was then placed onto the concrete pad, before steel steps, gantries and supports were fitted.

New pipelines were installed, lagged, and trace heated as required, in order to feed the correct tanks with leachate and discharge treated leachate to the main effluent dis-

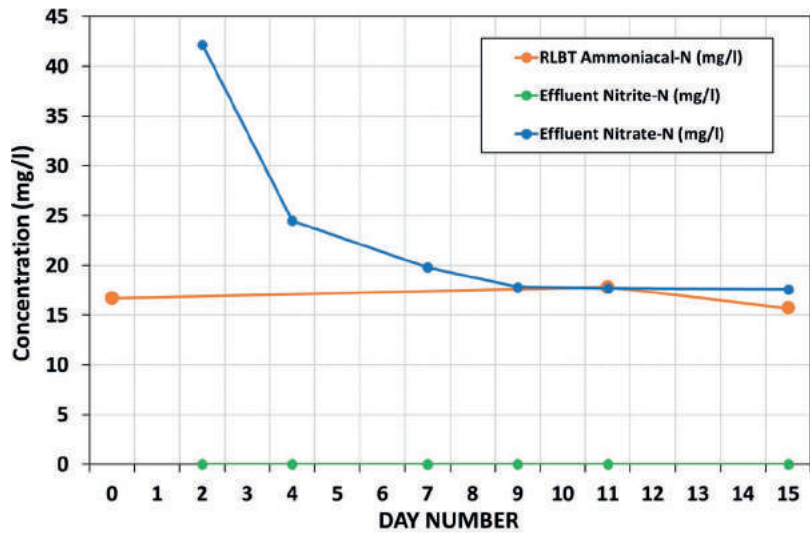


FIGURE 5: Raw leachate Ammoniacal-N concentrations compared to Effluent Nitrite-N and Nitrate-N concentrations.

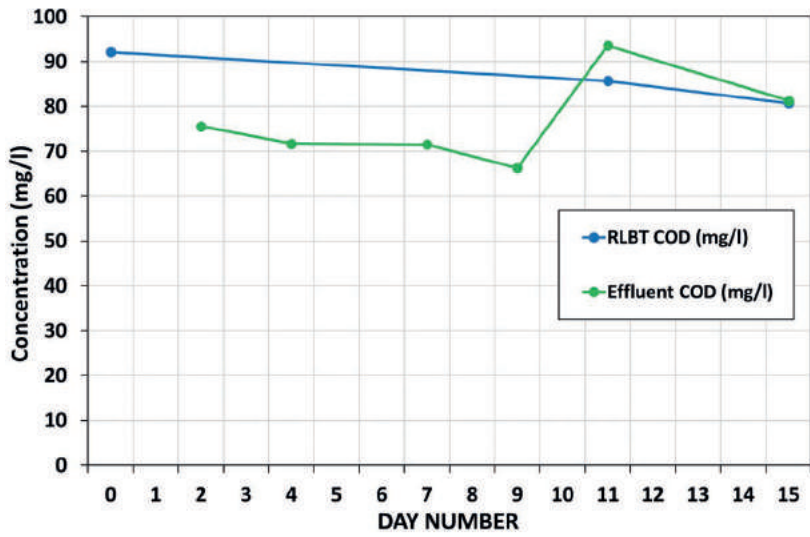


FIGURE 6: Raw leachate COD concentrations compared to Effluent COD concentrations.

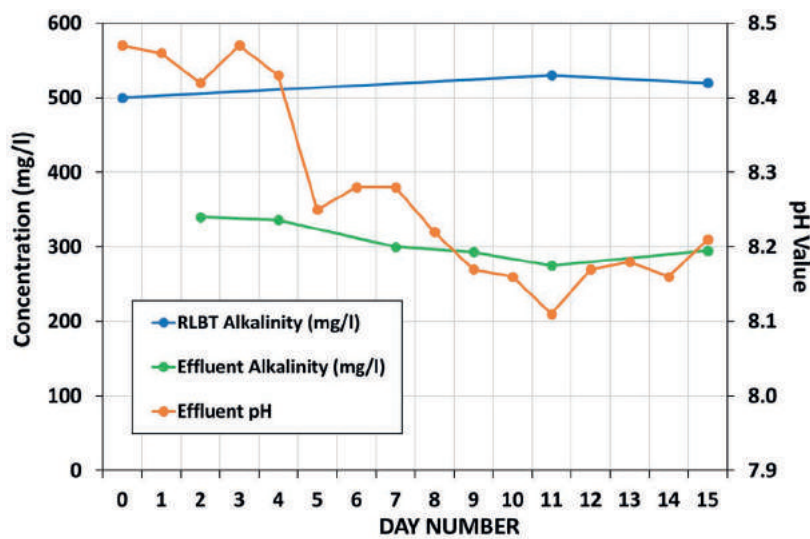


FIGURE 7: Raw leachate Alkalinity concentrations compared to effluent Alkalinity concentrations and pH.

**TABLE 2:** Raw leachate concentrations, process design parameters, and discharge permit for breakdown LTP.

Determinand	Design Blend (Sump, DP1 & DP2)	Design Loading at 60m <sup>3</sup> /day	Environment Agency Discharge Permit
COD	100 mg/l	6 kg COD/day	N/A
Ammoniacal-N as N	20 mg/l	1.2 kg Ammoniacal-N/day	5 mg/l (as Ammonia)
Alkalinity	500 mgCaCO <sub>3</sub> /l	Not less than 30 kgCaCO <sub>3</sub> /day	N/A
Suspended solids	N/A	N/A	130 mg/l
Temperature	N/A	N/A	25°C
Iron (Fe)	10 mg/l	N/A	6 mg/l
*PAH as Benzo (b) fluoranthene	< 0.1 ug/l	N/A	0.1 ug/l
pH-Value	N/A	N/A	6.0-8.5

\* PAH as Benzo (b) fluoranthene: This was not tested during the treatability trials. However, data on concentrations present in the leachate were supplied by the employer. On most occasions the concentration was below the recorded limit of detection <0.023ug/l. A marginally higher value of <0.046ug/l was recorded in the sump in February 2015 and January 2016. All these values are well below the Discharge Permit value of 0.1 ug/l, thus it is reasonable to assume a design blend value of <0.1ug/l.

charge point. The pipelines were fitted with flowmeters, so that incoming and outflowing volumes of leachate/effluents could be measured and recorded accurately.

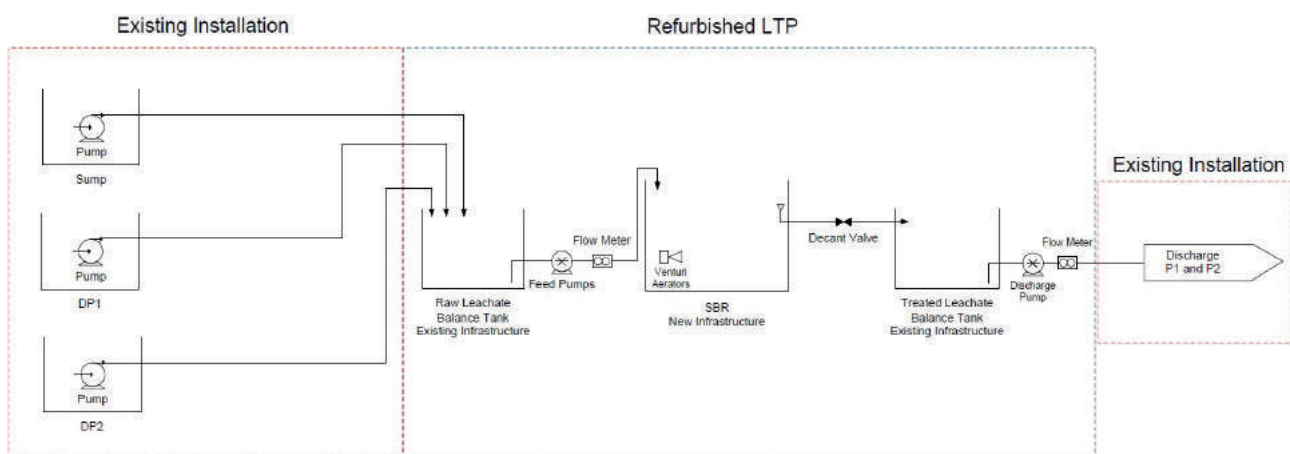
Following this work, all the electrical installation was completed, which involved fitting new valves (EAVs), flowmeters and instrumentation devices within the necessary tanks, before wiring these devices to control panels, and then back to the main control building. From the control building, the information from each device could be clearly displayed on the SCADA system.

Plate 5 shows the completed treatment plant during June 2017, following the biological commissioning. In the foreground the newly installed SBR tank is visible, which is used as the main treatment reactor. Following complete cleaning and refurbishment, the two pre-existing tanks were utilised as the RLBT and TLBT for raw leachate and treated leachate storage respectively. In the distance, the new control building is visible, at the end of the concrete foundations. The control building was constructed and fabricated within the small shipping container at Phoenix's premises in Cornwall, before being transported to site on the Isle of Wight. In order to enable monitoring on site,

CCTV was fitted to the control building, whilst 4G access enabled the SCADA and camera to be accessed remotely.

The treatment plant was biologically commissioned by Phoenix during June 2017, using seed sludge delivered from the same site in East Sussex which had provided seed sludge for the treatability trials. Thorough sampling work was carried out at the LTP and at the landfill leachate wells, which enabled the successful treatment process to be confirmed. Regular on-site analysis proved that all ammoniacal-N within the raw leachate feed was being removed through an effective nitrification process.

Once the treatment process had been established and was operating reliably, Phoenix were required to train up a local site technician, who would carry out fortnightly checks at the LTP and around the landfill. The technician would also perform routine monthly sampling of all leachate sources on the landfill site, in addition to a complete sampling suite at the LTP and the effluent discharge point. It was important that the site technician had a good understanding of the operation of the treatment plant, and the different reactors contributing to the process, particularly as between the fortnightly site visits the site would be



**FIGURE 8:** Process flow diagram for the new leachate treatment plant as installed at Bleakdown landfill.

unmanned, and only checked by Phoenix through remote access to the SCADA system.

## 6. OPERATION OF THE TREATMENT PLANT

As is common at similar leachate treatment plants, the SBR was to be fed with frequent small volumes of leachate at regular 15-minute intervals throughout the aeration phase. At a design flow rate of 60m<sup>3</sup>/day for the SBR (15m<sup>3</sup>/cycle) the feed pump is on for just over 3 minutes during each feed. This leaves a rest period of 11 minutes before the next feed call. Pump duty of the two feed pumps alternates on the hour, quarter past the hour, half past the hour and quarter to the hour.

The LTP was designed for a treatment capacity of at least 60m<sup>3</sup> per day, but operates satisfactorily at a lower throughput rate, such as the permit constraint of 50m<sup>3</sup> per day, or less. The 6-hour treatment cycle consists of an Aeration and Leachate Feed Period (4 hours), followed by a Settlement Period (1 hour), during which the treated leachate is separated from the biomass. The clarified supernatant is then decanted during the Decant Period (1 hour), as final effluent. In summary, the 6-hour treatment cycle within the SBR is operated as follows in Figure 9.

In order to operate and monitor the treatment within the SBR at Bleakdown LTP, the new Phoenix design of the treatment plant included the following plant and instrumentation:

- 1 x 3 kW venturi aerator, to provide complete aeration, mixing, and some heat input to the SBR.
- A depth transducer and a pH-value sensor were installed in separate stilling tubes.
- A DO probe was also fitted to assess the effectiveness of the aeration cycle.
- Float switch and support bracket, to control maximum depth in the SBR.

This instrumentation is fed back to the SCADA system, in order to effectively present the operational data



**PLATE 5:** The Bleakdown landfill leachate treatment plant (LTP) in June 2017, following the refurbishment works.

in a way that it could be viewed through a computer remotely.

The SCADA also stores data from monitoring devices in addition to displaying information regarding the instantaneous status of the various plant systems. The SCADA displays logs and trends, making data available for downloading to removable and remote storage devices. The system is password protected and open to interrogation by only named individuals to prevent casual interference.

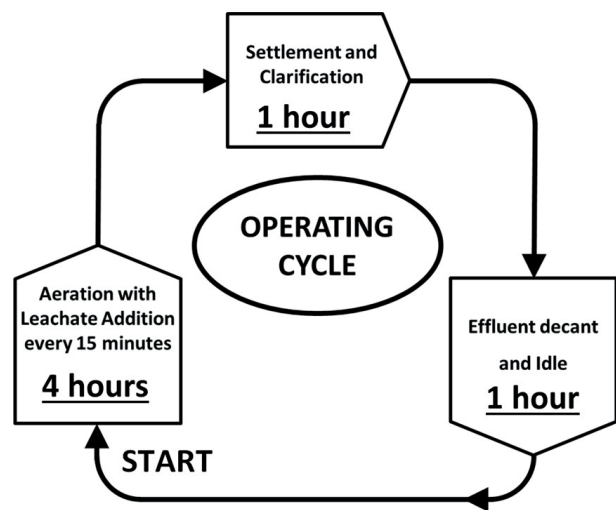
## 7. ROUTINE TESTING, MONITORING AND REPORTING

Following the outset of the operational contract in June 2017, there was a requirement to provide regular reporting of the operation of the treatment plant. This reporting involved monthly sampling of all of the leachates, process waters and effluents being produced by the treatment plant, in addition to the final discharge at the main discharge point from the site.

Phoenix were also contracted to carry out regular fortnightly checks across the leachate pumping locations, as well as thorough observations at the leachate treatment plant.

Following the monthly sampling and routine observations of the treatment plant and landfill site, a monthly update report is required by the client, Aggregate Industries. This update report highlights all data obtained during the month via the SCADA, including incoming leachate volumes and discharged effluent volumes. Phoenix are also able to compile a record of rainfall and weather data, which is collected at a local Bleakdown weather reporting station.

Samples that have been taken by the subcontractor at the start of each month are couriered to a laboratory, and tested for a routine suite of determinands. The results from these analytical tests are then emailed to Phoenix in time for the compilation of the monthly reports. These analytical results are used to confirm basic and routine on-site test strip analyses, and to prove that the discharge consent is



**FIGURE 9:** A single 6-hour treatment cycle, as performed four times every 24 hours at Bleakdown LTP.

met on a monthly basis. These results are also useful for observing the changes in leachate strength on a seasonal basis, which will be discussed later in the report.

In addition to monthly reporting, Phoenix are required to make six-monthly and annual visits to site at Bleakdown, to perform six-monthly maintenance works. On an annual basis, a condition report is produced, highlighting any changes in the condition of the treatment plant or the landfill site. The maintenance visits involve testing all electrical supplies, control panels, instrumentation, flow meters and pumps on the site, in addition to arranging for engineers to visit site to test aerators and heavy-lifting apparatus.

Regular contact with Aggregate Industries is maintained, in order to communicate data on operation of the treatment plant, in addition to pointing out any areas of the site and treatment plant that may require repair or upgrade works.

## 8. OPERATIONAL RESULTS FROM THE TREATMENT PLANT

Since summer 2017, the Bleakdown treatment plant has performed successfully and the strict discharge consent at the site has consistently been met. During the two years since the new treatment plant was commissioned at Bleakdown, a complete record of analytical results, daily rainfall, and daily leachate volumes has been kept, which has enabled accurate observation of the plant's operation to be observed. Figure 10 presents monthly rainfall and treatment volumes, highlighting the impact that seasonal changes in rainfall has on COD and Ammoniacal-N loads.

### 8.1 Rainfall data

At the end of each month, rainfall and weather data from the local Bleakdown weather station is compiled and compared against leachate and effluent flows passing through the treatment plant.

Figure 10 compares historic average monthly rainfall data between 1981 and 2010, to more recent monthly data during the operational period of the upgraded leachate treatment plant at Bleakdown Landfill Site. Figure 10 highlights several distinctive trends in rainfall over previous years, which can be noted below:

- Seasonal changes in rainfall on an average annual basis between 1981 and 2010.
- An exceptionally wet January during 2016.
- A very wet summer period between May and September 2017.
- A very dry summer in 2018.
- Prolonged heavy rainfall between November and December 2018.
- A very dry January in 2019.

### 8.2 Leachate flow volumes

On a monthly basis, daily logs of leachate volumes pumped to the leachate treatment plant and effluent totals flowing from the discharge point can be downloaded and compiled using the remote SCADA system at Bleakdown. Observation of the leachate totals and effluent volumes is

useful when considering the monthly rainfall volumes to see how volumes of rainfall influence leachate abstracted from the landfill site on a monthly basis.

Figure 11 highlights the changes in leachate volumes produced by the landfill site each month, during the operational period of the leachate treatment plant, from June 2017.

Figure 11 shows that the volumes of leachate abstracted at each pumping well are proportional to the changes in rainfall on a monthly basis. For example, following prolonged heavy rainfall during the winter of 2017/18, leachate volumes produced by the site continued to increase until March 2018. Likewise, after heavy rainfall experienced in November and December 2018, the volumes of leachate abstracted from DP2 and the Sump pumping line showed a sudden increase in volumes of leachate generated.

### 8.3 Analytical Data

Analytical data obtained through monthly sampling highlight the consistent and reliable treatment process that has been observed at Bleakdown since the commissioning period in June 2017.

Table 3 highlights that all parameters originally set as part of the Environment Agency's discharge permit have been achieved consistently throughout the 2-year period of operation. Importantly, Ammoniacal-N has consistently been reduced to trace levels (<0.2 mg/l), whilst iron concentrations have always been significantly below the consented concentration of 6 mg/l.

Figure 12 shows that complete nitrification has consistently been achieved at Bleakdown LTP since commissioning in June 2017. A mean concentration of 17 mg/l Ammoniacal-N is evident within the blend of leachate, which is fully nitrified to 17 mg/l (mean) of nitrate-N within the final effluent. This proves that the nitrification process being performed within the SBR reactor is being achieved successfully.

It is worth noting that Figure 12 highlights two periods where the concentrations of nitrate-N within the effluent spiked (September 2017 and July 2019). These results correspond with reseeded events (see Figure 17), where two different deliveries of biological sludge were made from a treatment plant where a leachate with a high ammoniacal-N was being treated (resulting in a high nitrate-N concentration within the sludge that was delivered to Bleakdown LTP).

Similar to the treatability trials, Figure 13 illustrates how removal of both COD and BOD was minimal, from the raw leachate to the final effluent being discharged. This was not an issue at Bleakdown, because the raw leachate contained low concentrations of both COD and BOD, and no set discharge consent exists for either determinant. In the same way that ammoniacal-N spikes on two occasions in Figure 12, the same effect can be highlighted in COD concentrations in Figure 13, where COD in the effluent increases after the initial delivery of biological sludge, containing a higher concentration of non-degradable COD.

Figure 14 highlights how pH remains stable throughout treatment, whilst the levels of alkalinity within the raw leachate are sufficient to buffer the acid-generating nitrification process within the SBR, as was the case within the treatment tank during the treatability trial. At sites where

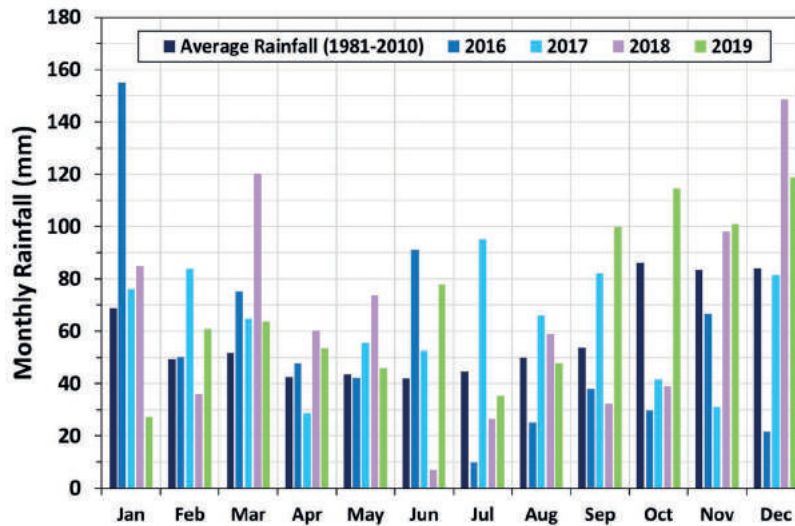


FIGURE 10: Average monthly rainfall volumes and recent monthly rainfall volumes experienced at Bleakdown LTP.

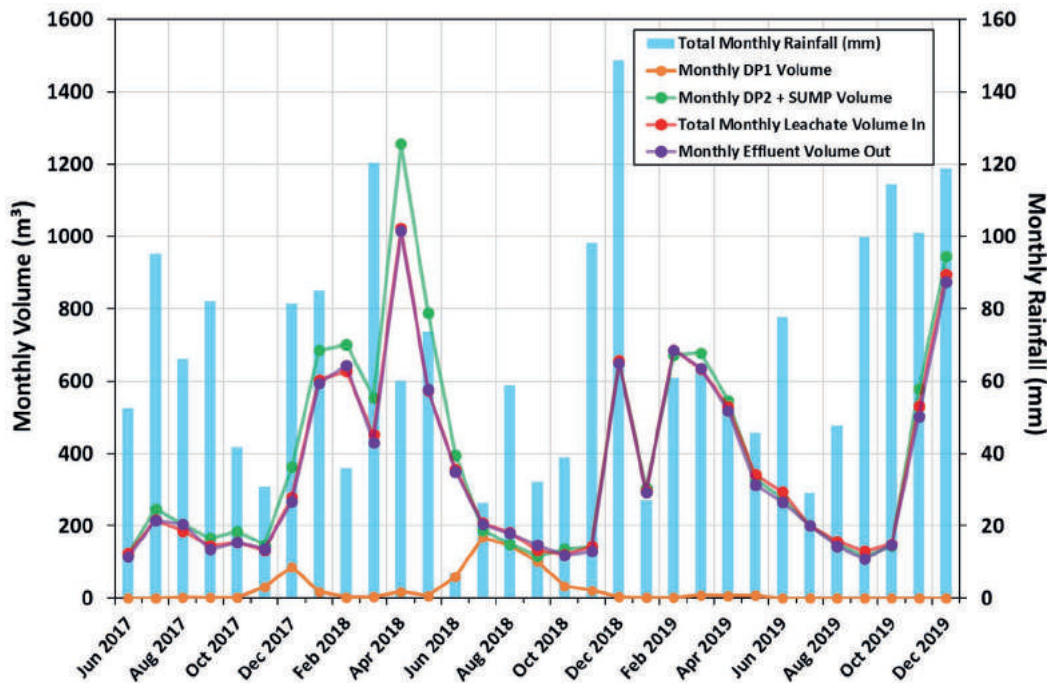


FIGURE 11: Monthly leachate volumes received at the LTP from each leachate pumping location, compared to the change in rainfall on a monthly basis.

stronger leachates are being treated, it is a necessity to add alkalinity to the nitrification treatment process.

### 8.4 Contaminant loading within leachate at Bleakdown

Using the monthly analytical data obtained from Bleakdown, the strength of leachate can be compared with volumes of leachate being produced, allowing loading calculations to be made. This means that observations can be made into how the strength of leachate varies on a seasonal basis, whilst also considering how this impacts the expected requirements of the treatment plant at different times of year.

Figure 15 and Figure 16 present the total volume of leachate treated by the LTP as bars, whilst Ammoniacal-N and COD are presented as lines on respective graphs. It is clear from these graphs that the loading of both COD and Ammoniacal-N is heavily influenced by the varying volumes of leachate being generated by the landfill site on a seasonal basis.

Table 4 shows that although Ammoniacal-N concentrations in raw leachate are influenced by the variations in rainfall and therefore dilution, COD values remains very similar throughout the year regardless of flow rates. Therefore, with a consistent COD value within the leachate, the COD loading is primarily influenced by the volume of lea-

**TABLE 3:** Mean results for the performance of Bleakdown LTP since biological commissioning during June 2017.

Design Parameter	Mean Leachate Blend (Sump, DP1 & DP2)	Mean Effluent Quality	Environment Agency Discharge Permit
COD	92.6 mg/l	107 mg/l	N/A
Ammoniacal-N as N	17.5 mg/l	<0.2 mg/l	5 mg/l (as Ammonia)
Nitrate-N as N	N/A	16.8 mg/l	N/A
Nitrite-N as N	N/A	0.5 mg/l	N/A
Alkalinity	548 mg/l	342 mg/l	N/A
Suspended Solids	N/A	32.7 mg/l	130 mg/l
Temperature	<25 °C	<25 °C	25 °C
Iron (Fe)	10 mg/l	0.4 mg/l	6 mg/l
*PAH as Benzo (b) fluoranthene	0.01 ug/l	0.0063 ug/l	0.1 ug/l
pH-Value	7.9	8.2	6.0-8.5

\*PAH as Benzo (b) fluoranthene: This was not tested during the treatability trials. However, data on concentrations present in the leachate were supplied by the employer. On most occasions the concentration was below the recorded limit of detection <0.023ug/l. A marginally higher value of <0.046ug/l was recorded in the sump in February 2015 and January 2016. All these values are well below the Discharge Permit value of 0.1 ug/l, thus it is reasonable to assume a design blend value of <0.1ug/l.

chate passing through the plant, hence the strong correlation with changing leachate volumes, shown in Figure 16.

Both COD and Ammoniacal-N loading are highest during winter months, from December to February. In contrast, during the autumn months (September to November), the loading for COD and Ammoniacal-N are at their lowest, corresponding with the significantly reduced rainfall when compared to other seasons. This seasonal loading variation is typical of leachate at many other landfill sites.

Because significantly higher volumes of leachate are treated during winter months, this causes elevated loading of both COD and ammoniacal-N. Table 4 shows that ammoniacal-N loading of 5,694 kg during the winter months (December to February) is approximately double the loading of 2,913 kg during autumn (September to November).

Although the volumes of leachate generated at Bleakdown vary significantly on a seasonal basis, it is clear that the loading of Ammoniacal-N throughout the year is not altered drastically, due to the varying strength of leachate at different times of year.

Figure 12 shows that the feed ammoniacal-N strength varies by a factor of ~5 over the course of a year, whilst Figure 11 shows monthly leachate volumes vary by a factor of ~10. Because these two parameters are inversely correlated, the net effect is that the ammoniacal-N loading only varies by a factor of ~2. Whilst this inverse correlation of leachate flow and strength fluctuations is common knowledge in a qualitative sense, this case study highlights a real data set, in order to quantify the extent of seasonal variations that can occur in both parameters, and the net effect this has on loading.

Regardless of the loading that the LTP experiences on a seasonal basis at Bleakdown Landfill Site, Table 3 proves that the treatment plant has been capable of consistently achieving the discharge consent as applied to the site by the UK Environment Agency.

### 8.5 Biological sludge concentrations

As noted earlier, the low concentrations of ammoniacal-N (17.5 mg/l) and BOD (2.23 mg/l) combined with the

high concentrations of iron (10 mg/l) and calcium (150 mg/l), could lead to the depletion of organic solids and the accumulation of inorganic solids within the SBR reactor at Bleakdown LTP. It is worth noting that the long term mean BOD concentration of 2.23 mg/l within the Bleakdown leachate is much lower than the original concentration of 28 mg/l litre that was used during the trials.

Figure 17 shows that occasional reseeded of biological sludge was needed, as was noted during the treatability trials. Following the initial seeding of the treatment plant, three additions of biological sludge have been required in order to maintain levels of organic matter within the SBR. These additions were made at between 10 and 12-month intervals, and were low cost to the process, because only a single small (18m<sup>3</sup>) tanker of concentrated sludge was required to be delivered to site.

On each occasion, sludge levels within the SBR reduced initially, before stabilising at a concentration that could be maintained for up to a 12-month period. Volatile suspended solids concentrations (VSS) have always changed proportionally to the total suspended solids (TSS), reducing significantly following reseeded, before stabilising at a lower concentration and eventually requiring an addition of fresh biological sludge after a 10 to 12-month period.

During July 2019, a modification was made to the leachate feeding arrangement, which meant that the discharge bellmouth was flushed before the effluent was decanted. This was to ensure that no sludge accumulated within the bellmouth prior to decant. The impact of this simple modification can be seen in Figure 17, when following the modification and addition of sludge, the rate of sludge loss was reduced significantly. Additionally, it is worth noting that suspended solids have never been a problem within the effluent being discharged to the local stream.

Going forwards, it is predicted that biological sludge additions into the SBR at Bleakdown will be necessary at less frequent periods of greater than 12 months.

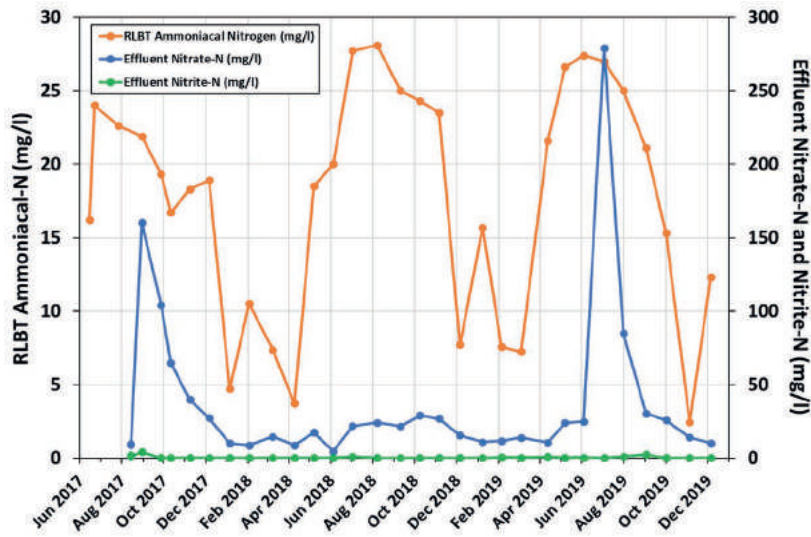


FIGURE 12: RLBT Ammoniacal-N concentration and Effluent Nitrate-N and Nitrite-N concentrations.

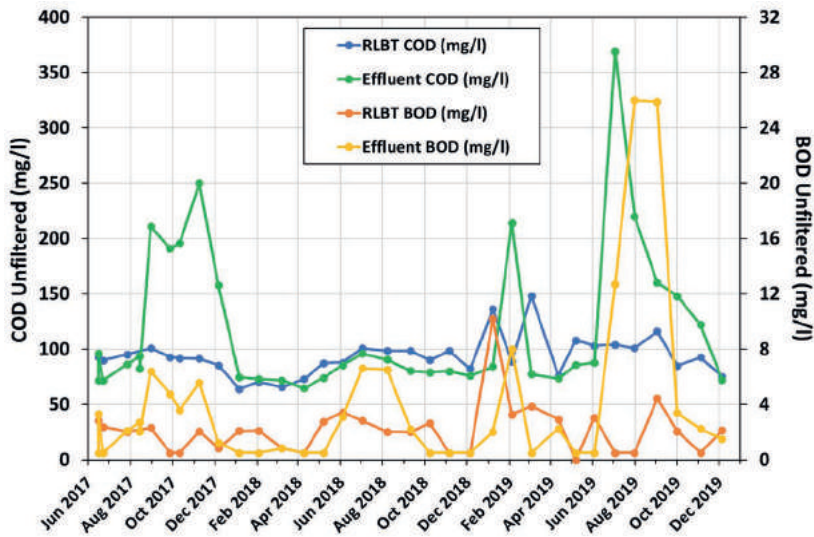


FIGURE 13: Raw leachate COD and BOD concentrations, compared with Effluent COD and BOD concentration.

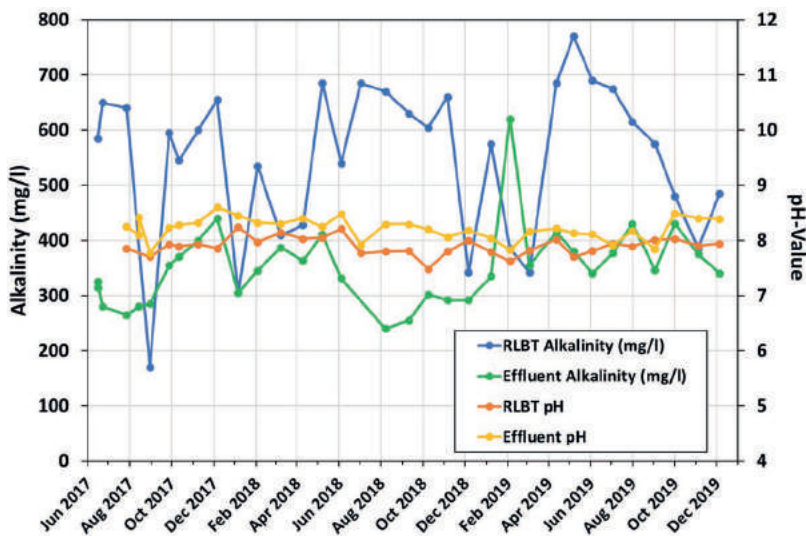


FIGURE 14: Raw leachate alkalinity and pH-value, compared with Effluent alkalinity and pH-value.



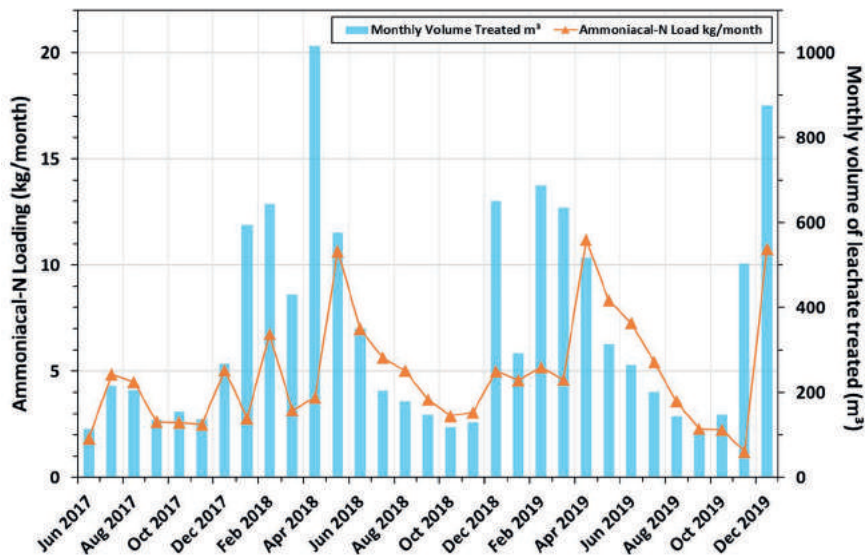


FIGURE 15: Ammoniacal-N loading results compared to the volumes of leachate treated by the LTP since biological commissioning during June 2017.

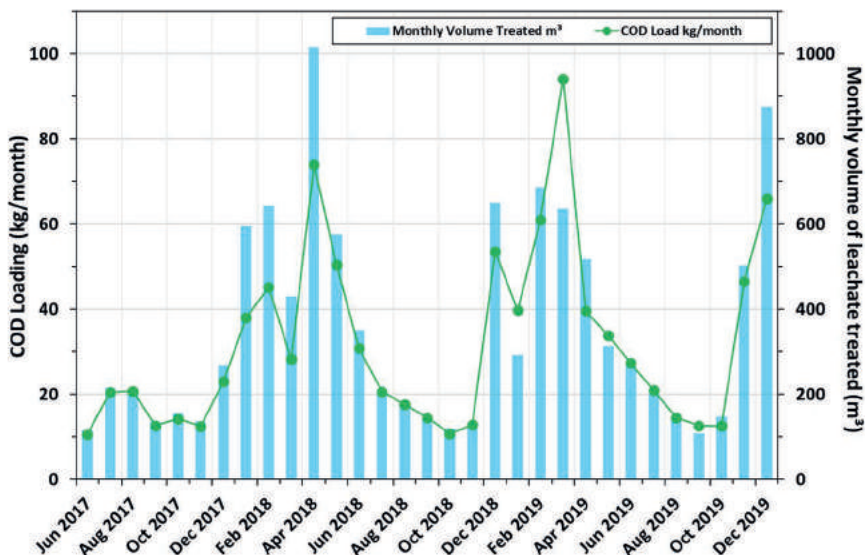


FIGURE 16: COD loading results compared to the volumes of leachate treated by the LTP since biological commissioning during June 2017.

## 9. FUTURE OPERATION OF THE TREATMENT PLANT

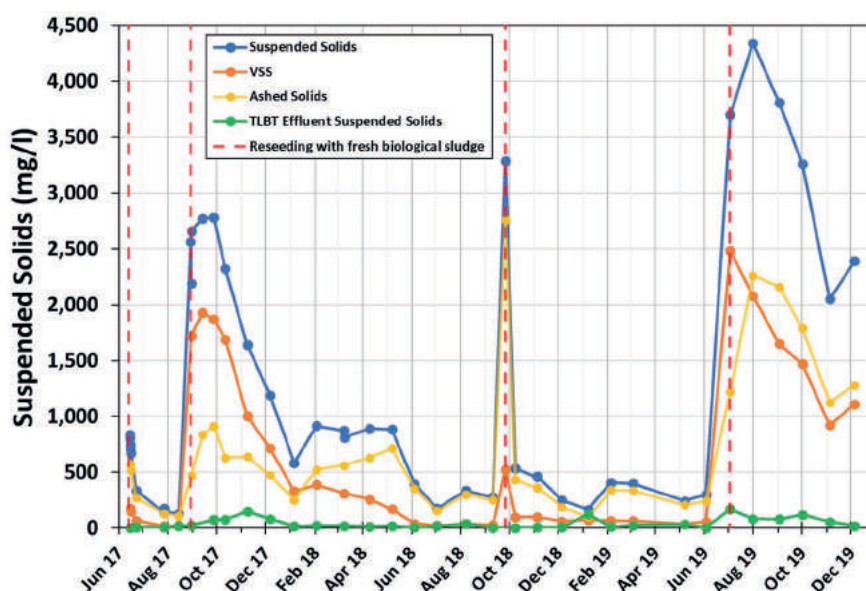
Having now operated successfully for more than two years, it is expected that the Bleakdown LTP will continue to fulfil its purpose in successfully treating the leachate abstracted from this landfill site.

A key factor in the ongoing success of the treatment plant is the routine testing, monitoring and sampling work performed at the plant. This work enables assessment of the effectiveness of the treatment plant, and the successful operation of all elements of Bleakdown LTP. The regular sampling enables observations to be made as to whether the treatment plant is achieving its design capacity, and also helps in monitoring any unexpected changes in leachate strength.

By regularly testing the SBR reactor for concentrations of suspended solids and volatile suspended solids, a record can be kept of the total organic sludge content within the process. This is beneficial because it means that any changes in sludge concentration can be addressed before any problems arise. At a small and simple treatment plant such as this, where relatively small volumes of leachate are being treated, it is only now an occasional requirement for biological sludge to need reseeded.

## 10. CONCLUSIONS

This paper presents a case study of Bleakdown Leachate Treatment Plant, which is a completely unmanned and remote site, where monitoring technicians are only required to briefly attend site twice per month in order to



**FIGURE 17:** Suspended solids, volatile suspended solids and inorganic solids within the SBR reactor at Bleakdown LTP, following commissioning in June 2017 up to December 2019.

monitor the biological process. Through an online SCADA control system, operation of the treatment plant can be monitored and controlled remotely, trends in results observed, and daily data and treatment records downloaded.

Routine reporting following monitoring and maintenance checks made on the site is used to inform Phoenix Engineering that the process is working effectively, and analytical results obtained from monthly sampling exercises support on site observations and analysis.

This treatment plant is a prime example of how leachate from old closed landfills can be effectively managed, with very low costs of operation, maintenance and site attendance, when compared to alternative solutions. In future it is expected that many more of these similar leachate treatment plants will be necessary at old, closed landfill sites, where relatively weak leachates are being generated and require treatment in order for stringent discharge consents to be achieved.

## ACKNOWLEDGEMENTS

Phoenix Engineering would like to acknowledge the assistance and cooperation of our client, Aggregate In-

dustries throughout the operation and maintenance of the Bleakdown leachate treatment plant and landfill site.

Phoenix would also like to thank both Tim Wilkins and CEC Systems for their support and efforts in carrying out routine maintenance, monitoring and sampling works at the leachate treatment plant.

## REFERENCES

- Carville, M., Last, S., Olufsen, J. and Robinson, H., (2003). Characterisation of contaminant removal achieved by biological leachate treatment systems. Paper presented to Sardinia 2003, the International Waste Management and Landfill Symposium, S. Margherita di Pula, Cagliari, Italy, 6-10 October 2003, 10pp.
- Last, S., Barr, M., Robinson, H., (1993). Design and operation of Harewood Whin landfill: an aerobic biological leachate treatment works. Paper presented to an open meeting of the North East Centre of the Institute of Wastes Management, held at Askham Bryan Agricultural College, York, on 12 March 1993. 10pp plus figures and plates. Published in Wastes Management Proceedings, October 1993, 9-16.
- Robinson, H., Maris, P.J., (1983). The Treatment of Leachates from Domestic Wastes in Landfills : I. Aerobic Biological Treatment of a Medium-strength Leachate. *Water Research*, 17(11), 1537-1548, November 1983.
- Robinson, H., Grantham, G., (1988). The treatment of landfill leachates in on-site aerated lagoon plants : Experience in Britain and Ireland. *Water Research*, 22 (6), June 1988, 733-747.

**TABLE 4:** Mean seasonal Ammoniacal-N and COD concentrations and loadings at Bleakdown since June 2017.

Season	Spring	Summer	Autumn	Winter
Determinand	March - May	June - Aug	Sept - Nov	Dec - Feb
COD (mg/l)	93.1	95.2	93.9	87.8
COD loading (total kg)	22,780	20,130	12,900	45,870
Ammoniacal-N as N (mg/l)	14.2	24.0	21.2	10.9
Ammoniacal-N loading (total kg)	3,480	5,070	2,910	5,690
Mean monthly rainfall (mm/month)	69.5	63.2	54.0	73.0
Mean monthly treated leachate volume (m <sup>3</sup> /month)	245	211	137	522

- Robinson, H., (1989). On site treatment of leachates from landfilled wastes. Paper presented to the annual conference of the Institution of Water and Environmental Management, IWEM 89 "Technology Transfer in Water and Environmental Management, at the Metropole Hotel, National Exhibition Centre, Birmingham, 12-14 September 1989. 1 Paper 15, 18pp, in Proceedings, and published in the Journal of the Institution of Water and Environmental Management, 4, (1), February 1990, 78-89.
- Robinson, H., (1990). On-site treatment of leachates from landfilled wastes. Journal of the Institution of Water and Environmental Management, 4 (1), February 1990, 78-89.
- Robinson, H., Luo, M.M.H., (1991). Characterisation and treatment of leachates from Hong Kong Landfill Sites. Journal of the Institution of Water and Environmental Management, 5 (3), June 1991, 426-335.
- Robinson, H., (1992). Leachate collection, treatment and disposal. Paper presented at the Institution of Water and Environmental Management Conference, "Engineering of Landfill - Problems and Solutions", held at the Wiltshire Hotel, Swindon, on 30 October 1991, 22pp. Published in the Journal of the Institution of Water and Environmental Management, 6 (3), June 1992, 321-332.
- Robinson, H., (1995). A Review of the Composition of Leachates from Domestic Wastes in Landfill Sites. Report No. CWM/072/95, prepared for the Wastes Technical Division of the UK Department of the Environment, under contract number PECD/7/10/238, in the series "The Technical Aspects of Controlled Waste Management". August 1995, 550pp.
- Robinson, H., Chen, C.K., Formby, R., Carville, M., (1998). Leachate treatment plants at Hong Kong landfill sites. International training seminar, Management and treatment of MSW landfill leachate. Cini Foundation, San Giorgio Venice, December 1998.
- Robinson, H., Harris, G., Last, S., (1999). The stripping of dissolved methane from landfill leachates prior to their discharge into sewers. Paper presented to Sardinia 99, the Seventh International Waste Management and Landfill Symposium, S. Margherita di Pula, Cagliari, Italy, 4-8 October 1999, Proceedings Volume II, 285-293pp.
- Robinson, H., (2000). Major UK study of trace contaminants in landfill leachate. Waste Management, April 2000, page 26.
- Robinson, H., Knox, K., Van Santen, A., Tempny, P.R., (2001). Compliance of UK landfills with EU pollution emissions legislation: development of a reporting protocol. Paper presented to Sardinia 2001, the Eighth International Waste Management and Landfill Symposium, S. Margherita di Pula, Cagliari, Italy, 1-5 October 2002, 10pp.
- Robinson, H., Knox, K., (2001). Pollution Inventory discharges to sewer or surface water from landfill leachates: Final Report to the UK Environment Agency, by Enviros and Knox Associates. Ref: REGCON 70, May 2001. 19pp plus Appendices and Figure.
- Robinson, H., Knox, K., (2003). Updating the Landfill Leachate Pollution Inventory tool: Report to the UK Environment Agency by Enviros and Knox Associates. R&D Technical Report No. PI – 496/TR (2), March 2003, 56pp.
- Robinson, H., Farrow, S., Last, S., Jones, D., (2003). Remediation of leachate problems at Arpley Landfill Site, Warrington, Cheshire, UK. Paper presented to Sardinia 2003, the Ninth International Waste Management and Landfill Symposium, S. Margherita di Pula, Cagliari, Italy, 6-10 October 2003, 10pp.
- Robinson, H., Carville, M., Walsh, T., (2003). Advanced leachate treatment at Buckden Landfill, Huntingdon, UK. Journal of Environmental Engineering and Science, 2, (4), 255-264, July 2003.
- Robinson, H., Olufsen, J., Last, S., (2004). Design and operation of cost-effective leachate treatment schemes at UK Landfills: Recent case studies. Paper presented to the 2004 CIWM Annual Exhibition and Conference, June 2004, Torbay.
- Robinson, H., (2007). The composition of leachates from very large landfills: An international review. Paper presented to Torbay 2006, The Annual Conference and Exhibition of CIWM "Changing the Face of Waste Management", Paignton, June 2006. Published in Communications in Waste and Resource Management, June 2007, 8 (1), pp. 19-32.
- Robinson, H., (2008). Operation of the UK's largest leachate treatment plant : 6 years of experience at Arpley Landfill. Paper presented to Waste 2008, "Waste and Resource Management – A Shared Responsibility", held at the Stratford Manor Hotel, Stratford-upon-Avon, Warwickshire, England, 16-17 September 2008, In Proceedings, 10pp.
- Robinson, H., Carville, M., Robinson, T., (2013). Biological Nitrification and Denitrification of Landfill Leachates. Paper presented to Sardinia 2013, the Fourteenth International Waste Management and Landfill Symposium, S. Margherita di Pula, Cagliari, Italy, 30 September - 4 October 2013, Proceedings P95 and on DVD ROM.
- Robinson, H., Wilson, K., Stokes, A., Olufsen, J., Robinson, T., (2017). Recent state-of-the-art leachate treatment plants in eastern England. Paper presented to Sardinia 2017, the Sixteenth International Waste Management and Landfill Symposium, S.Margherita di Pula, Cagliari, Italy, 2 – 6 October 2017, in Proceedings.
- Robinson, T., (2013). Aerobic Biological Treatability Studies on Landfill Leachate using Nitrification and Denitrification. Paper presented to Sardinia 2013, the Fourteenth International Waste Management and Landfill Symposium, S.Margherita di Pula, Cagliari, Italy, 30 September – 4 October 2013, 9pp, in Proceedings.
- Robinson, T., (2014). Aerobic Biological Treatability Studies on Landfill Leachate using Nitrification and Denitrification. Final Year Dissertation Project 2014, School of Environmental Sciences, University of East Anglia, Norwich, UK, 100 pages, Available from the UEA Library.
- Robinson, T., (2015). Use of pilot-scale treatability trials in the design of full-scale leachate treatment plants. Paper presented to Sardinia 2015, the Fifteenth International Waste Management and Landfill Symposium, S.Margherita di Pula, Cagliari, Italy, 5 – 9 October 2015, 128pp in Proceedings.
- Robinson, T., (2017). Robust and reliable treatment of leachate at a closed landfill site in Sussex, UK. Paper presented to Sardinia 2017, the Sixteenth International Waste Management and Landfill Symposium, S.Margherita di Pula, Cagliari, Italy, 2 – 6 October 2017, in Proceedings.
- Robinson, T., (2018). Robust and reliable treatment of leachate at a closed landfill site in Sussex, UK. Detritus. 1 (1), Pages 116-121. Available at: <https://digital.detritusjournal.com/articles/robust-and-reliable-treatment-of-leachate-at-a-closed-landfill-site-in-sussex-uk/30>
- Robinson, T., (2019). Aerobic Biological Treatability Studies on Landfill Leachate with Nitrification and Denitrification. Detritus. 7 (1), Pages 1-13. Available at: <https://digital.detritusjournal.com/articles/in-press/aerobic-biological-treatability-studies-on-landfill-leachate-with-nitrification-and-denitrification/235>
- Shuylar, R.G., (2013). What every operator should know about ORP. Water Environment and Technology, January 2013, 25, 68-69.
- UK Department of the Environment (1978). Cooperative Programme of Research on the Behaviour of Hazardous Wastes in Landfill Sites: Policy Review Committee Final Report, April 1978.

# INDEX TO EVALUATE CLOSED LANDFILLS BASED ON LEACHATE PARAMETERS

Claudio Fernando Mahler <sup>1,\*</sup>, Julia Righi de Almeida <sup>2</sup> and João Paulo Bassin <sup>1</sup>

<sup>1</sup> COPPE/ UFRJ, Federal University of Rio de Janeiro, COPPE/Civil Engineering Program, Rio de Janeiro/RJ, Brazil

<sup>2</sup> Federal University of Juiz de Fora, Department of Civil Engineering, Juiz de Fora, Brazil

## Article Info:

Received:  
6 June 2019  
Revised:  
5 March 2020  
Accepted:  
17 March 2020  
Available online:  
30 June 2020

## Keywords:

Closed landfill  
Leachate  
Polluting potential  
Deactivated landfill assessment  
index (DLAI)

## ABSTRACT

After the end of their useful life, waste landfills and their surroundings should continue to be monitored constantly. The main concern is the pollution of groundwater and surface water by leachate, which represents a serious risk to public health. In this work an index is proposed to assess the conditions of a landfill after closure. Insufficient data on the waste entering these areas causes uncertainty as to how long the material will continue to degrade. The presence of polluting elements in landfill leachate was evaluated by characterizing the effluent over a period of ten years. The leachate data were analyzed statistically to test the significance of Pearson's linear correlation coefficient. Multivariate statistical analysis was used to describe the similarity between the samples considering the total set of variables and their correlations. These results showed the importance given to certain parameters that are not relevant for Brazilian landfills, in which the presence of organic matter is high. The present work contributes by generating information for a better understanding of the impacts caused by landfills in Brazil and in most countries of the Third World, in which organic waste represents at least 50% of the waste discarded in landfills. Through the proposed Deactivated Landfill Assessment Index (DLAI), involving four-parameter analysis (pH, BOD, COD and ammoniacal nitrogen), possible pollution threats can be detected, allowing prioritizing areas for remediation and better allocation of resources.

## 1. INTRODUCTION

Upon completion of their useful life, landfills and their surroundings should continue to be monitored. The main concern is contamination of water from transport of the leachate generated. This effluent contains hundreds of chemical products, and its management is recognized as one of the major problems associated with the operation of landfills, especially after their closure. Areas that were previously used for waste disposal often become sites of low-income settlements. Since these old landfills can continue to produce effluents and contaminate the environment for many years, it is important that they not simply be abandoned. Closed landfills should instead be monitored to prevent their irregular occupation (Schueler and Mahler, 2008). More than 50% of the waste contained in landfills in Brazil is organic matter. The lack of public policies to prioritize and invest in composting, to prevent disposal of this waste in landfills, generates very high costs, mainly for the treatment of leachate. The concentrations of ammoniacal nitrogen, for example, tend to increase after the decommissioning of the landfill, increasing the treatment costs of the

effluent generated. Leachate from closed landfills may have equal or greater potential for contamination compared to that from active landfills, so post-closure remediation and monitoring actions should be continued until the leachate stabilizes and no longer poses a threat to the environment and health (Kumar and Alappat, 2005). The Leachate Pollution Index (LPI), originally proposed by Kumar and Alappat (2003) and later also applied in Kumar and Alappat (2005), Sharma et al. (2008), Rafizul et al. (2011), Bhalla et al. (2014), Krishnamurthy et al. (2015), Naveen et al. (2016) and Lothe and Sinha (2016), among others, was developed to enable comparing the pollution potential of leachate from different landfills. LPI is a single number ranging from 5 to 100. It represents the level of leachate contamination potential of a determined landfill. It is obtained from several leachate pollution parameters at a given moment.

However, the weights attributed to each of the leachate components do not seem to be the most suitable for application in Brazilian landfills, mainly because they do not take into account the importance of organic matter, the main fraction found in the wastes. Given the high number of dumps in Brazil and the lack of resources for the manage-



\* Corresponding author:  
Claudio Mahler  
email: mahler@coc.ufrj.br



ment of municipal solid waste, the number of parameters to be analyzed in the leachate could be reduced (compared to that proposed in the LPI), at least in the control analyses. The concentrations of most heavy metals, phenols and cyanides, for example, as shown by experience in Brazilian landfills, tend to fall drastically over time, as the pH increases and natural processes occur in this environment (Peixoto, 2007; Teixeira et al., 2007; Galvez et al., 2008; Queiroz et al., 2011). In this case, not all of the above parameters need to be analyzed. In this article, the main results obtained by monitoring a landfill for a period of 10 years are presented to support the method proposed, the Deactivated Landfill Assessment Index (DLAI).

The aim of this study was to investigate what parameters are really important to evaluate the contamination potential of the effluent and to propose an index that could help efforts in developing countries regarding the monitoring of closed areas and support decisions regarding the allocation of resources for remediation in the post-closure phase.

## 2. MATERIALS AND METHODS

### 2.1 Materials

#### 2.1.1 Studied area

The Sky Hill dumpsite is located in an area of approximately 180,000 m<sup>2</sup> in the Caramujo district of the municipality of Niterói, state of Rio de Janeiro, Brazil. Niterói has an estimated population of 497,883 (IBGE, 2016) and produces about 700 metric tons of waste per day.

The landfill was operated for 30 years (1983-2013), generally as a dump. As of 2005, on-site improvement works were implemented, which allowed it to be considered a controlled landfill as of 2008. This fact improved its aesthetic appearance and operating conditions, and over time its liquid and gaseous emanations declined.

#### 2.1.2 Monitoring of leachate, surface water and groundwater

The monitoring began in 2004 and was done during 10 years. Sixty-four effluent and water samples were collected, and in relation to the leachate, a series of parameters were analyzed in duplicate: pH, BOD, COD, phenols, cyanides, heavy metals and ammoniacal nitrogen. In addition to the leachate, wherein the concentration of its pollutants were compared within the effluent discharge standards set forth in CONAMA Resolution 430/2011, samples of surface and groundwater from areas surrounding the landfill were also analyzed, with the results being compared to the limits of CONAMA Resolution 420/2009, CONAMA Resolution 357/2005 and Edict 2914/2011 from the Ministry of Health, which establish standards of water quality of aquifers, water sources in general and water for human consumption and potability, respectively. Groundwater collections were carried out through a monitoring well in the landfill itself and the surrounding surface water samples were collected downstream of the disposal area. The collection of groundwater in the monitoring well was carried out with the aid of a plastic collection tube, which had a collection sealing system and tips for overflow. They were

stored in specific bottles made available by the laboratory responsible for the analysis and routed under specific temperature conditions required by the lab. For surface water, 500 mL samples were collected in all campaigns on the river banks (river and Floralia points), at a depth of up to 30 cm. After collection, the samples were placed in a Styrofoam box and transported to the laboratory following the standards of ABNT NBR 9897 and NBR 9898. The same procedure was used to transport the slurry samples, collected at all sites, from inside of a collection box inside the landfill. For the collection of these samples (using 500 mL vials), special care was required (use of masks and gloves), due to the toxicity of the liquid. The collection points are identified in Figure 1 and the methods used in the analyzes, carried out in certified laboratories, are summarized in Table 1. The results of the analyses presented in this article were extracted from the technical reports of the project coordinated by Mahler from 2004 to 2013.

In addition to the leachate, samples of surface and groundwater from areas close to the landfill were analyzed, which showed values above the limits of CONAMA, which changed with time as the landfill started to be controlled.

### 2.2 Methods

#### 2.2.1 Statistical analysis

The Statistica 7 program was used for statistical analysis of the results obtained from the landfill monitoring. Initially, descriptive statistics were used to summarize the data for all the compounds analyzed directly: mean, minimum and maximum values, standard deviation, etc. In order to verify the influence of chemical elements (effects of antagonism and synergism), the leachate data were treated and analyzed statistically to test the significance of Pearson's linear correlation coefficient. Multivariate statistical analysis (main components and clusters) was used both to describe the similarity between the samples considering the total set of variables and their correlations, and to find sets of variables that could be considered redundant. Principal component analysis (PCA) enabled transformation of the data into two dimensions, designed to transform the original variables into new uncorrelated variables. Hierarchical cluster analysis (HCA) was used to recognize patterns (similarities) of samples from a set of data obtained, presented in dendrograms. The results obtained from the statistical analysis performed with the leachate monitoring data from the Sky Hill dumpsite supported the choice of the parameters used to calculate the proposed index.

## 3. RESULTS AND ANALYSES

### 3.1 Parameters analyzed in the leachate and waters surrounding the Sky Hill Dumpsite

#### 3.1.1 pH, BOD and COD

At the start of a landfill, an acidic phase is expected with pH values below 7, followed by gradual elevation towards the methanogenic phase, with pH values above 7 (Pohland and Harper, 1985). In the Sky Hill dumpsite, the mean value observed for the entire monitoring period was 7.85, and in the last sample collected, with the landfill deactivated four



**FIGURE 1:** Collection points of leachate and water samples: well (22° 53' 32,3" S and 43° 04' 8,80" O), leachate (22° 53' 27,0" S and 43° 03' 59,3" O), river (22° 53' 31,0" S and 43° 04' 87,3" O) and floralia\*\* (22° 53' 9,90" S and 43° 03' 18,1" O).

years beforehand, the pH result was 8.71. Based on the data collected by Souto and Povinelli (2007), this range is within the most probable values for Brazilian landfills. Regarding BOD and COD, in the last analysis performed at the dumpsite, in 2017, the detected values were 255.9 mg/L and 990 mg/L, respectively. Several authors have reported that the leachate from young landfills is characterized by a very high COD, with values above 2000 mg/L, while in older disposal areas the COD is below 1000 mg/L. Initial-

ly, the BOD/COD ratio is typically greater than or equal to 0.5. Values between 0.4 and 0.6 indicate that the organic matter is readily biodegradable. In mature landfills, this ratio often varies between 0.05 and 0.2 (Ottoni, 2011). In the case of leachate from the Sky Hill dumpsite, the BOD/COD ratio found in 2017 was 0.26. In relation to surface and groundwater surrounding the landfill, concentrations above the limits established by CONAMA Resolution 357/2005 (5 mg/L) were found for BOD. The highest values were: 790

**TABLE 1:** Methods of the chemical analyses carried out over the years.

Parameters	2004	2005	2006	2010	2011	2012	2013	2017
COD	Dichromate in acidic medium - FEEMA 440-R1							Method 5.220 D, Closed Reflux - Col-orimetric. SMEWW, 20th Edition
BOD	Standard method FEEMA MF 439-R1						Method 5.210 B - Dilutions. SMEWW, 20th Edition	
pH	Potentiometric FEEMA MF 426							Method 4500 B. - Potentiometric. SMEWW, 20th Edition
ammoniacal nitrogens	Determination of Ammoniacal Nitrogen by Distillation - CETESB	Potentiometric with selective ion - SMEWW / Phenate standard method FEEMA MF 420	Standard method phenate FEEMA MF 420				Method 4.500 NH3 F - Indophenol. SMEWW, 20th Edition	
heavy metals	Atomic Absorption Spectrometry						USEPA 7061-A. 1992 (Atomic Absorption) / USEPA 7062. 1994 (Atomic Absorption) USEPA 6010-C. 2007; USEPA 7741-A.1994; USEPA 7742. 1994; USEPA 7061-A. 1992; USEPA 7062. 1994	Optical emission spectrometer with inductively coupled plasma source (ICP OES)/acid extraction

mg/L and 585 mg/L at the Floralia and river sites respectively. In 2010, the result in groundwater was 420 mg/L. In all other analyses, the values did not exceed 60 mg/L and the last result was 19.6 mg/L. As expected for the BOD values, the COD results were also quite high, particularly in the samples collected at the river site in 2011 and 2013. In both years, in periods of high rainfall (January 2013) and low rainfall (September 2011), COD values exceeded 500 mg/L. For groundwater, COD exceeded 250 mg/L in January 2013, but three months later, the values decreased to 81.5 mg/L.

### 3.1.2 Ammoniacal Nitrogen

During the entire monitoring period, the values found for ammoniacal nitrogen in the leachate of dumpsite were well above the established standards, which are 20 mg/L according to CONAMA Resolution 430/2011 and 5.0 mg/L according to INEA regulations (NT 202, revision 10). In general, the concentrations of ammoniacal nitrogen in the leachate of Brazilian landfills are very high. At the landfill site in Nova Iguaçu, located in the state of Rio de Janeiro, one of its cells was closed after 7 years of operation, with more than 3 million tons buried. The material received at the site was predominantly organic and the concentrations of ammoniacal nitrogen after its deactivation exceeded 1000 mg /L (Ottoni, 2011). Teixeira et al. (2007) presented analyses of slurry from a garbage dump in the state of Minas Gerais, which operated for 6 years and received about 800 thousand tons of disposed waste. Two years after its closure, the concentrations of ammoniacal nitrogen detected in the leachate exceeded 1,200 mg/L. Queiroz et al. (2011) characterized the leachate generated at the Bandeirantes and São João landfills, both in the state of São Paulo. The former operated for approximately 30 years and received more than 23 million tons of waste. Of this total, approximately 60% was organic. It was closed in March 2007 and leachate concentrations between May 2008 and February 2009 exceeded 2,390 mg/L. The São João landfill operated between 1992 and 2007 and received approximately 27.9 million tons of urban waste. The amount of leachate generated currently exceeds 1,800 m<sup>3</sup>/day and the concentrations of ammoniacal nitrogen measured in the leachate are in the range of 2,870 mg/L. Lins et al. (2011) reported that the concentrations of ammoniacal nitrogen in the Muribeca landfill in Pernambuco state varied between 1,125 and 2,900 mg/L, which corresponds to the maximum range for Brazilian landfills, according to Souto and Povinelli (2007). In all surface water samples collected near the Sky Hill dumpsite, concentrations were above the limit established by CONAMA, which can vary between 1 and 2 mg/L depending on the pH of the medium. In order to evaluate the results of this parameter in groundwater samples, the criteria were used of the Ministry of Health, indicated in Edict 2914/2011, which establishes a consumption acceptance standard of 1.5 mg/L for non-ionizable ammonia (NH<sub>3</sub>). In the case of samples collected from the well inside the Sky Hill dumpsite, the NH<sub>3</sub> concentration was 10 times higher than the limit established by this edict in 2011.

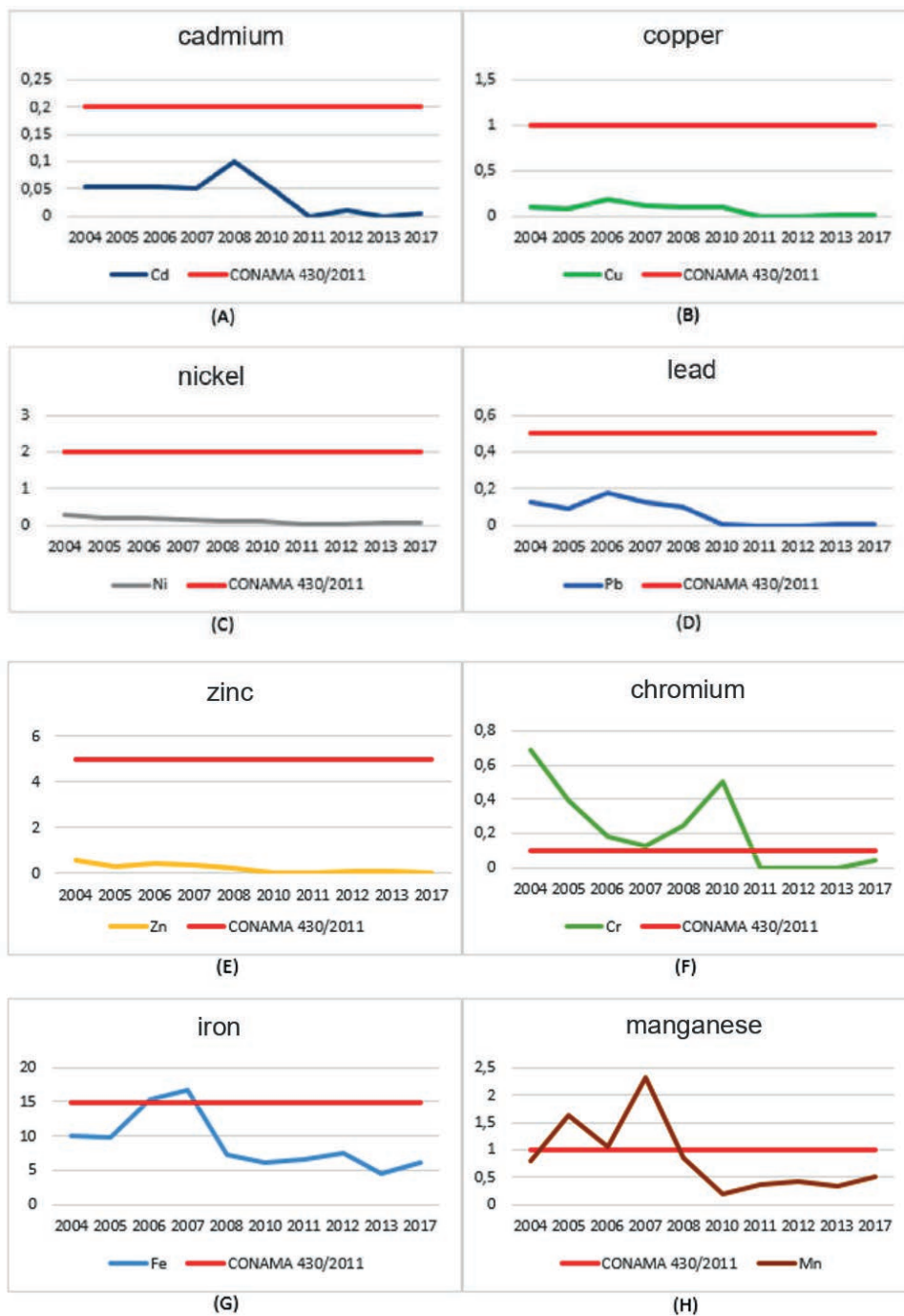
### 3.1.3 Heavy Metals

Slightly higher concentrations of metals are usually found in young landfills due to the high degree of solubilization of metals as a result of the low pH caused by the production of organic acids. As the age of the landfill increases, pH values tend to rise, resulting in a drop in metal concentrations, due mainly to the precipitation of hydroxides and sulfides. In the leachate of Sky Hill dumpsite, mean concentrations of Cd, Cu, Ni, Pb and Zn remained below the limits established by the legislation in force in all years, with a clear tendency to decrease over time. This behavior confirms the findings of Harmsen (1983) that there are low concentrations of heavy metals in landfill leachates in the fermentation stage due to metallic solubilization and complexation of volatile fatty acids. The average concentrations of the metals Cr (VI), Fe and Mn were above the established standards for effluent discharge at the beginning of the monitoring, but in 2017 they were below the allowable limits. The high concentrations of Fe found can be explained by the content of this metal present in the clay used as the cover layer of the Sky Hill dumpsite. The behavior of metals during the monitoring is shown in Figure 2.

The concentrations of heavy metals in surface and groundwater in the vicinity of Sky Hill dumpsite were monitored in order to evaluate the influence of the leachate in these media. At the beginning of the monitoring, with the exception of barium, all other elements were above the maximum limits determined by the regulations in force at the river site. Over the years, the metal concentrations fell and the Ag, Ba, Cr and Ni levels were below the limits established from 2010 onward. The same happened with Pb and Zn. Of all the heavy metals monitored in the groundwater well inside the landfill, the only ones that still were above the limits recommended by CONAMA Resolution 420/2009 and Health Ministry Edict 2914/2011 in 2013 were Fe and Mn, which can be explained by the natural composition of the soils of the region.

### 3.2 Selection of the parameters to obtain the Deactivated Landfill Assessment Index (DLAI)

In order for the proposed index to be applied in Brazil, the first step was to identify the type of waste that arrives in the largest quantity in landfills. Due to the lack of consolidated initiatives to exploit and recover the organic fraction, at least 70 million tons of this material was buried in 2016 (ABRELPE, 2017). The aggravating factor is that much of this waste goes to landfills that do not have any kind of soil waterproofing, drainage or leachate treatment, causing damage to the health of residents in these areas. For the proposed index, we therefore tried to evaluate the impact caused by the leachate discharge in the water bodies. For the quality of the water supply, for example, high levels of mineral salts, particularly sulfate and chloride, are associated with a tendency for corrosion of distribution systems, in addition to imparting a disagreeable flavor to the water. In order to classify and protect water bodies and to prevent health problems, CONAMA, in Resolutions 357/2005 and 420/2009, establishes maximum permissible values for total dissolved solids (TDS):



**FIGURE 2:** Results of metals in the Sky Hill Dumpsite leachate: (A) cadmium, (B) copper, (C) nickel, (D) lead, (E) zinc, (F) chromium, (G) iron, (H) manganese.

500 mg/L for surface water (class 1, 2 and 3) and 1000 mg/L for groundwater. Edict 2914/2011 from the Ministry of Health establishes a maximum value of 1000 mg/L of TDS for water for human consumption. Like for TDS, there are recommendations on the maximum limit of chloride in surface water as well as drinking water (both 250 mg/L). The fact is that the dilutive effect of chloride in water bodies generates concentrations normally below 250 mg/L, leading to the belief that it is not a pollutant that can cause long-term problems, and because of this,

it should not be considered as an important parameter for assessing the potential contamination from leachate. In addition, chloride and TDS are not even cited in CONAMA Resolution 430/2011, which provides effluent release standards. The same occurs with the coliform and total Kjeldahl nitrogen (TKN) parameters. This means there is no restriction on the release of these compounds, based on the belief that their concentrations will not significantly influence the quality of the water surrounding landfills. Christensen et al. (2001) stated that metals such as As,



Cd, Ni, Zn, Cu, Hg and Pb do not constitute a frequent problem in landfills containing domestic solid waste. It is therefore believed that for the composition of the pollutant potential of the leachate of deactivated landfill, the parameters related to heavy metals should not be included in the calculation, since their influence on the surroundings of the waste disposal area can be considered low. However, Kumar and Alappat (2003) suggested that metals such as iron ( $w_i = 0.045$ ), copper ( $w_i = 0.050$ ), nickel ( $w_i = 0.052$ ), zinc ( $w_i = 0.052$ ), lead ( $w_i = 0.064$ ), mercury ( $w_i = 0.062$ ) and arsenic ( $w_i = 0.061$ ) had higher weights and importance than pH ( $w_i = 0.055$ ), ammoniacal nitrogen ( $w_i = 0.051$ ), and in some cases equal to or greater than BOD ( $w_i = 0.061$ ) and COD ( $w_i = 0.062$ ). The LPI has been applied to several landfills in India, a country where, like in Brazil, organic matter is the main fraction of waste generated. We believe, therefore, that the weights for metals are overestimated, whereas the parameters that have direct relation with the potential pollutant of the organic matter do not receive proper importance in this index. The analysis of the main components of the leachate for predicting the behavior of the organic fraction is a fundamental condition for the creation of an index that can be applied to Brazilian landfills. The data from monitoring the Sky Hill dumpsite and research carried out in other Brazilian landfills indicate that concentrations of heavy metals, phenols, cyanides and chlorides in the leachate tend to fall over time (Teixeira et al. 2007; Ottoni, 2011; Lins et al, 2011; Queiroz et al., 2011). In addition, there is no great influence of these compounds in the water around these disposal areas. On the basis of this finding, we believe it is not necessary for the pollutants mentioned above to be present in the calculation of a leachate pollutant potential assessment index. Among other issues, the excessive number of components to be analyzed to verify polluting potential becomes unnecessary from a technical point of view, in addition to substantially complicating the monitoring. In the case of leachate from Brazilian landfills, we found that the analysis of the concentrations of four components (pH, BOD, COD and ammoniacal nitrogen) would be enough to evaluate a possible threat of pollution, allowing better allocation of resources for remediation processes. Next, the importance and justification for choosing each of these parameters are highlighted.

### 3.2.1 pH

Farquar and Rovers (1973) found that pH equal to or lower than 5.5 caused the total inhibition of the production of all gases, which thus corresponds to the total inhibition of the biological activity of the landfill. The concentration of a chemical species found in the leachate can vary depending on the pH of the sample. For values lower than 7, there may be buffering by volatile acids, which increases the solubility of some heavy metals. The opposite also occurs, since in alkaline media, and especially in environments with high content of organic matter, there may be reduced sulfate levels - since it can precipitate as hydroxides and/or sulfides, causing the metals to have low solubility. pH assessment is important, since this parameter affects the activity of enzymes and the toxicity of many compounds.

The most typical example is ammonia. In alkaline media, for example, it is possible to increase its concentration in the non-ionized form ( $\text{NH}_3$ ), which is toxic.

### 3.2.2 Ammoniacal Nitrogen

Waste landfills, because they are predominantly anaerobic environments, produce effluents with very low concentrations of nitrites and nitrates. On the other hand, the strong biological activity present in both the residue mass and the drainage system causes almost all of the organic nitrogen to be converted into ammoniacal nitrogen inside the landfill itself, and it is not used in significant quantities by any microbial group. Thus, there are high concentrations of ammonia in the leachate, considered an important tracer in the contamination of the water bodies (Souto and Povinelli, 2007). The oldest landfill leachate is typically rich in ammoniacal nitrogen due to the hydrolysis and fermentation of the nitrogenous fractions of biodegradable substrates. Free ammonia ( $\text{NH}_3$ ) is a very restrictive toxic substance to fish, and many species cannot withstand concentrations above 5 mg/L. For these reasons, the concentration of ammoniacal nitrogen is an important parameter for the classification of natural water bodies and is usually used in the constitution of water quality indexes (CETESB, 2009). Clément and Merlin (1995) argued that alkalinity and ammonia may be the main contributors to the toxicity attributed to leachate. In addition to compromising the quality of drinking water, in the short term human exposure to ammonia can cause severe burns to the skin, eyes, throat, lungs, mouth and stomach. In case of prolonged exposure, liver diseases, chronic respiratory problems and glaucoma are some of the maladies caused by this pollutant. In the case of enclosed landfills, and those with heightened risks because they are near rivers or important aquifers, the attention paid to this pollutant must be greater than for any other.

In the LPI, an index proposed by Kumar and Alappat (2003), the weight given to ammoniacal nitrogen is very low ( $w_i = 0.051$ ) compared to its importance in Brazilian or even Indian landfills, studied by Bhalla et al. (2014), Krishnamurthy et al. (2015) and Naveen et al. (2016). The organic matter is the predominant material in the mass of garbage, so ammoniacal nitrogen, whose concentration rises with the passage of time, should receive greater weight when calculating the index of polluting potential of Brazilian leachate. This means that, based on all the information presented on the impacts not only on the environment but also health, this parameter should be seen as the most important when assessing the need for remediation of an area.

### 3.2.3 BOD and COD

The high organic matter load present in leachate, due to the indiscriminate disposal of organic residues in landfills, can cause water pollution due to the consumption of dissolved oxygen by the microorganisms in their metabolic processes of using and stabilizing organic matter. In the choice of the parameters for composition of a new index for the classification of leachate from depleted landfills, in addition to ammoniacal nitrogen and pH, BOD and COD should also be considered, since the quantification of or-

ganic matter and its pollutant potential is traditionally evaluated through these methods. In addition, the BOD/COD ratio is considered a good indicator of the level of biological degradation of the effluent. Depending on the magnitude of this ratio, one can draw conclusions about the biodegradability of the waste, and from this forecast the necessary monitoring time. A high BOD/COD ratio signals the presence of a biodegradable fraction whereas a ratio less than 0.1 has been suggested as an indicator of stable leachate (Reinhart and Townsend, 1997; Barlaz et al., 2002). It is important to note that, like ammoniacal nitrogen, the parameters BOD and COD have important weights because the proposed index is tailored for application to Brazilian landfills. In addition, pH should also be considered when calculating the index, since depending on the alkalinity of the environment, the predominance of heavy metals can be evaluated.

### 3.3 Statistical analysis of results

The Statistica 7 program was used for statistical analysis of the results obtained from the landfill monitoring. Initially, descriptive statistics were used to summarize the data relating to all compounds analyzed in the leachate in a direct manner: mean, minimum and maximum values, standard deviation, etc. From the normalization of the data obtained through the annual averages of monitoring the leachate at the Sky Hill dumpsite, Pearson correlation coefficients were calculated, as presented in Table 2.

When analyzing the matrix, it is possible to see that although the pH had a negative correlation with most of the

variables, this parameter was not the only one that directly influenced the availability of metals. All metals varied inversely in relation to pH (negative values, as expected), but the correlations were low. Probably the greater variation of the metals is related to the presence of organic matter. In the same matrix, it is possible to note a high positive correlation between the metals, which may indicate they are associated with the same source. In the case of the Sky Hill dumpsite, we believe that metals come from industrial waste, since at the beginning of the operation there was no control over the material that came to the site. The statistics also show that BOD and COD, as expected, presented high positive correlation.

Multivariate statistical analysis (main components and cluster) was used both to describe the similarity between the samples considering the total set of variables and their correlations, and to find sets of variables that can be considered redundant. Principal component analysis (PCA) made it possible to transform the data into two dimensions. Factor 1 involved the elements Pb, Cu, Fe, Ni, Zn, phenols, cyanides and BOD and COD, influencing 48.69% of the sample as a whole. Although pH is not present in factors 1 and 2, it has an important influence on the other variables, since factor 3, which includes pH, influences 11% of the sample as a whole. In Figure 3 it is possible to visualize the table with the main factors and also the projection of the variables in the plane. Figure 4 shows the importance of each factor in the sample as a whole.

Through the dendrograms presented below, it is possible to recognize patterns (similarities) between samples

TABLE 2: Correlation Matrix (leachate variables).

	NH <sub>4</sub>	Ba	Cd	Pb	Cu	Fe	Mn	Ni	Ag	Zn	phenols	CrVI	cyanides	fluorides	BOD	COD	BOD/COD	pH
NH <sub>4</sub>	1.00	0.19	0.60	0.72	0.67	0.48	0.38	0.51	0.53	0.61	0.33	0.26	0.32	0.09	0.49	0.61	-0.11	-0.18
Ba	0.19	1.00	0.16	0.28	0.38	0.50	0.26	-0.26	0.62	-0.07	-0.48	-0.42	-0.03	0.18	-0.55	0.04	0.83	-0.52
Cd	0.60	0.16	1.00	0.70	0.77	0.38	0.42	0.54	0.31	0.51	0.50	0.64	0.39	-0.10	0.39	0.37	0.16	-0.31
Pb	0.72	0.28	0.70	1.00	0.89	0.84	0.68	0.81	0.79	0.88	0.62	0.42	0.68	-0.37	0.58	0.73	0.06	-0.16
Cu	0.67	0.38	0.77	0.89	1.00	0.75	0.55	0.70	0.78	0.67	0.48	0.55	0.62	-0.21	0.40	0.55	0.00	-0.28
Fe	0.48	0.50	0.38	0.84	0.75	1.00	0.82	0.62	0.93	0.71	0.37	0.13	0.69	-0.40	0.20	0.47	-0.24	-0.13
Mn	0.38	0.26	0.42	0.68	0.55	0.82	1.00	0.54	0.67	0.56	0.46	0.11	0.80	-0.39	0.19	0.42	-0.19	-0.09
Ni	0.51	-0.26	0.54	0.81	0.70	0.62	0.54	1.00	0.47	0.93	0.88	0.74	0.68	-0.43	0.83	0.70	0.46	0.08
Ag	0.53	0.62	0.31	0.79	0.78	0.93	0.67	0.47	1.00	0.55	0.18	-0.01	0.62	-0.31	0.13	0.49	-0.33	-0.15
Zn	0.61	-0.07	0.51	0.88	0.67	0.61	0.56	0.93	0.55	1.00	0.81	0.55	0.63	-0.35	0.78	0.75	0.29	-0.05
phenols	0.33	-0.48	0.50	0.62	0.48	0.37	0.46	0.88	0.18	0.81	1.00	0.74	0.73	-0.34	0.85	0.63	0.53	0.04
CrVI	0.26	-0.42	0.64	0.42	0.55	0.13	0.11	0.74	0.01	0.55	0.74	1.00	0.34	-0.11	0.63	0.30	0.57	-0.07
cyanides	0.38	-0.03	0.39	0.68	0.62	0.69	0.80	0.68	0.62	0.63	0.73	0.34	1.00	-0.38	0.49	0.58	0.10	-0.02
fluorides	0.09	0.18	-0.10	-0.37	-0.21	-0.40	-0.39	-0.43	-0.31	-0.35	-0.34	-0.11	-0.38	1.00	-0.28	0.09	-0.45	-0.72
BOD	0.49	-0.55	0.39	0.58	0.40	0.20	0.19	0.83	0.13	0.78	0.85	0.63	0.49	-0.28	1.00	0.80	0.64	0.14
COD	0.61	-0.04	0.37	0.73	0.55	0.47	0.42	0.70	0.49	0.75	0.63	0.30	0.58	-0.09	0.80	1.00	0.07	-0.25
BOD/COD	0.11	-0.83	0.16	0.06	0.00	-0.24	-0.19	0.46	-0.33	0.29	0.53	0.57	0.10	-0.45	0.64	0.07	1.00	0.69
pH	-0.18	-0.52	-0.31	-0.16	-0.28	-0.13	-0.09	0.08	-0.15	-0.05	0.04	-0.07	-0.02	-0.72	0.14	0.25	0.69	1.00

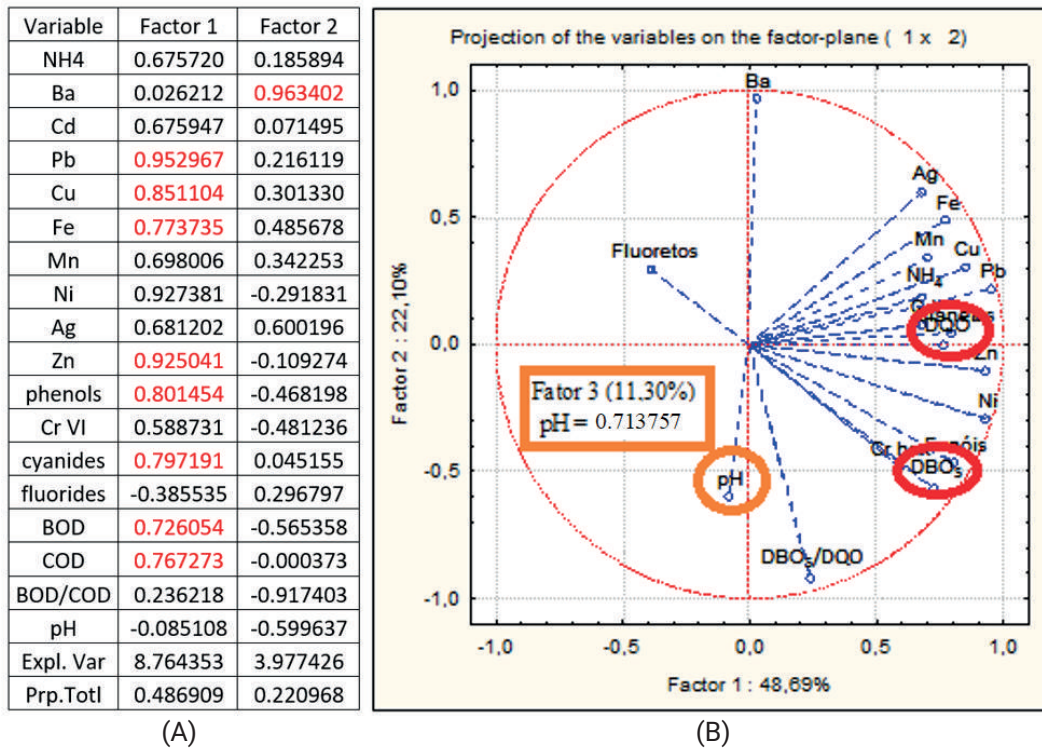


FIGURE 3: (A) Factor 1 and Factor 2 (ACP); Projection of the variables in the plane (detail for BOD and COD - Factor 1 and pH - Factor 3).

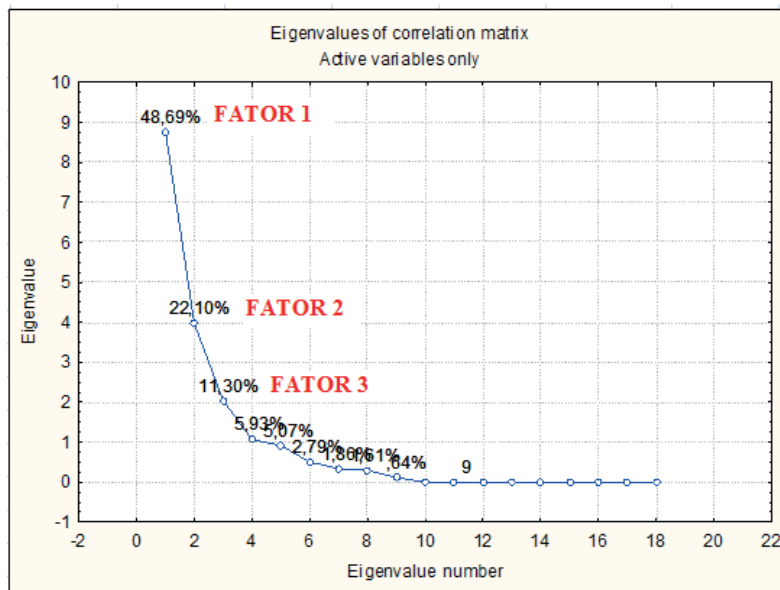


FIGURE 4: Factors 1, 2 and 3 of principal component analysis.

from a set of data, allowing the grouping of samples among them. The smaller the distance is between the points, the greater the similarity between the samples is.

### 3.3.1 Dendrogram (years)

In the first dendrogram (Figure 5a), two large groups of similarity are formed. The first, formed by the initial years 2004, 2005, 2006 and 2007, jibes with the history of the area, since the site was operated as a dump during this

period. The second group, formed by the years 2008, 2010, 2011, 2012, 2013 and 2017, indicates that with the beginning of control of the landfill, the area began to present similar behavior in 2008.

### 3.3.2 Dendrogram (variables)

In the second dendrogram, two large groups of similarity are formed (Figure 5b). The first is formed by the metals Mn, Ag, Fe, Cu, Pb and Cd, along with cyanides, fluorides

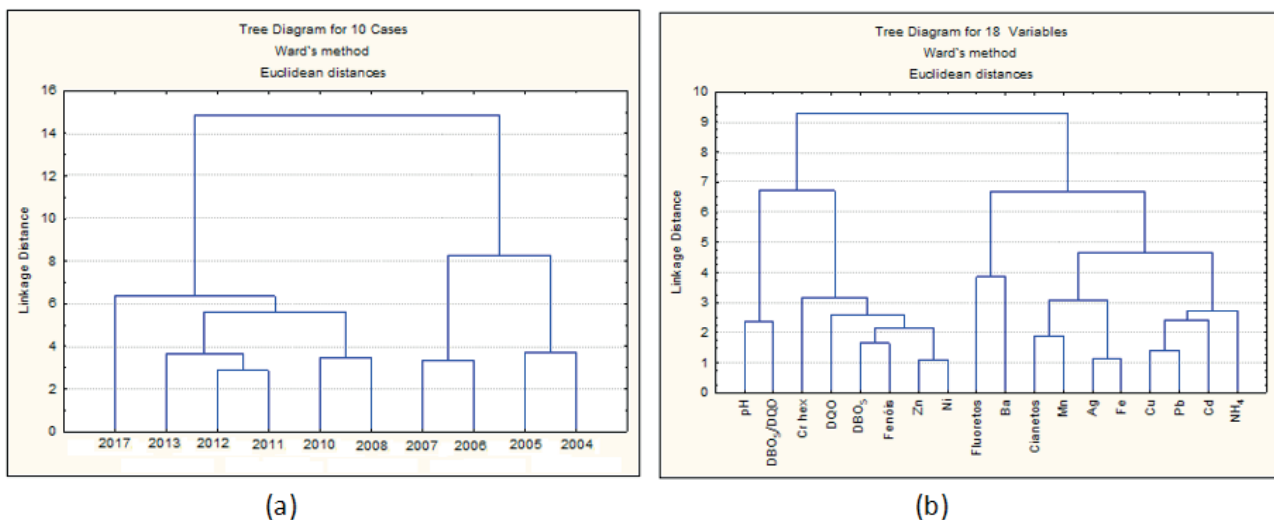


FIGURE 5: (a) Dendrogram of the years of operation, (b) Dendrogram of the variables.

and ammoniacal nitrogen. These results indicate greater similarity in the behavior of metals, cyanide and ammoniacal nitrogen, as well as greater similarity in the behavior of fluorides with barium, indicating they probably come from the same source. The second group is formed by BOD, COD, Zn, Ni, phenols, Cr (VI), BOD/COD ratio and pH. There is strong similarity between the pH and the BOD/COD.

D ratio, indicating that the behavior of the sample as a whole was directly influenced by the associated action of these two parameters. The phenols are associated, as expected, with BOD, COD, Zn and Ni. As in the correlation matrix, there is a high positive correlation between the elements Zn and Ni, which suggests they come from the same source.

### 3.4 Distribution of weights of the parameters chosen for DLAI calculation

For the four parameters cited, weights were assigned according to the potential impacts of these components on the environment and human health, in addition to treatment costs, as in the case of ammoniacal nitrogen. Therefore, we believe this parameter should receive the greatest weight among the four chosen to compose the index. Regarding pH, BOD and COD, we decided to distribute the same weights for the three parameters, all smaller than the one suggested for ammoniacal nitrogen, which is the greatest concern when analyzing deactivated waste disposal areas. Its presence at high concentrations throughout the life of the landfill makes it one of the main pollut-

TABLE 3: Weights of pollutants in the Deactivated Landfill Assessment Index (DLAI).

Pollutant	Weight (w <sub>i</sub> )
pH	0,15
BOD	0,15
COD	0,15
Ammoniacal nitrogen	0,55
Total	1

ants in leachate. According to Chu et al. (1994), after a period of 3 to 8 years, the concentration of ammoniacal nitrogen reaches values between 500 and 1500 mg/L, remaining at this level for at least 50 years. We believe that for a first analysis, shortly after the closure of a landfill, it is important to assess a wider range of pollutants present in the leachate, just to verify that the behavior of the area is in line with what is expected (low concentrations of metals, for example) and within the limits established in the standards with respect to leachate release. If the levels are below the limits, the monitoring can be continued only with the evaluation of the most relevant parameters, presented in Table 3, which were weighted for the calculation of the Deactivated Landfill Assessment Index (DLAI).

Despite the need to create a new index, where the weights and the individual importance of each parameter were changed to fit the reality of Brazilian landfills, the curves presented by Kumar and Alappat (2005) (Figure 6) are useful for determining the sub-index components analyzed.

Thus, the DLAI can be calculated using equation 1:

$$DLAI = \sum_{i=1}^n w_i p_i \quad \sum_{i=1}^n w_i = 1 \quad (1)$$

where: DLAI - Deactivated Landfill Assessment Index;  
w<sub>i</sub> - weight of the parameter evaluated;  
p<sub>i</sub> - score of the sub-index of the parameter evaluated;  
n - number of pollutant variables of the leachate used in calculating the DLAI.

The procedure for calculating the DLAI for the leachate must follow the three steps below:

1. Analysis of the 4 parameters (pH, BOD, COD and ammoniacal nitrogen).
2. Determination of the 'p<sub>i</sub>' subscript values from the curves presented by Kumar and Alappat (2005), based on the concentration of leachate pollutants (Figure 7).
3. Aggregation of 'p<sub>i</sub>' subscript values obtained for the parameters, multiplied by the respective 'w<sub>i</sub>' weights assigned to each parameter. The weighted sum of all parameters gives the DLAI.

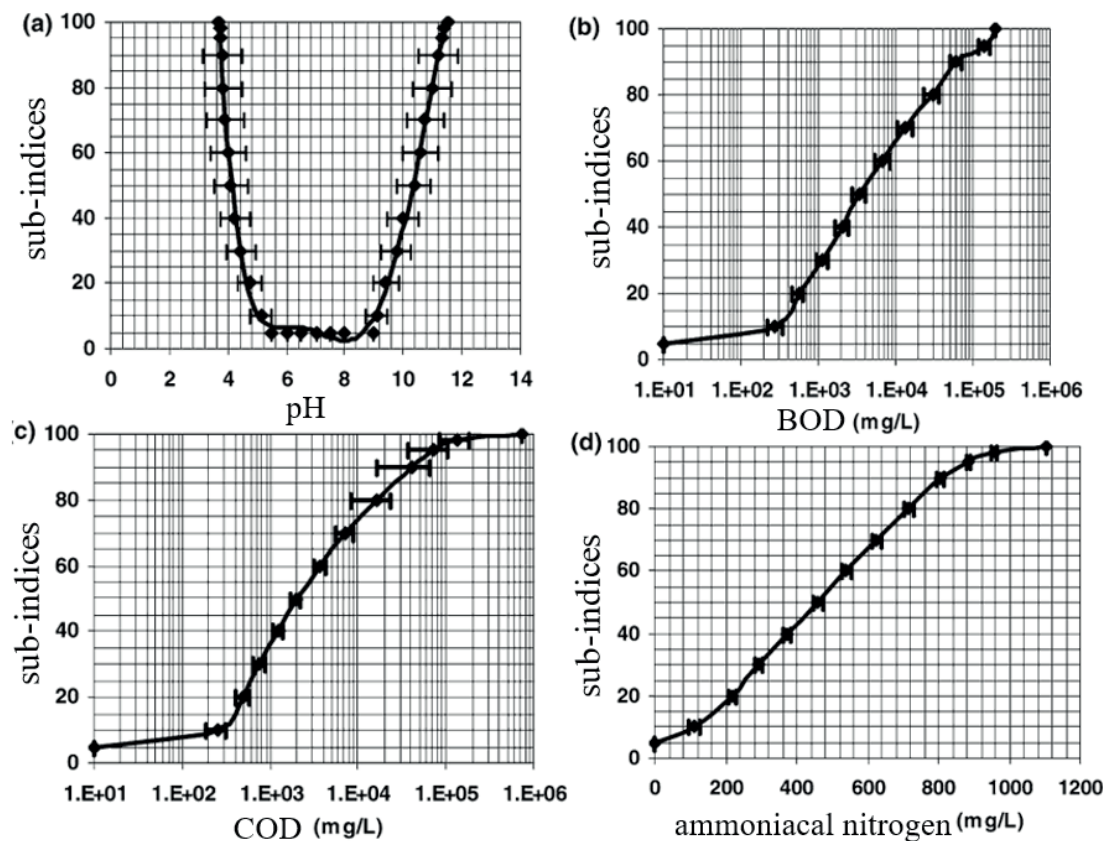


FIGURE 6: Subscript curves of (a) pH, (b), BOD, COD and ammoniacal nitrogen (Kumar and Alappat, 2005).

Like the LPI, the DLAI is represented by a number ranging from 5 to 100 (as a score), expressing the overall contamination potential of the leachate from a landfill based on the defined parameters. It is an increasing scale index, where a higher value indicates greater potential for contamination by the leachate.

### 3.5 Calculation of the DLAI for the Sky Hill dumpsite

The LPI value was calculated for the leachate at the Sky Hill dumpsite using the method proposed by Kumar and Alappat (2005), with weights distributed in 12 parameters (Table 4). Then, the calculations were redone with the weights proportional to the importance of the organic fraction in Brazilian landfills, taking into account pH, BOD, COD and ammoniacal nitrogen. In this new calculation, therefore, the contributions of heavy metals, chlorides, TDS and others were not considered, because they did not directly influence the contamination of the water around the landfill. In analyzing Table 5, it is possible to verify that the calculation of the DLAI for the leachate through the application of the method proposed for Brazilian landfills provides values with relevant changes. The pollutant potential of Sky Hill dumpsite, calculated with new parameters and weights, comes close to that in 2004 (LPI = 17.68, DLAI = 62.70) and 2006 (LPI = 17.94, DLAI = 64.55), quadrupled when compared to the LPI in the same year. If the DLAI were also applied in the deactivated landfills studied by Kumar and Alappat (2005) in Hong Kong and by Umar et al. (2010) in Malaysia, the results of these indexes would also

be quite different. In the case of the first study cited, the LPI values were 45.01 for the Ma Tso Lung (MTL) landfill and 15.97 for the Nagu Chi Wan (NCW). If the DLAI were applied to these landfills, the values would rise to 81.25 and 52.90, respectively. In the landfill evaluated by Umar et al. (2010), the value of the index would increase 46% if it were calculated from the parameters and weights suggested for the DLAI. The results found for the DLAI suggest that the pollutant potential of the leachate is much higher when one considers the parameters that really contribute most relevantly to the prolonged activity of the landfills. Calculation of the DLAI can assist in the first phase of low-cost landfill closure and recovery projects. The application of this index in waste disposal areas in Brazil can serve as a tool to prioritize remediation processes, by assessing which areas should undergo immediate intervention.

## 4. CONCLUSIONS

Organic matter is mainly responsible for the prolongation of the activity of a landfill, which means that pH, BOD, COD and ammoniacal nitrogen are the main parameters for the composition of a landfill closure assessment index. From the application of the LPI in Brazilian landfills, it was verified that the importance given to leachate components was not adequate. The DLAI was proposed to consider the conditions in the country and the garbage produced and buried, by assigning weights to each parameter according to the verification of the potential impacts of these components on the environment, human health and treatment

**TABLE 4:** Average values of the analyzed parameters in the Sky Hill leachate during the monitoring.

Parameters	2004	2005	2006	2007	2008	2010	2011	2012	2013	2017
1 pH	7.960	7.960	7.830	7.680	7.610	7.670	7.720	7.790	7.680	8.710
2 BOD (mg/L)	568,940	428,080	382,440	210,530	296,600	195,000	182,000	163,900	350,250	255,900
3 COD (mg/L)	2,101,630	1,876,250	2,166,330	1,684,080	1,580,000	1,020,000	1,276,100	969,270	2,051,500	990,000
4 NH <sub>4</sub> (mg/L)	855,440	795,500	975,330	846,220	927,000	723,100	492,870	788,090	841,600	706,200

**TABLE 5:** Comparison between LPI and DLAI values for each year of monitoring.

Parameters	Weight (wi)	2004		2005		2006		2007		2008		2010		2011		2012		2013		2017	
		Pi	pi*wi	Pi	pi*wi	pi	pi*wi	pi	pi*wi	pi	pi*wi	pi	pi*wi	pi	pi*wi	pi	pi*wi	pi	pi*wi	pi	pi*wi
pH	0.15	5	0.75	5	0.75	5	0.75	5	0.75	5	0.75	5	0.75	5	0.75	5	0.75	5	0.75	5	0.75
BOD	0.15	20	3.00	15	2.25	13	1.95	10	1.50	10	1.50	9	1.35	9	1.35	9	1.35	12	1.80	10	1.50
COD	0.15	52	7.80	46	6.90	53	7.95	45	6.75	41	6.15	35	5.25	37	5.55	35	5.25	51	7.65	35	5.25
NH <sub>4</sub>	0.55	93	51.15	89	48.95	98	53.90	93	51.15	97	53.35	83	45.65	49	26.95	88	48.40	92	50.60	79	43.45
LPI	12 parameters *	17.68		17.24		17.94		16.39		16.07		14.29		11.64		14.4		16.45		15.62	
DLAI	4 parameters	62.70		58.85		64.55		60.15		61.75		53.00		34.60		55.75		60.80		50.95	

\* Weights proposed by Kumar and Alappat, 2005  
 \*\* New weights

expenses. It was possible to conclude from the statistical analysis that the parameters BOD, COD and pH are important variables, with strong influence on the dataset, thus justifying their presence in the index. As expected, in the principal component analysis (PCA), the elements Pb, Cu, Fe, Ni, Zn, phenols, cyanides and BOD and COD, influence the sample as a whole. pH it has an important influence of the sample as a whole. Taking into account the lack of criteria to support decisions regarding the allocation of resources for remediation processes, the application of the DLAI can technically support the formulation of municipal actions for management and control of landfills, especially in the post-closure phase.

## ACKNOWLEDGMENTS

The authors would like to thank CAPES, CNPq and FAPERJ for supporting this study.

## REFERENCES

ABRELPE - BRAZILIAN ASSOCIATION OF PUBLIC CLEANING AND SPECIAL WASTE COMPANIES. Overview of Solid Waste in Brazil. 2015 Edition. São Paulo. 2015. Available at: <<http://www.abrelpe.org.br/Panorama/panorama2015.pdf>>. Accessed on: 20 Nov. 2016.

Barlaz, M.A., Rooker, A.P., Kjeldsen, P., Gabr, M.A., Borden, R.C., 2002. Critical Evaluation of Factors Required to Terminate the Postclosure Monitoring Period at Solid Waste Landfills. Environmental Science Technology, v. 36, p. 3457-3464.

Bhalla, B., Saini, M.S., Jha, M.K., 2014. Leachate contamination potential of unlined municipal solid waste landfill sites by leachate pollution index. International Journal of Science, Environment and Technology, v. 3, n. 2, p. 444-457.

CETESB - ENVIRONMENTAL COMPANY OF THE STATE OF SÃO PAULO. Manual of management of contaminated areas. São Paulo, 2009. Available at: <<http://www.cetesb.sp.gov.br/areas-contaminadas/manual-de-garagem-de-ACs/7/>>. Accessed on: 5 Aug. 2015.

Christensen, T.H., Kjeldsen, P., Bjerg, P.L., Jensen, D.L., Christensen, J.B., Baun, A., Albrechtsen, H., Heron, G., 2001. Biogeochemistry of landfill leachate plumes. Applied geochemistry, v. 16, n. 7, p. 659-718.

Chu, L.M., Cheung, K.O., Wong, M.H., 1994. Variations in the chemical properties of landfill leachate. Environmental Management. v. 18, No. 1, pp. 105-117, 1994.

Clément, B., Merlin, G., 1995. The contribution of ammonia and alkalinity to landfill leachate toxicity to duckweed. Science of the Total Environment. v. 170, n. 1-2, p. 71-79.

CONAMA - NATIONAL (BRAZILIAN) COUNCIL FOR THE ENVIRONMENT. Resolution No. 357, dated March 17, 2005, which provides the classification of water bodies and environmental guidelines for their classification, as well as establishing the conditions and standards for effluent discharge, and other matters. Available at: <<http://www.mma.gov.br/port/conama/legiabre.cfm?codlegi=459>> Accessed on: 28 Oct. 2015.; Resolution No. 420, dated December 28, 2009, which provides criteria and parameters of soil quality due to the presence of chemical substances and establishes guidelines for the environmental management of areas contaminated by these substances as a result of anthropic activities. Available at: <<http://www.mma.gov.br/port/conama/legiabre.cfm?codlegi=620>> Accessed on: 28 Oct. 2015.; Resolution No. 430 of 13 May 2011, supplements and amends Resolution No. 357/2005 on the conditions and standards for the discharge of effluents. Available at: <<http://www.mma.gov.br/port/conama/legiabre.cfm?codlegi=646>> Accessed on: 2 Nov. 2016. (In Portuguese)

Farquhar, G.J., ROVERS, F.A., 1973. Gas production during refuse decomposition. Water, Air, & Soil Pollution. v. 2, p. 483-495.

Harmsen, J., 1983. Identification of Organic Compounds in Leachate from a Waste Tip, Water Research, V. 17, No. 6, p. 699-705.

IBGE - BRAZILIAN INSTITUTE OF GEOGRAPHY AND STATISTICS, 2015. Available at: <<http://cidades.ibge.gov.br/xtras/perfil.php?codmun=510340>> Accessed on: 11 Aug. 2016.

INEA - STATE INSTITUTE OF THE ENVIRONMENT, 2013. Available at: <[www.inea.rj.gov.br](http://www.inea.rj.gov.br)>. Accessed on: 10 Oct. 2013.

Krishnamurthy, M.P., Sivapullaiah, P.V., SHAMBAVIKAMATH, 2015. Leachate Characteristics and Evaluating Leachate Contamination Potential of Landfill Sites Using Leachate Pollution Index. The Asian Review of Civil Engineering. v. 4 n. 1, p. 6-13.

Kumar, D., Alappat, B. J., 2003. A technique to quantify landfill leachate pollution. In: Proceedings of the 9th international landfill symposium. Cagliari, Sardinia, Paper n. 400.

Kumar, D., Alappat, B.J., 2005. Evaluating leachate contamination potential of landfill sites using leachate pollution index. Clean Techn Environ Policy. v.7, p. 190-197.

Lins, E. A. M., 2011. Study of the characteristics of the leachate from the Muribeca landfill before and after the closure. 26th Brazilian Congress of Sanitary and Environmental Engineering, Porto Alegre, RS.

- Lothe, A.G., Sinha, A., 2016. Development of model for prediction of Leachate Pollution Index (LPI) in absence of leachate parameters. Waste Management.
- Mahler, C.F. FUNDAÇÃO COPPETEC/FEDERAL UNIVERSITY OF RIO DE JANEIRO – Project Reports PEC 5556, on the Monitoring of Gases and Laboratory Analyses of Liquid Effluents from Sky Hill Dumpsite. Years: 2004 to 2013. (In Portuguese)
- MS - MINISTRY OF HEALTH. Edict 2914 dated December 12, 2001, which contains the procedures for controlling and monitoring the quality of water for human consumption and its standard of potability. Available at: <<http://portarquivos.saude.gov.br/images/pdf/2015/maio/25/Portaria-MS-no-2.914-12-12-2011.pdf>>. Accessed on: 28 Oct. 2016.
- Naveen, B.P., Mahapatra, D.M., Sitharam, T.G., Sivapullaiah, P.V., Ramachandra, T.V., 2016. Physico-chemical and biological characterization of urban municipal landfill leachate. Environmental Pollution. p. 1-12 in press.
- Otoni, V.A., 2011. Simulation of vertical flow in landfill of urban solid waste. Master's Dissertation, Federal University of Rio de Janeiro, COPPE, Civil Engineering Program, 176p.
- Pohland, F.G., Harper, S.R., 1985. Critical review and summary of leachate and gas production from landfills. EPA/600/2-86/073. Hazardous Environmental Research Laboratory, Office of Research and Development, United States Environmental Protection Agency. 165 p.
- Queiroz, L.M., Amaral, M.S., Morita, D. M., Yabroudi, S.C., Sobrinho, P.A., 2011. Application of physicochemical processes as an alternative of pre- and post-treatment of leachate from landfills. Sanitary and Environmental Engineering. v.16, p. 403-410.
- Rafizul, I., Alamgir, M., Islam, M. M., 2011. Evaluation of contamination potential of sanitary landfill lysimeter using leachate pollution index. Sardinia 2011 – Thirteenth International Waste Management and Landfill Symposium, S. Margherita di Pula, Cagliari, Italy.
- Reinhart, D.R., Townsend, T.G., 1997. Landfill Bioreactor Design & Operation. New York - Washington, D.C., CRC Press LLC.
- Schueler, A.S., Mahler, C.F., 2008. Evaluation system to classify areas for disposal of urban solid waste for remediation and post-occupation. Sanitary and Environmental Engineering, v. 13, p. 249-254.
- Sharma, A., Meesa, S., Pant, S., Alappat, B.J., Kumar, D., 2008. Formulation of a landfill pollution potential index to compare pollution potential of uncontrolled landfills. Waste Management and Research. v. 26, p. 474-483.
- Souto, G.D.B., Povinelli, J., 2007. Characteristics of landfill leachate in Brazil. 24th Brazilian Congress of Sanitary and Environmental Engineering. Belo Horizonte.
- Teixeira, G.P., Ritter, E., Lacerda, G.B.M., Ferreira, J.A., França, R.A., 2007. Considerations on the geotechnical and environmental remediation and monitoring of Salvaterra dump - Juiz de Fora / MG. 24th Brazilian Congress of Sanitary and Environmental Engineering. Belo Horizonte.
- Umar, M., Aziz, H.A., Yusoff, M.S., 2010. Variability of Parameters Involved in Leachate Pollution Index and Determination of LPI from Four Landfills in Malaysia. International Journal of Chemical Engineering. p. 6.

# SCALE AND IMPACTS OF LIVELIHOODS DEVELOPMENT ON WOMEN EMPOWERMENT IN THE SOLID WASTE SECTOR OF JORDAN

Motasem Saidan<sup>1,\*</sup>, Ammar Abu Draiss<sup>1</sup>, Ehab Al-Manaseer<sup>2</sup>, Murad Alshishani<sup>3</sup> and Colette Linton<sup>1</sup>

<sup>1</sup> Department of Chemical Engineering, University of Jordan, 11942 Amman, Jordan

<sup>2</sup> GreenPlans Environmental Consultation Ltd., 11118 Amman, Jordan

<sup>3</sup> UNDP, P.O. Box 941631, 11194 Amman, Jordan

## Article Info:

Received:  
12 November 2019  
Revised:  
21 February 2020  
Accepted:  
3 March 2020  
Available online:  
8 May 2020

## Keywords:

Women empowerment  
Livelihood development  
Host communities  
Refugees  
Solid waste  
Composting  
Recycling

## ABSTRACT

The present study outlines a cohesive compilation of analysis of the involvement of women in decision-making and leadership in the solid waste sector in Jordan. The socio-economic challenges have been catalyzed by the influx of Syrian refugees into the host communities and camps in Jordan. Hence, deterioration of municipal solid waste services have centered on and proposed that women engagement in the Solid Waste (SW) sector to provide opportunities that aim to improve livelihoods by producing an avenue for added income generation through the recycling and sorting scheme; as well as the cost revenue implications for the municipalities. Since 2015, projects added prospects for continued engagement of women and have drastically increased their involvement by filling management positions in the development and operation of municipal SW Transfer Stations (TSs), including heading the design and operation of the TS, and the recycling project. While 54 employment opportunities were created within North Shouneh SW pilot project; 37,794 women jobs of recycling and composting were made available by the cash for work initiative throughout 2016-2017, as well as, 60 women were employed in Zaatari camp. Moreover, when CBOs are directly involved, there has been more opportunity to engage women in employment in the solid waste sector.

## 1. INTRODUCTION

Solid waste management as an integrated system can be a gateway for innovation, leading to sustainable options for development and increased community resilience. Hence, the increased production of solid waste in communities experiencing population growth is leveraged as an opportunity to positively integrate solid waste back into the socio-ecological metabolic system. Notwithstanding that solid waste transforming into a valuable resource can promote shared goals around building resilience (i.e. job creation, recycling, reuse, reduction of waste, and the empowerment of women).

The natural resource demands of the increased population, resulting in part due to multiple refugee immigrations over the past decades in Jordan (Al-Addous et al., 2019; 2020; Al-Awad et al., 2018; Aldayyat et al., 2019; Al-Hamamre et al., 2017; Saidan et al., 2017a), have strained solid waste services and operations while increasing solid waste production, translating into seemingly unsurmounta-

ble challenges, which have been negatively restricting community resiliency and impacting public and environmental health (Alrabie and Saidan, 2018; Aboelnga et al., 2018; Jabr et al., 2019; Khasawneh et al., 2019). The total population in Jordan is estimated at 9.5 million, including about 2.9 million guests (Malkawi, 2015; Saidan et al., 2018; MWI, 2015; Saidan, 2019), consisting of Syrian, Iraqi, Palestinian and other populations. However, by 2050 it is expected to double (Saidan et al., 2019).

The design and implementation of innovative solutions is urgently needed to bridge the socio-economic resiliency and safeguard the existing natural resources of host communities is underscored in the national and regional strategies in Jordan (Saidan et al., 2020). Moreover, the governing the intended targets for the solid waste sector were laid out in the Jordan National Vision and Strategy and the National Municipal Solid Waste Management Strategy, followed by their rationalization into the Regional level for the North and Central Regions. Regions of core concern are those located in the north of Jordan, as their populations

\* Corresponding author:  
Motasem Saidan  
email: m.saidan@gmail.com



catalyzed and their infrastructure further strained by the influx of refugees since mid-2013. The distribution of registered Syrian refugees in the major governorates, as shown in Figure 1, are namely Amman (29.4%), Mafrq (24.3%), Irbid (21.0%) and Zarqa (14.5%) (UNHCR, 2018).

In searching for an alternative to the deterioration of solid waste services and efficiency, incorporating women into the development has been and continues to be investigated. Recent ongoing projects have centered on and proposed that women lead associations for recyclables collection at the household level, which are then collected and sorted at the municipal level. This in return offers economic and employment opportunities for women in Jordan. For instance, the newly established composting facilities have carved out specific roles for women in the production of such products that are socially acceptable while also impactful.

In this way, the potential inherent in the roles of women as proximate experts in the solid waste sector can evolve as a means to boost the socio-economic opportunities of refugees hosting communities. Moreover, this emphasizes the leadership capacity of women not only in deciding how waste is discarded, but also taking a hand in establishing a foundation for meeting waste generation, environmental,

climate and water-related challenges by contributing to solutions.

The participation of the female members in the municipal solid waste management is noteworthy, since they occupy the leading roles, and are able to overcome internal and external problems (GTZ, 2005). Several studies revealed the necessity to prioritize women in order to promote knowledge and attitude on effective MSW management since women are more aware of waste management specifically source separation, waste reuse and recycling (Bhawal Mukherji et al., 2016; Laor et al., 2018; Almasi et al., 2019), given their active role as the house manager is crucial (Moh, 2017). Moreover, although men are more willing-to-pay than women (Ezebilo, 2013; Bernad-Beltran et al., 2014), however, females are more willing-to-participate in waste reduction and recycling (Bench et al. 2005; Saphores et al., 2006). Iyer and Kashyap (2007) highlight the role of gender and strongly recommend the involvement of women in the promotion of recycling schemes. Notwithstanding, there has been no widely published research that has tackled the women empowerment role in the solid waste sector.

The formation of women recycler cooperatives has gained impetus in Asia and Latin America Recuperar, based in Medellin (Columbia), was created in 1983 and has 1,000

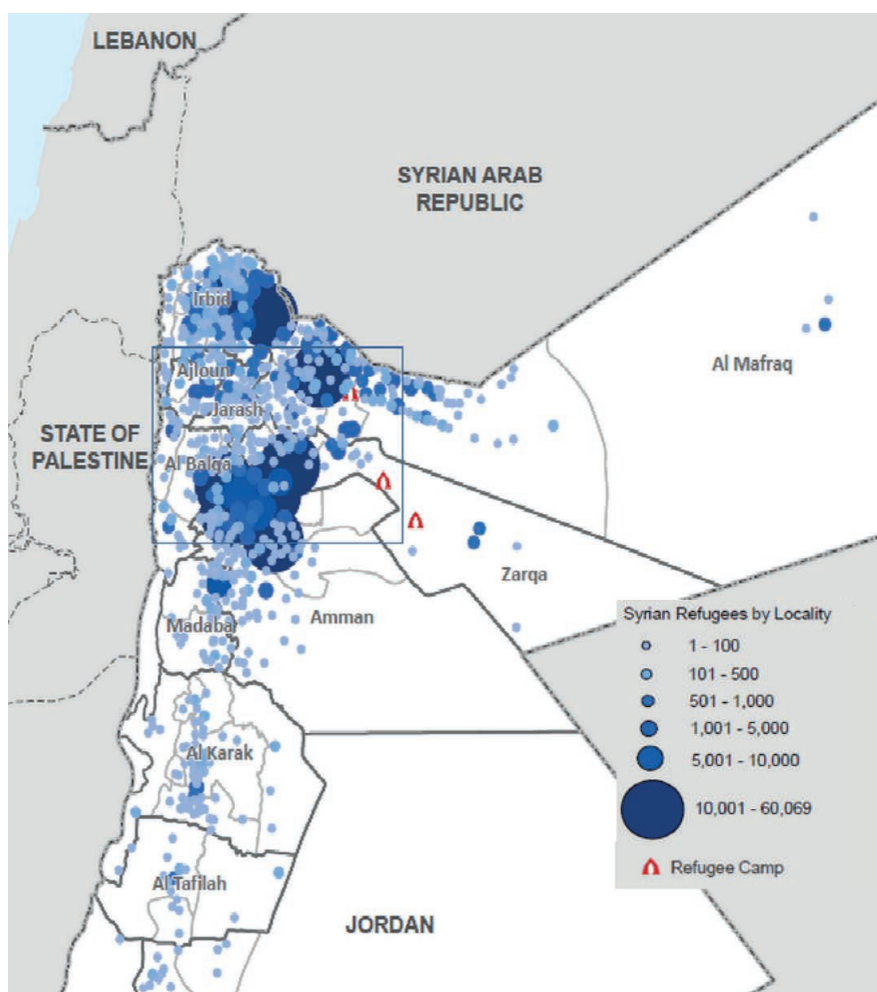


FIGURE 1: Distribution of Syrian refugees in Jordan (UNHCR, 2018).

members, 60% of them women. In Manila (Philippines) the NGO group Women's Balikatan Movement developed as a formalized system of waste pickers and itinerant buyers of recyclables working now 17 cities and towns that comprise Metro Manila (GTZ, 2005). In Vietnam, women constitute almost 50% of employees in the MSW management industry (4500 as itinerant buyers and 500 as shopkeepers) and contribute significantly to MSW management (Mehra et al., 1996). In India more than 20,000 women work as paper pickers in the city of Ahmedabad, and up to 150,000 waste pickers in the municipal corporation of the Delhi area (Ahmed and Ali, 2004).

Before 2015, women had limited involvement in the solid waste sector at both governmental and communal levels in Jordan, despite of the active solid waste management projects in Jordan that were stimulated by the Syrian refugees influxes to the northern region of Jordan. The main objective of the present study is to provide an overview of the solid waste management projects undertaken in Jordan, as well as, the added prospects for continued engagement of women and their growing role in the solid waste sector. The focus of the present study is on the established a community-based waste sorting and recycling project in North Shouneh at Irbid Governorate, which aims at facilitating the income creation opportunities and maximizing the women involvement in the solid waste management (SWM). The "Cash for Work" initiative, which has been unleashed in refugees' camps and hosting communities, is also highlighted in the present study since women are targeted along with Syrians and youth as so-called vulnerable groups. The initiative gave an advocacy role to female Syrian Refugee workers to educate the community at the household level to sort dry wastes.

## 2. METHODOLOGY

### 2.1 Case study area

The study area includes the Tabaqet Fahel, Mo'ath Bin Jabal and Sharhabeel Bin Hasna Municipalities of the Northern Shouneh, as shown in Figure 2. Each municipality of the study area is comprised of many localities, those localities are distributed alongside with the geographic extension of the municipality.

More than half of the localities of the three municipalities have a population parentage less than 2% while almost half of them has a population percentage above 2%. However, the approach of the present study included only the most populated localities with more than 2% of population percentage, which are 10 out of 23 localities. The population of these selected localities are shown in Figure 3.

In Northern Shouneh, approximately 13,145 ha of land are cultivated on annual basis, agricultural land use consisted of fodder crops (1,131 ha), fallow fields (1,662 ha), greenhouses/greenhouse crops (33 ha), fruit crops (6,458 ha), fallow (3,061 ha). The amount of agricultural wastes generated from crop production varies by crop type.

### 2.2 Data gathering

A desk study was carried out for the available baseline documents (i.e. unpublished, monthly progress reports,

internal memos, and minutes of meetings) and other references for collecting the technical data. Semi-structured interviews with funding agencies (i.e. UNDP, GIZ, etc.) involved in the ongoing projects targeting the host communities of Syrian refugees project, to obtain information on staffing, infrastructure, costing and working conditions. Information obtained through the interviews was cross-checked with the objective to reassess gaps and divergences of information.

### 2.3 Gender statistics: women in Jordan

Although females and males in Jordan achieve increasingly equal educational success, however, the economic participation of women remains relatively low. In terms that according to the World Bank ranking, Jordan ranked as the eight worst among MENA countries (Schwab and Sala-i-Martin, 2017), and with lowest percentages in the MENA region for the percentage of female labor force, which is at 14.4% (World Bank, 2017). Moreover, approximately 80% of women in Jordan are excluded from the labor force completely; whereas 82% of working-age men are employed or looking for work, and only 21% of women are reported with the same analogy.

At the local governmental and municipal level, women's participation in decision making roles is comparably low. Although the use of quotas has increased women's participation in government overall in Jordan, the percentage of women on municipal councils remained constantly un-

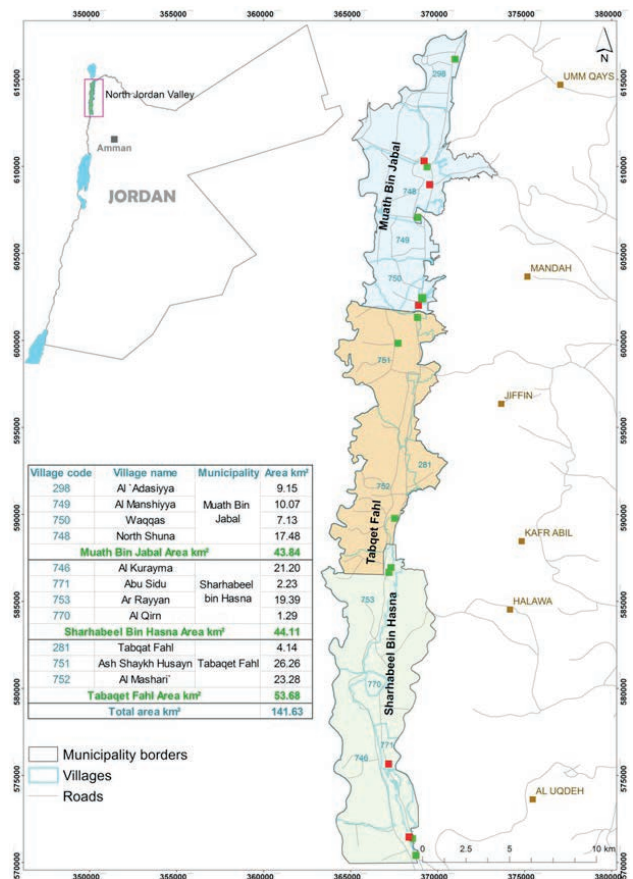


FIGURE 2: Map of selected municipalities in the study area.

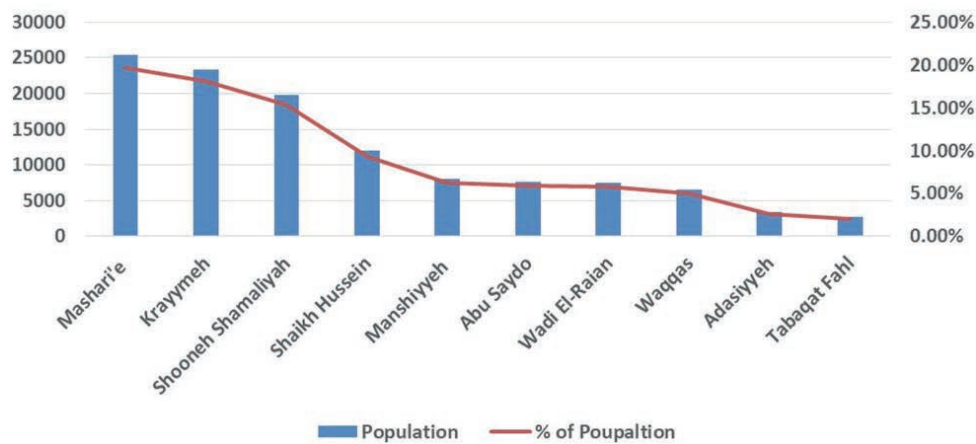


FIGURE 3: Population in all localities of the target municipalities (2017).

der 25% between 2006 and 2016 (Al Kharouf and Al-Jribia 2016). Women's involvement in local government and municipal decision making as members of municipal councils was not only low, but decreased from 27.4% to 24.8% between 2007 and 2013 (Al Kharouf and Al-Jribia, 2016). However, Jordan set a new record in 2018 for the number of female ministers in the history of Jordan, surpassing 24% of women participation, totaling 29 women in the Cabinet (Ibanez Prieto, 2018). International indicators tracking gender equality, however, reported a decline in equality while stating a drop in economic and political participation on the part of women (UNDP, 2015). In terms of employment, the reported gender gap is wider for Jordan's most vulnerable women. For those with only a primary education, the statistic can be up to six men work for everyone working woman, given the same level of capacity (UNDP, 2015). The marital status statistics also showed that while 29% of never-married women participated in the labor market, only 15% of married women were involved (UNDP, 2015). Despite these statistics, the World Bank found that 92% of female college students are planning to work after graduation (UNDP, 2015). This is one of many studies indicating that Jordanian females desire to participate in the labor market, but due to cultural and/or economic reasons cannot achieve that. It is also noteworthy that women will likely embrace the opportunity to conduct meaningful work and contribute to their families and communities, if such an opportunity is offered in a way that is culturally sensitive.

While women may be motivated to seek employment following graduation, the cultural expectation remains that women who enter the workforce should not allow their work to disrupt their household and familial responsibilities, as these duties and expectations are delegated to women. In Jordan, for example, women are the primary caretakers of children. Women take most of the workload in family health and hygiene. Women are responsible for household waste management (Tarawneh and Saidan, 2013). Women and children drop the plastic bags with solid waste into the communal solid waste bins. Mothers educate their children in household and community hygiene and hence are the first choice to function as change agent in waste-related behaviour.

### 3. RESULTS AND DISCUSSION

#### 3.1 Women Involvement in SWM: Women as Proximate Experts

Women involvement in the SWM sector in Jordan is still in its beginning stages with the exception of some interventions that are almost in the final stages of implementation. The involvement of women in SWM sector is meant to offering women potential leadership roles, community engagement and auxiliary roles in SWM projects, with exclusion of roles in the physical collection, transportation and handling of wastes.

International project implementers have been looking to make headway in SWM services by incorporating women, addressing the gaps in SWM services, and assessing the socio-economics. The following projects bear such components (i.e. job provision). The incorporation of women, while a more difficult aspect due to the traditional responsibilities of women in addition to the perception overall that SWM jobs are less prestigious, these projects have struck a chord with individuals and households who are in need of an additional financial income. However, where this has been a challenge, one project in particular is trying to transform it into a leverage point, engaging women to take a leadership role as proximate experts.

Mechanisms Development for Operation of the Community Based Recyclables Receiving Stations in the framework of the UNDP-Canada led project "The Establishment of a Municipal Final Sorting Center in Northern Shouneh and the Facilitation of Local Women Engagement in Waste Recycling and Reuse Business". Developing successful mechanisms for the operation of the community-based Recyclables Receiving Stations (RRSs) was seen as a crucial challenge for the project area with the main goal of the project to encourage waste recycling practices within the targeted municipalities.

In order to develop the customized recycling mechanism within the project area (North Shouneh, Tabaqat Fahel, Mo'ath Bin Jabal and Sharhabeel Bin Hasna) a public event was initiated at an early stage of the project in order to encourage the widespread, ongoing and meaningful participation of all key stakeholders with a focus on vulnerable

groups (i.e. elderly, women, children) in order to mobilize the public, the stakeholders of the project will be made fully aware of the intent, design, schedule impact and overall objectives of the project.

Using of the population data and relevant MSW generation rates, the MSW quantities in the study area are estimated to reach a total amount of 57,546 tons during the year of 2019 with an estimated annual quantity of 19,193 tons, 19,524 tons, and 18,829 tons for Sharhabeel Bin Hasna Municipality, Tabaqet Fahel Municipality, and Mo'ath Bin Jabal Municipality, respectively. Figure 4 presents a projection of the expected solid waste generation during the period from 2019 to 2041 in the three municipalities (MoMA, 2015).

According to the National Municipal Solid Waste Management Strategy, issued officially in 2015, the waste composition varies according to the urbanization index. Accordingly, 100 municipalities in Jordan are classified into three Classes: A, B, and C; where the urbanization index for these classes are 75-100%, 50-75%, and 25-50%, respectively (MoMA, 2015). Based on the proposed municipal solid waste composition according to Class C- Urbanization Index, 65% of the original solid waste quantities is food waste, 9% is paper and cardboard, 9% is plastic, 2% is metal, 2% glass, 3% is textile, 5% is yard waste, and 5% is other waste types (MoMA, 2015).

The activities of pilot project were undertaken in four sessions (ten working days in each session) throughout June, July, August, September, and November 2019. The working time was 5 hours per day (9:00 AM-2:00 PM). The total number of women engaged in the project during the reporting period is (54) women, who were distributed as of the following:

- 16 women worked at the Final Sorting/Recycling Center, exists at the Northern Shouneh Transfer Station (JSC-Irbid);
- 12 women worked in the field for collecting waste at community level in Mo'ath Bin Jabal;
- 9 women worked in the field for collecting waste at community in Tabaqet Fahel;

- 16 women worked in the field for collecting waste at community in Sharhabeel Bin Hasna.

The final sorting/recycling center has been operated during the reporting period on a daily basis to receive and sort waste of marketing value into subcategories. Women had mainly practiced a limited waste processing activities on: cardboard baling, cardboard shredding, plastic baling, and waste sorting line operating. Plastic shredding is not applicable because the machine is crushing only the hard plastics. No activities for producing briquettes/ pellets from organic waste are reported as the machine is out of service.

The positioning of the container was optimized during the reporting period and the collection team were aware of the new locations. The modifications aimed to increase the filling up and optimize the efficiency. All of the containers are coded with specific numbers and the coordinates were identified. The collection timing and routes were updated during the reporting period in line with what recommended in waste routing collection plan.

To increase the waste recycling rates within the project area, Green points were established. Green Points - a single-stop for the reception of multiple receptacles (paper, plastic, glass and metals). The project sought out the assistance of interested community based organizations (CBOs) which would be capable of providing continuous support and technical assistance to the women managing the Green Points. In this way, the women involved in the cooperative framework for the collection of recyclables could benefit from an incentive mechanism: the more recyclables received at the Green Points, placed throughout the neighborhoods of the selected regions in northern Jordan, the greater the incentive they would receive. The mechanism provides opportunities that aim to improve livelihoods by producing an avenue for added income generation through the recycling and sorting scheme; as well as the cost revenue implications for the municipalities. Accordingly, the total number of the existing Green Points established over the projects area is shown in Table 1 according to the existing distribution.

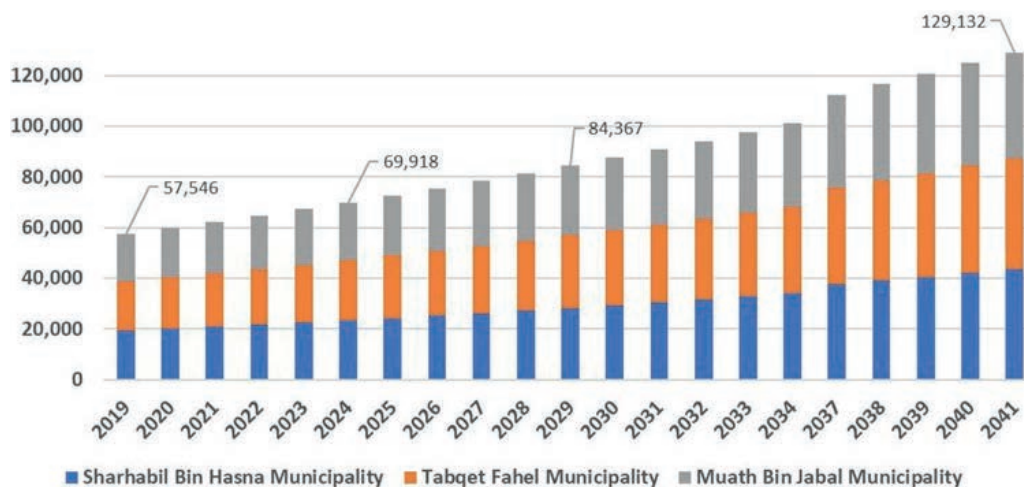


FIGURE 4: Projection of municipal solid waste generation (2019-2041) (MoMA, 2015).

**TABLE 1:** Total number of the existing Green Points established over the projects area.

Municipality/ Area	No. of Green Points established	Total no. of plastic bins (770 liter)	Total no. of steel cages (2000 liter)
Mo'ath Bin Jabal	12	31	4
Tabaqet Fahel	11	29	4
Sharhabeel Bin Hasna	6	14	3
Total	29	74	11

The women had collected around 63.3 tons since the start of June 2019 from the entire study area. Figure 5 shows the total waste amounts collected in the pilot project by women in June, July, August, September, and November 2019.

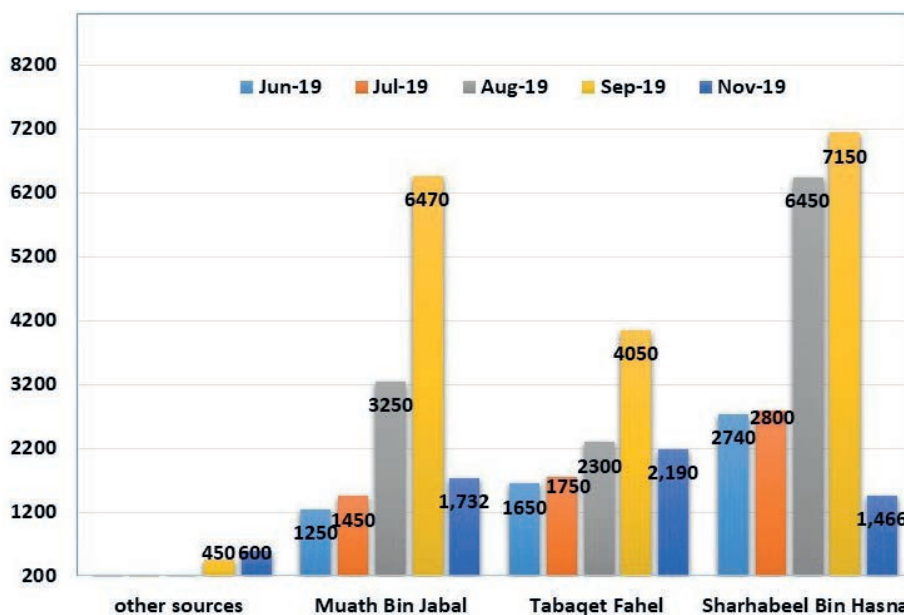
The proposed MRF lies within the Northern Shouneh district in Irbid Governorate at an existing old dumpsite (to be closed upon rehabilitation of the transfer station). The transfer station there is already serving many Municipalities, as a transfer station to other landfills where the number of served municipalities will decrease by the establishment of another transfer station at Al-Taybeh. The transfer station will continue working as a solid waste transfer facility. Added to that a sorting center (final sorting of solid waste) will be constructed. The project includes rehabilitation and upgrade existing facilities and construction of a new sorting center. This will decrease the delivery of waste to the landfill, and this will increase the lifetime of the destination landfill. It will be used to provide Livelihood opportunities, capacity building and proper training for more than 60 women and men from the local community to run such facility through collection, sorting and marketing. This station will serve as a final sorting facility of solid waste collected at the Green points from Mo'ath Bin Jabal, Tabaqet Fahel and Sharhabeel Bin Hasna. The site lies on a total area of 80 dunums, of which, 10 dunums will include the transfer station as well as the new intended Sorting Center. It must be noted that the location was used as solid waste

landfill for about 30 years. Officially is supposed to be closed, but, still used in many cases of breakage of vehicles.

Furthermore, through the aforementioned project, the feasibility and viability of establishing a briquettes production plant from organic, agricultural materials, as well as, paper and cardboards by women associations is to be evaluated, given its potential benefits to the community. It is estimated that approximately 3,500 tons of agricultural waste are generated annually. However, the proposed briquettes production unit shall have a design capacity of about 100 tons per year and will utilize the locally available agricultural waste, scrap wooden furniture and non-recyclable paper and cardboard as input materials for the plant.

Based on comprehensive assessment on the project scope of the recyclables quantities for each target municipality. The projected recyclables quantities assessment results are shown in Figure 6 for Sharhabeel Bin Hasna, Tabaqet Fahel and Mo'ath Bin Jabal municipality respectively.

As shown in Figure 6, Tabaqet Fahel municipality has the highest quantities of paper and cardboard and plastic with 1,757 tons and 2,576 tons in 2019 and 2029, respectively. Metal quantities is almost the same among all municipalities, where 384 tons, 390 tons and 377 tons is expected to be generated from Sharhabeel Bin Hasna, Tabaqet Fahel and Mo'ath Bin Jabal municipality, respectively in 2019, while the quantities are estimated as 565 tons, 573 tons and 550 tons in 2029 for the same municipalities, respectively. Glass quantities also represents the



**FIGURE 5:** Total waste amounts (kg) collected by women in in June, July, August and September 2019.

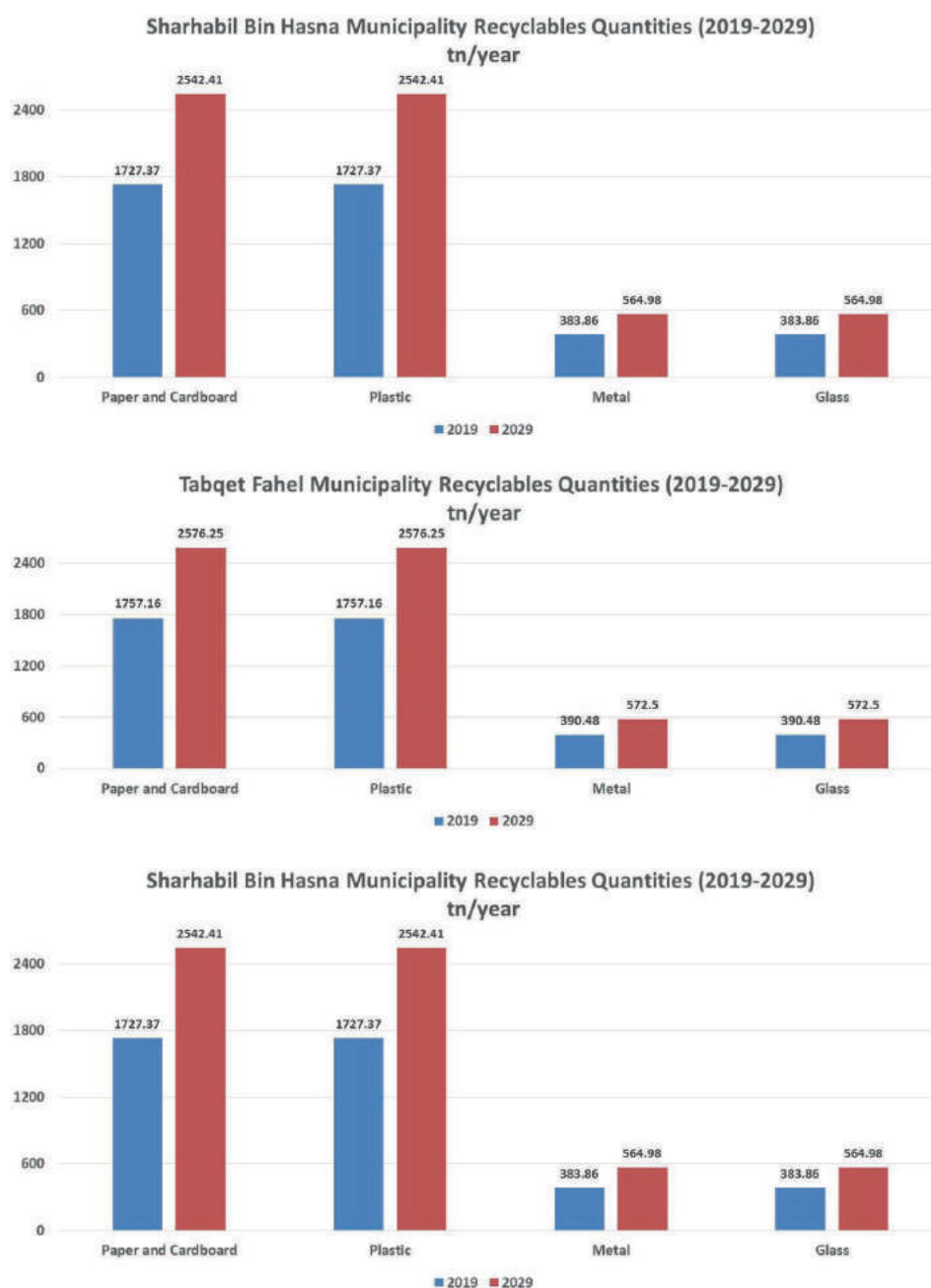


FIGURE 6: Potential quantities of collected recyclables in the three municipalities.

same amounts for the three municipalities with 384 tons, 391 tons and 377 tons are expected to be generated from Sharhabeel Bin Hasna, Tabaqet Fahel and Mo'ath Bin Jabal municipality in 2019, respectively, compared with 565 tons, 573 tons and 550 tons in 2029, respectively.

### 3.2 Establishment of umbrella cooperative

The participation of community based organizations (CBOs) in the recyclables collection scheme translated into livelihood opportunities for women in this mechanism. According to UNDP parallel project "Livelihoods Intervention" which aims to engage woman in the field of waste management and to generate employment opportunities within North Shouneh, a total of 20 full time positions (13

Green Points Operators, 7 Support Staff) and 13 part time positions (women for waste collection) are to be opened up to women in the communities to operate the community based Green Points (16 CBOs hosting Green Points in total), participating and innovating the collection of recyclables and ensuring their delivery into the designated bins located within their community. Figure 7 shows photography of different activities for the women engaged in the project. The location of the CBOs facilitate accessibility for the women workers, who are tasked with collecting recyclables from residential areas and turning them over to the Green Points.

The means for propelling the women participation and incentivizing collection of recyclables also take another



(a) Processing activities at the final sorting center



(b) Processing activities at the final sorting center



(c) Further waste sorting activities at the center



(d) Sorting of plastic according to the sub-categories



(e) Paper sorting and baling



(f) Scarp waste processing



(g) Further plastic sorting at the final recycling center



(h) Baling of steel/iron waste and aluminum





(i) On-job training activities for the women engaged in the project

**FIGURE 7 a-i:** Pictures of different activities for the women engaged in the project.

form: the establishment of an Umbrella Cooperative to coordinate efforts and manage the shares of accrued revenues from recycling operations, distributing monthly salaries through cooperative revenues and others as shares, as well as, designating funds in ways to additionally incentivize collection, pride in recyclables and SWM sector work and uplifting the communities. The Umbrella Cooperative also is a mean for the workers based at the CBOs, as well as, at the sorting station to gain shares in both the collection of recyclables and sorting station operations. This is of particular importance for the women who start their works at the sorting station. To ensure the sustainable operations of the sorting facility, during the first 4 years (2019 to 2022) the facility will employ 10 individuals (supervisors, operators, mechanics, etc., in addition to the women sorting workers). The number of employees will increase to 18 for the following 4 years (2023 to 2026), and to 22 for the following 3 years (2027 to 2029), reflecting increases in amounts of waste processed.

### 3.3 Female factor: Innovation and value-added contribution

The socio-economic context of Jordan is largely attributed as the driving fuel for women motivations to take part in employment opportunities that previously would not have been readily available to them. Particularly in the northern part of Jordan, women views on employment in the solid waste management activities can be summarized as of the following:

- Women in the northern Jordan would be willing to work in waste separation and recycling; guaranteed that suitable working conditions would be made available.
- Given women's primary household responsibility and chores, women and men may have different roles that are determined by the community, giving men the space of freedom in the public sphere, and leaving the private sphere to women.
- Women economic situation is a critical factor that affects society acceptance and support of economic participation the women in the solid waste activities by surpassing the set social norms. Despite the diversity

of opinions regarding what is culturally acceptable in terms of women in the workforce, the poor economic situation and the guarantee of a decent living drive women to work in any sector.

- Women economic activity can generally generate higher incomes for their families, as well as the possibility of becoming empowered decision makers.
- Women should be pioneers and manage the implementation of the project, but the participation of women in community decision-making on waste disposal is largely a missing element, requiring explicit facilitation by the employer and/or project.
- Raising awareness and training on the right mechanism of solid waste management are essential in achieving the desired project objectives. This cannot be effectively achieved without women taking part due to the fact that women are responsible for managing the household waste, and are the primary actors in reusing solid waste (proximate experts).
- There are many challenges facing women working in the solid waste sector which include socio-cultural factors related to gender roles, norms and stereotypes, in addition to the subjective and economic factors which are relevant to rewards of this activity.

While these characteristics can be obstacles to increasing women inclusion in the workforce, there are some opportunities to promote skilled labor that draws a connection to traditional roles and translating them into meaningful, skilled work in the solid waste sector. Specifically, as women are positioned at the helm of deciding what items are purchased; and how, what, and when they are discarded.

Globally, 70-80% of all consumer purchases are driven by women, through a combination of their purchasing power and influence. When it comes to typical household items that will eventually make their way to the curb for recycling, the purchasing power is even higher. In addition, since women generally make up the majority of municipal service users, hence, this makes them the ideal beneficiaries of solid waste management projects, because they usually provide improvement for services, a higher priority than men (Asi et al., 2013).

Previous and ongoing projects in Jordan have offered the women the role to lead associations for recyclables collection at the household level, which are subsequently collected and sorted at the municipal level. In return this offers economic and employment opportunities for women in Jordan. Moreover, as a central component to current and future projects in the solid waste management, women are determined to be proximate experts since they are capable of contributing to this sector improvement from the bottom-up.

### 3.4 Other cross cutting SWM projects and women empowerment

UNDP's "Community Based Composting to Convert Manure Waste to Resource and Create Livelihood Opportunities", implemented by Future Pioneers in Empowering Communities (FPEC), which aims to create job opportunities through compost production paired with a formidable business model. To date, the project has established a packaging facility at Al Khaldyeh women society. The compost packaging operations employ 16 women on a part-time basis.

Started in 2017, a GIZ funded project titled "Waste to positive Energy" and conducted by international NGO Action Against Hunger (ACF) in Jordan, has helped around 1,194 vulnerable individuals (550 women) around Irbid on a 50-day-fixed-term contract, where they collected and sorted waste through cleaning campaigns in the local area, later turning them into salable items to increase theirs and their families' livelihood.

For example, under GIZ's "Cash for Work" initiative, encompassed within the project entitled "Supervising the Commissioning of Composting and Sorting Plants, Their Operation, and the Marketing of Recycled Products and Compost by Municipalities" women are targeted along with Syrians and youth as so-called vulnerable groups. One of the objectives of the project is to develop a participatory system to establish labor intensive materials recovery and processing systems (sorting and recycling stations as well as composting sites) to create income generation for these vulnerable groups. It was envisioned that community groups be trained to conduct public awareness activities and increase the acceptance and public respectability of SWM activities. The project is underway in the municipalities of Greater Irbid, West Irbid, Al-Wassatya, Al-Taybeh, Greater Mafrq, Deir-Alla, Greater Madaba and Al-Karak.

Through GIZ's Cash for Work initiative, the following jobs figures were achieved (Roy and Schmid, 2018):

- 16,723 vulnerable Jordanians and Syrian refugees (22.6% women) were employed - Direct partnership with 9 municipalities construction of recycling and composting facilities throughout 2016-2017,
- 790 vulnerable Jordanians and Syrian refugees were employed outside the camps, and 4059 refugees took part in inside the camps.

Oxfam project also utilized the Cash for Work incentive program. In this case, the setting was the Zaatari Camp in

the Mafrq Governorate where Cash for Work workers collected wastes while encouraging households to separate their dry wastes. Thus, by covering about 18% of the working age population in Zaatari, this becomes as an integral part of people survival and livelihoods strategy (OXFAM, 2017). The initiative gave an advocacy role to female Syrian Refugee workers. Approximately, 200 workers (30% women and 70% men) educate the community on recycling, collect recyclable materials from households, and process the waste into materials that can be sold to traders (UNHCR, 2017). Saidan et al. (2017) investigated the potential solid waste recycling in the camp, and proposed a feasible recycling model based on the recyclables market prices in Jordan (Saidan et al., 2017b). However, 4,237 tons of recyclables can be collected per year (over three folds of what is collected currently) with massive expansion of the existing recycling program the project will come closer to covering its running costs (OXFMA, 2017).

The projects mentioned above largely incorporate women into administrative roles and have attempted to avoid the labor- or operations-related work. In contrast, when NGOs and CBOs are directly involved, there has been more opportunity to engage women in employment on another level, as NGOs/CBOs can offer sustained services, such as providing a babysitter or coordinated carpooling, that are tailored to women who have dual roles: household and workplace responsibilities. Additionally, in either case, creating a workplace wherein segregated work spaces can be provided (in certain regions this aspect becomes more important) depending on the type of work required (physical – segregated; administrative – integration is acceptable).

### 3.5 Incentive mechanism

The direct incentives will include "cash for trash" scheme; the scheme will be designed based on points credit system whereby participating residents are encouraged to deposit their recyclable waste at the nearest Green Point in exchange for credit.

The waste deposited by the participating residents will be weighed by the employees of the supervising CBO, who will be trained on the required technology that will transfer the assigned credit to each participant based on graweight, type of recyclable, prevailing market price, as well as, on how to process credit transactions. As part of a digitized and periodically audited system that connects the local Green Points, Umbrella Cooperative, Military/Civil Consumers Cooperative, and Sorting Facility, each bale of waste generated from participating residents will need to be tagged with the appropriate serial number. This is to identify the exact amount of waste deposited by residents and weighed by CBOs.

Initial calculations illustrate that the amount allocated to reimburse participating residents might not be relatively competitive enough to incentivize broad communal participation and the depositing of average household waste volumes. It is therefore crucial to highlight that the success of this aspect of the project will depend in great part on the active participation of a minority of residents who will be able to deposit voluminous amounts of waste, as well as,

the participation of the CBOs' part-time collection workers, who will be reimbursed according to the amount and type of waste they collect.

This incentive mechanism has yet to connect the benefits and revenues of the recycling operations to the larger community. As the establishment of Green Points and their operations are conducted by a select number of women and local CBOs, this represents an opportunity for the CBOs to promote the recycling activities. CBOs could use their new involvement with the community to survey their (the community) ideas for small-scale projects to improve public spaces, host public events, and/or other activities upon discretion of the community. The local CBOs would then pitch the projects to the Umbrella Cooperative that would have a cache of funds from project revenues to facilitate small-scale community improvement/cohesion projects.

#### 4. CONCLUSIONS

As exemplified in this study, projects implemented by international organizations are institutionalizing a trickle-down effect, making women roles as core aspects of their projects in the solid waste management. Even though these positions are small in their number or in the scope of the women responsibilities, as cultural norms have a preference for segregated workstations as well as labor that avoids direct contact with collection points on the street (i.e. dumpsters, etc.), the economic pressure that confronts these women and their families has led to them looking for employment opportunities. In turn, this has given project implementers the opportunity to expand projects that bridge the needs of the solid waste sector with the needs of local, vulnerable households in Jordan. Women taking the lead as proximate experts has yet to fully take shape on the ground, yet project implementers are strategizing for the successful integration of women in such roles of responsibility, in which they coordinate and mobilize communities around the interests of improving solid waste management at the local level.

#### ACKNOWLEDGMENT

The authors in general, and GreenPlans for Environment Co. authors, are grateful for the support and facilitation received from United Nation Development Program (UNDP), GIZ, and OXFAM.

#### REFERENCES

- Aboelnga, H., Saidan, M., Al-Weshah, R., Sturm, M., Ribbe, L., Frechen, F.B., 2018. Component analysis for optimal leakage management in Madaba, Jordan. *J. Water Supply Res. T.* 67(4): 384-396
- Ahmed, S., Ali, M., 2004. Partnerships for solid waste management in developing countries: linking theories to realities. *Habitat Int.* 28: 467-479
- Al-Addous, M., Saidan, M.N., Bdour, M., et al., 2019. Evaluation of Biogas Production from the Co-Digestion of Municipal Food Waste and Wastewater Sludge at Refugee Camps Using an Automated Methane Potential Test System. *Energies* 12(1): 1-11
- Al-Addous, M., Saidan, M.N., Bdour, M., et al., 2020. Key aspects and feasibility assessment of a proposed wind farm in Jordan. *International Journal of Low-Carbon Technologies*, doi:10.1093/ijlct/ctz062
- Al-Awad, T.K., Saidan, M.N., Gareau, B.J., 2018. Halon management and ozone-depleting substances control in Jordan. *International Environmental Agreements: Politics, Law and Economics* 18(3): 391-408
- Aldayyat, E., Saidan, M.N., Abu Saleh, M.A., Hamdan, S., Linton, C., 2019. Solid Waste Management in Jordan: Impacts and Analysis. *J Chem Technol Metall* 54(2): 454-462
- Al-Hamamre, Z., Saidan, M., Hararah, M., et al., 2017. Wastes and biomass materials as sustainable-renewable energy resources for Jordan. *Renewable Sustainable Energy Reviews* 67: 295-314
- Al Kharouf, Al-Jribia, 2016. The Evolution of Women's Political Participation in Various Public Offices in Jordan
- Almasi, A., Mohammadib, M., Azizi, A., Berizi, Z., Shamsi, K., Shahbazi A., Mosavi S.A., 2019. Assessing the knowledge, attitude and practice of the kermanshahi women towards reducing, recycling and reusing of municipal solid waste. *Resources, Conservation and Recycling* 14: 329-338
- Alrabie, K., Saidan, M.N., 2018. A preliminary solar-hydrogen system for Jordan: impacts assessment and scenarios analysis. *International Journal of Hydrogen Energy* 43(19): 9211-9223
- Asi, E., Busch, G., Nkengla, L., 2013. The Evolving Role of Women in Sustainable Waste Management in Developing Countries – A Proactive Perspective?. *National Conference on Integrated Waste Management and Green Energy Engineering*. April 15-16
- Bench, M., Woodard, R., Harder, M., Stantzos, N., 2005. Waste minimization: home digestion trials of biodegradable waste. *Resour. Conserv. Recycl.* 45: 84-94
- Bernad-Beltran, D., Simo, A., Bovea, M.D., 2014. Attitude towards the incorporation of the selective collection of biowaste in a municipal solid waste management system. A case study. *Waste Manage.* 34: 2434-2444
- Bhawal Mukherji, S., Sekiyama, M., Mino, T., Chaturvedi, B., 2016. Resident knowledge and willingness to engage in waste management in Delhi, India. *Sustainability* 8 (10): 1065
- Ezebilo, E.E., 2013. Willingness to pay for improved residential waste management in a developing country. *Int. J. Environ. Sci. Technol.* 10: 413-422
- GTZ, 2005. Private Sector Involvement in Solid Waste Management-Avoiding Problems and Building on Successes. *Deutsche Gesellschaft für Technische Zusammenarbeit (GTZ) GmbH, Eschborn, Germany*
- Ibanez Prieto, A., 2018. Women Rights Movement Hails Unprecedented Number of Women in Government. *The Jordan Times*. <http://www.jordantimes.com/news/local/women-rights-movement-hails-unprecedented-number-women-government> (accessed on 10 October 2019)
- Iyer, E.S., Kashyap, R.K., 2007. Consumer recycling: role of incentives, information, and social class. *J. Consum. Behav.* 6: 32-47. <https://doi.org/10.1002/cb>
- Jabr, G., Saidan, M., Al-Hmoud, N., 2019. Phosphorus Recovery by Struvite Formation from Al Samra Municipal Wastewater Treatment Plant in Jordan. *Desalination and Water Treatment*, doi: 10.5004/dwt.2019.23608
- Khasawneh, H., Saidan, M., Al-Addous, M., 2019. Utilization of hydrogen as clean energy resource in chlor-alkali process. *Energy Exploration & Exploitation* 37(3): 1053-1072
- Laor, P., Suma, Y., Keawdounlek, V., Hongtong, A., Apidechkul, T., Pasukphun, N., 2018. Knowledge, attitude and practice of municipal solid waste management among highland residents in Northern Thailand. *J. Health Res.* 32 (2): 123-131
- Malkawi, K., 2015. Refugees constitute third of Jordan population – World Bank Official. *The Jordan Times*, Jordan
- Mehra, R., Du, T., Nghia, N., Lam, N., Chuyen, T., Tuan, B., Tran, P., Nhan, N., 1996. Women in waste collection and recycling in Ho Chi Minh city. *Popul. Environ.* 18: 187-199
- Ministry of Municipal Affairs (MoMA), 2015. Development of a National Strategy to Improve the Municipal Solid Waste Management Sector in the Hashemite Kingdom of Jordan. Amman, Jordan
- Ministry of Water & Irrigation, MWI, 2015. National Water Strategy 2016-2025, Amman, Jordan
- Moh, Y., 2017. Solid waste management transformation and future challenges of source separation and recycling practice in Malaysia. *Resour. Conserv. Recycl.* 116: 1-14
- OXFAM, 2017) TRASH TALK- Turning waste into work in Jordan's Za'atari refugee camp. *Oxfam Discussion Papers*. Oxfam International August 2017

- Saidan, M.N., Ansur, L.M., Saidan, H., 2017a. Management of Plastic Bags Waste: An Assessment of Scenarios in Jordan. *J. Chem. Technol. Metall.* 52 (1): 148–154.
- Saidan, M.N., Abu Draiss, A., Al-Manaseer, E., 2017b. Solid waste composition analysis and recycling evaluation: Zaatari Syrian Refugees Camp, Jordan. *Waste Manage.* 61:58–66.
- Saidan, M.N., Al-Yazjeen, H., Abdalla, A. et al., 2018. Assessment of on-site treatment process of institutional building's wastewater. *Processes* 6(4):1-13
- Saidan, M.N., 2019. Cross-sectional survey of non-hazardous waste composition and quantities in industrial sector and potential recycling in Jordan. *Environ. Nanotechnol. Monit. Manage.* 12:100227
- Saidan, M., Khasawneh, H.J., Aboelnga, H., Meric, S., Kalavrouziotis, I., Hayek, B.O., Al-Momany, S., Al Malla, M., Porro, J.C., 2019. Baseline carbon emission assessment in water utilities in Jordan using ECAM tool. Baseline carbon emission assessment in water utilities in Jordan using ECAM tool. *J Water Supply Res T.* 68:460–73
- Saidan, M.N., Abu Draiss, A., Linton, C. et al., 2020. Solid Waste Characterization and Recycling in Syrian Refugees Hosting Communities in Jordan. In: Negm AM and Noama E (eds) *Waste Management in MENA Regions*, Earth and Environmental Sciences Series, Applied Environmental Science and Engineering for a Sustainable Future, Springer International Publishing AG, part of Springer Nature
- Saphores, J., Nixon, H., Ogunseitan, O., Shapiro, A., 2006. Household willingness to recycle electronic waste – an application to California. *Environ. Behav.* 38:183-208
- Schwab, K., Sala-i-Martin, X., 2017. *The Global Competitiveness Report 2017 – 2018*. World Economic Forum
- Roy, N., Schmid, L., 2018. Labour-Intensive Cash for Work Measures and Structured Employment Promotion for Refugees and Vulnerable Groups. GIZ Jordan, 17<sup>th</sup> May, 2018 UNHCR
- Tarawneh, A., Saidan, M., 2013. Households awareness, behaviors, and willingness to participate in E-waste management in Jordan. *Int J Ecosys* 3(5): 124-131
- The World Bank, 2017. *Progress Towards Gender Equality in the Middle East and North Africa Region: A descriptive note on progress and gaps towards gender equality and women's empowerment in the MNA region*, produced to provide the situational context to the World Bank Group's Regional Action Plan (RGAP) FY18-23
- UNDP, 2015. *Socio-economic Inequality in Jordan*. Amman, Jordan
- UNHCR, 2017. *Cash for Work in Za'atari Camp. Basic Needs and Livelihoods Working Group*. April 2017. <http://reliefweb.int/sites/reliefweb.int/files/resources/April2017CfWfactsheet.pdf>

Extra contents  
**COLUMNS AND SPECIAL CONTENTS**



## BOOKS REVIEW



### Ecotoxicology

Edited by  
Elisabeth Gross and Jeanne Garric

*New Challenges and New Approaches*

ISTE  
PRESS



### ECOTOXICOLOGY, NEW CHALLENGES AND NEW APPROACHES

Edited by Elisabeth Gross and Jeanne Garric

Ecotoxicology is a relatively young field resulting initially from a series of studies concerning pollution accidents affecting humans and the environment in the 1950s. At the same times, there was the birth of the concept of chemical ecology. Both fields have a somewhat different focus, yet they have more in common than just the prefix “eco”. Both look at the impact of compounds on organisms; while ecotoxicology focuses mainly on anthropogenic pollutants, chemical ecology concentrates on natural metabolites produced by certain species and affecting others.

The main idea behind the book, which consists of 6 chapters by different authors, is to highlight current challenges and emerging approaches in ecotoxicology. One of the most important challenges is the better inclusion of

chemical ecology in ecotoxicology.

The individual chapters are diverse in their focus on different aspects, but they all aim to highlight the complexity of situations under which pollutants act at different levels of organisms in our ecosystems.

The book starts with a broad introduction to the different as well as complementary views of the fields of chemical ecology and ecotoxicology, both developed as independent research fields since the late 1950s. The first chapter continues with the following topics: the chemical ecology of aquatic and terrestrial habitats; the impact of selected pollutants on allelochemical interactions; the current knowledge in the chemical ecology of natural biocides; the use of chemical ecology response factors as alternate endpoints in ecotoxicology

The second chapter outlines the different questions of intra- and interspecific variability of tolerance, or cross-tolerance to pollutants. The ability of many different aquatic organisms to cope with the chemical stress resulting from many different toxic contaminants is here discussed. Besides, substantial developments are analysed, considering the mechanisms responsible for such tolerance as well as the ecological consequences, including operational aspects for environmental risk assessments and biomonitoring.

In the third chapter, it is shown how cyanobacterial toxins and selected pollutants differentially affect native and alien mussels.

In the fourth chapter, the authors provide a detailed overview of the interaction of individual and co-infections by parasites with pollutant effects on aquatic organisms. Here, the parasites are introduced as confounding factors that can influence the uptake, retention and bioaccumulation of contaminants and biomarker responses. Thus, the interaction between chemical stressors and parasites could have serious implications for environmental monitoring studies.

In the fifth chapter, the book presents an overview of the distribution, fate and behaviour of microplastics in the aquatic environment, and the interactions as well as the potential toxicity of plastic particles towards the aquatic biota through laboratory and field studies.

In the sixth chapter, “Omics” technologies, such as genomics, transcriptomics, proteomics and metabolomics, are presented. These techniques can offer a better view of the mechanisms of toxicity of certain pollutants, and provide an overview of the effects on physiological processes that are affected.

In summary, there is a wealth of information within the covers of this book on how new approaches can be ap-



plied to better investigate the effects of pollutants in the ecosystem. I am personally convinced that the reading of the book will instil in the reader a different point of view on facing the field of potential environmental pollution from waste treatment plants. Therefore, the book represents a useful reference for professionals (researchers, managers, engineers) working into this field.

Alberto Pivato  
DICEA, Civic, Environmental and Architectural Engineering,  
University of Padova, Italy  
e-mail: alberto.pivato@unipd.it

## ABOUT THE EDITORS

### Elisabeth Gross

*Elisabeth Gross is a specialist in aquatic chemical ecology. After a PhD at MPI Limnology, Germany, and a postdoc at*

*Cornell University, USA, she joined Konstanz University, Germany, and is now Professor for ecotoxicology at LIEC, University of Lorraine, France.*

### Jeanne Garric

*Jeanne Garric is the Head of research at IRSTEA (National Research Institute of Science and Technology for Environment and Agriculture), with an expertise in ecotoxicology. She obtained the Legion of Honour in 2013 for her whole scientific career and her role in the emergence of ecotoxicology.*

### Book Info:

*Editors: Elisabeth Gross, Jeanne Garric*

*Imprint: ISTE Press - Elsevier*

*Year of publication: 2020*

*Page Count: 224*

*Paperback ISBN: 9781785483141*



## ENVIRONMENTAL FORENSICS

### ENVIRONMENTAL FORENSICS: THE WHAT? WHEN? WHERE? WHY? AND HOW?

The term “environmental forensics” has been in explicit use in scientific literature since 1994. McGee and Block (1994) - the earliest article noticed in literature to use the term “environmental forensics” – discussed the failure of environmental forensics to emerge as a discipline. Rusk (1996) presented environmental forensics as a mechanism for technical support to complex, controversial and high stakes environmental litigation. The emergence of environmental forensics as an important area of study can be attributed to the Comprehensive Environmental Response, Compensation and Liability Act (CERCLA) or Superfund legislation of the United States of America that made the polluters pay for their role in pollution since the 80’s (Varghese and Alappat, 2012). Identifying the source(s) of pollution and providing a technical framework for allocating the responsibility among the polluter(s) using scientific methods were understood to be the fundamental purposes of the field of environmental forensics in the initial years of the field’s evolution.

But pollution crimes, such as the illegal emission or discharge of substances into air, water or soil, form only a part of the larger spectrum of environmental crimes, including, for example: the illegal trade in wildlife, illegal trade in ozone-depleting substances, illegal transport, shipment or dumping of waste.

INTERPOL has identified environmental crime as a growing international crime area having an extremely detrimental impact on the planet, biodiversity, the global economy and human life. A 2016 INTERPOL report estimates the position of environmental crime as the fourth largest crime in the world (91–258 billion USD) after drug trafficking (344 billion USD), counterfeit crimes (288 billion USD) and human trafficking (157 billion USD), by value (Nellemann et al., 2016). This calls for extensive use of science and technology in combating environmental crimes, yet this type of crime is commonly overlooked in terms of investment. Environmental forensics, being the area primarily looked upon for technical solutions to environmental crimes, needs to widen its scope to address the expanding realm of environmental crimes. Further, there is a need to foster more research in the area of environmental forensics to respond to the evolving challenges.

Given the requirement of expanding its scope, there is a need to modify the traditional definition of environmental forensics, which primarily addressed pollution crimes. In the new context environmental forensics may be defined as “a multidisciplinary science which aims to apply scien-

tific methods and knowledge to the diverse range of environmental concerns in the context of a regulatory and legal framework”. This definition goes beyond the identification of the source and age of a contaminant which has been used to describe environmental forensics in the past (Morrison and Murphy, 2005).

Despite the importance of the subject, to the knowledge of the authors only one indexed journal, “Environmental Forensics” published by Taylor & Francis, exists in this field. There is an urgent need to augment the publication avenues in the field of environmental forensics, which the ‘Detritus Journal’ plans to meet, at least partially. With reference to the aims of Detritus Journal, the following topics will be included: illegal waste trafficking, illegal landfills, misclassified waste streams, release of contaminants in terror threats, oil spill identification, crime scene investigation techniques, detection and identification of particular contaminants, wildlife crime, emerging pollutants and the methods for their detection, the role of the public in environmental forensics, case studies, historical environmental crimes and, the fate & transport of pollutants.

Finally, from a scientific point of view, it is worth mentioning the parallelism between the scientific approach and the forensic approach graphically represented in Figure 1. In the latter, the phase of the experiment designing is replaced by the use of the well known “Six W’s of Investigation” (what, where, who, when, why and how).

As an example, we can refer to a pollution crime represented by an uncontrolled leachate leakage from an old landfill. As environmental technical experts, we can apply an investigation approach that schematically includes a modelling phase of the transport of leachate from the source to the groundwater and a collection and interpretation phase of the monitoring data of a long time period (leachate quality and quantity, groundwater quality, etc.).

By this approach, we can try to answer technically the “Six Ws”:

**WHAT:** Can we identify a conceptual model of the event including the fundamental elements of source-fate and transport-target? Which are the chemicals (heavy metals, ammonia, organics, etc.) that can affect the groundwater when they are released from the landfill to the environment?

**WHERE:** Can we identify the extent of the pollution in groundwater?

**WHO:** Can we identify the source of pollution beyond a reasonable doubt among the potential sources (industrial areas, agriculture activities, etc.)

**WHEN:** Can we identify when the pollution occurred and how long it lasted?

## SCIENTIFIC APPROACH

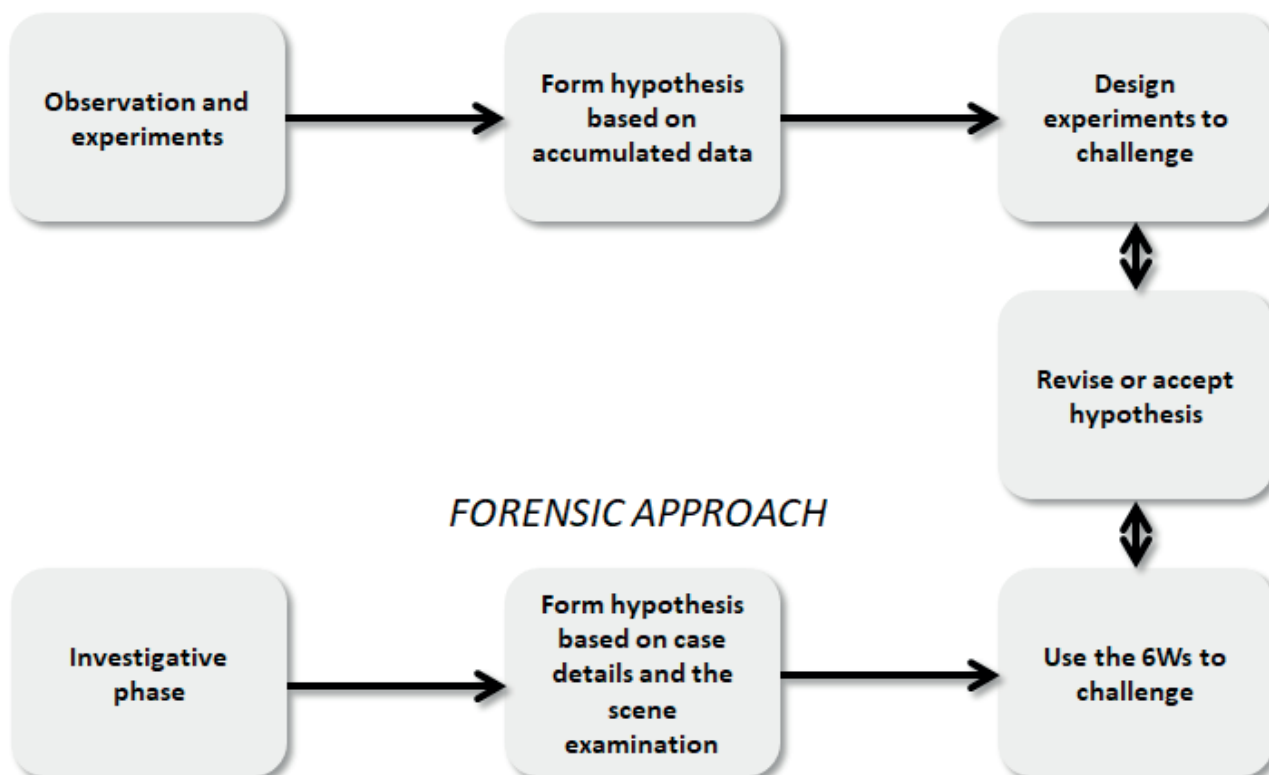


FIGURE 1: The similitude between the scientific and the forensic approach.

WHY: This is a matter for the judiciary to decide.

HOW: These are the processes that influence the fate and the transport of chemicals in the environment.

In summary, environmental forensics represents an important but often overlooked part of the criminal justice system. The breadth of different environmental crime types is such that a diverse range of approaches are required to investigate them. These multidisciplinary approaches originate from all science disciplines and bring together environmental science and forensic science techniques for the purposes of combating crimes to the environment.

Alberto Pivato, *University of Padova (IT)*  
alberto.pivato@unipd.it

Claire Gwinnett, *Staffordshire University (UK)*  
C.Gwinnett@staffs.ac.uk

GeorgeVarghese, *NIT Calicut, Kozhikode (IN)*  
gkv@nitc.ac.in

## REFERENCES

- McGee, Robert W. and Walter E. Block. 1994. Pollution Trading Permits as a form of market socialism and the search for a real market solution to Environmental Pollution. *Fordham Environmental Law Journal* 6: 51-77
- Morrison, R. D and Murphy, B. L. 2005. *Environmental Forensics: Contaminant Specific Guide*. Academic Press. <https://doi.org/10.1016/B978-0-12-507751-4.X5021-6>
- Rusk, G. A. 1996. Environmental forensics: Technical support of complex environmental litigation. In *Hazardous and Industrial Wastes: Proceedings of the Twenty-Eighth Mid-Atlantic Industrial and Hazardous Waste Conference*, ed. A. Scott Weber, 760-774. Basel, Switzerland: Technomic Pub Co.
- Nellemann, C. (Editor in Chief); Henriksen, R., Kreilhuber, A., Stewart, D., Kotsoyova, M., Raxter, P., Mrema, E., and Barrat, S. (Eds). 2016. *The Rise of Environmental Crime – A Growing Threat to Natural Resources Peace, Development and Security*. A UNEPINTERPOL Rapid Response Assessment. United Nations Environment Programme and RHIPTO Rapid Response–Norwegian Center for Global Analyses, [www.rhipto.org](http://www.rhipto.org)
- Varghese, G. K. & Babu J. Alappat (2012) National Green Tribunal Act: A Harbinger for the Development of Environmental Forensics in India?, *Environmental Forensics*, 13:3, 209-215, DOI: 10.1080/15275922.2012.702330

Info from the global world

## THE SOURCE OF WASTE AND THE END OF WASTE: COVID-19, CLIMATE, AND THE FAILURE OF INDIVIDUAL ACTION

Marc Kalina

University of KwaZulu-Natal, South Africa; email: [marc.kalina@gmail.com](mailto:marc.kalina@gmail.com)

---

After COVID 19, time to have a specific column on developing countries is over: the pandemic highlighted - if ever necessary - the need to think as a whole.

The new corner called "Info from the global world" wants to collect thoughts and impressions from different parts of the world, with the aim of promoting cultural intersections on issues affecting circular waste management, environmental protection and human health. We will discuss how gender inequality and environmental racism can also be combated through truly sustainable waste management and how the circular economy and Sustainable Developing Goals can contribute to worsening already precarious situations.

The first issue concerns COVID19, supplementary article to the editorial of this first issue of Detritus after the start of the global health emergency.

Maria Cristina Lavagnolo, University of Padova, Italy

---

The Covid-19/Coronavirus pandemic, which has gripped the globe for the first half of 2020, has patently demonstrated the fallacy of emphasising the role of individual action as a determinant step in addressing our waste and climate change challenges. Throughout the first half of 2020, as states across the globe have enforced lockdowns, quarantines, and stay-at home orders, individuals have retreated: into themselves, as social connections grow distant, and from public space into private, domestic life. On a societal level, we have witnessed a collective experiment to determine how much any one person can do to reduce their level of consumption and individual carbon footprint: no air travel and severely curtailed travel by car; shuttered shops and malls leading to fewer purchases; restaurants and entertained venues closed, driving individuals to creative ways to entertain and feed themselves within their homes, and; renewed interest in urban farming and household food production, etc. Yet, although these actions have all surely added up, and carbon emissions have visibly dipped (see (UNEP, 2019), it has not been enough.

The Covid-19 pandemic has revealed the true depths of our climate crisis, and has starkly illustrated the changes necessary to correct our catastrophic trajectory. Of course, the pandemic has been accompanied with positive environmental impacts. Though many of the fantastic stories of ecological regeneration and renewal that have circulated on social media have proven to be fabrications or wishful thinking (and have often carried less than subtle eco-fascist tones, as well), the air quality impacts of stay-at-home orders in major cities, for instance, have been very real,

and for residents, highly visible (see (Chen et al., 2020)). Nonetheless, despite the radical changes that many individuals across the globe have accepted to their lives and livelihoods, which have collectively forestalled hundreds of millions of tonnes of CO<sub>2</sub> emissions, these individual efforts will not be enough to prevent further global heating. A 2019 report by the UNEP paints this picture unambiguously. According to models based on current carbon-cutting pledged, they estimate that we can expect a potentially disastrous 3.2oC rise in global temperatures over pre-industrial levels by 2030 (UNEP, 2019). To achieve a moderate and hopefully more manageable, warming rate of only 1.5o they estimate that total annual emissions would need to be cut by 7.6%.

And yet....

Despite this knowledge, the numerous existing carbon reduction agreements in place, and the historically unprecedented impact of the Covid-19 pandemic, analysis by Carbon Brief (2020) suggests global emissions for 2020 are only expected to drop by approximately 5.5%. This sharply reveals the limits of individual action. Travelling less helps, but not enough to make a difference. Differences in purchasing, consumption, and choice, limited without our current crisis, have not been enough to meaningfully shift the climate change equation. There is of course nuance to the data. For instance, a 5.5% reduction is preferable to the likely increase in total annual carbon dioxide emissions we would be facing in a normal year, and keeps us further from the more precarious consequences of a 2o or

30 increase. However, these are near-impossible choices to have to make, and in a time of such overwhelming hardship and grief for so many across the globe, society must be driven to think bigger, and do better. As Valentine (2020) observed, individuals are currently doing about as much as you could reasonably ask from them, and it has not been enough. Individual action is not the solution to our climate crisis and it will not be the solution to our waste crisis.

Waste management academic discourse has historically centred on the role of individual agency within our interrelated waste and crises. For instance, a brief literature search reveals multiple authors linking increased personal consumption (often within nations in the Global South) to the creation of unprecedented amounts of waste, inundating our rivers and oceans with plastic (see (Sanni, 2019; Van Rensburg et al., 2020; Zambrano-Monserrate & Ruano, 2020)). However, often, within these narratives, individual action is also presented as the panacea, through sustainable choice and switching to multiple-use products, the consumer is presented as both the cause and the solution to waste (see (Cohen, 2017; Moss, 2018; Willis et al., 2019)). Likewise, individuals have also often been represented as the linchpin around which our waste management systems turn. We may be the cause of waste, but if we source separate, reuse, and recycle we can all become cogs in a more circular economy (Bernstad, 2014; Khattab & El Hagggar, 2016; Roustia et al., 2016; Zoroufchi Benis et al., 2019). This outlook has also become entrenched at the intersection between waste and climate change. By choosing to go 'zero waste' we can each reduce our individual carbon footprint, and do our part to combat climate change (see (Korst, 2012; Song et al., 2015; Wunsch & Simon, 2018)). Within these narratives, the individual has become both the problem and the solution: the source of waste and the 'end of waste'; the protagonist, antagonist, and deus ex machina of the climate change story. This observation is not meant to cynically detract from the power of the individual as a force for positive change. Moreover, we should be sceptical of any attempt to deny agency to any community, particularly the most marginalised and vulnerable. However, by shifting responsibility to the individual, we fundamentally ignore the systemic, socio-economic, and socio-political conditions that have created, and continue to create, our interrelated waste and climate problems. While small steps are important, and studies which centre individual action certainly remain interesting or potentially illuminating, they are, as Tallie (2020) points out, inherently non-transformative. Rather they tend to individualise responsibility for ecological failure instead of pointing to the large structural oppressions of global capitalism.

Others within our field have, within recent years, tried to widen the scope of analysis to account for the systemic factors driving waste creation and management globally. For instance, Doeland (2019) has alluded to the danger of 'zero waste' narratives normalising and stigmatising unsustainable capitalist consumption, while Hawkins (2019) and Loibron (2014) have written on disposability as a fundamental (in-disposable), component of modern capitalist economies. Moreover, within the context of Covid-19, Kalina and Tilley (2020) have discussed the in-

herent structural inequalities within waste management systems globally, which have, and will continue to, shape different nations' ability to respond to the pandemic. I myself, have advocated for a return to Marxist analytics within waste management discourses, in order to foster greater critical engagement with class and capitalist production and accumulation, as the principal barrier to access for waste management services, and the root cause of waste, respectively (Kalina, 2020). However, although these modes of analysis have begun to gain traction within waste management discourses, it has taken a crisis to emphasise the urgent need for broad-based, systemic socio-economic change. Meaningful change can only be structural change, and as academics, we must adjust the focus of our analyses towards informing a more just transition.

## REFERENCES

- Bernstad, Anna. (2014). Household food waste separation behavior and the importance of convenience. *Waste Management*, 34(7), 1317-1323. doi: <https://doi.org/10.1016/j.wasman.2014.03.013>
- Brief, Carbon. (2020). Analysis: Coronavirus set to cause largest ever annual fall in CO2 emissions. In S. Evans (Ed.), *Global Emissions: Carbon Brief*.
- Chen, Kai, Wang, Meng, Huang, Conghong, Kinney, Patrick L., & Paul, Anastas T. (2020). Air Pollution Reduction and Mortality Benefit during the COVID-19 Outbreak in China. *medRxiv*, 2020.2003.2023.20039842. doi: 10.1101/2020.03.23.20039842
- Cohen, Steven. (2017). Understanding the Sustainable Lifestyle. *The European Financial Review*, 7-9.
- Doeland, L. (2019). LETTING REMAINDERS GET STUCK IN OUR THROATS. *Detritus*, 7, 1-3.
- Hawkins, G. (2019). Disposability. *Discard Studies*.
- Kalina, M. (2020). TREATING THE SYMPTOM? A MARXIST REFLECTION ON 'ZERO WASTE' AND SARDINIA 2019 SYMPOSIUM. *Detritus*, 9, 4-10.
- Kalina, Marc, & Tilley, Elizabeth. (2020). "This is our next problem": Cleaning up from the COVID-19 response. *Waste management*, 108, 202-205. doi: <https://doi.org/10.1016/j.wasman.2020.05.006>
- Khattab, Mianda, & El Hagggar, Salah. (2016). Beyond Zero Waste Concept: A Revolution for Sustainable Community. *Int. J. of Sustainable Water & Environmental Systems*, 8(1), 13-19.
- Korst, A. (2012). *The Zero-Waste Lifestyle: Live Well by Throwing Away Less*. Berkeley, CA: Ten Speed Press.
- Loibron, M. (2014). Modern Waste as an Economic Strategy. Retrieved from <https://discardstudies.com/2014/07/09/modern-waste-is-an-economic-strategy/>
- Moss, Steve. (2018). Striving for a low-waste lifestyle. *MRS Bulletin*, 43(7), 559-560. doi: 10.1557/mrs.2018.174
- Roustia, Kamran, Bolton, Kim, & Dahlén, Lisa. (2016). A Procedure to Transform Recycling Behavior for Source Separation of Household Waste. *Recycling*, 1(1), 147-165.
- Sanni, Lukman Oladimeji. (2019). Environmental Impact of Sachet Water Consumption in Saki Town, Oyo State, Nigeria.
- Song, Guobao, Li, Mingjing, Semakula, Henry Musoke, & Zhang, Shushen. (2015). Food consumption and waste and the embedded carbon, water and ecological footprints of households in China. *Science of the Total Environment*, 529, 191-197.
- Tallie, T.J. (2020). Facebook Comment, in response to Geoff Williams. Facebook. [https://web.facebook.com/ttallie/posts/10107582158645124?comment\\_id=10107582568239294&notif\\_id=1589999150128095&notif\\_t=feedback\\_reaction\\_generic](https://web.facebook.com/ttallie/posts/10107582158645124?comment_id=10107582568239294&notif_id=1589999150128095&notif_t=feedback_reaction_generic)
- UNEP. (2019). *Emissions Gap Report 2019*. Nairobi, Kenya: United Nations Environment Programme.
- Valentine, M. @mckinleaf. (2020). Individuals are currently doing about as much as you could ask for in terms of reducing consumption: no air travel, much fewer car trips, less take-away and home delivery food, etc. Carbon emissions have dipped but not by much. Individual action is not the answer. Twitter. <https://twitter.com/mckinleaf/status/1255413545447108609>

## DETRITUS & ART / A personal point of view on Environment and Art by Rainer Stegmann

Artists seldom provide an interpretation of their own work; they leave this to the observer. Each of us will have his/her own individual view of a specific piece of art, seeing different contents and experiencing a range of own feelings and emotions. Bearing this in mind, I created this page where you will find regularly selected masterpieces from different epochs and I express my thoughts on what the work conveys to me personally. My interpretation will refer specifically to the theme "Environment". Any comments or suggestions regarding this column should be addressed to [stegmann@tuhh.de](mailto:stegmann@tuhh.de).



**KARL KLUTH** / 1931 Coast in Northern Schleswig.

My first impression looking at this artwork was somehow spooky or mystic; dark sky with huge clouds partly illuminated by the full moon, dark sea with white foam waves and a green landscape dominated by a high dike in the moonlight. Looks like that at the foot of the dike are some buildings, surrounded by grassland and water areas. The high dike retains the water and hinders it from flooding the land below sea level. Perhaps the water areas down on land originate from sea- water overflowing the dike during stormy weather.

For very long time humans have an impact on nature; this is also the case when protecting land from the sea. In times of climate change this impact experiences a new dimension: extreme weather conditions appear more frequently and ice is melting in the pole areas, which leads to continuous rise of sea water levels (1901 – 2010 from 1,7 mm/a - 3,2 mm/a). Until end of this century humans can

expect a sea-level rise of 26-55 cm if appropriate actions are taken (otherwise 45-82 cm) (IPCC (International Panel of Climate Change)). Wide areas of countries like the Maldives may be flooded. As a consequence existing dikes will be raised and new ones have to be constructed. High amounts of resources as sand, clay and plastic liners will be necessary associated with enormous costs and high environmental impact.

When Karl Kluth painted this picture in the year 1931 climate change was not an issue. He would be surprised establishing a connection between his painting and climate change, interpret his artwork as a kind of eye opener for the danger of further sea-level rise. The dike dominates the painting, it enables the safety of people, land and habitats, but the big dark clouds around the moon create a bit scary atmosphere reminding us of the risks of stormy weather and further sea level rise. For me this artwork underpins the necessity to take more immediate actions against global warming to reduce sea-level rise and extreme weather conditions like big storms.

Humans have to control nature in the future to a much higher extent; by these means world will become more vulnerable, more artificial. We all have to make a bigger effort to reduce these increasing risks.

But despite these thoughtful reflections we can see also the beauty in this painting for enjoying and encouraging us.

*Next issue: I will present the famous sculpture "Bull's Head" of Pablo Picasso, which he created in 1942. Picasso is one of the most well known artists of our time; he was born in Malaga, Spain in 1881 and died in Mougins, France in 1973. He used different expressions and techniques in his around 50 000 paintings, drawings, graphics, ceramics and sculptures. Picasso influenced substantially art of the 20th century.*

- Van Rensburg, Melissa L., Nkomo, S'phumelele L., & Dube, Timothy. (2020). The 'plastic waste era'; social perceptions towards single-use plastic consumption and impacts on the marine environment in Durban, South Africa. *Applied Geography*, 114, 102132. doi: <https://doi.org/10.1016/j.apgeog.2019.102132>
- Willis, Kathryn, Hardesty, Britta Denise, Vince, Joanna, & Wilcox, Chris. (2019). The success of water refill stations reducing single-use plastic bottle litter. *Sustainability*, 11(19), 5232.
- Wünsch, Christoph, & Simon, Franz-Georg. (2018). The Reduction of Greenhouse Gas Emissions Through the Source-Separated Collection of Household Waste in Germany. In R. Maletz, C. Dornack & L. Ziyang (Eds.), *Source Separation and Recycling: Implementation and Benefits for a Circular Economy* (pp. 269-287). Cham: Springer International Publishing.
- Zambrano-Monserrate, Manuel A, & Ruano, Maria Alejandra. (2020). Do you need a bag? Analyzing the consumption behavior of plastic bags of households in Ecuador. *Resources, Conservation and Recycling*, 152, 104489.
- Zoroufchi Benis, Kh, Safaiyan, A., Farajzadeh, D., Khalili Nadji, F., Shakerkhatibi, M., Harati, H., Sarbazan, M. H. (2019). Municipal solid waste characterization and household waste behaviors in a megacity in the northwest of Iran. *International Journal of Environmental Science and Technology*, 16(8), 4863-4872. doi: 10.1007/s13762-018-1902-9

## A PHOTO, A FACT, AN EMOTION



*"I made this shot in Sylhet, Bangladesh. It is a place where all of the garbage of the city is collected and burnt together."*

### **"LIFE AND WASTE"**

Sylhet, Bangladesh

**Nafiul Islam, Bangladesh**



This photo was selected to participate in the third edition of Waste to Photo in 2019, the photo contest connected to the Sardinia Symposium, International Waste Management and Landfill Symposium organised by IWWG.

Waste to Photo is conceived with the specific aim of recreating a scenario representing the global situation with regard to waste and landfills, ranging from the developing countries to the more industrialised nations.

The 3rd edition of the contest officially closed on 31st May, receiving over a hundred entries. During the Symposium, a photography exhibition was set up using a selection of the most significant shots and a jury consisting of members of the IWWG Managing Board and professional photographers voted for the best photo.

In this shot, Mr. Nafiul Islam shows a widespread situation in many countries of the world.

Garbage dumps are mostly inhabited by vulnerable populations, including those who face extreme poverty, severe illness and/or disability, and lack of educational opportunities. Dumps are the only place in these areas where

people can live for free and find items that they can keep for their families or sell for profit, which incentivizes vulnerable populations to stay there.

In almost all garbage dumps, recycling garbage offers opportunities for small wages for those willing to filter through the contents – a wage that allows individuals and their families to survive, but not a high enough wage for them to leave.

Elena Cossu  
*Studio Arcoplan, Italy*  
email: [studio@arcoplan.it](mailto:studio@arcoplan.it)

## ABOUT THE AUTHOR

### **Nafiul Islam**

He is a passionate photographer from Bangladesh. He is currently studying at the University of Bremen, Germany. He started his photographic journey with the hand of Shahjalal University Photographers' Association (SUPA) about 9 years ago. This photographic journey has helped him to travel and meet many people and to capture their stories.



(Contents continued from outside back cover)

**Columns**

<b>BOOKS REVIEW</b>	
Ecotoxicology, New Challenges and New Approaches .....	I
<b>ENVIRONMENTAL FORENSIC</b>	
Environmental Forensics: The What? When? Where? Why? and How? .....	III
<b>INFO FROM THE GLOBAL WORLD</b>	
The source of waste and the end of waste: covid-19, climate, and the failure of individual action .....	V
<b>DETRITUS &amp; ART / A personal point of view on Environment and Art</b>	
Karl Kluth / Coast in Northern Schleswig .....	VIII
<b>A PHOTO, A FACT, AN EMOTION</b>	
Life and waste, Sylhet, Bangladesh .....	IX

## CONTENTS

### Editorial

- “CLOSING THE LOOP” OF THE CIRCULAR ECONOMY AND COVID19  
M.C. Lavagnolo ..... 1

### Biological treatment

- EVALUATION OF NEW SMALL-SCALE COMPOSTING PRACTICES WITH ENERGY RECOVERY  
R.G. Lima Jr. and C.F. Mahler..... 3

- EVALUATION OF TEMPERATURE CHANGES IN ANAEROBIC DIGESTION PROCESS  
S.Ö. Cinar and K. Kuchta ..... 11

### Recycling and enhanced landfill mining

- UTILIZATION OF DEMOLITION WOOD AND MINERAL WOOL WASTES IN WOOD-PLASTIC COMPOSITES  
P. Jetsu, M. Vilkki and I. Tiihonen ..... 19

- CASE STUDY ON ENHANCED LANDFILL MINING AT MONT-SAINT-GUIBERT LANDFILL IN BELGIUM: MECHANICAL PROCESSING, PHYSICO-CHEMICAL AND MINERALOGICAL CHARACTERISATION OF FINE FRACTIONS <4.5 MM  
D. Vollprecht, J.C. Hernández Parrodi, H. Lucas and R. Pomberger ..... 26

- CASE STUDY ON ENHANCED LANDFILL MINING AT MONT-SAINT-GUIBERT LANDFILL IN BELGIUM: PHYSICO-CHEMICAL CHARACTERIZATION AND VALORIZATION POTENTIAL OF COMBUSTIBLES AND INERT FRACTIONS RECOVERED FROM FINE FRACTIONS  
J.C. Hernández Parrodi, D. Vollprecht and R. Pomberger ..... 44

### WEEE

- SILVER RECOVERY FROM END-OF-LIFE PHOTOVOLTAIC PANELS  
L.S.S. de Oliveira, M.T. Weitzel Dias Carneiro Lima, L. H. Yamane and R.R. Siman ..... 62

- END-OF-LIFE MANAGEMENT OF PHOTOVOLTAIC PANELS IN AUSTRIA: CURRENT SITUATION AND OUTLOOK  
T. Dobra, M. Wellacher and R. Pomberger ..... 75

### Sewage Sludge

- CHARACTERISATION OF BACTERIAL DIVERSITY IN FRESH AND AGED SEWAGE SLUDGE BIOSOLIDS USING NEXT GENERATION SEQUENCING  
K.R. Little, H.M. Gan, A. Surapaneni, J. Schmidt and A.F. Patti ..... 82

- EFFECTS OF THE DIFFERENT IMPLEMENTATION OF LEGISLATION RELATING TO SEWAGE SLUDGE DISPOSAL IN THE EU  
T. Bauer, L.E. Burgman, L. Andreas and A. Lagerkvist ..... 92

### Waste to energy

- BIOGAS FROM CASSAVA PEELS WASTE  
F.A. Aisien and E.T. Aisien ..... 100

- ROLE OF BIOGENIC WASTE AND RESIDUES AS AN IMPORTANT BUILDING BLOCK TOWARDS A SUCCESSFUL ENERGY TRANSITION AND FUTURE BIOECONOMY – RESULTS OF A SITE ANALYSIS  
A. Schüch, J. Sprafke and M. Nelles ..... 109

### Landfill

- USE OF ALTERNATIVE COVER MATERIALS TO CONTROL SURFACE EMISSIONS (H<sub>2</sub>S AND VOCs) AT AN ENGINEERED LANDFILL  
Y. Le Bihan, D. Loranger-King, N. Turgeon, N. Pouliot, N. Moreau, D. Deschênes and G. Rivard ..... 118

- DETECTION AND ANALYSIS OF METHANE EMISSIONS FROM A LANDFILL USING UNMANNED AERIAL DRONE SYSTEMS AND SEMICONDUCTOR SENSORS  
I. Daugela, J.S. Visockiene and J. Kumpiene ..... 127

- LANDFILL AIR POLLUTION BY ULTRAFINE AND MICROPARTICLES IN CASE OF DRY AND WINDLESS WEATHER CONDITIONS  
E. Hroncová, J. Ladomerský and D. Ladomerská ..... 139

### Semi aerobic landfilling

- THE ELEVATED TEMPERATURE AND GAS COMPONENT WITHIN AN OPERATING SEMI-AEROBIC LANDFILL  
V.Q. Huy, Y. Kohata and H. Yoshida ..... 147

- OPTIMISED MANAGEMENT OF SEMI-AEROBIC LANDFILLING UNDER TROPICAL WET-DRY CONDITIONS  
V. Grossule and M.C. Lavagnolo ..... 160

### Landfill leachate

- TECHNO-ECONOMIC EVALUATION OF LANDFILL LEACHATE TREATMENT BY HYBRID LIME APPLICATION AND NANOFILTRATION PROCESS  
R. de Almeida, F. de Almeida Oroski and J.C. Campos .. 170

- TREATMENT OF LANDFILL LEACHATE AT A REMOTE CLOSED LANDFILL SITE ON THE ISLE OF WIGHT  
T. Robinson ..... 182

- INDEX TO EVALUATE CLOSED LANDFILLS BASED ON LEACHATE PARAMETERS  
C.F. Mahler, J. Righi de Almeida and J.P. Bassin ..... 200

### Waste Management in DCs

- SCALE AND IMPACTS OF LIVELIHOODS DEVELOPMENT ON WOMEN EMPOWERMENT IN THE SOLID WASTE SECTOR OF JORDAN  
M. Saidan, A.A. Drais, E. Al-Manaseer, M. Alshishani and C. Linton ..... 212

*(Contents continued on inside back cover)*